C55 402. G51/v.2

PROCEEDINGS

PENNSYLVANIA STATE UNIVERSITY
JUL 17 1985
DOCUMENTS COLLECTION

First International Symposium on Precise Positioning with the Global Positioning System

POSITIONING WITH GPS—1985

Volume II

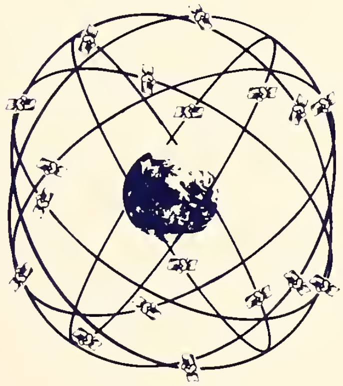

Rockville, Maryland
April 15-19, 1985

U.S. DEPARTMENT OF COMMERCE
National Oceanic and Atmospheric Administration
National Ocean Service

May 1985

PROCEEDINGS

First International Symposium on Precise Positioning with the Global Positioning System

POSITIONING WITH GPS—1985

Volume II

Rockville, Maryland
April 15-19, 1985

Clyde C. Goad
Convenor

Symposium sponsored by:

International Union of Geodesy and Geophysics
International Association of Geodesy

U.S. Department of Defense
Defense Mapping Agency

U.S. Department of Commerce
National Oceanic and Atmospheric Administration

in cooperation with
American Society of Civil Engineers

U. S. Depository Copy

For sale by the
National Geodetic Information Center, NOAA
Rockville, MD 20852

Mention of a commercial company or product does not constitute an endorsement by the National Oceanic and Atmospheric Administration. Use for publicity or advertising purposes of information from this publication concerning proprietary products or the test of such products is not authorized.

The following are registered trade names:

Macrometer is a trademark of Aero Service Division, Western Geophysical Company of America.

Wild Heerbrugg is a registered trademark owned by Wild Heerbrugg Ltd., Switzerland.

Magnavox is a registered trademark owned by North American Philips Corporation, U.S.A.

Any omission of other registered trademarks within these proceedings is unintentional.

PREFACE

This symposium was conceived at the International Union of Geodesy and Geophysics general meeting in Hamburg, 1983, by the executive council of the International Association of Geodesy (IAG). At that general meeting only two papers were presented on the subject of precise positioning with the Global Positioning System. It was clear at that time, however, that interest in this subject was very high, and an attendance of around 450 persons was expected for the symposium in Rockville two years later. After scheduling by the IAG, the Defense Mapping Agency and the National Oceanic and Atmospheric Administration agreed to support the meeting. In addition, the American Society of Civil Engineers advertised the symposium in its various journals. Their support is gratefully acknowledged.

Almost 600 persons attended "Positioning with GPS-1985," approximately one-third more than had been expected. Nearly 30 percent of the attendees were from outside the United States. Eighty-eight papers were presented within a four-day format. Approximately 420 enjoyed themselves at the Thursday evening banquet and heard a very entertaining talk given by Dr. Charles Whitten.

These proceedings contain the written versions of all the talks, as submitted by the authors.

The local technical organizing committee, composed of Dr. Benjamin Remondi, Dr. Alan Evans, and Mr. Larry Hothem, is responsible for the successful meetings format which allowed so many papers to be given in four days. Other support from Ms. Peggy Morrish, Ms. Grace Sollers, Mr. John Gergen, and Mr. Bernard Chovitz is also acknowledged with gratitude.

I am very grateful to the National Geodetic Survey's editor, Mrs. Eleanor Andree, for her effort in organizing these volumes.

Clyde Goad
Convenor

CONTENTS

Preface..iii

SESSION 1: OVERVIEW, STATUS, AND POLICY
Moderator: C. C. Goad

Vol. I

GPS Instrumentation and Federal Policy
J. D. Bossler and C. W. Challstrom.................................... 1

Transition from NAVSTAR to GPS Geodesy
R. Anderle.. 11

NAVSTAR Global Positioning System: 1985
W. H. Wooden 23

Civil Use of the Global Positioning System Precision Positioning Signal
P. Baker and F. Zedeck... 33

SESSION 2: GPS TIME AND ORBITS
Moderator: C. C. Goad

On-Orbit Frequency Stability Analysis of NAVSTAR GPS Clocks and the Importance of Frequency Stablity to Precise Positioning
T. B. McCaskill and J. A. Buisson.................................... 37

NSWC's GPS Orbit/Clock Determination System
E. R. Swift.. 51

Interferometric Determination of GPS Satellite Orbits
R. I. Abbot, Y. Bock, C. C. Counselman III, R. W. King, S. A. Gourevitch, and B. J. Rosen.. 63

GPS Orbit Improvement and Precise Positioning
E. J. Krakiwsky, B. Wanless, B. Buffett, K. P. Schwarz, M. Nakiboglu..... 73

Force Modelling for GPS Satellite Orbits
C. Rizos and A. Stolz... 87

Modelling and Estimating the Orbits of GPS Satellites
G. Beutler, W. Gurtner, I. Bauersima, R. Langley......................... 99

The GPS Radiation Force Model
H. F. Fliegel, W. A. Feess, W. C. Layton, and N. W. Rhodus...............113

GPS Satellite Orbit Determination from Radio Interferometry Data
J. B. Zieliński and E. Butkiewicz....................................121

SESSION 3: USER EQUIPMENT
Moderator: A. Stolz

An Alternative Concept for the Design of a Low Cost C/A Code NAVSTAR GPS Receiver
M. T. Allison and P. Daly..127

Capabilities of the TR5S Sercel GPS Receiver for Precise Positioning
C. Boucher and G. Nard....................135

The First Wild-Magnavox GPS Satellite Surveying Equipment: WM-101
T. A. Stansell, Jr., S. M. Chamberlain, and F. K. Brunner....................147

Static Point Positioning with an L1, C/A Code GPS Receiver
A. K. Brown and M. A. Sturza....................161

The Macrometer II™ Dual-Band Interferometric Surveyor
J. W. Ladd, C. C. Counselman III, and S. A. Gourevitch....................175

Codeless Systems for Positioning with NAVSTAR-GPS
P. F. MacDoran, R. B. Miller, L. A. Buennagel, and J. H. Whitcomb....................181

SESSION 4: USER EQUIPMENT TESTING
Moderator: A. Stolz

Geodetic Applications of the Texas Instruments TI 4100 GPS Navigator
D. J. Henson, E. A. Collier, and K. R. Schneider....................191

Precise Baseline Determination with a New Codeless GPS Receiver
J. Collins....................201

New Results on the Accuracy of the C/A Code GPS Receivers
J. Ashjaee....................207

Experiences with TI 4100 NAVSTAR Navigator at the University of Hannover
G. Seeber, D. Egge, A. Schuchardt, J. Siebold, and G. Wübbena....................215

Phase Center Variation in the Geodetic TI 4100 GPS Receiver System's Conical Spiral Antenna
M. L. Sims....................227

Collocation Tests of an Advanced Geodetic Global Positioning System Receiver
A. G. Evans, B. R. Hermann, D. S. Coco, and J. R. Clynch....................245

SESSION 5: MODELING AND PROCESSING
Moderator: A. G. Evans

Three-Dimensional Geodetic Control by Interferometry with GPS: Processing of GPS Phase Observables
Y. Bock, R. I Abbot, C. C. Counselman III, R. W. King, and S. A. Gourevitch....................255

Integrated Modelling of GPS-Orbits and Multi-Baseline Components
G. W. Hein and B. Eissfeller....................263

Improved Second Order Design of the Global Positioning System - Ephemerides, Clocks, and Atmospheric Influences
E. W. Grafarend, W. Lindlohr, and A. Stomma....................273

Magnet-4100 GPS Survey Program Processing Techniques and Test Results
R. Hatch and K. Larson....................285

GPS Interferometric Phase Algorithms
V. Ashkenazi, L. G. Agrotis, and J. H. Yau....................299

On the Elimination of Biases in Processing Differential GPS Observations
P. Vaníček, A. Kleusberg, R. B. Langley, R. Santerre, and D. E. Wells....315

SESSION 6: MODELING AND PROCESSING
Moderator: A. G. Evans

Modeling the GPS Carrier Phase for Geodetic Applications
B. Remondi....325

Oasis - A New GPS Covariance and Simulation Analysis Software System
S. C. Wu and C. L. Thornton....337

Precise Relative Position Determination Using Global Positioning System Carrier Phase Measurements in a Nondifference Mode
C. C. Goad....347

GPS Carrier Phase Ambiguity Resolution Over Long Baselines
P. L. Bender and D. R. Larden....357

Evaluation of GPS Carrier Difference Observations: The Bernese Second Generation Software Package
W. Gurtner, G. Beutler, I. Bauersima, and T. Schildknecht....363

The Case for Ranging in GPS Based Geodetic Systems
W. G. Melbourne....373

SESSION 7: MODELING AND PROCESSING
Moderator: D. E. Wells

Concept of the Geodetic Interferometer "RYSY" for Baseline Determination with GPS
Z. J. Krysiński and K. K. Vorbrich....387

Multi-Station GPS with Orbit Improvement
E. G. Masters and A. Stolz....395

Software Developments for Geodetic Positioning with GPS Using TI 4100 Code and Carrier Measurements
G.Wübbena....403

Reduction of Multipath Contamination in a Geodetic GPS Receiver
F. R. Bletzacker....413

GPS Satellite Multipath: An Experimental Investigation
L. E. Young, R. E. Neilan, and F. R. Bletzacker....423

SESSION 8: APPLICATIONS (PART I)
Moderator: D. E. Wells

Absolute Calibration and Precise Positioning between Major European Time Observatories and the U.S. Naval Observatory Using GPS
J. A. Buisson, O. J. Oaks and H. Warren....433

Sensitivity of GPS Caribbean Baseline Performance to the Location of a Southerly Fiducial Station
P. M. Kroger, C. L. Thornton, J. M. Davidson, S. A. Stephens, and B. C. Beckman....447

A Survey of GPS Satellite System Alternatives and Their Potential for Precise Positioning
K. D. McDonald and R. L. Greenspan....................................457

GPS Accuracy While Surveying Arrays of Deep Ocean Transponders
L. A. Anderson..473

Application of GPS in a High Precision Engineering Survey Network
R. Ruland and A. Leick..483

Interferometric Processing of NNSS Doppler Observations
Sz. Mihaly, T. Borza, and I. Fejes....................................495

SESSION 9: SURVEY POSITIONING RESULTS
Moderator: B. W. Remondi

Vol. II

GPS Positioning Software at the Ohio State University: Franklin County Results
Ziqing Wei..509

Precise Relative Positioning with the Macrometer V-1000 Interferometric Surveyor: Experiences at the Geodetic Survey of Canada
D. McArthur, N. Beck, K. Lockhead, D. Delikaraoglou...................521

Baseline Determination in Geodetic First Order Networks - A Comparison of GPS Results with ERS-1 and POPSAT Simulations
H. Wilmes and K. Kaniuth..533

High-Precision, Three-Dimensional Differential Positioning Using GPS
W. E. Strange...543

A Comparison between Global Positioning System and Very Long Baseline Interferometry Surveys in Alaska and Canada
G. L. Mader and M. D. Abell...549

SESSION 10: SURVEY POSITIONING RESULTS
Moderator : B. W. Remondi

The Quebec 1984 Macrometer™ Test: Comparison of Phase-difference Processing and Network Solution Methods
R. Moreau, G. Beutler, J. G. Leclerc, B. Labrecque, R. B. Langley, and R. Santerre...557

Macrometer Measurements 1984 in the Inn Valley Network
H. Heister, A. Schödlbauer, and W. Welsch.............................567

Comparison of Survey Results from Different Types of GPS Receivers
A. Kleusberg, R. B. Langley, R. Santerre, P. Vaníček, D. E. Wells, and G.Beutler...579

Recovery of a 1700 km Baseline Using Dual Frequency GPS Carrier Phase Measurements
E. Cannon, G. Lachapelle, and C. C. Goad..............................593

The March 1985 Demonstration of the Fiducial Network Concept for GPS Geodesy: A Preliminary Report
J. M. Davidson, C. L. Thornton, C. J. Vegos, L. E. Young, and T. P Yunck...603

GPS - A User's Critique
R. W. Leeman H. D. MacAulay, and L. B. Fletcher.......................613

SESSION 11: PRACTICAL ASPECTS OF GPS GEODETIC SURVEYS
Moderator : C. C. Counselman III

Comparing the Predicted Positioning Costs of Doppler and GPS Technology
J. K. Crossfield.....625

Factors To Be Considered in Development of Specifications for Geodetic Surveys Using Related Positioning GPS Techniques
L. D. Hothem and G. E.Williams.....633

On The Establishment of 3-D Geodetic Control by Interferometry with the TI 4100 GPS Receiver
D. Delikaraoglou, N. Beck, D. McArthur, and K. Lochhead.....645

Network Adjustment of Correlated Coordinate Difference Observations
D. G. Milbert and W. G. Kass.....657

Variance Analysis of Satellite Networks
W. M. Welsch and W. Oswald.....667

Analysis of Macrometer Networks with Emphasis on the Montgomery (PA) County Survey
J. Collins and A. Leick.....677

SESSION 12: PRACTICAL ASPECTS OF GPS GEODETIC SURVEYS
Moderator : C. C. Counselman III

The Re-adjustment of the First Order Local Geodetic Network in Franklin County, Ohio, Incorporating the Results of the Global Positioning System
L. Sliwa.....695

The Montgomery County Pennsylvania Global Positioning Geodetic Control Project
G. Cuppels and J. Collins.....705

Local Reference Systems in Geodetic Survey Under Consideration of Terrestrial and Satellite Positioning Methods
A. Schödlbauer.....713

Transformation between Geodetic Reference Systems Without Height Information
J. Bittencourt de Andrade.....723

GPS - Considerations for the Potential Geodetic User
J. Hannah.....731

The Impact of VLBI and GPS on Geodesy in Canada
D. Delikaraoglou and R. R. Steeves.....743

SESSION 13: DYNAMIC POSITIONING
Moderator : V. Ashkenazi

Applying GPS to Range Tracking Requirements
C. E. Hoefener and J. Clark.....753

Kinematic Positioning with an Integrated INS-Differential GPS
J. M. Goldfarb and K. P. Schwarz.....757

GPS/IMU Navigation in a High Dynamics Environment
D. Eller.....773

Radio Interferometry in a Moving-Base Application
R. C. Merenyi, S. J. Brzezowski, and W. G. Heller.....783

Performing Centimeter Accuracy Relative Surveys in Seconds Using GPS Carrier Phase
B. W. Remondi....789

Precise Ship's Velocity from GPS: Some Test Results
D. E. Wells, A. Kleusberg, S. H. Quek, J. McCullough, and J. Hagglund....799

SESSION 14: DYNAMIC POSITIONING
Moderator : V. Ashkenazi

Orbit Determination of High-Altitude Earth Satellites: Differential GPS Approaches
S. C. Wu....809

The Use of GPS for Determining the Position of Small Buoys
E. E. Westerfield....819

An Application Study for Using Differential GPS in Airborne Gravity Surveying
W. R. Gumert, G. F. Wertz, and R. M. Iverson....829

Performance Experience of and Design Goals for the SATRACK I & II Missile Tracking Systems
D. J. Duven, C. W. Meyrick, J. R. Vetter, and M. M. Feen....833

Real-Time GPS Tracking for Peacekeeper Test Flights
E. P. Oppenheimer, D. J. Duven, E. E. Westerfield, and J. B. McConnell....843

Predicted Topex Positioning Accuracy with Differential GPS Techniques
S. M. Lichten, S. C. Wu, J. T. Wu, and T. P. Yunck....853

SESSION 15: APPLICATIONS (PART 2)
Moderator : L. D. Hothem

The Present Status and the Plan of Geodetic Applications of Space Technology Including the Global Positioning System in Japan
Y. Baba....863

Results from GPS - Research Projects in Norway
J. C. Blankenburgh, R. Ekseth, T. Hals, and S. Holte....873

Time from GPS
W. J. Klepczynski, K. A. Kingham, M. Imae, and M. Urazuko....879

Geodetic Constraints on Strain Rates in the Vicinity of the 1886 Charleston, South Carolina, Earthquake
W. H. Prescott, S. W. Krueger, and M. D. Zoback....887

A 406 MHz GPS/Emergency Location Transmitter (ELT) for SARSAT Operations
K. P. Maine....897

Recommended GPS Terminology
D. E. Wells....903

List of Registered Participants....933

GPS POSITIONING SOFTWARE AT THE OHIO STATE UNIVERSITY: FRANKLIN COUNTY RESULTS

Ziqing Wei[1]
Dept. of Geodetic Science and Surveying, Ohio State University
Columbus, Ohio 43210-1247

ABSTRACT. The GPS interferometric positioning software at The Ohio State University was designed to process Macrometer^{TM} observations in the single-, double- and triple-differenced phase modes with the capability of estimating relative positions of stations and baseline length, along with their statistics. Inter-station clock epoch offsets are also estimated in the single-difference mode. The correlations between double observables and between triple observables are taken into account. Cycle slips are considered by introducing additional bias (ambiguity) unkonwns in the adjustment.

Test computations were made, using the mainsframe IBM 3081-D computer to determine ten baselines ranging in length from 2-20 km. The OSU baseline solutions agree well with those of the National Geodetic Survey. The results demonstrate that the double-difference mode with bias (ambiguity) fixed provides the best solution among all processing modes so far developed. The single-difference mode, the double-difference mode with bias (ambiguity) free and the triple difference mode are, in the case of no cycle slips, capable of detemining the baselines with the same accuracy. In addition, the clock offset can be estimated to subnanoseconds.

1. INTRODUCTION

GPS geodetic applications generally operate through three approaches: pseudo-range, integrated Doppler and interferometry (Fell 1980). Although each approach has its advantages and uses, at the present stage the interferometric approach seems to be the most attractive to the geodetic community and has come into wide use in practice.

It is expected that carrier phase difference observations are potentially the most precise geodetic measurements that can be made using the GPS system. Tests and operations with the Macrometer V-1000 have demonstrated that an accuracy better than 5 ppm (usually 2-3 ppm) of relative positions have been achievable over baselines of varying lengths of hundreds of meters to several thousand kilometers (Hothem and Fronczek 1983, Bock et al. 1983), and that several-meter accuracy of single point positioning has been obtainable (Bock et al. 1983). It is believed that with the availability of the two-frequency instrument the accuracy of the GPS interferometric positioning will be further improved and will find more applications in surveying, geodesy and geodynamics.

In view of the importance of the GPS interferometric positioning in geodetic applications we have developed three types of software for relative positioning on single baseline basis: the single-(SD), double-(DD), and triple-difference(TD) processing programs. The test run was made on the mainframe IBM 3081-D to process the data set collected by the National Geodetic Survey (NGS) with the Macrometer V-1000 in 1983 in Franklin County, Ohio. The results are encouraging and agree well in general with the NGS results.

---

[1] Visiting scholar from Research Institute of Surveying and Mapping of the Shaanxi provincial Bureau of Surveying and Mapping, Xian, China.

2. DATA PREPROCESSING AND MATHEMATICAL MODELS

2.1 Data Preprocessing

Data preprocessing is intended to detect cycle slips and to edit blunders. To our knowledge there are several approaches in practice for tackling the problem. The commonly used approach is to manually edit the data by examining residuals on the computer screen after the usual single- and double-difference solutions. Another approach is to fit the piecewise continuous SD and DD observations to a time polynomial, and then to correct slipped observations (Beutler et al. 1984). The above approaches are interactively performed, somewhat based on the operator's experience. After data editing, a small error may still remain in the related observations. The third approach is using the triple-difference solution, in conjunction with the SD or DD solution to automatically deal with the cycle slips (Remondi 1985).

Our approach to handling cycle slips is simply the introduction in the main programs of an additional bias (ambiguity) unknown whenever cycle slips occur. The cycle slips should be ascertained in the data preprocessing stage. In doing so two steps are taken:

(1) To reject sparse data. If the loss of lock frequently occurs at a certain channel during a short period (usually when the satellite is near critical cut-off angle, ~25°-30°), the sparse observations, most likely undergoing cycle slips are meaningless for data processing. They need to be rejected.

(2) To ascertain when and where the loss of lock happened. First the delta single-differences (defined as the difference between two single differences at consecutive epoches) are formed for an individual satellite, and their prediction values are also evaluated using the known orbit, the approximate positions of the stations, and the measured clock offset and drift rate. Then the observations minus predicted values, called "O-C", are calculated. Finally the first differences of O-C are formed. If the first difference exceeds a selected criterion, a mark should be tagged to a specific single difference, indicating that cycle slip(s) had occurred at the related epoch. The criterion is unnecessarily too tight in view of the fact that once cycle slips happened, hundreds and thousands of cycles might be lost or gained.

The correctness of detecting cycle slips using the above procedure will be further tested with the help of the triple-difference of the (O-C)'s, formed by differencing the (O-C)'s, for two satellites in the same epoch interval. Knowing that the triple difference substantially reduces the effect of the instabilities of the receiver oscillators, the triple differences of the (O-C)'s should be very small (e.g., < 1 cycle), provided that the initial coordinates of the stations are good enough. Otherwise a blunder could be considered to exist instead of a cycle slip.

2.2 Single-Difference Mode

The observation equation for the single-difference phase is

$$\frac{fs}{c}\left(\frac{\bar{r}_2}{r_2}\,\overline{\Delta r}sta_2 - \frac{\bar{r}_1}{r_1}\,\overline{\Delta r}sta_1\right)+\left(f_S - f_S\,\frac{\dot{r}_2}{c} - \frac{\Delta f}{2}\right)\Delta T + N = l + v \qquad (1)$$

where

$l \quad = SD + \frac{f_S}{c}\,(r_2 - r_1)$

$v \quad$ = residual

$\overline{\Delta r}_{sta_1}$, $\overline{\Delta r}_{sta_2}$ = corrections to approximate positions of the stations

ΔT = clock offset between two station clocks

N = bias (ambiguity)

$\bar{r}_{1(2)}$ = $\bar{r}_s - \bar{r}_{sta_{1(2)}}$; $\bar{r}_s$, $\bar{r}_{sta_{1(2)}}$ are the respective position vectors of the satellite and the station 1(2)

$r_{1(2)}$ = $|\bar{r}_s - \bar{r}_{sta_{1(2)}}|$

$\dot{r}_2$ = rate of change of r_2

SD = observed single-difference phase, corrected for tropospheric refraction

Δf = $f_{R_2} - f_{R_1}$, frequency offset between the receivers

f_s = satellite frequency (1575.42 MHz)

c = the speed of light

In the standard algorithm, station 1 is held fixed, and the parameters to be solved for are $\overline{\Delta r}_{sta_2}$, N_i, $i=1, 2, \ldots, n$, where n is the number of observed satellites (Note: every time cycle slips occur, i is increased by one), and ΔT_j, $j = 1, 2, \ldots, m$, where m is the number of observation epochs. The reason for including so many unknowns ΔT is to isolate the clock error from the position parameters to be estimated. As a by-product we obtain the time synchronization error between stations to subnanosecond level (see section 3.4).

As seen from eq. (1), the coefficient of ΔT is close to a constant; ΔT and N are highly correlated. To avoid the singularity problem it is necessary to fix ΔT_1, the offset at the first epoch, at its measured value. It should be pointed out that if cycle slips occur at all channels at a certain epoch, the solutions to the clock offsets and, in turn, to the relative position, are usually not so strong. It is also necessary to constrain the clock offset at the epoch when cycle slips occur, to measured value, which can be evaluated by eq. (3) (see next section).

Solving for numerous unknowns ΔT could be readily manageable in the least squares process without wasting storage area and computational time.

2.3 Double-Difference Mode

The observation equation for the double difference is formulated by differencing two SD equations, corresponding to the satellites j and k, at the same epoch. That is,

$$\frac{f_s}{c}\left(\frac{\bar{r}_2{}^k}{r_2{}^k} - \frac{\bar{r}_2{}^j}{r_2{}^j}\right) \overline{\Delta r}_{sta_2} - \frac{f_s}{c}\left(\frac{\bar{r}_1{}^k}{r_1{}^k} - \frac{\bar{r}_1{}^j}{r_1{}^j}\right) \overline{\Delta r}_{sta_1} + \frac{f_s}{c}\left(\dot{r}_2{}^j - \dot{r}_2{}^k\right) \Delta T +$$

$$+ \left(N^k - N^j\right) = \left(l^k - l^j\right) + v \qquad (2)$$

The comparison of eq. (2) with eq. (1) shows that the coefficient of ΔT in the DD case is reduced by a factor of $c/\dot{r} \approx 10^5$, resulting in the insensitivity of DD to the clock offset. So it is impossible to accurately recover clock parameters from this mode. Taking advantage of the insensitivity we could gain the high accuracy of positioning from the DD mode. Then it is necessary to model ΔT as

$$\Delta T = C_0 + \dot{C}(t - t_0) \qquad (3)$$

the C_0 and $\dot{C}$ being the clock offset and the clock rate, usually held fixed at their a priori values, either measured or estimated in the SD mode, though solvable as options. In the standard algorithm, only the position of station 2 and biases are solved for.

Suppose m+1 is the number of satellites observed at an observing session, the independent combinations of $(N^k - N^j)$ are m, implying only m bias parameters in this mode. It should be pointed out that a choice is left to select an arbitrary satellite as reference from one epoch to the next. (This is often unavoidable because of the visibility of the satellite, or the malfunction of the instruments.) When the reference satellite is not the original one (suppose it is designated as ℓ), we have to introduce two unknowns $(N^k - N^\ell)$ and $(N^j - N^\ell)$ into the present observation equation resulting from differencing the single differences, corresponding to the satellites k and j.

It is apparent that the correlations only exist between DD's at the same epoch, assuming SD's are independent. There are several ways of dealing with the correlations (Remondi 1984, Beutler et al. 1984). The following method is used in our program.

Suppose the satellites observed at the epoch i are numbered 1, 2, 3, ..., m_i, m_{i+1}. Without loss of generality, let the first satellite be chosen as a reference. The relation between DD's and SD's can be expressed as

$$\begin{bmatrix} DD(1,2,i) \\ DD(1,3,i) \\ \vdots \\ DD(1,m_i,i) \end{bmatrix} = \begin{bmatrix} -1 & 1 & & & & 0 \\ -1 & 0 & 1 & & & \\ -1 & 0 & 0 & 1 & & \\ \vdots & \vdots & \vdots & \vdots & & \\ -1 & 0 & 0 & 0 & \ldots & 1 \end{bmatrix} \begin{bmatrix} SD(1,i) \\ SD(2,i) \\ SD(3,i) \\ \vdots \\ SD(m_{i+1},i) \end{bmatrix} \tag{4}$$

Realizing that the individual SD is independent, with variance σ^2, we get the covariance matrix of DD's

$$\Sigma_i = \sigma^2 \begin{bmatrix} 2 & 1 & 1 & \ldots & 1 \\ 1 & 2 & 1 & \ldots & 1 \\ \vdots & \vdots & \vdots & & \vdots \\ 1 & 1 & 1 & \ldots & 2 \end{bmatrix} \tag{5}$$

The weight matrix is

$$P_i = \sigma^2 \Sigma_i^{-1} = \frac{1}{m_i+1} \begin{bmatrix} m_i & -1 & -1 & \ldots & -1 \\ -1 & m_i & -1 & \ldots & -1 \\ \vdots & \vdots & \vdots & & \vdots \\ -1 & -1 & -1 & \ldots & m_i \end{bmatrix} \tag{6}$$

The weight matrix for all DD observations are in the form

$$P = \begin{bmatrix} P_1 & & & 0 \\ & P_2 & & \\ & & \ddots & \\ 0 & & & P_n \end{bmatrix} \tag{7}$$

where subscripts 1, 2, ..., n are epoch number. In eq. (7), each submatrix on the leading block-diagonal has the same pattern as eq. (6). Because of the property of the weight matrix, the normal equation can be separately formed for each epoch, and the entire system of normal equations can be obtained simply by adding normal equations for individual epochs together.

The chi-squared quantity V^TPV, needed for the estimation of the variance of unit weight, can be calculated according to

$$V^{T}PV = \sum_{1}^{n} L_i^{T} P_i L_i - \hat{X}^{T} \sum_{1}^{n} A_i^{T} P_i L_i \tag{8}$$

where A_i, L_i are the respective design matrix and constant term vectors of the observation equations for the ith epoch, and $\hat{X}$ is the solution vector.

The baseline determination in the DD mode is insensitive to the instabilities of the oscillators of both the satellite and the receiver. It is expected that the bias, due primarily to the ambiguity per se and secondarily to instrumental factors and the atmospheric refraction effect (in our software no consideration is given to the ionospheric refraction correction), should be an integer for a short baseline, e.g., up to 30 km long. In order to exploit the bias integer feature after the primary least squares solution, a set of integer biases minimizing $V^{T}PV$ at a chosen confidence level are found. Then the least squares procedure is repeated with the biases fixed at the set of integers. In our program the double solution with bias fixed (designated as DD1) is optionally implemented.

2.4 Triple-Difference Mode

The observation equation for TD can be formed either by subtracting the DD equation for the current epoch from that for the next epoch, or by differencing the delta single-difference equations corresponding to two satellites in the same epoch interval. The equation need not be written here because of its straightforwardness.

The triple difference is insensitive to clock errors, and susceptible to isolation of blunders and cycle slips. Therefore, the triple-difference mode can serve as a powerful tool to edit blunders and to detect cycle slips.

It is impossible for the triple difference to take advantage of the bias-integer feature in data analysis. So in the case of a short baseline the results for the TD solution are likely to be less accurate than the DD bias fixed solution. But for longer baselines, this is no longer a problem.

The correlations exist between TD's both at the same epoch interval and between consecutive epoch intervals. It is easy to dervie the correlations. Suppose the satellites observed during the observation session are numbered j, k, ℓ, m, n in that order. Naturally not all of them are observed at a certain epoch. Suppose the satellite with the lowest number always is chosen as reference at each epoch, then the general rules for creating the covariance matrix are (Remondi 1984):

a. for the same epoch i

$$\mathrm{cov}[\mathrm{TD}(k,\ell,i),\ \mathrm{TD}(k,m,i)] = \sigma^2 \begin{bmatrix} 4 & 2 \\ 2 & 4 \end{bmatrix} \tag{9}$$

b. for the consecutive intervals i, i+1

$$\mathrm{cov}[\mathrm{TD}(k,\ell,i),\ \mathrm{TD}(m,n,i+1)] = \begin{cases} -2\sigma^2 & \text{if } k=m \text{ and } \ell=n \\ -\sigma^2 & \text{if } k=m \text{ or } \ell=n\text{, but not both} \\ \sigma^2 & \text{if } k=n \text{ or } \ell=m \\ 0 & \text{otherwise} \end{cases} \tag{10}$$

The covariance matrix for all TD observations is in the form

$$\Sigma = \begin{bmatrix} V_{11} & V_{12} & & & & 0 & \\ V_{21} & V_{22} & V_{23} & & & & \\ & V_{32} & V_{33} & V_{34} & & & \\ & & & \ddots & V_{n-1,n-2} & V_{n-1,n-1} & V_{n-1,n} \\ & 0 & & & & V_{n,n-1} & V_{nn} \end{bmatrix} \qquad (11)$$

in which V_{ij} is formed according to eqs. (9) and (10), $V_{ij} = V_{ji}^T$, n is the number of effective epoch intervals.

Remondi gave a method for solving the normal equations for the triple difference in an attempt to save time and storage (Remondi 1984). Analogous to his scheme we developed a procedure for reducing the normal equation, which appears somewhat more efficient.

Given the normal equation

$$A^T \Sigma^{-1} AX = A^T \Sigma^{-1} L \qquad (12)$$

the least squares solution $\hat{X}$ is desired. Let

$$Z^T = A^T \Sigma^{-1} \qquad (13)$$

Then eq. (12) becomes

$$Z^T AX = Z^T L \qquad (14)$$

It follows that the key to solving eq. (12) lies in finding Z. Transposing eq. (13)

$$Z = (\Sigma^{-1})^T A = \Sigma^{-1} A \qquad (15)$$

we get

$$\Sigma Z = A \qquad (16)$$

According to Eq. (16) the matrix Z can be sought by first reducing forwards the matrix A and then substituting backwards, both on epoch interval basis. It is not required to store V_{ij}. Furthermore, it is convenient to incorporate part of the computation of $V^T\Sigma^{-1}V$ into the process of reducing A. In fact, from the expression

$$V^T \Sigma^{-1} V = L^T \Sigma^{-1} L - X^T Z^T L \qquad (17)$$

we can see that in order to obtain $L^T\Sigma^{-1}$ it is only necessary to augment A into (A,L) and to reduce (A,L) in the same manner as that for reducing A.

3. NUMERICAL EXPERIMENTS

3.1 Observation Data

The survey observations available to us are the Macrometer V-1000 data, which are single differences in the form of a tape file. The contents of the file contain the epoch number, satellite ID, modified Julian day and its fraction, single difference phase, signal-to-noise ratio and tropospheric refraction correction. Detailed information about the single difference file may be found in (Remondi 1984).

Fig. 1 is a sketch showing the observation stations involved and the approximate lengths of individual baselines. The observation data were collected by NGS in

Franklin County, Ohio, on November 8, 9, 10 and 15, 1983. One observing session was accomplished each day. During the first three sessions up to six satellites were simultaneously observed with three Macrometers at as many stations. For the last session only two instruments were used to determine a single baseline. Each session lasts nearly three hours, containing 41-59 equally spaced epochs.

The satellites observed were SV4, SV5, SV6, SV8, SV9 and SV11. Of these, SV4 was visible only at a very late stage of the observation sessions.

3.2 Observation Statistics

Included in Table 1 is the number of observations used in the SD, DD and TD modes and the estimated uncertainties of observations. For comparison, the uncertainties of the NGS solutions are also included.

It is noted that the SD observations used in both the SD and the DD modes are exactly the same, while the SD observations used in the TD mode is probably slightly less than those used in the SD mode due to the triple-difference formation. Also note that the numbers of the TD observations used in our and NGS' analyses are not exactly equal for most of the baselines.

For most cases the uncertainty of observation is designated by its standard deviation, defined as $\sqrt{V^TPV/DF}$, where Df is degrees of freedom. For the cases of baselines 7, 8, 9 and 10 for the DD mode, the uncertainty is computed by $\sqrt{V^TV/DF}$, regardless of correlations for computational convenience. For the TD (NGS) case the statistics given in Table 1 are RMS of fit. And no wonder the statistics of NGS differ from ours.

As shown in Table 1, the standard deviations are nearly identical for the three modes, of course with the exception of baselines 7, 8, 9 and 10 for the DD solution. Note that the standard deviations for the double difference mode with bias fixed might be slightly larger than those for the DD mode. The estimated standard deviations in the DD1 mode should more realistically represent the observation accuracy, which disperses between 0.08 and 0.2 half cycles, with the mean of 0.135 half cycles. We find at a glance that the observations associated with the baseline 1883-SMIT are of very poor quality. The related standard deviation reaches 0.74 cycles! The reason for the abnormality needs to be investigated.

3.3 Baseline Solutions

The baseline lengths with their uncertainties are summarized in Table 2. It can be found that the discrepancies between the SD and DD solutions range from 0.3 to 2.7 cm, with an absolute average of 1.0 cm and that the discrepancies between the SD and TD solutions are within 3.6 cm, with most of them centered at 0.0 cm. For both cases above the maximum discrepancies occurred with the baseline CLAR-BRIT, for which cycle slips occurred in the observations at only two effective channels at the 15th epoch. A similar situation happened to the baseline BRIT-SHAN.

In the case of baselines 1-6, and 9, where no cycle slips occur, the three modes provide essentially the same solutions without regard to the insignificant discrepancies between the solutions and between their uncertainties. No evidence was found that geometric strength of structure for positioning was noticeably degraded by differencing single differences, as one would expect.

The comparisons between the double difference solutions with bias free and with bias fixed, show that the bias-fixed solutions are appreciably superior to the bias-free solutions. The standard deviations for the former are much lower than those for the latter. There is no doubt that the double-difference mode with bias fixed could provide us with a baseline solution with the best accuracy among all types of solutions.

It can be seen from Table 2 that our SD or DD solutions agree with NGS' TD solutions within 1 cm for most baselines. The maximum departure reaches 3.1 cm for baseline CLAR-BRIT, for which cycle slips happened to the observations related. The agreements between our TD solutions and NGS TD solutions are also satisfactory, again with the exception of the baselines BRIT-SHAN and CLAR-BRIT. The discrepancies of -2.6 and -6.7 cm probably become understandable if we take into account the fact that the different data editing techniques and slightly different observations were used in processing, and that the ephemerides used by NGS and us come from different sources.

Table 3 summarizes the uncertainties of the components of the baseline vectors in terms of north, east and up. it can be seen from Table 3 that for the SD and DD modes, characterized by the bias being a real number, and for the TD mode, free of bias parameters, the error in longitude is consistently larger than in latitude, indicating that the nonambiguity ingredient of bias (i.e., the fractional part of bias) primarily maps into longitudinal direction. It is interesting to note that for the DD1 mode (bias fixed), the error in height becomes dominantly larger than that in horizontal components because uncorrected ionospheric and residual tropospheric refraction then manifest themselves in being major contributors to the error sources.

3.4 Clock Offset Estimation

As described earlier, the clock offset estimates are part of the solutions in the SD mode, and they are useful for the purpose of time transfer. As an example, the typical behavior of the variations in clock offsets between clocks 914 and 908 at the endpoints of baseline 1883-HOWE (18.72 km) is illustrated in Fig. 2. It is not unusual that clocks have the excursion of a few nanoseconds over one epoch interval, as seen from Fig. 2. It is expected that in the case of no cycle-slips one can achieve the offset estimates accurate to the subnanosecond level for the clocks at least a few tens of kilometers apart. The standard deviations of the clock offset estimates for the specific pair of clocks range from 0.031 to 0.054 ns.

Our experience demonstrates that if cycle slips occur at all channels at a certain epoch, it is hardly possible to accurately recover the offset parameters.

4. CONCLUSIONS

The software packages for processing Macrometer data developed at The Ohio State University have proven to work well through the test run using ten baselines ranging from 2-20 km. It is shown that the agreements between our and NGS results are fairly good, though remarkable discrepancies exist for few baselines.

Among all modes of data processing, the double-difference mode with bias fixed provides the best solution in terms of standard deviation.

For the observation session without breaks, the single-difference mode, the double-difference mode with bias free, and the triple-difference mode yield essentially the same solution for baseline determination, provided that proper considerations are given to the correlations between double differences and between triple differences. For the observation session with breaks, the three modes appear to give slightly different solutions, caused by slightly different processing techniques used in the three modes.

For short baselines (e.g., shorter than 20 km in our case), the accuracy of the relative positions is dependent on bias treatment. In the mode with bias free or free of bias parameters, the error in longitude is higher, whereas in the mode with bias fixed, the error in height becomes dominant.

The three modes are all powerful tools for solving the relative positioning problem. Each approach possesses its own advantages and uses. In addition to positioning, the single difference mode has the capability of estimating clock synchronization to the subnanosecond level. The double-difference mode enables taking advantage of integer bias feature in the case of short baselines, by which the highest accuracy would be achieveable. The triple difference mode is absolutely free of bias parameter, and therefore convenient for data editing; it might be even more useful in the multistation solution.

Cycle slips can be effectively handled by introducing an additional bias unknown. It is necessary to identify in advance where and when cycle slips occur.

The above conclusions are based only on the limited results of the ten baselines. More and longer baselines are needed to be processed to further test our software. Some possible improvements are to be devised with emphasis on the capability of data editing.

Acknowledgements

I wish to express my gratitude to the Department of Geodetic Science and Surveying of the Ohio State University for its extensive support and arrangements for this investigation. I would like to thank the National Geodetic Survey for kindly providing us with Macrometer data and the Massachusetts Institute of Technology for the GPS ephemerides. I am grateful to Dr. Ivan I. Mueller for his valuable suggestions and advice during this investigation and for his comments on this manuscript. Many thanks are due to Dr. Y. Bock for instructive discussions which were very useful and helpful in developing our software. I am also grateful to the extensive computer support provided by the Instruction and Research Computer Center of the Ohio State University.

References

Beutler, G., D.A. Davidson, R.B. Langley, R. Sauterre, P. Vanicek and D.E. Wells, 1984: Some Theoretical and Practical Aspects of Geodetic Positioning Using Carrier Phase Difference Observations of GPS Satellites, Dept. of Surveying Engineering Tech. Rep. 109, Univ. of New Brunswick, Fredericton, N.B. Canada.

Bock, Y., R.I.Abbot, C.C. Counselman, S.A. Gourevitch, R.W. King and A.R. Paradis, 1983: Geodetic Accuracy of the Macrometer Model V-1000, presented at IUGG XVIII General Assembly, Hamburg, FRG.

Fell, P.J., 1980: Geodetic Positioning with a Global Positioning System of Satellites, Dept. of Geodetic Science Rep. 299, Ohio State Univ., Columbus.

Hothem, L.D. and C.J. Fronczek, 1983: Report on Test and Demonstration of Macrometer^{TM} Model V-1000 Interferometric Surveyor, Federal Geodetic Control Committee: FGCC-IS-83-2, Rockville, MD.

Remondi, B.W., 1984: *Using the Global Positioning System (GPS) Phase Observable for Relative Geodesy: Modelling, Processing, and Results*, PhD dissertation, Univ. of Texas at Austin.

Remondi, B.W., 1985: Global Positioning System Carrier Phase: Description and Use, submitted for publ. in *Bull. Geodesique.*

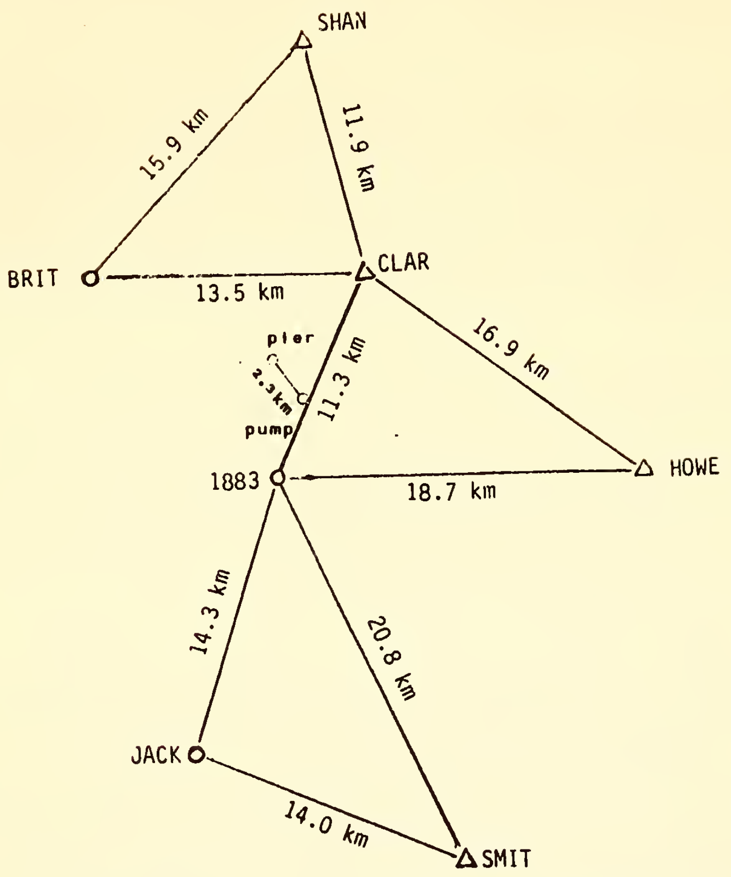

Fig. 1 Observation stations and approximate baseline lengths.

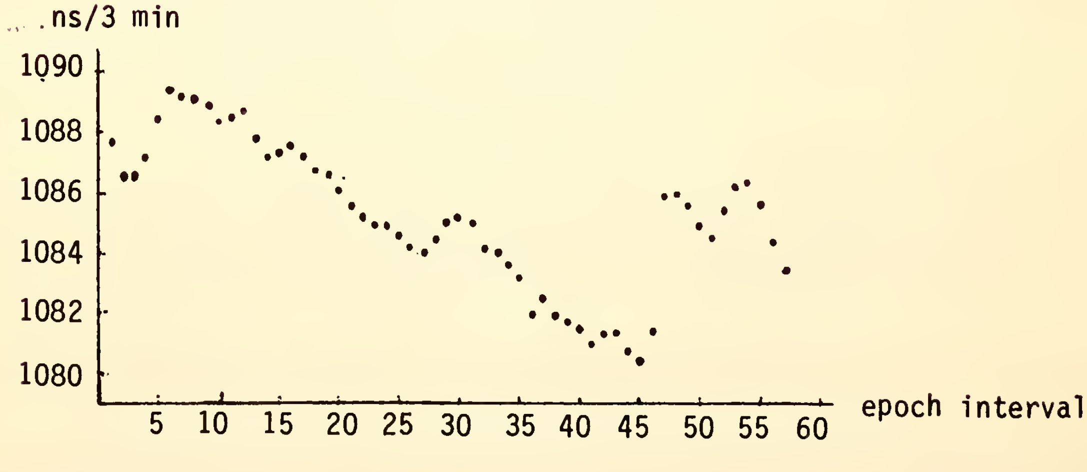

Fig. 2 **Behavior of clock drift between clocks 914 and 908**

Table 1 Number of Observations Used in Various Modes with Their Uncertainties

No.	Baseline	Number of Observations Used					Uncertainties (in half cycles)				
		SD	DD	DD1	TD	TD(NGS)	SD	DD	[1]DD1	TD	[2]TD(NGS)
1	1883-CLAR	213	154	154	150	154	0.102	0.100	0.110	0.100	0.134
2	1883-HOWE	233	174	174	170	172	0.169	0.161	0.171	0.167	0.156
3	CLAR-HOWE	212	153	153	149	149	0.184	0.176	0.200	0.180	0.166
4	1883-JACK	250	191	191	186	185	0.131	0.128	0.138	0.130	0.194
5	1883-SMIT	242	183	183	178	178	0.740	0.738	—	0.732	0.334
6	JACK-SMIT	243	184	184	179	181	0.088	0.086	0.112	0.088	0.121
7	BRIT-SHAN	156	115	115	108	107	0.088	*0.120	0.122	0.084	0.138
8	CLAR-BRIT	153	110	110	104	103	0.105	*0.132	0.142	0.111	0.133
9	CLAR-SHAN	207	151	151	147	149	0.131	*0.186	0.137	0.130	0.156
10	PIER-PUMP	217	161	161	155	156	0.078	*0.097	0.079	0.077	0.112

[1] Double difference made with bias fixed.

[2] The statistics in this column mean RMS of fit.

*Computed by $\sqrt{V^TV/DF}$, with correlations neglected.

Table 2 Baseline Lengths (m) with Their Uncertainties (cm)

No.	Baseline	SD	DD	[1]DD1	TD	TD(NGS)
1	1883-CLAR	11312.468	11312.465	11312.471	11312.468	11312.462
		0.3	0.2	0.2	0.2	
2	1883-HOWE	18720.484	18720.467	18720.495	18720.485	18720.476
		2.0	1.9	0.3	2.0	
3	CLAR-HOWE	16927.483	16927.468	16927.506	16927.483	16927.474
		3.1	3.0	0.4	3.1	
4	1883-JACK	14257.928	14257.931	14257.945	14257.928	14257.929
		0.4	0.4	0.2	0.4	
5	1883-SMIT	20808.917	20808.914	—	20808.917	20808.926
		7.7	7.7	—	7.6	
6	JACK-SMIT	13996.732	13996.724	13996.757	13996.731	13996.724
		1.1	1.1	0.2	1.0	
7	BRIT-SHAN	15884.369	15884.383	15884.357	15884.355	15884.381
		0.7	0.9*	0.2	1.2	
8	CLAR-BRIT	13526.461	13526.488	13526.426	13526.425	13526.492
		1.9	2.4*	0.3	3.4	
9	CLAR-SHAN	11885.131	11885.134	11885.112	11885.131	11885.135
		1.7	2.4*	0.3	1.7	
10	PIER-PUMP	2295.408	2295.413	2295.394	2295.408	2295.413
		1.0	1.3*	0.2	1.0	

[1] Double difference mode with bias fixed.

*Based on variance of unit weight $\sigma^2 = V^TV/DF$, with the correlations neglected.

Table 3 Uncertainties of Baseline Components (cm)

No.	Baseline	SD			DD			[1]DD1			TD		
		σ_N	σ_E	σ_H	σ_N	σ_E	σ_H	σ_N	σ_E	σ_H	σ_N	σ_E	σ_H
1	1883-CLAR	0.9	1.5	0.8	0.9	1.4	0.7	0.2	0.2	0.6	0.9	1.4	0.7
2	1883-HOWE	1.2	1.9	1.2	1.1	1.8	1.1	0.3	0.3	0.8	1.2	1.9	1.2
3	CLAR-HOWE	1.7	2.6	1.4	1.6	2.5	1.4	0.4	0.4	1.1	1.7	2.6	1.4
4	1883-JACK	0.8	1.4	0.9	0.8	1.3	0.8	0.2	0.2	0.6	0.8	1.3	0.9
5	1883-SMIT	4.9	8.2	5.0	4.9	8.2	5.0	–	–	–	4.8	8.1	5.0
6	JACK-SMIT	0.6	1.0	0.6	0.6	0.9	0.6	0.2	0.2	0.5	0.6	1.0	0.6
7	CLAR-BRIT	1.4	1.7	1.6	1.8	2.2	2.2	0.2	0.3	0.7	1.7	2.7	1.6
8	CLAR-SHAN	1.5	2.0	1.8	1.9	2.4	2.3	0.3	0.3	0.9	2.0	3.4	2.2
9	BRIT-SHAN	1.3	2.0	0.9	1.9	2.8	1.3	0.2	0.3	0.7	1.3	2.0	0.9
10	PIER-PUMP	0.6	0.9	0.7	0.7	1.1	0.9	0.1	0.1	0.4	0.6	0.8	0.7

[1] Double difference mode with bias fixed.

Note: The underlined statistics are based on variance of unit weight $\sigma^2 = V^TV/DF$, with correlations neglected.

PRECISE RELATIVE POSITIONING WITH THE MACROMETER V-1000 INTERFEROMETRIC SURVEYOR: EXPERIENCES AT THE GEODETIC SURVEY OF CANADA

D. McArthur, N. Beck, K. Lochhead, D. Delikaraoglou
Geodetic Survey Division
Surveys and Mapping Branch
Energy, Mines and Resources
615 Booth Street
Ottawa Canada
K1A 0E9

ABSTRACT. During the summer of 1983 the Earth Physics Branch (EPB) and the Canadian Geodetic Survey (CGS) of the Federal Department of Energy, Mines and Resources leased two Macrometer (TM) V-1000 GPS receivers in order to evaluate this latest surveying technology and test various independent sets of processing software. The results of this campaign on a precise GPS test network in the Ottawa area led CGS to use, in a subsequent campaign, four Macrometer receivers simultaneously, to survey a 22-station network in the province of Manitoba during the summer of 1984.

This paper summarizes the results obtained during this campaign, with emphasis on the surveying logistics and the practical aspects of surveying with the Macrometer V-1000 receiver, data processing approaches and adjustment methods of the data.

INTRODUCTION

Precise relative positioning is 'a part of the broader mandate of CGS, encompassing the entire spectrum of surveying operations, mapping and positioning services. It is with this goal in mind that the use of the Global Positioning System (GPS) for geodetic and geodynamic applications has received serious attention over the past few years.

In the summer of 1983, EPB and CGS conducted the first evaluation in Canada of the the Macrometer V-1000 Interferometric Surveyor on a precise calibration network in the Ottawa area, established by CGS for the purpose of evaluating various GPS receivers (McArthur, 1985).

The results of this test (Beutler et al, 1984; Valliant et al, 1985) and reported results of tests conducted by other organizations have encouraged CGS to use Macrometer V-1000 receivers for conducting a control survey near Gimli, Manitoba. This paper presents some practical aspects of planning and conducting such a survey, the data processing approach and the results of the survey in Manitoba.

PRACTICAL ASPECTS

The objective of the Gimli area survey was to obtain high accuracy relative 3-D coordinates (2 ppm or better) for 22 existing stations using four Macrometer V-1000 receivers. Embedded in this primary objective, three additional objectives were to: (a) gain some hands on experience in planning such multi-receiver GPS operations; (b) to provide the data necessary for conducting further analyses relating to future deployment strategies and data handling; and (c) evaluate the impact of the single frequency only capability of the V-1000 in measuring baselines up to 150 km.

In planning the survey, control points were selected around the perimeter of the survey area which had either been observed with TRANSIT Doppler or which were part of the national framework. To ensure redundancy, every internal point was to have three vectors measured to it (Hothem et al, 1984) preferably during at least two different sessions. A 5-hour observation period was chosen to provide us data for all visible satellites in the present constellation. Satellites 4, 6, 8, 9, 11, 13 (see Figure 2) were observed whenever they were visible between about 13:00 and 18:00 local time (a time when the state of the ionosphere is rapidly changing).

To avoid unnecessary delays once the receivers arrived on site, reconnaissance was done prior to their arrival. Each site was visited to check for obstructions over 15 degrees of elevation (some trees were cleared at one site), to determine the best access, and to ensure that the receiver vehicles would get within 30-60 metres of the site. Three base locations were selected to be used throughout the project to minimize the daily driving times. In spite of this, the one-way driving time to some stations was up to three hours.

The four-receiver systems and vehicles were driven to the Gimli area from GEO/HYDRO Washington. Three 4-WD vehicles and one station wagon were used for receiver deployment. An extra station wagon was used as a backup vehicle. The backup was forced into operation several days into the project when one vehicle blew an engine.

Vehicles and power supplies (batteries, AC generators, inverters) are all vital, integral parts of the V-1000 system. Although AC generators failed at times (or ran out of fuel), backup battery systems kept the systems going during these periods. Only on two occasions was there a total loss of data due to a power problem.

Upon arrival at a site the antenna had to be centered above the monument on standard survey tripods. Optical plummets in standard tribrachs were used. The plummet was removed and the "unwieldy" 19 kg antenna was placed into the tribrach, often causing the tribrach to move, especially on windy days. Rather than restart the procedure, plumb-bobs were used to re-center the antenna. One antenna arrived with a malfunctioning pre-amp, this hardware problem was repaired within a couple of days by field personnel.

Clock calibration logs were kept daily: the recommended clock sychronization procedures of synchronizing one receiver to the Geosynchronus Orbiting Earth Satellite (GOES) and then to one another were followed, resulting in all receiver clocks being referenced to UTC to within a millisecond. At the end of each day´s observing session, the differences in the receiver clocks relative to one another were recorded to ensure that good a priori estimates for clock offsets and drift rates could be used in the baseline solution. Meteorological information, wet and dry bulb temperatures, and pressure were recorded every hour during observations and recorded in logs at each receiver site. A site obstruction diagram log was maintained along with equipment and project logs detailing the daily operations.

A P-1000 processing system had been brought along in order to generate receiver control files (A-files) for each site daily. Unfortunately the computer system failed during the very first day of operation and was not repaired until the last day. In the mean time A-files had to be sent daily via telephone lines from GEO/HYDRO office in Washington. Because we were in a rural area, the communication lines were quite poor, so that often, transfer of the A-files took three to four hours to complete. With such poor communication lines, attempts to transmit observed data to GEO/HYDRO for verification were soon aborted. On the last day of operation, after the P-1000 was repaired, a simple data verification program (DALOOK) was run to examine all the collected data. The program output indicates the signal quality for the data recorded for each tracker at every epoch. No baseline had to be reobserved on the basis of this output so demobilization could begin.

In all, from August 6 (day 219) to August 22 (day 230) the V-1000 units were deployed 65 times. Only 3 times was data lost or not collected for the reasons already stated. However, had there been no failures, the campaign would have been completed in 12 days instead of the 17 days it eventually took.

DATA PROCESSING

The phase as received from one satellite at one epoch is referred to as a "one-way phase" measurement. The errors in this measurement are due to the random and systematic variations caused by clock errors of the satellite and receiver oscillators, receiver measurement noise and delays as well as atmospheric delays of the signal.

The portion of the systematic errors, which are common to the two stations can be effectively removed by differencing the phase data received simultaneously by two stations to form the single difference observables. Differencing again, this time between satellites yields the so-called double differences. It is this "observable" which is used by GEO/HYDRO for baseline determination between stations observing simultaneously up to six satellites (i.e. current maximun number of satellites the V-1000 is capable of tracking). Errors which remain in this type of observation are the residual ionospheric and tropospheric refraction on the propagation of the signals and the residual satellite ephemeris errors.

GEO/HYDRO program LSQT, uses the double difference observations and solves for the three components of the position of the unknown end of the baseline, and outputs the associated standard deviation and correlations of these components. Although four receivers were used simultaneously, the collected data was processed in a "baseline-by-baseline" fashion which yields only a partial set of results since it does not account for the inherent relationships between various baselines. This necessitated a subsequent network adjustment to arrive at a consistent set of final coordinates.

In order to use the LSQT output values as input to our network adjustment program CASPER, several transformations were required. After transforming the LSQT correlations ρ into a right-handed coordinate system by taking

$$\begin{aligned} \rho_{\phi\lambda} &= -\rho_{\phi\lambda} \\ \rho_{\phi h} &= \rho_{\phi h} \\ \rho_{\lambda h} &= -\rho_{\lambda h} \end{aligned} \tag{1}$$

the covariance matrix (C) of the baseline components was transformed into a local geodetic (LG) right-handed system. From the LSQT standard deviations (σ) and correlations

$$\rho = \frac{\sigma_{ab}}{\sigma_a \, \sigma_b} \tag{2}$$

it then follows readily that

$$P_{(LG)} = \begin{vmatrix} \sigma^2_\phi & \sigma_{\phi\lambda} & \sigma_{\phi h} \\ & \sigma^2_\lambda & \sigma_{\phi h} \\ & & \sigma^2_h \end{vmatrix} = \begin{vmatrix} \sigma^2_\phi & \rho_{\phi\lambda}\sigma_\phi\sigma_\lambda & \rho_{\phi h}\sigma_\phi\sigma_h \\ & \sigma^2_\lambda & \rho_{\lambda h}\sigma_\lambda\sigma_h \\ & & \sigma^2_h \end{vmatrix} . \tag{3}$$

In the next step the local geodetic covariance matrix was transformed to the conventional terrestrial (CT) system through the well-known covariance propagation law

$$C_{(CT)} = R^T \, C_{(LG)} \, R \tag{4}$$

where

$$R = \begin{vmatrix} -\sin\phi \cos\lambda & -\sin\phi \cos\lambda & \cos\phi \\ -\sin\lambda & \cos\lambda & 0 \\ \cos\phi \sin\lambda & \cos\phi \sin\lambda & \sin\phi \end{vmatrix} \tag{5}$$

Similarly the coordinate differences provided by the LSQT program needed only to be changed to a right-handed system i.e.

$$\Delta X_{CT} = -\Delta X_{LSQT} \tag{6}$$

$$\Delta Y_{CT} = +\Delta Y_{LSQT} \tag{7}$$

$$\Delta Z_{CT} = -\Delta Z_{LSQT} \tag{8}$$

The data, now in the form of a total of 84 sets of coordinate differences and their associated covariance information, was ready for input to network adjustment program CASPER. At this point of the processing, there are a number of possible approaches one may choose to treat these coordinate difference observations in a network adjustment. In the sequel we shall dwell briefly on three of them pointing out their relative merits and disadvantages, and summarize the CGS philosophy on the matter.

The optimal way of differencing and combining the one-way phase data collected simultaneously by n (n>2) receivers has been attracting considerable attention recently (cf. Vincenty, 1984; Bock et al, 1984). So far, in the majority of GPS surveys, even if more than two receivers were deployed, the "baseline-by-baseline" mentality has persisted in handling the data. To date, the general approach has been to reduce the data for each pair of stations of n(n-1)/2 baselines and then combine these partial results into an "occupation" adjustment, enforcing the closure relations between baselines forming closed loops. The problem with this approach is that the correlations between the various combinations of vectors are not known, since instead of producing (n-1) independent vectors it yields n(n-1)/2 vectors. The obvious question is then what to do with the redundant ones.

Three possible data processing approaches are examined in this paper in order to observe the impact on the results: 1) select n-1 vectors per session from the possible total of n(n-1)/2 and reject the rest of the so-called "trivial" vectors (e.g. for differential observations from two sides of a triangle of stations, observations from the third side are perfectly redundant - assuming perfect matching observation schedules at each site); 2) combine all n(n-1)/2 vectors observed during one session in one adjustment and then combine these session adjustment results (n-1 sets of coordinate differences)in an overall network adjustment; or 3) use all the observed vectors from the entire campaign in a unified network adjustment.

Method 1 is appealing because it reflects the correct number of "observations". However, in most cases, some observational data may be ignored: for example, data points contributing to the rejected trivial vector(s) that are unique to this determination are not necessarily used for the determination of the other vectors. The selection of trivial vectors is essentially arbitrary and can lead to a very high number of possible combinations of baseline configurations. During the Gimli campaign, where normally 4 receivers observing simultaneously were used, there are 16 possible combinations per session in selecting the 3 vectors to be used in the adjustment. Our overall strategy for selecting these vectors was to ensure that there was a minimum of three vectors to each station included in the network adjustment, in order to maximize the geometrical strength.

Method 2 seems to be the most rigorous since each session adjustment reflects the geometric contributions of all observations through the resulting covariance matrix for n-1 sets of coordinate differences, in addition to producing the correct number of degrees of freedom. A problem which still remains however is that the coordinate differences used in the session adjustments are weighted as if each vector was an independent observation. However, this is not the case, since data from each site are used more than once, so that there exist strong correlations which cannot be represented properly. This problem might be overcome by processing the data after scaling the corresponding covariance matrix of each determination by n/2 as suggested by Vincenty (1984) or more rigorously by processing all observations in a network simultaneously in a "short arc" analysis, akin to the familiar TRANSIT Doppler approach, as suggested by Delikaraoglou et al, (1985), in these proceedings.

Method 3 uses all observations n(n-1)/2 whether they are independent or not. Again with this method, as in method 2, relative weighting is a problem because all trivial vectors are included.

RESULTS

For the purposes of this paper, since the control coordinates are less accurate than those provided by this data, the various results are compared against each other.

Several checks were performed using the output of the LSQT program. The first check was to form triangle closure checks in order to detect any gross blunders due to observational or processing errors. These closures are computed for the daily sessions, and are formed by the vectorial addition of the sides of the triangles. Table 1 shows 48 triangles formed from the observations and a ppm value representing the ratio of the triangle misclosure to the total distance around the triangle. This check is not a definitive test on the overall results, but indicates the internal consistency of the session and points outs vectors that may have larger errors than anticipated. For day 222 we see that the triangle 82R338, 82R339, 82R353 has a small misclosure in relation to the other three triangles for this session. Station 82R311 is common to the three triangles with the higher misclosures. This supports the notion of a less reliable observation from that station on this particular day. Furthermore, examination of the receiver data and the LSQT outputs, it is noticeable that the standard deviations of the solutions involving 82R311 are higher than results involving the other stations for this day.

Comparisons of all vectors observed more than once are summarized in Table 2. All but four of the fifteen vectors agree within 1 to 2 ppm (which is within the stated accuracy of the V-1000) including a 111 kilometer line. In one case the agreement was at 10 ppm for a 9 kilometer line. Discrepancies like this add credibility to statements (e.g. Hothem et al, 1984) that stations must be occupied more than once for redundancy so that possible erroneous determinations are revealed.

The differences between the three methods of adjusting the data are summarized in Table 3. Methods 2 and 3 show the best agreement, but statistically all methods give equivalent results, within the a posteriori standard deviations of the positions. Table 4 presents standard deviations generated by the adjustment for the adjusted positions. Method 1 produces the highest standard deviations of the components; this is likely caused by the loss of geometrical strength when removing trivial vectors. Methods 2 and 3 produce identical standard deviations. This can be explained: the same relative weighting is used and the vectors are treated as independent observations in both methods; different adjustment strategies are used but method 2 produces the correct number of degrees of freedom.

Finally it should be noted from the triangle misclosures (Table 3) that the latitude misclosures are in most cases less than either the longitude or height misclosures; this is also reflected in Table 4 which shows that the latitude component has lower standard deviations associated with it. The polar plot (Figure 2) of the satellite geometry seems to indicate that there should be a stronger latitude determination, since most passes are in a north-south direction as opposed to a east-west direction.

SUMMARY

This paper attempts to outline various aspects of performing control surveys with the Macrometer V-1000. Practical aspects, data processing and results have been discussed.

Concerning the practical aspects: it is prudent to occupy a station a minimum of two times to obtain the highest accuracy and to be able to detect any observational errors, such as centering and vertical offsets.

We have been able to learn a good deal about deployment strategy, however further analysis of optimal ways of deploying four or more receivers is still necessary. An optimum design and deployment strategy can only be arrived at after critical pre-analysis of the network and a decision on post-processing and adjustment techniques to be used.

The many baselines that were observed more than once show repeatability at the 1-2 ppm level. The triangle misclosures for the daily sessions are also better than 2 ppm, showing, as well, good internal consistency.

Demonstrated here were the practical difficulties in the combined adjustment of vectors which have been processed in a "baseline-by-baseline" approach. Three different methods were used to adjust the data with no significant differences in results between the methods. However, due to the neglect of interstation correlation, and the arbritrariness of selecting the vectors to be used in these network adjustments, the apparent procedure for processing and adjusting the data is clearly the one of an overall simultaneous adjustment, which accounts for these inherent problems with the "baseline-by-baseline" approach. In the near future we plan to reprocess all of the raw data with our GPS reduction and adjustment software, which uses the "short-arc" mode and to compare those results with those presented here.

ACKNOWLEDGEMENTS

The authors are indebted to Mario Bérubé for the many hours he spent modifying program CASPER to suit our needs.

DISCLAIMER

No product endorsement is intended or implied by this report.

TRADEMARK

Macrometer (TM) is a trademark of Aero Services Division, Western Geophysical Company of America.

REFERENCES

BEUTLER, G., D.A. Davidson, R.B. Langley, R. Santerre, P. Vaníček, and D.E. Wells (1984): "Some Theoretical and Practical Aspects of Geodetic Positioning Using Carrier Phase Difference Observations of GPS Satellites", Technical Report No. 109, UNB, Fredericton, N.B.

BOCK, Y., R.I. Abbot, C.C. Counselman, S.A. Gourevitch, B.J. Rosen and R.W. King (1984): "Establishment of Three-dimensional Geodetic Control by Interferometry with the Global Positioning System", submitted to Journal of Geophysical Research.

DELIKARAOGLOU, D., N. Beck, D. McArthur, K. Lochhead (1985): "On the Establishment of 3-D Geodetic Control by Interferometry with the TI-4100 GPS Receiver", these proceedings.

ENERGY, MINES & RESOURCES (August 1984): "GPS Gimli Test Network", Geodetic Survey Report of Field Operations.

HOTHEM, L.D., and C.J. Fronczek (1983): "Report on Test and Demonstration of Macrometer Model V-1000 Interferometric Surveyor", Federal Geodetic Control Committee, Report FGCC-IS-2, NGS, NOAA, Rockville, Md.

HOTHEM, L.D., C.C. Goad, B.W. Remondi (1984): "GPS Satellite Surveying - Practical Aspects", Proceedings Canadian Institute of Surveying, 1984 Annual Convention, Quebec, Canada, May 1-4, 1984.

MCARTHUR, D.J. (in preparation): "Ottawa 3D Test Net", Canadian Geodetic Survey, Department of Energy, Mines and Resources.

VALIANT, H.D., (1984): "Canadian Evaluation of the Macrometer Interferometric Surveyor", Earth Physics Branch, File No. 84-4, Ottawa.

VINCENTY, T., (1984): "On the Use of GPS Vectors in Network Adjustments", U.S. NGS, personal communication.

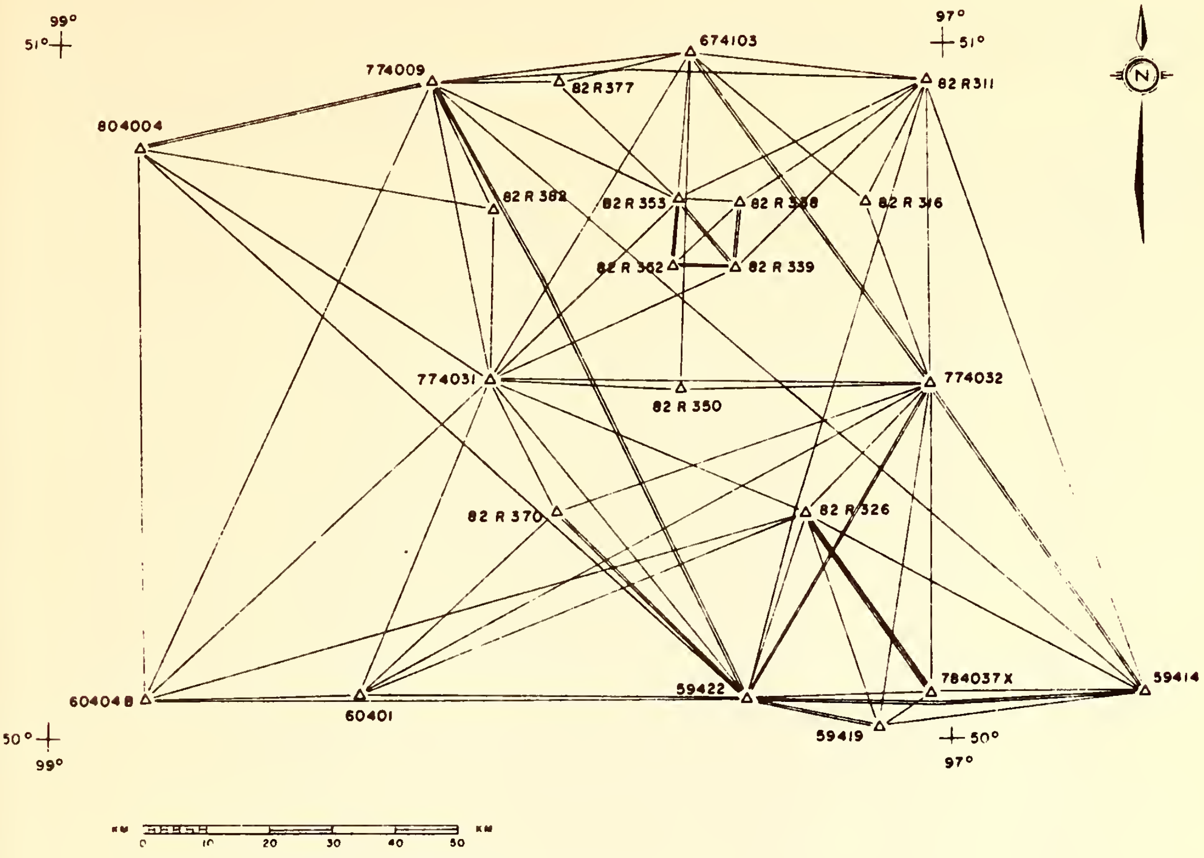

FIGURE 1: Gimli GPS Network
Each line represents an observed baseline

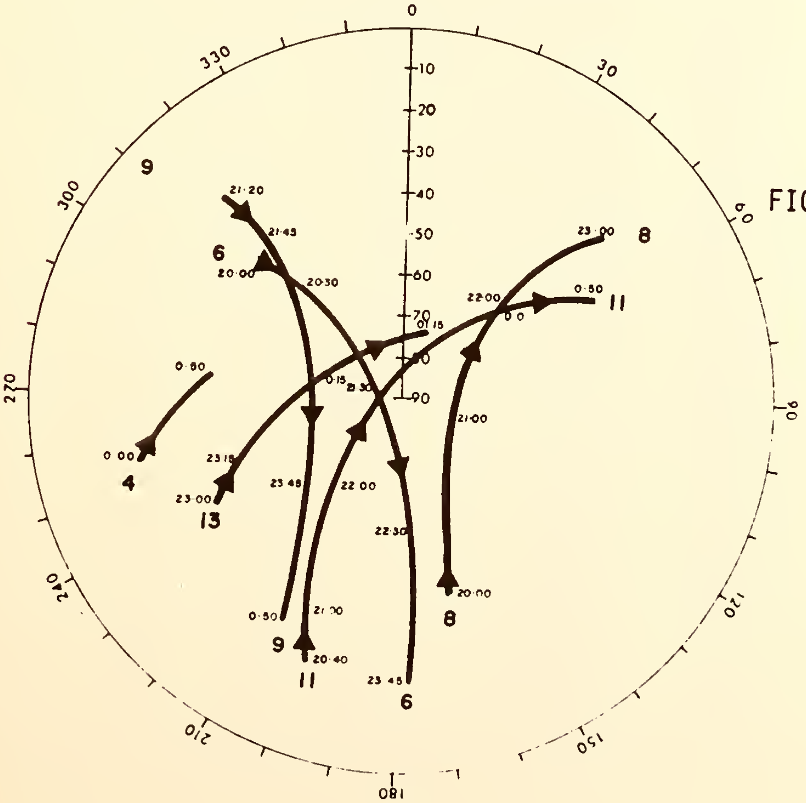

FIGURE 2: Polar Plot showing satellite geometry as a function of azimuth, elevation and time on Aug. 7, 1984 (Day 220)

TABLE 1: TRIANGLE MISCLOSURES OF ALL TRIANGLES AVAILABLE FOR A SESSION

DAY	TRIANGLE			MISCLOSURES (mm)			
				Δφ	Δλ	Δh	ppm
DAY 220	59422	59419	784037X	-6	43	-3	.7
	784037X	82R326	59422	11	-29	-20	.4
DAY 221	59422	59419	774302	18	-21	6	.2
	59422	59419	59414	-72	215	32	1.8
	774032	59414	59419	4	25	-18	.2
	774032	59414	59422	-86	262	9	1.5
DAY 222	82R311	82R353	824338	-25	-73	11	.9
	82R311	824353	82R339	-1	-25	-53	.6
	82R338	82R339	82R311	-26	-47	67	1.0
	82R338	82R339	82R353	-2	1	3	.1
DAY 223	774032	82R316	674103	-4	9	26	.2
	774032	82R316	82R311	-5	31	-7	.3
	82R311	674103	774032	-2	3	-50	.3
	82R311	674103	82R316	-2	-19	-17	.3
DAY 224	774032	674103	774031	-6	-17	64	.3
	774032	674103	82R350	5	31	11	.2
	82R350	774031	674103	5	48	-27	.4
	82R350	774031	774032	-6	1	26	.2
DAY 225	59422	59414	82R311	-2	-1	3	.0
	59422	59414	774009	9	-18	5	.1
	82R311	774009	59422	18	-36	-42	.2
	82R311	774009	59414	07	-18	-34	.1
DAY 226	82R353	82R339	82R352	-54	116	-36	3.9
	82R353	82R339	774031	2	-14	9	.2
DAY 227	674103	82R353	774009	28	-8	82	.8
	674103	82R377	82R377	20	-34	12	.6
	774009	82R377	82R353	05	-17	-27	.3
	774009	82R377	674103	13	9	44	.6
DAY 228	774009	804004	774031	2	-5	9	.1
	774009	804004	82R382	2	-1	5	.0
	774031	82R383	774009	3	-10	4	.1
	774031	82R382	804004	3	-15	8	.1
DAY 229	774009	804004	59422	-23	29	111	.4
	774009	804004	60404B	5	1	-18	.1
DAY 230	774031	82R370	59422	-4	-22	-18	.2
DAY 231	60404B	60401	82R326	0	8	6	.0
	60404B	60401	774031	-1	4	12	.1
	774031	82R326	60401	0	3	1	.0
	774031	82R326	60404B	-1	0	6	.0
DAY 232	82R339	82R352	82R338	0	3	-4	.1
DAY 233	60401	774032	82R370	-3	-7	-4	.0
	60401	774032	59422	1	15	6	.1
	59422	82R370	60401	-1	0	-2	.0
	59422	82R370	774032	-5	22	-11	.2
DAY 234	784037X	59414	82R326	-11	-43	-30	.4
	784037X	59414	774032	-3	-56	-37	.5
	774032	82R326	784037X	1	1	-6	.1
	774032	82R326	59414	-7	15	0	.1

TABLE 2: CONSISTENCIES BETWEEN REPEATED MEASUREMENTS

(units are in millimetres)

OBSERVATION DAYS		BASELINE STATIONS		Δφ	Δλ	Δh	ΔL	ΔL ppm	L
225	229	59422	774009	27	-57	-144	22	.2	111 km
230	230	59422	82R370	-6	41	-53	22	.5	43
222	226	82R339	82R353	-4	2	6	3	.2	14
226	235	82R353	82R352	-30	-11	-93	-30	2.8	11
226	232	82R339	82R352	-98	-74	36	-98	9.9	10
222	232	82R338	82R339	-15	-35	27	-18	1.8	9
223	224	774032	674103	13	55	1	32	.5	65
221	234	774032	59414	-11	-21	-1	-19	.3	60
221	233	774032	59422	-54	89	-11	-3	.0	57
219	220	784037X	82R326	-119	107	-15	-70	2.0	35
219	234	784037X	82R326	-111	82	-85	-68	1.9	35
220	234	784037X	82R326	9	-26	-50	2	.1	35
220	221	59422	59414	-8	-22	3	-24	1.1	21
221	225	59422	804004	44	-217	72	-214	3.4	63
228	229	774009	804004	18	131	-5	132	2.8	47

TABLE 3: DIFFERENCES IN POSITIONS BETWEEN DIFFERENT METHODS

(Units are in millimetres)

STATION	ALL VECTOR - COMBINED SESSIONS method 3 - method 2			ALL VECTOR - TRIVIAL REMOVED method 3 - method 1			COMBINED SESSIONS - TRIVIAL REMOVED method 2 - method 1			
	Δφ	Δλ	Δh	Δφ	Δλ	Δh	Δφ	Δλ	Δh	
774032	0	0	0	0	0	0	0	0	0	FIXED
59414	-3	3	-4	14	-28	-22	17	-31	-18	
59419	-13	13	-2	28	-38	-1	40	-52	2	
59422	-2	-4	0	12	-34	15	13	-30	15	
60401	4	2	3	1	9	-2	-3	7	-5	
60404B	-9	1	3	5	10	41	14	9	38	
674103	11	-2	-9	4	7	3	-7	9	12	
774009	5	6	0	8	-29	17	3	-34	17	
774031	2	4	1	9	-31	18	7	-35	18	
784037X	-24	27	-15	1	13	-1	25	-15	14	
804004	6	5	-4	9	-2	52	3	-7	56	
82R311	4	6	-1	10	-9	-16	6	-14	-15	
82R316	0	4	2	6	-6	-9	6	-11	-11	
82R326	39	7	3	16	16	0	-23	9	-3	
82R338	11	10	1	9	-37	9	-2	-48	8	
82R339	9	9	1	11	-36	9	2	-45	7	
82R350	3	1	3	6	-12	10	3	-13	7	
82R352	13	9	5	15	-30	14	2	-39	9	
82R353	8	7	1	10	-35	5	2	-42	4	
82R370	3	2	0	9	-20	9	6	-22	9	
82R377	6	5	0	7	-21	8	1	-27	8	
82R3B2	5	2	-1	9	-29	20	4	-32	21	

TABLE 4: COMPARISON OF POST-ADJUSTMENT STANDARD DEVIATIONS
(Units are in millimetres)

STATION	TRIVIAL VECTORS REMOVED Method 1			COMBINED SESSIONS Method 2			ALL VECTORS Method 3			
	$\sigma\phi$	$\sigma\lambda$	σh	$\sigma\phi$	$\sigma\lambda$	σh	$\sigma\phi$	$\sigma\lambda$	σh	
774032	0	0	0	0	0	0	0	0	0	FIXED
59414	7	31	18	4	21	12	4	21	12	
59419	6	24	17	4	15	11	4	15	11	
59422	5	23	13	3	15	9	3	15	9	
60401	9	40	23	5	24	14	5	24	14	
60404B	11	55	31	9	43	23	9	43	23	
674103	8	37	22	5	22	13	5	22	13	
774009	7	35	20	5	25	14	5	25	14	
774031	6	30	17	4	20	12	4	20	12	
784037X	6	29	17	4	15	10	4	15	10	
804004	11	54	31	7	32	18	7	32	18	
82R311	6	27	17	4	19	11	4	19	11	
82R316	5	24	14	4	19	12	4	19	12	
82R326	7	31	18	4	15	10	4	15	10	
82R338	9	40	25	6	27	18	6	27	18	
82R339	8	40	24	6	27	16	6	27	16	
82R350	7	32	18	6	29	16	6	29	16	
82R352	9	40	25	6	27	17	6	27	16	
82R353	9	40	24	6	27	16	6	27	16	
82R370	6	30	17	5	21	12	5	21	12	
82R377	9	41	24	7	34	20	7	34	20	
82R382	7	33	19	5	25	15	5	25	15	

BASELINE DETERMINATION IN GEODETIC FIRST ORDER NETWORKS
- A COMPARISON OF GPS RESULTS WITH ERS-1 AND POPSAT SIMULATIONS -

H. Wilmes and K. Kaniuth
Deutsches Geodätisches Forschungsinstitut (DGFI), Abteilung I
Marstallplatz 8, 8000 München 22, FRG

ABSTRACT. At the end of 1983, 11 baselines between 6 stations of the first order triangulation network in the FRG were derived from GPS measurements performed with 4 Macrometer V-1000 receivers. From a two-day observation campaign baseline accuracies of between 2 and 19 cm were achieved.

The same network configuration was simulated both for the ERS-1 spacecraft, which is due to be launched by the ESA in 1989, and for the proposed POPSAT system. Both satellite systems apply microwave range and range rate measurements (experiment name PRARE) as well as, for orbit determination, assistant laser tracking. The simulations, using the covariance analysis technique, yielded the following estimates for baseline precision:

POPSAT: 1-2 cm
ERS-1: 2-4 cm

From the results obtained it can be concluded in particular that the use of the PRARE system on board the ERS-1, although the low orbit of the satellite was not selected for geodetic purposes, will offer a means for improving geodetic triangulation networks.

INTRODUCTION

Since 1983 national survey agencies in the Federal Republic of Germany (FRG) have carried out several experiments in determining relative coordinates of trigonometric points within their first or second order triangulation networks applying the Global Positioning System (GPS). All these campaigns were performed using one-frequency receivers Macrometer V-1000 and aimed in particular at
- obtaining a measure of the efficiency of the GPS system compared to terrestrial surveying methods,
- gaining some experience in applying this new data type in traditional geodetic triangulation networks,

but not at finding the utmost attainable accuracy of the system.

One of these networks was a relatively small 6 station first order network which was observed in autumn 1983 on two days running with 4 Macrometers V-1000. The Deutsches Geodätisches Forschungsinstitut (DGFI) has been involved in this project in so far as it has performed an analysis of the results and transformations into the German Triangulation Network (Schwintzer and Reigber 1984).

Figure 1 shows the network configuration and indicates the precision resulting for each baseline length from the Macrometer measurements. It should be mentioned that due to the fact that in the FRG the terrestrial networks are of high standard and that precise geoid undulations are available a comparison of the GPS results with the terrestrial data makes sense: after applying a similarity transformation (residuals given in parentheses) the consistency of both data sets turned out to be in the range of the quoted standard deviations.

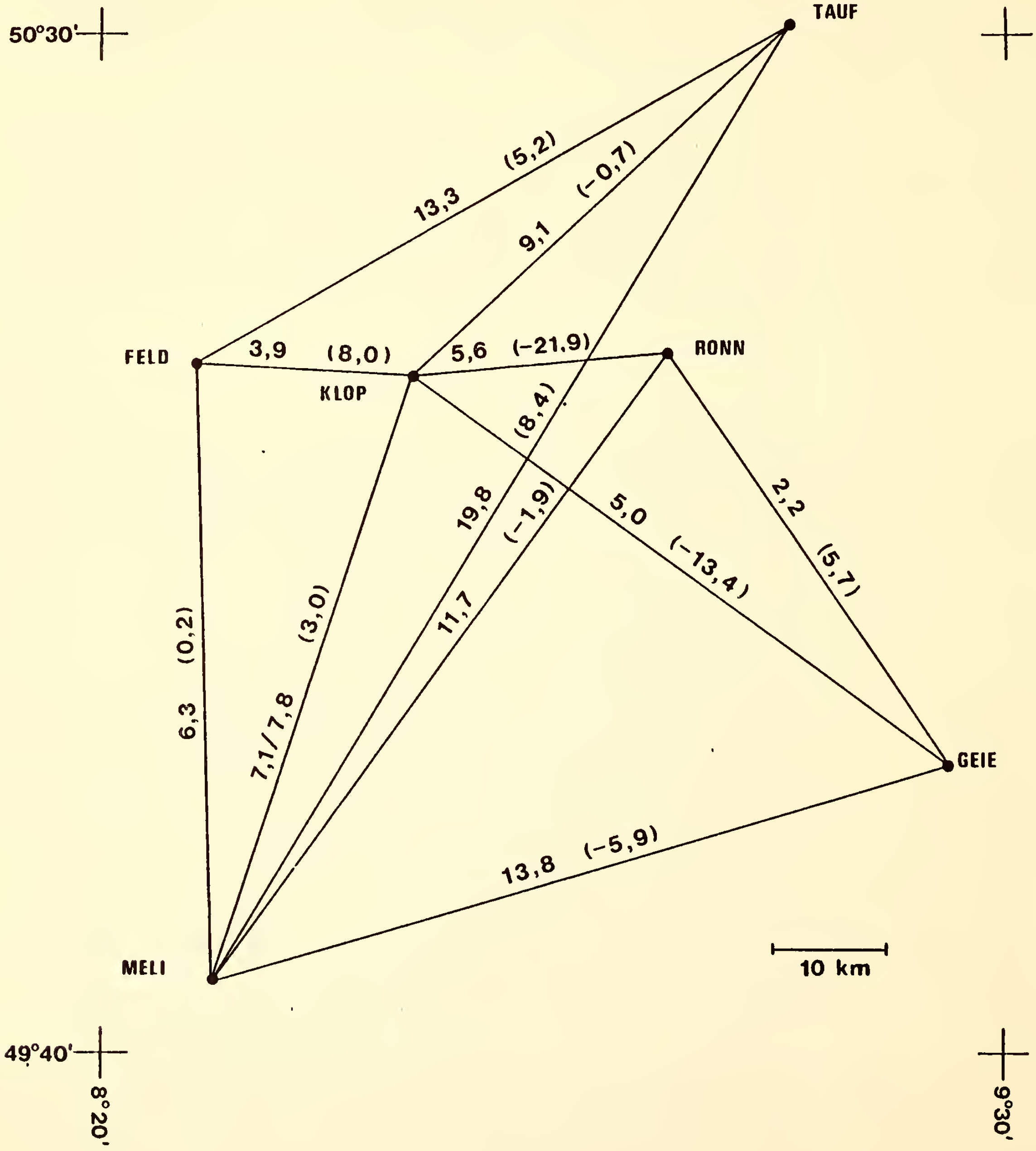

Fig. 1: First order network observed with Macrometers V-1000, baseline length precisions and residuals from a similarity transformation (in parentheses) [cm] (Schwintzer and Reigber 1984)

Although the numbers given in Figure 1 by no means indicate the utmost relative positioning capability of the GPS system it seemed to be appropriate to simulate the same configuration also for the two future satellite systems ERS-1 and POPSAT both to be flown by the European Space Agency (ESA).

THE ERS-1 AND POPSAT SATELLITE SYSTEMS

The ERS-1 satellite, presently in development phase C and definitely due to be launched by the ESA in 1989, will mainly be an oceanographic mission. Therefore, the spacecraft itself and the orbit have not been optimized for geodetic applications. The system will include a radar altimeter and Laser retroreflectors. Moreover, the ESA has accepted a proposal made by (Hartl and Reigber 1982) to accommodate on board the spacecraft an advanced Microwave Tracking System (MTS) and the German Ministry for Research and Technology has decided to finance the MTS space segment as well as some ground stations for the ERS-1 mission. Besides its main purpose of orbit determination for ERS-1, this additional payload also provides the opportunity to exploit the system for relative positioning or baseline determination respectively.

The MTS, bearing the experiment name PRARE (Precise Range and Range Rate Equipment), is essentially identical with the tracking system designed for ESA's POPSAT project. POPSAT will be a dedicated solid earth physics mission consisting of a single satellite the launching of which is at present envisaged for 1992 possibly to be followed by a second spacecraft in 1995/96. The system has been extensively studied (ESA 1982 and 1983) and a compact description is given in (Reigber et al. 1984). The baseline determination performance was also investigated not only for the single spacecraft but also for a multi-POPSAT satellite system (Kaniuth et al. 1984).

Table 1 summarizes the characteristics of both the ERS-1 and the POPSAT system as far as they are relevant to the objective of this paper. In addition, the following few features should be pointed out:

- The MTS is capable of performing two-way and two-frequency Range (R) and Range Rate (RR) measurements; the time delay between the two downlink frequencies 2 GHz and 8 GHz is measured on the ground thus allowing to nearly fully compensate for the ionospheric path delay.

- The estimated R and RR performance assumes a minimum elevation angle of 30° and, in the case of RR, is based on an integration interval of 5 seconds (ESA 1983).

- An essential difference between both systems with regard to the simulations performed consists in the spacecraft structure and the orbital height; ERS-1 due to its relatively low altitude is much more affected by the earth's gravity field than POPSAT, and moreover the surface forces modelling is more complicated.

Table 1: Summary of ERS-1 (PRARE) and POPSAT system characteristics

	ERS-1 (PRARE)	POPSAT
Geodetic Objectives	- Orbit determination as support to radar altimetry - Relative point positioning and baseline determination respectively over short and medium distances - Absolute point positioning for applications requiring only moderate accuracy	- Monitoring of polar motion and earth rotation on an operational basis - Absolute point positioning in a well defined geocentric reference frame - Relative positioning and baseline determination respectively over short to very long distances
Orbit Parameters:		
Semimajor axis	7140 km	13370 km
Eccentricity	< 0.005	< 0.005
Inclination	98.6°	98.6° (double launch with ERS-2)
Space Segment	Box structure with load carrying side panels Area/mass ratio ~ 0.01 m²/kg	Gravity gradient stabilized octahedron with 1.1 m radius Area/mass ratio < 0.005 m²/kg
Tracking Principle	Spaceborne Microwave Tracking System (MTS) - Two-way Range (R) and Range Rate (RR) measurement - Two-frequency downlink (S- and X-band) and one-frequency uplink (X-band) - Simultaneous operation of up to 4 active ground stations - Pseudo noise coded signal - Data collection on board - Data transfer between spacecraft and command ground station for mission control and regular data dump	
	Additional laser tracking assumed	Additional laser tracking possible; Unlimited access for passive ground stations with one-way/two-frequency (X-/S-band) RR capability

Table 1 continued:

	ERS-1 (PRARE)	POPSAT
MTS Performance: Estimation	R noise 5 cm, bias 4 cm RR noise 0.06 mm/s, bias 0.02 mm/s } slightly elevation dependent	
Applied in Simulations	R noise 10 cm, bias 12 cm RR noise 0.10 mm/s, bias 0.12 mm/s	
Ground Segments	Low cost transponders designed for automatic operation, parabolic antenna of 60 cm diameter	
Tracking Network Applied in Simulations	Global network consisting of 11 presently operational Laser stations and 12 PRARE stations performing R + RR microwave measurements	Global network of 16 Mission Execution (MEX) stations performing R + RR microwave measurements and providing nearly total coverage of the orbit

SIMULATIONS

The same network configuration as the one actually observed with Macrometer V-1000 (Figure 1) was applied in the simulations performed for ERS-1 and POPSAT respectively. As with the GPS measurements the total observation period was limited to 2 days in the case of ERS-1 whereas for POPSAT it could be completed in only 24 hours. Due to the properties of the MTS, it was assumed that only 4 stations were being tracked quasi simultaneously. The simulations of baseline determination were performed by covariance analysis (Hatch et al. 1973) and the various error types considered and their propagation are shown in the diagram of Figure 2. However, some comments on the assumptions made for the major error sources should be made:

- It was assumed that the uncertainty of the earth gravity field, projected onto the envisaged launching dates around 1990, could be described by 25% of the standard deviations which resulted for the coefficients of the GRIM3 model (Reigber et al. 1983). This assumption in the case of POPSAT leads to orbit errors of about 15 - 20 cm. In (ESA 1983) it has been proved that orbit accuracies of this order can already be achieved at present, and this is confirmed by the progress in gravity field modelling indicated by the recently derived GRIM3-L1 model (Reigber et al. 1985) withrespect to GRIM3.

- For the reference stations belonging to the global tracking networks the following position errors were introduced:

ERS-1	PRARE stations	1 m	in each coordinate
	Laser stations	10 cm	
POPSAT	MEX stations	10 cm	

  In the case of POPSAT simulations (ESA 1983) indicated that these MEX stations themselves could be absolutely positioned with about 4 cm accuracy from few days tracking. Concerning ERS-1 the tracking network applied was composed of presently operational Laser stations and of some other well positioned geodetic stations (e.g. Doppler) equipped with PRARE transponders.

- The noise and bias of the MTS R and RR data at 5 sec. observation intervals, which were applied in the simulations for both the reference and the baseline stations, are listed in Table 1. From a comparison of these numbers with those resulting from a thorough estimation it is obvious that a considerable margin has been allowed. The Laser data noise was assumed to be 10 cm while the strong weather dependency was accounted for by applying a 25% probability factor for selecting the successfully observed passes from all theoretically possible passes.

- The mismodelling of the tropospheric refraction was assumed to be 2.5 cm in zenith and systematic over the total tracking period of 1 or 2 days respectively. Moreover, this effect was considered to be uncorrelated from station to station. In fact this is a rather pessimistic assumption in particular for a small network with an extent of only about 100 by 100 km. The ionospheric path delay estimation was also assumed to be in error by 1% although this effect is almost totally accounted for by the two frequencies chosen.

- For all other parameters of the geometric and the dynamic model listed in Figure 2, the following errors were introduced:

Polar Motion	0."002	in each component
Air drag	5 %	of the total effect
Solar radiation	3 %	
Albedo radiation	20 %	
Tides	10 %	in K_2, h_2 and l_2

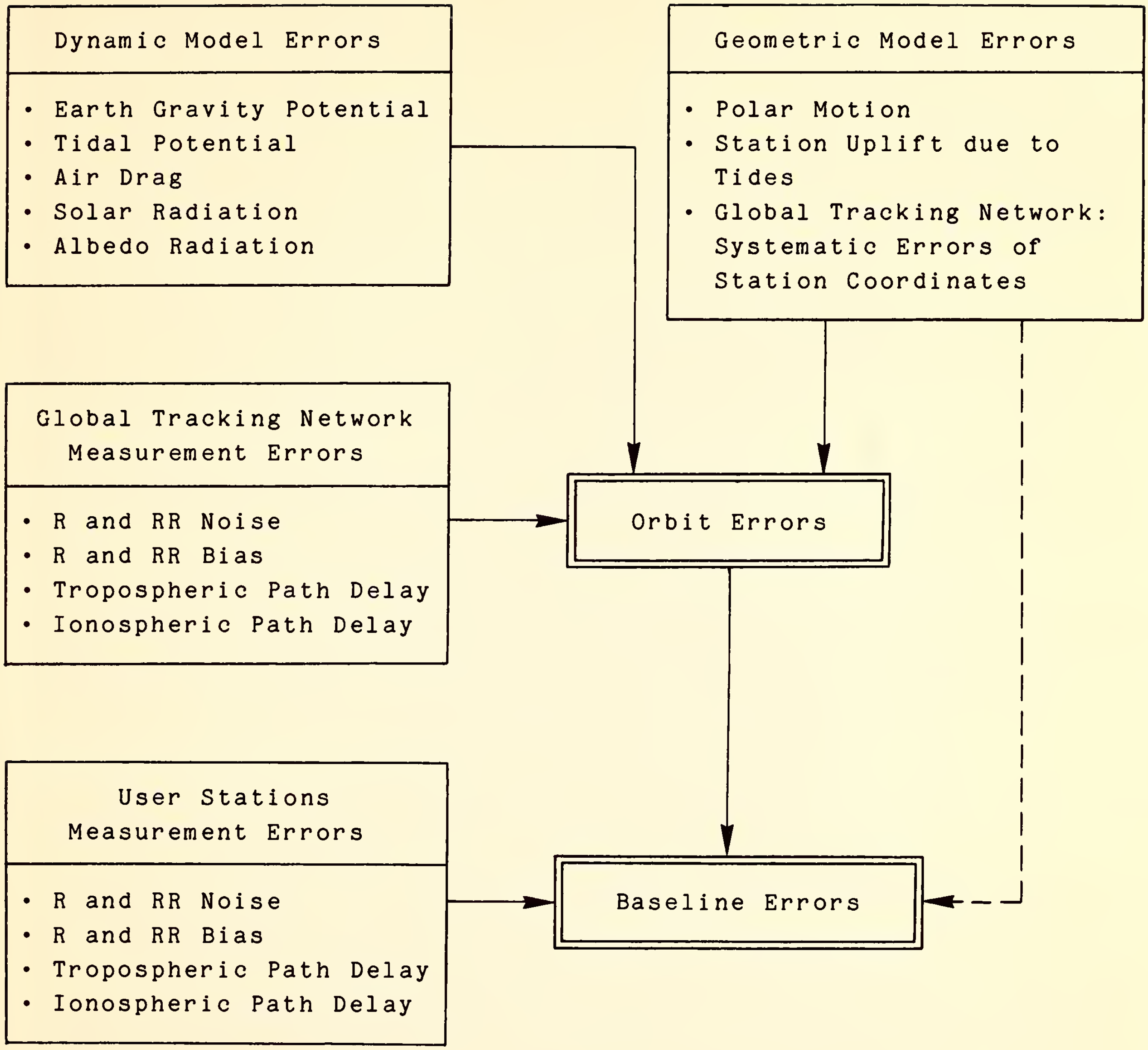

Figure 2: Error model applied in the simulations

Table 2: Total baseline errors and individual error contributions [cm] resulting from 2 days ERS-1 (PRARE) range and range rate data and additional Laser tracking

Baseline	Length (km)	Individual Error Contributions					Total Error (RSS)
		Noise	Trop. Refr.	Grav. Pot.	Solar Rad.	Stat. Coord.	
FELD-MELI	58.0	0.3	2.1	0.1	0.1	0.4	2.2
FELD-KLOP	19.5	0.6	1.0	0.2	0.4	1.4	1.9
FELD-TAUF	62.6	0.6	1.3	1.6	1.2	3.0	3.9
MELI-KLOP	55.4	0.2	2.1	0.1	0.0	0.2	2.1
MELI-TAUF	96.8	0.3	2.1	0.4	0.4	1.1	2.5
MELI-RONN	64.8	0.4	2.0	0.0	0.3	0.9	2.3
MELI-GEIE	60.2	0.6	1.1	0.8	1.1	3.9	4.3
KLOP-TAUF	47.6	0.5	1.7	1.1	0.7	1.6	2.7
KLOP-RONN	23.8	0.6	0.5	0.4	0.6	1.7	2.0
KLOP-GEIE	61.1	0.6	0.9	1.0	0.9	3.7	4.1
RONN-GEIE	45.6	0.4	1.6	0.4	0.3	1.7	2.4

Table 3: Total baseline errors as well as noise and tropospheric refraction error contributions [cm] as resulting from POPSAT range and range rate data for two different one-day arcs

Baseline	Length (km)	Day I			Day II		
		Contribution		Total Error (RSS)	Contribution		Total Error (RSS)
		Noise	Trop. Refr.		Noise	Trop. Refr.	
FELD-MELI	58.0	0.6	1.3	1.4	0.5	1.3	1.4
FELD-KLOP	19.5	0.7	0.7	1.0	0.4	0.4	0.6
FELD-TAUF	62.6	0.7	0.2	0.7	0.4	0.8	0.9
MELI-KLOP	55.4	0.7	1.1	1.3	0.5	1.3	1.4
MELI-TAUF	96.8	0.7	0.9	1.1	0.5	1.3	1.4
MELI-RONN	64.8	0.8	0.8	1.1	0.5	1.2	1.3
MELI-GEIE	60.2	0.7	0.1	0.7	0.4	0.7	0.8
KLOP-TAUF	47.6	0.8	0.6	1.0	0.5	1.1	1.2
KLOP-RONN	23.8	0.7	0.3	0.8	0.4	0.4	0.6
KLOP-GEIE	61.1	0.6	1.0	1.2	0.4	0.6	0.8
RONN-GEIE	45.6	0.6	1.1	1.3	0.4	1.0	1.1

RESULTS

As can be seen from the brief discussions given in the previous section, the assumptions made for some of the model errors introduced into the simulations are pessimistic, especially in view of the progress which can be expected in some areas over the next years. Thus, the baseline errors resulting from the covariance analysis cannot be considered as too optimistic estimations.

Both for ERS-1 and POPSAT several simulations were performed modifying the geometry satellite - ground network within the specifications of the fixed orbital parameters, inclination, eccentricity and semimajor axis. These various simulations were not aimed at finding any optimal solution in regard to baseline precision but at giving an indication of the possible scatter of the results.

Typical examples of the covariance analysis results are given in Tables 2 and 3. The total baseline length errors as well as the effects of individual error sources reaching an order of at least a few mm are listed, in the case of ERS-1, for one two-days arc and, in the case of POPSAT, for two one-day arcs.

Summarizing the results given in both Tables and bearing in mind those left unquoted, the following conclusions can be drawn:

- With POPSAT a tracking period of 1 day, corresponding to 3-4 observed passes at mid latitudes, is sufficient to achieve a 1-2 cm precision for baselines of up to 100 km in length. Apart from the noise being in the order of 0.4-0.8 cm the tropospheric refraction is the only remarkable error source. In the case of a strong correlation of the troposphere at both baseline stations accuracies of better than 1 cm would be feasible.

- In the case of ERS-1, two days of observation are necessary to achieve a 2-4 cm precision for baselines as considered here because
  - the spacecraft due to its relatively low orbit is affected to a greater extent by gravitational and non gravitational perturbations, and
  - the observation period per pass is limited to a few minutes.

  The dominant errors arise from tropospheric refraction as with POPSAT but, unlike with POPSAT also in the same order of magnitude from the earth gravitational potential, solar radiation and even position errors of the global tracking network.

- In the view of the fact that POPSAT is a dedicated geodetic mission its performance is not surprising. However, it should be emphasized in particular that also the oceanographic satellite ERS-1 with the PRARE payload, an approved project, will offer a means for precise baseline determination. Furthermore, it can be stated that the achievable accuracy will be not degraded as much with increasing baseline length as it is in the case of GPS. It should be added that both systems, ERS-1 (PRARE) and POPSAT, will also provide the capability of real time position determination from one-way/two-frequency range rate observations.

REFERENCES

ESA, 1982: System and Ground Segment Definition and Feasibility Study of an Earth Kinematics Satellite System for Precise Orbit Positioning, Final Report prepared by Deutsches Geodätisches Forschungsinstitut, Delft University of Technology, Groupe de Recherches de Geodesie Spatiale, Observatoire Royal de Belgique, Technische Universität Berlin; ESA contract No. 4591/80/F/DD/SC

ESA, 1983: POPSAT - A Candidate Satellite System for Solid Earth Applications and Sciences, Final Report prepared by Dornier System, Deutsches Geodätisches Forschungsinstitut, Universität Stuttgart, Aeritalia; ESA contract No. 5309/83/F/CG/SC

Hartl, Ph., 1984: The Precise Range and Range Rate Equipment (PRARE) and its Possible Support to the Radar Altimeter Measurements for ERS-1, Proceedings of a Workshop on ERS-1 Radar Altimeter Data Products, Frascati (Italy) May 1984, ESA SP-221, 153-160

Hartl, Ph., Reigber Ch., 1982: Precise Range and Range Rate Equipment (PRARE), Experiment Description

Hatch, W., Goad, C., Martin, C.F., 1973: Mathematical Description of the ORAN Error Analysis Program, Wolf Research and Development Corp., Riverdale

Kaniuth, K., Müller, H., Reigber, Ch., 1984: Baseline Determination Performance of a Multi-POPSAT Satellite System - Simulation Results - , Proceedings of the International Symposium on Space Techniques for Geodynamics, Sopron (Hungary) July 1984, Vol. 1, 324-334

Reigber, Ch., Balmino, G., Moynot, R., Müller, H., 1983: The GRIM3 Earth Gravity Field Model, Manuscripta Geodeatica Vol. 8, 93-138

Reigber, Ch., Hieber, S., Achtermann, E., 1984: POPSAT - An Active Solid Earth Monitoring System, IUGG XVIII General Assembly Hamburg 1983, Proceedings of the IAG Symposia, Vol. 2, 380-4o7

Reigber, Ch., Müller, H., Bosch, W., Balmino, G., Moynot, B., 1985: GRIM Gravity Model Improvement Using Lageos (GRIM3-L1), in press in Journal of Geophysical Research

Schwintzer, P., Reigber, Ch., 1984: Macrometerbeobachtungen im Deutschen Hauptdreiecksnetz (Macrometer-Netz "Hessen") - Auswertung und Vergleich mit den terrestrisch bestimmten Punktkoordinaten - , Deutsches Geodätisches Forschungsinstitut (DGFI), Internal Report, Ref. PS/CR/23/84/DGFI/Abt.I

High-Precision, Three-Dimensional Differential Positioning Using GPS

by

William E. Strange
National Geodetic Survey, Charting and Geodetic Services
National Ocean Service, NOAA
Rockville, Maryland 20852

ABSTRACT. Various reduction methods were tested to determine the maximum currently attainable precision for differential positioning with GPS using data obtained in southern Arizona. For line lengths up to 50 km it was possible to achieve rms repeatability at about ± 2 cm level in the vertical and to better than ± 1 cm in the horizontal. This repeatability was achieved using 4 hours of observational data taken by single frequency instruments. Repeat determinations were separated in time by as much as 2 weeks. In order to achieve this level of repeatability it was necessary to use single difference processing to adequately account for satellite/receiver time offsets and to enforce the requirement that satellite specific bias parameters be integers. To achieve separation of variables a minimum of about 3 hours of observations was required. Reduction of a limited number of repeat observations separated in time by more than 1 year suggests that long term repeatability may be as good as short term repeatability.

INTRODUCTION

In March and April 1984 a series of GPS measurements were carried out at bench marks along level lines and at horizontal control stations in southern Arizona. Three, single-frequency model V-1000 Macrometer^{tm} receivers were used. The primary purpose of the measurements was to evaluate the applicability of GPS to the monitoring of subsidence caused by ground water withdrawal. Therefore, multiple independent measurements were made of numerous base lines ranging in length from 8 to 50 km. These multiple measurements made the data especially valuable for evaluating the short-term repeatability of GPS three-dimensional differential positioning. To the degree that short-term repeatability is equivalent to long-term repeatability the results from this Arizona test represent the precision with which GPS can presently determine the relative positions of stations separated by up to 50 km. This precision then represents the accuracy with which three-dimensional differential crustal motions can be monitored using GPS over these distances.

DESCRIPTION OF SURVEY

Observations were carried out using three model V-1000 Macrometer^{tm} single frequency receivers in flat-desert areas of southern Arizona. Measurements were made at night due to satellite availability. Receiver clocks were synchronized relative to one another and to the GOES system timing before and after each observation period. Observations were made at 4-minute intervals during a 4-hour observation period. Data were obtained from five different satellites. However, only two of the satellites were observed for the entire 4-hour period and no more than four satellites were observed simultaneously.

Macrometer^{tm} is a trademark of Aero Service Division, Western Geophysical Company of America.

There was a total of 19 observing days. During the first 8 days all equipment functioned satisfactorily. For the remainder of the time one of the instruments malfunctioned intermittently causing temporary losses of lock and the introduction of frequent cycle slips. Except for one day it was possible to correct for the cycle slips during processing and obtain results with satisfactory formal errors.

REDUCTION METHODS

All data reductions were carried out using the precise ephemeris provided by the Naval Surface Weapons Laboratory, Dahlgren, Virginia. Reductions were undertaken using single-difference and triple-difference processing. The details of these procedures are described elsewhere (Goad and Remondi, 1984; Remondi, 1984; Remondi, 1985) and will not be repeated here. Each base line was reduced independently to get differential positions without any attempt to enforce closure for the three base lines obtained during a single day.

Using single-difference processing as implemented at the National Geodetic Survey, the following unknowns may be either computed during the soluion or fixed to some a priori values:

$\Delta x, \Delta y, \Delta z$ = components of the differential position between stations

δ_i = time offset between receiver clocks at the initial epoch

$\Delta\delta_i$ = $(\delta_i - \delta_1)$ = difference between receiver clock offset at epoch i and offset at epoch 1(i=2,60)

N_R = difference between integer cycle ambiguity for the two stations for a satellite selected as the reference satellite

ΔN_j = $(N_j - N_R)$ where N_j is a quantity analogous to N_R for satellite j

ξ = common time offset between satellite time and receiver time at the initial epoch.

In triple difference processing the only parameters which may be estimated are $\Delta x, \Delta y, \Delta z$ and δ_1.

All of the data were reduced using triple-difference processing with δ_1 held fixed in each solution to a value obtained using pre- and post-synchronization results. Using the triple difference results it was possible to fix cycle slips on a substantial portion of the data, including all of the data taken prior to equipment malfunction. For lines where cycle slips could be fixed, single-difference solutions were undertaken. Three types of single-difference solutions were carried out. In type 1 solutions δ_1 and ξ were held fixed to values obtained using pre- and post-synchronization results and the remaining parameters estimated. In solutions designated as type 2 only δ_1 was held fixed. In solutions designated as type 3, not only was δ_1 held fixed, but the ΔN_j values were constrained to be integers. The integer values to which the ΔN_j were constrained were obtained from analysis of the values of ΔN_j obtained in type 1 and 2 solutions. Although by definition the ΔN_j must, in reality, be integers they will differ somewhat from the correct integer values in type 1 and type 2 least squares solutions because of the existence of errors and correlations between satellite ambiguities and other parameters. At the time of the reductions discussed here considerable effort was required to fix the ΔN_j to the correct integer values. Subsequently, Goad (per comm., NGS, 1985) has developed an automated procedure for obtaining the ΔN_j values. This procedure was used to verify the ΔN_j values for the longer lines. While N_R must also be an integer it is not desirable to try to fix it. As discussed by Remondi (1985), N_R and δ_1 are almost totally correlated. Thus with δ_1 held fixed to the value estimated from pre and post calibration, the value obtained for N_R in the least squares solution will contain a correction for any error in δ_1.

RESULTS

Two or more independent determinations of differential position were obtained for a number of station pairs. These independent determinations were derived either from simultaneous occupation of the two stations or from combining results on two days, i.e., the differential position between A and B on one day is combined with the differential positon between A and C on day two.

In examining the independent determinations obtained from triple-difference solutions it was found that, while the repeatability of differential height and differential latitude determinations was near the ± 1 to 2 cm level needed for crustal motion studies, the differential longitudes were much poorer. Subsequent reductions indicated that while type 1 and type 2 single difference solutions gave better overall repeatability than triple-difference solutions, they were still not satisfactory for longitude determination. Once the bias parameters were held fixed in type 3 solutions the longitude repeatability was as good as height and latitude repeatability. The results shown in table 1 suggests that ζ, ΔN_j, and differential longitude are highly correlated in the solutions and that imposing the requirement that the ΔN_j be integers largely removes the damaging effects of the correlations. Tests in which 1 to 2 hours of data were used indicated that reliable separation of ζ, ΔN_j and differential longitude was not possible unless about 3 hours of data was available.

The remainder of the repeatability analyses was undertaken using type 3 single-difference processing results. Repeatability comparisons were done for line length and height. Most of the lines used are oriented NW-SE. Also, for the short lines used line length and height are almost orthogonal. Therefore, line length repeatability provides a good measure of GPS capability for monitoring horizontal crustal motions.

Table 2 summarizes the short-term repeatability in line length and height obtained in the Arizona test. This repeatability is expressed in terms of the maximum variation between repeat measurements. The tables do not indicate any correlation between line length repeatability and magnitude of line length for lines 8 to 50 km long. For heights there is indication of a slight degradation in repeatability with increased line length. The rms deviation from the mean for repeated line lengths is ± 1.2 cm; for differential heights it is ± 0.5 cm. The difference between line length and height repeatability is expected since unmodeled refraction causes greater error in the vertical coordinate.

If the GPS measurement precision indicated in table 2 is representative, GPS can be successfully used today to monitor many types of vertical and horizontal crustal motions with sufficient accuracy to provide useful information. There is no reason to believe the results in table 2 are unique. Table 3 shows repeatability obtained in other surveys with, in one case, a time separation between measurements of more than a year. These results are compatible with the results shown in table 2. Nevertheless, additional tests are needed to assure that the repeatability values reported here are generally attainable under all conditions. In particular, additional tests of long-term repeatability are needed. Also needed are tests where tropospheric and ionospheric refraction modeling are more difficult, particularly since the observations analyzed here were obtained during times of low ionospheric activity. Variations in orbit accuracy, number and geometry of satellites observed, and agreement between the fixed ground station and the satellite coordinate systems can also affect the accuracy of results.

REFERENCES

Goad, C. C. and Remondi, B. W., 1984: Initial relative positioning results using the Global Positioning System, Bulletin Geodesique, 58(2), 193-210.

Remondi, B. W., 1984: Using the Global Positioning System (GPS) phase observable for relative geodesy: modeling, processing, and results, Ph.D. Dissertation, Center for Space Research, The University of Texas at Austin, Austin, Texas, 360 pp, National Geodetic Information Center, NOAA, Rockville, MD 20852.

Remondi, B. W., 1985: Global Positioning System carrier phase: description and use, NOAA Technical Memorandum NOS NGS-42, National Geodetic Information Center, NOAA, Rockville, MD 20852, 21 pp.

Table 1.--Variation in longitude difference between independent determinations

Line length (km)	Variation (arc seconds)*			
	Triple difference	Single difference 1	Single difference 2	Single difference 3
50.1	0.00777	0.00207	0.00118	0.00040
44.6	0.00372	0.00093	0.00012	0.00022
24.2	0.00121	0.00186	0.00201	0.00010
18.6	0.00140	0.00163	0.00152	0.00022
14.4	0.00050	0.00016	0.00044	0.00011
8.0	0.00140	0.00123	0.00152	0.00022

*0.001 Arc Sec = 2.5 cm

Table 2.--Repeatability of independent determinations of differential positions for Arizona survey

Line length (km)	Maximum time between determinations (days)	Number of determinations	Maximum variation between determinations	
			Line length (cm)	Height difference (cm)
50.1	13	2	0.7	2.7
44.7	7	4	1.6	2.2
30.4	6	2	0.1	0.4
24.2	2	2	0.2	0.3
19.8	1	2	0.4	0.9
18.6	7	3	1.0	1.5
14.8	6	2	0.1	1.0
14.4	6	2	0.4	1.5
12.7	2	2	1.0	0.2
11.1	10	2	0.8	1.4
10.6	6	3	1.1	1.6

Table 3.--Repeatability of independent determinations of differential positions from other surveys

Line length (km)	Maximum time between determinations (days)	Number of determinations	Maximum variation between determinations	
			Line length (cm)	Height difference (cm)
22.1	413	3	1.7	1.9
13.4	3	2	1.2	0.7
9.8	2	2	0.9	1.2

A comparison Between Global Positioning System and Very Long Baseline Interferometry Surveys in Alaska and Canada

Gerald L. Mader
Michael D. Abell
National Geodetic Survey
Charting and Geodetic Services
National Ocean Service, NOAA
Rockville, Md. 20852

ABSTRACT. Survey results for five sites in Alaska and Canada, occupied during summer 1984 with TI-4100 GPS receivers and Mobile VLBI systems, are compared. For baseline lengths ranging from less than 300 to almost 1600 km the GPS and Very Long Baseline Interferometry (VLBI) results agree to better than 1 ppm. Average triangle closures for the GPS data are better than 1 ppm while GPS baseline lengths repeat over 2 days to better than 0.1 ppm.

Introduction

During the summer of 1984, the National Geodetic Survey (NGS) and the Jet Propulsion Laboratory operated Mobile VLBI systems in Alaska and Canada as part of a series of measurements by the National Aeronautics and Space Administration's Crustal Dynamics Project. Given the great expense and complex logistics of moving mobile VLBI systems to and around such a distant location, NGS decided to measure the same baselines by GPS in the hopes that as GPS technology and techniques mature and a history of GPS/VLBI comparisons emerge, these measurements may be performed solely by the less expensive GPS systems. These first measurements were made possible only by the cooperation of the Defense Mapping Agency and the Applied Research Laboratory of the University of Texas who supplied TI-4100 receivers and operating crews in Alaska and by the Department of Energy, Mines and Resources, Earth Physics Branch, who provided the same in Canada.

The sites occupied by both the mobile VLBI and GPS systems are shown in Figure 1. The site at Fairbanks was a VLBI base station using an existing 26 m diameter antenna. A second VLBI base station, MV-1, not shown in the figure, used a 9 m diameter antenna at Vandenberg Air Force Base, California. The two mobile VLBI systems, MV-2 and MV-3, are self contained VLBI observatories, fully equipped with the Mark III VLBI Data Acquisition System (NASA, 1982). Each system consists of an antenna transporter, an electronic van, and a diesel power generator (Trask et al., 1982). The MV-2 antenna is 4 m in diameter while the MV-3 is 5 m. The VLBI survey was organized in three segments. During the first segment MV-3 occupied Nome while MV-2 occupied Sand Point and Kodiak. MV-3 then moved to Sourdough while MV-2 occupied Yakataga and Whitehorse. The last occupation had MV-3 at Yellowknife while MV-2 was at Penticton (not shown in Figure 1).

The VLBI baseline measurements are made with respect to the intersection of the axis of the VLBI antennas. A local vector was measured at each site connecting the VLBI reference point to a monument in the ground. The GPS antennas were mounted on tripods directly above the same monuments occupied by the mobile VLBI systems and the observations were made within a few days or weeks of the

VLBI occupations. Using the measured heights of the GPS antennas, baselines measured by the two systems can be referred to the same set of ground monuments.

During this GPS/VLBI intercomparison, five TI-4100 GPS receivers were available. The original GPS observing plan was to occupy Nome, Fairbanks, Sourdough, Yakataga, and Whitehorse for 2 consecutive days. The second scheduled session kept the same receivers at Nome and Fairbanks and moved the other receivers to Sand Point, Kodiak and Yellowknife for 2 additional observing days. The principal observing session on each day consisted of two satellite scenarios. The first began in early afternoon local time, included SV's 6, 8, 9 and 11 and lasted almost 3 hours. This was immediately followed by the second scenario which included SV's 4, 9, 11, and 13 and lasted about 1 hour. The two scenarios were separated by 10 to 20 minutes as the tape cassettes were rewound and lock was acquired on the new satellites and reacquired on the common ones. This gap proved an inconvenience later for matching the satellite bias between the two scenarios. Because of the high latitude of these stations, the satellite coverage was very sparse in the western part of the sky. To compensate for this poor geometry, another session was scheduled approximately 12 hours after from the primary one with two satellites visible toward the west for a period of a few hours. These data have not yet been included in the solutions presented here.

The first observing occupation scheme went as planned and produced data that contained only a few cycle slips at one station on the second day. The second occupation scheme had to be severely modified as it lasted for the next 2 weeks due to receiver failures in Alaska. Coincidentally these data are heavily burdened with cycle slips, making the data processing a lengthy and painstaking task. The results given here will only compare GPS and VLBI results between Nome, Fairbanks, Sourdough, Yakataga, and Whitehorse.

VLBI Data Processing

The mobile VLBI systems include hydrogen masers as frequency standards to record data of approximately 400 MHz bandwidth at x-band and 80 MHz at s-band. The data recorded at each site are then cross correlated to produce a series of delay and delay-rate measurements for each baseline. The VLBI data acquisition sessions were 48 hours in duration during which about 200 separate delay and rate measurements of about 15 sources were scheduled for each baseline. These s and x band delay and delay-rate measurements are corrected for tropospheric effects using surface meteorological measurements and then combined to remove ionospheric effects. Baseline components along with clock models and atmospheric scale height are estimated using least-squares. The details of VLBI processing in general and at NGS have been described elsewhere (Herring et al. 1981, Robertson and Carter, 1982).

The VLBI data for all baselines between Fairbanks, Vandenberg, Nome, Sourdough, Yakataga, and Whitehorse were combined in a single solution in which the Fairbanks position was held fixed. Table 1 summarizes the computed VLBI baseline lengths. These lengths are referred to the ground monuments using preliminary site vectors between the ground monuments and the VLBI reference points. Baseline components were not compared at this time but are planned for the future using changes in earth orientation parameters between the time of the VLBI and GPS measurements. The VLBI and GPS baselines are also computed in two different coordinate systems which differ in scale, orientation and offset.

This is an additional reason why the baseline components have not yet been compared. However, only a scale difference is required to compare the baseline lengths. The VLBI scale has been determined from several years of measurements between fixed observatories with a repeatability of better than 0.01 ppm. Nevertheless, the lengths will be compared in the WGS 72 system because it currently may be more familiar to most readers. These rescaled VLBI baseline lengths (to the WGS 72 system) are listed in Table 1, where the scale factor has been determined from previous comparisons of VLBI and doppler measurements (Hothem, 1985) and found to be about 0.3 parts per million.

GPS Data Processing

The GPS data have been processed for this analysis as a single-difference phase observable as described by Remondi (1985). The computer programs used to process the data are developmental versions written in the Geodetic Research and Development Laboratory of NGS. The technique allows adjustments of station positions, the relative clock term between two stations at each epoch with respect to the difference at the initial epoch, the initial clock differences between two stations, the offset of one station clock with respect to GPS time, a bias term for a designated reference satellite and bias terms for the remaining satellites with respect to the reference satellite.

Surface measurements of temperature, pressure, and relative humidity before each GPS session were used in the Marini tropospheric model (1974) to estimate average path length corrections for the entire GPS observing session. These corrections are applied directly to the input phase data. The ionospheric effects are minimized by scaling each phase observable by its frequency and differencing the L1 and L2 observations.

Solutions have been obtained separately for each baseline between Fairbanks, Nome, Sourdough, Yakataga, and Whitehorse for both L1, L2, and L1/L2 combined. The data were collected at 30 second intervals but only data at 2 minute intervals were used in the solutions. Furthermore, the second satellite scenario containing SV's 4 and 13 has not been used here because of the uncertainty in the continuity of SV's 9 and 11 across the gap between the two scenarios. For all these solutions the WGS 72 position of Fairbanks was held fixed at x = -2281475.664, y = -1453751.199, and z = 5756976.681 m.

Results

The five stations included in this comparison yield 10 separate baselines. From these 10 baselines, 10 separate triangles can be formed, each of which can be used to examine the closure of GPS solutions in each of the vector components of the baselines. The closures are presented for each of the 2 observing days (208 and 209) in Tables 2 and 3. The closures are given on each day for the L1 and L2 and the dual frequency (L1/L2) solutions and are expressed in centimeters and fractional accuracy in parts per million (in parentheses). The average fractional accuracy for each component is given at the bottom of the tables.

The consistency of the GPS results was again examined by differencing the baseline components and lengths for each baseline on days 208 and 209 as seen in Table 4). Again, the numbers given are differences in centimeters and ppm with average fractional acuracies at the bottom.

The comparison between the GPS and VLBI solutions is summarized in Table 5, where the rescaled VLBI baseline lengths have been subtracted from the GPS baselines. The differences are again in centimeters with fractional accuracies given in ppm for both days 208 and 209. Table 5 also includes some results obtained by Clyde Goad of NGS for day 208 with the PHASER program described earlier in this symposium (Goad, 1985). These results were obtained in a solution where four stations (Fairbanks, Nome, Yakataga, and Whitehorse) were adjusted simultaneously. This solution also includes all the data collected at 30 second intervals and for both satellite scenarios of the principal observing session.

Discussion

The triangle closures for the GPS data shown in Tables 2 and 3 are slightly poorer for the L2 data than the L1. This behavior would be expected due to the lower L2 frequency and the uncorrected effects of the ionosphere. When the ionospheric effects are removed as shown by the L1/L2 results, the closures show significant improvement for both days. The closures are not the same in each component. The closures in y are about 0.1 ppm while the z closures are several ppm. Two factors primarily contribute to these differences; first, the vertical component which is generally more poorly determined shows up primarily in the z-component at these high latitudes and second, the poor distribution of satellites over the sky at this latitude must contribute systematically to the errors in each component. An overall average fractional precision of better than 1 ppm obtained from the dual frequency solutions is consistent with orbital errors, generally no larger than 20 m.

The difference of the GPS results over the 2 days of observations shown in Table 4, exhibits the same relation between L1, L2 and L1/L2 seen above. Furthermore, the magnitudes of the average precisions are not significantly different from the corresponding values in each component for the triangle closures. Table 4 also includes the baseline lengths which repeat on average to better than 0.1 ppm. This actually compares favorably with the repeatibility of Mobile VLBI results. As seen from Kroger et al. (1984), multiple measurements of the same Mobile VLBI baselines repeat to a precision of 0.05 to 0.1 ppm. It should be noted however that the mobile VLBI measurements are separated by several months while the GPS results here are on successive days.

The GPS-VLBI baseline length results shown in Table 5 continue to show the same behavior for L1, L2, and L1/L2, although the differences are not as large. The average agreement between the GPS and VLBI lengths are only slightly better than 1 ppm, which is an order of magnitude worse than the repeatability of GPS results only (Table 4), but consistent with the triangle closures (Tables 2 and 3). The results obtained with PHASER (Goad, 1985) are about a factor of 2 better than the single baseline solutions quoted above. PHASER provides an adjusted solution for four stations while no adjustment is attempted for the single-baseline solutions. Since the VLBI results come from an adjusted solution, this feature alone may account for part of this difference. Furthermore, the adjusted PHASER solutions include baselines of various orientations and would tend to distribute orbital errors resulting in a more favorable agreement with the VLBI results. There is also an apparent systematic effect in these GPS-VLBI results. The GPS L1/L2 single baseline lengths are generally longer than the VLBI lengths while the opposite appears to be the case for the PHASER results. In either case a scale factor could adjust the GPS-VLBI differences to zero mean but would not improve the average agreements significantly. While it is tempting to attribute most of the GPS-VLBI differences to orbit error, some work may be necessary in reconciling these two coordinate systems.

References

Goad, C. C., Precise Relative Position Determination Using Global Positioning system Carrier Phase Measurements in a Non-difference Mode, Proceedings of First International Symposium on Precise Positioning with the Global Positioning System, 1985.

Herring, T. A., Corey, B. E., Counselman, C. C., Shapiro, I. I., Ronnang, B. O., Rydbeck, O. E. H., Clark, T. A., Coates, R. J., Ma, C., Ryan, J. W., Vandenbert, N. R., Hintegger, H. F., Knight, C. A., Rogers, A. E. E., Whitney, A. R., Robertson, D. S., Shupler, B. R., Geodesy by Radio Inteferometry: Intercontinental Distance Determinations with Subdecimeter Precision, J. Geophys. Res., 86, 1647-1651, 1981.

Hothem, L. D., National Geodetic Survey, private communication, 1985.

Kroger, P. M., Allen, S. L., Beckman, B. L., Davidson, J. M., Harold, J. B., Jordan, J. E., Mar, A., Merken, L., Nelson, M. A., Patterson, J. E., Slade, M. A., Spitler, J. S., Stephens, S. A., Wieland, F. P., Mobile VLBI Data Base, JPL, 1984.

Marini, J., Goddard Space Flight Center, private communication, 1974.

National Aeronautics and Space Administration, Goddard Space Flight Center, Crustal Dynamics Project, Mark III VLBI Data Acquisition Terminal, 1982.

Remondi, B. W., Global Positioning System Carrier Phase: Description and Use NOAA Technical Memorandum NOS NGS-42, 1985.

Robertson, D. S., Carter, W. E., Earth Rotation Information Derived From MERIT and POLARIS VLBI Observations in High Precision Earth Rotation and Earth-Moon Dynamics, O. Calame (ed), D. Reidel Publishing Co., 1982.

Trask, D. W., Brunn, M. L., Cohen, E. V., Davison, J. M., Fanselow, J. L., MacDoran, P. F., Miller, R. B., Niell, A. E., Parks, G. S., Resch, G. M., Skjerve, L. J., Vegos, C. V., Wallace, K. S., Mobile VLBI Surveying: Instrumentation, Operating Procedures and Results of ARIES, Proceedings of Symposium No. 5: Geodetic Applications of Radio Interferometry, NOAA Technical Report NOS 95 NGS 24, 1982.

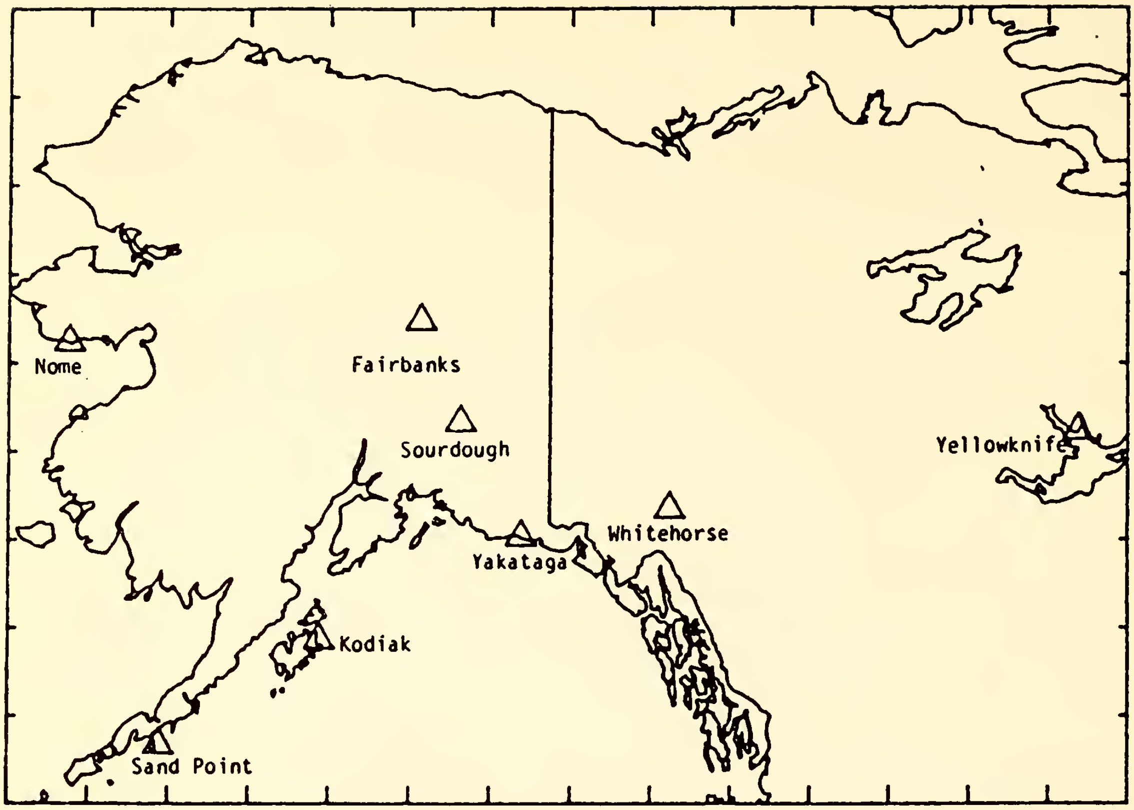

FIGURE 1 GPS and VLBI sites in Alaska and Canada

TABLE 1 VLBI BASELINE LENGTHS (monument - to - monument)

Baseline*	L (VLBI)	L (WGS72)
NF	848396.800	848396.545
FY	602983.864	602983.683
FS	276325.109	276325.026
FW	788753.160	788752.923
NY	1276160.556	1276160.173
NS	1003587.336	1003587.035
NW	1591080.616	1591080.139
YS	329299.252	329299.153
YW	414189.640	414189.516
SW	591316.604	591316.426

* N = NOME, F = FAIRBANKS, Y = YAKATAGA, S = SOURDOUGH, W = WHITEHORSE

TABLE 2 GPS TRIANGLE CLOSURES FOR DAY 208

	L1			L2			L1/L2		
	X	Y	Z	X	Y	Z	X	Y	Z
NFY	-27(2.1)	-13(.1)	-49(2.1)	-35(2.7)	-14(.1)	-64(2.7)	-16(1.2)	-11(.08)	-26(1.1)
NFS	-18(.7)	-9(.09)	-34(3.6)	-22(.9)	-10(.1)	-43(4.6)	-11(.5)	-8(.08)	-19(2.0)
NFW	-31(.7)	-7(.05)	-31(1.6)	-36(.8)	-9(.06)	-43(2.2)	-21(.5)	-4(.03)	-13(.7)
NYS	11(.5)	4(.04)	19(2.0)	15(.6)	4(.04)	27(2.9)	4(.2)	3(.03)	7(.7)
NYW	-11(.2)	-19(.1)	-49(2.5)	-11(.2)	-21(.1)	-53(2.7)	-11(.2)	-17(.1)	-42(2.1)
NSW	-18(.4)	-2(.01)	-19(1.0)	-22(.5)	-2(.01)	-27(1.4)	-11(.2)	-1(0)	-9(.5)
FYS	1(.07)	0(0)	4(.3)	3(.2)	1(.05)	6(.5)	-1(.07)	0(0)	1(.09)
FYW	-8(1.2)	-25(.3)	-67(3.1)	-10(1.5)	-25(.3)	-74(3.4)	-6(.9)	-24(.3)	-55(2.5)
FSW	-5(.7)	-4(.05)	-22(1.0)	-8(1.2)	-3(.04)	-26(1.2)	-1(.1)	-5(.07)	-15(.7)
YSW	4(.2)	21(.8)	48(13.6)	5(.2)	23(.9)	54(15.3)	4(.1)	19(.7)	40(11.3)
Average	(.7)	(.15)	(3.1)	(.9)	(.17)	(3.7)	(.4)	(.14)	(2.2)

TABLE 3 GPS TRIANGLE CLOSURES FOR DAY 209

	L1			L2			(L1/L2)		
	X	Y	Z	X	Y	Z	X	Y	Z
NFY	-31(2.4)	-4(.03)	-37(.16)	-41(3.2)	-1(.01)	-48(2.0)	-15(1.2)	-9(.07)	-21(.9)
NFS	-6(.3)	-4(.04)	-24(2.5)	-2(.1)	-2(.02)	-28(3.0)	-13(.5)	-6(.06)	-17(1.8)
NFW	-45(1)	5(.04)	-22(1.1)	-59(1.3)	9(.06)	-40(2.0)	-20(.5)	-3(.02)	-8(.4)
NYS	15(.6)	0(0)	14(1.5)	26(1.1)	-1(0)	20(2.2)	-1(.06)	2(.02)	4(.5)
NYW	-33(.7)	-7(.04)	-29(1.5)	-51(1.1)	-5(.03)	-38(1.9)	-8(.2)	-13(.09)	-26(1.3)
NSW	-44(1)	8(.05)	-8(.4)	-66(1.5)	13(.08)	-19(.9)	-11(.2)	0(0)	-2(.1)
FYS	-9(.7)	0(0)	1(.05)	-13(.9)	0(0)	1(.04)	-3(.2)	0(0)	1(.04)
FYW	-19(2.9)	-17(.2)	-44(2.1)	-34(5.1)	-15(.2)	-47(2.1)	-3(.4)	-19(.3)	-40(1.8)
FSW	-5(.8)	-1(.01)	-10(.5)	-10(1.5)	2(.03)	-7(.3)	-3(.5)	-3(.05	-12(.5)
YSW	4(.1)	16(.6)	35(9.8)	11(.3)	17(.6)	40(11.4)	-4(.1)	15(.6)	28(8.1)
Average	(1.05)	(.10)	(2.0)	(1.6)	(.2)	(2.6)	(.4)	(.12)	(1.54)

TABLE 4 GPS BASELINE DIFFERENCES (208-209)

	L1				L2				(L1/L2)			
	X	Y	Z	L	X	Y	Z	L	X	Y	Z	L
NF	-44(1.2)	1(.01)	-24(12.4)	21(.2)	66(1.7)	-6(.07)	27(13.6)	25(.3)	11(.3)	11(.1)	21(10.5)	15(.2)
FY	-5(.2)	-19(.4)	11(.4)	-13(.2)	-8(.3)	-28(.6)	13(.5)	-20(.3)	0(0)	-6(.1)	7(.3)	-2(.03)
FS	-27(2.0)	-10(.5)	12(1.1)	-16(.6)	-42(3)	-14(.7)	13(1.2)	-26(.9)	-4(.3)	-3(.2)	10(.9)	0(0)
FW	25(3.8)	8(.1)	-11(.5)	7(.09)	43(6.5)	15(.2)	-10(.4)	16(.2)	4(.7)	1(.02)	1(.03)	2(.02)
NY	52(4.1)	-10(.08)	-2(.07)	-5(.04)	80(6.3)	-21(.2)	2(.1)	-12(.1)	9(.7)	7(.05)	-8(.4)	6(.05)
NS	60(2.5)	-3(.04)	-2(.3)	11(.1)	88(3.7)	11(.1)	1(.1)	10(.1)	16(.7)	9(.09)	-8(.9)	12(.1)
NW	84(1.9)	22(.14)	-26(1.3)	41(.26)	131(3)	28(.2)	-33(1.7)	59(.4)	15(.3)	13(.09)	-15(.8)	15(.09)
YS	12(1.1)	-10(.4)	-4(.3)	-6(.2)	18(1.6)	-14(.5)	-5(.4)	-8(.3)	2(.2)	-3(.1)	-3(.2)	-3(.09)
YW	10(.3)	19(.7)	44(12.4)	24(.6)	11(.4)	33(1.2)	50(14.2)	34(.8)	9(.3)	3(.1)	22(6.3)	10(.2)
SW	-3(.1)	15(.3)	-34(3.3)	7(.1)	1(.03)	24(.4)	-42(4.1)	15(.3)	-2(.09)	3(.06)	-13(1.3)	0(0)
Average	(1.7)	(.23)	(3.2)	(.24)	(2.6)	(.4)	(3.6)	(.4)	(.4)	(.09)	(2.2)	(.08)

TABLE 5 GPS-VLBI BASELINE COMPARISONS

	208				209		
	L1	L2	L1/L2	PHASER	L1	L2	L1/L2
NF	117(1.4)	101(1.2)	141(1.7)	-6(.1)	96(1.1)	76(.9)	126(1.5)
FY	-93(1.5)	-130(2.2)	-36(.6)	-59(1.0)	-80(1.3)	-110(1.8)	-34(.6)
FS	-47(1.7)	-67(2.4)	-17(.6)		-31(1.1)	-40(1.4)	-17(.6)
FW	-16(.2)	-35(.4)	12(.2)	-36(.4)	-23(.3)	-51(.6)	11(.1)
NY	-32(.3)	-72(.6)	29(.2)	-67(.5)	-27(.2)	-60(.5)	23(.2)
NS	35(.3)	9(.1)	75(.7)		24(.2)	-1(0)	63(.6)
NW	91(.6)	64(.4)	132(.8)	-33(.2)	50(.3)	5(0)	118(.7)
YS	-46(1.4)	-66(2.0)	-16(.5)		-40(1.2)	-57(1.7)	-13(.4)
YW	122(2.9)	133(3.2)	106(2.6)	2(.1)	99(2.4)	99(2.4)	96(2.3)
SW	42(.7)	61(1.0)	59(1.0)		53(.9)	46(.8)	59(1.0)
	(1.1)	(1.3)	(.9)	(.4)	(.9)	(1.0)	(.8)

THE QUEBEC 1984 MACROMETER ^{TM} TEST

Comparison of phase-difference processing and network solution methods

R. Moreau
Ministère de l'Energie et des Ressources (MER)
1995 ouest, boul. Charest (1.01 B)
Sainte-Foy, Québec
Canada G1N 4H9

G. Beutler
University of Bern (UB)
Astronomical Institute
Sidlerstrasse 5, CH-3012
Bern, Switzerland

J.G. Leclerc, B. Labrecque
Université Laval (UL)
Sciences géodésiques (Pavillon Casault)
Sainte-Foy, Québec
Canada G1K 7P4

R. B. Langley and R. Santerre
University of New Brunswick (UNB)
Dept. of Surveying Engineering
Fredericton P.O.B. 4400
Canada E3B 5A3

ABSTRACT. This paper describes a 5-day test (January 1984) of three MACROMETER^{TM} V-1000 GPS receivers, conducted by MER in Sainte-Foy, Quebec. The initial purpose was to: 1) ascertain conformity of phase-difference results with Quebec requirements for urban/suburban control densification ($\leq$ 20 mm sd relative to peripheral networks); 2) verify instrumental behaviour in adverse conditions such as very low temperatures and an environment favouring multi-path signal reception. The test base comprised 16 ground points, with spacings 200 to 2000 metres: especially meticulous terrestrial methods provided the classical geodetic parameter values for purposes of comparison. Eighteen independent lines were measured by GPS. Phase difference processing results obtained by INTRFT/LSQT and PRMAC-3 are compared and found almost identical. In the comparison between GPS coordinates and terrestrial values, it is found that, after removal of inter-system distortion and terrestrial random error, estimated GPS densification accuracies are better than 5 mm rms in each coordinate. It is shown also that rigorous network processing by PRMNET yields better formal accuracy estimates than standard geodetic computations applied to single-line GPS results. It is concluded that despite adverse observation conditions, much better accuracy than initial requirements has been achieved, and that many applications more stringent than urban/suburban densification may also benefit from GPS.

INTRODUCTION

Early information, eg (FGCC 1983) encouraged MER to investigate further on the capabilities of the MACROMETER. A test was designed in the fall of 1983 in order to verify three-dimensional accuracies obtainable on short lines ranging from 200 to 2000 metres, for purposes of control densification in urban/suburban areas (present Quebec specifications require a sd of ± 20 mm or less on lines in such networks). Existing points determined by conventional methods were chosen as two test bases: a 13-point configuration in the Sainte-Foy network and a 3-point configuration on Université Laval campus. Field preparation and general coordination of the MACROMETER experiment were contracted to Michel Perron et Associés (MPA) of Ville St-Laurent, Quebec; measurements and computations were subcontracted by MPA to Geohydro (GH) of Maryland. The measurements took place during the last week of January, 1984. Thus the test was conducted in a difficult environment (multi-path reception due to the variety of flat surfaces found in urban areas) and under adverse climatic conditions. The GPS results of the 18 independent lines were furnished by MPA/GH in March 1984 (processing by programs INTRFT/LSQT). Terrestrial coordinates for the test bases were provided by Service de la géodésie du Québec and UL.

In the following sections, comparisons will be made between LSQT results and those obtained by PRMAC-3 (UB/UNB with collaboration of UL), internal and external consistencies of GPS results will be shown, and network solutions will be discussed, in particular program PRMNET (UB/UNB). The paper will be concluded by practical and technical considerations from MER and UL.

TEST BASES

The high-quality terrestrial measurements of the 70-point Sainte-Foy network were processed by standard least-squares programs TOGAS and ASTRAL for horizontal and vertical adjustments respectively. Figure 1 shows the 13-point configuration chosen from the said network for the purpose of GPS testing. Though of somewhat better quality than usual urban networks, the Ste-Foy test base cannot be regarded as "absolute truth": some distortion is to be expected from various causes such as constraint to so-called "higher-order" points, measurement and centering uncertainties amounting to several mm and also possibility of slight movement of the points themselves between the terrestrial and GPS measurements. Coordinates and formal accuracy estimates may be found in (Champagne 1984). The Université Laval points however, can be considered of ultra-high stability; also the length and levelling measurements were very precise; they are indicated in (Jobin 1984).

MACROMETER MEASUREMENTS

Simultaneous phase-variation measurements were obtained by means of three MACROMETER V-1000 GPS receivers. The 5-to-6 hour "visibility periods" of the NAVSTAR system were divided in two for the Sainte-Foy configuration, resulting in 4 independant lines being measured per day; the full period was exploited for the 2 UL lines. In all, 5 days were spent on the test (Jan 26 to 30 incl.) as initially scheduled, no time having been lost. The day by day production of GPS lines is symbolized in Figure 1. The coordinate differences, relative to the indicated "base" points, and resulting from the INTRFT/LSQT processing are listed in (Perron 1984).

SINGLE-LINE SOLUTIONS

The line-by-line computations of the GPS coordinate differences were obtained at UNB using program PRMAC-3 (Beutler 1984). Comparisons between these results and those from INTRFT/LSQT are shown in Table 1 (Beutler et al 1985) for all except two of the lines. The results on these were not comparable for reasons of data editing (06-27) and of a mistake in the UT1-UTC correction in the LSQT processing (33-29). For both programs, much the same observations were input (see n_1 and n_2). Also coordinates of the pole, universal time parameters, as well as satellite ephemerides (Macrometrics T-files), were identical in both cases. As can be concluded from Table 1, agreement is excellent between the two programs: rms differences being less than 1 mm in latitude and longitude and little more than 1 mm in height.

SIMPLIFIED NETWORK SOLUTIONS

Under this heading are summarized the detailed initial analyses and comparisons from (MOREAU 1984). The GPS coordinate-difference values are those computed by INTRFT/LSQT programs. The network solutions are termed "simplified" in that they treat the GPS single-line results as any other geodetic measurement.

Planimetry (internal consistency)

When considering only the independent lines in the Sainte-Foy network, there is little redundancy. To obtain as detailed a view as possible of the internal consistency of the GPS measurements, a traverse approach was initially used, in opposition to simultaneous least squares processing which in certain cases might "spread about" local inconsistencies. Using as origins two points (30 and 32) which had also been held fixed in the conventional adjustment of the terrestrial values, GPS coordinate differences (Perron 1984) were cumulated, yielding 2 values for 33, one each for 17, 20 and 77, and 3 each for 06 and 43. Discrepancies with respect to the means at 33,06 and 43 are shown in Table 2. Values of "n" indicate discrepancies due to one line (point 33) or to two lines (other two points). In this manner single-line rms dispersion is found to be 3.4 and 2.7 mm in North and East respectively.

A classical simultaneous least-squares adjustment was also exercised on the same portion of the GPS network ("free" adjustment except for translation constraint at 30 and 32). Each independent GPS line was expressed in azimuth and length weighted identically. Error ellipse information indicated practically identical standard deviations for each line: approximately 2.5 mm in each of N and E. Thus the least-squares solution gives a slightly more optimistic view of the internal consistency within the redundant part of the GPS network. It was noted that independently of the method used, the "free GPS" coordinates obtained for the extreme points 06 and 43 were identical.

Heights (internal consistency)

In similar fashion, GPS height differences were accumulated from point 33 out to points 06 and 43. In this case six discrepancies are available, as shown in Table 2. The rms result is for a single line (initial result divided by $\sqrt{2}$): ± 5.1 mm.

The corresponding least-squares free adjustment yielded a slightly better estimate of GPS height-difference internal consistency: standard deviation ± 4.1 mm. As with planimetry, the "free GPS" heights obtained for 06 and 43 were identical between the traverse and least squares solutions.

Planimetry (external consistency)

The method adopted for comparing GPS with terrestrial values is the same as that recommended for doppler densification (Moreau 1981). A minimum of three base points is required, and their official (terrestrial) values are assumed correct. In this case, the mid-point between 30 and 32 serves as the base point (p = 30/32) of zero correction, since the official terrestrial values were there assigned to the GPS network. The discrepancies noted at points 06 and 43 are then used to establish corrective terms by bilinear interpolation for all the GPS values. This is meant to remove not only scale and orientation differences but also local distortion between the two systems. In the particular case of the Sainte-Foy network, the corrections at the bases were found to be: $CN_{30/32} = 0$; $CN_{06} = -21$ mm; $CE_{06} = + 8$ mm; $CN_{43} = + 1$ mm, and $CE_{43} = + 7$mm (N and E stand for North and East, C stands for correction to the GPS value to convert it to the terrestrial value). For the general point "p", corrections are

$$CNp = FN' \times \Delta Np + FE' \times \Delta Ep \tag{1}$$
$$CEp = FN'' \times \Delta Np + FE'' \times \Delta Ep \tag{2}$$

Where ΔN and ΔE are plane coordinate differences between 30/32 and p, and FN and FE are the conversion factors computed after solving equations 1 and 2 using above numerical values for the C's at 06 and 43. Values of CN and CE are applied to the initial discrepacies DN and DE to give final discrepancies δN and δE. These are now assumed corrected for the systematic part of the TERR (terrestrial) system error: however they still contain the random TERR uncertainties. According to (Champagne 1984) the standard deviation of a coordinate difference is ± 7 mm: this must be subtracted quadratically from the global "σ" to obtain an estimation of σ_{GPS}. Numerical values observed and computed are shown in Table 3. Thus, after removal of inter-system distortion and the estimated random part of the terrestrial coordinate errors, it is found that GPS discrepancies are approximately 4 mm rms in each axis for two-hour observations and about 1 mm for 5-hour observations, on lines within 200 to 2 000 metres.

Heights (external consistency)

As in the preceding section a zero-point was chosen, in this instance no 33: $CH_{33} = 0$. Numerical values $CH_{06} = + 43$ mm and $CH_{43} = + 29$ mm resulted from the traverse and free adjustment computations previously mentionned. The equation for the correction at point "p", with Δ's counted from 33, was found to be:

$$CHp = - 0.01613 \times \Delta Np + 0.00705 \times \Delta Ep \tag{3}$$

where CH is in mm and ΔN, ΔE in metres. It is to be noted here that the conversion factors represent the tangents (x 10^3) of the components of the deviation of the vertical, since GPS values are deemed relative to the spheroid whereas MSL (terrestrial) values are considered relative to the geoid. Table 4 shows the detailed discrepancy values; for the final evaluation of σ_H for GPS alone, the formal estimations (Champagne 1984) of the MSL height difference uncertainties are subtracted quadratically from the global rms values of δH. Thus, after removal of the apparent geoidal slope effect and the estimated terrestrial random error, the estimated GPS uncertainty for one line (elevation difference) is nearly 5 mm rms for 2-hour observations and around 3 mm for 5-hour observations, on lines 200-2000 metres long. As mentioned in (Beutler et al 1985), loop misclosure analysis has pointed to the strong possibility of a blunder in antenna-height measurement on one of the lines in the redundant part of the Ste-Foy network: the dilution of this error throughout the network could well account for a slightly larger sd in heights than in planimetry.

RIGOROUS NETWORK SOLUTION

In this section information contained in (Beutler et al 1985) is summarized. The network solution developped by UB/UNB is embodied in program PRMNET which uses as input the GPS single-difference phase outputs produced by Macrometrics' program INTRFT. PRMNET derives the so-called "double-differences", simultaneously optimizes the ambiguity parameters and performs a three-dimensional least-squares solution (Beutler et al 1984). The Sainte-Foy observations were used in a free adjustment centered on point 77. The formal sd values obtained for coordinate differences in the redundant part ot the network were $\sigma_N \approx 1$ mm, $\sigma_E \approx 1.5$ mm and $\sigma_H \approx 2$ mm, which values are 50% smaller than the formal sd's of the classical least-squares solutions exercised individually in planimetry and heights. Also, in comparison with the independent single-line solutions, PRMNET introduced a substantial improvement (ratio 2.5 to 1) in the fractional part of the non-integer estimates of the ambiguity parameters. For comparing with the terrestrial coordinates, a Helmert tranformation centered on the centroid of all 13 points was performed. Resulting differences (GPS minus TERR) were 9.4, 6.1 and 7.5 mm rms in N, E and H respectively. The fact that such a transformation does not account for distortion as does the bilinear one, explains the larger horizontal discrepancies. However in the vertical, where the inter-system difference is essentially due to geoid slope, and both the Helmert and bilinear methods are essentially equivalent, it is noted that PRMNET is superior.

It is therefore expected that the best manner of computing GPS data for densification comprises an initial free adjustment using a rigorous approach such as with PRMNET, completed by constraint to the three official peripheral base points by means of the bilinear interpolation method. In cases where a group of GPS points could be tied to more than three official geodetic base points, it is suggested that a transformation lending itself to taking distortion into account, such as an affine transformation, be used following PRMNET.

CONCLUSIONS

To a high degree of certainty it is concluded that:

1. GPS phase-variation measuments easily meet accuracy criteria for Quebec urban/suburban densification, even in the presence of adverse observational conditions.
2. Other more stringent applications such as for earth works deformations and geodynamics measurements, are feasible.
3. Macrometrics' as well as the independently-developped software at UB/UNB correctly process the GPS phase-variation data for the short lines of the test.

Further investigation is in progress at UL since a preliminary study in 1983/84 (Leclerc 1984). Particular attention is being given to predicting behaviour of signals on longer lines, especially in the matters of refraction and of the effect of earth rotation between the times of arrival at the various receivers.

On the question of cost-effectiveness, it was pointed out in (Moreau 1984) that there is a high probability of GPS costs for urban/suburban densification becoming lower than those of actual methods when the full NAVSTAR constellation becomes operational. However immediate cost-effective applications can be found in engineering and geodynamics especially in cases where line-of-sight methods are difficult, such as when suitably stable reference points are relatively far from the points to be monitored, and standard methods require many costly intermediate points.

REFERENCES

Beutler, G., 1984: GPS carrier-phase difference observation software, University of New Brunswick, Fredericton, N.B.

Beutler, G., Davidson, D.A., Langley, R.B., Santerre, R., Vanicek, P., Wells, D.E., 1984: Some theoretical and practical aspects of geodetic positionning using carrier-phase difference observations of GPS satellites, University of New Brunswick, Fredericton, N.B.

Beutler, G., Langley, R.B., Santerre, R., 1985: UNB contribution to the Quebec 1984 Macrometer test, University of New Brunswick, Fredericton, N.B.

Champagne, M., 1984: Coordonnées terrestres du réseau de Sainte-Foy, Service de la Géodésie du Québec, Sainte-Foy, Québec.

Federal Geodetic Control Commitee (FGCC), 1983: Report on test and demonstration of MACROMETER V-1000, report FGCC-IS-83-2, Rockville, Maryland.

Jobin, J., 1984: Coordonnées terrestres du réseau de l'Université Laval, Département des sciences géodésiques et de télédétection, Université Laval, Sainte-Foy, Québec.

Leclerc, J.G., 1984: Etude préliminaire du récepteur Macrometer, Département des sciences géodésiques et de télédétection, Université Laval, Sainte-Foy, Québec.

Moreau, R., 1981: Integrated densification by doppler, ACSM technical papers, 1981 Fall Meetings, San Francisco, CA.

Moreau R., 1984: Projet GPS 1983/84, Domaine territorial/recherche-développement, Sainte-Foy, Québec.

Perron, M., 1984: Positionnement GPS à l'aide de l'équipement Macrometer, Michel Perron et Associés, Ville St-Laurent, Québec.

FIGURE 1

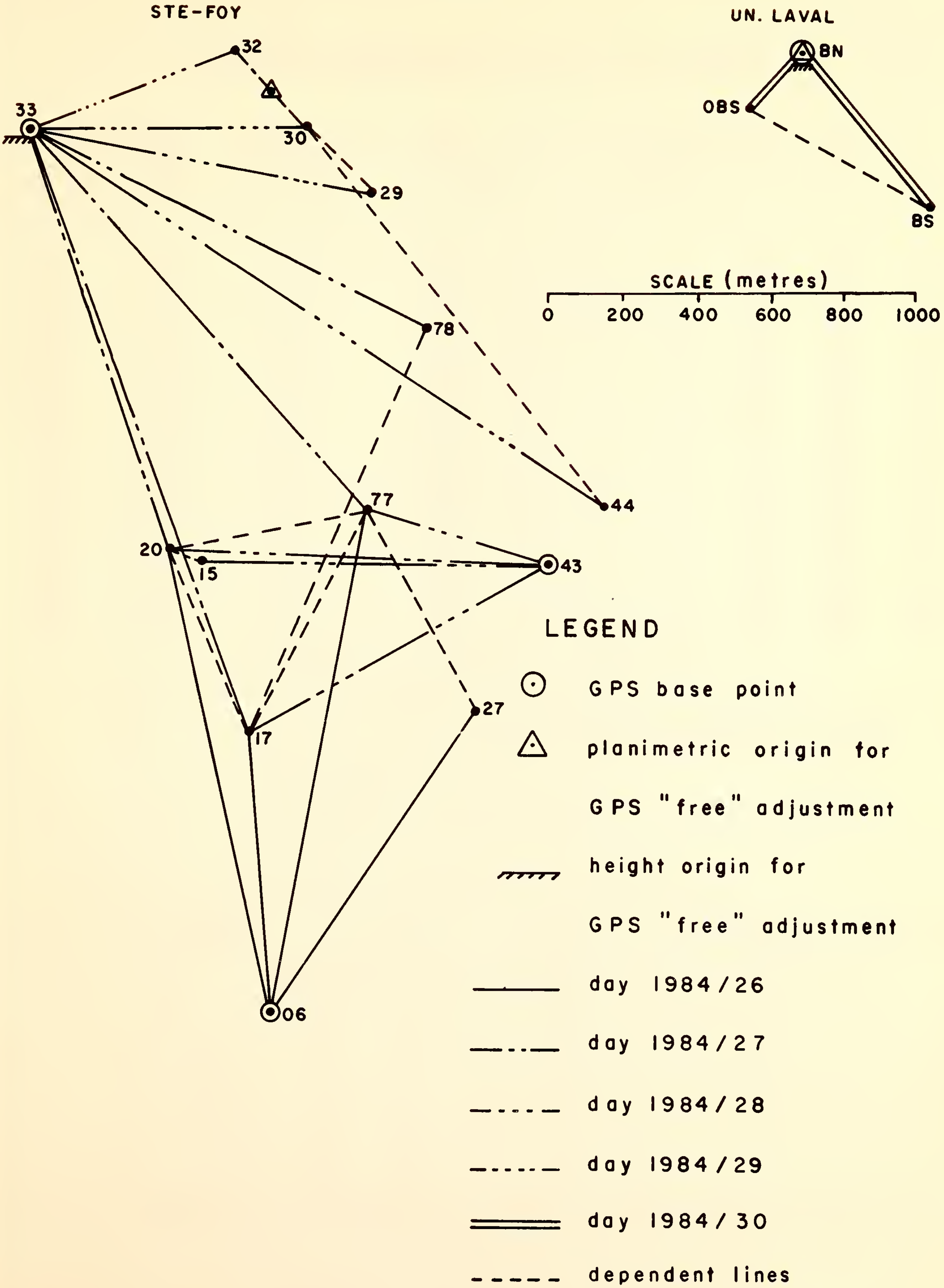
STE-FOY
32
33
30
29
78
44
77
20
15
43
17
27
06
UN. LAVAL
BN
OBS
BS
SCALE (metres)
0
200
400
600
800
1000
LEGEND
GPS base point
planimetric origin for
GPS "free" adjustment
height origin for
GPS "free" adjustment
day 1984/26
day 1984/27
day 1984/28
day 1984/29
day 1984/30
dependent lines

TABLE 1

COMPARISON OF SINGLE-LINE PROCESSING METHODS
(PRMAC-3 MINUS INTRFT/LSQT)

LINE	N1	N2	DELTA LAT. (MM)	DELTA LONG. (MM)	DELTA HGT. (MM)	DELTA LENGTH (MM)	DELTA LENGTH (PPM)
06,17	104	106	-0.6	0.4	-2	-0.5	0.7
06,20	103	105	-0.3	0.4	-1	-0.4	0.3
06,77	112	124	-0.6	0.6	0	-0.4	0.3
33,20	96	96	0.6	0.4	1	-0.6	0.5
33,77	106	112	0.9	-0.8	1	-1.4	1.0
33,17	126	130	0.3	-0.6	0	-1.0	0.6
33,78	121	135	0.9	-0.2	-2	-1.2	1.0
43,77	115	118	0.3	0.4	0	0.0	0.0
43,17	118	120	0.6	-1.0	2	0.3	0.3
43,20	132	141	-0.9	0.2	2	0.2	0.2
43,15	127	139	-1.2	0.0	2	0.1	0.1
33,32	116	120	-1.2	0.6	-2	0.3	0.5
33,30	116	120	-1.2	1.0	1	0.9	1.2
33,44	125	135	-0.3	0.4	0	0.1	0.1
NO.SU	150	149	-1.2	0.4	0	0.6	1.1
NO.OA	149	147	-0.3	0.2	0	-0.1	0.4
SU.OA	152	152	0.3	-0.2	0	0.7	1.2
			rms: ±0.8	±0.6	±1.3		

N1: NUMBER OF OBSERVATIONS USED IN INTRFT/LSQT
N2: NUMBER OF OBSERVATIONS USED IN PRMAC-3

TABLE 2

TRAVERSE SOLUTIONS-INTERNAL GPS CONSISTENCY

Point no.	DETERMINATION	δN(mm)	n	δE(mm)	n	δH(mm)	n
33	1	+2	1	+1	1		
33	2	-2	1	-1	1		
06	1	-8	2	+6	2	+5	2
06	2	+1	2	-5	2	-9	2
06	3	+7	2	-1	2	+4	2
43	1	-5	2	+5	2	+4	2
43	2	+1	2	-2	2	-11	2
43	3	+4	2	-3	2	+7	2
rms values for single line:		±3.4 mm		±2.7 mm		±5.1 mm	

TABLE 3 - PLANIMETRY

COMPARISON BETWEEN GPS AND "TERRESTRIAL" COORDINATES

DETERMINATION FROM	TO	DN(GPS-TERR) mm	CN mm	δN mm	DE(GPS-TERR) mm	CE mm	δE mm
Sainte-Foy							
30	33	+19	-11	+08	-06	+01	-05
32	33	+15	-11	+04	-07	+01	-06
33	17	+09	-15	-06	+08	-06	+02
33	20	+19	-15	+04	-04	-03	-07
33	77	-03	-05	-08	+04	-05	-01
17	06	+13	-21	-08	+14	-08	+06
20	06	+22	-21	+01	+03	-08	-05
77	06	+28	-21	+07	+07	-08	-01
17	43	-06	+01	-05	+12	-07	+05
20	43	00	+01	+01	+05	-07	-02
77	43	+03	+01	+04	+04	-07	-03
43	15	+11	-13	-02	+03	-05	-02
06	27	+05	-06	-01	+17	-07	+10
33	29	-16	+02	-14	-05	-02	-07
33	78	-09	+01	-08	+13	-04	+09
33	44	-20	+05	-15	+07	-07	00
			rms:	±7.2			±5.3

global rms (GPS + TERR): $\sqrt{7.2^2 + 5.3^2}$ = 9 mm
sd of TERR alone = 7 mm
estimated sd of GPS line $\sqrt{9^2 - 7^2}$ = 5.7 mm
estimated sd of GPS: $\sigma_N \approx \sigma_E \approx$ 4 mm

Université Laval

BN BS length difference (GPS-TERR) = -1.2 mm
BN OBS length difference (GPS-TERR) = -0.6 mm

TABLE 4 - HEIGHTS

COMPARISON BETWEEN GPS AND MSL HEIGHTS

DETERMINATION FROM	TO	DH(GPS-MSL) mm	CH mm	δH mm
Sainte-Foy				
33	17	-25	+31	+06
33	20	-27	+20	-07
33	77	-17	+23	+06
33	78	-17	+16	-01
33	29	+06	+08	+14
33	30	-09	+05	-04
33	32	-02	00	-02
33	44	-29	+27	-02
17	06	-38	+43	+05
20	06	-52	+43	-09
77	06	-39	+43	+04
17	43	-25	+29	+04
20	43	-40	+29	-11
77	43	-22	+29	+07
06	27	-50	+34	-16
43	15	-09	+21	+12
			rms:	± 8.1
			s.d. of MSL alone:	± 6.5
		estimated s.d. of GPS:	$\sqrt{8.1^2 - 6.5^2}$	± 4.8 mm
Université Laval				
BN	BS	-02	+07	+5
BN	OBS	-01	+02	+1

MACROMETER MEASUREMENTS 1984
IN THE INN VALLEY NETWORK

Hansbert Heister
Albert Schödlbauer
Walter Welsch
Universität der Bundeswehr München
Institut für Geodäsie
Werner-Heisenberg-Weg 39
8014 Neubiberg
Federal Republic of Germany

ABSTRACT. Macrometer observations were carried out on the eight trigonometrical points of the three dimensional (25 km x 25 km x 1,3 km) Inn Valley Network in November 1984. The experiences and the results proved the ability and the efficiency of the system. By reason of the achieved high accuracy, these results are considered to be an essential contribution to the improvement of the network, too.

1. INTRODUCTION

The capability of the Macrometer technology based on the NAVSTAR-GPS-system, has been proved in several missions, see e.g. GOAD/REMONDI (1983), SOLTAU (1983), LINDSTROT (1984), SCHMIDT (1984), STRAUSS (1984/1, 1984/2), BOCK/ABBOT/COUNSELMAN et.al. (1984). The evaluation of the GPS signals using this technology yield coordinate differences (baseline vectors) in a cartesian coordinate system for each pair of stations being equipped with Macrometer receivers. The procedure of data receiving and processing does not need any knowledge of the code, which in the GPS standard technology is the necessary key for the access to the system; see e.g. BOCK/ABBOT/COUNSELMAN et al. (1983), SEEBER (1984), SCHRICK (1984): By means of electronic manipulations the phase of the L1 carrier wave ($f = 1{,}575$ GHz $\hat{=}$ $\lambda = 19$ cm), which is modulated with a pseudo random signal of the C/A-code, is restored and its relation to a reference phase is measured. The phase relation (modulo phase), realized by two receivers on two stations, is the observable from which the coordinate differences can be deduced.

With two simultaneously recording receivers one baseline vector can be determined; with three receivers we obtain three vectors (the three sides of a triangle), with four receivers six (the four sides and the two diagonals of a quadrangle). But we have to note, that within the three receiver configuration only two baseline vectors are independent; the four receiver configuration provides three out of six independent baselines (due to geometrical and physical correlations even these "independent" baselines show a certain degree of dependence). From the ratio of the number of independent baselines to the number of employed receivers (1/2 = 0,5; 2/3 = 0,67; 3/4 = 0,75) we see that the four receiver configuration is more efficient than the three and the two receiver configuration. This should be taken into consideration if networks and campaigns are projected.

The Macrometer measurements reported on in this paper were intended for

- getting acquainted with the Macrometer surveying procedure
- monitoring the accuracy of the GPS Macrometer technology by comparison with a precise 3D terrestrial network and - if possible -
- strengthening the Inn Valley Network by GPS derived baseline vectors.

2. THE INN VALLEY NETWORK

Since 1979 the Institut für Geodäsie of the Universität der Bundeswehr München has established a precise test network round about the Inn valley on the northern slope of the Alps ("Inn Valley Network"). The network, covering a space of appr. 25 km x 15 km x 1,3 km, comprises the following eight points:

1 - Autobahn
2 - Immelberg
3 - Steinkirchen
4 - Hochries
5 - Heuberg
6 - Wendelstein
7 - Farrenpoint
8 - Eckersberg;

see figure 1.

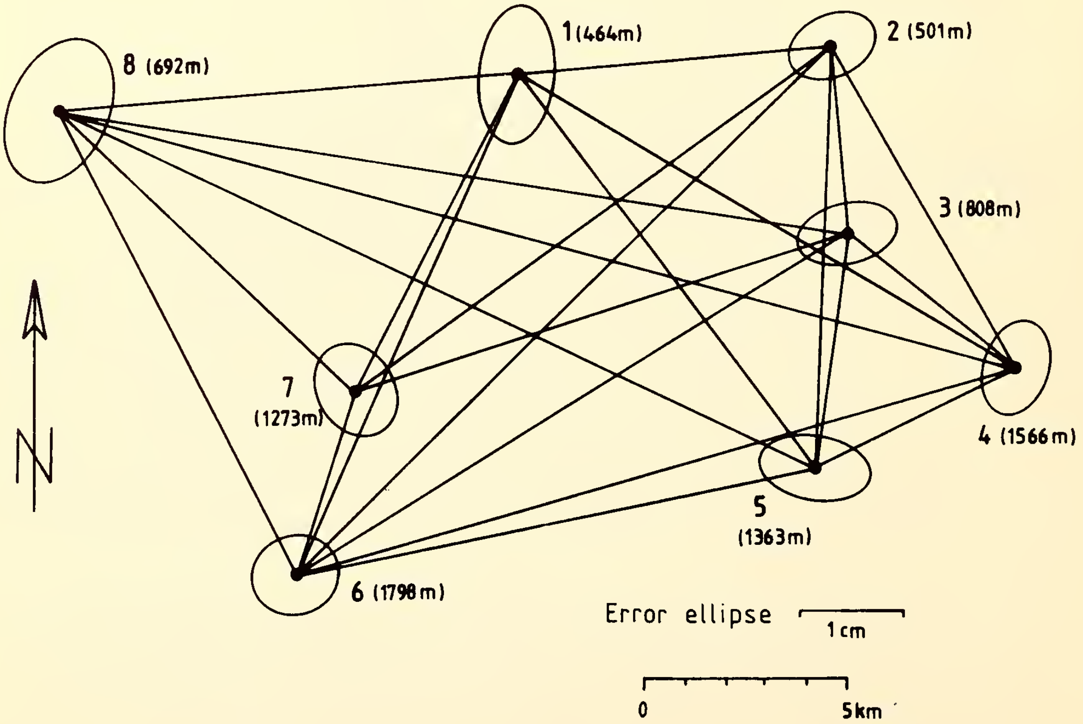

Figure 1: Inn Valley Network

All points but station No.3 are monumented by concrete pillars, see figure 4. The terrestrial measurements are composed of

- 48 slope distances (AGA Geodimeter 14 and 8, K & E Rangemaster III, Wild DI 20, Hewlett Packard HP 3808 A)
- 44 horizontal directions (Kern DKM 2AM)
- 44 zenith angles (Kern DKM 2AM)
- 8 (x 2 components) relative deflections of the vertical (Zeiss Ni-2 astrolabium).

The network was adjusted in a minimum constraint three-dimensional mode. The horizontal datum was taken over from the national horizontal control network (Deutsches Hauptdreiecksnetz, datum Potsdam, Bessel ellipsoid); the vertical datum was derived from the national vertical network (Deutsches Haupthöhennetz, datum "Normalnull"). The network was connected to the national horizontal and vertical datum by the following constraints: $x_6 = \bar{x}_6$, $y_6 = \bar{y}_6$, $x_4 = \bar{x}_4$, $h_3 = H_3$ (i.e. the scale was taken from the distance measurements).

The height differences determined by means of trigonometrical heighting are of the type ellipsoidal heights. As the given normal orthometric height $\bar{H}_3$ of point No.3 does not refer to the reference ellipsoid, all heights provided by the network adjustment differ from ellipsoidal heights by an unknown constant. Moreover, the reference surface of the height differences is not parallel to the surface of the reference ellipsoid because the relative deflections of the vertical were not minimized. Since, however, due to the nature of Macrometer measurements only coordinate differences can be compared, these shortcomings do not affect the analysis, so that all heights can be treated as ellipsoidal.

In tables 1 and 2 the terrestrial coordinates of the Inn Valley Network are documented. The mean horizontal (Helmert) point error is $\bar{m}_p = \pm 6$ mm, the mean error in heights is $\bar{m}_h = \pm 36$ mm.

Table 1 gives the Transverse Mercator coordinates x, y (Northing, Easting minus 500 km, scale factor $m_o = 1$) and the ellipsoidal heights h : $\underline{x}^K = (x,y,h)$. The x,y coordinates refer to the Bessel ellipsoid and to the meridian 12^o east of Greenwich. Table 2 shows the corresponding cartesian coordinates $\underline{x}^G = (X,Y,Z)$.

Point No.	x [m]	y [m]	h [m]
1	5 297 125,777	6 762,065	469,551
2	5 297 711,709	14 294,432	502,325
3	5 293 287,832	14 736,956	809,054
4	5 289 915,290	18 756,784	1 567,992
5	5 287 709,218	13 982,326	1 364,179
6	5 285 129,240	1 196,590	1 800,557
7	5 289 446,556	2 775,788	1 274,151
8	5 296 284,637	-4 497,898	698,058

Table 1: Terrestrial transverse Mercator coordinates and heights $\underline{x}^K$

Point No.	X [m]	Y [m]	Z [m]
1	4 195 742,851	898 746,313	4 702 827,398
2	4 193 765,317	906 027,239	4 703 235,977
3	4 197 079,902	907 184,942	4 700 490,468
4	4 199 178,479	911 743,412	4 698 777,156
5	4 201 642,813	907 384,479	4 697 151,419
6	4 206 466,332	895 335,688	4 695 749,282
7	4 202 665,835	896 142,566	4 698 264,346
8	4 198 845,207	887 893,215	4 702 433,221

Table 2: Terrestrial cartesian coordinates $\underline{x}^G$

For comparison with Macrometer results some spatial distances are derived from the terrestrial point coordinates of tables 1 and 2: ee table 3. Their relative mean square error is $m_{\bar{s}}/S = \pm$ 0,6 ppm.

Baseline	S	m_s/S [ppm]	Baseline	S [m]	m_s/S [ppm]
7 - 8	10 001,425	0,5	5 - 4	5 264,623	0,7
8 - 6	12 575,651	0,5	4 - 1	14 040,391	0,3
6 - 5	13 053,953	0,5	1 - 2	7 555,757	0,5
6 - 7	4 628,215	0,7	1 - 8	11 294,677	0,5
5 - 3	5 657,669	0,6	1 - 3	8 857,731	0,7
3 - 4	5 302,746	0,6	2 - 3	4 456,969	0,6

Table 3: Terrestrial spatial distances (adjusted) $\underline{S}$

3. THE INN VALLEY MACROMETER CAMPAIGN 1984

In November 1984 the campaign was carried out by employing four Macrometers type V 1000. The measurements were executed by a commercial company by order of and supported by the Institut für Geodäsie of the Universität der Bundeswehr München. Due to budgetary restraints the number of Macrometer observables was limited to twelve baselines. Altogether five institutions were involved in this campaign by supporting either the general organization, the observations or the logistics:

- Dr.-Ing. O. Schuster, ÖbVI, Mühlheim a.d.R., contractor
- GEO/HYDRO Inc., Rockville, Maryland, USA, subcontractor
- Hessisches Landesvermessungsamt, Wiesbaden

- Heeresfliegerregiment 20, Neuhausen o.E.
- Institut für Geodäsie der Universität der Bundeswehr München.

The observations started November 06, 1984 (day 311) at 3.00 a.m. and were completed November 11, 1984 (day 316) 7.00 a.m. All 6 NAVSTAR satellites available at that time (Nos. 1,3,4,6,8,9) could be received for roughly 3.5 hours each day. Within this period about 140 phase measurements could be obtained for each baseline. Since four receivers were scheduled, three almost independent baselines should be observed every day. Proceeding from these assumptions an optimization of the second order design resulted in a distribution of the observables as shown in figure 2.

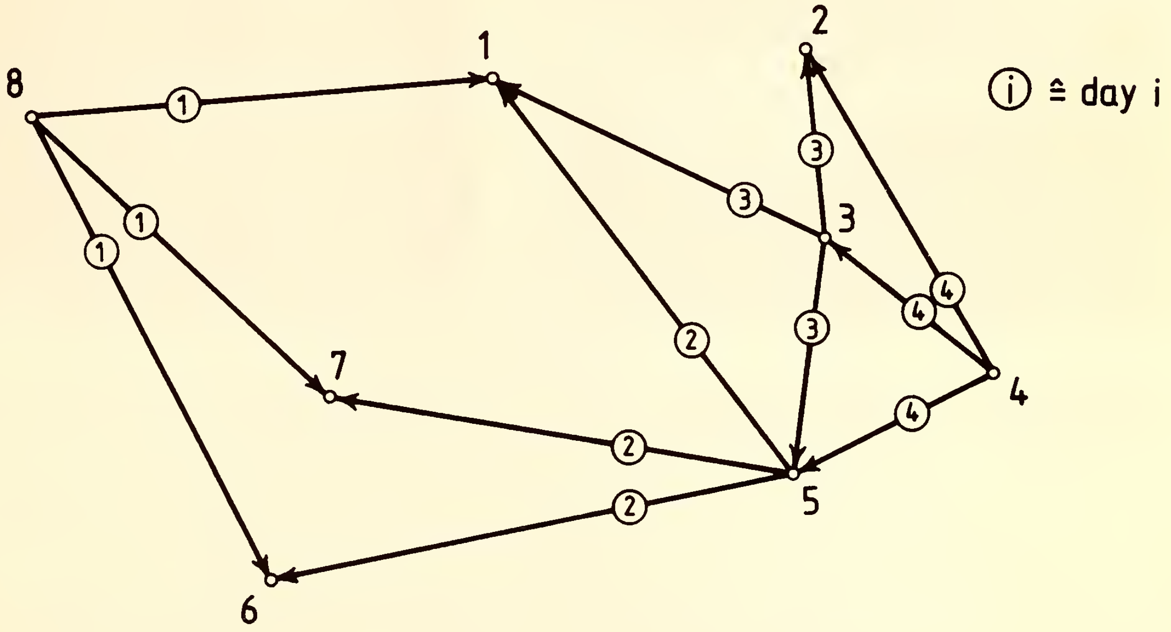

Figure 2: Observation plan for the use of 4 Macrometers

The evaluation of the received satellite signals demands precise synchronization of the internal clocks both relatively to all the other receivers involved and absolutely to the official time standard. Therefore the oscillators or the clocks respectively of two receivers were calibrated by the hydrogen maser time standard of the Geodetic Reference Station Wettzell. After synchronization the time delay was as little as 0.6 µs, which is well within the limit of 2 µs.

As three of the eight stations are located on rough crags high in the mountains the total instrumentation was daily carried up to the stations and down to the master clock for time tuning by a helicopter; see figure 3.

Figure 4 shows the Macrometer antenna on one of the pillars.

Figure 3:
Transportation of the equipment
helicopter to station No. 5 (Heuberg)

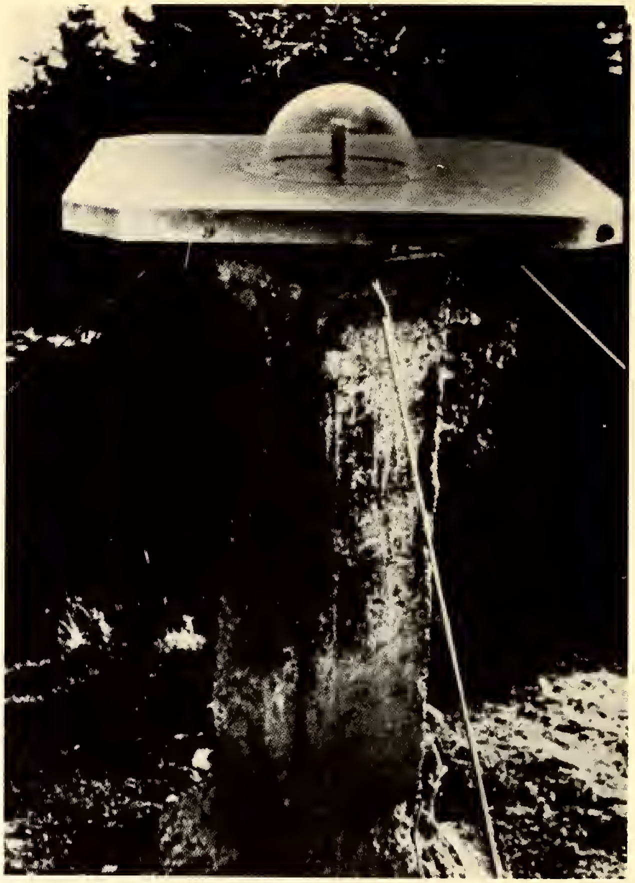

Figure 4:
Macrometer antenna on station No. 7
(Farrenpoint)

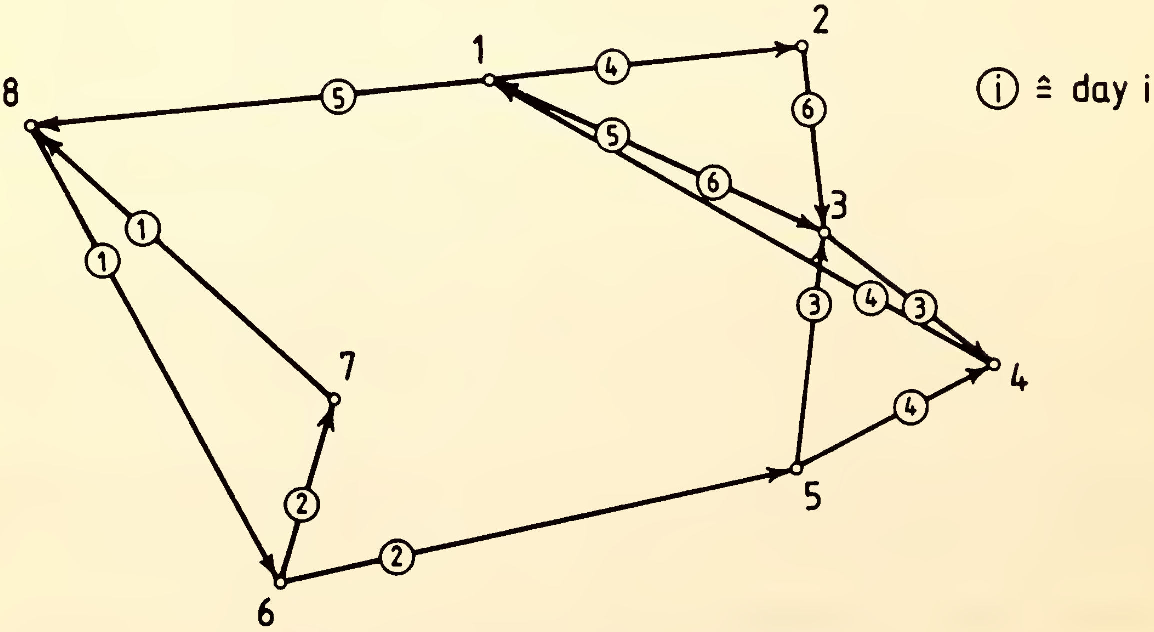

Figure 5: Observed baseline vectors

All helicopter flights had to be done in daytime. Consequently, the observer crews as well as the receivers had to remain over night close to the stations. Since the logistic conditions were quite difficult and the temperature in this season had already dropped below 0°C the campaign was a challenge for both man and equipment.

Possibly due to the rough environmental influences almost every night one of the four receivers failed (e.g. frequency drift, time jumps, break down of the power supply). Hence the observations initially planned could not be performed. After six days the network had been observed as shown in figure 5.

4. RESULTS OF THE MACROMETER CAMPAIGN

Baseline		$\Delta X'_M$ [m]	$\Delta Y'_M$ [m]	$\Delta Z'_M$ [m]	S'_M [m]
1	7 - 8	-3 820,427	- 8 249,325	4 169,032	10 001,392
2	8 - 6	7 620,949	7 442,490	-6 684,046	12 575,611
3	6 - 5	-4 823,592	12 048,681	1 401,923	13 053,855
4	6 - 7	-3 800,526	806,833	2 515,018	4 628,206
5	5 - 3	-4 562,890	- 199,536	3 339,053	5 657,655
6	3 - 4	2 098,391	4 558,454	-1 713,553	5 302,736
7	5 - 4	-2 464,479	4 358,924	1 625,506	5 264,613
8	4 - 1	-3 435,194	-12 997,039	4 050,760	14 040,379
9	1 - 2	-1 977,720	7 280,895	408,364	7 555,764
10	1 - 8	3 102,378	-10 853,040	- 394,148	11 294,626
11	1 - 3	1 336,798	8 438,567	-2 337,233	8 857,714
12	2 - 3	3 314,524	1 157,682	-2 745,589	4 456,967
13	3 - 1	-1 336,793	- 8 438,572	2 337,233	8 857,718

Table 4: "Observed" Macrometer coordinate differences $\Delta \underline{x}^{G}_{M}{}'$ and distances $\underline{S}'_M$

Baseline		ΔX_M [m]	ΔY_M [m]	ΔZ_M [m]	S_M [m]	m_s/S [ppm]
1	7 - 8	-3 820,426	- 8 249,325	4 169,032	10 001,392	0,5
2	8 - 6	7 620,948	7 442,489	-6 684,047	12 575,611	0,3
3	6 - 5	-4 823,644	12 048,660	1 401,913	13 053,854	1,0
4	6 - 7	-3 800,522	806,836	2 515,015	4 628,202	0,7
5	5 - 3	-4 562,880	- 199,534	3 339,054	5 657,647	0,7
6	3 - 4	2 098,394	4 558,457	-1 713,550	5 302,739	0,5
7	5 - 4	-2 464,486	4 358,923	1 625,504	5 264,615	1,0
8	4 - 1	-3 435,191	-12 997,029	4 050,780	14 040,374	0,3
9	1 - 2	-1 977,726	7 280,892	408,360	7 555,762	0,6
10	1 - 8	3 102,372	-10 853,044	- 394,149	11 294,628	1,2
11	1 - 3	1 336,797	8 438,572	-2 337,230	8 857,718	0,3
12	2 - 3	3 314,523	1 157,680	-2 745,590	4 456,966	0,4
13	3 - 1	-1 336,797	- 8 438,572	2 337,230	8 857,718	0,3

Table 5: Adjusted Macrometer coordinate differences $\Delta \underline{x}^{G}_{M}$ and distances $\underline{S}_M$

Table 4 represents the "observed" Macrometer coordinate differences $\Delta\underline{x}_M^{G}{}' = (\Delta X_M' , \Delta Y_M' , \Delta Z_M')$ in a cartesian coordinate system and the corresponding spatial distances $\underline{S}_M'$. The measurements were evaluated by GEO/HYDRO Inc. As a result adjusted coordinate differences $\Delta\underline{x}_M^G = (\Delta X_M , \Delta Y_M , \Delta Z_M)$ and adjusted spatial distances $\underline{S}_M$ were obtained, see table 5, with a relative mean square error of $m_s^{-}/S = \pm\, 0{,}7$ ppm.

Table 6 depicts the Macrometer results as WGS 72 cartesian coordinates $\underline{x}_M^G = (X_M , Y_M , Z_M)$ making use of the geocentric point vector $\underline{x}_S^G$ determined on the occasion of the Inn Valley Doppler Campaign in 1983 (HEISTER/GLASMACHER, 1984). The corresponding Transverse Mercator coordinates ($m_o = 1$, reference meridian: 12^o E) and WGS 72 ellipsoidal heights are given in table 7. The mean horizontal (Helmert) point error was found to $\bar{m}_P = \pm 19$ mm, the mean square error in heights by $\bar{m}_h = \pm 18$ mm.

Point No.	X_M [m]	Y_M [m]	Z_M [m]
1	4 196 381,489	898 755,274	4 703 274,536
2	4 194 403,764	906 036,166	4 703 682,897
3	4 197 718,286	907 193,846	4 700 937,306
4	4 199 816,680	911 752,303	4 699 223,757
5	4 202 281,166	907 393,380	4 697 598,253
6	4 207 104,810	895 344,720	4 696 196,340
7	4 203 304,288	896 151,556	4 698 711,355
8	4 199 483,862	887 902,231	4 702 880,387

Table 6: Macrometer cartesian coordinates $\underline{x}_M^G$

Point No.	x_M [m]	y_M [m]	h_M [m]
1	5 297 566,404	6 638,007	519,983
2	5 298 152,330	14 170,322	552,307
3	5 293 728,486	14 612,838	858,992
4	5 290 355,957	18 632,677	1 617,604
5	5 288 149,943	13 858,230	1 414,193
6	5 285 570,034	1 072,704	1 851,125
7	5 289 887,299	2 651,843	1 324,565
8	5 296 725,272	-4 621,813	748,761

Table 7: Macrometer Transverse Mercator coordinates and heights $\underset{\sim}{x}_M^K$

5. COMPARISON AND ANALYSIS

In order to evaluate the results $\underline{x}^G$, $\underset{\sim}{x}^K$, $\underline{S}$ of the terrestrial observations (chapter 2, tables 1,2,3) on the one side and the results $\underline{x}_M^G$, $\underset{\sim}{x}_M^K$, $\underline{S}_M'$, $\underline{S}_M$ (chapter 4, tables 6,7,4,5) of the Macrometer measurements on the other side we compared

- firstly the corresponding coordinates ($\underline{x}^G \leftrightarrow \underline{x}_M^G$, $\underset{\sim}{x}^K \leftrightarrow \underset{\sim}{x}_M^K$) by means of a seven parameter similarity transformations minimizing the residuals $d\underline{x}_M^G$ resp. $d\underset{\sim}{x}_M^K$ (Helmert transformation),

$$d\underline{x}^G = \underline{x}^G - m^G \cdot \underline{R}^G \cdot (\underline{x}_M^G - \underline{x}_{oM}^G) \; ; \quad d\underline{x}^G = (dX,\ dY,\ dZ)$$

$$d\underset{\sim}{x}^K = \underset{\sim}{x}^K - m^K \cdot \underline{R}^K \cdot (\underset{\sim}{x}_M^K - \underset{\sim}{x}_{oM}^K) \; ; \quad d\underset{\sim}{x}^K = (dx,\ dy,\ dh) \ ,$$

see tables 8 and 9, and

- secondly the corresponding distances ($\underline{S} \leftrightarrow \underline{S}_M'$) , obtaining absolute and relative distance residuals

$\underline{r}_s' = \underline{S} - \underline{S}_M$ and $\underline{r}_s' / S$ or minimizing the residuals $\underline{r}_s' / S$ by introducing a scale factor m^s ,

$$\underline{r}_s = \underline{S} - m^s \cdot \underline{S}_M' \quad \text{and} \quad \underline{r}_s / S \ ,$$

see table 10.

Point No.	dX [mm]	dY [mm]	dZ [mm]	$\lvert d\underline{x}^G \rvert$ [mm]
1	-90	9	-94	131
2	- 4	- 7	-16	18
3	-10	2	4	11
4	67	7	115	133
5	-46	2	-47	66
6	-14	-36	-58	70
7	47	- 1	15	50
8	51	37	83	104
m^G = 0,999 996 16				± 85

Table 8: Residuals "Macrometer-terrestrial" in terms of Cartesian coordinates: $d\underline{x}^G$

Point No.	dx [mm]	dy [mm]	r_h = dh [mm]	$\lvert d\underset{\sim}{x}^K \rvert$ [mm]	$r_p = \sqrt{dx^2+dy^2}$ [mm]
1	0	28	-128	128	28
2	-8	-6	-14	17	10
3	9	5	-4	11	10
4	30	-22	126	131	37
5	2	12	-65	66	12
6	-24	-32	-58	70	40
7	-24	-11	42	50	26
8	13	26	100	104	29
m^K = 0,999 988 35			± 80	± 85	± 26

Table 9: Residual "Macrometer-terrestrial" in terms of Transverse Mercator coordinates and heights: $d\underset{\sim}{x}^K$

Baseline		S [m]	r_S' [mm]	r_S'/S [ppm]	r_S [mm]	r_S/S [ppm]
1	7-8	10 001	+33	+3,3	+ 8	+0,8
2	8-6	12 576	+40	+3,2	+ 9	+0,7
3	6-5	13 054	+98	+7,5	+66	+5,1
4	6-7	4 628	+15	+3,2	+ 4	+0,9
5	5-3	5 658	+14	+2,5	0	0,0
6	3-4	5 303	+10	+1,9	- 3	-0,6
7	5-4	5 265	+10	+1,9	- 3	-0,6
8	4-1	14 040	+17	+1,2	-18	-1,3
9	1-2	7 556	- 7	-0,9	-26	-3,4
10	1-8	11 265	+51	+4,5	+23	+2,0
11	1-3	8 858	+17	+1,9	- 5	-0,6
12	2-3	4 457	+ 2	+0,4	-9	-2,0
13	3-1	8 858	+13	+1,5	-9	-1,0
m^S = 0,999 99753				+2,47		0,0 ±2,0

Table 10: Absolute and relative distance residuals: $\underline{r}_S'$, $\underline{r}_S'/S$, $\underline{r}_S$, $\underline{r}_S/S$

The results using Cartesian (table 8) and Transversal Mercator coordinates, extended by h (table 9), are equivalent (as they are expected to be). For the further analysis the results out of table 9 are more suitable, as they allow to distinguish x/y- and h-residuals. This distinction is also required to the corresponding coordinates derived from terrestrial measurement. Note the significant differences between the mean terrestrial horizontal point error and the mean error in height: Terrestrial coordinates: $\bar{m}_p$ = ± 6 mm vs. $\bar{m}_h$ = ± 36 mm; but Macrometer coordinates: $\bar{m}_p$ = ± 19 mm and $\bar{m}_h$ = ± 18 mm.

In general, these accuracies are also reflected by the residuals of table 9. They result in a mean horizontal component $\bar{r}_p = \sqrt{\Sigma(dx^2 + dy^2)/8} = \pm$ 26 mm and, in contrast, in a mean vertical component $\bar{r}_h = \pm$ 80 mm. While $\bar{r}_p = \pm$ 26 mm is an excellent result, $\bar{r}_h = \pm$ 80 mm has to be questioned. Considering the terrestrial mean square error $m_H = \pm$ 36 mm, one has to admit that due to refraction influences the terrestrial heights are much weaker than the horizontal positions. Therefore, the conclusion can be drawn that the Macrometer measurement cannot be burdened with the discrepancy. On the contrary, the terrestrial measurements have obviously to be strengthened for their h-component to be able to compete with the Macrometer heights.

Further analyses are done by Welsch/Oswald (1985).

As a conclusion we can state the Macrometer technology as a powerful competition to terrestrial surveying methods. Current shortcomings (as reported in chapter 3) might be eliminated by the rapid development of instrumental techniques.

6. REFERENCES

Bock, Y., Abbot, R.I., Counselman, C.C., Gourevitch, S.A., King, R.W.: *Establishment of Three-Dimensional Geodetic Control by Interferometry with Global Positioning System.* Submitted to the Journal of Geophysical Research December 1984

Bock, Y., Abbot, R.I., Counselman, C.C., Gourevitch, S.A., King, R.W., Paradis, A.R. (1984): *Geodetic Accuracy of the Macrometer Model V - 1000.* Bulletin Géodesique 58, 1984, pp. 211-221

Goad, C.C., Remondi, B.W.: *Initial relative Positioning Results using Global Positioning System.* Paper XVIIIth General Assembly of the International Union of Geodesy and Geophysics, Hamburg, 1983

Heister, H., Glasmacher, H.: *Satelliten-Dopplermessungen im Testnetz Inntal.* In Schödlbauer, A., Welsch, W. (editors): Satelliten-Dopplermessungen. Beiträge zum geodätischen Seminar 24./25. September 1984, p. 307-325. Schriftenreihe des Wissenschaftlichen Studiengangs Vermessungswesen der Hochschule der Bundeswehr München, Heft 15, Neubiberg, 1984

Lindstrot, W.: *Ergebnisse von Makrometermessungen in Nordrhein-Westfalen und Vergleiche mit anderen Verfahren,* BDVI Forum, 1984, p. 477-486

Schmidt, R.: *Das neue interferometrische GPS-Vermessungsgerät Makrometer und sein Einsatz in der TP-Netzerneuerung 2. Ordnung Nordeifel,* Allgemeine Vermessungsnachrichten 91, 1984, p. 138-148

Schrick, K.-W.: *Das Global Positioning System (GPS) und seine Bedeutung für die praktische Landesvermessung,* BDVI Forum, 1984, p. 447-464

Seeber, G.: *Die Rolle des NAVSTAR Global Positioning Systems für die Lösung geodätischer Aufgaben,* Zeitschrift für Vermessungswesen 109, 1984, p.1-11

Strauß, R.: *Makrometermessungen in Hessen,* BDVI Forum, 1984, p. 487-497

Strauß, R.: *Makrometermessungen im Deutschen Hauptdreiecksnetz,* In Schödlbauer, A., Welsch, W. (editors): Satelliten-Doppler-Messungen. Beiträge zum Geodätischen Seminar 24./25. September 1984, p. 361-368. Schriftenreihe des Wissenschaftlichen Studiengangs Vermessungswesen der Hochschule der Bundeswehr München, Heft 15, Neubiberg, 1984

Welsch, W., Oswald, W.: *Variance Analysis of Satellite Networks.* Paper submitted to First International Symposium on Precise Positioning with the Global Positioning System, Rockville, Maryland, 1985

COMPARISON OF SURVEY RESULTS FROM DIFFERENT TYPES OF GPS RECEIVERS

Alfred Kleusberg
Richard B. Langley
Rock Santerre
Petr Vaníček
David E. Wells
Department of Surveying Engineering
University of New Brunswick
Fredericton, N.B.
Canada E3B 5A3

Gerhard Beutler
Astronomical Institute
University of Bern
CH-3012 Bern
Switzerland

ABSTRACT. Observation equations for single and dual frequency GPS carrier phase measurements and their single and double differences are derived. The effects of dispersive refraction on the observables and on derived relative position vectors are discussed. Results from processing single frequency MACROMETER^{TM} V-1000 and dual frequency Texas Instruments TI 4100 observations on the Ottawa test network both in 'baseline mode' and in 'network mode' are presented.

INTRODUCTION

Simultaneous GPS carrier phase observations have become one of most precise methods for relative geodetic positioning. Several instruments based on different hardware philosophies have been developed and their usefulness for establishing geodetic control is presently being investigated. The analysis of observations from different types of receivers and the comparison of the relative positioning results is the primary goal of this paper. Accordingly we will derive the observation equations for GPS carrier phase measurements and show the necessary modifications for 'squaring type' receivers and dual frequency observations. These equations are the basis for the differential positioning software DIPOP developed at the University of New Brunswick (Vanicek et al, 1985). This software has been applied to the reduction of observations using MACROMETER V-1000 and Texas Instruments TI 4100 receivers on the Ottawa Geodetic Test Network shown in figure 1.

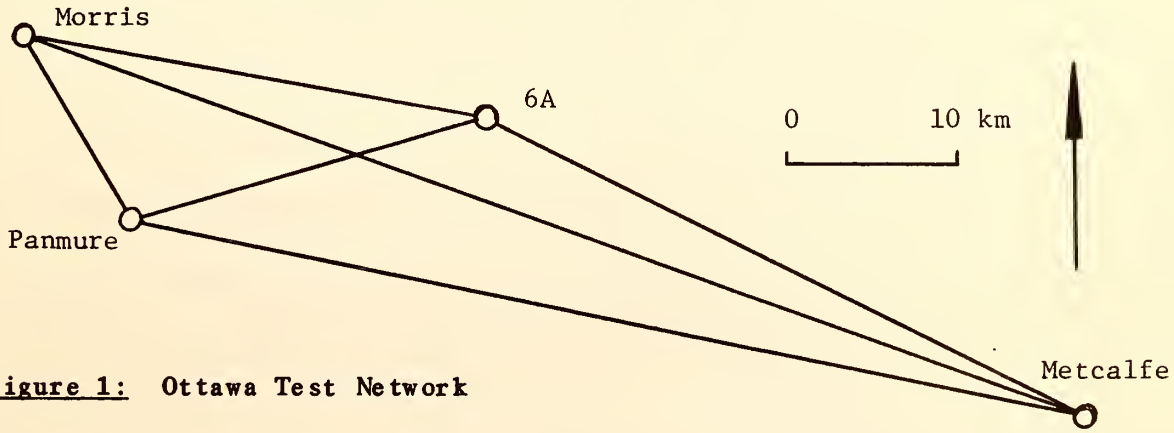

Figure 1: Ottawa Test Network

During the summer of 1983, the Earth Physics Branch of Energy, Mines and Resources Canada through a contract with GEO/HYDRO of Rockville, MD conducted Macrometer V-1000 GPS carrier phase observations on the network. The observation schedule is given in Table 1. In the spring of 1984, the network was reobserved by Nortech Surveys (Canada) Inc. of Calgary for the Geodetic Survey of Canada using Texas Instruments TI 4100 GPS receivers. The observation sessions are listed in Table 2. Further details concerning the Macrometer observations have been given by Valliant (1984). The TI 4100 observations have been discussed by McArthur (1984) and Vanicek et al. (1985).

Table 1: Macrometer V-1000 observations

Baseline	Number of Sessions	Observation time per Session [h]	Approximate length [m]
Pammure - Morris	2	5/5	12844
Pammure - 6A	4	5/5/5/5	21590
Morris - 6A	4	5/5/5/5	26489
Metcalfe - 6A	4	5/5/5/5	40295
Metcalfe - Pammure	4	5/5/3/3	57931
Metcalfe - Morris	3	5/5/5	66269

Table 2: Texas Instruments TI 4100 observations

Baseline	Number of Sessions	Observation time per Session [h]	Approximate length [m]
Pammure - Morris	2	5/5	12844
Pammure - 6A	2	5/5	21590
Morris - 6A	2	5/5	26489
Metcalfe - 6A	1	5	40295
Metcalfe - Pammure	1	5	57931
Metcalfe - Morris	1	5	66269

CARRIER PHASE OBSERVATION EQUATION

The basic GPS carrier phase observable is the phase P_i^k of the intermediate frequency signal (IF signal), corrupted by an unknown integer number of cycles (e.g. Bauersima, 1983):

$$P_i^k(t_{i\beta}) = P_r^k(t_{i\beta}) - P_i(t_{i\beta}) + N_i^k \tag{1}$$

where

$t_{i\beta}$ is the observation epoch β on the time scale t_i of receiver i

$P_r^k(t_{i\beta})$ stands for phase of received signal transmitted by satellite k

$P_i(t_{i\beta})$ is the Phase of oscillator of receiver i at signal reception time

N_i^k denotes the Phase ambiguity of observation P_i^k (integer number of cycles)

The phase of the received signal at reception time is equal to the phase P^k of the transmitted signal at transmission time. Thus we obtain from eqn.(1)

$$P_i^k(t_{i\beta}) = P^k(t^k(t_{i\beta})-\Delta t_i^k) - P_i(t_{i\beta}) + N_i^k \tag{2}$$

where

$t^k(t_{i\beta})$ denotes the time of satellite k at signal reception time, $t_{i\beta}$

Δt_i^k is the signal propagation delay between satellite k and receiver i

At observation epoch β, the receiver time t_i and satellite time t^k are assumed to be closely aligned to some independent time t (e.g. GPS time or UTC) according to the following expressions:

$$\begin{aligned} t^k(t_\beta) &= t_\beta^k + dt_\beta^k \\ t_i(t_\beta) &= t_{i\beta} + dt_{i\beta} \\ t^k(t_{i\beta}) &= t_\beta^k + dt_\beta^k - dt_{i\beta} \end{aligned} \tag{3}$$

with small time offsets dt_β^k and $dt_{i\beta}$. This leads to

$$\begin{aligned} P^k(t^k(t_{i\beta})-\Delta t_i^k) &= P^k(t_\beta^k+dt_\beta^k-dt_{i\beta}-\Delta t_i^k) \\ &= f \cdot (t_\beta^k+dt_\beta^k-dt_{i\beta}-\Delta t_i^k) + A^k, \end{aligned} \tag{4}$$

where we have denoted the nominal frequency of the satellite oscillator by f and its initial phase by A^k. Similarly, we replace the receiver oscillator phase by

$$P_i(t_{i\beta}) = f_R \cdot t_{i\beta} + A_i \tag{5}$$

with nominal receiver frequency f_R and initial phase A_i. The nominal receiver oscillator frequency f_R may be offset from the nominal satellite oscillator frequency by

$$df = f - f_R. \tag{6}$$

Using further the frequency-time relation

$$f \cdot t_\beta^k = f \cdot t_{i\beta} \tag{7}$$

and equations (4) through (6), we obtain from eqn.(2)

$$P_i^k(t_{i\beta}) = f \cdot (dt_\beta^k-dt_{i\beta}-\Delta t_i^k) + df \cdot t_{i\beta} + N_i^k + A^k - A_i. \tag{8}$$

The signal propagation delay is modelled by

$$\Delta t_i^k = (\rho_i^k + dI_i^k + dT_i^k) / c \tag{9}$$

where

ρ_i^k is the geometric signal path length between satellite and receiver

dI_i^k is the signal path lengthening due to ionospheric refraction

dT_i^k is the signal path lengthening due to tropospheric refraction

and c the vacuum speed of light. Inserting eqn.(9) in eqn.(8) and replacing c/f by the carrier wavelength λ, we obtain finally:

$$\lambda \cdot P_i^k(t_{i\beta}) = c \cdot (dt_\beta^k - dt_{i\beta}) - \rho_i^k - dI_i^k - dT_i^k + \lambda \cdot (df \cdot t_{i\beta} + N_i^k + A^k - A_i) \tag{10}$$

CARRIER PHASE DIFFERENCES

Two receivers at the i-th and j-th station may observe carrier phases of a signal transmitted by satellite k. Taking the difference between carrier phases observed at the same nominal time, we obtain the so called 'carrier phase single difference' (Davidson et al., 1983):

$$\begin{aligned} \lambda \cdot P_{ij}^k(t_{i\beta}, t_{j\beta}) &= \lambda \cdot (P_j^k(t_{j\beta}) - P_i^k(t_{i\beta})) \\ &= -c \cdot dt_{ij\beta} - \rho_{ij}^k - dI_{ij}^k - dT_{ij}^k + \lambda \cdot (N_{ij}^k + A_{ij}) \end{aligned} \tag{11}$$

where we have abbreviated

$$(\cdot)_j - (\cdot)_i = (\cdot)_{ij}.$$

In taking the observation difference, the initial phase of the satellite oscillator and the offset of the satellite clock are removed from the observation equation.

Subtracting the single difference observed on the signal transmitted by satellite k from that observed at the same nominal time on the signal transmitted by satellite n leads to the 'carrier phase double difference':

$$\begin{aligned} \lambda \cdot P_{ij}^{kn}(t_{i\beta}, t_{j\beta}) &= \lambda \cdot (P_{ij}^n(t_{i\beta}, t_{j\beta}) - P_{ij}^k(t_{i\beta}, t_{j\beta})) \\ &= -\rho_{ij}^{kn} - dI_{ij}^{kn} - dT_{ij}^{kn} + \lambda \cdot N_{ij}^{kn}. \end{aligned} \tag{12}$$

In taking the observation double difference, the initial phase of the receiver oscillator and the receiver clock offset are removed from the observation equation. The first term on the right hand side of eqn.(12) represents the double difference of geometric distances according to Figure 2. The distances from the i-th receiver to the satellites are referred to satellite positions slightly different from those from the j-th receiver to the satellites. This effect is due to different signal propagation delays and errors in the synchronization of the two receiver clocks and has to be taken into account when linearizing eqn.(12) for the purpose of a least squares adjustment.

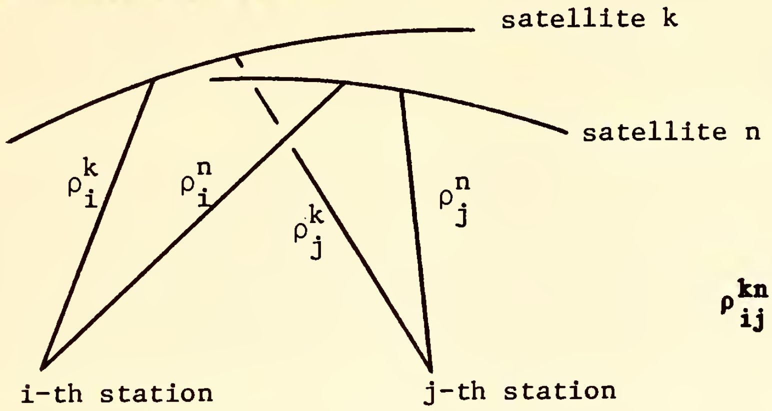

$$\rho_{ij}^{kn} = \rho_j^n - \rho_j^k - \rho_i^n + \rho_i^k$$

Figure 2: Double difference geometry

Equation (12) is the basis for the reduction of carrier phase observations by DIPOP. Two modifications are introduced to account for the specifications of the Macrometer V-1000 and the Texas Instruments TI 4100 observations. The V-1000 is a squaring type receiver and the effective wavelength in the observation equation is half the carrier wavelength (Beutler et al., 1984):

$$\lambda/2 \cdot P_{ij}^{kn}(t_{i\beta}, t_{j\beta}) = -\rho_{ij}^{kn} - dI_{ij}^{kn} - dT_{ij}^{kn} + \lambda/2 \cdot N_{ij}^{kn}. \tag{13}$$

The TI 4100 provides phase observations on both GPS carriers L1 and L2. Denoting the carrier by the subscript q we write

$$\lambda_q \cdot P_{ijq}^{kn}(t_{i\beta}, t_{j\beta}) = -\rho_{ij}^{kn} - dI_{ijq}^{kn} - dT_{ij}^{kn} + \lambda_q \cdot N_{ijq}^{kn}, \quad q = 1,2 \tag{14}$$

and using a first order approximation for the dispersive ionospheric delay

$$dI_{ij1}^{kn} = f_2^2/(f_2^2 - f_1^2) \cdot (dI_{ij1}^{kn} - dI_{ij2}^{kn}), \tag{15}$$

we obtain a linear combination of the L1 and L2 observations free of first order dispersive refraction:

$$C \cdot (P_{ij1}^{kn}/\lambda_1 - P_{ij2}^{kn}/\lambda_2) = -\rho_{ij}^{kn} - dT_{ij}^{kn} + C \cdot (N_{ij1}^{kn}/\lambda_1 - N_{ij2}^{kn}/\lambda_2) \tag{16}$$

with

$$C = c^2 / (f_2^2 - f_1^2). \tag{17}$$

The differential tropospheric delay dT in eqns.(13), (14) and (16) can be modelled with the well known Hopfield model (Hopfield, 1969) and standard atmospheric parameters. The use of actual temperature, air pressure and humidity seems not to be necessary for the present level of accuracy, at least on baselines with lengths shorter than about 65 km (Valliant, 1984). Due to the lack of a reasonably accurate model for the ionospheric delay, we have neglected the ionospheric refraction effect dI in the analysis of single frequency carrier phase double differences.

It has been shown by several authors (e.g. Bauersima, 1983, Davidson et al., 1983), that for baselines shorter than about 100 km the double difference observable depends only weakly on the absolute position of the receivers and the satellites. On the other hand, it is strongly dependent on the relative position of the observing stations. Therefore, if reasonably accurate orbital information is available (satellite position uncertainty less than about 50 m), no estimation of orbital parameters is performed to obtain baseline uncertainties approaching one part per million.

Thus the remaining unknowns in equations (13), (14) and (16) are the relative station coordinates and the carrier phase ambiguities.

EFFECT OF DIFFERENTIAL DISPERSIVE DELAY

To examine the effect of neglecting the differential ionospheric delay in the adjustment of single frequency carrier phase measurements, several TI 4100 dual frequency observation records have been reduced in three different ways. Firstly, we used only the L1 observations in eqn.(14), secondly, we used only the L2 observations in eqn.(14) and thirdly, we combined L1 and L2 observations for the use of eqn.(16). Before looking at the results, we note:

1) In combining L1 and L2 observations we amplify the measurement noise. Assuming some noise σ_s in the single frequency observations, uncorrelated between L1 and L2, the law of error propagation gives for the linear combination of eqn.(16)

$$\sigma_d \sim 4.1\,\sigma_s. \tag{18}$$

Hence, if the differential dispersive delay dI is negligibly small (or constant in time, see below), the only result of combining L1 and L2 observations is an increase in the measurement noise level.

2) Any differential ionospheric delay dI, constant in time, distorts only the estimation of the carrier phase ambiguity N and does not affect the estimation of relative coordinates (c.f. equation (14)). As long as the ambiguity estimate is not forced to be an integer number, the constant part of the neglected differential dispersive delay will not show up in the residuals of a least squares adjustment.

However, if the differential ionospheric delay is not constant during the observation time span, its neglect in the modelling of the observation may cause a distortion in the estimation of the relative coordinates and will increase the estimated a posteriori variance factor of the adjustment. A typical example for this case is depicted in Figure 3, which shows the least sqares residuals of carrier phase double differences observed on the 40 km baseline Metcalfe - 6A of the Ottawa Test Network during the single TI 4100 observing session. The adjustment included

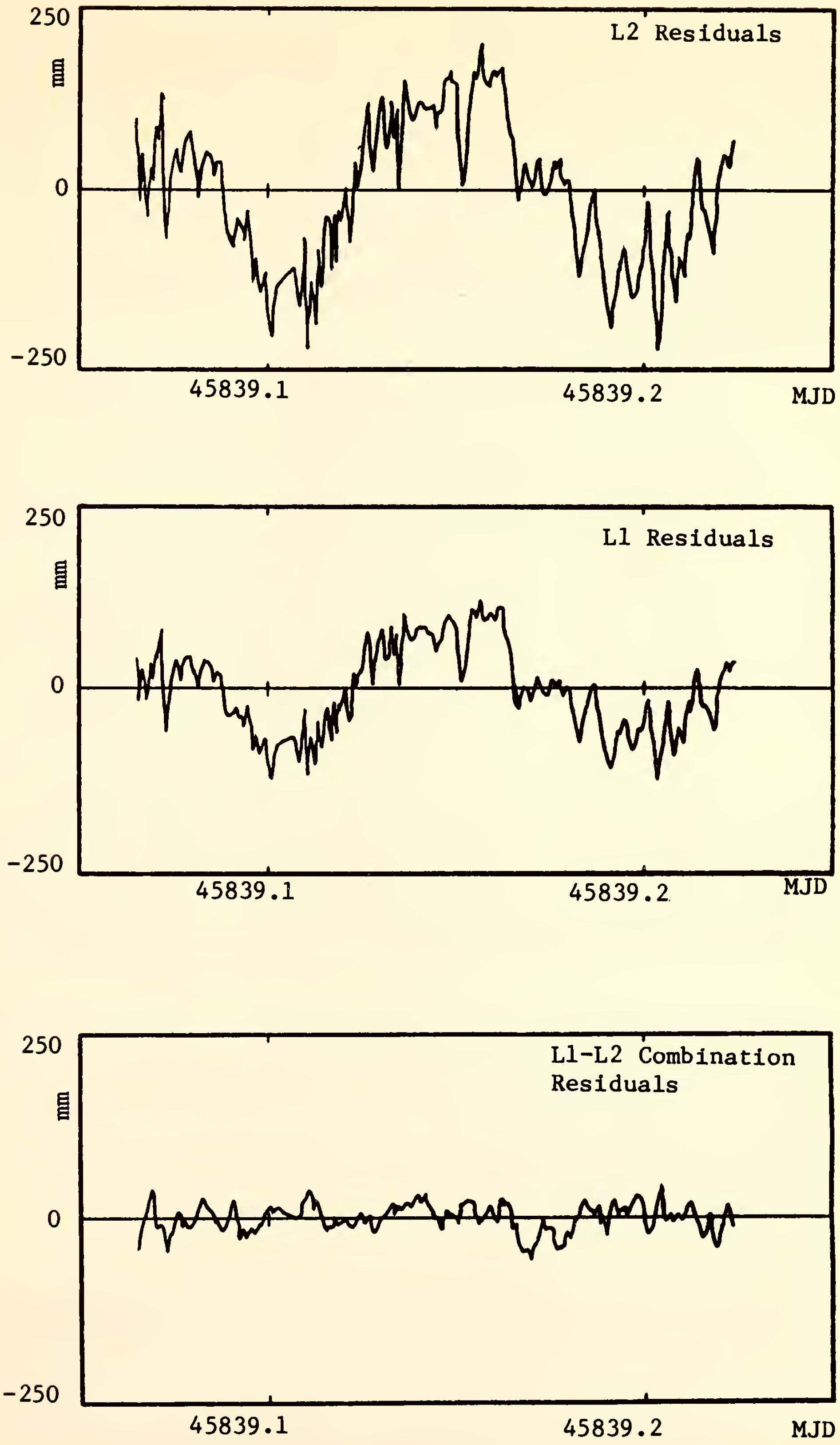

Figure 3: Single and dual frequency carrier phase double difference residuals

five hours of observations to five different GPS satellites. For the sake of clarity, only the residuals of carrier phase double differences between satellites 6 and 8 (PRN identification) are shown. A comparison of the first two plots demonstrates the dispersive character of the residuals quite clearly. The rather large systematic variations in the residuals disappear when combined observations according to eqn.(16) are used in the adjustment. The estimated precision of the carrier phase double difference observation for L2, L1 and L1-L2 combination based on the r.m.s. of the residuals was 88 mm, 55 mm and 22 mm respectively.

Table 3 gives the baseline component numerical results for the three separate adjustments. Also included are the corresponding 'ground truth' values from terrestrial measurements .

Table 3: Results for baseline Metcalfe - 6A using different carriers (Station 6A held fixed)

	Lat.Diff.	Long.Diff.	Hgt.Diff.	Length
L2 only	9'21.7883''	27'50.0261''	26.472 m	40295.542 m +/- 28 mm
L1 only	9'21.7868''	27'50.0261''	26.411 m	40295.522 m +/- 18 mm
L1-L2 comb.	9'21.7844''	27'50.0261''	26.316 m	40295.491 m +/- 7 mm
terrestrial	9'21.7935''	27'50.0170''	26.260 m	40295.429 m

The terrestrial values were obtained from the Geodetic Survey of Canada (McArthur, 1985). It can be seen, that in this particular sample only a relatively small difference exists between the baseline lengths derived from L1 only and the L1-L2 combination. The situation is quite different for the baseline components, especially the height coordinate. The height difference from the L1-L2 combination agrees with the terrestrial value reasonably well whereas the L1 solution is off by some 15 cm.

For the shorter baseline Morris - Panmure (13 km), no dispersive character such as that shown in Figure 3 was found in the residuals. The precision of a carrier phase double difference observation on this baseline was estimated as 19 mm, 12 mm and 22 mm for the L2, the L1 and the L1-L2 combined solution. The previously described increase in noise level in the combined solution compared with the L1 solution is obvious. Numerical results for the corresponding estimations of baseline components are given in Table 4.

Table 4: Results for baseline Morris-Panmure using different carriers (Station Morris held fixed)

	Lat.Diff.	Long.Diff.	Hgt.Diff.	Length
L2 only	6'15.4780''	4'14.2375''	64.432 m	12843.746 m +/- 13 mm
L1 only	6'15.4783''	4'14.2381''	64.447 m	12843.760 m +/- 8 mm
L1-L2 comb.	6'15.4788''	4'14.2389''	64.471 m	12843.782 m +/- 15 mm
terrestrial	6'15.4787''	4'14.2329''	64.540 m	12843.725 m

COMPARISON OF 'BASELINE' SOLUTIONS WITH 'NETWORK' SOLUTIONS

This section deals with the comparison of solutions for repeated Macrometer V-1000 observations of the same baseline with the solution from a network adjustment. For the three baselines involving station 6A, Table 5 gives the estimate of the station height difference and baseline length for each of the four observing sessions (denoted by day number), for the combined solution for all sessions on a particular baseline and for the network solution involving all observations of the network. Also given are the estimated uncertainties based on the observation residuals. For all 'baseline' solutions, one point of the baseline was held fixed whereas in the 'network' solution all a priori coordinates were given a weight matrix (see next section).

Table 5: Macrometer V-1000 baseline and network solutions

Baseline		Height Difference	Length
6A - Morris	Day 205	12.142 m +/- 11 mm	26488.993 m +/- 22 mm
	Day 211	12.133 m +/- 11 mm	26489.076 m +/- 22 mm
	Day 217	12.132 m +/- 6 mm	26488.955 m +/- 22 mm
	Day 223	12.109 m +/- 6 mm	26488.955 m +/- 22 mm
	All Days	12.127 m +/- 4 mm	26488.984 m +/- 7 mm
	Network	12.150 m +/- 5 mm	26489.007 m +/- 7 mm
6A - Panmure	Day 206	76.584 m +/- 9 mm	21590.242 m +/- 14 mm
	Day 212	76.557 m +/- 7 mm	21590.287 m +/- 12 mm
	Day 218	76.574 m +/- 10 mm	21590.279 m +/- 12 mm
	Day 224	76.551 m +/- 15 mm	21590.255 m +/- 27 mm
	All Days	76.574 m +/- 5 mm	21590.266 m +/- 7 mm
	Network	76.575 m +/- 5 mm	21590.235 m +/- 6 mm
6A - Metcalfe	Day 204	26.294 m +/- 13 mm	40295.442 m +/- 27 mm
	Day 210	26.271 m +/- 12 mm	40295.489 m +/- 24 mm
	Day 216	26.361 m +/- 10 mm	40295.460 m +/- 18 mm
	Day 222	26.372 m +/- 29 mm	40295.466 m +/- 27 mm
	All Days	26.317 m +/- 6 mm	40295.446 m +/- 11 mm
	Network	26.289 m +/- 6 mm	40295.454 m +/- 8 mm

It can be seen from Table 5, that the combined solution for all sessions agrees with the network solution in length at the 1 ppm level. The agreement for the height differences is better than 3 cm. However, the single session solutions disagree with the network solution by up to 3 ppm in length and 8 cm in height differences.

Figure 4 depicts the discrepancies between the single session solutions and and the combined solution for the horizontal baseline components relative to station 6A and their error ellipses (95% confidence level). It can be seen, that the single session solutions and the combined solution for the baselines 6A-Panmure and 6A-Metcalfe agree within their estimated error ellipses whereas for baseline 6A-Morris the result of day 211 is off by about 10 cm.

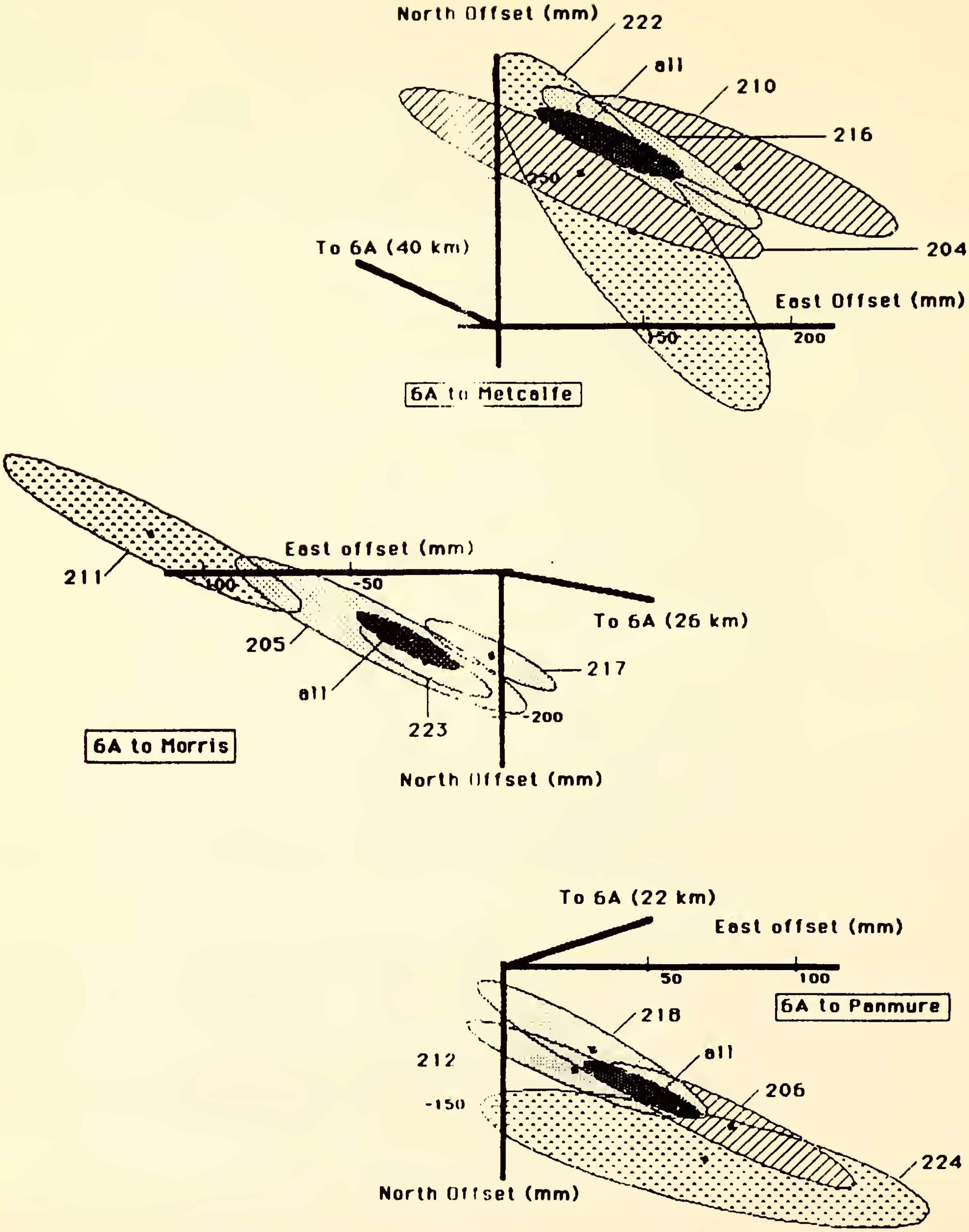

Figure 4 : Comparison of single session solutions with combined solution for all sessions

COMPARISON OF MACROMETER V-1000 AND TEXAS INSTRUMENTS TI 4100 RESULTS

In this section we compare 'network solutions' of DIPOP for the Macrometer V-1000 and Texas Instruments TI 4100 observations on the Ottawa Test Network described in the introduction. The TI 4100 results discussed here are derived from linear combinations of L1 and L2 observations according to eqn.(16). We restrict ourselves to a rather short description, more details can be found in Vanicek et al., (1985a).

The a priori coordinates of the stations were obtained from the Geodetic Survey of Canada (McArthur, 1985). These coordinates were given an a priori weight corresponding to a standard deviation of 1 m. The numerical results for estimated baseline components and baseline lengths are given in Table 6.

Table 6: Comparison of V-1000 and TI 4100 network results

Baseline		Diff. in Latitude	Diff. in Longitude	Diff. in Height	Length
6A - Morris	terr.	2'38.5068''	-19'57.4134''	11.98 m	26488.986 m
	V-1000	2'38.5012''	-19'57.4157'	12.150 m	26489.007 m
	TI 4100	2'38.4990''	-19'57.4125''	12.136 m	26488.926 m
6A - Panmure	terr.	-3'36.9719''	-15'43.1806''	76.52 m	21590.268 m
	V-1000	-3'36.9771''	-15'43.1764''	76.575 m	21590.235 m
	TI 4100	-3'36.9796''	-15'43.1739''	76.592 m	21590.209 m
6A - Metcalfe	terr.	-9'21.7935''	27'50.0170''	26.26 m	40295.433 m
	V-1000	-9'21.7848''	27'50.0238''	26.289 m	40295.454 m
	TI 4100	-9'21.7839''	27'50.0275'	26.319 m	40295.516 m
Morris-Panm.	terr.	-6'15.4787''	4'14.2329''	64.54 m	12843.725 m
	V-1000	-6'15.4783''	4'14.2393''	64.425 m	12843.773 m
	TI 4100	-6'15.4785''	4'14.2385''	64.455 m	12843.773 m
Morris-Metc.	terr.	-12'00.3003''	47'47.4304''	14.28 m	66268.707 m
	V-1000	-12'00.2860''	47'47.4394''	14.138 m	66268.752 m
	TI 4100	-12'00.2828''	47'47.4400''	14.182 m	66268.734 m
Panm.-Metc.	terr.	-5'44.8216''	43'33.1975''	-50.26 m	57930.717 m
	V-1000	-5'44.8077''	43'33.2002''	-50.286 m	57930.702 m
	TI 4100	-5'44.8042''	43'33.2014''	-50.273 m	57930.713 m

The baseline length estimated from V-1000 and TI 4100 observations agree at the ppm level with the exception of baseline 6A-Morris with a length discrepancy of 81 mm or 3 ppm. The height difference agreement is surprisingly good: the largest difference between V-1000 and TI 4100 results is 44 mm for the 66 km baseline Morris-Metcalfe. On the other hand, the GPS solutions disagree with the terrestrial height differences by as much as 17 cm in the baselines involving station Morris.

The differences in horizontal coordinates relative to station 6A between the GPS solutions and the terrestrial values are sketched in Figure 5. These discrepancies are as large as 35 cm, whereas the differences between the two GPS solutions do not exceed 10 cm. The rotation about the vertical axis between the terrestrial

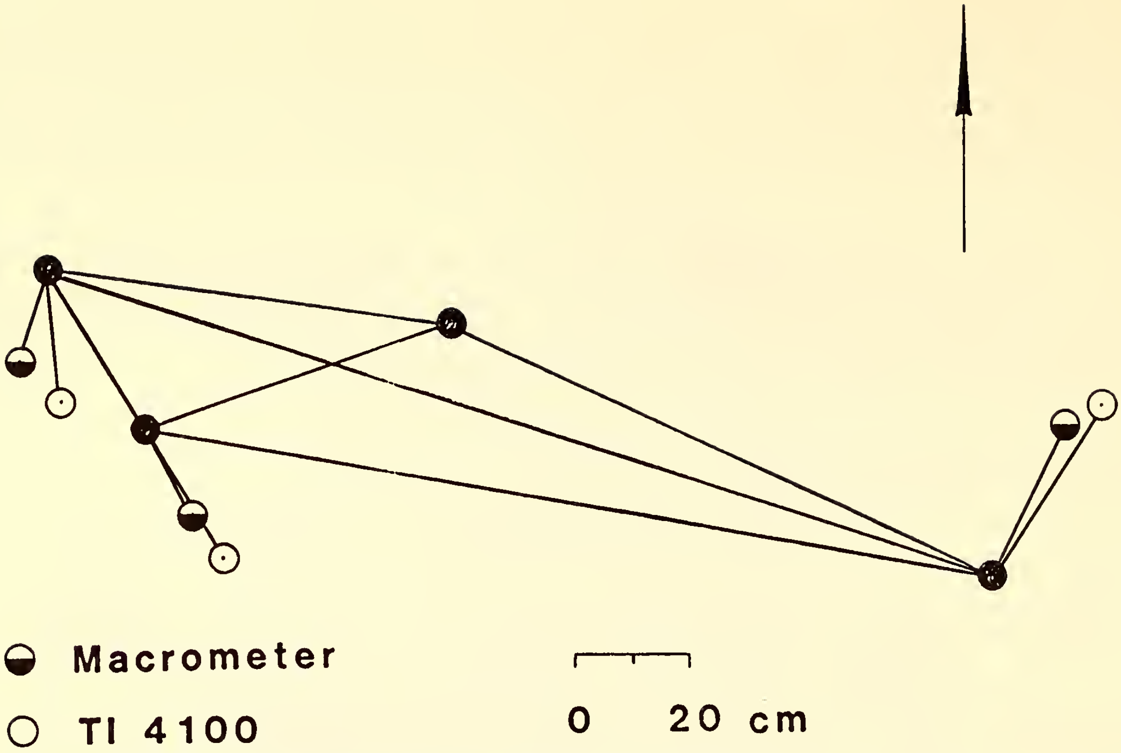

Figure 5: Discrepancies between GPS solution and terrestrial coordinates relative to station 6A

coordinates and the solutions from GPS observations is quite obvious, it amounts to 1.5'' for the Macrometer V-1000 result and 2.0'' for the TI 4100 result. More detailed information on the horizontal discrepancies of Figure 5 and the estimated accuracies of the baseline components can be taken from Figure 6. This Figure shows for each of the three baselines involving station 6A the horizontal offset of the GPS solutions with respect to the terrestrial coordinates for the other involved. Also plotted are the error ellipses (95% confidence level) based on the r.m.s. of the observation residuals.

CONCLUSIONS

We summarize our results obtained with the program DIPOP as follows:

The differential ionospheric delay may introduce errors up to 1 ppm in estimations of baseline lengths of several tens of kilometers.

Differences in baseline length obtained from single session and single baseline solutions and a combination network solution are at the 1 ppm level.

The network solutions for observations from two different receiver types agree on the 1 ppm level.

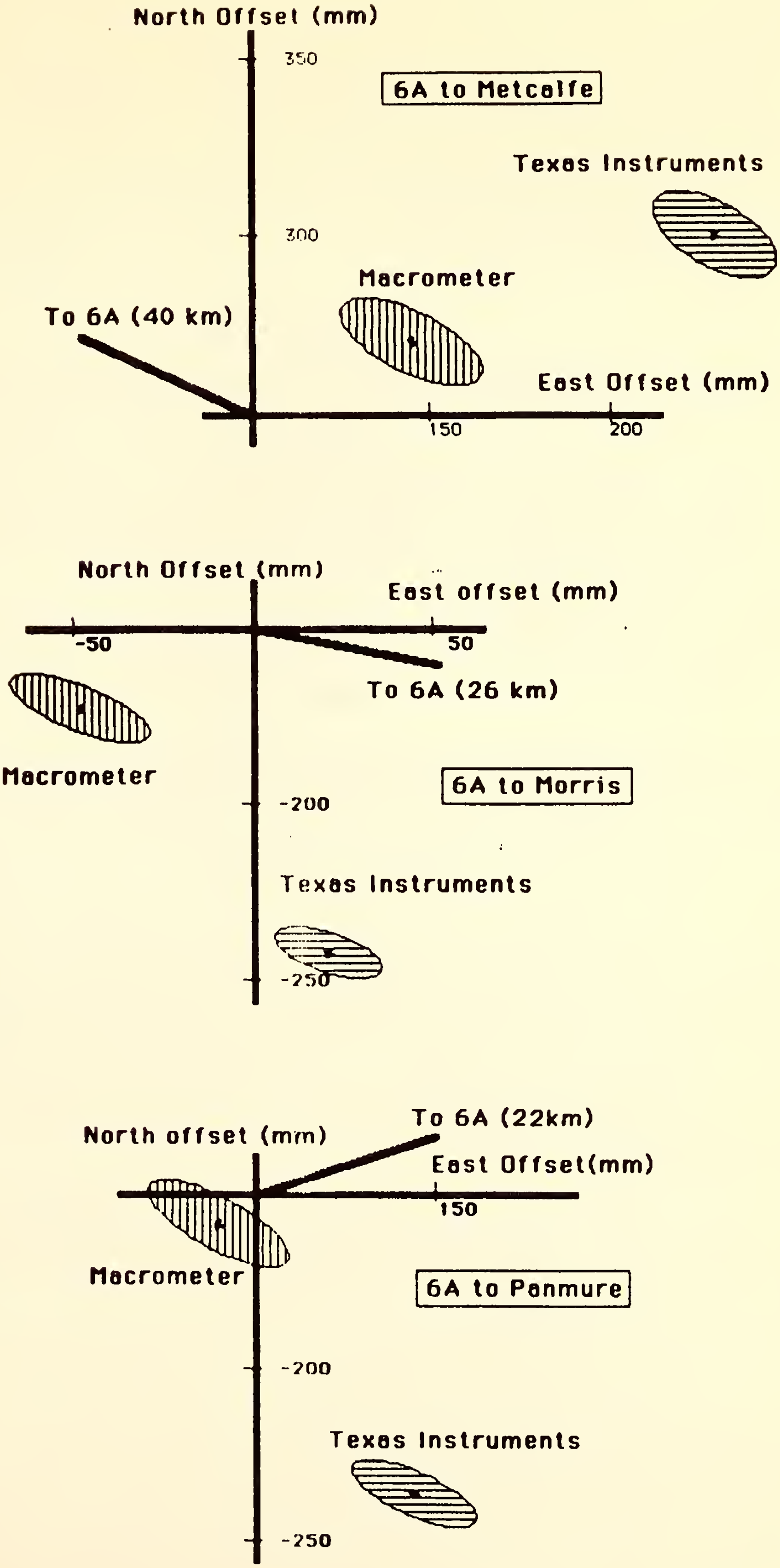

Figure 6: Offset of GPS solutions and their error ellipses with respect to terrestrial coordinates

ACKNOWLEDGEMENTS

Parts of the work reported herein were funded by the Natural Sciences and Engineering Research Council of Canada and a research contract with the Geodetic Survey of Canada. The Earth Physics Branch of Energy, Mines and Resources Canada supplied the Ottawa Macrometer data and the Geodetic Survey of Canada provided the Ottawa TI-4100 data.

REFERENCES

Bauersima, I., 1983: NAVSTAR/Global Positioning System (GPS) III, Mitteilungen der Satelliten-Beobachtungsstation Zimmerwald Nr. 12, Druckerei der Universitaet Bern

Beutler, G., D.Davidson, R.Langley, R.Santerre, P.Vanicek, D.Wells, 1984: Some Theoretical and Practical Aspects of Geodetic Positioning Using Carrier Phase Difference Observations of GPS Satellites, Technical Report No. 109, Dept. of Surveying Engineering, University of New Brunswick

Davidson, D., D.Delikaraoglou, R.Langley, B.Nickerson, P.Vanicek, D.Wells, 1983: Global Positioning System Differential Positioning Simulations, Technical Report No. 90, Dept. of Surveying Engineering, University of New Brunswick

Hopfield, H.S., 1969: Two-quartic Tropospheric Refractivity Profile for Correcting Satellite Data, Journal of Geophysical Research, Vol. 74, 4487-4499

McArthur, D.J., 1984: TI 4100 Observations at the Geodetic Survey of Canada, R+D Section, Geodetic Survey of Canada, Ottawa

McArthur, D.J., 1985: Personal communication, Geodetic Survey of Canada, Ottawa

Valliant, H., 1984: Canadian Evaluation of the Macrometer Interferometric Surveyor, EPB Open File No. 84-4, Earth Physics Branch of Energy, Mines and Resources, Ottawa

Vanicek, P., A.Kleusberg, R.B.Langley, R.Santerre, D.E.Wells, 1985: On the Elimination of Bias in Processing Differential GPS Observations, Paper presented at the First International Symposium on Precise Positioning with the Global Positioning System, Rockville, MD, 15-19 April

Vanicek, P., G.Beutler, A.Kleusberg, R.B.Langley, R.Santerre, D.E.Wells, 1985a: DIPOP: Differential Positioning Program Package for the Global Positioning System, Final Report for DSS Research Contract No. OST83-00353, Dept. of Surveying Engineering, University of New Brunswick

RECOVERY OF A 1700 KM BASELINE USING DUAL FREQUENCY GPS CARRIER PHASE MEASUREMENTS

E. Cannon
G. Lachapelle
Nortech Surveys (Canada) Inc.
309 - 2nd Avenue S.W.
Calgary, Alberta T2P OC5

C. Goad
National Geodetic Survey
Charting and Geodetic Services
National Ocean Service, NOAA
Rockville, MD 20852

ABSTRACT. Simultaneous GPS observations were carried out on three different days in January, 1984, between Calgary, Canada, and Southern California using a Nortech-owned TI 4100 and three TI 4100's loaned by Texas Instruments Inc. The dual frequency P-code phase measurements obtained over this 1700 km baseline were reduced using the phase observable in a nondifference mode. The successive use of L1 and L1/L2 (ionospherically corrected) phase data allowed the effect of the ionosphere over such a baseline to be taken into account. Data were processed using post-mission ephemerides. Analysis of results revealed a consistency of the order of 1.0 ppm between the daily solutions for each of the three coordinates. Methods of further improving GPS long baseline determinations are suggested.

INTRODUCTION

In January, 1984, Nortech Surveys (Canada) Inc. and the Defence Mapping Agency (DMA), jointly participated in a three day campaign to collect GPS P-code carrier phase data. Nortech collected data at a station in Calgary, while DMA simultaneously collected data at three stations in California, giving rise to baselines of approximately 1700 km.

Data were collected on two P-code frequencies for approximately 4 hours during the 4 satellite coverage period. The GPS equipment utilized was a Nortech owned TI 4100 in Calgary, and three TI 4100 receivers in California. On each of three observation days, data was only collected at two of the three California stations, resulting in two baseline determinations (California - Calgary) for each day.

A brief description of the methodology applied in the reduction of the phase data is given, along with an analysis of results of L1, L2 and L1/L2 solutions. Possible effects that may hamper the achievable accuracy of long baselines are discussed and some possible solutions sited.

METHODOLOGY

The carrier phase was reduced using the method described in (Goad 1985). Only a brief description is given. The phase measurements are used in each undifferenced mode. There are 3 stations tracking the carrier phase on each of the three days, and due to the strengthening of the solution by the vector closure, all three data sets were processed simultaneously. However, the combination of more than one baseline in simultaneous processing can lead to correlation amongst the measurements. For example, in single difference processing (Remondi 1984), if one baseline is considered, the measurements are uncorrelated as they appear only once in the model. If another station is added, hence two more baselines, the phase measurements appear more than once and are correlated. In double difference mode, the measurements are correlated for one baseline thus processing can become very difficult for multi-station solutions. However, the model itself is less complex than the single difference model as satellite and receiver clock differences are cancelled. Its form is given by:

$$\phi^{i,j}_{\ell,m}(t_k) = \phi^{i}_{\ell,m}(t_k) - \phi^{j}_{\ell,m}(t_k)$$
$$= \frac{f}{c}\,(\rho^i_m - \rho^i_\ell - \rho^j_m + \rho^j_\ell) + N^j_\ell - N^j_m - N^i_\ell + N^i_m \qquad (1)$$

where i,j ... are satellites

ℓ,m ... are receivers

$\phi^{i,j}_{\ell,m}(t_k)$ ... is the double difference phase observable at epoch t_k

$\phi^{i}_{\ell,m}(t_k)$ ... is the single difference phase observable for satellite i

$\phi^{j}_{\ell,m}(t_k)$ ... is the single difference phase observable for satellite j

f ... frequency of satellite oscillator

c ... speed of light

ρ ... range from satellite to receiver

N ... initial integer ambiguity.

Inherent to double differences is the integer nature of the bias. When long baselines are considered, say over 30 km, the biases may no longer resemble integers because of other factors such as orbit and atmospheric effects. This integer quality of the double differences is exploited in the "base station-base satellite" concept (Goad 1985) which is used here. This concept allows for the processing of multi-station data simultaneously with the measurements being uncorrelated. Assuming 2 stations and 2 satellites, with station ℓ as the base station and i as the base satellite, the phase measurements can be written as:

$$\phi^i_\ell(t_k) = -\frac{f}{c}\rho^i_\ell + \bar{N}^i_\ell \qquad (2a)$$

$$\phi^i_m(t_k) = -\frac{f}{c}\rho^i_m + \bar{N}^i_m \qquad (2b)$$

$$\phi^j_\ell(t_k) = -\frac{f}{c}\rho^j_\ell + \bar{N}^j_\ell \qquad (2c)$$

$$\phi^j_m(t_k) = -\frac{f}{c}\rho^j_m + \bar{N}^j_m \qquad (2d)$$

where $\bar{N}^{sat}_{rec} = N^{sat}_{rec} + \phi^{sat} - \phi_{rec}$ (2e)

Letting $K^j_m = (\bar{N}^j_m(t_k) - \bar{N}^i_m(t_k)) - (\bar{N}^j_\ell(t_k) - \bar{N}^i_\ell(t_k))$ (3a)

or, equivalently, $K^j_m = N^j_m - N^i_m - N^j_\ell + N^i_\ell$ (3b)

This allows $\phi_m^j(t_k)$ to be rewritten as,

$$\phi_m^j(t_k) = -\frac{f}{c}\rho_m^j + K_m^j + N_m^i(t_k) + N_\ell^j(t_k) - N_\ell^i(t_k) \tag{4}$$

The K variable is a linear combination of the integral ambiguities and is constant throughout the observation period if there is no loss of lock. Since $\phi_m^j(t_k)$ does not involve the base station (ℓ) nor the base satellite (i), the K formulation is used. The K values are the same as if double differences were formed, but this allows the data to remain uncorrelated. Thus, the measurements remain the same except if a non-base station and a non-base satellite are considered. For details on technique and ionospheric considerations see Goad (1985). Cycle slips in the data are detected and fixed automatically by viewing successive double differences from a previous triple difference solution.

Before the phase adjustment was performed, the time offset of each receiver was computed from pseudo-range solutions at each end of the baseline. The time offsets are needed to ensure that no receiver clock errors occur. They are calculated at every epoch where phase measurements are to be extracted to explicitly determine any clock drift that may be present in any of the three receivers. Also, this method will detect any receiver clock jumps that may occur during the observation period.

RESULTS AND ANALYSIS

Data were collected on January 26, 29 and 30, 1984 in Calgary and Southern California. The three stations in California are Mojave, Barstow and Venus. On days 29 and 30 pseudo-range and phase measurements were extracted every 24 sec, while on day 26, the data were only available every 60 sec.

Pseudo-Range Analysis

The pseudo-range solutions were computed twice for each station on each day, first using the broadcast ephemerides and second, using the precise ephemerides. Time offsets between the receivers were determined to about the 10 to 30 nanosecond level. The rms values of the two solutions are given in Table 1. It is readily apparent that the rms values between the data sets collected on Days 26 and 30 vary significantly for both the broadcast ephemerides and the precise ephemerides solutions. This may be due to the fact that in January, 1984, the Nortech TI 4100 was equipped with the TI Phase I software (the software has since been replaced to Phase II). These relatively low rms values assure that there are no significant clock errors in the data and the resulting time offsets are determined with sufficient accuracy for the phase adjustment. The rms values only improve slightly when the precise ephemerides are used. On Day 29, the rms values are significantly higher than on Days 26 and 30. This is likely due to the broadcast clock parameters. The U.S. Naval Observatory Report (February 2, 1984) states that SV 9 had clock frequency movements and that navigation data was less accurate than normal. This, in itself, could degrade the solution to the 14 m rms level.

Phase Data Analysis

Three stations were adjusted simultaneously using the program PHASER (Goad 1985) for each of the three observation periods. The data were processed three ways, L1 only, L2 only and ionospherically corrected L1/L2, to assess the effect of the ionosphere over such a long baseline. Only the precise ephemerides were used. A modified Hopfield model with standard atmospheric parameters corrected the data for tropospheric effects.

Cycle slips were first detected and fixed amongst the three data sets being processed. This was not difficult between the two Californian stations as they were close together (12 - 27 km) and small cycle slips were readily apparent. However, with the inclusion of the Calgary data, the cycle slips were much harder to detect. The reason is that such a long baseline induces range differences that change rapidly with time. Therefore phase data were used every 24 sec (60 sec for Day 26) to minimize this problem. The two Californian stations were held fixed during the adjustment as their baseline components were known accurately.

Table 2 shows the results for the ionospherically corrected data. The standard deviations of the Δx's are noticeably larger than those of the other two components. It is approximately one order of magnitude greater. The reason for this is unfavorable satellite geometry. In Table 3, the correlations between the Δx-component and the satellite biases from SV's 8, 9, 11 are given. SV 6 is not included as it is the base satellite (refer to Methodology). On all three days the correlations are very large. This suggests that any error that may occur in the biases will be directly reflected in the Δx-component. The determination of the satellite biases is a direct function of the satellite coordinates, and therefore, of the orbit itself. The rms value of the observed phase measurements varies from .40 cycles to .80 cycles which is approximately 8 cm to 16 cm. The true baseline components between Calgary and California are not available to a suitable accuracy which prevented any attempt to compare the GPS-derived baselines components to the actual ones.

A comparison of L1 vs L1/L2 results is summarized in Table 4. Since no true baseline components are known, it cannot be confirmed that the L1/L2 results are, in fact, any better than the L1 only or L2 only results. However, it is known that the data is influenced by the ionosphere and should therefore be corrected for it. The change in the baseline itself varies from 0.1 to 0.7 m which is approximately 0.06 to 0.4 ppm. However, the baseline components vary to a larger degree, 0.1 to 1.7 ppm. These values are significant if accuracies of 0.5 - 1.0 ppm are desired.

The L2 vs L1/L2 results show that the differences are greater than of L1 vs L1/L2 (see Table 5). This is to be expected since L2 is modulated on a lower frequency. Differences in baselines range from .2 to 1.1 m (.1 to 1.2 ppm) while those of the components range from .2 to 2.0 m (.2 to 2.9 ppm).

Since observations were carried out over three days, the repeatability between the baselines can be studied. These comparisons are given in Table 6. It is evident that the best results are between Mojave and Calgary with the repeatability of the baseline being better than 1.0 metre (.3 ppm). The repeatability of the three components is in the 1.0 metre range.

The repeatability for the other two baselines is significantly worse, with Barstow-Calgary having the highest discrepancies. Venus-Calgary gives .7 ppm as the baseline repeatability and component repeatabilities in the 2-3 m range. For Barstow-Calgary, the baseline repeatability, increases to a maximum of 1.2 ppm while the components have a discrepancy of approximately 2-7 metres. It is interesting to note that both Barstow-Calgary and Venus-Calgary, while Mojave-Calgary does not. Day 29 has previously been tagged (see Pseudo-Range Analysis) as a day where there may have been errors in the clock parameters and problems with SV 9. These may have contributed to the computed baseline components on Day 29 in such a manner that there accuracy was degraded. The rms value for that day was significantly higher (see Table 2) than the other two days.

The discrepancy in the Δx-component is generally higher than that of the other two components. This is due to satellite geometry and is reflected in the statistics. Overall, the repeatability in each of three components is approximately 2 m. Considering the baseline is 1,700 km and the satellites are approximately 20,000 km above the earth's surface, a 20 m error in the orbit would result in about a 2 m error in the baseline. This is the order of orbital error that is to expected with the precise ephemerides.

SUMMARY AND CONCLUSIONS

The reduction of GPS P-code carrier phase data using the measurements in a nondifference mode proved very successful for processing multi-station information. The lack of correlation amongst the phase measurements minimized the adjustment complexity.

Detection of small cycle slips became difficult for the long baseline, so data were chosen at a smaller interval (24 sec, 60 sec) than that of a shorter baseline (usually 60-180 sec). This minimized the problem of not detecting small cycle slips although processing time was slightly increased with the added measurements.

The degradation of the results using L1 vs L1/L2 ionospherically corrected data was in the 0.1 to 1.7 ppm range. For L2 vs L1/L2 the discrepancy was increased to .2 to 2.9 ppm. These values are significant if results of 0.5 to 1.0 ppm are desired and show that data must be corrected for the ionosphere.

The repeatability of this 1700 km baseline and its components is dependent on two main factors, namely clock parameter accuracy and orbit accuracy. The clock parameters appeared degraded on Day 29 which resulted in poorer results for that day. This became apparent when the repeatability between observation days included data from Day 29. The repeatability was better on Days 26 and 30 (Table 6). Assuming an orbit accuracy of 20 m for the precise ephemerides, this would propagate into approximately a 2 m error in the baseline. This is the range of error that is present between the three days.

ACKNOWLEDGEMENTS

Part of this work was sponsored by the Nortech-Alberta Research Council Joint Venture.

REFERENCES

GOAD, C.C., 1985: Precise Relative Position Determination Using Global Positioning Determination Using Global Positioning System Carrier Phase Measurements in a Nondifference Mode, First International Symposium on Precise Positioning with Global Positioning System, Rockville, MD. April 15-19.

REMONDI, B.W., 1984: Using the Global Positioning System (GPS) Phase Observable for Relative Geodesy: Modelling, Processing and Results, Ph.D. Dissertation, pp. 360, The University of Texas at Austin, Texas.

TABLE 1

COMPARISON OF RMS VALUES OF PSEUDO-RANGE SOLUTIONS USING BROADCAST AND PRECISE ORBITS

Station	Day, 1984	Broadcast rms (m)	Precise rms (m)
Mojave	26	3.44	2.92
Barstow	26	3.81	3.55
Calgary	26	5.85	5.89
Barstow	29	14.70	12.64
Venus	29	14.92	14.91
Calgary	29	14.52	12.49
Mojave	30	4.41	4.05
Venus	30	4.36	4.11
Priddis	30	5.51	5.16

TABLE 2

RESULTS FOR 1,700 KM BASELINE OVER THREE DAYS USING IONOSPHERICALLY CORRECTED PHASE DATA*

Line**	Day	RMS (cycles)	ℓ (m)	Δx (m)	$\sigma_{\Delta x}$ (m)	Δy (m)	$\sigma_{\Delta y}$ (m)	Δz (m)	$\sigma_{\Delta z}$ (m)
M-C	26	.58	1 734 016.8	-696 881.3	.26	-969 938.5	.07	-1 257 135.7	.06
B-C	26	.58	1 760 707.3	-707 883.0	.26	-981 942.3	.07	-1 278 585.6	.06
B-C	29	.80	1 760 705.2	-707 877.5	.17	-981 945.3	.05	-1 278 583.5	.04
V-C	29	.80	1 742 091.4	-691 277.0	.17	-798 811.3	.05	-1 264 494.7	.04
M-C	30	.40	1 734 016.2	-696 879.9	.13	-969 939.5	.03	-1 257 134.9	.04
V-C	30	.40	1 742 092.7	-691 281.0	.13	-978 809.3	.03	-1 264 496.0	.04

* - no antenna heights have been applied.

** M: Mojave, California
B: Barstow, California
V: Venus, California
C: Calgary, Canada

TABLE 3

CORRELATION OF Δ X-COMPONENT WITH THE SATELLITE BIASES*

Day	Correlation with SV 8	Correlation with SV 9	Correlation with SV 11
26	-.96	.95	.74
29	.97	.98	.88
30	-.97	.97	.85

* SV 6 is the base satellite so it is not included.

TABLE 4

COMPARISON OF L1 ONLY VS L1/L2 BASELINE COMPONENTS*

Line	Day	ℓ (m)	$\delta\ell$ (m)	Δx (m)	$\delta\Delta x$ (m)	Δy (m)	$\delta\Delta y$ (m)	Δz (m)	$\delta\Delta z$ (m)
M-C	26	1 734 016.7	-.1	-696 881.6	-.3	-969 938.7	-.2	-1 257 135.2	.5
B-C	26	1 760 707.1	-.2	-707 883.2	-.2	-981 942.5	-.2	-1 278 585.1	.5
B-C	29	1 760 705.9	.7	-707 878.7	-1.2	-981 945.1	.2	-1 278 583.9	-.4
V-C	29	1 742 092.1	.7	-691 278.2	-1.2	-978 811.1	.2	-1 264 495.1	-.4
M-C	30	1 734 016.9	.7	-696 880.6	-.7	-696 939.6	-.1	-1 257 135.3	-.4
V-C	30	1 742 093.4	.7	-691 281.7	-.7	-978 809.4	-.1	-1 264 496.4	-.4

* No antenna heights have been applied.

TABLE 5

COMPARISON OF L2 ONLY VS L1/L2 BASELINE COMPONENTS*

Line	Day	ℓ (m)	$\delta\ell$ (m)	Δx (m)	$\delta\Delta x$ (m)	Δy (m)	$\delta\Delta y$ (m)	Δz (m)	$\delta\Delta z$ (m)
M-C	26	1 734 016.6	-.2	-696 881.8	-.5	-969 938.9	-.4	-1 257 134.9	.8
B-C	26	1 760 707.1	-.2	-707 883.4	-.4	-981 942.6	-.3	-1 278 584.8	.8
B-C	29	1 760 706.4	1.2	-707 879.5	2.0	-981 944.9	.4	-1 278 584.2	1.2
V-C	29	1 742 092.5	1.1	-691 279.0	2.0	-978 811.0	.3	-1 264 495.4	.7
M-C	30	1 734 017.4	1.2	-696 881.0	-1.1	-969 939.7	-.2	-1 257 135.7	-.8
V-C	30	1 742 093.9	1.2	-691 282.2	-1.2	-978 809.5	-.2	-1 264 496.7	-.7

* No antenna heights have been applied.

TABLE 6

REPEATABILITY OF BASELINE COMPONENTS

Line	Day	Freq.	$\delta\ell$ (m)	ppm	$\delta\Delta x$ (m)	$\delta\Delta y$ (m)	$\delta\Delta z$ (m)
M-C	26,30	L1	.2	.1	1.0	-.9	-.1
		L2	.8	.5	.9	-.8	-.8
		L1/L2	-.6	.3	1.4	-1.0	.8
V-C	29,30	L1	1.3	.7	-3.5	1.7	-1.3
		L2	1.4	.8	-3.2	1.5	-1.3
		L1/L2	1.3	.7	-4.0	2.0	-1.3
B-C	26,29	L1	-1.2	.7	4.5	-2.6	1.2
		L2	-.7	.4	3.9	-2.3	.6
		L1/L2	-2.1	1.2	3.8	-6.8	2.1

THE MARCH 1985 DEMONSTRATION OF THE FIDUCIAL NETWORK CONCEPT FOR GPS GEODESY: A PRELIMINARY REPORT

J. M. Davidson, C. L. Thornton, C. J. Vegos,
L. E. Young and T. P. Yunck
Tracking Systems and Applications Section
Jet Propulsion Laboratory
California Institute of Technology
Pasadena, California 91109

ABSTRACT. The first field tests in preparation for the NASA GPS Caribbean Initiative were conducted in late March and early April of 1985. GPS receivers were located at the POLARIS VLBI stations at Westford, Massachusetts; Richmond, Florida; and Ft. Davis, Texas; and at the Mojave, Owens Valley, and Hat Creek VLBI stations in California. Other mobile receivers were placed near Mammoth Lakes, California; Pt. Mugu, California; Austin, Texas; and Dahlgren, Virginia. These sites were equipped with a combination of GPS receiver types, including SERIES-X, TI-4100 and AFGL dual frequency receivers. The principal objectives of these tests were the demonstration of the fiducial network concept for precise GPS geodesy, the performance assessment of the participating GPS receiver types, and the conduct of the first in a series of experiments to monitor ground deformation in the Mammoth Lakes-Long Valley caldera region in California. Other objectives included the testing of the water vapor radiometers for the calibration of GPS data, the development of efficient procedures for planning and coordination of GPS field exercises, the establishment of institutional interfaces for future cooperative ventures, the testing of the Phase I GPS Data Analysis Software, and the establishment of a set of calibration baselines in California. Preliminary reports of the success of the field tests, including receiver performance and data quality, and on the the status of the data analysis software are given.

INTRODUCTION

The development of geodetic surveying systems based on the Global Positioning System (GPS) satellites is motivated by the promise of high performance, mobility and low cost. The large number of measurements which can be economically made using GPS-based systems will enable the resolution of many geophysical questions which are inaccessible to the more costly VLBI or laser techniques. However, the use of GPS receivers for high precision geodesy is still in its infancy, and much work remains in assessing system performance and understanding sources of error. Two major system components are still in the developmental or validation stage. These are the water vapor radiometers (WVR's) and the GPS receivers themselves. A third system element, the fiducial network, has received considerable investigation via covariance analysis (e.g., Thornton et al. 1983; Kroger et al. 1985) but has not yet been tested in the field. The WVR's are currently undergoing extensive testing, with preliminary results reported elsewhere in this program (Janssen 1985).

In this paper, we report the results of recent field tests of the GPS receivers and of the fiducial network concept. These tests took place between March 28 and April 4, 1985. GPS receivers were placed at the NOAA/NGS POLARIS VLBI stations (Carter et al. 1984) in Westford, Massachusetts; Richmond, Florida; and Ft. Davis, Texas; and at the Mojave, Owens Valley, and Hat Creek stations in California. Additional GPS receivers located near Mammoth Lakes, California; Austin, Texas; and Dahlgren, Virginia; (Figure 1) also recorded data during the test. The sites were equipped with a combination of GPS receiver types, including SERIES-X, TI-4100 and Air Force Geophysical Laboratory (AFGL) dual-frequency receivers; Three of the sites in California were equipped with WVR's (Table 1). In all, seventeen different institutions made contributions to this test (Table 2).

Table 1. Receiver, WVR Deployment

Austin, TX	ARL TI-4100
Dahlgren, VA	ARL TI-4100
Ft. Davis, TX	TDH TI-4100
Hat Creek, CA	TI TI-4100, DSN R04 WVR
Mammoth Lakes, CA	ARL TI-4100
Mojave, CA	SERIES-X, TI TI-4100, CDP Retrofit WVR
Owens Valley, CA	SERIES-X, TI TI-4100, CDP Prototype WVR
Pt. Mugu, CA	PMTC TI-4100
Richmond, FL	AFGL dual-frequency, ARL TI-4100
Westford, MA	AFGL dual-frequency, ARL TI-4100

Table 2. Participating Institutions and Organizations

NASA Geodynamics Program
Applied Research Laboratory
Air Force Geophysical Laboratory
Bendix Coorporation
California Institute of Technology
Crustal Dynamics Project
Defense Mapping Agency
Goddard Space Flight Center
Haystack Observatory
Interferometrics Incorporated
Jet Propulsion Laboratory
National Geodetic Survey
Naval Surface Weapons Center
Pacific Missile Test Center
Texas Department of Highways
Texas Instruments Corporation
United States Geological Survey
University Navstar Consortium

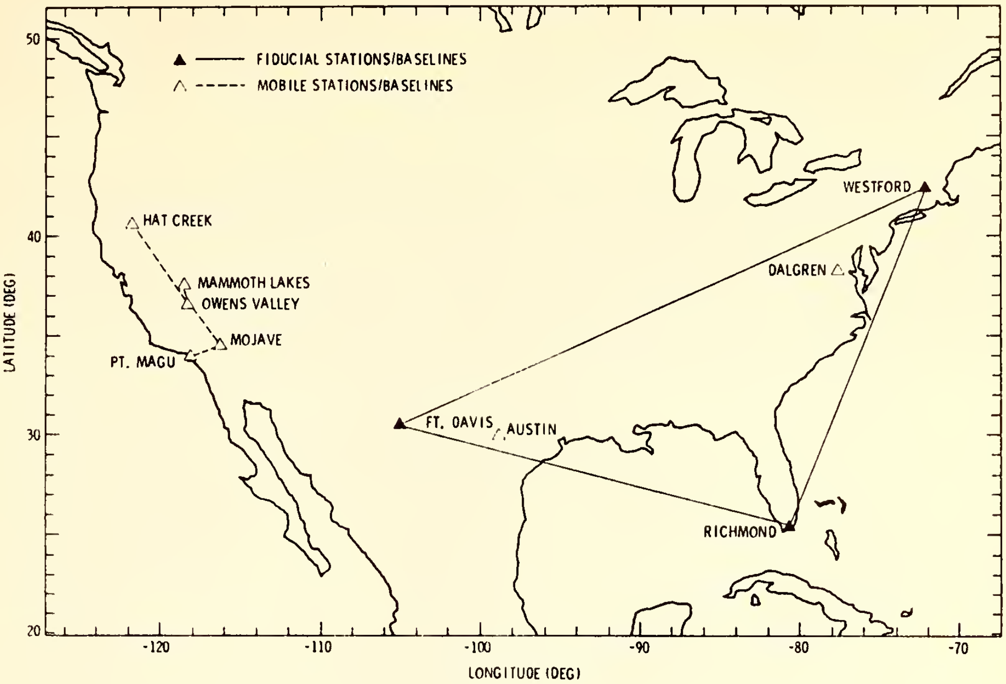

Figure 1. The locations of the fiducial and mobile GPS receivers involved in the March 1985 demonstration of the fiducial network concept are shown.

THE FIDUCIAL NETWORK CONCEPT

The accuracy of GPS-based baseline measurements depends in part on the accuracies with which the GPS satellite orbits are known. For baselines of 100 km length, simple geometric arguments show that orbit accuracies of order 2.5 m are required to attain baseline accuracy of 1 cm (Figure 2). For baselines lengths of several hundred km or more, orbit accuracies of better than 50 cm are required. Currently available GPS ephemerides are in error at the level of ten meters or more. Hence, results of geodetic quality are limited to baselines of no more than a few tens of km, unless a method of improving satellite ephemerides is devised.

A fiducial network approach has been proposed by JPL for improving satellite orbit accuracy (Fanselow and Thomas 1983). In the fiducial network approach, three or more GPS receivers are placed at sites, called fiducial stations, whose positions are well-established by an independent geodetic technique, such as VLBI or satellite laser ranging (SLR). Other receivers, called mobile receivers, are placed at sites of geodetic interest. During a GPS geodetic experiment, the fiducial receivers record data jointly with the mobile receivers (Figure 3), enabling the simultaneous determination of accurate GPS satellite orbits and geodetic baselines. The effectiveness of the fiducial approach depends strongly on the locations of the fiducial receivers and on the accuracy with which the fiducial baselines are known a priori. Covariance analysis has shown that orbit accuracies of better than 3 meters are attainable using current systems, involving the POLARIS VLBI sites as fiducial stations and integrated GPS carrier doppler as the data type. Orbit accuracies of better than 50 cm could be attainable using a system which delivers unambiguous carrier ranging data and which may include a fiducial station located in the northern part of South America. (C. L. Thornton et al. 1984, P. M. Kroger et al. 1985). The feasibility of such a system is currently being investigated at JPL (Yunck 1984). If it proves feasible, and if planned receiver developments proceed smoothly, such a system could be operational by 1989.

It should be noted that the location of the fiducial receivers at VLBI stations has the advantage of automatically placing the GPS satellite orbits in the coordinate frame of the quasi-stellar radio sources. This has the aesthetic appeal of tying the GPS results to an absolute frame of reference. Further, it unifies the VLBI and GPS geodetic frames, enabling simultaneous display and easy intercomparison of GPS and VLBI three-dimensional baseline results.

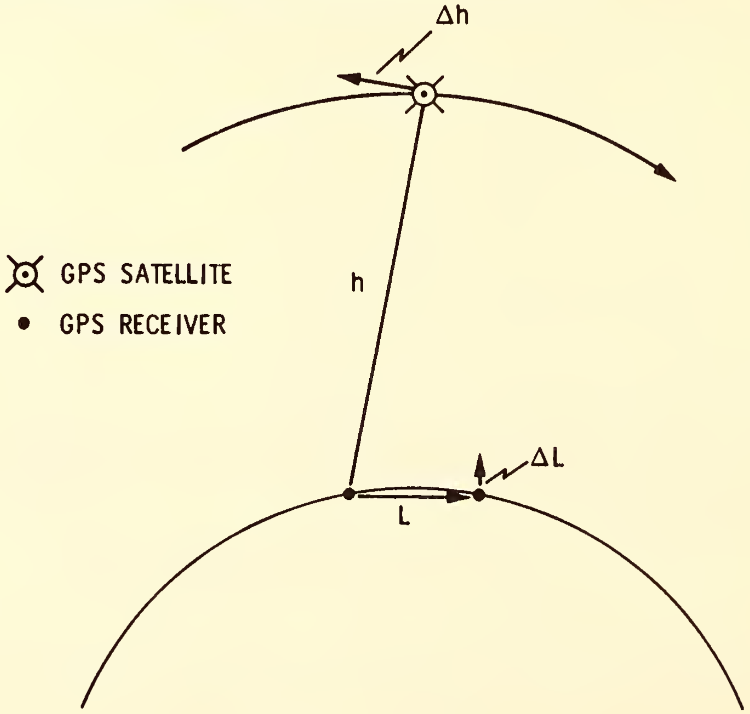

Figure 2. The qualitative dependence of baseline accuracy on orbit accuracy is illustrated. Ground stations track a GPS satellite. An error Δh in the satellite position results in an error ΔL in the baseline vector, such that $\Delta L \approx L/h * \Delta h$, where L is the baseline length and h is the satellite altitude. For L = 100 km, $\Delta L \approx \Delta h/250$.

TEST SITE SELECTION

The relative locations of the fiducial stations must be known to a few cm. Practical considerations limite the choices to locations which have some past history of VLBI (or SLR) measurement. For this reason, the VLBI stations of the POLARIS Project at Westfored, MA, Richmond, FL, and Ft. Davis, TX, were chosen. (Fiducial stations for future GPS experiments may include additional sites which presently at least have the facilities available for making these measurements.

The selection of the mobile sites was done to establish a set of calibration baselines and initiate a series of measurements to monitor ground deformation in the Long Valley caldera region of California. The stations at Mojave, Owens Valley and Hat Creek were selected as the endpoints for the calibration baselines. These stations were selected because of their easy access from JPL and from most of the

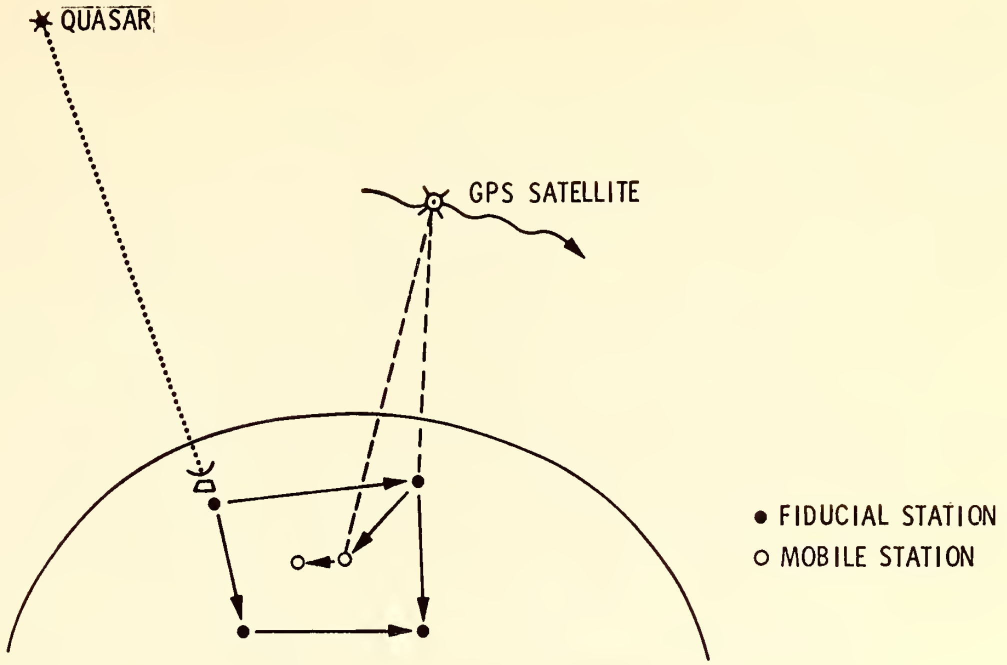

Figure 3. A schematic illustration of the fiducial network method for precision GPS geodesy is shown. Data from the fiducial stations enables accurate orbit determination, which in turn enables accurate mobile baseline determination. VLBI observations from the fiducial sites (not necessarily simultaneous with the GPS observations) determine fiducial baselines and tie the GPS results to the inertial frame of the quasi-stellar radio sources.

participating organizations and because they involve colocations with VLBI and SLR geodetic systems. Hence, high geodetic quality intercomparison data are available. Further, baselines between these three sites are approximately colinear. For this case, errors in the baselines due to orbit uncertainties will be similar in character, but will scale with baseline length (Figure 2) and should be separable from other error sources.

The Mammoth Lakes site was established as part of a JPL-Caltech program designed to supplement ongoing measurements by the U.S. Geological Survey of vertical motion associated with uplift of resurgent dome in the Long Valley caldera, currently believed to be due to an intrusion of magma into a shallow (< 10 km) crustal reservoir, and to monitor lateral motion associated with the strike-slip displacement along a newly-active fault on the Southern margin of the caldera (Dixon 1985).

TEST RESULTS

Receiver Performance

Three receiver types were involved in these field tests: the SERIES-X, the TI-4100 and the AFGL dual-frequency receivers. The SERIES-X receivers were built at JPL under the sponsorship of the Oceanic Processes Office of NASA's Office of Space Science and Applications; the TI-4100 receivers were developed by the Texas Instruments Corporation; and the AFGL dual-frequency receivers were developed by

Macrometrics Incorporated for the Air Force Geophysical Laboratory (AFGL). Each of the ten participating stations in the test was equipped with one or more of these receivers (Table 1). All three receivers recorded data at both L-band frequencies broadcast by the GPS satellites, thus enabling reduction of ionosphere corruption of the data. Data were recorded each day by all receivers throughout a six-hour viewing window when the current constellation of seven usable GPS satellites was visible over North America. This six-hour window extended from approximately 5:00 to 11:00 GMT (9:00 P. M. to 3:00 A. M. PST). The TI-4100 receivers recorded data for two hours more than the others, beginning at 3:00 GMT. During this window, the TI-4100 and the AFGL receivers recorded data from four GPS satellites; the SERIES-X receivers recorded data from all visible satellites. Throughout the eight days of the test, WVR's at Mojave, Owens Valley and Hat Creek recorded data continuously, with no data loss. A map of the Western Hemisphere, showing fiducial and mobile stations, satellite ground tracks for the full eight-hour viewing period, and 15 degree horizon masks is presented in Figure 4. In all, 106 station days of data recording were scheduled. Of these, only six station days of data were not recorded for various reasons. In general, the receivers operated smoothly and without technical problems. Tape changes were required only once every six hours with all receivers. Hence, tape changes were required only once a day. The

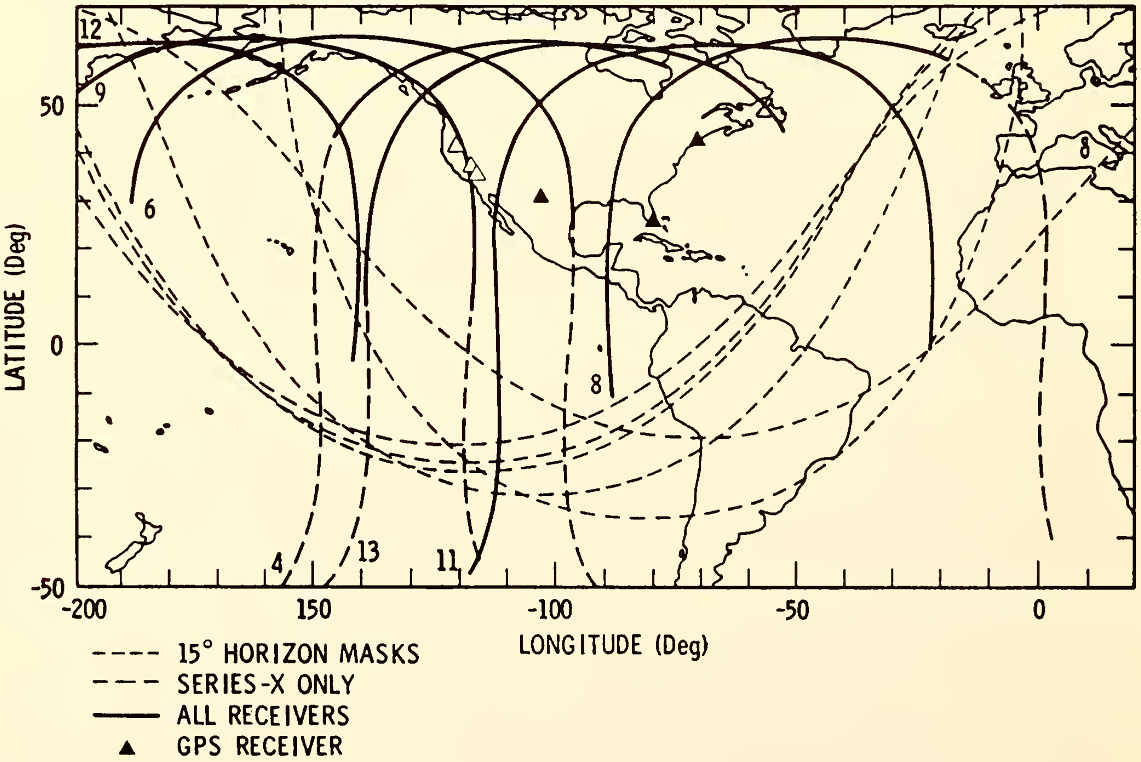

Figure 4. A map of the Western Hemisphere is shown, with stations at Westford, Richmond, Ft. Davis, Mojave, Owens Valley, and Hat Creek indicated. (See Figure 1.) The light dashed lines denote the fifteen-degree horizon masks for these six stations. GPS satellite ground tracks are denoted by heavy solid or dashed lines. The solid lines indicate when the satellites were scheduled for viewing by all three receiver types; the dashed lines indicated where the satellites were viewed only by the SERIES-X receivers. The GPS satellite number is given at the beginning of each track.

acquisition of new satellites as they rose was fully automated by the field system computers, as was the deacquisition of setting ones. It was particularly noted by the authors, all of whom have experience with VLBI systems, that the operation of the GPS receiver systems seemed relatively uneventful, even dull.

At this writing, less than a week since the completion of data collection, little is known of the quality of the data recorded. In the case of the SERIES-X receivers, initial processing is currently under way at JPL. Data from all satellites has been successfully recovered for the first few days of the test and the receivers appear to have operated properly.

Fiducial Network Performance

The principal objective of the March 1985 field test is the demonstration of the feasibility of the fiducial network concept. The proof will lie in the degree to which the accuracy of the mobile station baselines is improved over that attainable in the absence of a fiducial network. Since data collection was completed scarcely a week ago, considerable analysis remains before this question can be answered. In the mean time, it is instructive to describe the improvement expected

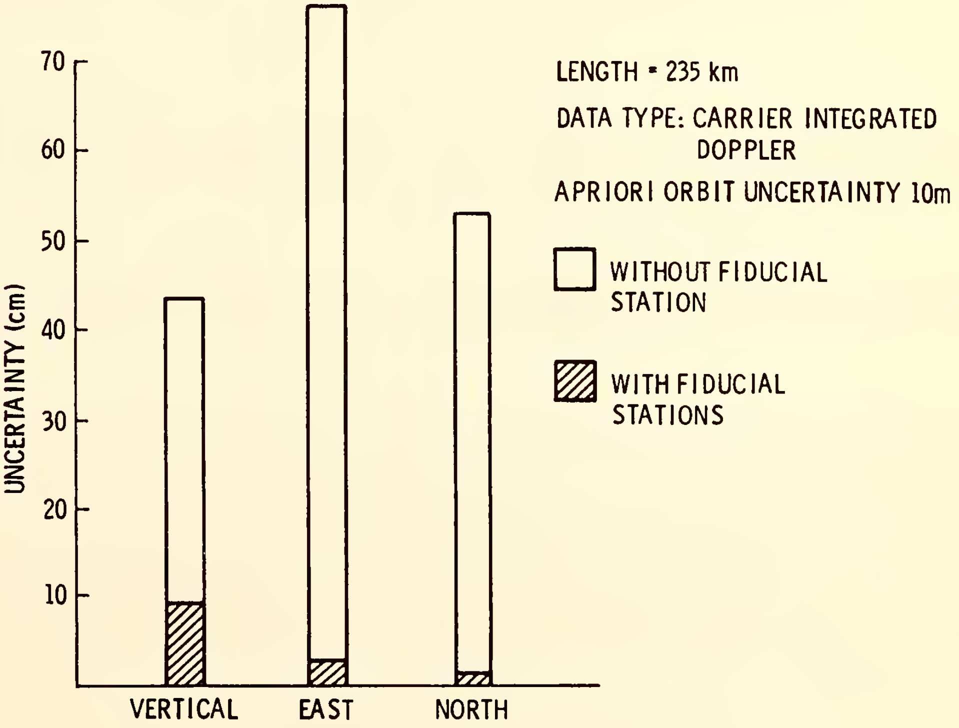

Figure 5. Covariance analysis results show expected baseline accuracies from the March 1985 field tests for the Mojave/Owens Valley baseline. Two scenarios are displayed, illustrating the improvement in accuracy expected as a result of the utilization of a fiducial station network.

based on covariance analysis. Figure 5 presents results for the Mojave/Owens Valley baseline, based on the actual observing scenario for the March field tests. The error model assumptions made in this analysis were as follows. Data noise was taken to be 2 cm; zenith troposphere calibration was taken to be 2 cm at stations where there were WVR's and 5 cm otherwise; fiducial baseline accuracy was taken to be 3 cm in all coordinates; a priori satellite position and velocity at epoch were taken to be 10 meters and 1 mm/sec, respectively; uncertainty in geocenter location was taken to be 20 cm in all coordinates; modeling of solar radiation pressure on the GPS spacecraft was assumed to be accurate to within 5% of the total effect; the product of GM was taken to be accurate to a part in 1.E+08; and the error in the gravity model was taken to be 10% of the difference between the GEM6 and APL5.0 models; the elevation angle cutoff at each station was taken to be 15 degrees; and the data type used was carrier integrated doppler. These error model assumptions are standard ones for the current systems and are justified in detail elsewhere (Davidson et al. 1985). Two analyses of the March scenario were run, one in which the satellite epoch states were estimated (i.e., using the fiducial network) and one in which they were fixed at their a priori values (i.e., as if it were a two-station experiment with no fiducial network). An intermediate case in which there are ten GPS stations in the network and in which satellite orbits are estimated, but in which none of the GPS receivers have a priori known relative locations gives results between the two extremes shown in Fig. 5. As Figure 5 shows for the case of the Mojave/Owens Valley baseline, the use of a fiducial network is expected to improve accuracy for this baseline by factors of from five in the vertical to forty in the north. This improvement is dependent on baseline length and orientation and in general increases with baseline length.

Other Test Objectives

As outlined earlier, it was also among the objectives of the March field tests to develop efficient procedures for conducting large-scale GPS field operations and to establish institutional interfaces for future cooperative ventures. We feel that these objectives were attained.

Data from the field test will be used to test the Phase I GPS Data Analysis Software. The software tests will be conducted over the next several months.

Delivery of Data

The raw data (observables, uncertainies and time tags) from this test will be made available to all participating organizations. In addition, important ancillary information (WVR and meteorology data, site eccentricities and fiducial baseline vectors) will also be available. These data should be available by early June, 1985. Processed results (calibrated observables, ionosphere data, GPS satellite orbits and station locations and observables) will also be available to the test participants, but the delivery of these will lag the raw data delivery by several months.

CONCLUSIONS

The March 1985 field tests described in this paper were conducted as preparation for the NASA GPS Caribbean Initiative. It would be premature at this time to make any definitive evaluation of the data quality or of the feasibility of GPS as a geodetic technology. However, as of now, the overall effort seems to have been a success. Pending final evaluation of the results from this test, plans for an initial deployment to one of the Caribbean countries will soon be developed. This deployment could take place as soon as late 1985. As with the recently completed test, future efforts will be collaborative.

ACKNOWLEDGMENT

The research described in this publication was carried out by the Jet Propulsion Laboratory, California Institute of Technology, under a contract with the National Aeronautics and Space Administration. One of the authors (CJV) expresses his particular thanks to all participating organizations who contributed to the success of the recently completed field tests.

REFERENCES

Carter, W. E., Robertson, D. S., Pettey, J. E., Tapley, B. D., Schutz, B. E., Eanes, R. J., and Lufeng, M., 1984: "Variations in the Rotation of the Earth", Science 224, 957-961.

Davidson, J. M., Thornton, C. L., Beckman, B. C., Kroger, P. M., Stephens, S. A., and Wu, S.-C., 1985: "Covariance Analysis for Geodetic Measurements in the Caribbean Utilizing the Global Positioning System Satellites", Journal of Geophysical Research (in preparation).

Dixon, T. H., 1985: private communication.

Fanselow, J. L. and Thomas, J. B., 1983: private communication.

Kroger, P. M., Thornton, C. L., Davidson, J. M., Stephens, S. A., and Beckman, B. C., 1985: this issue.

Janssen, M. A., 1985: "A New Water Vapor Radiometer for Troposophere Path Correction: Preliminary Test Results," this issue.

Thornton, C. L., Davidson, J. M., Beckman, B. C., Young, L. E., Thomas, J. B., Dixon, T. H., Trask, D. W., 1983: "System Study for Global Positioning Satellite (GPS) Geodesy in the Caribbean", Jet Propulsion Laboratory Document D-941.

Thornton, C. L., Davidson, J. M., Wu, S. C., Beckman, B. C., Kroger, P. M., Allen, S. L., 1984: "Determination of GPS Satellite Orbits Using a VLBI-Based Fiducial Network", Transactions of the American Geophysical Union 65, 856.

Yunck, T. P., 1984: "A GPS Measurement System for Precise Satellite Tracking and Geodesy", Proceedings Conf. on Precise Electromagnetic Measurements, August 20-24, 1984, Delft, The Netherlands.

GPS - A USER'S CRITIQUE

Roger W. Leeman
H. Douglas MacAulay
W.D. Usher & Associates Ltd.
#101, 10335 - 172 Street
Edmonton, Alberta T5S 1K9

L. Bruce Fletcher
Alberta Bureau of
Surveying and Mapping
50th Street Atria
4949 - 94B Avenue
Edmonton, Alberta T6B 2T5

ABSTRACT

The firm of W.D. Usher & Associates Ltd. recently completed a project for the Alberta Bureau of Surveying and Mapping (ABSM) wherein approximately 200 cadastral survey monuments were located, assessed and positioned within a remote area of northeastern Alberta. The survey covered an area in excess of 26,000 square kilometres. The monuments were positioned with four Macrometer V-1000 Interferometric GPS receivers, each mounted in a Bell 206B helicopter. The paper concentrates on the positioning phase of the project. An overview of the purpose and specifications of the project is presented. Topics covered in detail include planning, field organization, logistics, site preparation, data gathering and data processing. Problems encountered due to the nature of the technology being utilized and the large size and remoteness of the project area are described.

This paper is similar in content to a paper (Leeman et al 1985) to be presented at the Canadian Institute of Surveying Annual Convention in Edmonton, Alberta, Canada, May 28-31, 1985.

BACKGROUND

On April 1, 1982, the Land Survey Branch of ABSM assumed the responsibility for planning, developing and implementing a program to upgrade the record of coordinates for the Alberta Township System (ATS) which was first generated in 1976/77 based on a math model which simulated the layout of the Dominion Land Survey System. The main objective in upgrading the ATS file was to improve the accuracy of the coordinates to such a degree that they would be satisfactory for plotting the township grid on the 1:20,000 provincial mapping series which went into production in April 1984. The Land Survey Branch, through professional surveying services contracts, is gathering field data which connects the Alberta Township System to the Alberta Survey Control System. In particular, the northeast corner of every township (NE 36) is being tied to Alberta Survey Control.

Using the township corner coordinates derived from the above mentioned field connections in conjunction with the official Ottawa township plots which show the bearings and distances for each quarter section, the Land Survey Branch ABSM is computing upgraded coordinates for every quarter section in the Province.

Given the current level of funding for the acquisition of the field connections from the Alberta Survey Control System to the Land Survey System, it is estimated that the ATS upgrade will be completed in 1990.

OBJECTIVES

The primary objectives of this contract were:

(1) to find or re-establish each surveyed township corner in the project area

(2) to connect every found or re-established land survey monument to the Alberta Survey Control System

(3) to prepare a re-establishment of corners plan for any monuments re-established, and

(4) to derive adjusted coordinates for each positioned land survey monument in the project area.

The specification for accuracy was written such that all land survey monuments positioned under the contract were to meet or exceed 3rd order Energy, Mines and Resources specifications with respect to adjacent Alberta Survey Control Markers.

INTRODUCTION

The project described in this paper is the largest non-military project undertaken to date using the NAVSTAR Global Positioning System. Approximately 200 monuments within the Alberta Township System were positioned in this remote expanse which covered 135 kilometres westerly from the Alberta/Saskatchewan border and 230 kilometres northerly from latitude 55°N.

With the exception of the City of Fort McMurray and a few scattered native communities, this part of Alberta is virtually unsettled. The region consists predominantly of flat expanses of muskeg covered by spruce and tamarack. Those areas exhibiting improved drainage characteristics are forested with poplar, pine and mature spruce stands. The land has remained virtually unchanged since the original surveys were conducted in the first two decades of this century. The tarsands projects to the north and the network of cutlines and clearings associated with petroleum exploration activities throughout the west central portion of the project area represent the only physical disturbances to the natural environment.

The original meridian, baseline and township surveys were performed, for the most part, during the period from 1909 to 1918 and a conservative estimate would indicate that nearly two thirds of the monuments investigated had not been revisited since the day they were erected. Lines which were hand cleared during the original surveys have subsequently grown over. Only under exceptional circumstances could traces of these lines be seen from the air and on land they were virtually indistinguishable.

Location of the physical survey evidence on the ground proved to be one of the most difficult and certainly most interesting challenges associated with this project. Those interested in procedures used to locate the survey evidence are referred to (Leeman et al 1985).

The weather conditions tested both man and machine. These conditions included dense ground fog, heavy rainfall throughout much of September and early October, and arctic conditions in late October and November when temperatures fell to -30°C.

The field component of the project ran ten weeks in duration, from September 4, 1984 to November 13, 1984 when the observing window for the NAVSTAR satellite constellation was suitable for daylight operations.

GLOBAL POSITIONING SYSTEM

The positioning phase of this project was conducted with the new NAVSTAR Global Positioning System (GPS) which is presently under development by the United States Department of Defense. GPS is a space based satellite system which will eventually consist of a constellation of eighteen production satellites and three spares. Six satellites will be deployed in each of three different orbital planes which will be inclined at 55° to the equator (Remondi 1984). The satellites will orbit 20,200 kilometres above the earth with a period of twelve hours (Rizos et al 1984). Present plans indicate that deployment of the production satellites by the space shuttle will commence in late 1986. The full constellation of eighteen satellites is expected to be in place sometime in 1989. The eighteen satellite constellation, when fully deployed, will enable a minimum of four GPS satellites to be viewed from anywhere on earth at any time. This in turn, will provide full-time, world-wide, all-weather, real-time, three-dimensional navigation and positioning.

Each satellite will be equipped with an atomic clock. Two signals will be continuously transmitted at L-band carrier frequencies of 1575.42 MHz (L1) and 1227.60 MHz (L2) (Hothem et al 1984). These carrier frequencies are modulated with a precise code (P code), a coarse acquisition code (C/A code) and a navigation message. Frequency L1 is modulated with both codes and the navigation message, while frequency L2 contains only the P code and navigation message. Basically, the codes are time marks emitted by the satellites and are used by receivers to determine the transit time of the signal from satellite to receiver.

Receivers developed to date can be divided into two main categories: (1) pseudo-range receivers which access the satellite codes, and (2) codeless receivers or receivers which do not demodulate the satellite codes. The first type of receiver is capable of single point positioning and real-time navigation. These receivers use the codes transmitted by the satellites to determine the transit time and therefore, the range from the satellite to the receiver. The navigation message is read and used to determine the position of the satellite at any instant in time. Ranges are determined to three or more satellites simultaneously and therefore the three-dimensional coordinates of the receiver can be computed by simple intersection. The P code enables the transit time and therefore the ranges to be determined much more accurately than does the C/A code. Access to the P code may be denied (Collins 1984) to civilian users in the future for reasons of U.S national security. The second type of receiver that has been developed is meant to be used in the translocation or differential mode and as mentioned the satellite codes are not required. Generally, these receivers employ a method of phase measurement between the signal broadcast by the satellite and a reference signal generated by the receiver. The phase measurements made simultaneously at two receivers are combined and differenced enabling a difference in range from the two receivers to the same satellite to be determined. This procedure is continued over a period of time with a number of satellites to determine the baseline or vector between the two receivers.

There are presently seven useable GPS prototype satellites in orbit which allow use of the system for a few hours each day. NAVSTAR 1 is operating with only a crystal clock which makes it unsuitable for pseudo-range measurement. It can however be used by those receivers employing the codeless differential GPS mode of operation.

MACROMETER V-1000 GPS RECEIVER

Four Macrometer V-1000 GPS receivers were used on this project. The receivers were leased by W.D. Usher & Associates Ltd. from GEO/HYDRO, Inc. of Rockville, Maryland, U.S.A. The V-1000 is a codeless GPS receiver which must be used in a differential mode of operation. It measures a three-dimensional vector or baseline between two receivers. One receiver, if placed on a known station, will enable the coordination of the station occupied by the second receiver.

The V-1000 receiver consists of an electronics box (60 x 60 x 75 cm weighing approximately 50 kg), an antenna assembly (90 x 90 x 10 cm weighing approximately 19 kg), a small DEC cassette tape drive (weighing approximately 3 kg) and a small remote control/display unit (CDU). The V-1000 requires both 115 VAC and 12 VDC power supplies. The 115 VAC power supply operates all parts of the receiver with the exception of the crystal clock. The clock must be connected to a 12 VDC source at all times to maintain a stable frequency standard. On this project, power was supplied by portable Honda generators (115 VAC) and standard lead acid batteries (12 VDC).

NETWORK DESIGN

The survey network measured with the Macrometer V-1000 GPS receivers is shown in Figure One. The network consists of a total of 200 stations which include seven Geodetic Survey of Canada (GSC) primary doppler control stations, 178 Alberta Township System (ATS) land survey monuments, seven Alberta Survey Control (ASC) markers and eight eccentric stations. Unfavourable topography which restricted satellite visibility at eight ATS monuments dictated the establishment of the eccentric stations. Conventional survey ties were made to an additional six ATS monuments from control stations positioned by GPS. Conventional survey ties were also performed to tie an additional eighteen ASC markers to the GPS survey. Basically the network can be thought of as a series of interconnected traverses, each leg of which was measured with the V-1000 receivers. A moderate degree of redundancy was provided to ensure network strength. Seventeen baselines or vectors were measured with a four hour observation period. These vectors were intended to act as a high accuracy framework for the network and were essentially measured between the primary doppler control stations. Two hundred and twenty three vectors were measured with an observation period of one to two hours in length. These vectors were measured between adjacent monuments and acted as the various traverse legs. The detailed network design was completed before the field work began. A network computer pre-analysis was also conducted at that time to ensure that the required accuracy specifications could be achieved. Only slight changes to the originally conceived network were made in the field.

SITE PREPARATION

Certain steps were necessary to ensure that each site was prepared for the actual satellite observations. Using software developed by Macrometrics, Inc., visibility tables (V-files) were prepared for a site near the center of the project area and for a day within the planned observing schedule. The V-file consists of a digital representation of the NAVSTAR satellite tracks with respect to the observer's location. This digital information includes the time (UTC) of each of sixty measuring epochs for the day chosen and the elevation angle and azimuth to each visible NAVSTAR satellite at each of the specified times. This information is also presented in the form of a track plot. The daily observing schedule and site clearing requirements were designed using this information.

As previously mentioned, the vast majority of the project area was forest covered. This of course, made the clearing of sites necessary for reasons of satellite visibility. Generally speaking, Macrometer specifications call for unrestricted visibility to a 70° zenith angle in all directions from the observer's location. By examining the satellite tracks, it was determined that some segments of the circle of visibility did not have to be cleared at all and that other segments required less than a 70° zenith angle. This in fact reduced the required site clearing by approximately 50%.

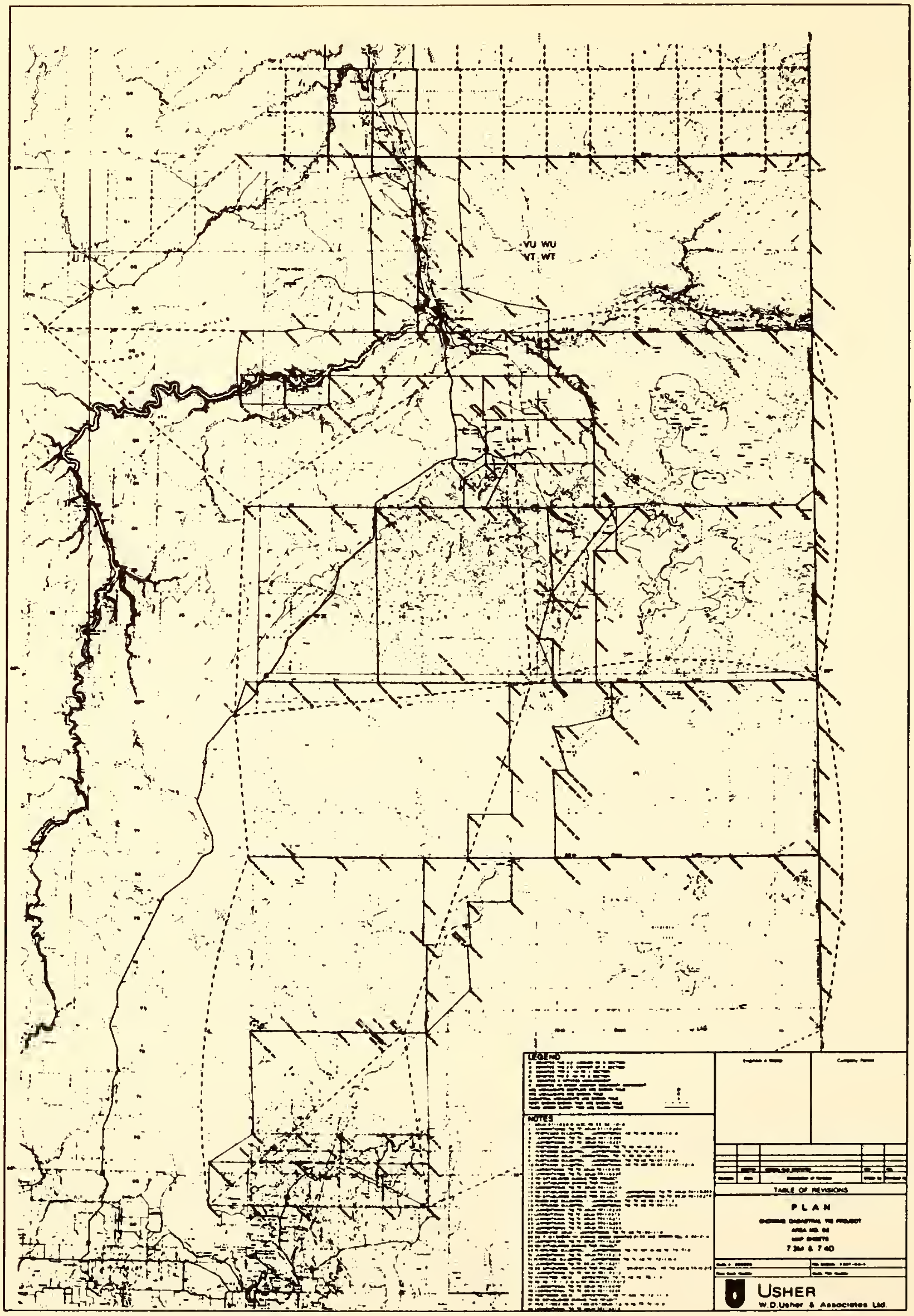
VU WU
VT WT
LEGEND
NOTES
TABLE OF REVISIONS
P L A N
7 3M & 7 4D
USHER
W.D.Usher & Associates Ltd.

FIGURE 1

The site clearing was performed by four 3-man crews. The crews were transported to the sites by Bell 206B helicopters. Each crew was equipped with three chainsaws, axes, safety equipment, two-way radios, compass, clinometer, spare equipment and personal effects. The party chief on each crew was responsible to ensure that each site was properly cleared. A few sites did not require any clearing while others required two days or more to clear. A landing location was provided at each site within thirty metres of the monument to be positioned. It was necessary to construct helicopter pads at approximately 50% of the sites due to the wetness of the terrain.

DATA ACQUISITION

Four Macrometer V-1000 receivers were used to collect the positioning data. Each of the four receivers was mounted in a Bell 206B helicopter. This necessitated the removal of the rear seats of each helicopter. It was possible to mount the large V-1000 electronics box in the rear seat section of the helicopter with room for the 12 VDC lead acid automobile battery (clock power supply) on the floor. This configuration filled approximately 50% of the rear seat area. The remainder of this area was used to transport the V-1000 antenna assembly and if necessary, a second passenger could be squeezed in beside the antenna. The remainder of the required equipment was transported in the storage compartment in the rear of each helicopter. This equipment included a Honda generator, tripod, tribrach and forty metres of antenna cable. The receiver operator travelled in the front passenger seat of the helicopter. Due to weight restrictions, it was not desirable to carry a second passenger when the helicopter required a full fuel load or when the sites visited required a great deal of hovering to land and take off.

The observation window available during the project was approximately 5.5 hours in length. The four hour observations were designed to enable the receivers to record data during the central four hours of the observation window. This made it possible to measure three quasi-independent (explained below) vectors each day using four receivers. A one to two hour observation measuring scheme was designed that enabled the measurement of nine quasi-independent vectors per day. This required three measurement periods within the daily observation window. Approximately thirty minutes were available between measurement periods to move three of the four receivers to the next sites, generally a distance of 39 kilometres. Due to very tight time constraints, proper planning and organization of this phase of the project was imperative. A great deal of map reading skill was required by the receiver operators and helicopter pilots and there was very little time for navigational errors of any kind.

The concepts of "quasi-independent" and "trivial" (Bock et al 1984) are now explained. Using n receivers simultaneously, n(n-1)/2 vectors are measured; however, only (n-1) of these can be thought of as statistically independent or in fact quasi-independent vectors. The remainder are defined as trivial vectors. A simple example helps to illustrate this concept. If three GPS receivers are simultaneously deployed on three survey stations forming a triangular figure, the three measured sides will always result in a zero closure regardless of the observational errors. Therefore, we define any (n-1) vectors or in this case two sides of the triangle as being quasi-independent and the third side as being trivial.

The observational scheme implemented each day was planned the previous day by the project coordinator. Each night almanac files (A-files) were prepared on a DEC LSI 11 micro computer and stored on cassette tape. To prepare the A-files, the time of observation, an estimate of the site coordinates and predicted satellite ephemeris information was required. The A-files were read into the receiver memories prior to each measurement period. They control the measurement sequence and the acquisition and tracking of the NAVSTAR satellites. Once the receiver was turned on and the A-file loaded, the receiver operator had only to monitor the display on the CDU to ensure that the observation was proceeding smoothly.

Another important consideration during each observing day was the synchronization of the V-1000 clocks. Before each day's observation period, one of the V-1000 receivers, designated as the master receiver for the project, was compared to universal coordinated time (UTC) using a GOES satellite time signal broadcast receiver. The two time signals were compared by using an HP 5314A Universal Frequency Counter. If the two time signals were found to differ by more than a few milliseconds then the V-1000 crystal oscillator (clock) was synchronized to UTC. Next, each of the other three receivers was synchronized to the master receiver to within a few microseconds. After each day's observing session was complete, the difference between the master receiver and UTC and the difference between the master receiver and the other three receivers were again determined. This information was recorded in a daily log book to be used later during processing.

It should be noted that NAVSTAR 10 was launched during this project in October, 1984. This increased the number of useable satellites for relative codeless GPS positioning to seven. This turned out to be quite fortunate. During the latter part of the project, as the time between first light and the beginning of the observation window continued to decrease (approximately eight minutes per day), it became increasingly difficult, due to flying restrictions, to deploy the receivers for the first measurement period. The use of NAVSTAR 10 allowed the observation window to be lengthened which in turn, allowed for a later start time for measurement period 1.

Although there were a few vectors which had to be re-measured due to clock errors or generator breakdown, receiver failure was practically nonexistent. This was quite remarkable considerng the harsh environment and the poor weather experienced during the project. The poor weather proved to be by far the biggest problem encountered and in fact made it impossible to fly on a great many days.

DATA PROCESSING

The data processing was conducted in two phases. The first phase was performed by GEO/HYDRO, Inc. staff in their Rockville, Maryland office. They performed their computations on a DEC LSI 11 micro processor using software developed by Macrometrics, Inc. This software required a great deal of user interaction and was extremely time consuming to use. The raw data files (R-files) of phase information collected at each receiver were transferred from cassette tape to disk tape files. The appropriate files were then merged into phase difference files (I-files). The I-files were combined with the appropriate satellite ephemerides and each baseline or vector was solved by a least squares technique. The satellite ephemerides, except for NAVSTAR 10, were commercially available from Aero Service Division, Western Geophysical Company of America. A total of twenty nine vectors were observed using data received from NAVSTAR 10. The satellite ephemerides for NAVSTAR 10 were not available commercially. Special thanks is given to the Naval Surface Weapons Centre who granted a special request and supplied the appropriate information.

Only one serious processing problem was encountered during the vector computation phase. During one observation period, the clock in one of the Macrometer receivers was offset from the other three receivers by thirteen seconds. The Macrometrics, Inc. software is unable to reduce data with clock offsets in excess of one second. Special thanks is given to Dr. Ben Remondi of National Geodetic Survey who processed the vector with software he developed (Remondi 1984).

The computed vectors were supplied to W.D. Usher & Associates Ltd. for phase two of the data processing which was conducted on their HP 1000 mini computer system. This project only required the computation of horizontal positions and therefore a two-dimensional approach was followed. Each of the three-dimensional vectors was reduced to a difference in geographic coordinates on the reference ellipsoid. These differences were then reduced to the corresponding ellipsoidal azimuths and distances. These quasi observations were input into the two-dimensional least squares adjustment computer program GEOPAN (Steeves 1978). In GEOPAN, the observations were further reduced to grid bearings and distances and the adjustment was performed on the 3° Transverse Mercator mapping plane.

Several network adjustments were performed beginning with an unconstrained adjustment wherein only one of the primary control stations was fixed. A brief explanation of the weighting scheme used in the adjustment is worth noting. The Macrometrics, Inc. software computed a formal statistical summary of each measured vector. This summary included standard deviations and a correlation matrix for the difference in latitude, longitude and ellipsoidal height between each pair of stations. These values were rigorously reduced to the corresponding two-dimensional covariance matrix for each ellipsoidal azimuth and distance. The resulting variances were used to weight the observations. Unfortunately, the GEOPAN software does not presently accept the input of observational covariances to be used for the formation of the weight matrix.

Due to the proprietary nature of the Macrometrics, Inc. software, the exact algorithm used to compute the formal statistics of each measured vector is unknown. It is a general observation that the formal standard deviations seem to be overly optimistic, especially in those cases where the satellite signal biases were fixed. In these cases, standard deviations for vectors of nine to ten kilometres in length were in the order of 0.3 to 0.5 ppm. Standard deviations for these vectors were increased by a factor of ten to be used in the formation of the weight matrix for the horizontal adjustment.

Only quasi-independent vectors were included in the network adjustment (trivial vectors were not included). These vectors were treated in the adjustment as being statistically independent where in fact they are not (thus the term quasi-independent). Obviously, vectors which are observed simultaneously are affected similarly by atmospheric conditions, errors in satellite ephemerides and receiver errors.

Notwithstanding the above weighting limitations, the results of the unconstrained adjustments were very good. An interesting analysis of the residuals from the unconstrained adjustment yields the following.

OBSERVATION TYPE	NUMBER	MEAN ACCURACY	LENGTH OF OBSERVATION
Azimuth	17	4.9 10^{-6} rad)	4 hours
Distance	17	2.7 ppm)	
Azimuth	223	4.1 10^{-6} rad)	1 to 2 hours
Distance	223	4.0 ppm)	
Azimuth	240	4.2 10^{-6} rad)	Combination of above
Distance	240	3.9 ppm)	

Generally, these results indicate that the accuracy level achieved with a one to two hour observation is four ppm. It is interesting to note that although the longer observation period improved the distance accuracy (2.7 ppm), the corresponding azimuth accuracy (4.9 microrad) was not improved and in fact decreased slightly. The lines measured with the four hour observation period were all significantly longer in length than those measured with the one to two hour observation period. At the time of this writing, it is speculated that the increased rotational error on the longer lines may have been caused by a lack of ionospheric modelling.

In addition to the unconstrained adjustment, two constrained adjustments were conducted. The seven primary control stations previously noted were held fixed in each of these adjustments. In the first, the coordinates used for these stations were the published Alberta Survey Control values (NAD27). Preliminary NAD83 coordinates prepared by Geodetic Survey of Canada were used in the second constrained adjustment. An estimation of the goodness of the results from all three adjustments can be made by examining the estimated variance factor of each adjustment.

ADJUSTMENT	DEGREES OF FREEDOM	ESTIMATED VARIANCE FACTOR
Unconstrained	82	1.58
Constrained NAD27	94	25.98
Constrained NAD83	94	2.69

Generally speaking, if the estimated variance factor from an adjustment approximates unity, then the residuals from the adjustment closely approximate the corresponding estimated observational standard deviations and the results from the adjustment can be accepted with a high degree of confidence. This is the case with the unconstrained adjustment. However, as one would expect, the estimated variance factor from the adjustment using the ASC coordinates is very high and indicates that the observations have been heavily constrained by the fixed stations. This high value indicates that there are some fairly large distortions in the terrestrial geodetic networks in this part of Alberta. It is distortions of this magnitude which have led to the 1983 North American Datum (NAD83) project which is to be a comprehensive continental adjustment of all North American geodetic horizontal control networks. Preliminary values from this adjustment were used in the final constrained adjustment. As can be seen from the estimated variance factor from this adjustment (2.69), the preliminary coordinate values are very compatible with GPS observations. This speaks well for both the horizontal re-adjustment of the North American datum and the accuracy of GPS.

SUMMARY

From the outset, it was anticipated that this project would provide invaluable experience and insight for all parties concerned, as well as, an intense field test and assessment of a relatively new positioning technology. Site preparation, although physically demanding, went according to schedule and presented very few logistical problems. The Macrometer V-1000 GPS receivers were extremely rugged and dependable despite their heavy and bulky nature and provided three-dimensional relative positioning information at the 2.5 to 4.5 ppm level throughout the project. Mother Nature dealt the harshest blow accounting for 21% of the project field component as Alberta experienced one of the worst autumns in many years. The data processing component of the project provided adjusted coordinate positions for all land survey monuments, as well as, several Alberta Survey Control markers within the project area. Due to the design of the project, it was possible to combine all observations into an all inclusive homogeneous network adjustment. The redundancy which was designed into the network provided for good network strength and valuable statistical testing of the adjustment results.

Geodetic GPS receivers which are small in size, light weight, weather resistant and require less input power are presently being developed and will make the logistics of a project of this nature much simplier. Software should be developed and in fact is being developed at the University of New Brunswick, Fredericton, New Brunswick, Canada (Beutler et al 1984) and National Geodetic Survey, Rockville, Maryland, U.S.A. (Remondi 1984) which will allow for more automated processing of GPS data. Software should be developed which will allow for the computation of the formal covariance matrix for all n(n-1)/2 simultaneously measured vectors using n receivers. Network adjustment results should be improved if the proper weight matrix accounting for the correlated nature of simultaneously observed vectors could be determined. A source of GPS satellite ephemeris information should be established in Canada.

The project was considered an unqualified success. Every expectation and objective was surpassed significantly with the 200 monuments being located, assessed, prepared for observation and positioned within a 71 day period.

REFERENCES

Beutler, G., D.A. Davidson, R.B. Langley, R. Santerre, P. Vanicek and D.E. Wells 1984. Some Theoretical and Practical Aspects of Geodetic Positioning Using Carrier Phase Difference Observations of GPS Satellites, Department of Surveying Engineering Technical Report No. 109, University of New Brunswick, Fredericton, New Brunswick, Canada.

Boch, Yehuda, R.I. Abbot, C.C. Counselman III, S.A. Gourevitch and R.W. King 1984. Establishment of Three Dimensional Geodetic Control by Interferometry With the Global Positioning System, Submitted to Journal of Geophysical Research.

Collins, J. 1984. GPS Satellite Surveying - A Review of the First Years Results, ACSM Bulletin, Number 88, American Congress on Surveying and Mapping, February, pp.23-26.

Hothem, Larry D., Clyde C. Good and Benjamin W. Remondi 1984. GPS Satellite Surveying - Practical Aspects, The Canadian Surveyor, Vol. 38, No. 3, Autumn, pp.177-192.

Leeman, Roger W., L.B Fletcher and H.D. MacAulay 1985. Geographical Positioning of the Alberta Township System by Global Positioning System Technology, to be presented at the Canadian Institute of Surveying Annual Convention in Edmonton, Alberta, Canada, May 28-31, 1985.

Remondi, Benjamin W. 1984. Using the Global Positioning System (GPS) Phase Observable For Relative Geodesy: Modelling Processing and Results, Doctoral Dissertation, Centre for Space Research, University of Texas, Austin (NOAA Reprint).

Rizos, C.A. Stolz and E.G. Masters 1984. Surveying and Geodesy in Australia with GPS, The Australian Surveyor, Vol. 32, No. 3, September, pp. 202-225.

Steeves, R.R. 1978. A Users Manual For Program GEOPAN Geodetic Plane Adjustment and Analysis, Department of Surveying Engineering Technical Report No. 54, University of New Brunswick, Fredericton, New Brunswick, Canada.

COMPARING THE PREDICTED POSITIONING COSTS OF DOPPLER AND GPS TECHNOLOGY

James K. Crossfield
Department of Civil and Surveying Engineering
California State University, Fresno
Fresno, California 93740

ABSTRACT. Quality, cost effective, horizontal geodetic control survey positioning is often required for land and mineral surveys, construction projects, mapping activities, control densifications and geodetic investigations. Doppler Satellite Positioning and the Global Positioning System, two techniques currently available, have different use, productivity and cost characteristics. Both of these systems are compared with respect to project equipment, manpower, and transportation requirements for local control densifications. These two generic areawide geodetic control positioning situations are also analyzed with respect to the projected productivity and costs of both Doppler and GPS technologies. The equipment rental or purchase threshold is explored and per station cost trends are developed.

INTRODUCTION

Development of a horizontal geodetic control survey cost model (Crossfield, 1984) that included Doppler and GPS positioning cost model components was initiated to formulate a generalized approach for finding the most economical positioning technology for establishing horizontal coordinate values on uniformly spaced area-wide geodetic control networks. These area-wide networks may be considered as fundamental building blocks in the geodetic reference framework component of evolving multipurpose cadastres. Availability of applicable cost models makes it easier for managers of multipurpose cadastres to select the least costly geodetic reference framework implementation or densification scheme.

Per point cost data can be misleading or easily misinterpreted because they ignore the dynamic nature of geodetic positioning technology costs. The positioning costs for any situation are totally dependent upon the specifics associated with the particular situation being analyzed. Additionally, it must be understood that more than one positioning technology may be used to satisfy any given positioning requirement. Situations do exist for which both Doppler satellite and GPS are applicable positioning tools. Several such common situations are used here to compare the costs associated with these satellite positioning techniques.

DOPPLER COST MODEL

The following equation (Crossfield, 1984) correlates the continuous number of days (D) that a given configuration of Doppler satellite receivers (NR) must occupy a given set of survey points, the latitude (PHI) of the project in degrees, the spacing of those survey points (S) in meters, and the allowable positioning error ratio (AE). This is based on use of the MAGNET adjustment program (Stansell, 1981).

$$D = 0.001172(115 - PHI)/((NR - 1)(S)^2(AE)^2) \qquad (1)$$

This equation is the basis for the Doppler cost model. 20 different input variables are used to drive the overall Doppler cost model. Four variables dictate the situation geometry, five are used to mirror equipment costs, seven relate the transportation status, one specifies the final required network positioning accuracy, and three are used to indicate labor costs.

The total time required to conduct any given Doppler positioning project is computed in days, and the total required transportation distance is tabulated. Then, five component costs--equipment, data reduction, labor, transportation, and planning--are generated and added together to equal the total Doppler cost.

Doppler Limitations and Assumptions

This model is designed to estimate the positioning costs associated with establishment of an area-wide horizontal geodetic control network by Doppler saellite. An area between 20 and 60 latitude is assumed. Monumentation costs are not included, so any applicable area with monuments in place (but not positioned) could be modeled. Uniformly spaced control points are necessary. A single ground transportation vehicle is assumed. Receiver security is not directly addressed, but careful input of the crew size variable might compensate, if necessary.

While up to 10 points may be adjusted simultaneously, the number of days of continuous operation (D) should not exceed about 4.0 because the accuracy improvements become negligible after that. Existing horizontal geodetic survey control points are considered to be essentially error-free.

Contracting for or rental of Doppler positioning equipment is considered. Discount rates and inflation are not evaluated, however. Input cost data must be an average projected over the expected project duration. Per diem labor costs must be added to daily crew costs.

Good input data are essential. The final outcome of a particular cost estimate will depend entirely on the quality and reliability of the input data. Any one or several of the 20 input values could cause a significant error if incorrectly estimated. Significant knowledge about the local situation is required before an effective evaluation may be conducted. Applicability of this model to specific geographical regions is based upon the knowledge and experience of the user.

The minimum allowable error (AE) is assumed to be 20 centimeters (NRC, 1983). This significantly restricts the applicability of Doppler satellite positioning to area-wide control. The minimum spacings for 1:5,000, 1:10,000, 1:20,000 and 1:50,000 control are 1,000, 2,000, 4,000, and 10,000 meters, respectively. Finally, it is assumed that only two-thirds of predicted passes are actually usable for positioning data reduction. One-third of all potentially available satellite passes are considered unavailable due to the combined effects of battery failure and transmission or receiving difficulties.

GPS COST MODEL

The following equation (Crossfield, 1984) correlates the allowable positioning error ratio (AE) to the time (TOS) required in hours to observe continuously four GPS satellites with two simultaneously operating Macrometer Series 1000 Interferometric Surveyors:

$$TOS = 1/(50{,}000(AE)) \qquad (2)$$

This equation is the basis for the GPS cost model, which is driven by 16 different input variables. Two inputs dictate the situation geometry, three are used to mirror equipment costs, six relate the transportation status, one specifies required network accuracy, and four are used to indicate labor costs. Each receiver is considered to be nonfunctioning one-third of the time, due to maintenance problems.

The GPS cost model was constructed so that the least expensive option (two or three receiver operation) is selected. This model must be constrained by the length of the observing window (when four simultaneous satellite passes are ongoing) each day. The availability of the four satellites is set at six hours per day for cost evaluations here. The GPS cost model may be changed easily to accomodate longer or shorter daily availability, depending on the appropriate satellite configuration.

Five component costs--equipment, labor, data reduction, planning, and transportation--are generated after computation of the total number of required project days and tabulation of the total required transportation distance. The five component costs are added together to generate the total GPS cost.

GPS Limitations and Assumptions

Only two or three receivers are considered here. While networks of many simultaneously observing receivers are necessary for fast quality Doppler positioning, such is not the case with GPS. Fast quality GPS positions are obtainable from just two simultaneously operating receivers, one of which is at a known point. Based on the operating characteristics of the Macrometer Series 1000, simultaneous use of more than three receivers would rarely be worthwhile.

The GPS cost model may be applied to virtually any horizontal positioning project requiring uniformly spaced points. The effects of nearby obstacles are significantly less than with the Doppler system. One vehicle is used for each receiver. Monumentation costs are not included. Only one new point is assumed t be observed at a time. Per diem labor costs must be included i the daily crewperson cost if required. The known point at whic one receiver operates continuously is assumed to be of reliably known horizontal position. A first order station would usually be satisfactory.

Contracting for or renting GPS equipment is also considered in this model. Very large scale projects may be more cost efficient, even with equipment purchase. This is evaluated with the GPS cost model by conducting a run without any equipment cost input and adding the computed cost of the project to the purchase cost of the equipment. Discount rates and inflation are not evaluated. Input and output costs must be for a given base year.

Good input data are again essential, because the final computed cost is totally dependent upon the quality of the 16 different input variables. The applicability of these cost models to specific geographic regions is based upon the knowledge and experience of the user. For example, vehicle rate of travel and receiver setup and pickup times are very sensitive to the quality and quantity of the available road network.

EXAMPLE COST PREDICTIONS

A series of nine hypothetical cost prediction tests was developed and analyzed. The situations were selected so that both the Doppler satellite and the Global Positioning System would be applicable for positioning. A 500-square-mile (1,300-square-kilometer) area was chosen. Several transportation input variables and the daily planning cost input variable common to both technologies were kept constant for all nine tests. Technology-specific labor and equipment-related input variables were also kept constant for all tests. Three different allowable positioning errors and three different new point spacings were used to create nine possible test situations. Table 1 lists constant input values; Table 2 lists the changing input values for each test.

An infinite number of possible situations could be analyzed with the Doppler and GPS cost models. The situations examined here are provided as a convenient medium for comparing (for one particular set of circumstances) the costs of GPS and Doppler positioning technologies.

The results of these hypothetical cost prediction tests are graphically represented in Figure 1. The top three curves represent Doppler, while the bottom three represent GPS.

Cost Comparisons

Based upon these nine specific test situations for which Doppler and GPS positioning costs were computed, GPS positioning is most cost effective. Throughout this range of point spacings, the Doppler cost curves are flatter, suggesting that Doppler costs tend to be more constant across these varying point spacings. The GPS cost curves are less flat, suggesting that

CONSTANT INPUT VALUES FOR EXAMPLE COST PREDICTIONS

Common Input Variable Values	
10	Vehicle Miles per Gallon
$24	Vehicle Rental per Day
$100	Driver Salary per Day
$1.25	Fuel Cost per Gallon
$0.125	Additional Vehicle Maintenance Cost per Kilometer
20	Kilometers from Office to Project Area
30	Kilometers/Hour Vehicle Travel Rate
$350	Daily Planning Cost
Doppler Specific Input Variable Values	
43	Latitude of Project Area
10	Receivers Available for Simultaneous Use
3	Receivers Continuously Used on Known Control Points
$250	Daily Receiver Rental Cost
0.7	Hours Required to Setup and Takedown 1 Receiver
$250	Crew Person Daily Cost
$300	Per Station Data Reduction Cost
GPS Specific Input Variable Values	
0.4	Hours/Day/Receiver Calibration Time
$700	Daily Receiver Rental Cost
$250	Data Reduction Costs/Hour
0.5	Hours Required to Setup and Takedown 1 Receiver
$300	Crew Person Daily Cost

TABLE 1

throughout this range of spacings, the GPS system is favored more and more as the spacing decreases (or number of points increases) in a given area.

The cost curves are consistent for each technology in that ultimately a smaller required positional error tolerance will cost more. Based upon these typical input costs, it appears that GPS per point positioning costs are about half the Doppler per point positioning costs for moderately spaced area-wide control densification projects. Relaxation of error tolerances appears to reduce Doppler costs much more than it reduces GPS costs.

While these curves appear to suggest a total economic dominance for GPS, such is not always true. Extrapolation of the curves in Figure 1 to the right suggests that GPS costs may be greater than Doppler costs for situations requiring very long spacings between points.

Two GPS receivers were the preferred (least costly) GPS approach for these situations, but in order to insure continued progress, one additional receiver must be available. A total of three GPS receivers, costing about $350,000 (Macrometrics, 1982) would support a GPS productivity of about 7 points per day, while a total of 10 Doppler receivers, costing about $500,000, would support a Doppler productivity of about 12 points per day. This suggests a productivity of about 2.3 points per GPS receiver day and about 1.2 points per Doppler receiver day for the specific situations analyzed here.

The particular crew and vehicle transportation requirements are essentially fixed for these test situations. GPS requires one crew member and one driver for each vehicle and receiver, while Doppler requires three crew members and a driver in one vehicle for all 10 receivers. Doppler technology is modeled so as to require more than one daily crew shift, if that will produce an overall lower cost. Three daily crew shifts would be required for all but one of these test situations. Two daily crew shifts would be required in the one other case.

TEST SITUATIONS

Test #	Specific Conditions		
	# New Points	Spacing	Accuracy
1	15	7,000m	1:20,000
2	31	5,500	1:20,000
3	70	4,000	1:20,000
4	15	7,000	1:10,000
5	31	5,500	1:10,000
6	70	4,000	1:10,000
7	15	7,000	1:5,000
8	31	5,500	1:5,000
9	70	4,000	1:5,000

TABLE 2

A SPECIFIC SET OF DOPPLER AND GPS POSITIONING COST PREDICTIONS

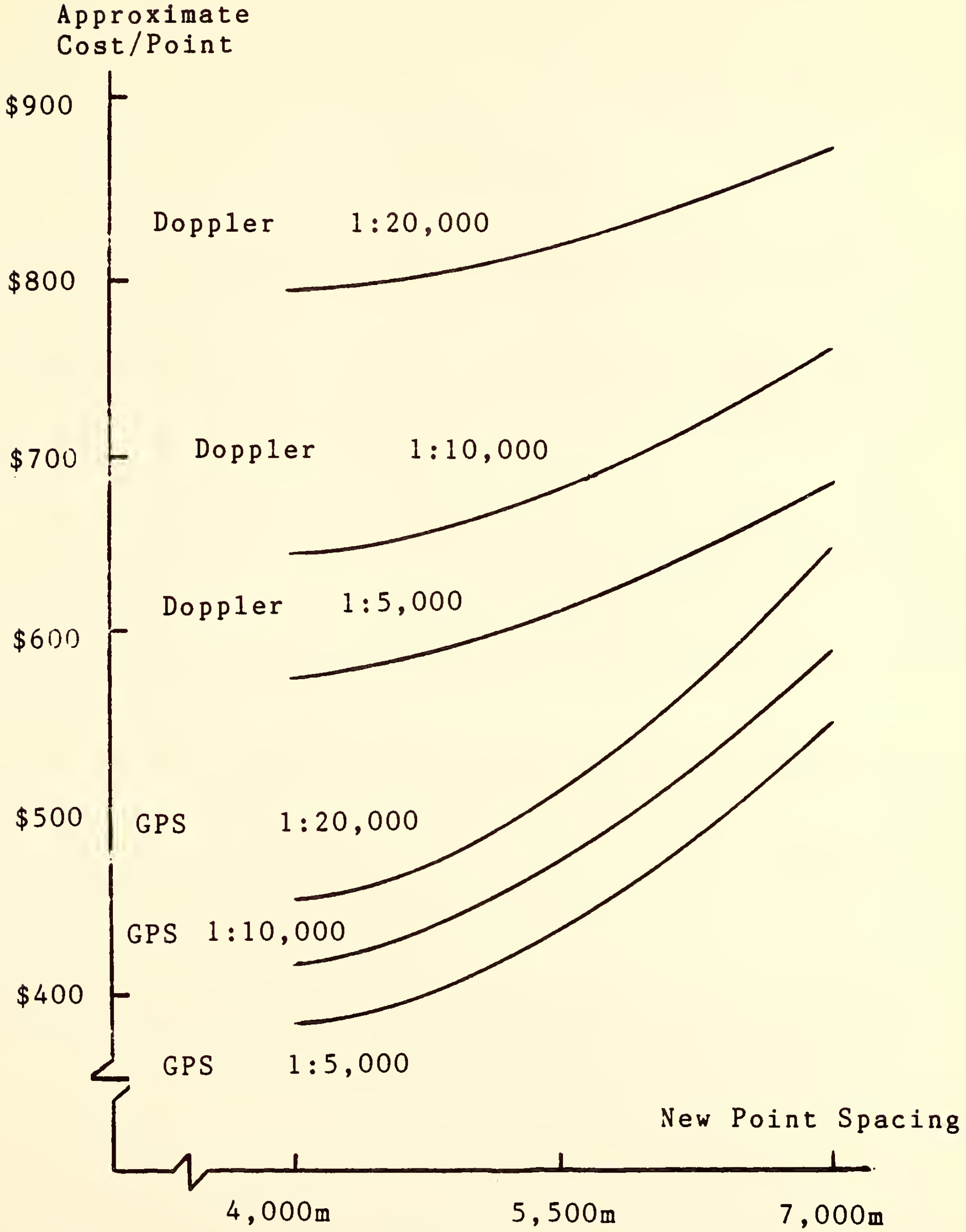

FIGURE 1

EQUIPMENT PURCHASE THRESHOLDS

Equipment purchase is deemed justified when total receiver rental costs are greater than the purchase costs of the receivers. Purchased technologies must be evaluated on a case by case basis. Many positioning tasks would be best satisfied by use of private consultants who specialize in advanced positioning technology or by direct short-term rental of the equipment. Ultimately, heavy long-term use of satellite positioning technology will create an economic environment in which direct equipment purchase is beneficial. The results of several positioning cost projections for Dane County, Wisconsin (Crossfield, 1984) suggest that purchase of three Macrometer 1000S GPS receivers would be justified when more than 1,200 1/2-mile-spaced corners require 1:20,000 positioning in a given area. Purchase of 10 Doppler receivers for precise area-wide corner positioning for 1/2-mile-spaced control was not justified for any reasonably conceivable application.

CONCLUSIONS

1. When supplied with appropriate input variable values, the GPS and Doppler positioning cost models are valuable control densification planning and cost estimation tools.

2. A flexible, technology-specific cost estimation procedure can answer site-specific per point positioning cost questions, but flexibility makes such procedures very sensitive to input.

3. While Doppler positioning has restricted applicability in terms of point spacing due to accuracy limitations and GPS positioning has much wider applicability, both of these satellite positioning systems are jointly applicable to a tremendous array of possible positioning applications.

4. Doppler costs were approximately double the GPS costs for each of the 9 hypothetical situations presented here.

5. GPS and Doppler cost comparisons and equipment purchase threshold determinations are only valid on a case by case basis.

6. Generalizations about positioning technology per point costs should not be made.

REFERENCES

Crossfield, J.K., 1984: The Cost of Establishing Horizontal Geodetic Survey Control on Remonumented Public Land Survey Corners, pp. 43-73, 119-146, 244-249, 265-270, Ph.D. Thesis, University of Wisconsin-Madison.

Macrometrics, Inc., 1982: Macrometer 1000 Series Interferometric Surveyor (information brochure), Woburn, MA.

National Research Council, 1983: Procedures and Standards for a Multipurpose Cadastre, p.32, Washington, D.C., National Academy Press.

Stansell, T.A., 1981: The Continuous Evolution of Satellite-based Geodetic Positioning and Survey Navigation Capabilities, Offshore Technology Conference Technical Paper, Houston, TX.

FACTORS TO BE CONSIDERED IN DEVELOPMENT OF SPECIFICATIONS FOR GEODETIC SURVEYS USING RELATIVE POSITIONING GPS TECHNIQUES

Larry D. Hothem and George E. Williams
National Geodetic Survey
Charting and Geodetic Services
National Ocean Service, NOAA
Rockville, MD 20852

ABSTRACT. Since 1983 the National Geodetic Survey has completed some 30 GPS survey projects designed to meet a variety of control requirements. The practical experience gained in performing these surveys, our analysis of the results, and the published results of others are the basis for the compilation of factors that will be considered in development of revised geodetic survey standards and proposed specifications for GPS three-dimensional relative positioning surveys. The revisions to the standards are designed to meet classification requirements for the high-level precision achieved from GPS relative positioning techniques. The specification factors cover network design and geometry, instrumentation, calibration procedures, field procedures, and office processing and analysis procedures.

INTRODUCTION

The rapidly growing use of the Global Positioning System (GPS) for geodetic surveying applications has now reached the point where the need for acceptable survey standards and specifications has become critical. Specifications are essential to promote maximum efficiency in the conduct of field operations and facilitate classification of surveys.

Since early 1983 the National Geodetic Survey has gained considerable field and office experience from about 30 GPS survey projects carried out by NGS field teams. These projects were designed to meet a variety of control requirements including connection of new points to the national geodetic horizontal and vertical reference systems, establishment of base measurements for the monitoring of horizontal and vertical motion, and determination of geoid height differences for use in refining our geoid modeling efforts. The NGS has also been involved in the review and approval of plans for six GPS geodetic surveys commissioned by other Federal and local government agencies and performed by commercial firms.

The extensive GPS survey field experience and numerous reports on the analysis of results for GPS survey projects were the basis for compilation of factors that will be considered in the development of specifications for GPS geodetic surveys. These factors were compiled from unpublished NGS GPS project reports and in published findings such as Beck et al. (1984), Bock et al. (1984), Collins and Leick (1985), Goad and Remondi (1983), Hothem and Fronczek (1983), Hothem et al. (1984) and Langley et al. (1984). The specification factors are only for control surveys performed by GPS relative positioning techniques where two or more receivers are collecting data simultaneously.

Specifications are defined as the field methods required to meet a particular survey standard. Survey standards are defined as the minimum accuracies that are necessary to meet specific objectives. The present FGCC (Federal Geodetic Control Committee) standards for accuracy are not well suited to control established by three-dimensional relative positioning methods. The standards for horizontal coordinates are based on minimum distance accuracies where the most stringent standard is 1:100,000 (10 ppm)(FGCC 1984). This is classified as a first-order standard. On the other hand, the FGCC standards for vertical (orthometric) coordinates, which are based on maximum elevation difference accuracy, are much more stringent than the first-order horizontal standard. Depending on the classification, the elevation difference accuracy standard for bench marks spaced 1 to 100 km apart ranges from 2.0 to 0.05 ppm.

Experience has shown that in any component of GPS relative position, the precisions are typically five times to as much as 100 times better than 1:100,000 (i.e., 2 to 0.1 ppm). If 1-cm level precision is achieved for crustal motion survey applications for stations spaced more than 1000 km apart, this is 1000 times better than 1:100,000 (i.e., 0.01 ppm).

Additionally, the present standards do not include criteria for ellipsoid height differences and geoid height differences. Accuracy standards for geoid height differences and ellipsoid height differences are essential since they will dictate the accuracy and classification for orthometric height differences determined from GPS surveys. Because the present standards are not adequate for classifying the results of high-precision, three-dimensional relative position surveys, revisions to the accuracy standards will be developed. Two groups of standards are being considered: a **general** classification for general purpose geodetic control and a **special** classification for special high-precision geodetic surveys.

Consistent with the format in the current edition of the FGCC document for standards and specifications for geodetic control networks (FGCC 1984), the specification factors includes network design and geometry, instrumentation, calibration procedures, field procedures, and office processing procedures.

After the proposed revisions to the accuracy standards and GPS survey specifications have been developed, they will be subject to further review within NGS before submission to the FGCC for final consideration. The FGCC, a U.S. interagency committee, is officially responsible for the adoption of standards and specification for geodetic control networks.

BACKGROUND

GPS satellite surveying is a three-dimensional measurement system based on observations of the radio signals of the NAVSTAR Global Positioning System. The GPS observations are processed to determine station positions in Cartesian coordinates (X,Y,Z), which can be converted to geodetic coordinates (geodetic latitude and longitude and height above reference ellipsoid). With adequate connections to vertical control network points and a priori knowledge of the shape of the geoid, orthometric heights or elevations can be computed for the points with unknown elevations.

There are two methods by which station positions can be derived: point positioning and relative positioning. In the point positioning method, data from a single station are processed independently to yield the station coordinates. The present accuracy of this method ranges from 50 cm to 10 m (1 sigma) depending on the accuracy of the ephemerides and period of the observations.

To perform decimeter-level or better geodetic surveys, one must employ the relative positioning method. In relative positioning, two or more GPS geodetic receivers simultaneously receive signals from the same set of satellites. These observations are processed to obtain the components of the base line vectors between observing stations (station coordinate differences). When the coordinates for one or more stations are known, the coordinates for new points can be determined after adjusting for the differences between the reference system for the GPS satellites and local geodetic network control. The GPS satellite coordinate data are currently computed in the World Geodetic System 1972 (WGS-72), an Earth-centered and Earth-fixed coordinate system. A new World Geodetic System is currently being considered for adoption as the GPS satellite coordinate reference system (Leroy 1982).

There are three basic GPS signal measurement types that have been used for relative positioning techniques: pseudorange, integrated Doppler frequency, and carrier beat phase. Although these observables have different characteristics, they are all functions of the instantaneous ranges between satellite and ground stations and their time derivatives. The most precise geodetic measurements are presently achieved from processing of carrier beat phase observations.

Carrier beat phase observations are measurements of the phase difference of received signals emitted by the satellite's oscillator and the nominal carrier signal generated by the receiver's oscillator (Remondi 1985). There are several receivers capable of making phase measurements of the L1 signal (1575.42 MHz) and others of both the L1 and L2 (1227.6 MHz) signals (Remondi 1983).

The processing of carrier beat phase data can be performed in at least four modes: single base line single difference, single base line double difference, single base line triple difference, and multiple base line phase data (Beutler et al. 1984, Bock et al. 1984, Remondi 1984, and Goad 1985). In the multiple base line data processing mode, the data are processed simultaneously for a single observing session or for multiple observing sessions. The multiple session mode is also called a network solution and is only practical if there are adequate links or common stations between the observing sessions.

The present estimated accuracy of the precise ephemeris for the GPS satellites is 20 to 50 m, or 1 to 2.5 parts-per-million (ppm). The accuracy of the broadcast ephemeris is about 5 ppm. When the GPS orbit coordinates are fixed in the data processing for base line determinations, the errors in the orbits will propagate directly into the results for the base lines. To obtain precise results at the 0.1 or 0.01 ppm level, the average allowable orbital errors are 2 m and 20 cm, respectively.

In session and network (multiple observing sessions) processing of phase observations, the satellite orbit coordinates may either be fixed or allowed to adjust while simultaneously determining the base line vectors. If allowed to adjust, the solution should include simultaneous observations from a minimum of three receivers.

STANDARDS

Classification Standards

In a report by Rizos et al. (1984), it was proposed that accuracy requirements be classified into four broad categories of potential users ranging from those satisfied with 100 ppm accuracies to those engaged in ultra-high precision crustal motion surveys requiring accuracies of 0.1 ppm or better. To meet a wider range of accuracy requirements and to incorporate the present FGCC accuracy standards, it is proposed that two sets of classification standards be adopted: general and special. The **general** classification standards would incorporate the present

FGCC accuracy standards and would be for general purpose geodetic surveys. The **special** classification standards are for high-precision and special geodetic surveys. Each classification has different levels of accuracy or orders of a survey. In some cases each level of accuracy is subdivided further by a class designation.

For the near future, a **special** classification would be based on the internal consistency of a GPS relative positioning network adjusted independently of the local network control. On the other hand, a **general** classification would be based on the results of a constrained adjustment where GPS stations connected to the local network control are held fixed to vertical and horizontal coordinates in the National Geodetic Reference System. Surveys receiving a **special** classification are for such purposes as crustal motion, subsidence monitoring, and special high precision engineering surveys. These standards would also be applicable for other high-precision measurement methods such as Very Long Baseline Interferometry and satellite laser ranging. When a survey is adjusted into the local network control system, it would receive a **general** classification with an order that would be dependent on the accuracy of the existing horizontal and vertical network control, and the accuracy of a priori geoid height differences.

The **special** classification standards would be based on three-dimensional relative positioning error. Networks are classified according to the ratio of maximum semi-major axis of the relative error ellipsoid for a network to the distance between points at the one-sigma probability level. The use of the error ellipsoid assumes that all surveys share a common origin. **General** classification standards would be based on minimum distance accuracies, azimuth accuracies, geoid height difference accuracies, ellipsoid height difference accuracies, and the order of the existing network control.

Table 1 summarizes the proposed **special** classification relative positioning standards for various high-precision survey categories. Six classifications are proposed for minimum accuracies ranging from 2 ppm to 0.01 ppm. The minimum accuracies apply to minimally constrained, correctly weighted, least-squares adjusted networks. For each **special** accuracy standard, the maximum allowable one-sigma ellipsoid semi-major axis in centimeter for the relative position precision can be computed for a corresponding station spacing. The relative position precision is the propagated maximum semi-major axis for the relative error ellipsoid of the vector base line measurement (three-dimensional relative coordinates) between stations.

Table 1. -- Proposed **special** classification three-dimensional relative accuracy standards

General Survey Categories	Classification		Minimum Accuracy (ppm)
	Order	Class	
Global dynamics, vertical and horizontal motion..	1	I	0.01
Regional dynamics..............................	1	II	0.01
National Geodetic Reference System (Primary).....	2	I	0.1
Local dynamics.................................	2	II	0.1
Network connections, densification.............	3	I	1
High-precision engineering surveys.............	3	II	2

Table 2 summarizes the proposed **general** classification standards. Except for the addition of the minimum distance accuracy of 1:300,000, the classification and distance accuracy standards are consistent with the 1984 FGCC standards. The minimum distance accuracy of 1:300,000 was added to meet the expected accuracy of the horizontal network control after readjustment into the North American Datum of 1983. Although this table currently excludes minimum accuracy standards for azimuth, ellipsoidal height difference, and geoid height difference, these standards are being developed. Azimuth accuracies will be based on a minimum spacing between the azimuth and station mark.

The heights produced from GPS surveys are with respect to a reference ellipsoid. To convert these ellipsoid heights (geodetic) to orthometric heights or elevations, the survey must include adequate connections to network control points with orthometric heights referenced by geodetic leveling to the National Geodetic Vertical Datum (NGVD). Then with good estimates for the geoid height differences between all stations of the project, orthometric heights derived from the GPS survey results can be computed. The accuracy of the GPS-derived orthometric heights will depend on the precision of the GPS ellipsoidal height differences, the accuracy of the orthometric heights of the bench marks, and the accuracy of geoid height differences. Standards for geoid height difference accuracy are being developed.

Table 2. -- Proposed **general** classification accuracy standards

General Survey Categories	Classification		Minimum Distance Accuracy	
	Order	Class	(ppm)	
National Geodetic Reference System (secondary)...	1	I	3.33	1:300,000
Cadastral, engineering, urban, surveys..........	1	II	10	1:100,000
Cadastral surveys, mapping......................	2	I	20	1: 50,000
Cadastral surveys, mapping......................	2	II	50	1: 20,000
Geophysical exploration and land surveys.........	3	I	100	1: 10,000
Geophysical exploration and land surveys.........	3	II	200	1: 5,000

Monumentation

The type of marker best suited for a given type or condition of terrain will depend on factors such as local conditions, transportation, materials available, equipment available for setting marks, and cost. When the sites for new points are being selected, surveyors should attempt to locate the new points on existing bench marks tied to the National Geodetic Vertical Network. Underground monumentation is optional for two reasons: (1) the cost of reestablishing the surface mark may be less than the cost of setting the underground mark, and (2) the underground mark is not acceptable for preserving the three-dimensional coordinates. Reference marks are optional except in special circumstances such as stations established in support of the National Crustal Motion Network, the primary National Geodetic Reference System, or for other precise geodetic applications where recovery of the main station is important. To meet requirements for permanent monumentation, the mark may be made of corrosion-resistant metal disks set in a large concrete mass or a rock outcrop, or long metal rods or stakes driven deep into the ground.

SPECIFICATIONS

The specification factors given in this section are based on considerable practical experience. Studies are underway to finalize proposed parameters for each factor. Significant changes are expected as progress is made in refining the processing techniques, as more satellites become available for observations resulting in improved geometry, and as we learn more about how to deal with other critical factors affecting field operations such as the effect of obstructions and reliability and accuracy of the antenna plumbing and height measurements. Also, it is expected the specification parameters will become less conservative and there will be more flexibility in the field procedures once the full 18-satellite GPS constellation is deployed by the end of this decade.

Network Design and Geometry

The location and relative disposition of the control points do not depend on factors such as network shape or intervisibility (except when establishing azimuth reference points) but rather on optimum layout for carrying out the intent of the survey.

The factors that will be considered for the network geometry specifications are:

1. Station spacing, minimum and maximum range in kilometers.
2. Minimum number of vertical network control points.
3. Minimum number of horizontal network control points.
4. Station spacing of existing network control, maximum in kilometers.
5. Distribution of existing network control (relative to center of project), specified in terms of the four quadrants.
6. Azimuth reference, distance from station (in meters) not less than __.

Checks should be made to ensure that all existing network control points have not been moved or disturbed. It may be necessary to occupy more than the minimum number of network control points to ensure the survey is tied into points with sufficient accuracy or internal consistency. If bench marks are located in areas subjected to vertical motion, it may be necessary to perform a vertical survey by differential leveling or precise trigonometric methods to ensure all bench marks are connected to a common epoch.

It is stated in the present FGCC specifications that whenever the distance between two unconnected survey points is less than 20 percent of the distance between those points traced along existing or new connections, a direct connection should be made between those survey points (FGCC 1984). Validity in scope of application of this rule for GPS relative positioning surveys should be thoroughly analyzed.

If azimuth marks are required, the azimuth reference can be established by GPS surveys. Some reasons for considering the establishment of azimuth reference by GPS relative positioning techniques rather than conventional astronomical methods are: (1) GPS surveys may be less costly, (2) two stations will be located close to each other with coordinates established at the same order of accuracy, and (3) repeat observations between the azimuth mark and main station can be used to verify the relative stability of the two marks in all three dimensions.

Table 3 summarizes minimum spacings between the azimuth and station mark in relation to expected relative position precisions for the GPS surveys and possible azimuth accuracies.

Table 3. -- Minimum spacings for establishing azimuth marks by GPS surveys

Spacing between azimuth and main station mark, less than (meters)	Azimuth reference accuracy in seconds of arc (1 sigma)				
	1	2	4	6	10
	GPS relative position precision (mm) (1 sigma)				
100	-	-	-	3	5
200	-	2	4	6	10
300	-	3	6	9	14
400	2	4	8	12	19
500	3	5	10	14	24
600	3	6	12	18	29

Instrumentation

GPS geodetic receivers may receive one or both carrier frequencies transmitted by the GPS satellites. Two frequency receivers are required for the most precise survey to correct for the effects of ionospheric refraction. The receivers must record the phase of the satellite signals, the receiver clock times and the signal strength. To help ensure data collected with different receivers can be combined in the processing, the measurement interval should be selectable in multiples of 3 seconds (e.g., 3, 15, 30, 60 seconds, etc.).

Generally, GPS satellite geodetic surveying equipment will consist of three major components: the antenna, receiver/processor, and recording unit. Depending on type of cable used, the lengths will range from 10 to 60 meters. The maximum length and type of cable may depend on the manufacturer's specifications. The receiver must have the capability to track a minimum of four GPS satellites simultaneously. Some receivers may have multiple data ports for handling printer output, data input from automatic weather instruments, and remote control operations. It should be possible to operate the receiver in the unattended mode. However, when commanded, information should be available for display to ensure the the receiver is functioning normally and the data quality meets acceptable standards.

The receivers may be of the so-called codeless type or have the capability to receive and decode the P and/or CA coded data. If it is the codeless type, the receiver must have the appropriate output and input ports for synchronizing the clocks relative to a UTC (Universal Coordinated Time) standard.

The reference frequency should be stable to within $5.0(10^{-11})$ per 100 second. The drift rate should be within a maximum of 10 μs/hour or $2.8(10^{-9})$; however, it is recommended that the drift rate be maintained to within 1 μs/hour or $2.8(10^{-10})$. For the most precise surveys, it is recommended that a rubidium or cesium atomic standard be used as the reference frequency. Atomic standards exhibit long-term stabilities that are typically better than $1(10^{-12})$. All GPS receivers should have a signal input port for an external frequency standard.

The best estimate of the mean electrical (phase) center of the antenna should be clearly marked at a standard location for the same model antennas. If the antenna is designed to receive both L1 and L2 frequencies, there should be a mark for each frequency. These marks will be the reference point for all height-of-antenna measurements. If L1 and L2 data are combined in the base line solutions, a mean of the location of the two phase centers will be used as the reference point.

Calibration Procedures

The receiver should be deployed on a test network at least once a year to ensure confidence in the receiver operation and in the data reduction software. The test network should comprise three or more stations spaced 10 m to 1 km apart. The standard will be three-dimensional relative position measurements with a precision of better than 2 mm (1-sigma) in each component.

If different receivers and/or different model antennas are used in a survey, it will be necessary to conduct calibration tests to determine whether significant biases exist. For example, if the markings for the location of the phase center are not at the true location for different antennas, this will cause a bias in the height component of the GPS base line measurements. Other tests may be needed to determine procedures to ensure optimum orientation of the antenna and optimum resistance to multipath effects.

Field Procedures

The precision of the GPS vector base line results depends on the number of satellites visible simultaneously from each station during an observing session, their geometric relationships, duration of the period when the desired number of satellites can be observed simultaneously, and the length of line. The number of possible observing sessions per observing day is a function of the required survey accuracy, satellite availability, and project logistical considerations such as transit time required between session station setups.

Currently, the incomplete GPS satellite constellation (seven of the 18 satellites) limits the observing period when three or more satellites are available to approximately 6 hours each day. This period of availability varies depending on the location of the project. When the 18-satellite constellation is available, at least four satellites will be available for simultaneous observations from anywhere on Earth at all times.

The factors that will be considered for the field procedure specifications are:

1. Two frequency observations required? (If yes, but two-frequency observations are not possible, an alternate method for estimating the ionospheric refraction will be necessary, such as modeling the ionosphere using two-frequency data obtained from other sources.)

2. Minimum number of receivers observing simultaneously.

3. Period of observation (in hours) not less than __.

4. Maximum time interval (in seconds) between observations or data collection rate.

5. Minimum independent occupations per station. (When two or more independent occupations of each station are specified, this will be for the purpose of detecting observation errors such as those caused by receiver biases, antenna centering, and height offset errors. When a station is occupied during two

or more sessions, back-to-back, the antenna/tripod will be reset and replumbed between sessions to meet the criteria for an independent occupation.)

6. Minimum base lines from each station.

7. Number of satellites observed during session, not less than __.

8. Minimum number of satellites observed simultaneously.

9. Minimum period for each three-satellite combination observed simultaneously in minutes.

10. Minimum number of quadrants with satellite observations.

11. Number of antenna phase center height measurements per session not less than __.

12. Maximum cutoff angle in degrees above horizon for observations.

13. Minimum meteorological observations per observing session.

14. Water vapor radiometer measurements required?

15. Frequency standard warm-up time in hours: crystal and atomic.

Although there has not been any report of interference affecting quality of data, the antenna should be located where potential radio interference is minimal for the 1227.6 and 1575.42 MHz frequencies (GPS L1 and L2 signals). High-powered radar and transmission antennas should be avoided.

The antenna must be stably located within 0.5 mm (1 sigma) over the station mark for the duration of the observations. The height difference between the mark and the reference point for the antenna phase center will be measured to the nearest 0.5 mm (1 sigma). If an antenna is moved during an observing session, the set of observations for that session is not acceptable.

The power source for the survey equipment must be stable and continuous to minimize unnecessary breaks in the observations or damage to the equipment that would affect the quality of the data.

Observations of temperature and relative humidity should be collected at or near the location of the phase center of the antenna. Observations of wet-bulb and dry-bulb temperature readings should be recorded to the nearest 0.5°C. Barometric readings at the station site should be recorded to the nearest millibar and corrected for any significant difference in height between the antenna and barometer. The meteorological instruments should be brought together and compared at least once per week and compared against a standard at least once per month.

Office Procedures

The criteria for processing and determining the quality of GPS relative positioning results are as follows:

1. The cutoff angle for data points should be 15°.

2. The coordinates for the station held fixed in the base line solutions must be referenced to the satellite datum (presently WGS-72). It must be accurate

to ± 10 meters. These coordinates may be determined from a point position reduction of GPS or Transit Doppler observations, or by transforming known coordinates in the North American Datum to the satellite datum.

3. Processing must account for the offset of antenna phase center relative to the station mark in both horizontal and vertical components.

4. The number of phase data observations rejected (excluding cutoff angle and nonsimultaneous observations) for a solution should be less than 10 percent of the total.

5. Depending on the number of observations, quality of data, method of reduction, and length of base lines, the standard deviation of the range residuals in the base line solution should be between 0.1 and 2 cm. It should not exceed 2 cm.

6. The formal standard errors of base line components should be less than 2 cm.

Triangle and loop closures, and differences in repeat base line measurements will be computed to check for blunders and to obtain initial estimates for the internal consistency of the GPS network. After correcting for any blunders, the user should perform a minimally constrained least squares adjustment and examine the normalized residuals. The observation weights should be verified as realistic. Vector component (relative position) standard errors computed by error propagation between points in a correctly weighted minimally constrained least squares adjustment will indicate the maximum achievable precision for the **special** classification.

The constrained least squares adjustment will use models which account for: the reference ellipsoid for the network control, the orientation and scale differences between the satellite and network control datums, geoid-ellipsoid relationships, the distortions in the network control, and instability in the control network due to horizontal and/or vertical motion. Length relative accuracy computed by error propagation in a correctly weighted minimally constrained least squares adjustment will indicate the maximum achievable accuracy for the **general** classification level. The final classification should not exceed the order for the existing network control.

A summary of factors which will aid in the classification of minimally constrained least squares adjusted results are:

1. Triangle and loop closure (valid only when two or more base lines in the triangle or loop analysis were determined from independent observations).

   a. In any component, average in centimeters not to exceed ___.

   b. In any component, maximum in centimeters not to exceed ___.

   c. Overall, in any component, maximum rms in centimeters not to exceed ___.

2. Repeated base lines

   a. In any component, average difference in centimeters not to exceed ___.

   b. In any component, maximum difference in centimeters not to exceed ___.

   c. In length, average difference in centimeters not to exceed ___.

d. In length, maximum difference not to exceed (cm)

SUMMARY

Revisions to the FGCC standards of accuracy are proposed to meet the classification requirements for high-precision surveys performed by GPS relative positioning techniques and other measurement systems such as VLBI and satellite laser ranging. The proposed revisions would be incorporated into two sets of classification standards: **special** and **general.**

Factors are given that will be considered in development of specifications for geodetic surveys performed by GPS relative positioning techniques. These factors are based on extensive field and office experience gained at the NGS over the past 2 years and from reports prepared by numerous researchers within and outside of the United States.

After the proposed revisions to the accuracy standards and preliminary specifications for geodetic surveys by GPS relative positioning methods have been subjected to further review within NGS, they will be submitted to the U.S. Federal Geodetic Control Committee for final consideration. The FGCC, a U.S. interagency committee, is officially responsible for the adoption of standards and specifications for geodetic control networks. Comments will also be solicited from experts in GPS relative positioning techniques. After this review and approval have been completed, they will be incorporated into the FGCC Standards and Specifications for Geodetic Control Networks.

REFERENCES

Beck, N., D. Delikaraoglou, K. Lochhead, D.J. McArthur and G. Lachapelle, 1984: Preliminary results on the use of GPS positioning for geodetic applications, presented at the Position Location and Navigation Symposium, San Diego, CA, November 28-30, 6 pp.

Beutler, G., D.A. Davidson, R.B. Langley, R. Santerre, P. Vanicek and D.E. Wells, 1984: Some theoretrical and practical aspects of geodetic positioning using carrier phase difference observations of GPS satellites, Technical Report No. 109, University of New Brunswick, Fredericton, N.B., 83 pp.

Bock, Y., R.I. Abbott, C.C. Counselman, S.A. Gourevitch, R.W. King, and A.R. Paradis, 1984: Geodetic accuracy of the Macrometer^{TM} model V-1000, Bulletin Geodesique, 58 (2), pp. 211-221.

Collins, J. and A. Leick, 1985: Montgomery County (PA) GPS survey, Technical Papers of the 45th Annual Meeting of the American Congress on Surveying and Mapping, Washington, D.C., March 10-15, 1985, pp. 512-527.

Federal Geodetic Control Committee, 1984: Standards and Specifications for Geodetic Control Networks, National Geodetic Information Center, NOAA, Rockville, Md., 20852, 34 pp.

Goad, C.C., and B.W. Remondi, 1983: Initial relative positioning results using the Global Positioning System, Bulletin Geodesique 58 (2), pp. 193-210.

Goad, C.C., 1985: Precise relative position determination using Global Positioning System carrier phase measurements in a non-differencing mode, Preceedings of the First International Symposium on Precise Positioning with Global Positioning System, April 15-19, Rockville, MD

Hothem, L.D., and C.J. Fronczek, 1983: Report on test and demonstration of Macrometer^{TM} model V-1000 interferometric surveyor, Federal Geodetic Control Committee, Report FGCC-IS-2, National Geodetic Information Center, NOAA, Rockville, MD, 36 pp.

Hothem, L.D., C.C. Goad, and B.W. Remondi, 1984: GPS satellite surveying - practical aspects, The Canadian Surveyor, Vol. 38, No. 3, Autumn, pp. 177-192.

Langley, R.B., G. Beutler, D. Delikaraoglou, B. Nickerson, R. Santerre, P. Vanicek, and D.E. Wells, 1984: Studies in the application of the global positioning system to positioning, Technical Report No. 108, Department of Surveying and Engineering, Univ. of New Brunswick, Fredericton, N.B., 295 pp.

Leroy, C.F., 1982: The impact of GRS80 on DMA products, Proceedings of the Third International Geodetic Symposium on Satellite Doppler Positioning, Las Cruces, New Mexico, February 8-12, pp. 129-150.

Remondi, B.W., 1983: GPS geodetic receivers - a status update report, Proceedings of the ACSM/ASP Convention, Washington, DC, March 13-18, pp. 441-448.

Remondi, B.W., 1984: Using the global positioning system (GPS) phase observable for relative geodesy: modeling, processing, and results, Ph. D. dissertation, CSR-84-2, Center for Space Research, The University of Texas at Austin, Austin, TX, National Geodetic Information Center, NOAA, Rockville, MD, 360 pp.

Remondi, B.W., 1985: Global Positioning system carrier phase: description and use, NOAA Technical Memorandum NOS NGS-42, National Geodetic Information Center, NOAA, Rockville, MD, January, 21 pp.

Rizos, C., A. Stolz and E.G. Masters, 1984: Surveying and geodesy in Australia with GPS, The Australian Surveyor, Vol. 32, No. 3, pp. 202-225.

ON THE ESTABLISHMENT OF 3-D GEODETIC CONTROL BY INTERFEROMETRY WITH THE TI-4100 GPS RECEIVER

Demitris Delikaraoglou, Norman Beck, Dave McArthur and Kim Lochhead

Geodetic Survey Division
Surveys and Mapping Branch
Energy, Mines and Resources
615 Booth Street, Ottawa
Ontario, CANADA K1A 0E9

ABSTRACT. We consider some theoretical and practical problems in establishing 3-D multistation, geodetic control networks using interferometric type observations of the Global Positioning System collected with Texas Instruments TI-4100 GPS receivers. The Canadian Geodetic Survey has established a precise calibration network in the Ottawa area where baselines ranging from 13 to 102 km were observed in 1984 with TI-4100 GPS receivers. Six of these baselines were previously measured using the Macrometer V-1000 Interferometric Surveyor which provides an extra comparison with the TI-4100 results. Results of the TI-4100 campaign are presented with emphasis on the associated analysis techniques and the comparison of the horizontal and vertical accuracies against independent terrestrial determinations.

INTRODUCTION

During May 1984, the Canadian Geodetic Survey (CGS) in cooperation with Nortech Surveys (Canada) Ltd. conducted an evaluation of the Texas Instruments TI-4100 geodetic receiver. The test was the second (the first was conducted in 1983 with the Macrometer V-1000 Interferometric Surveyor) in a series of evaluations of currently available geodetic receivers that use radio signals from the satellites of the Global Positioning System (GPS). The collected data were processed to determine precise 3-D positions of the survey stations without requiring interstation visibility. Five stations located in the vicinity of Ottawa, Ontario were occupied during the test. Two cesium clock aided TI-4100 receivers were employed to obtain simultaneous P-code and carrier phase measurements in two frequencies in a total of 13 sessions. The evaluation and analysis of the data was focused on the operational aspects, data processing techniques and the accuracy of the estimated positions.

In this paper we consider some theoretical and practical aspects particularly with regard to (a) the use of an efficient short-arc orbit computation comparable in ease of use to the broadcast orbit approximation but with orbit shape accuracy comparable to that of the precise ephemerides, (b) the approach of differencing data from two stations to determine their relative position vector leading to (c) a more generalized approach of combining the measurements on several baselines into one "short-arc" analysis in which some orbital parameters are estimated simultaneously with the station coordinates of all the stations in the network.

ON THE MODELLING OF THE GPS SATELLITE ORBITS

With the TI-4100 receivers, which can decode the GPS signal, the orbital information needed for processing the collected data is obtained by occasional dumps (typically every hour) of the broadcast ephemeris reports (Texas Instruments, 1984). These broadcast ephemerides are based on 24 hourly predictions from historical and near-real time tracking by the U.S. DoD. Although no detailed assessment of the orbits they represent is currently available, the satellite positions computed from the broadcast message are believed to be accurate to 5 to 20 m. For differential applications, although far less sensitive to orbital uncertainties than point positioning, baseline determinations using the carrier phase observations are still limited in accuracy by orbit errors. The problem with the broadcast orbits is that although they are seemingly adequate for a few parts per million (ppm) relative positioning, they must be fresh, i.e. they should only be used for the one hour for which they are intended. Extrapolation beyond that leads to an exponential growth of truncation error (van Dierendonck et al, 1978). Even if no extrapolation is attempted, satellite positions for the same epoch determined from two adjacent broadcast messages tend to show significant discontinuities of the order of several metres which can severely bias the final results. In particular, a distorted orbital shape can affect the relative positioning accuracy especially for large station separations and a short time span of data.

Alternatively, short-arc orbit computations by numerical or analytical integrations of the equations of motion can be used, although such procedures can be relatively involved and computationally expensive. In this connection, at CGS we have investigated the use of short-arc orbits evaluated more efficiently by means of least squares approximations of the second derivatives $\ddot{x}$, $\ddot{y}$, $\ddot{z}$ of the GPS satellites evaluated from a low degree and order geopotential model. This approach, which has been applied successfully in the past in our TRANSIT Doppler GEODOP software (Kouba, 1983), essentially uses a least squares approximation by Tchebychev polynomials for positions, velocities and accelerations. The latter are evaluated from the well known equations of motion

$$\begin{aligned} \ddot{x} &= \frac{\partial V}{\partial x} + 2\omega\dot{y} + \omega^2 x \\ \ddot{y} &= \frac{\partial V}{\partial y} - 2\omega\dot{x} + \omega^2 y \\ \ddot{z} &= \frac{\partial V}{\partial z} \end{aligned} \qquad (1)$$

where ω is the angular rotation rate of Earth and V is Earth's gravitational potential obtained from a truncated expansion at degree and order N of a series of spherical harmonics (Vanicek and Krakiwsky, 1982)

$$V = \frac{GM}{r} \{ 1 + \sum_{n=2}^{N} \sum_{m=0}^{n} (\frac{a}{r})^n P_{nm}(\sin\phi) [C_{nm} \cos m\lambda + S_{nm} \sin m\lambda]\}. \qquad (2)$$

Here GM is the product of the mass of Earth and the gravitational constant; a is the major semi-axis of the reference ellipsoid; r, ϕ and λ are the satellite radius, geocentric latitude and longitude; and $P_{nm}(\sin \phi)$, C_{nm} and S_{nm} are normalized Legendre functions and geopotential coefficients respectively.

In principle only six initial conditions at some time t_0, e.g. x_0, y_0, z_0 and $\dot{x}_0$, $\dot{y}_0$ and $\dot{z}_0$, and accelerations evaluated according to equ. (1) at regular intervals are required for the Tchebychev approximation leading to the solution of the differential equations of motion via the Tchebychev polynomials. The latter and their first derivatives at t_0, and their second derivatives at the regular intervals are computed by recursive formulae (e.g. Davies, 1975). In practice however, several state vectors are usually used. For the case of the GPS satellites, at CGS we make use of adjacent broadcast (hourly) ephemeris reports to evaluate initial boundary conditions at regular epochs

$$t_i = t_{oe} + i\ \Delta t,\ t_i\ \varepsilon [t_{oe} - 5\ \text{min};\ t_{oe} + 5\ \text{min}], \qquad (3)$$

$$i \varepsilon [\ldots, -2, -1, 0, 1, 2, \ldots]$$

where t_{oe} is the reference epoch of the particular broadcast ephemeris segment and Δt is a a specified interval usually chosen as 1 minute.

This in effect results in (a) taking advantage of the nearly correct (with respect to the true orbit) representation of the broadcast orbit in the vicinity of the ephemeris reference time, and (b) averaging the initial conditions over these points in several segments to minimize coordinate system (i.e. position and orientation) changes in the longer arc orbits we try to represent by the Tchebychev polynomials, and hence smooth out the otherwise discontinuous orbital arcs represented by the hourly broadcast segments.

Table 1 summarizes some representative results on the differences between the short-arc (5 hours in this case) orbit computations based on the Tchebychev approximation and the corresponding hourly segments of the broadcast ephemeris of each satellite visible in Ottawa on the days 139 and 147, 1984. As is apparent from Table 1, the mean differences for all satellites are well within the error bounds of the broadcast ephemeris and they reflect, we believe, errors in the broadcast segments rather than the continuous and smooth Tchebychev orbit. Supporting this argument from Figure 1, the forementioned deviations (discontinuities) of the adjacent broadcast segments from the smoothed 9th order Tchebychev polynomial orbit (using GEM-9 to degree and order 10) are readily apparent. The small remaining slopes and curvatures are likely due to both the polynomial approximation itself, the model truncation, the neglected lunisolar body attractions, the radiation pressure, etc. and to a lesser extend the difference in the two gravity field models used, i.e. GEM-9 and NSWC-10F which is used for the broadcast orbit generation.

TI-4100 DATA ANALYSIS

One of the observables obtained from the TI-4100 receivers is the one-way phase of the signal received from each of up to four satellites each with respect to a reference signal that is derived from the receiver oscillator. The phases of all four received carrier signals are tracked simultaneously at specified times governed by the receiver clock: usually at 3 sec epochs throughout a user specified time span. Each satellite is tracked continuously and the phase is accumulated from the first measurement onward. A major source of error in these one-way phase measurements is the variation of the phase of the transmitting and the receiving reference oscillators. In an attempt to eliminate or greatly reduce these errors, it is convenient to start the processing by differencing the phases of the signals received simultaneously at two stations because in this way the effects of the errors which are common to both measurements being differenced are nearly completely removed. Such measurements can be differenced across receivers, across satellites and across time with each successive level of differencing leading to the fundamental single, double and triple difference observables respectively [Delikaraoglou et al., in prep]. If the stations are closely spaced the differencing cancels most of the effects of the atmospheric refraction and most of the satellite modelling errors. The residual errors of both the atmospheric and orbital mismodelling are then affecting the results by a factor approximately proportional to the length of the baselines, i.e. the baseline determination uncertainties tend to be proportional to the ratio of the satellite altitude and the baseline length.

On the practical side, the optimal way of differencing the one-way phase data collected simultaneously by $n(n > 2)$ receivers and combining the double or triple difference observations to determine the coordinates of all the stations in the network can be a thorny problem. This is because the reduction of the GPS signals in this case can be performed in two ways: (a) in the simultaneous mode, akin to the familiar TRANSIT Doppler multistation translocation or VLBI processing, or (b) in the vector mode where the baseline-by-baseline approach is used in handling the data. So far, the majority of GPS surveys (including the Ottawa TI-4100 campaign) have involved the measurement of one baseline per day, requiring two receivers. Some networks have been surveyed using three (e.g. Bock et al, 1984) and occasionally more receivers (e.g. McArthur et al, 1985 in these proceedings) and splitting the available daily GPS coverage into two observing sessions, with a time gap for travel between stations. However, even in these cases, the "baseline-by-baseline" mentality has persisted in handling the data. To date, the general approach has been to reduce the data for each pair of stations of $n(n-1)/2$ baselines and then combine these partial results into an "occupation" adjustment enforcing the closure relations between baselines forming closed loops. The problem of this approach is that it suffers from the theoretical disadvantage that the correlations between the various combinations of vectors are not known, since instead of producing $(n-1)$ independent vectors, it yields $n(n-1)/2$ vectors. So the obvious question is what to do with the redundant ones. The practical difficulties in choosing the so called "trivial" baselines (e.g. for differential observations from two sides of a triangle of stations, observations from the third side are perfectly redundant - assuming perfect matching of observation schedules in all three sites) which are not to be used in a separate network adjustment has an unappealing arbitrariness (cf. Vincenty, 1985; McArthur et al, 1985 in these proceedings). The alternative approach of orthonormalizing the observations as suggested by Bock et al (1984) is not without its drawbacks, especially when using data series with frequent breaks and cycle slips.

To overcome these practical difficulties, at CGS we have opted for analyzing the data collected in a network of stations in one program run, whereby the station coordinates are adjusted to fit all the observations simultaneously in a "short-arc" analysis, very much as it is often done with TRANSIT Doppler observations, in which up to six orbital parameters can be estimated as well.

NUMERICAL COMPARISONS

The five stations occupied during the TI-4100 test campaign had first-order elevations and observed deflections and were all part of the national geodetic primary network. The baseline lengths between the sites varied between 12 km and 102 km as shown in Figure 2 and Table 2.

In order to assess the accuracy of the TI-4100 determinations of baseline lengths, azimuths, and ellipsoidal height differences, terrestrial surveys combined with TRANSIT were used as standards for comparison. The "ground truth" coordinates were computed by a 3-D adjustment of all available terrestrial observations in some 329 primary framework stations, and Doppler TRANSIT observations at 8 stations including the 5 GPS sites. A summary of the baseline lengths between the GPS occupied sites as derived from the combined adjustment and the Doppler reductions alone is given in Table 2. All the vertical undulations given in Table 2 were determined using CGS geoid software based on a Stokes integration and collocation approach using a combination of spherical harmonics (GEM-10B), gravity and observed deflections. The estimated 1σ accuracy for the absolute geoid heights is about 30-50 cm. However, the 1σ accuracy for geoid height differences is significantly better: in this case better than a decimetre because there was a good distribution of astronomic stations and the slope of the geoid is quite small.

In reducing the TI-4100 data collected during the campaign many different software options produced slightly different results making it often difficult to ascertain which result was the best. For this paper, we have opted for the following considerations: (a) to reduce the data using the triple difference observables; (b) to compare the results with the available terrestrial "truth" positions; (c) to include a comparison of "baseline" vs. "network" solutions; and (d) to compare the results for processing the data with or without estimation of residual clock synchronization errors, and with or without short-arc orbit improvement.

Decision (a) was justified because triple differences allow an easier automatic editing of existing cycle slips in the data, most satellite and receiver errors drop out in this approach, and because less modifications were needed in our software to accept TI-4100 data. The observation equation model for this type of observable is of the form [cf. Delikaraoglou et al, in prep]

$$
\begin{aligned}
\Delta^3\Phi^{jk}_{\alpha\beta}(\tau_1,\tau_2) &= \Delta^2\Phi^{jk}_{\alpha\beta}(\tau_2) - \Delta^2\Phi^{jk}_{\alpha\beta}(\tau_1) \\
&= \frac{f}{c}\{(\Delta\rho^{j}_{\alpha\beta}(\tau_2) - \Delta\rho^{k}_{\alpha\beta}(\tau_2)) - (\Delta\rho^{j}_{\alpha\beta}(\tau_1) - \Delta\rho^{k}_{\alpha\beta}(\tau_1))\} \\
&+ \frac{f}{c}\{(\dot\rho^{j}_{\beta}(\tau_2) - \dot\rho^{k}_{\beta}(\tau_2))\,\Delta T_{\beta}(\tau_2) - (\dot\rho^{j}_{\beta}(\tau_1) - \dot\rho^{k}_{\beta}(\tau_1))\,\Delta T_{\beta}(\tau_1)\} \\
&- \frac{f}{c}\{(\dot\rho^{j}_{\alpha}(\tau_2) - \dot\rho^{k}_{\alpha}(\tau_2))\,\Delta T_{\alpha}(\tau_2) - (\dot\rho^{k}_{\alpha}(\tau_1) - \dot\rho^{k}_{\alpha}(\tau_1))\,\Delta T_{\alpha}(\tau_1)\} \\
&+ f\{(\delta A^{j}_{\beta}(\tau_2) - \delta A^{j}_{\alpha}(\tau_2) - \delta A^{j}_{\beta}(\tau_1) - \delta A^{j}_{\alpha}(\tau_1)) \\
&- (\delta A^{k}_{\beta}(\tau_2) - \delta A^{k}_{\alpha}(\tau_2) - \delta A^{k}_{\beta}(\tau_1) - \delta A^{k}_{\alpha}(\tau_1))\} \qquad (4)
\end{aligned}
$$

where f denotes the L_1 GPS frequency, the $\Delta\rho_{\alpha\beta}$ terms denote differential ranges from the ground stations α and β to the satellite, $\dot{\rho}$ range rates, ΔT receiver clock errors (currently modelled as a polynomial in time) with respect to GPS time, τ denotes the time tag of the observations (the same for both stations), and δA denotes the combined ionospheric and troposheric effect on the signals.

The carrier phase data collected at each station were first edited for quality following the procedure described in Beck (1985) and differenced between stations to form single, double and triple difference observables (Delikaraoglou et al, in prep). Although for this campaign we collected data only on one baseline at a time, we felt that processing all the data from the baselines shown in Figure 1 from all observing sessions in one program run and computing one set of coordinates for the stations in the network, was the best possible way of analyzing the data. In all comparisons station PA was held fixed, so that for the baseline determinations, PA was considered the "reference end" and in the network solutions the "reference" station. All the reductions were involved with data for the period (about one hour) when three or four (SV 6, 8, 9 and 11) and occasionally five satellites (plus SV 4) were visible. The observations were adjusted in a sequential adjustment whereby the normal equations for the coordinates of the stations in the network were accumulated until all the data were processed. Since our software can eliminate or add new parameters between stages in the sequential adjustment, handling a variable number of clock and orbital parameters (i.e. estimating new clock offsets from day to day, and new orbit relaxation parameters) between sessions were not a problem.

In the following tables, all the results are with respect to the WGS-72 geocentric ellipsoid. Differences are given in cm for the latitude, longitude and height for the free end of the baseline, and for the azimuth and the length of each baseline (from antenna to antenna) emanating from the fixed station. In these solutions the ionospheric effects were removed by applying the standard two frequency first-order correction, whereas the tropospheric effects were modelled using Hopfield's model. We also used the option of estimating orbital parameters and station coordinates simultaneously. In essence, for each session the program can choose the orbital elements to be estimated according to a priori covariance information assigned by the user. For these runs given the one hour short-arcs and the relatively short to medium baseline lengths, we essentially constrained the orbital elements except the semi-major axis of the orbit and the offset in the time of the perigee passage for which we use an a priori sigma of 10 m and 1 sec respectively. Since the velocity of the GPS satellites is roughly 4 km/sec this allowed dealing with along-track errors up to 4 km. Residual clock synchronization errors were also estimated in the form of an offset from GPS time.

In Table 3, solution B1 compares three "baseline" solutions against the terrestrial survey values. All differences are well with the uncertainties of the terrestrial values. However, a comparatively larger orientation and scale difference is noted for the baseline PA-MO. In solution N1 we combine the data from the baselines in B1 and added the data from MO-6A and 6A-ME to get the extra redundancy in the determination of the coordinates of the three free stations. Immediately noticeable is the better agreement in the height component of both 6A and ME, but the same high difference in orientation and scale for the line PA-MO. Adding the data from the MO-ME session (solution N2) improved the mean and rms statistics somewhat but did not change the results significantly. From the practical viewpoint, however, loosely stated it indicates that spending an extra session on this line did not contribute any new information other than an extra check on the results.

To test the impact of correcting for ionospheric refraction in the results, the same reduction as with solution N1 was carried out but using only the L1 data. Note that for the shortest of the baselines, i.e. PA-MO there is an 8.4 cm change in length (as compared to the N2 solution) although the determined value seems to be closer to the terrestrial one. What is also noticeable is the complete reversal in the difference of the orientation of the same line. Quite suprisingly, the rms difference statistics in all but the height component are improved significantly in this solution. A possible explanation is that since all observations took place at night, spatial and temporal variations in the ionosphere lead to significantly different effects than those predicted by the two-frequency model. This is, of course, an argument favouring Macrometrics' approach, which is to ignore the ionospheric effect completely on such short baselines.

Next, we processed the data connecting the new station RENFREW. Solution B2 in Table 3 summarizes the results of the "baseline solutions" in which station RE was always assumed to be the free station in each case. Immediately noticeable are the large differences in the height component of RE, supporting the notion that the value of the terrestrial elevation is in error at the decimetre level. Indeed a re-levelling of the station revealed that the original elevation was 23.9 cm too high which agrees remarkably well with the estimated mean difference of 18.9 cm.

Other interesting statistics from Table 3 are the mean and rms differences for the ellipsoid height component values. Although a large portion of the noted rms values is probably due to the uncertainties in the terrestrial elevations and geoidal heights, it is encouraging to see that for stations less than 100 km apart it is possible to determine ellipsoid height differences sufficiently precise for many useful applications. For instance when accurate differences in elevations and orthometric heights are known between stations, one could determine geoidal height differences to a few centimetres. Conversely, if an accurate determination of the slope of the geoid can be made relative to a station with known elevation, an elevation at the unknown station could be determined at the same level of accuracy.

CONCLUDING REMARKS

The results achieved from the TI-4100 Ottawa test agreed very well with the terrestrial coordinate standard. The consistency of the differences in baseline lengths and azimuths between the GPS and terrestrially-derived positions indicate very clearly that the coordinates of one system can be adjusted to be compatible with the other system to within a few tenths of an arcsec in orientation and better than 2 ppm in scale. The results demonstrated that positioning accuracies of 1-2 ppm are feasible for distances between 10 and 100 km. There is no question that this new technology will produce a major redirection of positioning methodology accelerating the development that started with TRANSIT Doppler and inertial positioning methods.

The testing and the evaluation of the instruments mentioned in this paper do not constitute an endorsement intended or implied by CGS.

REFERENCES

Beck, N. (1985) - "Pre-processing Texas Instrument 4100 GPS Data" Geodetic Survey of Canada, Ottawa.

Bock, Y., R.I. Abbot, C.C. Counselman, S.A. Gourevitch, B.J. Rosen and R.W. King (1984) - "Establishment of Three-dimensional Geodetic Control by Interferometry with the Global Positioning System", submitted to Journal of Geophysical Research.

Davies, P.J. (1975) - "Interpolation and Approximation", Dover, New York.

Delikaraoglou, D., N. Beck, D.J. McArthur and K. Lochhead (in prep) - "A Tutorial Comparison of Geodetic Positioning Techniques Using the code and Carrier Phase Difference Observations of GPS Satellites", Geodetic Survey of Canada, Ottawa.

Kouba, J. (1983) - "An Efficient Short-arc Orbit Computation", Bull. geod. 57, pp. 138-145.

McArthur, D.J., N. Beck, K. Lochhead and D. Delikaraoglou (1985) - "Precise Relative Positioning with the Macrometer V-1000 (TM) Interferometric Surveyor: Experience at the Geodetic Survey of Canada", First International Symposium on Precise Positioning with the Global Positioning System, Washington, D.C., April 15-19.

Texas Instruments Inc. (1984) - "TI-4100 NAVSTAR Navigator Owner's Manual", Lewisville, Texas.

van Dierendonck, A.J., S.S. Russell, E.R. Kopitze and M. Birnbaum (1978) - "The GPS Navigation Message", Navigation, Journal of the Institute of Navigation, 25 (2), pp. 147-165.

Vanicek, P. and E.J. Krakiwsky (1982) - "Geodesy: The Concepts", North Holland, Amsterdam.

Vincenty, T. (1984) - "On the Use of GPS Vectors in Network Adjustments", U.S. NGS, personal communication.

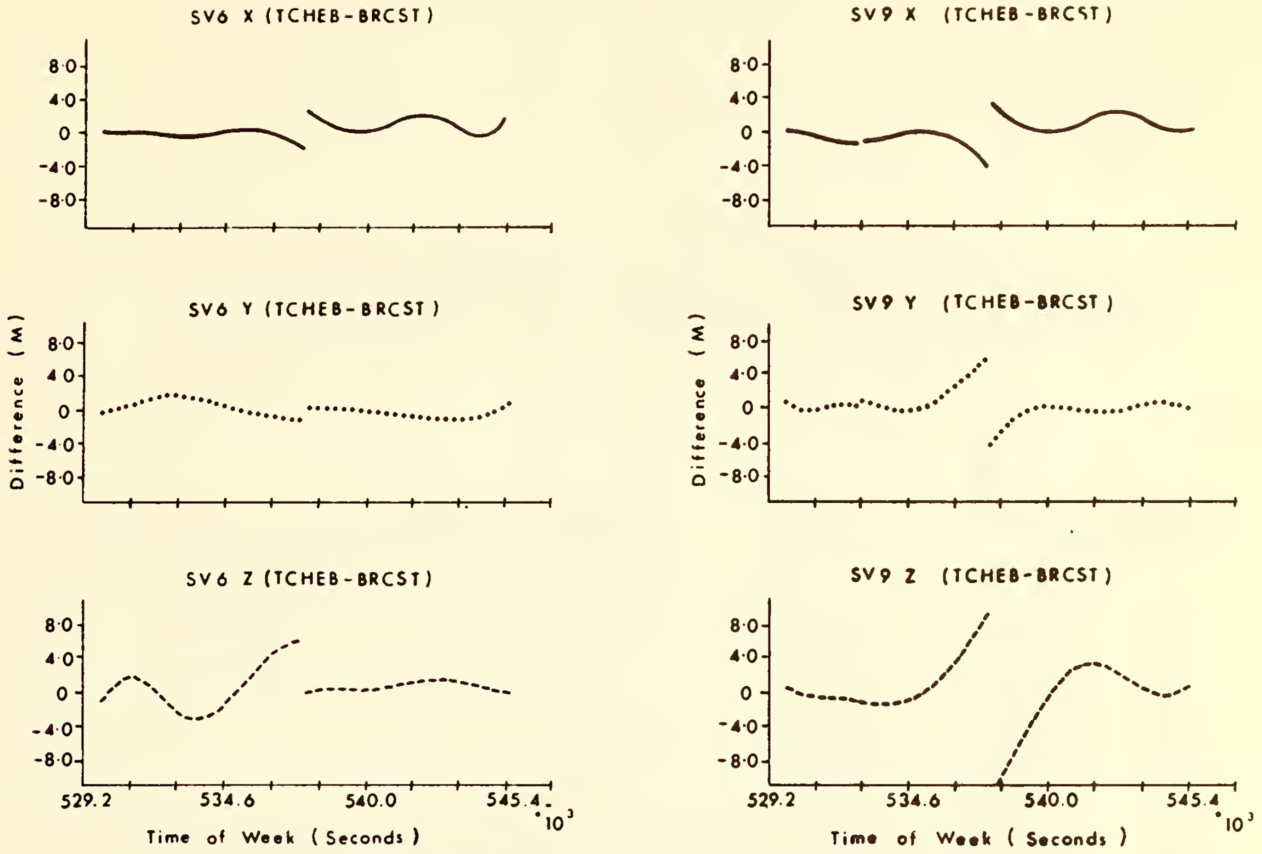

Fig. I TCHEBYCHEV APPROXIMATION - BROADCAST ORBIT DIFFERENCES (Day 147, 1984)

Fig. 2 OTTAWA GPS TEST NETWORK

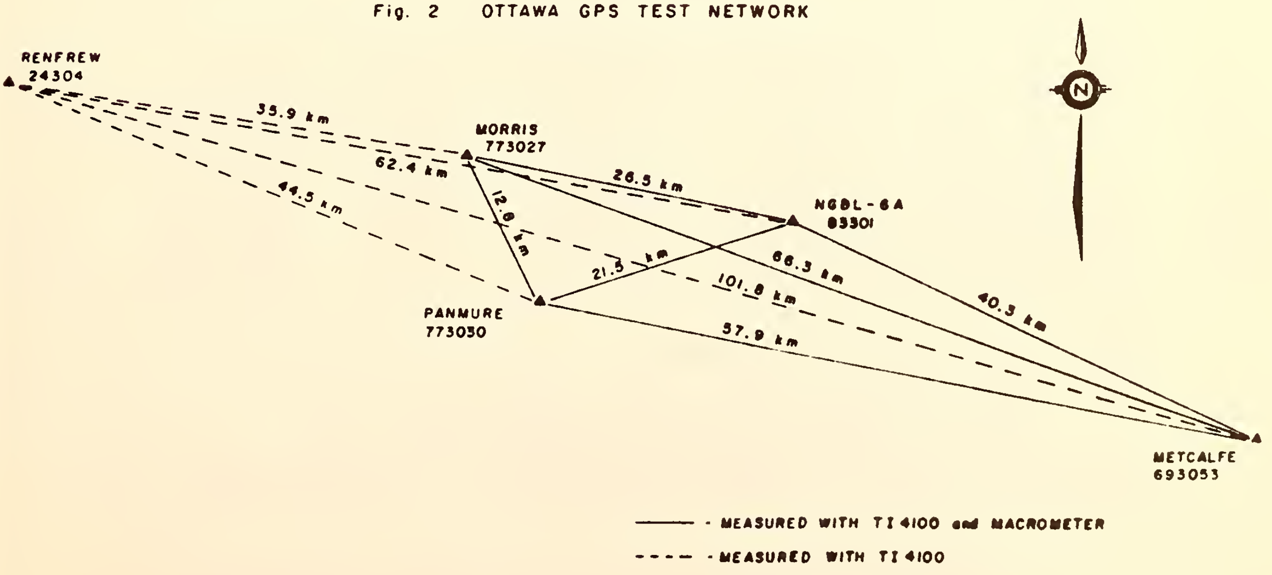

DAY		SAT #6			SAT #8			SAT #9			SAT #11		
		X	Y	Z	X	Y	Z	X	Y	Z	X	Y	Z
139	MEAN DIFF (m)	-0.0	-0.6	-0.2	1.2	1.7	0.0	-0.2	-0.7	-0.2	-2.0	1.6	-0.3
	RMS DIFF (m)	0.4	0.8	1.1	2.6	3.7	0.5	0.6	1.2	1.6	4.8	3.2	0.9
147	MEAN DIFF (m)	0.1	0.0	0.2	-0.0	-0.0	-0.1	0.1	0.1	-0.1	0.3	-0.1	0.0
	RMS DIFF (m)	0.4	0.4	1.0	0.6	0.2	1.6	0.7	0.8	1.9	0.9	0.6	0.4

TABLE 1

COMPARISON OF SHORT-ARC ORBITS COMPUTED FROM TRUNCATED GEM-9 POTENTIAL MODEL AND 9TH ORDER TCHEBYCHEV POLYNOMIAL APPROXIMATIONS WITH GPS BROADCAST EPHEMERIS

	TERRESTRIAL SURVEY BASELINE LENGTH (m)	TRANSIT DOPPLER	MACROMETER V-1000 BASELINE LENGTH (m)	n
PA-ME	57930.399	57930.853	57930.719 +/- 0.187	6
PA-MO	12843.828	12843.747	12843.671 +/- 0.061	4
PA-6A	21590.397	21590.545	21590.247 +/- 0.008	3
MO-ME	66268.762	66268.791	66268.743 +/- 0.126	3
MO-6A	26488.976	26489.138	26489.007 +/- 0.098	4
ME-6A	40295.446	40295.403	40295.423 +/- 0.041	4
PA-RE	44449.259	44449.698		
MO-RE	35905.169	35905.705		
ME-RE	101789.397	101790.014		
6A-RE	62388.116	62388.747		

n = number of independent baseline determinations

STATION DEFLECTIONS			HEIGHTS (m)			
			Ellipsoid	Orthometric	Geoid	Antenna
PAnmure	2.33	2.72	113.65	153.946	-40.30	1.60
6A	-0.30	1.69	37.13	77.085	-39.96	0.00
MEtcalfe	-1.33	2.12	63.39	102.730	-39.34	1.27
MOrris	0.21	2.51	49.11	89.605	-40.50	1.47
REnfrew	0.38	3.44	181.93	222.354	-40.66	1.46

TABLE 2

BASELINE LENGTHS, DEFLECTIONS AND HEIGHTS FOR THE OTTAWA TEST NETWORK (MACROMETER VALUES ARE UNWEIGHTED MEANS OF n DETERMINATIONS)

BASELINE	LENGTH (m)	Δφ	Δλ	Δh	ΔA	ΔL	(ppm)
BASELINE SOLUTIONS - B1							
PA-6A	21590.262	-2.6	-1.4	9.0	2.0	-2.1	0.9
PA-ME	57930.742	-0.8	1.1	-7.2	0.6	1.2	0.2
PA-MO	12843.810	9.9	1.3	3.4	5.4	8.4	6.5
Mean		2.1	0.3	1.7	2.7	2.5	2.5
Rms		6.7	1.5	8.2	2.5	5.4	3.4
NETWORK SOLUTION - N1 (ALL BASELINES IN B1 PLUS MO-6A, 6A-ME)							
PA-6A	21590.288	-0.2	0.5	0.2	0.3	0.4	0.2
PA-ME	57930.722	-2.3	-1.1	1.6	2.5	-0.7	0.1
PA-MO	12843.799	8.8	1.5	3.8	5.1	7.3	5.7
Mean		2.1	0.3	1.9	2.6	2.3	2.0
Rms		5.8	1.3	1.8	2.4	4.3	3.2
NETWORK SOLUTION - N2 (AS IN N1 PLUS MO-ME)							
PA-6A	21590.288	-0.2	0.5	0.2	0.3	0.4	0.1
PA-ME	57930.725	-1.4	-0.7	1.6	1.5	-0.4	0.1
PA-MO	12843.793	7.9	1.1	4.3	4.4	6.7	5.2
Means		2.1	0.3	1.9	2.0	2.3	1.8
Rms		5.0	0.9	2.1	2.1	3.9	2.9
NETWORK SOLUTION - N3 (AS IN N2 USING L1 DATA ONLY)							
PA-6A	21590.304	0.5	1.9	-7.8	0.1	2.0	0.9
PA-ME	57930.733	1.5	0.6	-0.9	-1.6	0.3	0.1
PA-MO	12843.709	-2.4	-1.1	2.3	-2.1	-1.6	1.2
Means		-0.1	0.5	-2.1	-1.2	0.2	0.7
Rms		2.0	1.5	5.2	1.2	1.8	0.6
BASELINE SOLUTIONS - B2							
PA-RE	44449.272	8.6	4.8	-11.3	9.7	-1.2	0.3
6A-RE	62388.130	-10.9	-5.3	-5.9	-11.6	3.4	0.5
ME-RE	101789.420	-0.1	2.8	-24.2	0.6	-2.9	0.3
MO-RE	25905.167	2.6	3.4	-34.3	3.0	-3.2	0.9
Mean		0.1	1.4	-18.9	0.4	-1.0	0.5
Rms		8.2	4.6	12.8	8.9	3.0	0.3

TABLE 3

COMPARISON OF GPS DETERMINED COORDINATES, AZIMUTHS AND BASELINE LENGTHS FOR OTTAWA TEST NETWORK IN CM

Network Adjustment of Correlated Coordinate Difference Observations

Dennis G. Milbert
William G. Kass
National Geodetic Survey
Charting and Geodetic Services
National Ocean Service, NOAA
Rockville, Maryland 20852

ABSTRACT

Although a variety of models have been proposed for processing Global Positioning System (GPS) carrier phase data, the models bear the common trait of reducing the data into a set of correlated coordinate differences. These coordinate differences (vectors) are then combined in a least squares adjustment. In this paper we explore different methods of parameterizing the vectors. The least squares adjustment of correlated vectors is then reviewed. Consideration is given to error propagation in large, sparse systems. Computation of redundancy numbers, variance factor estimates, and marginally detectable errors is discussed for large networks of correlated observations. Numerical examples from the adjustment of a GPS survey are presented. These examples are computed using program ADJUST, a portable computer program for the least squares adjustment of large networks of numerous types of geodetic observations.

INTRODUCTION

The processing of Global Positioning System (GPS) carrier phase data is usually divided into two steps. First, carrier phase measurements are combined with satellite ephemeris data to yield coordinate difference vectors in an Earth-centered, body-fixed (ECF) coordinate system along with associated covariance matrices. Second, these correlated coordinate difference "observations" are combined in a second least squares adjustment to produce the final coordinates. In this paper we will concentrate on this second adjustment and also explore the parameterization of coordinate difference vectors. Then we will turn our attention to the adjustment process for correlated observations, while giving special emphasis to large, sparse systems.

COORDINATE DIFFERENCE PARAMETERIZATION

The most natural model for coordinate difference vectors is the ECF system

$$\begin{bmatrix} \Delta X \\ \Delta Y \\ \Delta Z \end{bmatrix} = \begin{bmatrix} X_2 - X_1 \\ Y_2 - Y_1 \\ Z_2 - Z_1 \end{bmatrix} .$$

Here, the parameters (X,Y,Z) are referenced to the center of the earth.

Another alternative would be a Surface-Centered (SC) system,

$$\begin{bmatrix} \Delta X \\ \Delta Y \\ \Delta Z \end{bmatrix} = \begin{bmatrix} X_2' - X_1' \\ Y_2' - Y_1' \\ Z_2' - Z_1' \end{bmatrix} .$$

Here the parameters (X', Y', Z') are referenced to a point (X_o, Y_o, Z_o), usually in the center of the survey. The only advantage of the SC system is to allow computations with fewer significant digits of machine precision.

Next, one can rotate this SC system into the geodetic horizon at the reference point expressed as (X_o, Y_o, Z_o) or (ϕ_o, λ_o, H_o). This produces a Surface-Centered Geodetic Horizon (SCGH) system,

$$\begin{bmatrix} \Delta X \\ \Delta Y \\ \Delta Z \end{bmatrix} = R_o^{\,t} \begin{bmatrix} x_2 - x_1 \\ y_2 - y_1 \\ z_2 - z_1 \end{bmatrix}$$

where,

$$R_o = \begin{bmatrix} -\sin\lambda_o & \cos\lambda_o & 0 \\ -\sin\phi_o \cos\lambda_o & -\sin\phi_o \sin\lambda_o & \cos\phi_o \\ \cos\phi_o \cos\lambda_o & \cos\phi_o \sin\lambda_o & \sin\phi_o \end{bmatrix} .$$

The parameters (x,y,z) have a nominal orientation to east, north, and vertical.

Finally, one can generate a SCGH system at every control point, (X_i, Y_i, Z_i). This yields the Local Geodetic Horizon (LGH) system,

$$\begin{bmatrix} \Delta X \\ \Delta Y \\ \Delta Z \end{bmatrix} = R_2^{\,t} \begin{bmatrix} x_2 \\ y_2 \\ z_2 \end{bmatrix} - R_1^{\,t} \begin{bmatrix} x_1 \\ y_1 \\ z_1 \end{bmatrix} + \begin{bmatrix} X_2 - X_1 \\ Y_2 - Y_1 \\ Z_2 - Z_1 \end{bmatrix}$$

Now each parameter set (x_i, y_i, z_i) is oriented to the geodetic normal, and is referenced to its own unique reference point (X_i, Y_i, Z_i). More details on the LGH system may be found in Vincenty (1979).

The particular advantage of the LGH system is the ease with which one can model terrestrial measurements; that is, measurements which refer to the local gravity field, such as directions and zenith distances from a level theodolite. The observation equations are set up on the Local Astronomic Horizon (LAH) system, and are then rotated into the LGH system. It is easy to restrict parameter allocation and observation equation construction to yield vertical and horizontal adjustments (1-D and 2-D). And many times it is desirable to see variances and covariances expressed in a local horizon system. These come directly from the LGH system.

If one wishes to combine coordinate difference vectors with terrestrial data, then a LGH model is the method of choice. Otherwise, the ECF model is simplest. No matter which system is used to model the vectors, identical coordinates will be obtained in a full-rank system.

CORRELATED OBSERVATION ADJUSTMENT

Using the notation of Uotila (1967), the models discussed have the functional form

$$L_o = F(X_o) ,$$

where X_o is the initial estimate of our parameters. Let X_a be an improved estimate of our parameters where

$$X_a = X_o + X$$

and where X is a parameter correction. Then the misclosures, L, the residuals, V, and the actual observations, L_b, are related by

$$L = L_b - L_o ,$$

$$V = F(X_a) - L_b ,$$

when our model is linearized into observation equations

$$AX = L + V .$$

We compute corrections to our unadjusted model parameters by solving the normal equations

$$X = N^{-1} U = (A^t D^{-1} A)^{-1} A^t D^{-1} L .$$

To handle large adjustments, sparse matrix packages such as SPARSPAK by George and Liu (1978), LASSO (or BIBB) by Dillinger (1981) and HEART OF GOLD by Milbert (1984a) have been developed. Sparse matrix packages usually treat each observation equation as independent, and accumulate partial normal equations as

$$N + (1/d_i^2) A_i^t A_i \rightarrow N ,$$

where A_i is the row of A corresponding to the i-th observation.

To exploit such software for correlated observations, a transformation is applied to A and L,

$$A' = R^{-t} A$$
$$L' = R^{-t} L$$

where the prime notation denotes a result in a different vector space, and where

$$D = R^t R$$
$$R^{-t} = (R^{-1})^t .$$

That is, the rows of A and the associated elements of L which correspond to correlated observations are transformed using the Cholesky factor of the covariance matrix. These transformed observation equations are then accumulated into the normal equations. More detail on this method, sometimes known as observation decorrelation, may be found in Milbert (1985).

These sparse matrix packages have remarkable flexibility. Suppose one requires the diagonal elements of the covariance matrix of the residuals, D_v, for blunder detection. Following Uotila (1967),

$$D_v = D - D_a$$

where the covariance matrix, D_a, of the computed observations is computed as

$$D_a = A N^{-1} A^t .$$

This computation is not prohibitive. Hanson (1978) has shown that the inverse elements of a sparse, variable bandwidth profile can be computed in place, and can be computed at no greater cost than that incurred in computing only the diagonal elements of the inverse. And, the diagonal elements of D_a may be computed without involving any elements of the inverse outside a profile based on the elements of A which correspond to correlated observations.

El-Hakim (1981) considers a redundancy matrix

$$Q_r = D_v D^{-1} \ .$$

The diagonal values of this matrix are referred to as redundancy numbers and are used to indicate the reliability of the adjustment of individual observations. If D is correlated, then the property

$$0 \le q_{ii} \le 1$$

does not hold for all diagonal elements, q_{ii}. However we do have

$$0 \le \sum_{i}^{k} q_{ii} \le k \ ,$$

where q_{ii} is summed over the k rows of A which correspond to correlated observation.

Consider an alternative definition of the redundancy matrix,

$$Q_c = R^{-t} D_v R^{-1}$$

This may be easily computed by error propagation using the transformed observation equations,

$$Q_c = I - D_a' = I - A'N^{-1}A'^t$$

Again, the prime notation denotes the different vector space. For uncorrelated observations the diagonals of these matrices are equal. While this is not true for correlated observations, the sum of the diagonals, when summed over the k rows of A, are equal. That is,

$$\sum_{i}^{k} (q_{ii})_r = \sum_{i}^{k} (q_{ii})_c \ .$$

Recent work by Lucas (1985) on variance component estimation in large adjustments, using sparse matrix methods highlighted the Iterated Almost Unbiased Estimation (IAUE) method. In this procedure, one groups observations into k homogeneous sets, to each of which is associated a variance factor, f_i. In this case D could have the form

$$D = \begin{bmatrix} f_1 \ D_1^{\,0} & & 0 \\ & \ddots & \\ 0 & & f_k \ D_k^{\,0} \end{bmatrix}$$

The initial estimate of the k-th variance factor can be written as

$$f_k = \frac{(v^t D^{-1} v)_k}{tr(Q)_k} = \frac{(v'^t v')_k}{tr(Q)_k}$$

where Q can be Q_c. From the preceding discussion, it is seen that both the numerator and denominator are easily computed for cases of correlated observations. This is particularly important since the IAUE method is not always rapidly convergent.

As a measure of internal reliability, the i-th Marginally Detectable Error (MDE) can be computed by

$$\nabla_i = \left[\frac{\lambda}{(D^{-1} - D^{-1}AN^{-1}A^tD^{-1})_i}\right]^{\frac{1}{2}}$$

where the value of λ is selected based upon the α and β of the test (Baarda 1968). The MDE may be efficiently computed by

$$\nabla_i = \left[\frac{\lambda}{(D^{-1} - F\,N^{-1}F^t)_i}\right]^{\frac{1}{2}}$$

where

$$F = D^{-1}\,A\ .$$

One could compute F by back substitution using

$$R\ F = A'\ .$$

The needed elements of D^{-1} could be computed by a bordering method. That is, the diagonal elements of D^{-1} would be computed one at a time by reducing and backsolving a column containing one in the row of interest and zeroes elsewhere (Hanson 1978).

One can certainly question the utility of these marginally detectable errors for correlated observations. Both the correlated and the decorrelated GPS coordinate difference vector components are merely derived quantities that possess no special statistical significance. One should not rest content with "data snooping" on the individual components of a GPS coordinate difference vector or on the decorrelated values. For example, one step in the GPS surveying process is the measurement of antenna height. This step is subject to blunders and would profit by such "customized" error detection. A combination of GPS residual components on a specialized change of basis to highlight antenna height measurements is an intriguing possibility. However, the subject of test of hypothesis for GPS vectors (or any derived quantities) is quite broad and beyond the scope of this paper.

ADJUSTMENT EXAMPLES

We have selected a survey in Summit County, Ohio to illustrate these computations. This survey was conducted from September 20, 1983, through November 4, 1983, under operational conditions. Figure 1 shows a diagram of the survey. The survey contains seven horizontal control points, six vertical bench marks, and 25 new points. The survey spans about 50 km from east to west, and 35 km from north to south. The survey consists of 122 occupations in 56 sessions on 31 work days. Two receivers were used in 46 of the sessions, and three were used in 10 sessions. Typically, two, 2 1/2 hour sessions (each separated by 1/2 hour) were conducted each day. The receiver data were processed by a triple-difference model, which used a covariance decorrelation algorithm by Remondi (1984), to yield coordinate differences, or vectors, with associated covariance matrices. This algorithm is equivalent to a single-difference model over a baseline where cycle biases were not held fixed at integer values. This may have affected the accuracy of the results in a small way (Bock, et. al. 1984).

The following results were computed using a variant of ADJUST, the National Geodetic Survey (NGS) Horizontal Network Branch adjustment program (Milbert and Kass 1985). This program uses the LGH model described earlier due to its advantages in processing terrestrial data. Thirty eight points were adjusted in a survey network with 84 degrees of freedom. The large value of the variance of unit weight, 4.14, is due merely to the initial estimates of the GPS vector covariance and is not a reflection of gross systematic error (Milbert 1984b).

In order to compute the variance factor ratio (FGCC 1984), all horizontal terrestrial observations in the NGS data base were extracted from a geographic area bounding 40° 30' N to 41° 15' N and from 81° 0' W to 82° 15' W. All landmarks were deleted, and the "breakdown" survey for Portage County, Ohio was deleted, due to its large size and lower accuracy. Three hundred thirty points were adjusted in a combined network with 1387 degrees of freedom to yield a variance of unit weight of 0.80. The combined adjustment gave a variance factor for the GPS survey of 4.77. The ratio, 1.15, is well under an informal tolerance of 1.5. This tolerance, a threshold for significant systematic error, was computed in simulations by James R. Lucas of NGS. This is evidence that there is no detectable systematic error between the classical network and the Summit County GPS survey.

We next consider some results from the GPS survey without terrestrial observations. Table 1 provides examples of the redundancy numbers. The sum of the numbers for the components of selected vectors is given; the sum will range from 0 to 3. As the sum approaches 0, that observation is becoming "no-check". One such example is the line Air to 39 RHP. This line has the predominant strength on determining their relative position.

Table 1.--Some redundancy numbers

Line	Redundancy Sum
Louisville -- Square	1.21
Fire -- Square	1.92
Louisville -- Air	2.25
Air -- 39 RHP	0.39
39 RHP -- S 337	2.02
Hodge -- U 177	1.37
U 177 -- Baier	0.90
Air -- Chic	0.97
Chic -- Dorene	0.67
Dorene -- Manchester	0.41

Since we have 65 coordinate difference vectors in this adjustment of 84 degrees of freedom, we expect an average redundancy number sum of 1.3. We see that the "traverse" line, Manchester - Dorene - Chic - Air, tends to have lower redundancy numbers than other parts of the survey. This is not surprising. Even if Air and Manchester were absolutely determined by the remaining survey observations, the average value of the redundancy number sum along that line would be only 1.

Table 2 shows some values of the marginally detectable errors. These values are expressed as a range in millimeters for $\lambda = 9$. As mentioned earlier, one would not consider rejection of only one component of a coordinate difference vector. The values here do reflect the size of MDE's. These MDE's have been computed from formal values of the vector covariance matrices. They do not have the benefit of fixed integer biases. On the other hand, they have not been scaled by the a-posteriori variance of unit weight. These approximations should offset one another.

Table 2.--Some marginally detectable errors (λ=9)

Line		MDE range (millimeters)
Louisville	-- Square	11-29
Fire	-- Square	10-34
Louisville	-- Air	64-102
Air	-- 39 RHP	50-75
39 RHP	-- S 337	51-81
Hodge	-- U 177	25-72
U 177	-- Baier	19-56
Air	-- Chic	32-116
Chic	-- Dorene	32-116
Dorene	-- Manchester	32-116

In examining the values in table 2, recall that MDE's display the level at which an outlier is considered to be detected. Again, it is not surprising that the line, Manchester - Dorene - Chic - Air, possesses somewhat larger MDE's. Of course, if the same geometry were used with classical surveying methods, the MDE's would be much larger.

CONCLUSION

We have used the LGH system to model GPS coordinate differences in ADJUST. This parameterization has made the combination of GPS with terrestrial data painless and flexible. We also find that the various transformations of the observation equation coefficients provide efficient computation of the adjustment and supporting statistics. These preliminary results emphasize the need for more research in data snooping on correlated observations with special applications to GPS surveying.

REFERENCES

Baarda, W., 1968: A testing procedure for use in geodetic networks. Publications on Geodesy, New Series, Vol. 2, No. 5, Netherlands Geodetic Commission, Delft.

Bock, Yehuda, Abbot, R. I., Counselman III, C. C., Gourevitch, S. A. King, R. W., 1984: Establishment of Three-Dimensional Control by Interferometry with the Global Positioning System. Presented to American Geophysical Union Fall Meeting, San Francisco, California, December 3-7, 1984.

Dillinger, William H., 1981: Subroutine package for large, sparse, least squares problems. *NOAA Technical Memorandum*, NOS NGS 29, National Geodetic Information Center, NOAA, Rockville, Md. 20852, 18 pp.

El-Hakim, S. F., 1981: A practical study of gross-error detection in bundle adjustment. *The Canadian Surveyor*, 35(4), 373-386.

Federal Geodetic Control Committee, 1984: *Standards and Specifications for Geodetic Control Networks*. National Geodetic Information Center, NOAA, Rockville, Md., 20852.

George, Alan and Liu, Joseph W., 1978: User guide for SPARSPAK: Waterloo Sparse Linear Equations Package, *Report CS-78-30*, Department of Computer Science, University of Waterloo, Waterloo, Ontario.

Hanson, Robert H., 1978: A posteriori error propagation. *Proceedings of the Second International Symposium on Problems Related to the Redefinition of North American Geodetic Networks*, Washington, D.C., 427-445. National Geodetic Information Center, NOAA, Md. 20852.

Lucas, James R., 1985: A variance component estimation method for sparse matrix applications. *NOAA Technical Report NOS 111 NGS 33*, in press.

Milbert, Dennis G., 1984a: HEART OF GOLD: Routines for large, sparse least squares computations. *NOAA Technical Memorandum*, NOS NGS 39, National Geodetic Information Center, NOAA, Rockville, Md. 20852, 28 pp.

Milbert, Dennis, G., 1984b: Preliminary analysis of an operation global position system control survey. Presented to American Geophysical Union Fall Meeting, San Francisco, California, December 3-7, 1984.

Milbert, Dennis G., 1985: A note on Observation Decorrelation, Variances of Residuals, and Redundancy Numbers. *Bulletin Geodesique*, in press.

Milbert, Dennis G. and Kass, William, G., 1985: ADJUST: The horizontal observation adjustment program. *NOAA Technical Memorandum*, in preparation.

Remondi, Benjamin William, 1984: *Using the global positioning system (GPS) phase observable for relative geodesy: modeling, processing, and results*. Ph. D. dissertation, CSR-84-2, Center for Space Research, The University of Texas at Austin, Austin, Texas.

Uotila, Urho A., 1967: Introduction to adjustment computations with matrices (lecture notes), Department of Geodetic Science and Surveying, Ohio State University, Columbus, Ohio, 43210.

Vincenty, Thaddeus, 1979: The HAVAGO Three-Dimensional Adjustment Program. *NOAA Technical Memorandum* NOS NGS 17, National Geodetic Information Center, NOAA, Rockville, Md. 20852, 18 pp.

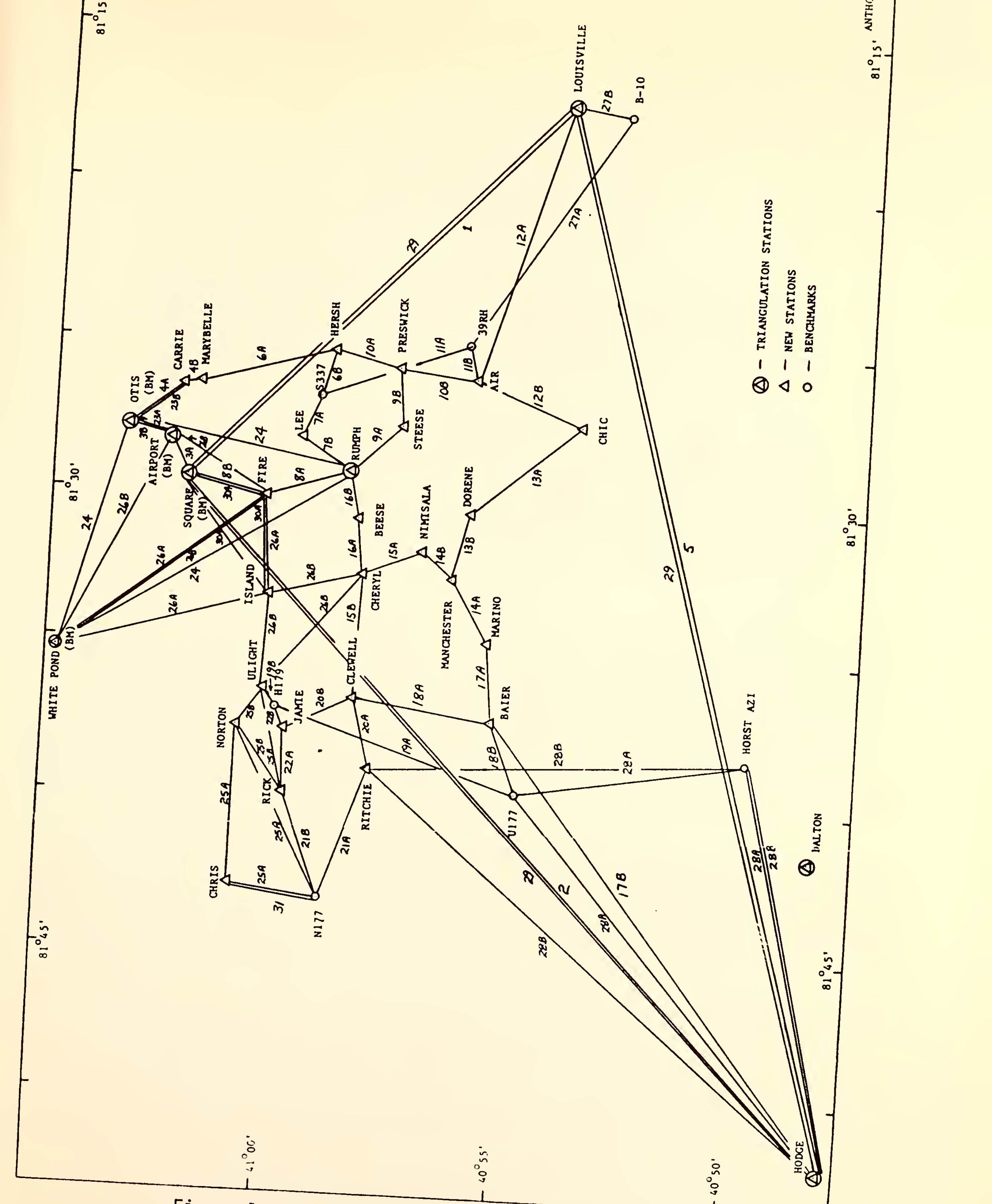

Figure 1.--Summit County, OH survey plan

VARIANCE ANALYSIS OF SATELLITE NETWORKS

Walter M. Welsch
Wolfgang Oswald
Universität der Bundeswehr München
Institut für Geodäsie
Werner-Heisenberg-Weg 39
D-8014 Neubiberg
Federal Republic of Germany

ABSTRACT. Programs being applied to the evaluation of satellite measurements provide besides the coordinates of the satellite network also their covariance matrix. However, it is difficult to decide definitely without further auxiliary data whether the covariance matrix obtained is correct.

In connection with the combined adjustment of a satellite network and the corresponding terrestrial network by applying techniques of variance-component estimation and S-transformations, one is in a position to check those results. It proves that the given covariance matrix of the satellite network adjustment has to be modified in order to obtain appropriate results for both the terrestrial and the satellite network. An example is given.

1. INTRODUCTION

The combination of classically performed terrestrial and satellite aided geodetic networks rank among the many tasks being attended with the establishment of satellite networks for national and engineering surveys. Doing so, several aspects are of importance. One of them is the functional connection of those heterogeneous networks. This is the problem of knotting together different reference systems whose interrelations are not clearly defined. As a rule the task is mastered by similarity transformations. It has often been treated as an extensive bibliography proves.

However, the stochastic problems occurring if different networks are combined, are hardly ever dealt with. Therefore, the investigations presented in the following intend to make a contribution by analyzing the accuracy of satellite networks. The analysis is exemplarily carried out by comparing two different satellite networks with a terrestrial network of high accuracy. For this purpose the terrestrial network takes in a way over the function of a comparator.

Before we go into particulars the procedure will be remarked on in general terms; some statistical tools will be explained, too.

2. THE GENERAL PROCEDURE OF NETWORK COMBINATION, AND THE ADJUSTMENT MODEL

Since the functional relations for the combination of a terrestrial and a satellite network are not subject of this paper, only the general procedure adopted is described.

In order to generate comparable coordinates, the satellite network was transformed onto the terrestrial network whose coordinates refer to the national geodetic datum. For the case being under consideration this transformation required the following steps:

- transformation of the cartesian geocentric satellite network coordinates X,Y,Z to coordinates φ,λ,h on the respective reference ellipsoid;
- projection of the ellipsoidal coordinates φ,λ,h to Gaussian coordinates x,y,h;
- 7-parameter similarity transformation of the Gaussian coordinates x,y,h onto the adjusted Gaussian coordinates x_T,y_T,h_T of the terrestrial network. The satellite coordinates, now x_S,y_S,h_S, can directly be compared with the terrestrial coordinates x_T,y_T,h_T;
- transformation of the covariance-matrix $C_{X,Y,Z}$ of the satellite network coordinates to the covariance-matrix $C_{x,y,h}$ of the transformed coordinates. For further particulars see Heister/Schödlbauer/Welsch (1985).

Several models have been established for the adjustment of network combinations. A relatively simple model regards the satellite coordinates as direct observations which are added to the observation equations of the terrestrial measurements. Therefore, the combined system of observation equations is

$$\begin{aligned} \ell_T + v_T &= Ax \ , \quad & P_T &= C_T^{-1} \\ \ell_S + v_S &= Ix \ , \quad & P_S &= C_{x,y,h}^{-1} \end{aligned} \tag{1}$$

(ℓ_T terrestrial observations, ℓ_S satellite coordinates x_S,y_S,h_S). The vector x of unknowns contains among others the point coordinates common to both types of networks.

In the case the satellite coordinates are used as approximate coordinates, $\ell_S = 0$. Then the normal equations are

$$(A^T P_T A + P_S)x = A^T P_T \ell_T \quad . \tag{2}$$

The cofactor matrix of the adjusted coordinates $\hat{x}$ is

$$Q_x = (A^T P_T A + P_S)^{-1} \quad . \tag{3}$$

From (3) one can immediately see that the weights of the coordinates of the terrestrial and of the satellite network are directly added. The interaction will depend on the respective size of the two parts and the resulting accuracies of the combined coordinates can be questioned in consideration of the nature (meaning, quality) of the terms of the sum. About this, investigations will be carried out in the following sections; they are essential part of this treatise.

3. VARIANCE COMPONENT ESTIMATION

When combining heterogeneous observations in one adjustment model, the difficulty arises how to adjoin proper weights to the individual groups of observations. If only one single type of observations is under consideration, it is by means of the estimated unit variance s_0^2 not difficult to find the proper weights. If, however, the network adjustment model contains several heterogeneous groups of interacting observations, the task becomes more complicated. This is all the more valid, if strongly geodetic datum affected observations or observation weights, e.g. coordi-

nate-observations and their covariance matrix, have to be processed. This dilemma can be overcome by the technique of estimating the variance components of the individual observation groups. Without any theoretical background, this technique will be illustrated briefly in the following (Welsch, 1981):
Starting point is the linear structure of the stochastic model of the observations. This allows the covariance matrix C of the observations to be dissected additively

$$C = \sigma_0^2 Q = \sigma_1^2 Q_{11} + \sigma_2^2 Q_{22} + \ldots + \sigma_k^2 Q_{kk} \quad . \tag{4}$$

σ_0^2 is the theoretical unit variance of all observations which is usually estimated by the empirical unit variance s_0^2. If the heterogeneous set of observations can be dissected into k homogeneous subsets, the cofactor matrix Q being the inverse of the weights $P = Q^{-1}$ can be split up correspondingly into submatrices $Q_{ii} (i \in 1,\ldots,k)$ for k uncorrelated groups of observations:

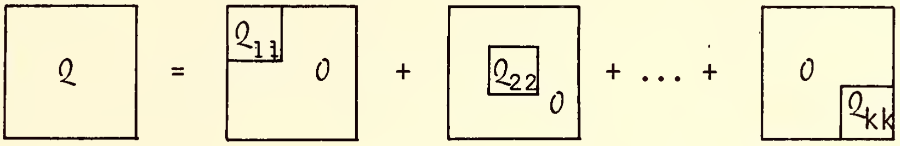

(5)

$$Q = Q_{11} + Q_{22} + \ldots + Q_{kk} \quad .$$

A variance component σ_i^2 belongs to the cofactor matrix Q_{ii} of each group of observations. Using the theory of variance component estimation (VCE), these components σ_i^2 can be estimated by

$$s_i^2 = \frac{v^T Q_{ii}^{-1} v}{\mathrm{tr}\{Q_{ii} Q^{vv}\}} \tag{6}$$

(v residuals, Q^{vv} their cofactor matrix). The estimation is iteratively repeated until all group variances converge. The results s_i^2 obtained are best, invariant and unbiased estimations of the group variances σ_i^2. Their knowledge is indispensable to the appropriate variance analysis and combination of networks of different types.

4. S - TRANSFORMATIONS

It is well-known that the covariance matrix of the adjusted coordinates is implicated in the geodetic datum constraints of the network. If, for instance, horizontal directions, spatial distances and zenith distances are introduced into a free three-dimensional network adjustment, the resulting datum defect is d = 4 (3 translations, 1 rotation around the h-axis). The remaining 3 datum dispositions are established by the scale of the distances and the plumbline of the vertical resp. of the zenith distances. Through these dispositions of 3 datum constraints the network is somehow restrained from being absolutely free. The restraints are reflected in the covariance matrix of the adjusted coordinates, too. Since this covariance matrix obtained from a "free" network adjustment is nevertheless affected by network external influences, it is called "external" covariance matrix C_x.

The actually obtained relative accuracy ("neighbouring" accuracy) has therefore to be represented by a covariance matrix released from any datum constraints. This "inner" covariance matrix C_x^1 (Rinner, 1969) can be derived from the external covariance matrix C_x by applying a 7-parameter S-transformation

$$C_x^i = (I - G\,(G^T G)^{-1}\,G^T)\; C_x\; (I - G\,(G^T G)^{-1}\,G^T)^T \;. \tag{7}$$

G is the coefficient matrix of the similarity transformation

$$G^T = \left|\begin{array}{cccccccc} 1 & 0 & 0 & 1 & 0 & 0 & \ldots \\ 0 & 1 & 0 & 0 & 1 & 0 & \ldots \\ 0 & 0 & 1 & 0 & 0 & 1 & \ldots \\ 0 & -z_1 & y_1 & 0 & -z_2 & y_2 & \ldots \\ z_1 & 0 & -x_1 & z_2 & 0 & -x_2 & \ldots \\ -y_1 & x_1 & 0 & -y_2 & x_2 & 0 & \ldots \\ x_1 & y_1 & z_1 & x_1 & y_1 & z_1 & \ldots \end{array}\right| \tag{8}$$

For the comparison of relative accuracies of network points all external influences have to be removed from the covariance matrices to be compared by applying the transformation (7). (This transformation does not affect the accuracy of estimable functions of the adjusted coordinates, as is well-known.) The difference between the external and inner covariance matrix will be made evident in the next sections.

5. THE TERRESTRIAL COMPARATOR "INN VALLEY NETWORK"

The INN VALLEY NETWORK of the Institut für Geodäsie of the Universität der Bundeswehr München covers a space of 25 km x 15 km x 1.3 km. All points but one are monumented by concrete pillars. The terrestrial coordinates were determined by 48 spatial distances, 44 horizontal directions, 44 zenith distances and 8 x 2 components of the deflections of the vertical. The network was adjusted in a minimum constraint three dimensional mode taking over the national geodetic datum. A more detailed description is given by Heister/Schödlbauer/Welsch (1985).

Due to lack of space only those results important for the comparison with the satellite networks are represented in a compressed form. Therefore, from the covariance matrices of the adjusted coordinates mean square values A and B for the major and minor semi axes of the error ellipses (1 σ - level) will be given, and the standard deviation s_h of the heights.

After VCE for the determination of the weights of horizontal directions, zenith distances and 3 types of spatial distances, the following accuracies are obtained (tab.1)

$${}_T C_x \;:\;\; A = \pm\, 4.9 \text{ mm},\; B = \pm\, 3.2 \text{ mm},\; s_h = \pm\, 36.4 \text{ mm}. \tag{9}$$

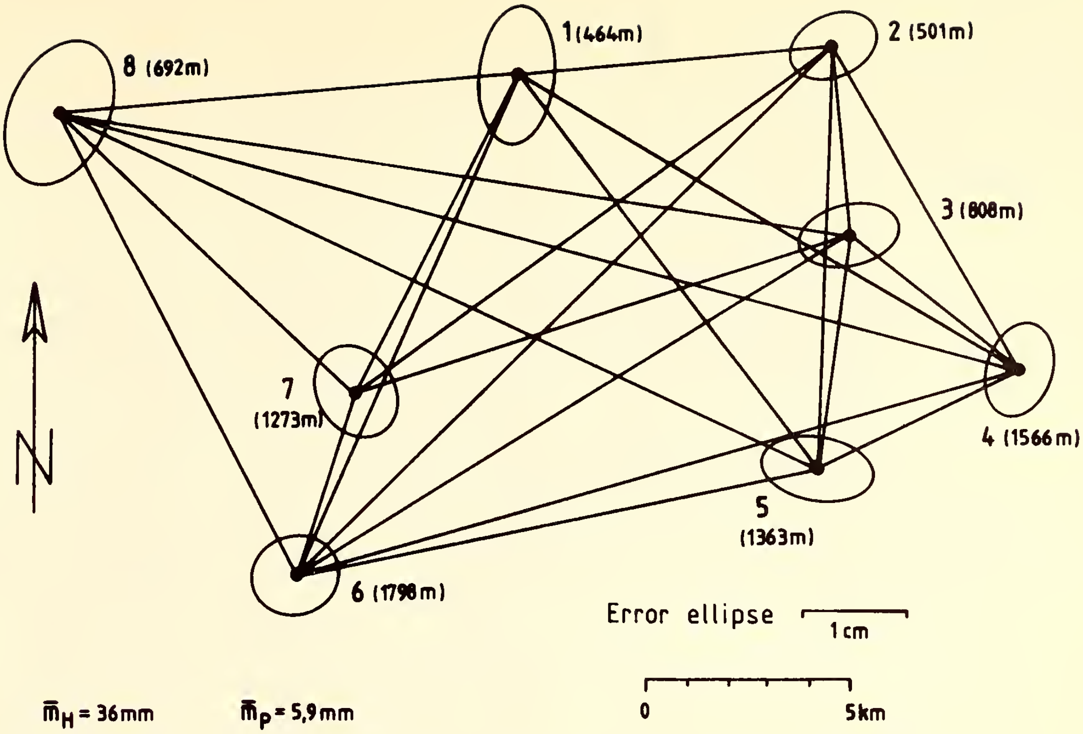

Fig.1: INN VALLEY NETWORK as terrestrial comparator

After S-transformation the corresponding values of inner accuracies are

$${}_{T}C_{x}^{i} : \quad A = \pm\ 4.6\ \text{mm},\ B = \pm\ 2.9\ \text{mm},\ s_h = \pm\ 21.3\ \text{mm}. \qquad (10)$$

As to be expected, the rotations around the x- and y- axes affect mainly the height accuracy from which strong datum effects are filtered off.

The accuracies (9) and (10) represent the terrestrial comparator in stochastic terms.

6. VARIANCE ANALYSIS OF A DOPPLER NETWORK

In October 1983 geocentric coordinates were determined (Magnavox MX 1502) for all the points of the INN VALLEY NETWORK (Heister/Glasmacher, 1984). Of course, the authors are conscious of the fact that the extension of the network with respect to satellite-Doppler measurements is small. Thus generally accepted conclusions can hardly be drawn. The variance analyses, however, lead nevertheless to some remarkable results (tab.1).

The multistation solution for the Doppler measurements (GEODOP 3) results in the external covariance matrix

$${}_{D}C_{x} : \quad A = \pm\ 648\ \text{mm},\ B = \pm\ 468\ \text{mm},\ s_h = \pm\ 198\ \text{mm}. \qquad (11)$$

Removal of all external influences leads to

$${}_{D}C_{x}^{i} : \quad A = \pm\ 84\ \text{mm},\ B = \pm\ 59\ \text{mm},\ s_h = \pm\ 50\ \text{mm}. \qquad (12)$$

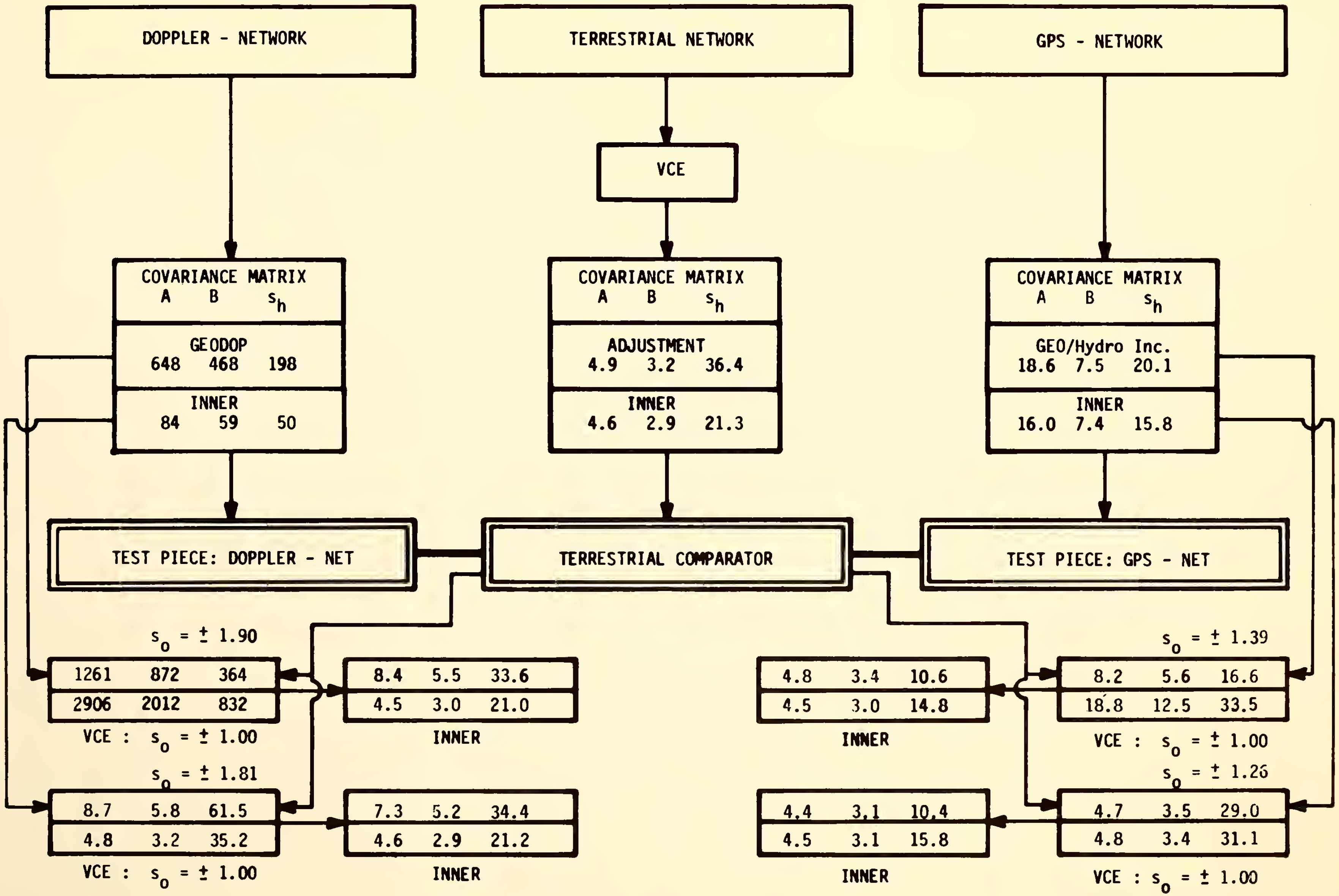

Table 1: VARIANCE ANALYSIS OF HYBRID NETWORKS
(all numbers are mm)

${}_{D}C_{x}^{i}$ proves the astonishingly high relative accuracy of Doppler measurements.

If at this stage the terrestrial observations are combined with the Doppler coordinates, one would, to begin with and for lack of better knowledge, introduce ${}_{D}C_{x}$ into the adjustment model (1) to obtain the weights P_S. The result, the covariance matrix ${}_{D+T}C_{x}$ of the combined coordinates, may surprise a little bit:

$$ {}_{D+T}C_{x} : \ A = \pm\ 1261 \text{ mm},\ B = \pm\ 872 \text{ mm},\ s_h = \pm\ 364 \text{ mm}. \tag{13}$$

However, $s_0 = \pm\ 1.90$ as the estimator of the unit standard deviation indicates a wrong relation between the weights of the terrestrial and the satellite observations resp. The tool VCE masters the difficulty. With $s_0 = \pm\ 1.00$ the following result is obtained:

$$ {}_{D+T}C_{x,VCE} : \ A = \pm\ 2906 \text{ mm},\ B = \pm 2012 \text{ mm},\ s_h = \pm\ 832 \text{ mm} \tag{14}$$

which seems even worse. The idea, both covariance matrices (13) and (14) were strongly influenced by external effects, is confirmed after S-transformations which yield from (13)

$$ {}_{D+T}C_{x}^{i} : \ A = \pm\ 8.4 \text{ mm},\ B = \pm\ 5.5 \text{ mm},\ s_h = \pm\ 33.6 \text{ mm}, \tag{15}$$

and from (14)

$$ {}_{D+T}C_{x,VCE}^{i} : \ A = \pm\ 4.5 \text{ mm},\ B = \pm\ 3.0\text{mm},\ s_h = \pm\ 21.0 \text{ mm}. \tag{16}$$

The inspection of (16) reveals that the comparatively inaccurate Doppler observations could expectedly not spoil the accuracy of the precise terrestrial measurements $({}_{D+T}C_{x,VCE}^{i} = {}_{T}C_{x}^{i})$.

In contrast, the adjustment resulting in the inner covariance matrix (15) affects the terrestrial observations due to an unqualified choice of weights. Thus this result as well as the result (13) has to be refused.

The nature of the influences causing the high inaccuracy (14) has to be questioned. How can in this context the values (11) obtained from the GEODOP-programs be interpreted? Compare Jenkins/Leroy (1979).

If, for an additional analysis, the inner covariance matrix ${}_{D}C_{x}^{i}$ (12) is utilized for the combination of the two networks (Reichsthaler, 1983), the external accuracy of the terrestrial network ${}_{T}C_{x}$ (9) succeeds after harmonizing the weights by VCE. The result is

$$ {}_{D_i+T}C_{x,VCE} : \ A = \pm\ 4.8 \text{ mm},\ B = \pm\ 3.2 \text{ mm},\ s_h = \pm\ 35.2 \text{ mm}. \tag{17}$$

The comparatively low internal accuracy of the Doppler network does not affect the external accuracy of the terrestrial comparator. The S-transformation applied to (17) results again in the expected values of the inner accuracies (10) or (16).

It can concludingly be stated that the internal subdecimeter accuracy of the Doppler observations could not conduce the precision of the small INN VALLEY NETWORK. Apart from the determination of absolute positions, a satellite network can only be conducive to a terrestrial network if the extension of the terrestrial network is such that the inner accuracies of both network types can compete with each other; or if the satellite network is so accurate that its inner accuracy can compete with the inner accuracy of a precise terrestrial network. An example for this case will be given in the next paragraph.

7. VARIANCE ANALYSIS OF A GPS NETWORK

In November 1984 coordinate differences for the INN VALLEY NETWORK points were determined by Macrometer V1000 measurements (Heister/Schödlbauer/Welsch, 1985).

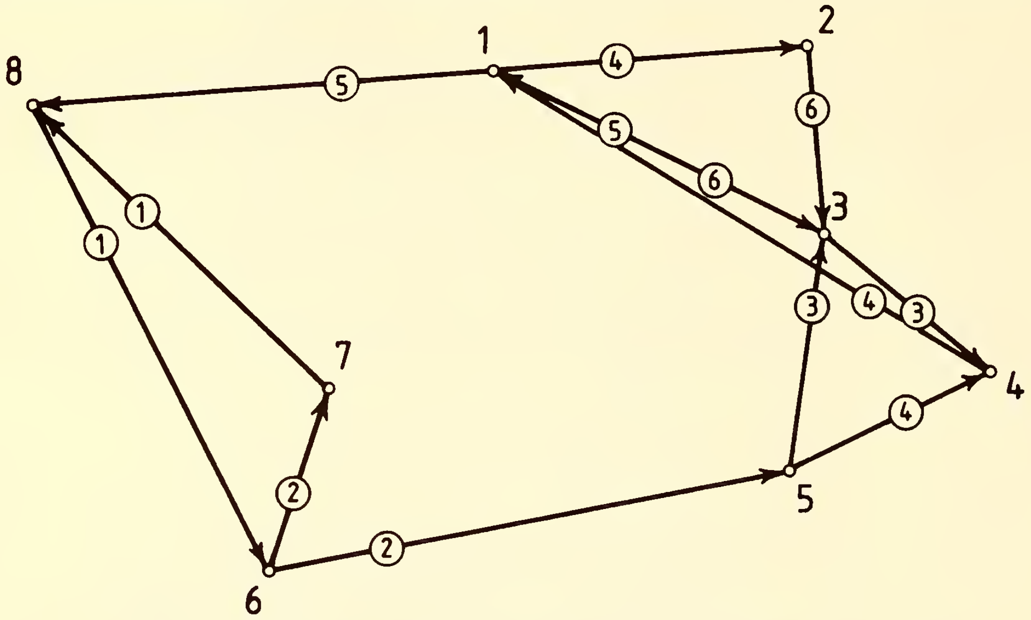

Fig.2: Observed baseline vectors (Macrometer V1000)

The covariance matrix of diagonal block structure of the adjusted coordinate differences was provided by GEO/HYDRO Inc. It shows the following characteristics:

$$ {}_{M}C_{x} : \quad A = \pm\ 18.6 \text{ mm}, \ B = \pm\ 7.5 \text{ mm}, \ s_{h} = \pm\ 20.1 \text{ mm}. \tag{18} $$

These values contain external effects. After their removal the inner covariance matrix is

$$ {}_{M}C^{i}_{x} : \quad A = \pm\ 16.0 \text{ mm}, \ B = \pm\ 7.4 \text{ mm}, \ s_{h} = \pm\ 15.8 \text{ mm}. \tag{19} $$

Again the change of the height accuracy is the clearest. And the question arises how ${}_{M}C_{x}$ has to be interpreted.

If one prosecutes the combination of the Macrometer and the terrestrial network (analogously to the Doppler measurements) one obtains the following results (tab.1):

$$ {}_{M+T}C_{x} : \quad A = \pm\ 8.2 \text{ mm}, \ B = \pm\ 5.6 \text{ mm}, \ s_{h} = \pm\ 16.6 \text{ mm}. \tag{20} $$

The unit standard deviation $s_{0} = \pm\ 1.39$ indicates inappropriate weighting. Therefore, variance components were estimated. However, due to the high inner accuracy of the Macrometer measurements, especially for the heights, the VCE was refined by establishing 6 separate groups of observations: directions, zenith distances, 3 groups of spatial distances, Macrometer observations. By this means the interaction of the satellite measurements and the individual groups of terrestrial observations could be studied thoroughly. It turned out that the zenith distances lost something of their significance for the determination of heights.

After VCE the covariance matrix shows the following values

$$_{M+T}C_{x,VCE} : \ A = \pm\ 18.8 \text{ mm},\ B = \pm\ 12.5 \text{ mm},\ s_h = \pm\ 33.5 \text{ mm}, \tag{21}$$

a result which seems unpleasant at the first glance. But one can suggest that again external influences (which have to be interpreted) falsify the picture. The inner accuracy appears after S-transformation. From (20) we achieve

$$_{M+T}C^{i}_{x} : \ A = \pm\ 4.8 \text{ mm},\ B = \pm\ 3.4 \text{ mm},\ s_h = \pm\ 10.6 \text{ mm}, \tag{22}$$

the results from (21) are

$$_{M+T}C^{i}_{x,VCE} : \ A = \pm\ 4.5 \text{ mm},\ B = \pm\ 3.0 \text{ mm},\ s_h = \pm\ 14.8 \text{ mm}. \tag{23}$$

The situation in (22) shows that a very high accuracy in height was calculated at the cost of accuracy in position. The relations were put right in (23). While the accuracy in position of the terrestrial network has been maintained, the better height accuracy of the satellite network has improved the respective accuracy of the terrestrial network. (23) represents the final result of the combined adjustment of the terrestrial and the satellite network: an astonishing result!

If one introduces finally the inner covariance matrix (19) into the combined adjustment, the result is with $s_o = \pm\ 1.26$

$$_{M_i+T}C_{x} : \ A = \pm\ 4.7 \text{ mm},\ B = \pm\ 3.5 \text{ mm},\ s_h = \pm\ 29.0 \text{ mm} \tag{24}$$

and after VCE only slightly modified

$$_{M_i+T}C_{x,VCE} : \ A = \pm\ 4.8 \text{ mm},\ B = \pm\ 3.4 \text{ mm},\ s_h = \pm\ 31.1 \text{ mm}. \tag{25}$$

With (25) again the external accuracy of the terrestrial network has succeeded.

After filtering off the external effects we obtain from (24)

$$_{M_i+T}C^{i}_{x} : \ A = \pm\ 4.4 \text{ mm},\ B = \pm\ 3.1 \text{ mm},\ s_h = \pm\ 10.4 \text{ mm}. \tag{26}$$

Again too accurate heights!

The transformation of (25) results in

$$_{M_i+T}C^{i}_{x,VCE} : \ A = \pm\ 4.5 \text{ mm},\ B = \pm\ 3.1 \text{ mm},\ s_h = \pm\ 15.8 \text{ mm}, \tag{27}$$

which is, compare (23), the inner accuracy of the combined networks.

The variance analyses confirm an essential improvement of the inner height accuracy by Macrometer measurements.

8. CONCLUSIONS

What have we learned from the variance analyses of combined terrestrial and satellite network adjustments:

- a terrestrial network comparator is an important means for variance analyses;
- variance component estimation is an indispensable tool for appropriate results;

- external (datum?) influences affect the covariance matrices of satellite and combined networks. The nature of those influences should be discussed;
- for the comparison of accuracies achieved either invariant functions or inner covariance matrices are suitable. These can be obtained by S-transformations;
- Doppler coordinates adjusted in combined networks can only improve the inner accuracy of widespread or comparatively inaccurate terrestrial networks - a well-known result;
- Macrometer measurements can improve even precise terrestrial networks especially for their accuracies in height.

The techniques described in this treatise and applied to a local network should also be employed for networks of regional and national extension.

REFERENCES

Heister, H., Glasmacher, H.: *Satelliten-Dopplermessungen im Testnetz Inntal,* in: Schödlbauer, A., Welsch, W. (editors): Satelliten-Doppler-Messungen, Schriftenreihe des Wissenschaftlichen Studiengangs Vermessungswesen, Heft 15, S. 307-326, Hochschule der Bundeswehr, München 1984

Heister, H., Schödlbauer, A., Welsch, W.: *Macrometer Measurements 1984 in the Inn Valley Network,* paper submitted to the First International Symposium on Precise Positioning with the Global Positioning System, Rockville, Maryland, 1985

Jenkins, R.E., Leroy, C.F.: *"Broadcast" versus "Precise" Ephemeris-Apples and Oranges,* Proceedings of the International Geodetic Symposium on Satellite Doppler-Positioning, Austin, 1979

Reichsthaler, K.: *Dreidimensionale Netzausgleichung im Testnetz Steiermark unter Berücksichtigung von Dopplermessungen,* Mitteilungen der geodätischen Institute der Technischen Universität Graz, Folge 46, Graz 1983

Rinner, K.: *Über die Ausgleichung von Prüfnetzen,* Nachrichten aus dem Karten- und Vermessungswesen, Sonderheft Gigas, Institut für Angewandte Geodäsie, Frankfurt 1969

Welsch, W.: *Estimation of Variances and Covariances of Geodetic Observations,* Australian Journal of Geodesy, Photogrammetry and Surveying, No. 34, pp. 1-14, 1981

ANALYSIS OF MACROMETER NETWORKS WITH EMPHASIS ON THE MONTGOMERY (PA) COUNTY SURVEY

James Collins
GEO/HYDRO, INC.
2115 E. Jefferson Street
Rockville, Maryland 20852

Alfred Leick*
AFGL/LWG
Hanscom AFB MA. 01731

ABSTRACT

An analysis of the 42 station Montgomery (PA) County survey is given. For this survey two lines were observed per observation period. A comparison with known orthometric heights reveals discrepancies at 2 stations which can either result from errors in the given data or from local geoidal features. A few remarks are made regarding the implementation of a GPS survey into the existing horizontal network. Data snooping is used to discover possible blunders in the observations. The network is analyzed regarding its internal and external reliability. The orientation of the error ellipsoids with respect to the configuration of the satellites is studied. Finally, the Montgomery County survey is compared with a similar survey of the Eifel region of Germany and the survey of the engineering netork at the Stanford Linear Accelerator. In the latter cases one line was observed per observation period.

THE MONTGOMERY (PA) SURVEY PROJECT

The Montgomery County survey was contracted by the Pennsylvania Department of Transportation (Penn DoT) as part of an on going geodetic control densification program. It was the first Macrometer densification survey submitted to the National Geodetic Survey (NGS) for inclusion in the national network. The network is shown in Fig. 1.

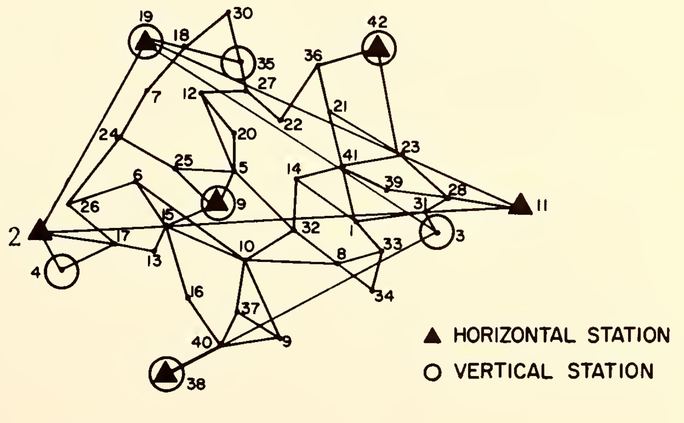

Figure 1: Montgomery (PA) County Network

The only significant (variable) aspect of performing GPS surveys is the length of time of the observations and the segment of the satellite "window" during which the observations are made. The window of opportunity at the time of the Montgomery County survey (summer, 1984) was five hours. For this particular project the V-1000 Macrometers were used so that the three points of a triangle were observed during a single session (simultaneous occupation). The five hour window was divided as follows: (1) first session 2-1/2 hours, (2) 1/2 hour move to second point, (3) second hour session 2 hours. On several occasions observations were lost due to equipment malfunctions, so that less than two hours of data were obtained.

---

* NRC Research Associate (On sabbatical leave from the University of Maine at Orono, Department of Civil Engineering, Orono, ME 04469)

The post observation processing consisted of computing the vectors (individually) between the stations and their covariance matrices. These computations are routinely carried out and have been explained on several occasions elsewhere. The focus in this paper is on the characteristics of GPS networks, which consist of these individually computed vectors.

THE PROGRAMS CATGPS AND CATOPT

CATGPS (Combined Adjustment of Terrestrial and GPS observations) and CATOPT (CAT OPTional) were developed to provide a user-friendly software package to the "GPS-surveyor" for use primarily in high precision engineering networks and for use in the densification of existing networks. They were developed by one of the authors (A.L.) during the summers of 1982 and 1983 while working at M.I.T. (Dept. of Earth, Planetary and Atmospheric Science), and also at the University of Maine.

CATGPS allows the separate adjustment of terrestrial observations and GPS vector observations as well as in combination. The mathematical model is strictly three-dimensional. Angular observations refer to the reference ellipsoid (ell. normal, ell. meridian, geodetic horizon). Astronomical latitude, longitude, and azimuth observations are not incorporated, since it is unlikely that a typical "GPS-surveyor" will ever observe them. Table 1 shows the various options of CATGPS. Each of these options can be excercised without changing the input data set. Exceptions are the weighted parameters. Each station coordinate (geodetic latitude, longitude or ell. height) is associated with several codes which make it possible to treat each coordinate separately as either an unknown, a parameter with associated weight, or as a fixed constant. Proper selection of

Table 1: The CATGPS Program

Options	Observation Types
	Spatial Distances
Angles (Directions) only	Azimuth
Distances only	Vertical Angle
Terrestrial Observations (Combined)	Horizontal Angle
GPS Vectors	(Short) Horizontal Dist.
Terrestrial Obs. + GPS Vectors	Height Differences
	GPS Vectors

these codes defines minimal constraints for coordinate system definition (reference ellipsoid), creates so-called 3D height-controlled adjustments, or degenerates the model to a 1D model to be used for adjusting leveling observations. Directions are treated as correlated angles. There are five options for handling refraction in vertical angles. All of them can be invoked interactively. The height difference observable is, of course, the ellipsoidal height difference. GPS vectors are treated line-by-line, i.e. as stochastically independent. Each vector is assigned a (3x3) covariance matrix. There is no need to reduce the observations to the station marker if the observation file contains the heights of the target and instrument. Adjusted observations always refer to the station marker. Options exist for excluding interactively individual stations contained in the input file or, conversely, for entering the stations which participate in the adjustment individually by name. The latter option is very convenient if components of the network are adjusted triangle by triangle or in small groups of stations for the purpose of analysis. A very simple blunder detection procedure can be invoked optionally in which case weights are changed if the respective residuals are beyond a certain threshold.

In the combination solution (i.e. terrestrial observations and GPS vectors combined in one adjustment), CATGPS estimates three rotation parmeters and one scale. These paramters are defined as follows:

$$\vec{\Delta X} = (1+S)\, R(\alpha,\xi,\eta)\, \vec{\Delta U} \qquad (1)$$

where $\vec{\Delta X}=(\Delta X,\Delta Y,\Delta Z)$ are the observed cartesian GPS vector components and $\vec{\Delta U}=(\Delta U,\Delta V,\Delta W)$ denote the respective coordinate differences in the terrestrial system (U). The rotation angles will generally not be zero if, e.g., the terrestrial system (U) is defined by adopting the astronomical positions of a station in order to make the ellipsoid tangent to the equipotential surface. In network densification these transformation parameters may absorb distortions. The combined adjustment is formulated in the system (U).

A parameterization in terms of cartesian coordiantes is implemented for analysing pure GPS networks. Not only are the observation equations linear in this case, but the inner constraints are very easy to formulate. Inner constraints are useful if one intends to inspect the standard deviations of the adjusted coordinates (or the error ellipsoids) in order to judge over-all homogeneity of the GPS-determined polyhedron of stations. As is well known, the minimal and inner constraint solutions yield identical estimates for the residuals and, consequently, for the adjusted observations and the a-posteriori variance of unit weight, and for any angle, distance, height, etc. computed from the adjusted coordinates. The same is true for the estimated variance-covariances of these quantities. Only the coordinates themselves and their covariance matrix change. Since GPS vectors determine the size and orientation of the station polyhedron, only three constraints are required to fix the translatory components. Minimal constraints are imposed by simply fixing one network station, whereas inner constraints fix the centroid of the polyhedron. The inner constraints are implemented by computing (Pope,1973)

$$N^{+} = (A^{T}PA + E^{T}E)^{-1} - E^{T}(EE^{T}EE^{T})^{-1}E \tag{2}$$

where N^{+} is the pseudo inverse of the normal matrix, P equals the weight matrix, A is the design matrix, and E equals

$$E = (I \; I \cdots I) \tag{3}$$

where I denotes the (3x3) identity matrix.

The program CATOPT was written to support the analysis and interpretation of the results obtained from CATGPS. The options of CATOPT can be invoked separately and repeatedly. They are:

1.) Data Snooping and Reliability of the Network. The respective theory underlying data snooping and internal and external reliability is found in Baarda (1968). An excellent overview is presented in Kok (1984) from where all the subsequent expressions are taken. Let V denote the residuals, then

$$\bar{V} = PV \tag{4}$$

$$Q_{\bar{V}} = P - PA(A^{T}PA)^{-1}A^{T}P \tag{5}$$

The symbol Q denotes the cofactor matrix. All other symbols have been defined earlier. Data snooping of the residuals is based on the test

$$t = \frac{|\bar{V}_i|}{\sigma_{\bar{V}_i}} > x_{1-\alpha_0} \tag{6}$$

The symbol σ denotes the standard deviation of the transformed observation (it is equal to the square root of the ith diagonal element of $Q_{\bar{V}}$ since the a-priori variance of unit weight is assumed to be known for this test). Finally, x denotes the square root of the chi-square distribution with 1 degree of freedom and significance level α_0. If the inequality (6) is true then the zero hypothesis, i.e. the ith observation contains no blunder, is rejected.

The internal reliability of the network is computed from

$$|\widetilde{\nabla L_i}| = \sqrt{\frac{\lambda_0}{Q_{\bar{V}_i}}} \tag{7}$$

where $|\widetilde{\nabla L_i}|$ is the marginally detectable error in L_i. The factor λ_0 is functionally related to the significance level α_0 and the power β_0. The values in Table 2 are taken from Baarda's (1968) charts.

Table 2: Probability Levels

α_0	β_0	λ_0	x
5.0%	80%	7.8	1.96
2.5%	80%	9.5	2.25
.1%	80%	17	3.29

The influence of each marginally detectable error $|\nabla L_i|$ on the coordinates is known as external reliability. CATOPT does not compute these coordinate changes explicitly. Instead, the simple expression

$$\lambda_i = \tilde{\nabla} L_{(i)}^T P \tilde{\nabla} L_{(i)} - \lambda_0 \qquad (8)$$

is computed for every observation. If these values are of the same order of magnitude, then the network is said to be homogeneous with respect to external reliability.

2.) Error Ellipses and Error Ellipsoids. Error ellipses are computed in the geodetic horizon and in the prime vertical plane. Relative error ellipses are also available. The size of the error ellipsoids and the orientation of their semi-major axis are computed.

3.) Transformation of the (3x3) Covariance Submatrices of the Station Coordinates into the Local Geodetic System (tangent to the ellipsoidal meridian and positive north, tangent to the parallel and positive east, ellisoidal normal). The standard deviations expressed in this system are especially useful for depicting the homogeneity of the network if inner constraints are used.

4.) Computation of Adjusted Quantities. The adjusted values of any spatial distance, azimuth, horizontal angle, ellipsoidal height difference, or vertical angle including their variances can be computed. It is even possible to enter instrument and target heights so that the computed quantity can be directly compared with observations.

5.) Computation of Conformal Mapping Coordinates for Adjusted Positions. Currently the Transverse Mercator and the Lambert Conformal Conic mappings are implemented.

MINIMALLY CONSTRAINED SOLUTIONS

The GPS vector observations are adjusted by least squares using minimal constraints, i.e. the solutions are free of possible constraints imposed by existing geodetic networks. All vectors are treated stochastically independent, i.e. if n stations observe simultaneously over the same observation period, only (n-1) "independent" vectors are included. The weight matrix of the observations, P, consists of (3x3) submatrices along the diagonal. The latter submatrices are the inverse of the covariance matrices obtained during the processing of the individual vectors using the manufacturer's software. See Bock et al. (1985) for additional information regarding the steps leading to this covariance matrix. For all adjustments the a-priori variance of unit weight is 1.

Search for Outliers (Data Snooping)

Initially a solution is carried out which includes all 68 observed vectors. Since the network consists of 42 stations, the degree of freedom is 81. Solution 1 in Table 3 shows that the a-posteriori variance of unit weight is 1.30. The symbol VPV denotes the quadratic norm which is minimized. Data snooping according to Eq.(6) is carried out with a significance level of 2.5%. Only vector (2-11) has all 3 components flagged. This line, therefore, is suspected of containing a blunder. Solution 2 contains vectors for which only one or two components are flagged. Since line (21-41) has the largest flagged residual (-112mm), this vector is deleted next. The residuals flagged in Solution 3 are generally small. Interestingly, some of the larger residuals which were still present in this solution, are not flagged. In order to investigate the significance of the remaining flagged observations several adjustments were made for small groups of stations. After lengthy comparison it was finally concluded that line (24-26) might also contain a blunder. The residuals, including the flags, of Solution 4 are shown in Table 4.

Table 3: Candidates for Outliers

Solution	Variance of Unit Weight	VPV	Vectors Excluded	Flags
1	1.30	105	none	22
2	1.20	94	2-11	16
3	1.13	85	2-11,21-41	11
4	1.03	74	2-11,21-41,24-26	8

In order to investigate the size of possible blunders, another adjustment is carried out in which the 3 questionable vectors are assigned very low weights. The resulting residuals, expressed in millimeters in the directions north,east,and height are: (2-11)-(32,47,30), (21-41)-(113,-109,-28), (24-26)-(58,-102,95). These values are very much like those found in Solution 1. The residuals for lines (21-41) and (24-26) are larger than expected for a typical Macrometer performance. Recomputation of both vectors from the double phase differences neither changed the vector components nor the covariance matrices. The computed residuals of line (2-11) are within the expected size considering that this line is 45km long. The coordinates (minimal constraint solution) between Solution 1 and Solution 4 differ by roughly 10mm or less. The only exception is station 11 which differs by (36,-24) millimeters in latitude and longitude respectively, and station 26 whose difference in height is 35mm.

The choice of the significance level, no doubt, is critical to the performance of data snooping. To demonstrate this, Solution 1 was tested again using a significance level of .1% (which is a frequently used value). Not a single observation is flagged in this case! More experience with GPS vector observations will, hopefully, help in identifying the most desirable significance level. Alternatively, analysing the observations using several significance levels is acceptable too, since the flagged observations are only "suspects".

Internal and External Reliability

Although it is very desirable to have small standard deviations for the station coordinates, it is equally important to analyze the network in terms of its internal and external reliability.

> "The sizes of marginally detectable errors, computed for all observations, are measures of the capability of the network to detect outliers of that size in an observation with the probability β_0. They constitute the internal reliability of the network. The influence of each of the marginally detectable errors on the unknowns of the adjustment (usually on the coordinates) is called the external reliability." (Kok, 1984)

The elements entering the reliability computations are the network geometry, the covariance matrix of the observations, and the power β_0 and significance level α_0. The network geometry is not very critical for typical GPS networks, since the design matrix contains only the elements 1 and -1 (cartesian parameterization). Only the number of vectors leading to a particular station impacts the "geometry". The covariance matrix of the observation is the most critical part, since it reflects the satellite-station geometry and the fact of whether or not the time biases could be fixed in the pre-processing. The significance level α_0 (the probability of Type I error, i.e. rejection of the null hypothesis when it is true) and the power of the test β_0 (probability that an error of specific size will be detected when present) are chosen in accordance with the tables given in Baarda (1968). The test procedure is based on the one-dimensional tests in which case one computes the magnitude of the blunders that can be detected with the same probability β_0. Table 4 lists all vectors of Solution 4 (X, Y, and Z components). The remaining flags are denoted by "*" in column 4. The marginally detectable errors which are computed from Eq.(7) and the probability levels specified at the top of the table are listed in column 5. The marginally detectable errors are substantially larger than the residuals and the standard deviations of the station coordinates (See below). The largest values are frequently in the X-components. Given the geographic location of the network, this property is in full agreement with the primarily east-west elongation of the error ellipses shown below. If a point is determined by only two vectors, than each vector has the same internal reliability. Column 6 displays the external reliability as computed from Eq.(8). The factor of variation is about 100. Generally, it is desirable that the external reliability be of the same size. Columns 7 and 8 refer to the

Table 4: Data Snooping and Reliability
(α_0=2.5%, β_0 =80%, λ_0=9.5)

1	2	3	4	5	6	7	8	1	2	3	4	5	6	7	8
19 3	32	55		97	12	416	4	29 25	6	-3		26	21	106	15
		-20		57	32					4		23	22		
		7		61	40					-8		23	21		
3 38	29	27		134	11	380	4	25 5	6	-6	*	26	19	104	12
		-19		65	22					0		23	21		
		12		68	32					-4	*	23	21		
19 2	20	15		113	15	280	5	5 29	4	-6	*	26	19	93	29
		-4		84	64					-1		23	19		
		-1		95	90					-4	*	23	20		
11 19	38	-43		192	10	491	4	16 15	7	-11	*	107	45	146	20
		6		132	44					37		119	20		
		3		175	94					7		132	38		
19 18	3	-1		77	958	222	315	15 29	5	6		57	14	138	36
		1		56	272					65		83	11		
		-2		56	350					-42		74	13		
18 7	4	-80		59	22	153	65	38 40	6	-2		134	310	380	232
		4		77	19					-6		65	78		
		89		71	20					8		68	76		
7 24	5	-6		59	60	153	47	40 16	6	3	*	107	364	146	35
		-8		77	149					3		119	562		
		8		71	86					-2		132	624		
24 25	6	-2		59	169	153	36	40 37	3	-3		107	4129	85	31
		-3		77	317					5		28	114		
		3		71	174					-1		32	204		
26 6	7	4		47	24	136	17	37 9	4	60		131	6	86	16
		11		67	25					-7		28	10		
		-15		59	23					25		35	8		
2 17	7	84		261	7	123	12	9 40	5	2		118	429	92	11
		-31		80	38					10	*	28	23		
		34		121	48					-3		34	34		
17 26	6	1		47	59	136	24	37 10	5	-95		154	10	108	20
		2		67	151					18		37	20		
		-3		59	115					-23		48	19		
2 4	4	2		107	419	123	48	10 9	8	157		186	7	124	8
		3		89	314					-25		38	10		
		-3		110	351					49		51	9		
4 17	6	-20		107	161	123	20	10 8	9	4		55	42	138	8
		34		89	55					9		64	64		
		-4		110	99					-12		64	74		
17 15	5	-4		44	9	80	9	8 32	5	17		56	18	103	18
		-12		61	8					6		73	13		
		17		53	8					-26		70	17		
15 13	2	2		47	25	79	57	32 10	6	16		134	16	115	18
		5		67	23					8		52	87		
		-8		59	24					-10		74	107		
18 35	6	4		54	39	107	13	8 33	4	67		44	10	78	14
		6		36	20					-12		63	9		
		-8		36	27					-81		56	10		
35 30	5	-2		165	496	116	28	33 34	4	-68		44	11	83	22
		-3		40	26					13		65	9		
		3		46	49					81		56	10		
35 27	2	0		55	1095	144	192	31 1	6	-14		44	33	119	15
		2		54	480					-12		37	29		
		-1		50	506					19		38	29		
27 12	4	-11		51	39	124	52	1 33	4	-1		62	295	114	51
		32		71	33					-1		72	523		
		-11		63	36					2		73	510		
36 22	6	0		65	79	177	47	28 31	3	-2		44	278	118	93
		1		58	86					0		36	91		
		2		57	76					2		37	131		
22 27	4	0		65	307	177	100	31 3	2	16		86	181	286	1306
		0		58	305					-12		68	51		
		0		57	320					-13		80	100		
42 36	6	-3		152	549	176	43	14 32	5	10		152	16	111	25
		-2		58	80					4		57	81		
		5		76	138					-8		78	86		
36 21	4	-3		62	70	157	96	32 5	8	-5		56	44	139	12
		-4		71	118					-12		66	75		
		4		72	120					10		66	72		
21 23	8	4		62	52	157	15	1 14	7	32		52	15	108	8
		-12		71	31					-4		83	12		
		1		72	42					-57		71	14		
23 42	10	-37		152	16	176	11	14 41	5	-13		53	54	101	22
		6		58	77					-14		52	68		
		-7		76	78					15		53	71		
41 23	5	44		113	9	112	22	41 1	5	-8		156	8	96	13
		-20		32	30					11		38	19		
		35	*	35	18					-30		48	13		
11 28	6	-8		192	227	491	353	10 6	13	36		55	5	178	6
		16		132	47					-41		83	4		
		0		175	117					7		71	5		
28 23	6	0		56	677	119	15	6 15	5	10		40	21	118	26
		5		32	86					3		59	19		
		-5		32	93					-12		50	20		
41 39	4	-2		50	109	119	41	15 10	8	1		38	536	127	9
		0		31	45					-2		49	389		
		-1		31	53					2		47	426		
39 28	6	-3		50	177	119	14	13 17	4	2		47	16	79	19
		1		31	24					7		67	16		
		-1		31	32					-9		59	16		
12 5	8	-5		39	9	117	7	30 18	6	-1		165	11	116	16
		31		58	8					-3		40	16		
		-17		50	9					5		46	11		
5 20	3	4		38	12	106	54	20 12	5	1		38	241	106	22
		-27		56	12					-3		56	283		
		16		49	12					1		49	303		
								34 8	4	0		44	330	83	21
										-1		65	273		
										1		56	269		

1:Line; 2: Distance (Km); 3: Residuals (mm);4: Flag (*);
5, 7: Internal Reliability; 6,8: External Reliability

hypothetical situation were the components of the vectors are stochastically independent and the standard deviations assigned to the components are proportional to the length of the vectors. A ratio of 1:250.000 was taken, since the a-posteriori variance of unit weight is close to unity in this case. Because of this specific stochastic model, the components of each vector have the same internal and external reliability respectively. Comparing columns 5 and 7 one recognizes that the actual stochastic model provides a much better internal reliability than the hypothetical one. In fact, one might conclude that internal and external reliability might benefit most from improvements in the stochastic model, e.g. by not neglecting the correlation between station vectors if the stations are occupied simultaneously.

It is generally recognized that the covariance matrix of the vector observations is a "weak element" in Macrometer surveying (Bock et al., 1985). This analysis should, therefore, be considered as merely giving a first insight into the reliability of GPS networks. This is even more true since "there is significant probability" that one or more of the many assumptions underlying statistical testing theory are violated. At the basis of the one-dimensional approach is the assumption that only one blunder is present. Any blunders in GPS surveying, however, are likely to affect at least all three components of a vector. A simple example is misreading the height of the antenna. To make sure that the internal reliability as computed above is, indeed, meaningful, several test computations were carried out in which the component of one vector was changed by known amounts. Indeed, as the known change exceeded the internal reliability, the respective component was flagged.

Adjusted Distances and Height Differences

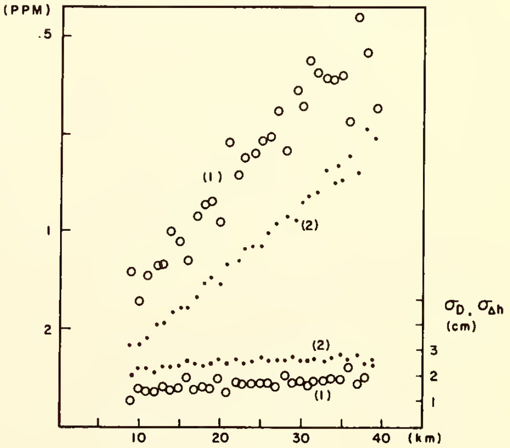

Figure 2: Std. Dev. for Distances and Height Differences

The Macrometer accuracy is generally quoted as being 1-2ppm of the length of the line. This value was derived by comparison with "known" ground truth. Causes for this accuracy limitation are limited knowledge (at this time) of the satellite ephemerides and the ionosheric effect (one frequency). This method of describing the accuracy of the Macrometer is very appropriate when referring to the measurement of single lines. The performance of the Macrometer within an areal network is a different matter. There are still questions regarding the error propagation characteristics of Macrometer networks and how these change with the station distribution. Figure 2 shows the standard deviations of the adjusted distances (1) and height differences(2). For each station, the combination to all other stations is computed and then averaged over 1km distance intervals. The graphs demonstrate a high degree of homogeneity of the network as the standard deviations are almost independent of the station separations.

Station Statistics

In the following table and figures the station statistics are represented in several ways. All values are derived from the inner constraint solution. Columns A, E and H in Table 5 represent the standard deviations in the local geodetic system (north, east, ell. height). Columns A, B, and C contain the minor, intermediary and major axes of the error ellipsoids, and columns AZI and Z denote the azimuth and the zenith distance of the major axes. Figures 3 and 4 show the error ellipses in the geodetic horizon and the prime vertical plane respectively. Figure 5 shows the foot points of the GPS satellites during the observation campaign. In order to relate the orientation of the error ellipsoids to the over-all positions of the satellites, this figure also shows the direction of the major axis of the error ellipsoids for each station. The high correlation between this direction and the center of the satellite configuration is very visible.

Table 5: Standard Deviations in Local Geodetic System and Error Ellipsoids

ST	N (mm)	E (mm)	H (mm)	A (mm)	B (mm)	C (mm)	AZI (0)	Z (0)
1	8	10	13	5	10	15	265	38
2	13	17	18	6	18	20	272	83
3	10	12	14	5	13	15	266	78
4	14	17	21	6	20	22	266	48
5	8	9	14	4	10	15	260	34
6	30	23	22	6	21	38	262	83
7	12	13	20	6	12	23	260	34
8	9	10	15	4	10	17	254	33
9	8	15	15	6	16	16	262	85
10	7	8	10	4	8	11	269	36
11	21	22	29	8	29	29	120	12
12	30	24	19	5	19	39	261	81
13	39	31	24	6	24	50	262	83
14	7	10	12	5	10	14	279	36
15	7	8	12	4	9	12	260	24
16	9	14	19	6	15	19	276	26
17	16	16	18	6	17	22	264	70
18	8	10	12	5	12	13	264	41
19	8	11	12	5	12	13	93	86
20	31	24	20	5	20	39	261	81
21	9	11	18	5	11	19	258	30
22	8	10	14	5	10	15	259	31
23	7	9	12	4	9	12	270	29
24	10	11	17	5	11	19	260	33
25	9	10	15	5	10	17	259	33
26	17	16	20	6	18	24	263	61
27	8	9	13	4	10	14	259	30
28	7	8	12	4	9	12	265	29
29	9	10	15	5	10	17	258	33
30	9	12	16	6	12	17	263	35
31	8	9	12	5	10	13	262	29
32	6	9	11	4	9	12	277	36
33	9	10	14	5	10	16	262	36
34	10	10	17	5	13	18	245	21
35	8	10	13	4	11	14	258	28
36	8	10	14	5	10	16	264	31
37	8	14	15	6	14	15	98	60
38	9	16	17	6	17	17	274	46
39	7	10	13	5	10	14	269	34
40	8	14	15	6	14	15	97	58
41	7	10	11	5	10	13	277	39
42	8	11	14	6	11	16	276	32

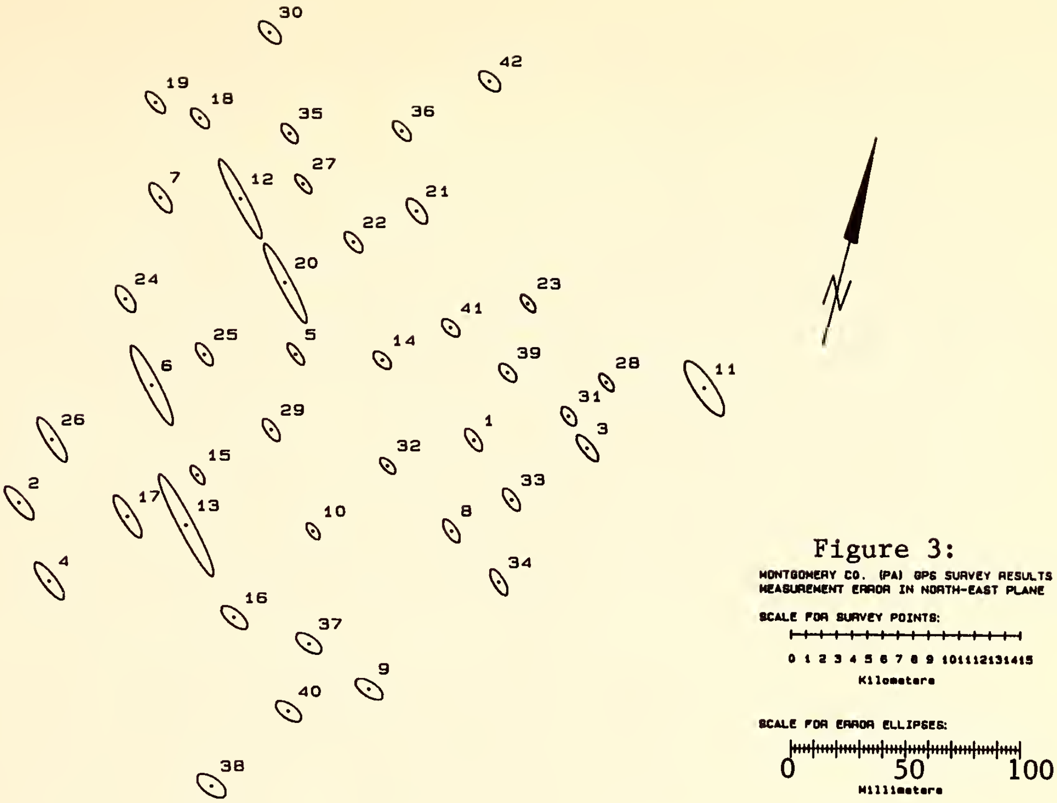

Figure 3:
MONTGOMERY CO. (PA) GPS SURVEY RESULTS
MEASUREMENT ERROR IN NORTH-EAST PLANE

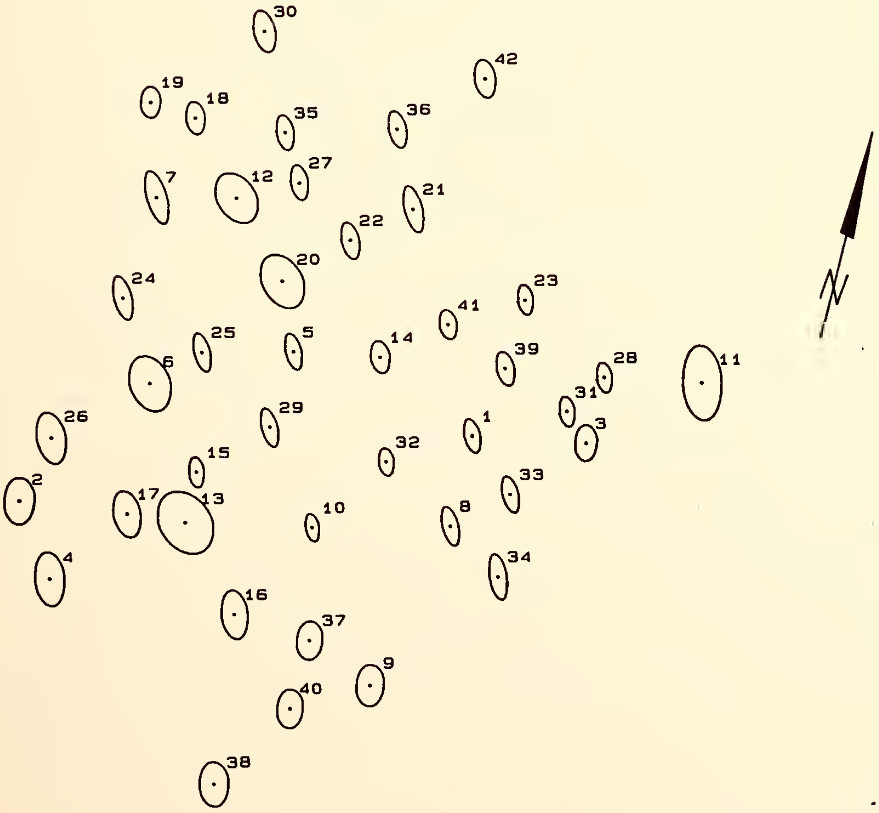

Figure 4:
MONTGOMERY CO. (PA) GPS SURVEY RESULTS
MEASUREMENT ERROR IN HEIGHT-EAST PLANE

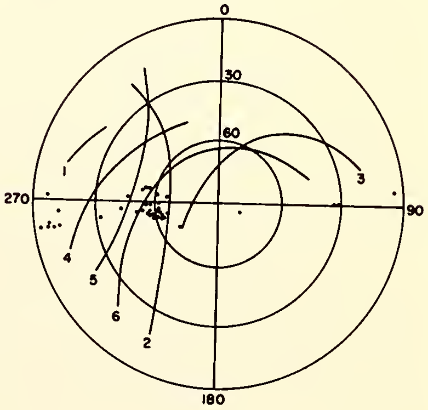

Figure 5: Satellite Configuration and Direction of Error Ellipsoids

COMPARISON WITH EXISTING VERTICAL CONTROL

The GPS polyhedron of stations can be used readily for determining geoid undulation by comparing ellipsoidal heights with known orthometric heights. Figure 6 shows the geoid undulation map for Montgomery County. The reference ellipsoid is arbitrarily defined (minimal constraints) through the ellipsoidal latitude and longitude of one station, in this case station 29, and by equating the orthometric and ellipsoidal height for that station. The orientation of this ellipsoid in azimuth is provided by the GPS vector observations themselves.

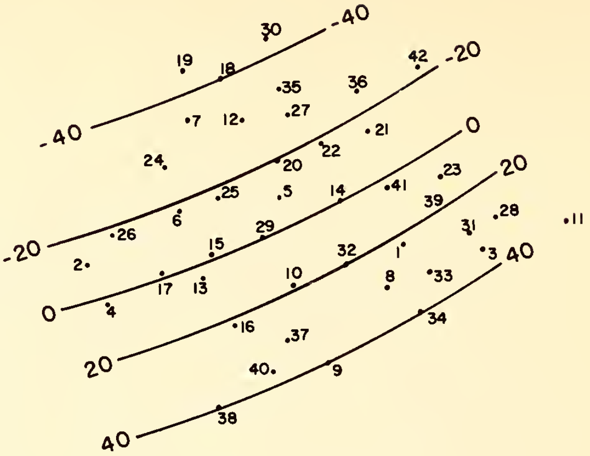

Figure 6: Geoid Undulations

A partial analysis (discovery) of local geoid features is possible with CATGPS, provided the known orthometric heights are well distributed. Solution 1 in Table 6 is yet another minimal constraint solution carried out for this purpose. The constraints are implemented by fixing the geodetic latitudes and longitudes of 2 stations and by equating ellipsoidal and orthometric heights for 3 other stations. Given these specifications the estimated rotation parameters (α , ξ , η) of Eq.(1) reflect the slope of the geoid (as defined by the 3 stations whose orthometric heights are held fixed). The scale factor contains the possible scale error of the existing network (as implied by the separation of the 2 fixed stations on the ellipsoid) and the effect of a constant, but unknown undulation. Table 6 shows that VPV for Solution 1 equals that of Solution 1 in Table 1, which is exactly the way it should be. In subsequent solutions the orthometric heights of the other stations are introduced as weighted parameters. It appears that at stations 4 and 38 the orthometric heights differ noticably from the Macrometer determined ellipsoidal heights. These discrepancies can

Table 6: Weighting Konwn Orthometric Heights
(Values in Parentheses denote the assigned Std.Dev)

Sol	Observed Height - Adjusted Height							VPV
	3	4	19	29	35	38	42	
1	0 (2)					0 (2)	0 (2)	105
2	-2.9 (4)	-4.6 (4)	.6 (4)	1.6 (4)	-.4 (4)	3.9 (4)	.9 (4)	109
3	.1 (2)	-6.7	-.8 (2)	1.0 (2)	-.2 (2)	4.8	.9 (2)	106
4	-.4 (1)	-6.3	-.4 (1)	.5 (1)	-.1 (1)	5.2	.4 (1)	107
5	-.9 (1)	-1.4 (1)	.2 (1)	.4 (1)	0 (1)	1.2 (1)	.4 (1)	123

principally be caused by errors in the Macrometer survey, the orthometric heights, or geoidal features. A resolution as to the significance of geoidal features requires the independent computation of geoid differences from other data, such as gravity anomalies (Englis et al.,1984).

IMPLEMENTATION INTO THE HORIZONTAL NETWORK

CATGPS provides at least two approaches for the densification of existing networks with GPS. One procedure is to treat the coordinates of common stations as weighted parameters. If only orthometric heights are available rather than ellipsoidal heights one can make use, again, of the transformation parameters to absorb the "model errors". The rotation parameters can be made zero by simply applying the undulation differences of Fig. 6 to the orthometric heights. The scale factor, once again, will absorb the effect of the undulations with respect to the (national) reference ellipsoid. It can be shown that this procedure yields acceptable results over a region of a typical county, considering the finite accuracy of the GPS survey, the quality of the existing network, and a typical size for the undulations. This procedure was used to compute a set of NAD coordinates for the Montgomery County (Collins and Leick, 1984). Alternatively, one could use two-dimensional transformations of ellipsoidal surfaces, in which case heights are not required explicitly (Leick,1984).

The disadvantage of the coordinate approach is that the neighborhood, i.e. the region of the network that is impacted by the new GPS observations, is limited to the common stations. In addition, station motion could have occured which is not yet reflected in the published coordinates. Clearly, a more desirable method is to perform a regional adjustment which includes all terrestrial observations and the GPS vectors using the combination option of CATGPS. Such regional adjustments could thus far not be done by the practicing surveying engineer, because the terrestrial observations were not yet available in computer readable form. As the new and innovative data base approach (Pendleton,1985) becomes operational, these practical difficulties will disappear, since it will be as easy to extract observations from the data base as it is to add them using telecommunication techniques. Hand in hand with this improved network maintenence capability one should promote the rethinking of the surveyors from coordinates to observables (non-estimable quantities to estimable ones). The earlier the surveyors learn how to operate in a "world of changing coordinates", the better are the prospects that the improved measurement capability is recognized, fully used, and accepted by the public. (This seems to be especially true for boundary surveying.)

SUMMARY AND CONCLUSIONS

It has been demonstrated that the Montgomery (PA) Macrometer network is very homogeneous and suitable for inclusion in the data base of the National Geodetic Survey. This "two line per observation period" network yields, on the average, a standard deviation of 2cm for the adjusted distance and 3cm for the adjusted height difference between stations. These values are practically independent of the station separation.

Data snooping identified several vector observations suspected of containing blunders. Three of these vectors had a significant impact on VPV. However, recomputation of these vectors did not reveal any error. Data snooping appears to be quite sensitive regarding the choice of the significance level.

The error ellipsoids are generally elongated with the major axis pointing towards the center of the satellite configuration. The major axis is roughly two or three times the length of the minor axis. The major axis of the error ellipses in the geodetic horizon have an azimuth of about 120 to 130 degrees. The satellite configuration is roughly symmetric about this direction.

The internal reliability is mostly below 10cm in the vector components. In several cases it is as large as 20cm. It is expected that improved computation procedures, e.g. not neglecting the correlation between vectors if stations are occupied simultaneously, will result in improved internal reliability and a more smooth external reliability. Even though the reliability computaion presented here should be regarded as preliminary, it is clear that reliability considerations should not be ignored when dealing with GPS networks.

Internal and external reliability of the Montgomery network were compared with the Eifel network for which one line had been observed per observation period. Internal reliability is only about 5cm for the Eifel network, and it is much more homogeneous with respect to external reliability than is the Montgomery network.

Finally, a comparison is made with an engineering network whose station separation is 1km or less. The internal reliability is about 1cm, and the standard deviations of the coordinates are in the range of millimeters. Yet, when four GPS points are compared with a higher standard (straight line of alignment laser), there is agreement within 1 millimeter! (See explanations at another place in these proceedings.) This comparison is significant, since one often does not have an adequate standard of comparison for Macrometer measurements.

REFERENCES

Baarda, W., 1968: A Testing Procedure for Use in Geodetic Networks, Netherlands Geodetic Commission, Vol 2, No.5

Bock, Yehuda, Abbot, Richard, Counselman, Charles, Gourevitch, Sergei, and Robert, King, 1985: "Establishment of Three-Dimensional Geodetic Control by Interferometry with the Global Positioning System", Journal of Geophysical Research (accepted for publication)

Collins, James, Leick, Alfred, 1985: "Montgomery County (PA) GPS Survey', Technical Papers 45th Annual Meeting ACSM, Washington, D.C., March 10-15

Englis, Theo, Rapp, Richard and Yehuda Bock, 1984: "Measuring Orthometric Height Differences with GPS and Gravity Data", AGU Chapman Conference on Vertical Crustal Motions: Measurement and Modeling. Harpers Ferry, West Virginia, Oct. 22-26

Kok, Johan, 1984: On Data Snooping and Multiple Outlier Testing, NOAA Technical Report NOS NGS 30

Leick, Alfred:, 1984: "Macrometer Surveying", Journal of Surveying Engineering, Vol. 110, No. 2

Pendleton, Dave, 1985: "Telecommunications Access to the National Geodetic Survey Intergrated Data Base",Journal of Surveying Engineering, Vol.111, No.1

Pope,Allen, 1973: "The Use of the Solution Space in the Analysis of Geodetic Network Adjustment", IAG Symposium on Computational Methods in Geometric Geodesy, Oxford, England

APPENDIX I: Eifel Network

The network in the Eifel region of West Germany was observed during the Fall of 1983 and the Spring of 1984. The results of this survey are discussed in detail in Bock et al. (1985). Their analysis is supplemented here with internal and external reliability computations. In contrast to the Montgomery survey, the Eifel network was observed with one observation per observation period, i.e. the full observation time span was used for each line. The observations upon which Table 7 is based, are the final (cleaned) set which were given to the German client. It is seen from the table that none of the observations is flagged by data snooping. The internal (5) and the external (6) reliability columns appear to be very smooth indeed. Comparing with the respective column of Table 4 for the Montgomery survey, it appears that the Eifel survey is unquestionably of higher quality. Since both networks are of the same type, with generally the same station spacing, it must be concluded that the improved Macrometer performance in the Eifel results from the full use of the whole observation window for each line.

Table 7: Data Snooping and Reliability
(α_0=2.5%, β_0=80%, λ_0=9.5)

1	2	3	4	5	6	1	2	3	4	5	6
19 8	13	-2		40	6	16 10	9	3		26	20
		9		43	7			4		33	18
		-15		46	6			-1		31	15
8 2	5	-4		29	15	13 15	9	0		35	9
		4		32	18			0		42	8
		-4		35	15			-12		35	10
2 1	7	-5		22	10	13 12	12	11		53	16
		-2		26	10			-5		60	12
		-1		25	10			11		52	14
3 2	9	1		26	8	15 10	10	5		30	14
		-6		30	8			-4		37	13
		-9		29	9			7		36	13
4 1	8	0		36	46	14 15	10	0		32	25
		-2		55	65			5		38	22
		-6		61	43			3		37	27
5 1	9	7		47	15	15 16	7	-3		28	18
		1		52	20			2		34	24
		-1		41	14			-5		34	23
6 5	8	4		47	15	13 11	8	-8		40	7
		-5		52	12			-9		43	9
		-4		41	16			-5		40	8
20 6	6	10		44	20	12 11	6	18		53	17
		-13		50	15			7		60	22
		-3		41	21			21		52	18
19 7	8	7		28	8	15 11	8	-2		38	53
		7		33	7			1		42	46
		13		31	7			-3		38	49
19 20	11	19		44	9	8 7	9	5		30	10
		-5		50	14			-3		34	9
		5		41	10			1		37	9
7 1	8	-1		23	10	18 8	18	0		83	43
		-3		25	10			-5		97	38
		-8		25	10			4		89	37
7 6	8	11		24	10	18 17	21	2		83	10
		10		26	11			17		97	10
		13		25	11			-8		89	10
4 3	8	4		36	8	16 9	9	-24		38	8
		11		55	5			-9		50	10
		28		61	6			-16		40	9
10 9	6	6		36	32	14 16	14	5		49	5
		-6		48	22			10		61	5
		2		37	34			27		69	4
17 9	18	1		83	64	13 14	11	0		36	14
		4		97	87			11		42	15
		-1		89	87			13		40	12
10 3	7	1		28	30	1 3	8	-1		25	13
		-1		32	38			-1		28	16
		-3		32	34			-2		29	15
2 7	8	2		23	12	19 6	9	-4		23	38
		9		27	10			-3		27	27
		0		27	11			-3		25	35
10 2	9	-2		28	13	6 1	12	7		25	12
		7		32	11			8		27	13
		8		32	11			15		26	11

1: Line; 2: Distance (km); 3: Residuals (mm);
4: Flag (*); 5: Internal Reliability;
6: External Reliability

APPENDIX II: Stanford Network

The Stanford Macrometer survey was carried out to support construction at the Stanford Linear Accelerator. In this network the length of the lines is typically about 1km. A detailed discussion of this survey is found elewhere in this proceeding (See paper by Ruland and Leick). The internal and external reliability computation is given here in order to have a ready comparison with the Montgomery and the Eifel networks. As expected, the reliability columns are very smooth. Internal reliability is about 1cm. The directions of the major axis of the error ellipsoids are all clustered around the center of the satellite configuration (See Fig. 7).

Table 8: Data Snooping and Reliability (α_0=2.5%, β_0=80%, λ_0=9.5)

*	1	2	3	4	5	6
	20 39	.5	-1		18	66
			-1		11	11
			1		10	11
	39 1	3.2	5		12	9
			3		14	6
			3		12	6
	1 33	3.5	-1		14	11
			-1		14	7
			-4		12	6
	35 20	.5	-8		31	4
			0		14	14
			1		13	15
	41 42	.2	2		12	44
			2		9	19
			-2		7	28
	42 19	1.1	-1		12	39
			0		10	28
			1		8	36
	19 10	.9	0		12	41
			1		10	26
			0		8	35
	10 1	1.0	-3		10	26
			-1		11	34
			1		9	47
	20 41	.3	-4		19	7
			2		11	17
			-1		9	20
	33 41	.5	0		13	29
			-3		11	14
			3		10	10
	33 19	1.6	1		27	4
			1		13	7
			-4		11	8
	39 10	2.3	-1		10	24
			-3		11	10
			-1		9	9
	33 10	2.5	-6		15	6
			1		15	5
			1		12	5
	39 42	.4	-8		20	5
			0		9	11
			2		7	14
	39 41	.4	-7		30	4
			4		9	12
			-4		8	9
	33 35	.6	0		28	173
			1		13	20
			-1		12	20
	1 35	4.1	2		56	3
			-6		17	7
			7		15	6

* See Table 7

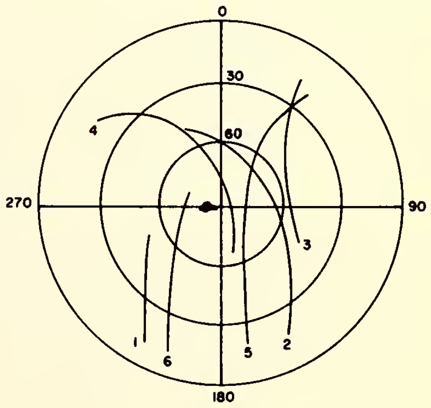

Figure 7: Satellite Configuration and Orientation and Error Ellipsoids

THE RE-ADJUSTMENT OF THE FIRST ORDER LOCAL GEODETIC NETWORK IN FRANKLIN COUNTY, OHIO, INCORPORATING THE RESULTS OF THE GLOBAL POSITIONING SYSTEM (GPS).

Ludwik Sliwa
4620 College Avenue
College Park, MD 20740

ABSTRACT. Adjustment procedures for observations obtained through the Global Positioning System are presented. The data is fitted into North American Datum 1927 using two different techniques: 1. Minimum constraint least squares technique and 2. minimum norm least squares technique. The results of these two adjustments have been compared to the adjustment results provided by Geo/Hydro, private contractor to Franklin County. The averages of the station coordinates provided by Geo/Hydro did not differ significantly from the average results obtained by the author. Three station coordinates, however, differed significantly when comparisons were made station by station. An attempt was made to locate the reasons for these differences, but lack of sufficient data did not allow to draw definitive conclusions.

INTRODUCTION

The re-adjustment procedure is referred to Geo/Hydro's survey which took place in June of 1983. It was performed in 3-D Cartesian geocentric coordinate system. Eleven 1st order control stations (Appendix), forming fourteen baselines were included in the adjustment. The geodetic coordinates of these stations, as adjusted by Geo/Hydro were adopted in order to compute the vector of the approximate values: Lo in geocentric system.

Raw geodetic coordinate differences submitted by Geo/Hydro to Franklin County's Engineer Office were used to compute the vector of observation: Lb. The input in the adjustment should include 3-D Cartesian geocentric coordinate differences: ΔX, ΔY, ΔZ. Since these were not available to the author, instead, raw geodetic coordinate differences were transformed to raw geocentric coordinate differences. These were used as input data.

ADJUSTMENT PROCEDURE

The adjustment was performed in 3-D Cartesian geocentric coordinate system. Our case was typical for the observation equation. The mathematical model was selected as:

$$La = F\ (Xa) \qquad (1)$$

where: La = adjusted values of the observed quantities
Xa = theoretical values of the parameters

In our case the parameters were the X,Y,Z, coordinates of the stations included in the adjustment. The "observed quantities" were the differences in 3-D Cartesian coordinates: ΔX, ΔY, ΔZ. So our mathematical model took the form:

$$\Delta X_{ij_a} = X_{j_a} - X_{i_a} \tag{2}$$

$$\Delta Y_{ij_a} = Y_{j_a} - Y_{i_a} \tag{3}$$

$$\Delta Z_{ij_a} = Z_{j_a} - Z_{i_a} \tag{4}$$

Due to limited access to available data, our observed quantities were not really observed: they were computed from raw geodetic coordinate differences (delta phi, delta lambda and delta h) and hence, ΔX, ΔY, ΔZ were correlated.

As presented by Leick (1984), the correlation coefficient could run as high as .57, with the negative correlation as high as .65.

The observation equation had the form:

$$V = AX + L \tag{5}$$

where: V = residuals of the observed quantities: delta X, delta Y and delta Z

A = coefficient matrix derived from the linearization of the model

X = alterations to approximate values of X,Y,Z coordinates of the stations

L = Lo-Lb = the difference between the approximate (Lo) and the observed (Lb) values of the observables

The approximate values of the observable Lo were computed from the approximate values of the parameters Xo:

$$Lo = F\ (Xo) \tag{6}$$

The approximate values of the parameters Xo were computed from Geo/Hydro's adjusted coordinates: phi, lambda, and h. The coefficient matrix A had the form as suggested by Leick (1984). The pattern of our observation equation is as follows:

PLATE 1. Design of Observation Equations

$$\begin{array}{lccccccccclll}
V\ = & & & & & A & & & & & X & +\ (Lo & -Lb) \\
V1 & 1 & 0 & 0 & 0 & 0 & 0 & -1 & 0 & 0 & X1 & L1o & L1b \\
V2 & 0 & 1 & 0 & 0 & 0 & 0 & 0 & -1 & 0 & X2 & L2o & L2b \\
V3 & 0 & 0 & 1 & 0 & 0 & 0 & 0 & 0 & -1 & X3 & L3o & L3b \\
. & . & . & . & . & . & . & . & . & . & .. & ... & ... \\
. & . & . & . & . & . & . & . & . & . & X33 & ... & ... \\
V42 & 0..1 & 0 & 0 & 0 & -1 & 0 & 0 & 0 & & & L42o & L42b
\end{array}$$

The normal equations had the form:

$$A^T PA\ X + A^T\ P\ L = 0 \tag{7}$$

where: P is the weight matrix. The weight matrix P was taken as P=I.

This was done because we did not have full information from Geo/Hydro and therefore, could not possibly imply another choice in designing matrix P. By denoting:

$$N = A^T P A \tag{8}$$

$$U = A^T P L \tag{9}$$

we can re-write equation (7) as:

$$NX + U = 0 \tag{10}$$

and solve for the unknowns:

$$X = -N^{-1}U \tag{11}$$

Our X-ses are the alterations to the approximate values of the parameters Xo.

The rank deficiency problem of matrix A was approached by rigidly fixing some of the parameters (X-ses) and assigning to them the corrections as equal to 0. Matrix A was broken into two sub-matrices: A1 and A2. Matrix A1 contained all columns of matrix A but three (corresponding to the station (Rhodes) with the coordinates fixed). Matrix A2 contained the three columns of the station held as fixed in the adjustment. The selection of the station held as fixed was arbitrary: it could be any of the stations included in the adjustment. Matrix N could then be re-designed as:

$$N = \left[\begin{array}{c|c} N11 = A1^T PA1 & N12 = A1^T PA2 \\ \hline N21 = N12^T = A2^T PA1 & N22 = A2^T PA2 \end{array}\right] \tag{12}$$

The vector of the corrections to unknowns then took the form:

$$X^* = \begin{bmatrix} X1^* \\ X2^* \end{bmatrix} = \begin{bmatrix} X1^* \\ 0 \end{bmatrix} \tag{13}$$

and the system of normal equations could be re-written as:

$$\begin{bmatrix} N11 & N12 \\ N21 & N22 \end{bmatrix} \begin{bmatrix} X1^* \\ X2^* \end{bmatrix} + \begin{bmatrix} U1 \\ U2 \end{bmatrix} = 0 \tag{14}$$

The solution was obtained in the following steps:

1. Compute:

$$X^* = \begin{bmatrix} X1^* \\ X2^* \end{bmatrix} = \begin{bmatrix} -N11^{-1} & U1 \\ & 0 \end{bmatrix} \tag{15}$$

This gives us a minimum constraint solution.

2. Compute:

$$V^T PV = L^T PL + X1^T U1 \tag{16}$$

The VTPV value was equal to 0.004823.

3. Compute:

$$\hat{\sigma}^2 = \frac{V^T PV}{n - u} \tag{17}$$

The numerical value of sigma-zero square was equal to 0.004019 m^2. It means that a posteriori standard deviation for any X,Y, Z is 0.063 m or 63 mm.

4. Compute:

$$E = \begin{bmatrix} -N11^{-1} & N12 \\ & I \end{bmatrix} \tag{18}$$

5. Find:

$$X = X^{*} - E(E^{T}E)^{-1} E^{T} X^{*} = TX^{*} \tag{19}$$

where: $$T = I - E(E^{T}E)^{-1}E^{T} \tag{20}$$

This solution is the "mimimum norm least squares solution" using the technique of the generalized inverse (Uotila, 1984).

6. Compute:

$$Qx^{*} = \begin{bmatrix} N11^{-1} & 0 \\ 0 & 0 \end{bmatrix} \tag{21}$$

This is a weight coefficient matrix for the minimum constraint solution,

7. Compute:

$$Qx = T\,Qx^{*}T \tag{22}$$

8. Compute:

$$\hat{\Sigma}_{x} = \hat{6}^{2}\,Qx \tag{23}$$

This is the variance-covariance matrix for the mimimum variance-mimimum norm solution.

9. Compute:

$$Xa = Xo + X \tag{24}$$

10. Compute V (equation 5)

11. Compute:

$$La = Lb + V \tag{25}$$

12. Use Xa to compute La values through the mathematical model:

$$F(Xa) = La \tag{26}$$

13. Check if:

$$N\,E = 0 \tag{27}$$

COMPUTATION OF GEODETIC COORDINATES FROM 3-D CARTESIAN GEOCENTRIC COORDINATES AFTER THE ADJUSTMENT

After the adjustment was completed, the conversion from 3-D geocentric to geodetic coordinate system was done. The aim was to compare the results with the adopted coordinates obtained by Geo/Hydro (Table 1) within the same coordinate system (i.e geodetic).

The conversion procedure was followed from the outline given in Heiskanen and Moritz (1967:181-184). The adjusted X,Y,Z geocentric coordinates were used as input data.

COMPUTATION OF THE STATE PLANE COORDINATES

The objective of this exercise was twofold: to check if using the mathematical formula from the US Department of Commerce (1973) will yield the same x and y values as those given by Geo/Hydro when applying their adjusted geodetic latitude and longitude as input data.[1] If so, then to compare our state plane coordinates (computed from the adjusted geodetic latitudes and longitudes) with Geo/Hydro's values.

The formulas used in the computation are fully elaborated in the publication quoted above (pp. 3,4,42,43). One must emphasize here, that the computation of the state plane coordinates (x,y) by us was optional: it was not essential to compute the state plane coordinates by us in order to comparre our results with Geo-Hydro's results.

PRESENTATION OF SELECTED RESULTS

The approxinate values of the parameters: Xo are presented in Table 1. They were computed from Geo/Hydro's adjusted coordinates: phi, lambda and h.

TABLE 1

These are Geo'Hydro's adjusted coordinates: X,Y, Z computed in geocentric system and used as Xo. The units are meters.

	X	Y	Z
18-83:	593219.1939	-4859538.3127	4074815.1125
BRITTON:	584418.0126	-4854211.9554	4082460.6097
BOLTON:	584754.9753	-4864483.0917	4070259.5615
JACKSON:	590077.6094	-4868746.7426	4064394.5533
HAMILTON:	606038.8727	-4865031.4982	4066484.3951
TRURO:	609079.1244	-4856547.3354	4076088.1054
HOOVER:	605724.1601	-4847638.4108	4087145.4913
CLARK:	597846.6778	-4852589.2865	4082448.3341
SMITH:	603352.6237	-4870501.7513	4060319.5433
HOWELL2:	611840.7495	-4857665.5649	4074390.2730
RHODES:	596659.7206	-4859301.4676	4074880.6590

---

[1] On page 3 of this publication there is the following statement:

> "These equations are not the only ones that can be used in computing Lambert coordinates. They may not even be the best. However, they yield coordinates which check values computed using the projection tables within a hundredth of a foot (or at most two hundredths)."

The numerical values of vector X^*, computed from equation (15) are listed in Table 2. This is a minimum constraint solution.

TABLE 2

This is the solution vector: X^*, computed with minimum constraint solution in geocentric system. Station Rhodes was held as fixed. The units are meters.

	X	Y	Z
18-83:	0.0649	-0.1719	0.1460
BRITTON:	0.1022	-0.2581	0.2343
BOLTON:	0.1220	-0.2209	0.2344
JACKSON:	0.1733	-0.2491	0.2067
HAMILTON:	0.0687	-0.0082	0.1233
TRURO:	0.0806	0.1334	0.0278
HOOVER:	0.0006	0.2354	0.0457
CLARK:	0.0306	0.0119	0.1648
SMITH:	-0.1500	0.0062	-0.0221
HOWELL2:	0.0184	0.0767	0.0192
RHODES:	0.0000	0.0000	0.0000

The numerical values for vector X, computed from equation (19), are shown in Table 3. This solution is the minimum norm least squares solution using the technique of the generalized inverse (Uotila, 1984).

TABLE 3

This is the minimum variance-minimum norm solution. The units are meters.

	X	Y	Z
18-83:	0.0184	-0.1413	0.0387
BRITTON:	0.0557	-0.2274	0.1270
BOLTON:	0.0755	-0.1902	0.1271
JACKSON:	0.1268	-0.2184	0.0994
HAMILTON:	0.0223	0.0224	0.0160
TRURO:	0.0341	0.1640	-0.0794
HOOVER:	-0.0458	0.2660	-0.0616
CLARK:	-0.0158	0.1498	0.0575
SMITH:	-0.1965	0.0369	-0.1294
HOWELL2:	-0.0281	0.1074	-0.0881
RHODES:	-0.0465	0.0307	-0.1073

The adjusted 3-D Cartesian geocentric coordinates, computed with minimum norm solution, are presented in Table 4.

TABLE 4

These are adjusted coordinates: X,Y,Z computed with minimum norm solution in geocentric system. The units are meters.

	X	Y	Z
18-83:	593219.21232	-4859538.45400	4074815.15125
BRITTON:	584418.06824	-4854212.18281	4082460.73674
BOLTON:	584755.05084	-4864483.28192	4070259.68864
JACKSON:	590077.73616	-4868748.96099	4064394.65276
HAMILTON:	606038.89499	-4865001.47573	4066484.41104
TRURO:	609079.15851	-4856547.17134	4076088.02597
HOOVER:	605724.11430	-4847638.14479	4087145.42971
CLARK:	597846.66192	-4852589.13675	4082448.39156
SMITH:	603352.42714	-4870501.71437	4060319.41397
HOWELL2:	611840.72143	-4857665.45749	4074390.18493
RHODES:	596659.67413	-4859301.43692	4074880.75171

Comparison between Geo/Hydro's and our geodetic coordinates is shown in Table 5. The differences were computed as: Geo/Hydro's minus our minimum norm solution.

TABLE 5

These are the differences between Geo/Hydro's and our minimum norm solution geodetic coordinates. The difference in latitude and longitude are expressed in arc-seconds, the differences in ellipsoidal height are in meters. The average value of the displacement vector is 0.123 m, and after neglecting Clark, it is 0.082 m.

	delta phi	delta lambda	delta h
18-83	0.0020	0.0000	-0.134
BRITTON	0.0017	0.0012	-0.260
BOLTON	0.0010	0.0022	-0.233
JACKSON	0.0024	0.0042	-0.242
HAMILTON	-0.0008	0.0030	0.005
TRURO	-0.0013	0.0023	0.172
HOOVER	-0.0041	0.0005	0.246
CLARK	-0.0170	0.0001	-0.243
SMITH	0.0020	-0.0080	0.130
HOWELL2	0.0001	-0.0006	0.141
RHODES	0.0019	-0.0018	0.097

Comparison between Geo/Hydro's and our state plane coordinates is presented in Table 6. The differences were computed as: Geo/Hydro's minus our minimum norm solution.

TABLE 6

These are the differences between Geo/Hydro's and our state plane coordinates. The magnitude of the residual vector is listed in the right column. The units are feet.

	delta y	delta x	$(x^2 + y^2)^{0.5}$
18-83	0.20	0.00	0.20
BRITTON	0.16	-0.09	0.18
BOLTON	0.09	-0.17	0.19
JACKSON	0.24	-0.33	0.41
HAMILTON	-0.08	-0.08	0.11
TRURO	-0.14	-0.18	0.23
HOOVER	-0.42	0.04	0.42
CLARK	-1.71	-0.02	1.71
SMITH	0.21	0.62	0.66
HOWELL2	-0.02	0.08	0.08
RHODES	0.19	0.15	0.24
	rms = 0.54	rms = 0.23	avg = 0.40

and after neglecting for Clark:

	rms = 0.20	rms = 0.25	avg = 0.27

CONCLUSIONS

1. Geo/Hydro's geodetic coordinates and ellipsoidal heights slightly differ from ours. The average differences are: in latitude 0.000" (rms=0.005"), in longitude 0.000" (rms=0.003"), in ellipsoidal height 0.029 m (standard deviation=0.187 m).

2. There was an indication that coordinates of station Rhodes, determined by Thomas Engineering and Surveying Company (TESCO) and used by Geo/Hydro, may be in error (Geo/Hydro, 1983). Based on the resultsof our investigation we may state that there is no indication that the coordinates of station Rhodes are possibly in error. The differences between the minimum constraint and the minimum norm solutions for station Rhodes are not greater than for other densified stations.

3. From the investigation it became evident that in some cases the re-evaluation of the precision in which the computations are carried out, may be in order. The accuracy in coordinate determination should be at least at the level of 1 mm. All intermediate steps should have ensured computational accuracy of one order higher (i.e. 0.1 mm).

4. The discrepancies between our and Geo/Hydro's adjusted state plane coordinates (X,Y) for the stations: Jackson, Clark and Smith were respectively (-0.33' & +0.24'). (-0.02' & -1.71') and (+0.62" & 0.21'). It is suggested

to re-check the entire procedure of their determination before the final coordinates will be published by NGS and transferred to NAD83 system.

5. When using GPS for the densification of geodetic networks it is necessary to outline the standard procedures for: data collection, data pre-processing, data treatment (adjustment), display (presentation) of results. In particular, the following seem to be desirable: to state what reference ellipsoid was used, to suggest what minimum degrees of freedom should be acceptable, to display the entire procedure for data-processing (in order to obtain the "raw coordinates" or "raw coordinate differences") , to state if geoid undulations were used for converting orthometric heights (H) to ellipsoidal heights(h), to state which method of adjustment was used and why, and what was the initial point taken to start the adjustment (if any), to provide the user with all the equations used for transformations from geocentric to geodetic to state plane coordinate system (and vice versa), to state who developed the software used (including the address), on what kind of system the computations were carried out, what language was used, in what precision the computations were carried out, what magnitude of round-off errors is to be expected and what are the significant digits that can be used for further computations.

6. It is suggested that, whenever possible, the geoid undulations should be included in the computation of the ellipsoidal heights from orthometric heights (particularly in hilly and mountaineous terrain). This, in turn, calls for improved knowledge of the gravity field in the area of the survey.

REFERENCES:

Geo/Hydro, Inc., 1983. "Project Report, Geodetic Survey, Franklin County, Ohio." Report Prepared for the Office of Engineers, Franklin County, Ohio. 25 pp. Rockville, Maryland.

Heiskanen, W.A. and H. Moritz, 1967. Physical Geodesy. Reprint Institute of Physical Geodesy, Technical University, Graz. 464 pp.

Leick, A., 1984. "Macrometer Satellite Surveying". Paper Presented at the F.I.G. Engineering Surveys Conference, March 10-11, 1984, Washington, D.C.

NOAA, 1974. "Classification, Standards of Accuracy and General Specifications of Geodetic Control Surveys.".US Department of Commerce, NOS, Reprint 1978. 30 pp.

Rapp, R.H., 1983. "Geometric Geodesy II, Advanced Techniques". Lecture Notes, Department of Geodetic Science and Surveying, The Ohio State University. 192 pp.

Sigl, R. (ed.), 1982. Proceedings of the International Symposium on Geodetic Networks and Computations of the International Association of Geodesy. August 31-September 5, 1982, Munich, Vol. 2-8, Deutsche Geodatische Kommission der Bayerischen Akademie der Wissenschaften, Reihe B, Heft Nr.258.

Sliwa, L., 1985. "The Re-Adjustment of the First Order Local Geodetic Network in Franklin County, Ohio, Incorporating Results of the Global Positioning System (GPS)". M.Sc. Thesis, Department of Geodetic Science and Surveying, The Ohio State University. 75 pp.

Steeves, R.R., 1983. "Mathematical Models for Use in the Re-Adjustment of the North American Geodetic Networks". Ottawa, Canada. 57 pp.

Uotila, U.A. 1984. "Advanced Adjustment Computation". Unpublished Lecture Notes for the Course GS 762, Department of Geodetic Science and Surveying, The Ohio State University.

U.S. Department of Commerce, 1973. "State Plane Coordinates by Automatic Data Processing". Environmental Science Service Administration, Coast and Geodetic Survey, Publication 62-4, 68 pp.

APPENDIX

FIGURE 1: Sketch of the Area of Densification with Densified Stations

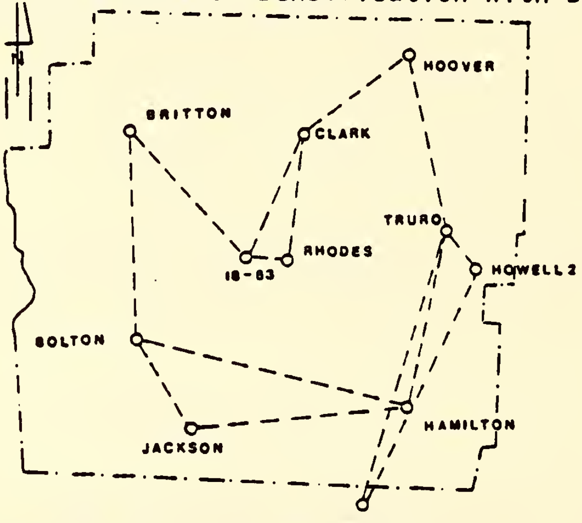

FIGURE 2: The Residual Vectors Between Geo/Hydro's and Our Adjustment (State Plane Coordinates, Lambert Projection, Ohio South Zone). The residual vectors are amplified 15 000 times. The units are feet.

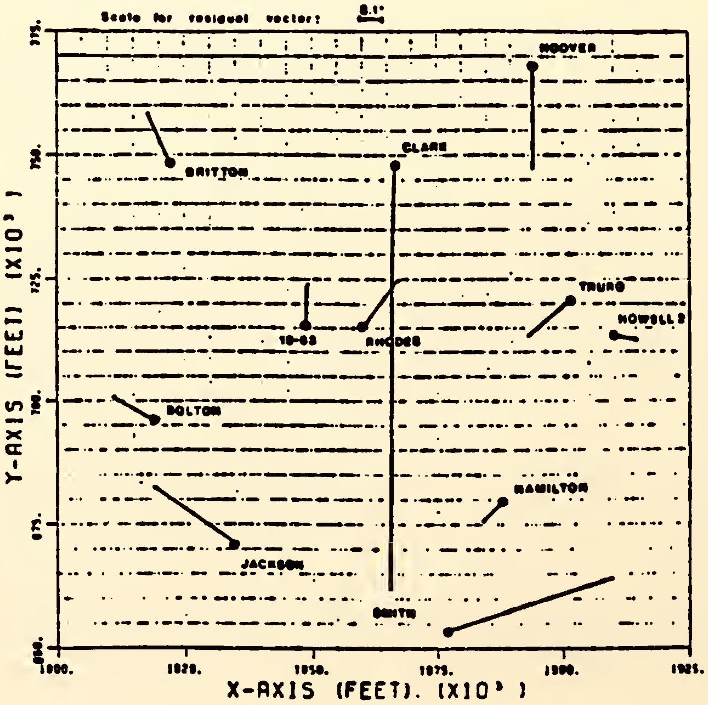

THE MONTGOMERY COUNTY PENNSYLVANIA GLOBAL POSITIONING GEODETIC CONTROL PROJECT

Gary Cuppels
Gilbert/Commonwealth, Inc.
P. O. Box 1498, Reading, Pennsylvania 19603

and

James Collins
Geo/Hydro, Inc.
2115 E. Jefferson Street
Rockville, Maryland 20852

INTRODUCTION

The Montgomery County Geodetic Survey is the result of over a decade of effort and lobbying by numerous individuals located in both state government and private engineering and survey practice. Most notable of which were personnel assigned to the Pennsylvania Department of Transportation and individual members of the Pennsylvania Society of Land Surveyors.

The culmination of those efforts occurred when the Pennsylvania State Legislature approved funding for a statewide geodetic survey project in 1982. Upon funding, the administration of the survey was assigned to the Bureau of Highway Design, Photogrammetry and Surveys within the Pennsylvania Department of Transportation. A geodetic control committee composed of a broad cross-section of the potential user community, Department of Transportation personnel, and a National Geodetic Survey advisor was subsequently appointed to serve the Department in an advisory capacity.

A survey of each of the 67 counties in Pennsylvania to determine need priorities was undertaken and a list of critical areas was developed by the Department of Transportation in association with the geodetic control committee and the National Geodetic Survey. The Montgomery county area which adjoins the city of Philadelphia was chosen as the initial project, due to the extreme lack of existing recoverable horizontal control monumentation in this area. Montgomery county is a suburb of Philadelphia and is experiencing the extensive growth patterns associated with this type of location. The lack of recoverable horizontal control monumentation had made the growth very difficult to manage and had added dramatically to the costs associated with the development of this area.

The project area was further defined to include the southern portion of Montgomery county bounded by Philadelphia county to the southeast Chester county to the southwest latitude and longitude 40° 07' 30", 75° 27' 45" to the northwest latitude and longitude 40° 17' 12", 75° 15' 53" to the north and Bucks county to the northeast. The total project area encompasses approximately four hundred square miles.

In March of 1983, the Department of Transportation advertised for a consultant qualified to perform geodetic control surveys for the state of Pennsylvania.

After an extensive selection process, Gilbert/Commonwealth, Inc. in association with Geo-Hydro, Inc. was selected in June of 1983 to provide the requested geodetic survey services.

The initial project planning was based on the utilization of standard steel tower triangulation and conventional geodetic control survey methods. The work to be performed was to be fully compatible and in conformance with the accuracy standards promulgated by the Federal Geodetic Control Committee's "Classification, Standards of Accuracy and General Specifications of Geodetic Control Surveys" dated February 1974 and reprinted January 1979. During the initial planning stage of the project, a number of events occurred that drastically altered the course of the project.

First the liability, maintenance and possible public resistance to the construction of 30 to 36 meter survey towers in this suburban to urban area would have added considerably to the project costs and would have impacted unfavorably on the location of control monumentation as it relates to subsequent user community usage and monument access. Second, the MACROMETER™ V-1000 interferometric surveyor global positioning instrumentation was in the final stages of being validated and approved for usage as a geodetic survey instrument by a variety of governmental agencies both domestically and internationally.

Third, the costs associated with conventional horizontal control survey techniques and the related steel tower erection would have serious impact on either the total project area or the number of survey points that could be positioned.

As a result of these factors, a decision to pursue global positioning via the MACROMETER™ was made in October of 1983. Efforts towards finalizing the initial project and commencing the site reconnaissance and monument location were started.

SITE RECONNAISSANCE

In January of 1984, Gilbert/Commonwealth, Inc. was authorized to commence the site reconnaissance for the project area. The reconnaissance was subsequently divided into a number of individual project tasks. The first task was to determine the current status of the existing horizontal and vertical control that could possibly be utilized as reference ties for the G.P.S. network. The existing control was recovered where possible and recovery descriptions were prepared for subsequent inclusion into the N.G.S. bluebook database.

The existing recoverable sites were reviewed for compatibility to G.P.S. survey methods utilizing the following criteria: an unobstructed site as it would relate to an open horizon and allow the G.P.S. system receiver antenna to receive the satellite signals. To insure this ability, the field reconnaissance team was provided with a "Pie" diagram which depicted the minimum horizon vertical angle for each sky quadrant. As there were not any satellites located in the southeast quadrant, large obstructions such as trees and buildings could be tolerated within that quadrant. Additional criteria considered included site access to the G.P.S. survey vehicle which was usually a "Jeep" CJ7 or a similar vehicle. The existing monumentation location related to the central project area was considered so as to minimize the travel time between observations. Ideally, it was desirable to limit travel time to not more than thirty minutes if two G.P.S. observations per day were to be obtained.

The second task conducted was the selection of sites for the establishment of new horizontal control monuments. In addition to the criteria used to select existing recoverable control sites, the selection of the new sites was based on the following criteria:

1. Accessibility for G.P.S. observations.
2. Sites that were located on public property to include road right of ways, public parks, public building ground such as local government office building sites, school yards, etc.
3. Sites that were permanent, accessible and where the control monuments could be set at ground level.
4. The distance between station sites was to be limited to four to five kilometers.
5. Sites were selected with consideration given to providing a minimum of one existing intersecting object such as water tanks, radio masts, or church spires so as to facilitate the establishment of additional landmark azimuth position.
6. The sites were reviewed so as to provide a location for adequate reference marks with particular emphasis being placed on the ability to install a permanent ground visible azimuth mark at least four hundred meters distant from the new station mark.
7. When possible, sites were selected that had unobstructed ground to ground lines of site between established stations.

Generally, all of the above criteria were adhered to with the exception of item number six. Due to the extensive development within the project area, only a limited number of sites are intervisible. Simultaneous to the site selection reconnaissance, descriptions were prepared for each of the selected sites. The descriptions provided accurate "To Reach" descriptions for each proposed station and information related to property ownership and the person to contact for site access.

Upon completion of the above referenced tasks, a reconnaissance report was prepared for submittal to both the Department of Transportation and the National Geodetic Survey. The reconnaissance report contained the following information:

- Project location sketch
- Recovered vertical control data including a summary sheet
- Recovered horizontal control data including a summary sheet
- Proposed horizontal control stations including detailed descriptive data

- A project reconnaissance sketch

The reconnaissance sketch was produced at scale and provided plotted data on all of the existing horizontal and vertical control that was searched for but not recovered, the positions of the proposed horizontal monumentation and a graphic breakdown of the MACROMETER™ observations into one per day observations and two per day observations.

In March of 1984, the reconnaissance sketch and report were completed and submitted for review by the above mentioned agencies. Simultaneous to the review of the report and sketch, efforts to secure the required permission for the instruction of the new monumentation was initiated. This effort involved contacting all of the affected property owners via a standardized letter, obtaining written approvals, securing underground utility information and actual field locations of utilities that might be in conflict with the proposed monumentation, and revising the proposed monumentation locations where conflicts with property owners or utilities occurred. By the end of April 1984, approval of the reconnaissance report and sketch was granted by both the Department of Transportation and the National Geodetic Survey.

MONUMENT CONSTRUCTION

The actual construction of the monumentation was started in April 1984 and was completed in May of the same year. During that span of time, thirty-one new horizontal stations were established, including reference marks and azimuth marks, and eight existing horizontal stations were improved or upgraded by the installation of reference marks and/or azimuth marks. In total, ninety-one (91) new concrete monuments were poured in the field and forty-seven standard discs were set in existing permanent objects or structures. All of the monuments established are in conformance with applicable National Geodetic Survey construction specifications and standards. All of the new horizontal control stations have underground reference discs that were set in bedrock or concrete.

PROJECT ACCURACY STANDARDS

The observational data and field procedures utilized during the course of this project were performed to support the "Classification, Standards of Accuracy and General Specifications of Geodetic Control Surveys" as promulgated by the Federal Geodetic Control Committee. The achieved results for this project meet and/or exceed all of these requirements. The project accuracy specifications specified by the Department of Transportation for the various tasks associated with the project are as follows:

o G.P.S Observations Primary Control Ties to First Order Monumentation Stations Fleck - 2, Arco, Mainland RM3	First Order
o All Other G.P.S. Observations	Second Order Class I
o Field Traverses	Second Order Class I
o Azimuth Determinations	Third Order Class I

o Horizontal Distances and Directions	Second Order Class I
o Vertical Control	Third Order

MACROMETER OBSERVATIONS

Field observations with the MACROMETER™ by Geo-Hydro personnel assisted by the Gilbert/Commonwealth project surveyor were started May 21, 1984 and were completed June 23, 1984. No observations were obtained during the period of June 10, 1984 through June 16, 1984 due to equipment failure and/or malfunctions. The observations were obtained using three V-1000 MACROMETER™ operating within a five hour observation window. For the purpose of tying the proposed control network to the available existing horizontal and vertical control stations one observation per day per station was used. For all stations to be established two observations per day were used. The observation window was divided as follows: The first session was two and one half hours, one half hour was used for travel and the remaining two hours provided the second observation.

The horizontal basis for this network was three first order control points Arco, Mainland RM3 and Fleck-2. Upon comparison of the observed data it became apparent that the published position for station Arco was suspect. The error was confirmed by a comparison of the "Free" adjustment of the MACROMETER™ observations with the constrained adjustment of the observations utilizing the published coordinate values for the existing control stations. The "Free" adjustment had a closure of 1:700,000 while the constrained adjustment closure was only 1:8,000. As a result of these findings the National Geodetic Survey was contacted. It was found that the published values for station Arco were in error due to a network adjustment constraint. Subsequently new coordinate values for station Arco were published and made available. Utilizing the revised coordinate values for station Arco, the constrained adjustment of the G.P.S. observations resulted in a closure of 1:60,000, well within the project specification of 1:50,000.

The vertical ties to existing benchmarks for this project were consistent and did not require any significant adjustment.

ANALYSIS OF THE RESULTS

The "free" adjustment of the Montgomery County network indicates that the observed data were more accurate that the existing geodetic control to which the survey was referenced. For this reason it is difficult to determine actual accuracies of individual points. An analysis was performed comparing each point's circular error computed from the Least Square Adjustment, with the circular "uncertainties" the result from the computation of each individual line vector. These two "circular errors" were differenced to give an indication of how well individual formal line errors predicted the actual errors as given by the Least Square Adjustment. It is recognized that this approach is flawed by the fact that individual line errors are highly correlated with the point errors computed in the Least Square Adjustment. However, the MACROMETER™ measures more accurately than conventional systems so that comparisons with "ground truth" are not possible.

In spite of the flawed nature of this comparison, several important results can be reported. Of the fifty-eight lines studied, eleven lines had less than 100 observations, with the remaining lines averaging about 120 observations (an observation is defined as one less than the number of phases observed during a single epoch). Five of the eleven lines gave higher than normal line uncertainties while only three of these five lines showed abnormally high circular errors resulting from the Least Square computation. None of the lines with over 100 observations exhibited unusually high errors.

This rather simple analysis shows that for the conditions encountered during this survey one can observe a minimum of 100 MACROMETER observations and be virtually assured of obtaining first-order results.

The duration of the two observing periods used was selected by simulating conditions encountered during the survey. An analysis of the accuracy achieved for the first and second periods shows no appreciable difference between sessions, so that actual observations conformed fairly well to the simulation.

In other G.P.S. surveys it has been noted that there is a direct relation between the ratio of the number of observations divided by the Chi square to the accuracy achieved. For example, when the Chi square value exceeds the number of observations by a factor of two, the accuracy of the vector determination decreased significantly. The highest ratio for this project was 1.97 for line 36 to 21; however, no decrease in accuracy was noted.

Several graphs plotting the Chi square to observation ratio and number of observations vs. accuracy were made. The plots showed completely random distribution and no particular trend was evident.

The G.P.S. observations for the Montgomery County survey exhibited both a high degree of reliability and accuracy. None of the vectors measured displayed unusually high residuals in the Least Square adjustment and, therefore, none of the lines was recomputed. The fact that the "uncertainties" resulting from individual vector computations closely agreed with the line standard errors shows that these "uncertainties" are a good indicator of survey accuracy.

Upon finalization of the adjustments of the observational data a control and adjustment report was prepared and submitted to the Department. Additionally, all of the G.P.S. observational data was formatted into a provisional bluebook format acceptable to the National Geodetic Survey. The formatting was accomplished using the NGS Computer Program MACAD with the end result being a 8-inch floppy disc which was submitted to the Department of Transportation along with the control and adjustment report.

CONVENTIONAL FIELD SURVEYS

In October 1984 the Department of Transportation authorized the survey field work, observation, and measurements necessary to finalize the project. This work involved obtaining the horizontal distance and angle between the newly established stations and their respective azimuth mark and station reference marks that were set previously in the project. Additionally, horizontal angles between the station azimuth marks and available landmarks were obtained and the final descriptive data for the new station and its peripheral marks including landmarks was obtained. Significant to this effort, station descriptions for all of the installed azimuth marks were prepared so as to render a "stand alone" description for the newly installed azimuth marks. This was done to satisfy a project requirement in that all of the azimuth positions be formatted in a manner acceptable to the National Geodetic Survey for final publishing of the azimuth position as an exact position rather than an approximate position. If adequate "stand alone" descriptions and separate station descriptions would not have been prepared, the azimuth mark position would have been published by the National Geodetic Survey with the distance between the station and the mark being rounded off to the nearest meter, and then being converted into kilometers or decimals of a kilometer.

Simultaneous to this effort by Gilbert/Commonwealth personnel, Department of Transportation personnel, under the direction of the National Geodetic Survey advisor, obtained astro-azimuth for each of the new stations and provided the calculated azimuth to Gilbert/Commonwealth for inclusion in the final project data and eventual inclusion in the bluebook database.

In order to provide for further redundancy of the positions obtained via the MACROMETER™ observations, provide a check on the validity of other existing horizontal control located within the project boundary and to eliminate the potential of a twenty percent violation. A traverse connection between existing horizontal and vertical station BQ197 and the newly established St. Basil was run using conventional Second Order Class One metropolitan survey procedures. The preliminary reduction of this traverse by the contractor substantiated the previous observations and field work.

FINALIZED DATA AND BLUEBOOKING

Upon the completion of the field work in December of 1984 efforts to finalize all of the data were commenced, project records were consolidated and put into final format, the project reconnaissance sketch was updated, information for inclusion into the final project report was compiled, and all data necessary to compile and format the field data into an acceptable N.G.S. bluebook database was assembled.

The N.G.S. bluebooking was accomplished utilizing the National Geodetic Survey computer program "Micro-tencol." The program was loaded on one of Gilbert/Commonwealth's IBM PC-XT computers. The computer was utilized fully to complete all of the bluebook formatting of the project data, and the eventual preparation of the final project database that was subsequently submitted to the Department of Transportation in February of 1985.

Also submitted to the Department at this time as part of the finalization of this project was a final project report. This document provides a chronological history of the project, a repository for relevant project information and a copy of the final project reconnaissance sketch in a concise, easily utilized document. By submittal of the above referenced data the Montgomery county project was officially completed.

CONCLUSION

The Montgomery County Geodetic Control Project has provided a wealth of practical information related to the utilization of the global positioning system for the accurate, reliable, cost-efficient and timely acquisition of geodetic control survey data. The project also demonstrates that this system is applicable to a variety of other typical land survey tasks that would formerly require extensive, costly and time consuming field surveys.

LOCAL REFERENCE SYSTEMS IN GEODETIC SURVEY UNDER CONSIDERATION OF TERRESTRIAL AND SATELLITE POSITIONING METHODS

Albert Schödlbauer
Institut für Geodäsie
Universität der Bundeswehr München
Werner-Heisenberg-Weg 39
D-8014 Neubiberg, Federal Republic of Germany

ABSTRACT. The utilization of satellite data for purposes of point positioning requires various curvilinear and Cartesian coordinate systems. This paper treats the transformation network linking these systems. New investigations were carried out on the direct relations between Local Geodetic Cartesian Coordinates on the one side and Geodetic Polar Coordinates and Transversal Mercator Coordinates on the other side.

1. INTRODUCTION

Two principally different kind of families of ellipsoid related coordinate systems are employed in geodetic survey:

- Firstly,
  the family of Curvilinear Coordinate Systems
  using Gaussian coordinate curves on the surface of a reference ellipsoid. In order to describe three dimensional point fields, the two-dimensional grids of parameter lines, generated by the Gaussian coordinate curves, have to be extended by normals to the surface as straight reference-lines of a third parameter.

  The most important representatives of this family are the following three coordinate systems

  $\underset{\sim}{x}^G = (\varphi, \lambda, h)$, the system of Geodetic Coordinates

  φ = geodetic latitude (geographical latitude on the reference ellipsoid)
  λ = geodetic longitude (geographical longitude on the reference ellipsoid)
  h = geometric height above the reference ellipsoid.

  $\underset{\sim}{x}^P = (\alpha_0, S, h)$, the system of Geodetic Polar Coordinates

  α_0 = geodetic azimuth of a geodesic on the reference ellipsoid
  S = length of a geodesic on the reference ellipsoid
  h = geometric height above the reference ellipsoid (ellipsoidal height).

  The coordinates refer to an origin P_0 with the geodetic coordinates

  $\underset{\sim}{x}^G_0 = (\varphi_0, \lambda_0, h_0 = 0)$; see figure 2.

  $\underset{\sim}{x}^K = (x, y, h)$, the system of Transversal Mercator Coordinates

  which is defined on a conformal mapping plane as well as on the surface of the corresponding reference ellipsoid.

x = northing
y = easting
h = geometric height above the reference ellipsoid (ellipsoidal height).

With the intention of simplifying the relations to the other coordinate systems treated in this paper, we refer the x^P-system to the meridian of P_0, the origin of the x^P and x^{LG}-system (but not to one of the prime meridians in the conventional raster related to the Meridian of Greenwich ($\lambda_0 = 0^o$, $\Delta\lambda = 6^o$) as used in the UTM-system); see figure 2.

- Secondly, the family of Three Dimensional Cartesian Coordinate Systems . Using them as a tool for state survey like the above mentioned systems $\underline{x}^G$, $\underline{x}^P$, $\underline{x}^K$, they have to be tied to the reference ellipsoid too, either in its center or on its surface:

$\underline{x}^G = (X^G, Y^G, Z^G)^T$, Ellipsoid Centered Cartesian Coordinate System .

The Z^G-axis coincides with the minor semi axis of the reference ellipsoid, directing to its north pole, X^G- and Y^G-axis put up the equator plane and create together with the Z^G-axis, a right-handed coordinate system. Moreover, the X^G-axis is situated in the ellipsoidal meridian plane of Greenwich.

$\underline{x}^{LG} = (X, Y, Z)^T$, Local Geodetic Cartesian Coordinate System .

The system is defined as follows: its origin is a point P_0 on the surface of the reference ellipsoid with the geodetic coordinates φ_0, λ_0, $h_0 = 0$. The Z-axis coincides with the ellipsoidal normal in P_0, the X-axis with the tangent vector of the meridian ellipse through P_0 directing to the northern branch of this curve. The Y-axis is chosen in a way that the system is left-handed; see figure 2. Note that the $\underline{X}^{LG}$-system determines angles of φ_0 and λ_0 with the $\underline{X}^{GL}$-system.

The family of coordinate systems mentioned firstly is appropriate for terrestrial surveying methods. Their orientation conforms to the direction of the vertical line. The second family is particularly suitable to the methods of satellite surveying. If we merge these methods, which has become more and more important in the wake of the progress of surveying techniques, we have to master the mutual relations. In particular, we need algorithms to transform the coordinates from one system into any other one, cf. VANIČEK/KRAKIWSKY (1982, p.321) or the synopsis given by SCHÖDLBAUER (1984).

Hitherto, the transformation from $\underline{x}^P$- and $\underline{x}^K$-coordinates into $\underline{x}^{LG}$-coordinates and vice versa (continuous line in fig. 1) had to be done by means of $\underline{x}^G$- and $\underline{x}^G$-coordinates. Extending the possibilities, SCHÖDLBAUER (1984) has made available formulas for the direct transformations $x^P \leftrightarrow \underline{x}^{LG}$ and $\underline{x}^K \leftrightarrow \underline{x}^{LG}$. The present paper makes up for the necessary derivations, which could not be communicated there. The mentioned transformations are of interest, if local geodetic networks based on terrestrial and satellite surveying methods are to be treated.

An associative diagram showing the significant excerpt of the network of pertinent transformations is presented in figure 1. Figure 2 is illustrating the geometrical relations between them.

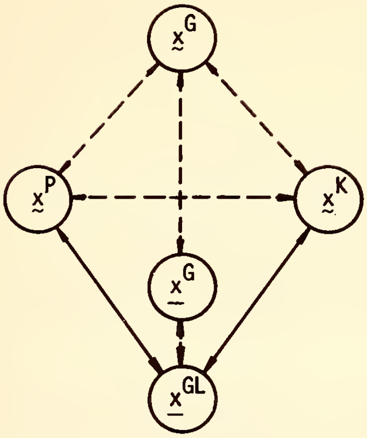

Figure 1

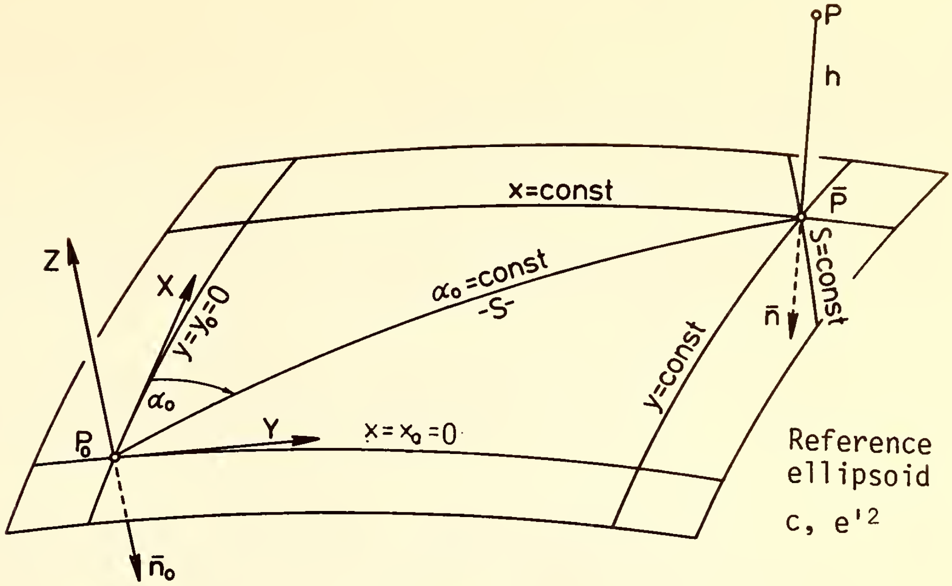

Figure 2

2. TRANSFORMATION

We denote

c = polar radius of curvature of the meridian ellipse) of the
N = c/V = radius of curvature in the prime vertical) reference
e' = second excentricity) ellipsoid

$\eta^2 = e'^2 \cdot \cos^2\varphi$; $V^2 = 1 + \eta^2$) auxiliary variables .
$u_0 = S \cdot \cos \alpha_0$ $v_0 = S \cdot \sin \alpha_0$)

The fundamental relation for solving the defined problem in a local approach are "Weingartens developments" (GROSSMANN, 1976, p.62), which are Taylor's series extensions with the increment S. That means, the scope of their applicability is limited. We consider that, using a diameter of not more than 200 km ($S \leq 100$ km) and ellipsoidal heights up to 2000 m ($h \leq 2000$ m) cm-granting accuracy is attainable. Thus we dare neglect terms of the order of $(S/c)^5 \cdot S$, $(S^3 \cdot h/c^4) \cdot S$, $e'^2 \cdot (S/c)^3 \cdot S$ and $e'^2 \cdot (S \cdot h/c^2) \cdot S$, and of higher order.

2.1 $\underset{\sim}{x}^P$ $(\alpha_0, S, h) \rightarrow \underline{x}^{LG}$ (X, Y, Z)

For solving this problem, SCHÖDLBAUER (1985) has given a direct solution on "Weingartens Developments" (GROSSMANN, 1976, p.62-66). These developments are based on differential geometric relations between two-dimensional ellipsoidal polar coordinates (α_0, S) of points $\bar{P}$ on the surface of an ellipsoid and three-dimensional local geodetic ($\underline{x}^{LG}$-) coordinates of these points.

$$\underline{\bar{x}}^{LG} = \begin{bmatrix} \bar{X} \\ \bar{Y} \\ \bar{Z} \end{bmatrix} = N_o \cdot \begin{bmatrix} \cos\alpha_o \cdot \sin\dfrac{S}{N_o} - \dfrac{\eta_o{}^2 \cdot (1+\cos^2\alpha_o) \cdot \cos\alpha_o \cdot S^3}{6 \cdot N_o{}^3} \\ \sin\alpha_o \cdot \sin\dfrac{S}{N_o} - \dfrac{\eta_o{}^2 \cdot \cos^2\alpha_o \cdot \sin\alpha_o \cdot S^3}{6 \cdot N_o{}^3} \\ -1 + \cos\dfrac{S}{N_o} - \dfrac{\eta_o{}^2 \cdot \cos^2\alpha_o \cdot S^2}{2 \cdot N_o{}^2} + \dfrac{\eta_o{}^2 \cdot \tan\varphi_o \cdot \cos\alpha_o \cdot S^3}{2 \cdot N_o{}^3} \end{bmatrix} . \qquad (1)$$

(1) represents the vector from the origin of the $\underline{x}^{LG}$-system to an S-variable point $\bar{P}$ on a geodesic which passes P_0 under the azimuth α_0. The principal normal of the geodesic in $\bar{P}$ which coincides with the normal of the surface $\underline{n}$ in the same point (directing from $\bar{P}$ to P), can be described by Frenets formulas (f.e. EISENHART, 1947, p.25, VANIČEK/KRAKIWSKY, 1982, p.39). According to these formulas, $\underline{n}$ can be found by differentiating $\underline{\bar{x}}^{LG}$ twice with respect to S and by normalizing it to the unit 1.

$$\underline{n} = \frac{\underline{x}^{LG''}}{|\underline{x}^{LG''}|} = \begin{bmatrix} X_n \\ Y_n \\ Z_n \end{bmatrix} = \begin{bmatrix} -\cos\alpha_o \cdot \sin\dfrac{S}{N_o} - \dfrac{\eta_o{}^2 \cdot \cos\alpha_o \cdot S}{N_o} \\ -\sin\alpha_o \cdot \sin\dfrac{S}{N_o} \\ -\cos\dfrac{S}{N_o} \end{bmatrix} . \qquad (2)$$

Putting (1) and (2) together, we find the solution

$$\underline{x}^{LG} = \underline{\bar{x}}^{LG} - h \cdot \underline{n} . \qquad (3)$$

On expressing the vectors (3) by its coordinate components we finally obtain

$$X = \cos\alpha_o \cdot \sin\frac{S}{N_o} \cdot (N_o + h) - \frac{\eta_o{}^2 \cdot (1+\cos^2\alpha_o)\, \cos\alpha_o \cdot S^3}{6 \cdot N_o{}^2} + \frac{\eta_o{}^2 \cdot \cos\alpha_o \cdot S \cdot h}{N_o} \qquad (4)$$

$$Y = \sin\alpha_o \cdot \sin\frac{S}{N_o} \cdot (N_o + h) - \frac{\eta_o{}^2 \cdot \cos^2\alpha_o \cdot \sin\alpha_o \cdot S^3}{6 \cdot N_o{}^2} \qquad (5)$$

$$Z = \cos\frac{S}{N_o} \cdot (N_o + h) - N_o - \frac{\eta_o{}^2 \cdot \cos^2\alpha_o \cdot S^2}{2 \cdot N_o} + \frac{\eta_o{}^2 \cdot \tan\varphi_o \cdot \cos\alpha_o \cdot S^3}{2 \cdot N_o{}^2} \qquad (6)$$

2.2 $\underline{x}^{LG}(X, Y, Z) \to \underset{\sim}{x}^{P}(\alpha_0, S, h)$

The wanted solution (α_0, S, h) can be found by inverting (4), (5), (6). In a first step h is extracted. For this purpose, we put together the squares of (4), (5), (6) by

$$X^2 + Y^2 + (Z+N_0)^2 = (N_0+h)^2 - \frac{(N_0+h)\cdot\eta_0^2\cdot\cos^2\alpha_0\cdot S^2}{N_0} + \frac{(N_0+h)\cdot\eta_0^2\ \tan\varphi_0\cdot\cos\alpha_0\cdot S^3}{N_0^2}\cdot \tag{7}$$

Extracting the square root and developing the right side yields

$$\sqrt{X^2 + Y^2 + (Z+N_0)^2} = N_0 + h - \frac{\eta_0^2\cdot\cos^2\alpha_0\cdot S^2}{2\cdot N_0} + \frac{\eta_0^2\cdot\tan\varphi_0\ \cos\alpha_0\cdot S^3}{2\cdot N_0^2}\ . \tag{8}$$

Hence we have

$$h = \sqrt{X^2 + Y^2 + (Z+N_0)^2} - N_0 + \frac{\eta_0^2\cdot\cos^2\alpha_0\cdot S^2}{2\cdot N_0} - \frac{\eta_0^2\cdot\tan\varphi_0\cdot\cos\alpha_0\cdot S^3}{2\cdot N_0^2}\ . \tag{9}$$

For the necessary final substitution of the parameters α_0 and S by X and Y in the terms containing η_0^2 we can extract from (4) and (5) sufficiently accurate $\cos\alpha_0\cdot S = X$ and $\sin\alpha_0\cdot S = Y$. Thus h is found to be

$$h = \sqrt{X^2 + Y^2 + (Z+N_0)^2} - N_0 + \frac{\eta_0^2\cdot X^2}{2\cdot N_0} - \frac{\eta_0^2\cdot\tan\varphi_0\cdot(X^3+X\cdot Y^2)}{2\cdot N_0^2}\ . \tag{10}$$

The second step to be done is to represent X and Y through inverting the equations (4) and (5) and substituting again $\cos\alpha_0\cdot S = X$ and $\sin\alpha_0\cdot S = Y$ in the terms with η_0^2. We obtain

$$\cos\alpha_0\cdot\sin\frac{S}{N_0} = \frac{X}{N_0+h} + \frac{\eta_0^2\cdot X^3}{3\cdot N_0^3} + \frac{\eta_0^2\cdot X\cdot Y^2}{6\cdot N_0^3} - \frac{\eta_0^2\cdot X\cdot h}{N_0^2} \tag{11}$$

$$\sin\alpha_0\cdot\sin\frac{S}{N_0} = \frac{Y}{N_0+h} + \frac{\eta_0^2\cdot X^2\cdot Y}{6\cdot N_0^3}\ . \tag{12}$$

Squaring and adding (11) and (12) and extracting the square root out of the sum on the one side, and dividing (11) and (12) by (13) on the other side yields

$$\sin\frac{S}{N_0} = \sqrt{(\cos\alpha_0\cdot\sin\frac{S}{N_0})^2 + (\sin\alpha_0\cdot\sin\frac{S}{N_0})^2} \tag{13}$$

$$\cos\alpha_0 = \frac{(\cos\alpha_0\cdot\sin\frac{S}{N_0})}{\sin\frac{S}{N_0}} \quad \text{resp.} \quad \sin\alpha_0 = \frac{(\sin\alpha_0\cdot\sin\frac{S}{N_0})}{\sin\frac{S}{N_0}} \;. \tag{14}$$

The representation of S and α_0 with the aid of (13) and (14) applying arccos and arcsin is obviously without any problem.

2.3 $\underset{\sim}{x}^K\,(x,y,h) \rightarrow \underline{x}^{LG}\,(X,Y,Z)$

Initial equation for solving this problem are functions $\underline{x}^{LG} = \underline{x}^{LG}(\underset{\sim}{x}^P)$ as we have obtained by (4), (5), (6) on the one hand and functions $\underset{\sim}{x}^K = \underset{\sim}{x}^K(\underset{\sim}{x}^P)$ f.e. according to HRISTOW (1955, p.187), GROSSMANN (1976, p.173), SCHÖDLBAUER (1982, p.229) on the other hand. From (4) and (5) we have, after developing sin (S/N_0) into series

$$\begin{aligned} X = {} & \cos\alpha_0\cdot S + \frac{\cos\alpha_0\cdot S\cdot h}{N_0} - \frac{\cos\alpha_0\cdot S^3}{6\cdot N_0{}^2} - \frac{\cos\alpha_0\cdot S^3\cdot h}{6\cdot N_0{}^3} \\ & - \frac{\eta_0{}^2\cdot(1+\cos^2\alpha_0)\cdot\cos\alpha_0\cdot S^3}{6\cdot N_0{}^2} + \frac{\eta_0{}^2\cdot\cos\alpha_0\cdot S\cdot h}{N_0} \end{aligned} \tag{15}$$

$$Y = \sin\alpha_0\cdot S + \frac{\sin\alpha_0\cdot S\cdot h}{N_0} - \frac{\sin\alpha_0\cdot S^3}{6\cdot N_0{}^2} - \frac{\sin\alpha_0\cdot S^3\cdot h}{6\cdot N_0{}^3} - \frac{\eta_0{}^2\cdot\cos^2\alpha_0\cdot\sin\alpha_0\cdot S^3}{6\cdot N_0{}^2} \;. \tag{16}$$

The other sources mentioned deliver, by spezializing $y_0 = 0$ and considering $1/R_0 = V_0/N_0 = 1/N_0 + \eta_0{}^2/(2\cdot N_0)$, and $1/R_0{}^2 = 1/N_0{}^2 + \eta_0{}^2/N_0{}^2$ respectively

$$x = \cos\alpha_0\cdot S + \frac{\cos\alpha_0\cdot\sin^2\alpha_0\cdot S^3}{3\cdot N_0{}^2} + \frac{\eta_0{}^2\cdot\cos\alpha_0\cdot\sin^2\alpha_0\cdot S^3}{3\cdot N_0{}^2} \tag{17}$$

$$\begin{aligned} y = {} & \sin\alpha_0\cdot S - \frac{\cos^2\alpha_0\cdot\sin\alpha_0\cdot S^3}{6\cdot N_0{}^2} + \frac{\sin^3\alpha_0\cdot S^3}{6\cdot N_0{}^2} \\ & - \frac{\eta_0{}^2\cdot\cos^2\alpha_0\;\sin\alpha_0\cdot S^3}{6\cdot N_0{}^2} + \frac{\eta_0{}^2\cdot\sin^3\alpha_0\cdot S^3}{6\cdot N_0{}^2} \;. \end{aligned} \tag{18}$$

Subtracting (17) form (15) and (18) from (16) yields

$$X-x = \frac{\cos\alpha_o\cdot S\cdot h}{N_o} - \frac{(1+2\cdot\sin^2\alpha_o)\cdot\cos\alpha_o\cdot S^3}{6\cdot N_o^2} - \frac{\cos\alpha_o\cdot S^3\cdot h}{6\cdot N_o^3}$$
$$- \frac{\eta_o^2\cdot(2+\sin^2\alpha_o)\cdot\cos\alpha_o\cdot S^3}{6\cdot N_o^2} + \frac{\eta_o^2\cdot\cos\alpha_o\cdot S\cdot h}{N_o} . \qquad (19)$$

$$Y-y = \frac{\sin\alpha_o\cdot S\cdot h}{N_o} - \frac{\sin^3\alpha_o\cdot S^3}{3\cdot N_o^2} - \frac{\eta_o^2\cdot\sin^3\alpha_o\cdot S^3}{6\cdot N_o^2} - \frac{\sin\alpha_o\cdot S^3\cdot h}{6\cdot N_o^3} . \qquad (20)$$

Here too, we have to eliminate $\cos\alpha_o\cdot S$ and $\sin\alpha_o\cdot S$, which can be expressed, inverting (17) and (18), by

$$\cos\alpha_o\cdot S = x - \frac{x\cdot y^2}{3\cdot N_o^2} \quad \text{and} \quad \sin\alpha_o\cdot S = y + \frac{x^2\cdot y}{6\cdot N_o^2} - \frac{y^3}{6\cdot N_o^2} . \qquad (21)$$

Thus we get from (19) and (20), after some contraction,

$$X = x + \frac{(1+\eta_o^2)\cdot x\cdot h}{N_o} - \frac{(1+2\cdot\eta_o^2)\cdot x^3}{6\cdot N_o^2} - \frac{(1+\eta_o^2)\cdot x\cdot y^2}{2\cdot N_o^2} - \frac{x^3\cdot h}{6\cdot N_o^3} - \frac{x\cdot y^2\cdot h}{2\cdot N_o^3} \qquad (22)$$

$$Y = y + \frac{y\cdot h}{N_o} - \frac{(2+\eta_o^2)\cdot y^3}{6\cdot N_o^2} - \frac{y^3\cdot h}{3\cdot N_o^3} . \qquad (23)$$

In order to display Z, we go back to (6), where $\cos\frac{S}{No}$ has to be developed into series:

$$Z = h - \frac{S^2}{2\cdot N_o} - \frac{S^2\cdot h}{2\cdot N_o^2} + \frac{S^4}{24\cdot N_o^3} - \frac{\eta_o^2\cdot\cos^2\alpha_o\cdot S^2}{2\cdot N_o} + \frac{\eta_o^2\cdot\tan\varphi_o\cdot\cos\alpha_o\cdot S^3}{2\cdot N_o^2} . \qquad (24)$$

As final result we obtain, after inserting (21) into (24) and arranging terms of the same kind and order,

$$Z = \left(1 - \frac{x^2+y^2}{2\cdot N_o^2}\right)\cdot h - \frac{(1+\eta_o^2)\cdot x^2}{2\cdot N_o} - \frac{y^2}{2\cdot N_o} + \frac{\eta_o^2\cdot\tan\varphi_o\cdot(x^3 + x\cdot y^2)}{2\cdot N_o^2}$$
$$+ \frac{(x^4 + 6\cdot x^2\cdot y^2 + 5\cdot y^2)}{24\cdot N_o^3} . \qquad (25)$$

2.4 $\underline{x}^{LG}\ (X, Y, Z) \rightarrow \underset{\sim}{x}^{K}\ (x, y, h)$

A formula for determining h by means of $\underline{x}^{LG}$ (X,Y,Z) was already found in (10). By taking into account the derivations

$$\left(1+\frac{(1+\eta_0^2)\cdot h}{N_0}\right)^{-1} = 1-\frac{(1+\eta_0^2)\cdot h}{N_0}+\frac{h^2}{N_0^2} \quad \text{and} \tag{26}$$

$$\left(1+\frac{h}{N_0}\right)^{-1} = 1-\frac{h}{N_0}+\frac{h^2}{N_0^2} \ , \tag{27}$$

the inversion of (22) and (23) with respect to x and y yields, in a first step,

$$x = \left(1-\frac{(1+\eta_0^2)\cdot h}{N_0}+\frac{h^2}{N_0^2}\right)\cdot\left(X+\frac{(1+2\cdot\eta_0^2+\frac{h}{N_0})\cdot x^3}{6\cdot N_0^2}+\frac{(1+\eta_0^2+\frac{h}{N_0})\cdot x\cdot y^2)}{2\cdot N_0^2}\right. \tag{28}$$

$$y = \left(1-\frac{h}{N_0}+\frac{h^2}{N_0^2}\right)\cdot\left(Y+\frac{(2+\eta_0^2+\frac{2\cdot h}{N_0})\cdot y^3}{6\cdot N_0^2}\right)\cdot \tag{29}$$

When we substitute in the terms of higher order finally

$$x = \left(1-\frac{h}{N_0}\right)\cdot X \quad \text{and} \quad y = \left(1-\frac{h}{N_0}\right)\cdot Y$$

we obtain

$$x = \left(1-\frac{(1+\eta_0^2)\cdot h}{N_0}+\frac{h^2}{N_0^2}\right)\cdot X + \frac{(1+2\cdot\eta_0^2-\frac{3\cdot h}{N_0})\cdot X^3}{6\cdot N_0^2}+\frac{(1+\eta_0^2-\frac{3\cdot h}{N_0})\cdot X\cdot Y^2}{2\cdot N_0^2} \tag{30}$$

$$y = \left(1-\frac{h}{N_0}+\frac{h^2}{N_0^2}\right)\cdot Y + \frac{(2+\eta_0^2-\frac{2\cdot h}{N_0})\cdot Y^3}{6\cdot N_0^2} \ . \tag{31}$$

3. REFERENCES

EISENHART, L.P. (1947): *An Introduction to Differential Geometry with Use of Tensor Calculus;* Princeton University Press, Princeton

GROSSMANN, W. (1976): *Geodätische Rechnungen und Abbildungen in der Landesvermessung.* Konrad Wittwer Verlag, Stuttgart, 1976

HRISTOW, W.K. (1955): *Die Gaußschen und geographischen Koordinaten auf dem Ellipsoid von Krassowsky.* VEB Verlag Technik, Berlin, 1955

SCHÖDLBAUER, A. (1982): *Rechenformeln und Rechenbeispiele zur Landesvermessung - Teil 2: Geodätische Berechnungen im System der Gaußschen konformen Abbildung eines Bezugsellipsoids unter besonderer Berücksichtigung des Gauß-Krüger und des UTM-Koordinatensystems im Bereich der Bundesrepublik Deutschland.* Wichmann Skripten, Heft 2, Teil 2, Herbert Wichmann Verlag, Karlsruhe, 1982

SCHÖDLBAUER, A. (1984): *Bezugssysteme der Landesvermessung unter Berücksichtigung terrestrischer und satelliten-geodätischer Meß- und Auswerteverfahren.* In Schödlbauer, A., Welsch, W. (Editors): *Satelliten-Doppler-Messungen, Beiträge zum Geodätischen Seminar am 24./25.09.1984,* S.62-153, Schriftenreihe des Wissenschaftlichen Studiengangs Vermessungswesen der Hochschule der Bundeswehr München, Heft 15, Neubiberg 1984

SCHÖDLBAUER, A. (1985): *Transformation räumlicher ellipsoidischer Koordinaten in cartesische topozentrische Koordinaten auf der Grundlage der "Entwicklungen von Weingarten".* In Festschrift zum 60. Geburtstag von Prof. Dr.-Ing. Gerhard Eichhorn, S.241-257, Darmstadt 1985

VANIČEK, P., KRAKIWSKY, E. (1982): *Geodesy: The Concepts.* North-Holland Publishing Company, Amsterdam, New York, Oxford, 1982

TRANSFORMATION BETWEEN GEODETIC REFERENCE SYSTEMS WITHOUT HEIGHT INFORMATION

J. Bittencourt de Andrade
Universidade Federal do Paraná
Curso de Pós-Graduação em Ciências Geodésicas
C.P. 19011 Jardim das Americas
80,000 Curitiba, Paraná
Brazil

ABSTRACT. In this paper is shown the feasibility to compute the transformation between two Geodetic Reference Systems with no height information, through a new mathematical model proposed here. A previous paper published by the author is also commented here and the results of basis compared. In the last case, the number of unknown parameters is too high. It is intuitive that a mathematical model with small number of parameters works better. In order to compare both approaches, a computation was carried out using the same data to find the transformation between WGS-72 and SAD-69. The GPS, due to the high accuracy offered, will be the tool to definitely solve the problems on transformation between geodetic reference systems and geoidal height determination in continental areas.

INTRODUCTION

A reference coordinate system can be defined but for practical purposes, it must be materialized.

The materialization of a reference coordinate system, called reference frame, (Mueller, I.I., 1985), requires accurate observations in order to be as close as possible to the defined reference coordinate system.

It is possible to establish a priori a mathematical model of transformations between defined reference coordinate systems and then adapt them to perform transformations between the corresponding materialized systems. It is not possible, however, to improve the materialization of a reference system, through transformations, unless the other system involved in the transformations is perfect.

It seems that the problems of transforming reference systems and the improvement of their materializations must, generally, be treated through different approaches. Consequently, from the practical point of view, it is more interesting for geodesists to find the transformation between materialized reference systems. This approach frequently requires the inclusion of additional parameters in the transforming model. Greater parameterization requires more accurate observations compatible with the required resolution.

Therefore the choice of a mathematical model must be the result of a careful analysis of parameters and observations, in addition to those concerning the necessary strength of geometry.

MATHEMATICAL MODEL

Veis (1963), Bursa (1962), Molodenskii et al. (1960) proposed models which are variations of the following: See for example, (Vaníček 1975) or (Gemael 1981) for details.

$$k' \begin{bmatrix} X' - X'_0 \\ Y' - Y'_0 \\ Z' - Z'_0 \end{bmatrix} = kR\ (\omega, \psi, \varepsilon) \begin{bmatrix} X \\ Y \\ Z \end{bmatrix} \tag{1}$$

The variations include:

1) the selection of the rotation point; and
2) the interpretation of the role of the scale factor.

The difficulty to use such models is that the position vectors of the points involved are required to be known in both systems.

One of the models discussed here was previously proposed by the author (Andrade 1984) and differs from the above (see equation 1), mainly due to the introduction of a new parameter per point. From figure 1,

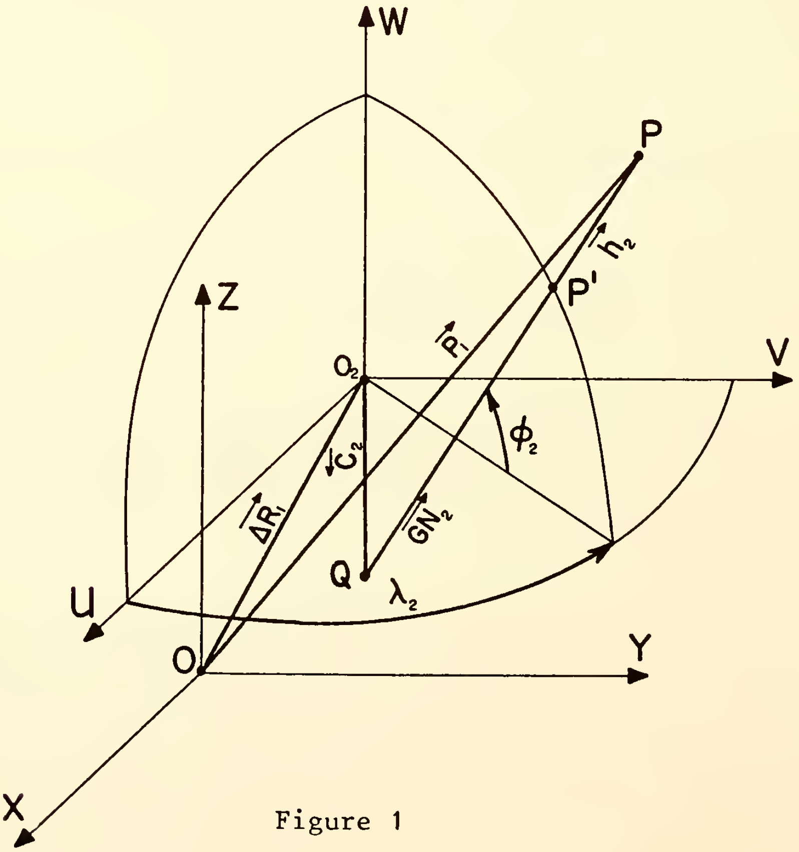

Figure 1

$$\vec{P}_1 = \Delta\vec{R}_1 + \vec{C}_2 + \vec{GN}_2 + \vec{h}_2 \text{ , but} \tag{2}$$

$$\vec{h}_2 = \vec{N}_2 + \vec{H} \text{ , then,} \tag{3}$$

$$\vec{P}_1 = \Delta\vec{R}_1 + \vec{C}_2 + \vec{GN}_2 + \vec{N}_2 + \vec{H} \text{ , where} \tag{4}$$

$\vec{P}_1$ = position vector of P in system $\underline{1}$: (X,Y,Z);

$\Delta\vec{R}_1$ = position vector of the origin of the system $\underline{2}$ in $\underline{1}$;

$\vec{C}_2$ = $-e_2^2 \,.\, \sin \phi_2 \,.\, \vec{GN}_2$, where

e_2 = excentricity of $\underline{2}$;

ϕ_2 = geodetic latitude of P in $\underline{2}$;

GN_2 = principal radius of curvature along the prime vertical in $\underline{2}$ (P'Q)

h_2 = geodetic height of P in $\underline{2}$;

H = "orthometric height" of P in $\underline{2}$;

N_2 = geoidal height at P in $\underline{2}$

$$\begin{bmatrix} X \\ Y \\ Z \end{bmatrix} = \begin{bmatrix} XO \\ YO \\ ZO \end{bmatrix} + \begin{bmatrix} 0 \\ 0 \\ GN_2 \; e_2^2 \,.\, \sin \phi_2 \end{bmatrix} + (GN_2 + N_2 + H) \begin{bmatrix} \cos\phi_2 \; \cos\lambda_2 \\ \cos\phi_2 \; \sin\lambda_2 \\ \sin\phi_2 \end{bmatrix} \tag{5}$$

where λ_2= geodetic longitude of P in $\underline{2}$.

The new parameter here can be either the geodetic height h_2 or the geoidal height N_2 when the orthometric height H is known.

Like in the model (1), scales and rotations also can be included here. However, because the accuracy of the observation does not allow it, no attempt was made to compute rotations or scale factors.

The second approach proposed here is based on a resection model.

Given the geodetic ellipsoidal coordinates of P in $\underline{2}$: ϕ_2, λ_2, one can compute the coordinates (UP', VP', WP') of P'. (See figure $\underline{1}$):

$$\begin{bmatrix} UP' \\ VP' \\ WP' \end{bmatrix} = \begin{bmatrix} GN_2 \,.\, \cos\phi_2 \,.\, \cos\lambda_2 \\ GN_2 \,.\, \cos\phi_2 \,.\, \sin\lambda_2 \\ GN_2 \,.\, (1-e_2^2) \,.\, \sin\phi_2 \end{bmatrix}_{a_2 \,, f_2} \tag{6}$$

and $C_2 = GN_2 \,.\, e_2^2 \sin \phi_2$

The collinearity conditions says:

$$\frac{UP'}{UP} = \frac{WP' - C_2}{WP - C_2}$$

$$\frac{VP'}{VP} = \frac{WP' - C_2}{WP - C_2} \tag{7}$$

where $\begin{bmatrix} UP \\ VP \\ WP \end{bmatrix}$ are the coordinates of P in system 2

but
$$\begin{bmatrix} UP \\ VP \\ WP \end{bmatrix} = \begin{bmatrix} X \\ Y \\ Z \end{bmatrix} - \begin{bmatrix} XO \\ YO \\ ZO \end{bmatrix} \qquad (8)$$

if no rotations or scale factors are considered.

$$\begin{aligned} UP'(Z-ZO-C_2) - (X - XO)\,(WP' - C_2) &= 0 \\ VP'(Z-ZO-C_2) - (Y - YO)\,(WP' - C_2) &= 0 \end{aligned} \qquad (9)$$

This simplified model (only three unknown) neither requires the knowledge of heights like model (1) nor introduces any unknowns like (5).

Scales and rotations can also be introduced into this model. However, due to the very reasons already explained no attempt was made to compute such parameters.

EXPERIMENTS

A set of 15 points were used to perform the experiments, as shown in figure 2.

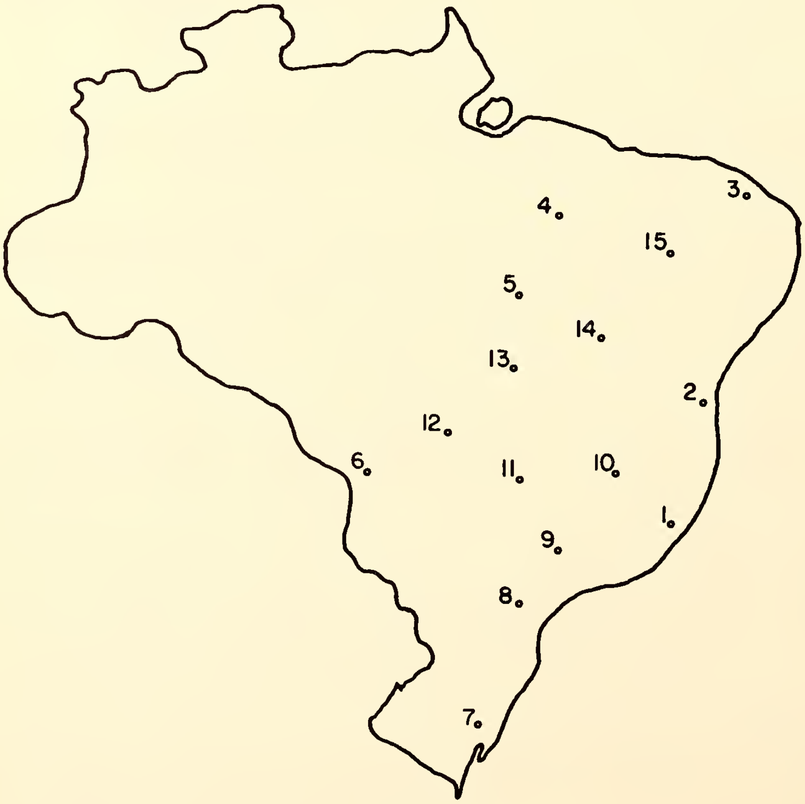

Figure 2

Table 1 shows the coordinates of the above points on WGS-72 and SAD-69.

TABLE 1 - List of Points

POINT	X, Y, Z (WGS-72) φ λ H (SAD-69)		
1 VITÓRIA	4575124.851 -20°09'45"10	-3865804.270 -40°11'45"48	-2184662.149 20.66
2 ILHÉUS	4787599.928 -14°46'50"28	-3889708.717 -39°05'30"33	-1616733.233 122.46
3 MOSSORÓ	5052233.350 -05°13'03"91	-3849945.772 -37°18'28"50	-576226.050 46.48
4 GRAJAÚ	4398656.860 -05°48'30"80	-4573990.172 -46°07 08"02	-641270.845 232.36
5 LUZIA	4145716.170 -09°55'24"15	-4722140.302 -48°43'06"59	-1092027.240 424.69
6 PROFESSOR MIGUEL	3278652.665 -16°04'28"22	-5180074.368 -57°40'05"65	-1754741.850 119.51
7 CANOAS	3464572.701 -29°52'52"12	-4316379.250 -51°14'48"48	-3159017.034 1.56
8 BOCAIUVA DO SUL	3780985.144 -25°13'04"85	-4364797.155 -49°05'55"59	-2701446.728 1041.61
9 OLHOS D'ÁGUA	4033873.208 -21°55'50"34	-4332958.276 -47°02'48"02	-2367617.402 716.37
10 VARZEA DA PALMA	4324898.527 -17°33'11"10	-4278324.307 -44°41'21"38	-1911492.342 503.57
11 FAZENDA LAGOA	3947699.145 -18°14'07"55	-4598476.920 -49°21'14"40	-1983456.101 793.14
12 FAZENDINHA	3760736.211 -16°02'55"19	-4842762.914 -52°10'03"45	-1752066.404 394.08
13 URUAÇU	4044198.814 -14°34'34"22	-4665959.959 -49°04'56"99	-1594949.404 543.77
14 BARREIRAS	4411356.924 -12°04'41"62	-4411323.526 -44°59'57"18	-1326075.730 737.36
15 TANQUE NOVO	-4749955.942 -07°51'13"70	-4167706.655 -41°15'49"78	-865884.163 463.23

Adjustments by the least square method were done using models (5) and (9). The results are shown on table 2.

TABLE 2 - Results

Model (5)

$X0 = -60.88m \pm 1.90m$ (SD)
$Y0 = -25.10m \mp 1.99m$ (SD)
$Z0 = -49.67m \mp 0.86m$ (SD)
$\sigma_0^2 = 1.000$
$P = I$
$\hat{\sigma}_0^2 = 2.561$ $\hat{\sigma}_0 = 1.60$
$\sigma_N = 3.21m$ D.F. = 27

Model (9)

$X0 = -60.85 \pm 1.90m$ (SD)
$Y0 = -25.12 \mp 2.00m$ (SD)
$Z0 = -49.68 \mp 0.87m$ (SD)
$\sigma_0^2 = 1.000$
$P = I$
$\hat{\sigma}_0^2 = 2.565$ $\hat{\sigma}_0 = 1.60$
D.F. = 27

	Model (5)				Model (9)		
POINT	N	VX	VY	VZ	VX	VY	VZ
1	6.38	-0.252	-0.285	-0.024	-0.246	-0.285	-0.011
2	10.04	0.564	0.126	1.357	0.571	0.137	1.354
3	20.76	0.272	0.322	0.228	0.281	0.336	0.217
4	-6.21	1.297	1.687	-3.117	1.307	1.698	-3.123
5	-4.10	1.292	1.062	0.309	1.295	1.067	0.300
6	9.31	-1.274	-0.334	-1.386	-1.282	-0.337	-1.392
7	-1.21	1.818	1.824	-0.495	1.804	1.814	-0.497
8	4.07	0.690	0.897	-0.481	0.707	0.906	-0.471
9	1.68	-1.179	-1.185	0.160	-1.177	-1.190	0.172
10	0.34	-0.806	-1.544	1.622	-0.802	-1.539	1.618
11	-5.01	-0.408	-1.480	2.601	-0.413	-1.485	2.604
12	0.10	-0.265	0.572	-2.136	-0.275	0.566	-2.139
13	-2.33	-2.700	-2.175	-0.480	-2.702	-2.179	-0.474
14	1.86	0.773	0.515	0.851	0.756	0.497	0.854
15	9.14	0.179	-0.004	0.991	0.177	-0.005	0.988

CONCLUDING COMMENTS

The results show that the models proposed, namely equations (5) and (9), work very well with no significant difference. In both cases the degree of freedom is the same for any number of points used. The main difference between them is the parameterization.

Loss of precision of about 50% was obtained, when comparing the predicted standard deviation of data versus the standard deviation of the computed parameters. To reach dm level geoidal determination it becomes necessary to use a better data set such as GPS observations may offer.

In the near future, the Parana Federal University expects to start a joint program with the University of Hannover (F.R.G.), using GPS receivers to improve geoidal mapping in Brazil.

REFERENCES

Andrade J.B. (1984), Determinação Simultânea de Parâmetros de Transformação entre Referenciais Geodésicos e Desníveis Geoidais. Boletim da Universidade Federal do Paraná - GEODÉSIA N.º 30, 16p. Curitiba.

Bursa, A.M. (1962). The theory of the Determination of the Nonparallelism of the Minor Axis of de Reference Ellipsoid Polar Axis of Inertia of the Earth, and Initial Astronomical and Geodetic Meridians from Observation of Artificial Earth Satellites. Studia Geophysica et Geodaetica N.6.

Gemael C. (1981). Referenciais Cartesianos Utilizados em Geodésia. Universidade Federal do Paraná, Curso de Pós-Graduação em Ciéncias Geodésicas, 41p. Curitiba. Brazil.

Molodenskii, M; Eremeev, V; Yurkina, M. (1962). Methods for study of the External Gravitational Field and Figure of the Earth. Translation from Russian. (1962). National Technical Information Service. Springfield, VA.

Mueller, I.I. (1980). Reference Coordinate Systems for Earth Dynamics: A Preview in Proc. of IAU Colloquium 56 on Reference Coordinate Systems for Earth Dynamics. E.M. Caposchkin and B. Kołaczek, eds. D. Reidel Publishing Company.

Vaníček, P. (1975). Report on Geocentric and Geodetic Datums. Technical Report. University of New Brunswick N 32, 26p, Fredericton.

Veis, G. (1963). Precise Aspects of Terrestrial and Celestial Reference Frames in The Use of Artificial Satellites for Geodesy. G. Veis ed. North-Holland Publishing Company. Amsterdam. The Netherlands.

GPS - CONSIDERATIONS FOR THE POTENTIAL GEODETIC USER

J Hannah
Department of Lands and Survey
Private Bag
Wellington, New Zealand

ABSTRACT. Living in a country not only far removed from the mainstream of developments in satellite positioning, but also with limited foreign exchange resources, the potential non U.S. geodetic user of the GPS is forced to undertake a rigorous evaluation of a number of factors, all of which will influence any decision as to if, when, or what to purchase. This paper elaborates upon the factors under consideration in New Zealand. It outlines the geodetic needs in New Zealand which could be met through the GPS, the specific problems which could arise (depending upon the positioning method adopted), possible user scenarios and economic evaluation criteria. In short, it provides the criteria upon which it is anticipated that New Zealand will significantly base any purchase decisions.

It is anticipated, however, that a majority of potential users will find themselves in a similar situation as ourselves, and for this reason, the paper also seeks to provide general guidelines applicable to all such users.

1 INTRODUCTION

As technology develops, so the number of tools available for geodetic positioning increments proportionally, each of these new positioning tools and techniques necessitating an independent evaluation by the potential user in order to assess the costs of such new technology against the perceived benefits of use. It is obvious that not all new technological items will prove to be a sound economic acquisition to all users, some preferring to hire or enter into joint venture arrangements of some description while others may choose to perform their positioning tasks by more traditional methods. In any event, realistic appraisals of new technological items are always necessary, especially so for agencies which hold the primary responsibility for the development and maintenance of their respective national geodetic networks. The Department of Lands and Survey in New Zealand is such an agency.

This paper outlines the considerations of the Department of Lands and Survey as a potential future user of the GPS. Initially it reviews both the relevant technical data concerning the GPS and the geodetic positioning techniques available through the GPS with sufficient detail to provide continuity and clarity of argument in the body of the paper which deals with the potential user considerations. The last section attempts to summarise these considerations and place them in more general terms.

2 TECHNICAL OVERVIEW OF THE GPS

By the time of full operational capability (1988) the GPS satellite constellation will consist of 18 satellites evenly spaced in each of six orbital planes. The orbits will be circular, at altitudes of approximately 20200 km, have inclinations of 55° and have 12 hr periods (Senus, 1983). This pattern should, for nearly all observers, provide at any instant a minimum of four satellites above an altitude of 9.5° and a minimum of five above the local horizon (Cook, 1984).

All NAVSTAR GPS satellites will have precise atomic frequency standards and will broadcast on two L band frequencies, L_1 at 1575.42 MHz and L_2 at 1227.6 MHz. Within each satellite there will be two code generators unique to that satellite, a P (Precision) code and a C/A (Coarse Acquisition) code. These codes, although precisely generated, appear to behave as if they are random noise and are thus often referred to as Psuedo Random Noise (PRN).

The L_1 and L_2 frequencies at which satellite transmission occurs are modulated by both these codes and also by a satellite navigation message (D code) containing satellite ephemerides, and the C/A to P signal "handover" information. Due to its short length, the C/A code is used for rapid signal acquisition and low order (navigation) positioning whereas the P code has greater noise suppression characterisics and is thus useful for more precise purposes. For much greater detail on these matters, one should consult Spilker (1980) or Hui (1982).

For geodetic point positioning purposes, a GPS receiver would normally need to complete three operations: (a) acquire and recognise the C/A code, (b) decode the satellite navigation message from the C/A code, (c) acquire and recognise the P code.

For geodetic baseline determinations (relative positioning) it is only necessary to be able to acquire the satellite signals at either or both the L_1 and L_2 frequencies. In this instance (assuming limited code access) the satellite ephemerides must be available from some independent external source.

3 GEODETIC POSITIONING TECHNIQUES

In using the GPS for geodetic purposes, four general positioning techniques are available:

- Range (psuedo range) positioning
- Doppler positioning
- Carrier phase methods
- Interferometric methods

These are well explained in Fell (1980), Mueller and Archinal (1981), Hui (1982), and Goad and Remondi (1984) and thus will not be detailed here. It is of importance, however, to draw attention to the following differences between these techniques.

(a) The first three methods, i.e. psuedo ranging, integrated Doppler and carrier phase all require a knowledge of the P code sequence if geodetic accuracy is to be obtained. No such knowledge is necessary for interferometric methods although the ephemerides of the GPS satellites are required.

(b) Hui (1982) notes that the first three measurement types require receivers which are quite similar in design, utilising similar hardware modules. Interferometric techniques, on the other hand, require hardware with considerably different characteristics and modules.

(c) The different measuring techniques have differing capabilities. The first two, for example, are suitable for single satellite, single receiver point positioning. While this is theoretically true for the third and fourth techniques, the high measurement resolution possible is negated by receiver clock instabilities and atmospheric delay effects. Receiver clock instabilities, however, can be negated by simultaneously tracking more than one satellite. Bock et al (1984b) comment upon initial interferometric type point positioning results.

All measurement techniques are suitable for baseline determinations.

(d) An investigation into the accuracies inherent in the different equipment types has been published by Hui (1982). For translocation (i.e. baseline determinations) using either carrier phase or interferometric techniques on a 100 km baseline and after 2 hr of averaging, these investigations show total error budgets of 0.03 m and 0.04 m for each technique respectively. These two techniques show far greater potential for very accurate baseline determination than either those of psuedo range or Doppler.

Simulations by Fell (1980) for point positioning show the psuedo range technique capable of one sigma accuracies of 50-80 cm after one day and 25-40 cm after five days. The corresponding Doppler simultations gave figures of 65-150 cm and 30-70 cm respectively.

(e) Actual interferometric type results are discussed by Hothem and Fronczek (1983), Bock et al (1984a), Bock et al (1984b) and by Goad and Remondi (1984). For baseline determinations using this technique, single wavelength measurements have been shown to agree consistently with their terrestrial counterparts to within 2.5 ppm on almost all measured lines. There is some evidence, however, (Hothem and Fronczek, 1983) of a systematic scale difference of approximately 2 ppm between the two. Resurveys of lines some months apart have shown repeatability between surveys to within 0.3 ppm.

Comparisons with VLBI baselines have shown agreement to 2 ppm on distances up to 2000 km (Bock et al, 1984b).

4 SPECIFIC USER CONSIDERATIONS

Having thus far reviewed basic aspects of the GPS, this discussion now focuses upon the specific considerations which we in New Zealand, as potential users, have given to this tool. Broadly speaking, this discussion will follow three avenues which we choose to define as its Potential Applications, the Policy Considerations and finally, the Practical Evaluation.

4.1 Potential Applications

As a necessary first step in the evaluation procedure it is of importance to define the tasks for which geodetic GPS receivers would be useful. Having defined these it then becomes important to ask two questions:

(a) Are existing geodetic techniques capable of meeting these needs?
(b) If so, do GPS techniques present significant cost benefits over and above existing methods?

This section will, with the exception of (b) above which is dealt with in Section 4.3, seek to address these issues.

The primary triangulation of New Zealand (covering approximately three quarters of the land area) was completed and adjusted by 1949. Since then it has been extended in a piecemeal fashion to cover all remaining areas. Although this triangulation is known to contain scale errors in excess of 6 ppm it is nevertheless more than adequate as a basis for both our national mapping and cadastral survey systems. We now find our primary geodetic positioning activities to be:

(a) Occasional (but almost complete) extensions to the primary network.
(b) Continuing second, third and fourth order breakdowns of the primary network (generally to provide control for basic mapping, specific project mapping, and local cadastre).
(c) Control for project engineering.
(d) Precise levelling.
(e) Earth Deformation Surveys (EDS's).
(f) The provision of control for the mapping of NZ Dependencies (e.g. Antarctica and certain Pacific Islands).

In considering the above we find little need for any point positioning capability to link NZ and her dependencies to a global geocentric datum beyond the approximately 25 points already established through the TRANSIT NNSS.

At present all the above activities are carried out using conventional (i.e. triangulation, trilateration and levelling) techniques. At this time the accuracies of the computed positions resulting from tasks (a) and (b) are limited by the 6 ppm scale error mentioned earlier although observing techniques and methods are used which give results beyond this accuracy limitation. This is done in recognition of the possible future use of this data for both earth deformation studies and for any readjustment of the NZ datum.

The control produced under task (c) often necessitates highest possible accuracies but only in very localised areas where line of sight and accessibility constraints are few. These tasks are completed relatively quickly with short range EDM and with few problems beyond those of ensuring ground mark stability.

Task (d), however, is aimed at producing a unified national height datum. In the New Zealand context it has been realised recently that the use of precise levelling alone is, for the following reasons, probably inappropriate:

- Primary precise levelling (as yet incomplete) began over 30 years ago.

- The areas which have been completed are, in general, composed of different sections which themselves have been observed at widely varying times. Such time discontinuities would represent little problem on a tectonically and geologically stable land mass. However, various recent geological estimates of land uplift suggest that parts of New Zealand are uplifting at rates approaching 10 cm/yr. Obviously such motion, should it exist, stands to invalidate the precise levelling data recorded 20-30 yrs ago but still needed to complete the national network.

- The resources of time, finance and manpower do not exist to re-observe, within a total time of 1-2 years, the entire existing network plus those portions still requiring initial observation.

It is our view that the transfer of highly accurate ellipsoidal height differences across the nation by means of the GPS, together with a comprehensive coverage of both gravity and astronomic data can significantly alleviate these problems by verifying the existence (or otherwise) of the differential land uplift suggested by the geologists, by enabling us to easily maintain a differential height reference system, and by enabling the linking of this reference system to the existing orthometric system.

Task (e) is of national importance due to the fact that New Zealand is considered to lie astride the Australian and Pacific crustal plate boundary. A national EDS program was instituted in 1973, consisting in part of eight triangulation/trilateration networks which cover extensive portions of the country. The intention is that these be remeasured every 10 years to highest possible accuracies. The first measurement program is complete and has produced networks with scale errors in the order of 1.25 ppm (Hannah, 1984). These surveys, however, are large and complex logistical operations often performed under severe alpine conditions. Costs are high both in terms of finance and physical stress on staff (Ricketts, 1984). It is thus anticipated that GPS techniques would be ideal for the remeasurement program.

In summary therefore, we perceive the primary geodetic uses for GPS technology within New Zealand to be related to the provision of general geodetic control, an accurate vertical reference network and to ongoing EDS's.

4.2 Policy Considerations

As was outlined in Section 3 of this paper, three of the four GPS positioning techniques require an a priori knowledge of the P code if geodetic accuracies are to be obtained. Senus (1983) outlines the system management considerations involved. In brief, it is anticipated that two unique and distinct services will be provided.

(a) Precise Positioning Service (PPS) utilising the P-code and available to both military users and selected civilian users. The users specified here will probably include those of nations who are both closely aligned militarily with the U.S.A. and who are working in their "national interest". The GPS will have in its design a selective availability feature with PPS users instrumented in such a way that they can read through the selective availability mechanisms in order to be able to extract the precise navigation information. A user fee (tentatively under review) of $3700 (U.S.) per annum has been set for this service.

(b) Standard Positioning Service (SPS) available to the world wide community of civil users and capable of providing positions to navigation accuracy only.

It is expected that significant pressure will be exerted by the civil community to have the P code released for general use. Even if this were done initially, continued long term access to the code obviously cannot be guaranteed, particularly when political and military factors influence such decisions.

An alternative scenario is to rely on the fourth positioning technique, that achieved by using interferometric measurements. As was mentioned in Section 2, an a priori knowledge of the satellite ephemerides are required. It is presently planned that the Defense Mapping Agency will compute precise ephemerides and release them on the same basis as is done with the existing NNSS precise ephemerides. Two potential problems exist with this arrangement. In the first instance it is again subject to political alignment and secondly, and perhaps most importantly for New Zealand, tracking stations in remote regions may not produce ephemerides in the vicinity of New Zealand with accuracies sufficient to meet all requirements. As a rule of thumb, the uncertainty in a measured baseline (Stolz, private communication) can be expressed as:

$$\frac{\text{Baseline Length}}{\text{Sat. Altitude}} \times \text{Ephemeris uncertainty}$$

Thus a 100 km baseline for which an accuracy of 0.1 ppm is required will necessitate ephemeris errors no greater than 2 meters. Such a level of accuracy is certainly desirable for the earth deformation studies outlined in Sec 4.1. Present estimates of the accuracy of the DMA precise ephemerides indicate uncertainities in the order of 10-20 metres (Bock et al, 1984a) while those produced independently by certain equipment manufacturers appear somewhat worse.

As a consequence of the above it is anticipated that New Zealand will work closely with Australia in considering the option of establishing local tracking and orbit generation facilities. It is recognised that such tracking facilities will necessitate the use of at least three sites well spread in the Australasian region, each equipped with an atomic frequency standard.

4.3 Practical Evaluation

To this point we have reached the conclusion that GPS technology has much to offer in terms of potential uses within New Zealand. We have also noticed that existing tasks indicate a need for a relative positioning rather than a point positioning capability. This in turn links nicely with the system management considerations which result in a present preference for the interferometric approach. We now move to the very practical issues of cost recovery and daily use.

4.3.1 Cost Benefit Studies

In any cost benefit study, the life cycle costs of the equipment are obviously vital issues. Such costs include:

- equipment capital cost
- ongoing operational costs
- data processing costs
- development and training costs
- maintenance costs

At this time, with the ongoing development of geodetic GPS receivers by a number of manufacturers, it is not prudent to attempt cost comparisons between such receivers as exist. Indeed, in attempting to perform a reasonable cost benefit study of the use of GPS technology, two immediate problems were apparent. In the first instance many receivers are still under development and thus a competitive market environment for geodetic GPS receivers has yet to develop. Consequently, capital costs are not yet well established. Secondly, actual productivity gains made by existing users are not well documented. Bossler and Hansen (1984) speak of a possible increase in the production of network control point positions by as much as 20 times, but the origin of this figure is not given. For this reason we have adopted a typical New Zealand EDS survey in rugged country as our model and costed the field portion of this survey (for which good documentation exists) by conventional triangulation/trilateration techniques. We have then attempted to cost the same survey by interferometric GPS techniques using both the Hothem and Fronczek (1983) and Bock et al (1984a) reports as a basis for typical field operations. These figures are given below.

Item	Conventional EDS (25 stations)	Cost (NZ$)
Vehicles:	1000 km/veh/wk for 6 weeks 10 vehicles @ 50c/km	30 000
Salaries:	25 men for 6 weeks @ $100/day	105 000
Overtime:	Equivalent to 600 man days @ $100	60 000
Helicopter:	120 hr @ $600/hr	72 000
Reconnaissance, beaconing etc		10 000
Accommodation and allowances:	1050 man days @ $25	26 250
		$303 250

Item	Equivalent GPS Survey	Cost (NZ$)
Vehicles:	1000 km/veh/wk for 3 weeks 4 vehicles @ 50c/km	6 000
Salaries:	8 men for 3 weeks @ $100/day	16 800
Overtime:	Equivalent to 85 man days	8 500
Helicopter:	100 hr @ $600/hr	60 000
Reconnaissance etc		5 000
Accommodation and allowances:	168 man days @ $25	4 200
		$100 500

The GPS survey has assumed the simultaneous use of four receivers with the completion of two new stations each day with an allowance for interruptions due to poor flying weather. It is, of course, anticipated that with intervisibility between stations no longer required, new stations will in time be established beside roads, thus largely eliminating the need for helicopter support. Thus on a typical EDS, the difference in cost of field operations alone between the two surveys is at least in the order of $203,000 (NZ).

On average, one such specialised survey is completed each year together with an ongoing re-equipmentation cost for such surveys of approximately $35,000 (NZ) per year. Such a cost would no longer be necessary under a GPS scenario thus leading to a total annual savings of approximately $238,000 (NZ).

By extending these same costing methods into our general geodetic control program, by recognising that line of sight constraints no longer apply, and by using GPS measurements as a substitute for part of our precise levelling programme, we conservatively anticipate $500,000 (NZ) savings per year on our existing programme. This in turn will allow significant redeployment of resources.

In order to determine the maximum allowable capital cost for GPS receivers to be economically viable, a discounted cash flow technique may be used. In order to use this technique, which takes account of both savings and costs over the total life of the equipment, it has been necessary to make a number of assumptions. In these we have attempted to be as realistic as possible.

(1) Maintenance costs on the receivers are zero for the first year of use and increase by 1% of the capital cost for each year which passes. By year eight they reach 7% and remain constant thereafter.

(2) The receivers have a useful life of 10 years at which time they have a "salvage value" of $25,000 (NZ) each.

(3) All equipment is acquired in a single bulk purchase at the beginning of the first year.

(4) The cost of capital is assumed to be 10% in real terms.

(5) Development and training costs in the first year of use are $20,000 (NZ) with fixed running costs of $10,000 per year thereafter.

Given these assumptions, Table 1 summarises the results of this cash flow in which the variable term "c" is the initial capital invested. All costs are given a negative sign and all savings a positive sign. The row in the table labelled "Discounted Nett" shows yearly costs and savings in real dollar terms and is obtained by taking the previous row and dividing by 1.0 for year 1, 1.1 for year 2, $(1.1)^2$ for year 3, $(1.1)^3$ for year 4 etc. The "Running Total" for each year is thus the nett present value of the investment up to that year. If, for example, the capital cost of four receivers plus ancilliary hardware were $2.0 M (NZ) then we find that the nett present value of the investment is - $119,000 in year 5, $123,000 in year 6 and $864,000 in year 10. In other words the investment pays itself off between years 5 and 6 and runs into significant cost savings by year 10. Clearly, for any other capital cost it is only necessary to insert it in place of "c" in the last row and the nett present value of the investment can be derived. Equally clearly many different scenarios exist. For example, equipment could be hired or it could be purchased over a number of years. Local tracking stations could be established thus significantly increasing capital cost. Obviously each potential user must decide on the most advantageous scenario in the light of their own geodetic needs and the costs they are willing to sustain in order to meet these.

4.3.2 Daily Use Issues

(a) Servicing. In general, the higher the capital cost of equipment, the more important it becomes that such equipment be kept in productive use. This implies that any servicing required be both rapid and efficient. Experience indicates that the primary factors affecting such servicing are those of distance to the servicing agents, their technical expertise and the strength (or otherwise) of their customer service.

In New Zealand we recognise that we are potentially a very small market for geodetic GPS receivers and thus cannot expect the same servicing benefits as, for example, users in the USA. Nevertheless, the

Table 1 ACQUISITION OF GPS RECEIVERS - DISCOUNTED CASH FLOW

Item	Year									
	1	2	3	4	5	6	7	8	9	10
Costs (Millions$)										
Capital	-C	Nil	Nil	Nil	Nil	Nil	Nil	Nil	Nil	Nil
Maintenance	Nil	-0.01C	-0.02C	-0.03C	-0.04C	-0.05C	-0.06C	-0.07C	-0.07C	-0.07C
Running	-0.02	-0.01	-0.01	-0.01	-0.01	-0.01	-0.01	-0.01	-0.01	-0.01
Total	-C-.02	-.01C-.01	-.02C-.01	-.03C-.01	-.04C-.01	-.05C-.01	-.06C-.01	-.07C-.01	-.07C-.01	-.07C-.01
Savings	0.5	0.5	0.5	0.5	0.5	0.5	0.5	0.5	0.5	0.6
Nett (Costs/ Savings	-C+.48	-.01C+.49	-.02C+.49	-.03C+.49	-.04C+.49	-.05C+.49	-.06C+.49	-.07C+.49	-.07C+.49	-.07C+.59
Discounted Nett (Discounting @ 10% p.a.)	-C+.48	-0.009C +0.445	-0.017C +0.405	-0.023C +0.368	-0.027C +0.335	-0.031C +0.304	-0.034C +0.277	-0.036C +0.251	-0.033C +0.229	-0.030C +0.250
Running Total	-C+.43	-1.009C +0.925	-1.026C +1.330	-1.049C +1.698	-1.076C +2.033	-1.107C +2.337	-1.141C +2.614	-1.177C +2.865	-1.210C +3.094	-1.240C +3.344

availability of good servicing close at hand in Australia, for example, would be seen as a significant asset in any purchase arrangement.

(b) Accuracy Limitations. Sec. 3 gave details on the potential accuracies of each of the measurement methods. For the current interferometric type GPS receivers, non hardware dependent accuracy limitations are due to:

- errors in the satellite ephemerides
- atmospheric variations
- receiver oscillator stabilities

Aspects relating to the satellite ephemerides were discussed earlier in Sec 4.2. The atmospheric variations referred to above are those due to both the ionosphere and the troposphere. The use of dual frequency (both L_1 and L_2 band) receivers should eliminate the ionospheric effects, Bock et al (1984b) reporting the reduction of such effects to the centimeter level on a 2045 km baseline.

Tropospheric effects, however, are significantly more difficult to eliminate. Although current processing techniques apply tropospheric corrections based upon atmospheric models (c.f. Goad and Remondi, 1984), this is not expected to be adequate for the most precise work on baselines of over 25-50 km in length, beyond which significant differential tropospheric effects can occur. The acquisition of water vapour radiometers could largely eliminate the problem, but at considerable monetary cost.

Receiver oscillator stabilities can be an important aspect of the ultimate accuracies achieved. Goad and Remondi (1984) comment upon this aspect noting, however, that the technique of differencing interferometric observables between two (or more) receivers simultaneously observing the same satellite at common epochs can be used to either eliminate or at least estimate relative clock drifts. They also note that baseline solutions are sensitive to constant relative clock offsets at the 10 microsecond level. Indeed, the manufacturers of one receiver, for example, specify that before going into the field receiver clocks be set to within ± 10 millisec of UTC and synchronised to within ± 1 microsec of each other. Any potential user should thus reckon this type of task into their pre-observational procedures for interferometric type positioning.

(c) Real Time Processing. Some organisations may desire a real time processing, or at least a field processing, capability. While we in New Zealand do not see this as an important requirement, we do, however, consider some means of field data verification as important. Although we anticipate future geodetic reference marks positioned through GPS means to be easily accessible (no line of sight requirement), the linking of these points into existing networks will still entail initial occupation of difficult alpine stations. Field data verification before leaving such stations would obviously be advantageous.

5 SUMMARY

The previous chapter of this paper has outlined the specific considerations which we in New Zealand are giving to the GPS. We now conclude by seeking to summarise and condense these into a series of steps which form a set of potential user guidelines.

Step 1 Define both the positioning tasks to be performed and the desired measurement accuracies.

Step 2 Decide on eligibility for P code access. If eligible, then all measurement types (i.e. psuedo range, Doppler, carrier phase and interferometric) are available for consideration. If not eligible, then only interferometric methods should be considered from here on.

Step 3 In the light of the positioning needs defined above and the general guideline given in Sec. 4.2, decide if the ephemerides available (either from specific manufacturers or, if eligible, from the Defence Mapping Agency) are sufficiently accurate for the necessary positioning tasks.

If so, proceed to the next evaluation step. If not, consider the option of establishing a local tracking network.

Step 4 In the light of the positioning tasks defined, decide on the need for both dual frequency receivers (to eliminate first order ionospheric refraction effects) and water vapour radiometers (to determine tropospheric refraction effects).

Step 5 Having adopted a measurement type and hardware scenario, compare available equipment in terms of cost, servicing, accuracy differences, reliability and real time processing (and/or software) capabilities.

Step 6 Investigate acquisition methods e.g. purchase, lease, joint venture arrangement.

Step 7 Perform cost/benefit analysis.

6 ACKNOWLEDGEMENTS

I am indebted to the Department of Lands and Survey and the Royal Society of New Zealand for making the presentation of this paper possible. Thanks are also due to Mr Ross Judge of the New Zealand Treasury and Mr Tony Bevin of the Department of Lands and Survey for their critical reading of the manuscript.

7 REFERENCES

Bock Y., R.I. Abott, C.C. Counselman , S.A. Gourevitch, R.W. King (1984a): "Establishment of Three-Dimensional Geodetic Control by Interferometry with the Global Positioning System", Submitted for publication in the Journal of Geophysical Research.

Bock Y., R.I. Abott, C.C. Counselman , S.A. Gourevitch, R.W. King, A.R. Paradis (1984b): "Geodetic Accuracy of the Macrometer Model V-1000", Bulletin Geodesique, Vol. 58, pp 211-221.

Bossler J.D., R.H. Hanson (1984): "The Impact of VLBI and GPS on Geodesy", Surveying and Mapping, Vol. 4, No. 2, pp 105-113.

Buennagel L.A., P.F. MacDoran, R.E. Neilan, D.J. Spitzmesser, L.E. Young (1984): "Satellite Emission Range Inferred Earth Survey (SERIES) Project : Final Report on Research and Development Phase, 1979 to 1983", JPL Publication 84-16. Available from JPL, California Institute of Technology, Pasadena, California.

Cook G.E. (1984): "Principles and Present Status of NAVSTAR GPS", International Hydrographic Review, Monaco, Vol. LX1, No. 2.

Counselman C.C., R.A. Abbot, S.A. Gourevitch, R.W. King, A.R. Paradis (1983): "Centimeter - Level Relative Positioning with GPS", Journal of Surveying Engineering 109 (ASCE), pp 81-89.

Fell P.J. (1980): "Geodetic Positioning using a Global Positioning System of Satellites", Report No. 299, Department of Geodetic Science, The Ohio State University, 1958 Neil Av., Columbus, OH 43210.

Goad C.G, B.W. Remondi (1984): "Initial Relative Positioning Results using the Global Positioning System", Bulletin Geodesique Vol. 58, pp 193-210.

Hannah J. (1984): "Accuracy Estimates of, and the Rejection Criteria used on the Observed Quantities from the New Zealand EDS Networks", Proceedings of Int. Symp. on Recent Crustal Movements of the Pacific Region, Royal Society of New Zealand, Wellington, New Zealand (in preparation).

Hothem L.D., C.J. Fronczek (1983): "Report on Test and Demonstration of Macrometer^{TM} Model V-1000 Interferometric Surveyor", FGCC Report: FGCC-IS-83-2, available from the Federal Geodetic Control Committee, 6001 Executive Boulevard, N/CGI,Room 1026, Rockville, MD 20852.

Hui P.J. (1982): "On Satellite Signal Processing Techniques Applicable to GPS Geodetic Equipment", The Canadian Surveyor, Vol. 36. No. 1, pp 43-55.

Mueller I.I., B. Archinal (1981): "Geodesy and the Global Positioning System", Proc. IAG Symposium on Geodetic Networks and Computations, Munich.

Ricketts L.S. (1984): "A Survey to Monitor Earth Deformation", Proceedings of Int. Symp. on Recent Crustal Movements of the Pacific Region, Royal Society of New Zealand, Wellington, New Zealand (in preparation).

Senus W.J. (1983): "NAVSTAR Global Positioning System Status" Proceedings of the IAG Symposia, Hamburg, FRG, August 15-27. Available from Department of Geodetic Science and Surveying, The Ohio State University, 1958 Neil Av., Columbus, OH 43210-1247.

Spilker J.J. (1980): "Signal Structure and Performance Characteristics", Reprint of Global Positioning System papers published in "Navigation". Available from the Institute of Navigation, 815 Fifteenth Street, Suite 832, Washington DC 20005.

THE IMPACT OF VLBI AND GPS ON GEODESY IN CANADA

Demitris Delikaraoglou and Robin R. Steeves

Geodetic Survey Division
Surveys and Mapping Branch
Energy, Mines and Resources Canada
615 Booth Street, Ottawa
Ontario, CANADA K1A 0E9

ABSTRACT. The rapid rate of evolution of space positioning systems such as LBI and GPS is changing the practice of geodesy as we have known it in the past few decades. There is already strong evidence that these new technologies may provide the means of achieving a long sought goal of geodesists - a unified, worldwide geodetic control network tied to an inertial reference frame. Repeated LBI determinations at regular and frequent intervals will provide a precise record of the dynamic behaviour of Earth on a global scale, as well as changes in the relative position of the antennas on Earth's surface with accuracies at the 5 to 10 cm level achievable over observation periods of less than a day. GPS will permit rapid, economical positioning with accuracies of a few centimetres over distances of 20-100 km or more, thus replacing terrestrial methods for most geodetic tasks.

In this paper possible scenarios currently under consideration at the Canadian Geodetic Survey (CGS) for the application of LBI and CGS in Canada will be reviewed, especially regarding the evolution of LBI and GPS geodetic networks, the improvement of the determination of the geoid, and the subsequent determination of orthometric heights.

INTRODUCTION

The two new technologies, namely Long Baseline Interferometry (LBI) and the Global Positioning System (GPS) are rapidly emerging as powerful new geodetic and geophysical tools. Realizing that the LBI and GPS era will undoubtedly bring fundamental changes to the practice of geodetic surveying, at the Canadian Geodetic Survey (CGS) we began to address such fundamental questions as: How can CGS best prepare for the support of the "GPS Surveyor" of tomorrow? What type of reference system will best provide a uniform reference fabric for positioning on a national scale? And how will the reference system and networks be realized? CGS is not alone asking such questions. Many others, including the Alberta Bureau of Surveying and Mapping, the U.S. National Geodetic Survey (NGS) and the Department of Transportation of the State of Texas are addressing these issues.

It is within this background that we have recently initiated a study aimed at examining various candidate near future scenarios for the combined application of the LBI and GPS technologies to geodesy in Canada. One such system based upon selected LBI and GPS stations and a number of automatic ground stations receiving non-coded data appears extremely attractive. Preliminary analyses indicate that this system should be capable of locating both satellites and ground receivers to the decimetre or sub-decimetre level at a reasonable cost.

In the sequel we shall discuss desirable system characteristics, the available coded and non-coded GPS system data types, the elimination of the need for very precise clocks, preliminary design of the network of Active Control Points (ACPs), requirements and predicted capabilities for orbit determination, precise positioning from covariance analyses, and the status of system demonstration tests currently in progress at CGS.

GEODETIC REQUIREMENTS

In Canada, the Geodetic Survey Division of the Surveys and Mapping Branch, EMR, is one of nine agencies involved in the upgrading and maintenance of the national geodetic networks to be based on the up-coming NAD83 geocentric coordinate system. The present effort for the re-adjustment of the North American networks will be completed approximately two years before the expected full deployment of GPS. The shortcomings of the newly completed NAD83 will be revealed by the new, higher accuracy GPS measurements. Thus it appears we may well see history repeating itself: as with EDM and TRANSIT satellite measurements before, GPS may force us into another re-adjustment. On the positive side, although future re-adjustments are inevitable, their impact on the surveying and mapping community will not be as disruptive as NAD83. Changes in coordinates of the reference framework would be smaller in magnitude than those being caused by NAD83, and the experience has led us to developments of proper data management tools required to handle such major overhauls. At this point in time it is rather difficult to be precise about the future geodetic requirements. By contrast, our future capabilities seem to be clearer:

(a) GPS will provide greater accuracy over distances of 100 km or more (0.1 ppm relative positioning accuracies in the 1990's) in shorter observation times (1-2 hours compared to 2-5 days) than the TRANSIT system. Therefore, it will be more economical to the user.

(b) Geodynamics support requires a relative accuracy of 0.1 to 0.01 ppm. Repeated such determinations at regular, frequent intervals by LBI will provide a precise record of the dynamic behaviour of Earth as a whole, as well as changes in relative positions between stations separated by as much as a few thousands of kilometres, and all that in observing periods of less than a week at the most.

(c) Especially because of the speed and economy of the GPS operations, definition of the geoid accurately enough to allow GPS to be useful in supporting the vertical control network at 200 km spacing (i.e. to control the propagation of systematic errors in levelling) is becoming all the more important for the purpose of accurate and economic height difference determinations using satellite technology.

(d) Finally, in addition to the fast evolution of geodetic (positioning) tools, computer hardware and telecommunications advances will (do) make it possible to handle large amounts of data in a timely manner.

CGS SCENARIOS FOR CONSIDERATION

Recognizing that the changes to be brought about by the GPS/LBI system are far more than replacing the old technology with a newer one in order to perform the same function, we at CGS have been exploring the following scenarios:

(a) A sparse network of 20 to 30 Active Control Points (ACPs) would provide the reference framework. These ACPs would consist largely of automated facilities at which satellite receiver equipment would operate continuously, tracking all visible satellites at all times. Data would automatically be transmitted to some central facility and hence to users on request in standardized formats. The data collected by these stations would be used to support orbit computations as well as network connections to users through translocations based on ACP and user data sets combined. Under such a scenario the present federal control network could be gradually phased out as a sufficient number of ACPs are put into operation.

(b) Because the current monumented control of some 7,000 primary control stations in Canada is naturally going to be used for some time, the scenario (a) above may be modified to include, in addition to the 20 to 30 ACPs, a portion (approximately 1000 stations) of the present federal network upgraded to 1 ppm (i.e. 10 cm in 100 km) in order to support GPS equipped surveyors. The 1000 or so chosen stations from the present control would involve 500 to 600 of the existing first-order (vertical) bench marks which are generally more accessible than triangulation stations. Users of GPS would employ several receivers to ensure high relative accuracy locally and ACPs would provide the required connections to the national framework. When users operate differentially but without using ACP data sets, they would be required to occupy one or more of the federal control stations (1000 stations would provide a 100 km spacing).

(c) If no ACPs are to be established, a dense (some 40 km) spacing of control points would be required in order to cover the settled areas of the country. Clearly the quality of the network would vary depending on the amount of GPS data included in the computation of station coordinates. This scenario is unlikely due to its high cost of implementation and maintenance.

Regardless of the chosen scenario, LBI would provide the overall strengthening of the national framework. LBI collocated with GPS stations would ensure consistent scale and orientation of the terrestrial networks positioned by GPS. In addition, such LBI observations would connect the Earth centered reference frame of GPS to an inertial reference frame. For experimentation, GPS receivers would be installed at sites where Canadian LBI terminals (CLTs) exist, e.g. the Dominion Radio Astrophysical Observatory (DARO) in Penticton, B.C., the Algonquin Radio Observatory (ARO) in Lake Traverse, Ont., and the Herzberg Institute of Astrophysics (HIA) in Ottawa, Ont. Because the GPS satellites are so high, there are no intervisibility restrictions so that all sites can be involved in these experiments. All sites are well equipped with hardware and technical support. ARO has a hydrogen maser available as a frequency standard; DARO and HIA would use much cheaper rubidum standards, particularly if the current Canadian research effort directed towards development of a satellite link that measures the relative phase of local oscillators at widely separated observatories is proven to be satisfactory in permitting corrections to be applied to the data to compensate for relative drifts of the frequency standards (Canadian Astrophysical Society, 1982).

PRIMARY ACP TRACKING SYSTEM CHARACTERISTICS

There are four most desirable features required by the ACP system: automatic tracking stations, tracking system design capable of collecting both coded and non-coded GPS data (preferably non-coded data because of their higher quality), ability to generate precise position estimates with data taken over short time spans, and ability to verify the capabilities of the system.

Automation

The planned operations of the ACPs require that all functions of the system are computer controlled on site with most operations (satellite receiver control, data handling, monitoring, etc.) normally accomplished by software residing on the controlling computer without interruption of satellite tracking functions.

Each ACP station would relay, to the network control and processing centre, the phase data from the GPS observations, and other auxiliary information. The task of automation would be much easier if each station does not require precision clocks, steerable antennas, or water vapor radiometers (WVR).

The studies under development at CGS, to be outlined below, indicate that high precision clocks may not be required if the analysis of the collected data is done in a differential mode. Tests for non-directional antennas (e.g. omni, phase-array or others) would have to be carried out, and experiments with WVR may be necessary to determine the requirements and whether it may be possible to select station locations where WVR are not needed.

Non-coded vs coded GPS data

For precision (i.e. sub-decimetre) geodetic applications of GPS, two significant departures from the nominal navigation mode (Vanicek et al., 1984) must be undertaken. First, the phase of the GPS L_1 and L_2 carrier signals are tracked as well as the code modulations (Delikaraoglou et al, in prep.). Carrier phase data yield very precise measures of the change with time of the range between a satellite and receiver: the phase changes by one cycle whenever the satellite-to-receiver distance changes by one wavelength of the carrier frequency (e.g. about 20 cm for the L_1 carrier compared to about 30 m for one P-code chip). Second, the observations must be differential in nature, i.e. streams of observations from more than one station must be differenced between stations to obtain differential phase delays. The latter should be routinely obtained with an accuracy typically of 1% of the carrier wavelength, so that when corrected for ionospheric refraction, it would yield range change measures with sub-decimetre precision. By comparison, from P-code modulations the precision would only be several decimetres.

Currently, because of the likelihood of the restrictions on the availability of the P-code under the U.S. DoD selective availability policy (Scull, 1984), development studies at CGS have been concentrated on techniques which can provide high precision results utilizing code or carrier phase GPS data. These techniques would require accurate orbit parameters which can only be incorporated through post mission processing after the field measurements have been completed and hence are within national security considerations.

Short-arc vs Long-arc Solutions

The GPS interferometric techniques of relative positioning currently under consideration are very similar to the ones used in LBI. Nevertheless, GPS applications differ from LBI in two major aspects: the proximity, and the rapid angular velocity of the signal sources, i.e. the GPS satellites. Therefore, the LBI techniques appropriate for distant "stationary" radio sources need to be modified for GPS positioning by properly accounting for the GPS satellite motions. In that respect, the lack of precise orbital information is a major limiting factor if accuracies of 0.1 ppm are to be achieved, particularly for long baselines.

If estimates of the satellite and station positions can be derived from data taken over short time spans (e.g. 1 to 2 hours) the estimation process can be simplified enormously since almost all of the modelling requirements are substantially relaxed (Nakiboglu et al., 1984; Vanicek et al., 1985). This is because position solutions made with data taken simultaneously using a multi-station configuration are essentially geocentric in character, and hence there is no need for any dynamic modelling. By contrast, as longer arcs are observed, the perturbing forces likely to contribute significantly to GPS satellite motion (such as the non-central part of Earth's gravitational field, third body effects of the sun and the moon, and perhaps drag and solar radiation pressure effects) must be modelled by elaborate force models. Clearly, any imperfections in the dynamical modelling of the satellite motion arising from gravity field uncertainties and other non-gravitational processes would effectively cause some information loss when the satellites are not tracked. In this connection, the data from the ACP-based tracking system, because they would be continuous and geometrically well distributed, would greatly reduce the rate of information loss even for long arc solutions.

One of the major advantages envisaged for short span, short-arc solutions based on the ACP data, is that they would allow a continuous monitoring and separation of various station position solutions from the "signals" of various Earth dynamical models, a process which would conceivably provide a powerful source of information to those interested not only in satellite positioning but also in Earth dynamics.

ACP CONFIGURATION

The ACP system is currently visualized in three major segments: 20-30 continuously tracking GPS receivers spaced uniformily throughout Canada, a central processing site, and a communications network.

The choice of GPS receivers to be employed in these stations has not been reached yet. It is envisaged that the timing requirements of the system can easily be met with microsecond quality clocks which are widely available as well as appropriate processing techniques such as using doubly differenced data (see follow-up discussion), or auxiliary parameters. However, if higher precision clocks are available, a significant improvement can be made in both satellite and ground positioning.

In the initial phase of the project, the currently existing TRANET stations in Ottawa, Ontario and Calgary, Alberta operated by the Department of Energy, Mines and Resources would be upgraded to become GPS Tracking sites. Co-location of GPS receivers at the existing CLT sites (DARO, ARO and HIA) is also the next obvious choice. Since the positions of these stations can be located with LBI techniques to a few centimetres, they would serve as reference mark positions to which other stations may be referenced by short-arc GPS interferometric solutions. The remaining ACP stations would then be progressively established throughout the country with a suitable spacing between stations. When the full GPS constellation is operational, the ACP tracking performance should not be sensitive to the location of the ACP sites, so that the particular ACP sites may be selected for security, power, convenience of access or other factors. For instance, the sites may be conveniently chosen to minimize tropospheric effects and thus avoid the need for expensive water vapour radiometers.

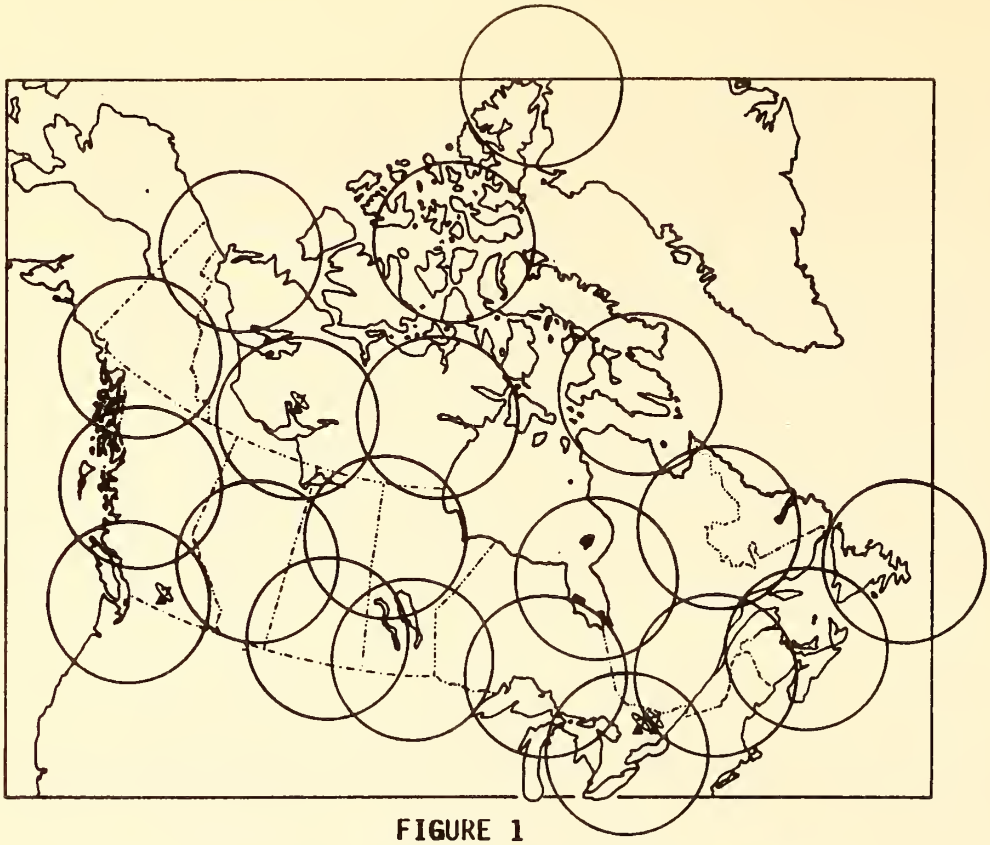

FIGURE 1

ONE POSSIBLE CONFIGURATION OF THE ACP NETWORK

Fig. 1 shows one of several possible configurations of the ACP network. The "effective" areas of differential operations within which surveyors can make effective use of the ACP data are shown here with circles of 500 km radii. Although theoretically the effective range of differential GPS can be of the order of thousands of km due to the high GPS orbits, in practical terms, the optimal effective range wil be somewhat limited by the correlation distance of atmospheric conditions affecting refraction. This is typically about 200-300 km.

Once the data are collected at the ACP sites, they would be transmitted regularly to the central processing site where they will be edited, compressed and archived in a suitable form to be made available on request to the general user operating in the "effective area" of the specific ACP. In addition, a larger amount of data from the entire ACP network would also be used to monitor the GPS orbits and to determine ground positions of non-ACP stations. Thus the ACP network would provide a dual function: orbit refinement, and translocation measurements in support of user activities. Geodetic (or other) positioning would then be directly related to the national coordinate system in this way without the requirement to occupy the active control stations. Especially for real-time applications (navigation and general use by the public), these stations would provide a precise, dynamic positioning capability. By being placed in selected Canadian airports or strategic coastal locations, these stations would provide a valuable service to on-shore as well as off-shore navigation and positioning applications.

TYPE	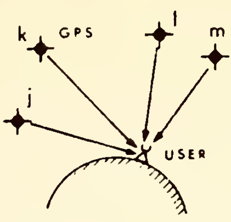	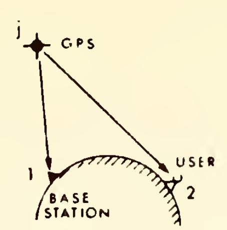	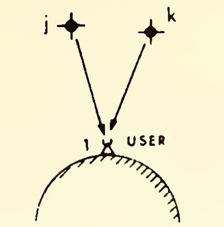	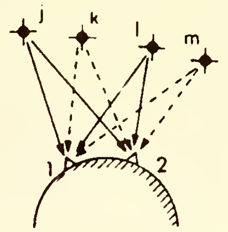
DATA	$\rho_1^j\ \rho_1^k\ \rho_1^l\ \rho_1^m$	$\Delta\rho_{12}^j = \rho_2^j - \rho_1^j$	$\nabla\rho_1^{jk} = \rho_1^k - \rho_1^j$	$\Delta\rho_{12}^{jk}$, $\Delta\rho_{12}^{lm}$
LIMITATIONS	PRECISION CLOCKS GPS AND STATIONS GPS EPHEMERIDES	STATION CLOCKS	GPS CLOCKS	SOME GEOMETRY INFORMATION LOSS CROSS-CORRELATIONS
ADVANTAGES	NO GEOMETRY LOSS	GPS ERRORS CANCEL	STATION CLOCK ERRORS CANCEL	GPS ERRORS CANCEL NO STATION CLOCK REQUIREMENTS (< μsec)

FIGURE 2

DIRECT AND DIFFERENTIAL TRACKING BY GPS

The communication requirements necessary to return the collected GPS data to the central facility are perhaps the most stringent because of the continuing cost elements of any type of communication system. Part of current Canadian research in satellite communication technologies, together with the use of the Canadian communication satellites, would conceivably make possible the regular use of satellite communications. For the ACP plans the communication system would include the general functions of providing communication between external peripherals such as dedicated lines, dial-up lines, and the EMR's CYBER, IBM or VAX mainframes.

PRECISION CLOCK REQUIREMENTS VS SPECIAL PROCESSING TECHNIQUES

GPS measurements can be combined in a variety of ways to remove or greatly reduce the effect of particular error sources inherent in the positioning process. The conventional way of using the GPS data, as shown for instance in fig. 2, is to carry out range code measurements over short time spans and solve for station clock bias and position. Clearly, any clock biases involved in this process results in an equivalent range error equal to the clock bias multiplied by the speed of light, i.e. about 30 cm for every nanosecond of clock synchronization error. For decimetre position determination such operations would require clocks with an accuracy of 10^{-13}. Using the code or carrier GPS measurements in a differential mode however, greatly reduces this requirement, because in this way the effect of errors which are common to both measurements being differenced are nearly completely removed. GPS measurements can be differenced across receivers, across satellites and across time (Paradissis and Wells, 1984). Although many difference combinations are possible, the present convention for GPS measurement differencing is to perform it in the above order (cf. fig. 2), i.e. first across receivers (single difference observables), then across satellites (double difference observables) and lastly across time (triple difference observables). Single differences remove or greatly reduce the effect of errors associated with the satellites, i.e. satellite clock errors and to a great extent (depending on baseline lengths which are short compared to the 20,000 km GPS satellite altitudes) satellite ephemeris and atmospheric refraction errors; double differences reduce the effects associated with any station clock misalignment (which is a common contributor to both single differences) with respect to the reference time scale used (e.g. UTC or GPS System Time); triple differences similarly reduce the effects of residual satellite and receiver clock errors, and in the case of carrier phase measurements, of the phase ambiguity errors.

Clearly, double or triple difference data can produce quality measurements to support GPS satellite or station positioning operations without the need of precise clocks. The clocks in the GPS sites need have only modest stability performance that is required to maintain accurate time tagging of the observation records. For the GPS satellites moving at about 4 km/sec, this translates to about 1 msec time-tag epoch accuracies, i.e. clocks that support 1 msec synchronization anywhere in the ACP network is all that is needed. Such clocks are readily available.

On the disappointing side, double, and to a greater extent triple, differencing operations result in some information loss in terms of geometry, in addition to the increased complexity of rigorously keeping track of the cross-correlated nature of the differenced observables. Current analyses at CGS and elsewhere show for instance that double differencing leads to about 40% increase in orbit error over that obtained from single difference data assumed to be taken with perfect clocks (Crow et al., 1984). Nevertheless, in an operation like the ACP network, the nominal double or triple difference observables are not likely to be used without a more rigorous, optimal modelling applied to the data streams that better reflects the stochastic properties of the clocks.

ACP TECHNOLOGY PROOF-OF-CONCEPT TESTS

To date, ACP proof-of-concept tests at CGS have been limited to a series of GPS differential positioning tests and receiver evaluations which were conducted over the past year for the purpose of, in addition to gaining some hands-on experience with various receiver systems, establishing the degree of maturity of the technology, and extrapolating from the results obtained from these tests to validate the theoretical accuracy predictions for the full ACP network. Details of these test results can be found in Delikaraoglou et al. (1985) and McArthur et al. (1985) in these proceedings. These preliminary tests were carried out in an effort to study the performance of the instrumentation (so far we have only tested the MACROMETER V-1000 and TI-4100 receiver systems), the effects of the environment (i.e. multipath, ionospheric and tropospheric effects), and the effects of error sources originating at the GPS satellites (i.e. their ephemerides). This evaluation did not address the problem of establishing our own orbit determination capabilities. This would have entailed many more receivers and considerably more time and resources than we had available at that time. Instead, we concentrated on evaluating the instrumentation and its performance in terms of accuracy and stability (repeatability) in recovering the baseline vectors over a variety of baseline lengths. The repeatability of the results and the level of agreement with "ground truth" measures of the corresponding vectors provided a fairly definite picture of the readiness of this type of operation.

CONCLUDING REMARKS

Although the NAD83 project for the re-adjustment of the North American geodetic network is near completion, it is apparent that we are at the beginning of a new era in the positioning field. The new data management requirements and the new advances in the LBI and GPS technologies will affect the entire spectrum of our surveying operations. Economics will require it. The present system of some 7,000 monumented control points in Canada will be used for some time, but we must accept the challenge of exploring the new technologies that are now becoming available to us to their full potential. And we must do it now to ensure that Canadians are provided with the full benefits. In this paper, we have described one concept which is in the process of being studied in Canada. Considerably more study will be needed before we can be confident enough to present it to our government as an operational proposal to be funded.

ACKNOWLEDGEMENTS

The many fruitful discussions with Norman Beck,Research and Development Section, CGS are gratefully acknowledged and greatly appreciated.

REFERENCES

Canadian Astrophysical Society (1982) - "The Canadian Long Baseline Array", report to the Natural Sciences and Engineering Council, and the National Research Concil of Canada, Ottawa, September

Crow, B.R., F.R. Bletzacker, R.J. Najarian, G.H. Purcel Jr., J.I. Statman and J.B. Thomas (1984) - "Series-X Final Engineering Report", Jet Propulsion Laboratory, August.

Delikaraoglou, D., N. Beck, D.J. McArthur and K. Lochhead (1985) - "On the Establishment of 3-D Geodetic Control by Interferometry with the TI-4100 receiver", First International Symposium on Precise Positioning with the Global Positioning System, Washington, D.C., April 15-19.

Delikaraoglou, D., N. Beck, D. McArthur and K. Lochhead (in prep.) - "A Tutorial Comparison of Geodetic Positioning Techniques using the Code and Carrier Phase Difference Observations of GPS Satellites", Geodetic Survey of Canada, Ottawa.

McArthur, D.J., N. Beck, D. Delikaraoglou and K. Lochhead (1985) - "Precise Relative Positioning with the Macrometer V-1000 Interferometric Surveyor: experiences at the Geodetic Survey of Canada", First International Symposium on Precise Positioning with the Global Positioning System, Washington, D.C., April 15-19.

Nakiboglu, M., K.P. Schwarz, E.J. Krakiwsky, B. Barrett and B. Wanless (1984) - "A Multi-pass, Multi-station Approach to Orbital Improvement and Precise Positioning", PLANS '84, San Diego, December.

Paradissis, D. and D.E. Wells (1984) - "GPS Standardization - Status and Problems", International Sympsosium on Space Techniques for Geodynamics, Sopron, Hungary, July.

Scull, D.C. - "U.S. Radionavigation Plan", NAV'84 Conference, London, United Kingdom, May.

Vanicek, P., R.B. Langley, D.E. Wells and D. Delikaraoglou (1984) - "Geometrical Aspects of Differential GPS", Bull. Geod. 58, pp. 37-52.

Vanicek, P., G. Beutler, A, Kleusberg, R.B. Langley, R. Santerre and D.E. Wells (1985) - "DIPOP: A Differential Positioning Program Package for the Global Positioning System", Contract report to Geodetic Survey of Canada, Ottawa, March.

APPLYING GPS TO RANGE TRACKING REQUIREMENTS

Carl E. Hoefener
Interstate Electronics Corporation
Anaheim, CA 92803
and
John Clark
CAST Inc.
Los Alamitos, CA 90720

ABSTRACT. If Global Positioning System (GPS) receivers are to be used for range tracking, they must be specially designed to take into consideration some of the unique problems encountered. For navigation, precise position at selected points in time are required to plan subsequent action. For range tracking, however, precision trajectory determination is mandatory, and during violent maneuvering, precise position is required for instrumentation purposes. Therefore, a unique receiver design must be considered

When considering the use of the GPS for instrumentation applications, the subtle differences between the requirements of general navigation and precision trajectory determination must be taken into account. For navigation, precise position at selected points in time are required to plan subsequent action (course change, weapon release, etc.). Measurements can be made generally at the operator´s convenience and are not normally required during highly dynamic maneuvers.

After the maneuver (say, for example, a dogfight), the pilot can select his course home based on his current position. Generally, however, position determination is not a continuous requirement. On the contrary, for range tracking instrumentation applications, precision trajectory determination is mandatory. During violent maneuvering precise position is required for instrumentation purposes. Therefore, a whole set of unique problems exists when applying GPS to range tracking requirements. A second major difference when considering instrumentation applications of a GPS receiver is that the receiver will generally be temporarily installed on an operational aircraft for a particular series of tests, and the aircraft will usually not be modified for the test. This means that the GPS receiver will be mounted in a container (say, for example, a five-inch-diameter pod such as that used in the Range Applications Joint Program Office (RAJPO) program), and this pod will be mounted at an existing weapon station on the aircraft. Most often this is an underwing or wing tip pylon and varies from test to test.

This can cause severe operational constraints on the GPS receiver and its associated processing. Consider the following:

- The receiver must operate on existing power sources at a normal weapon station.
- Because the receiver may be mounted on a wing tip, it will be subjected to much more extreme environmental characteristics than if it were mounted on the aircraft centerline.

- As the receiver may be mounted under a wing, antenna masking may be severe, allowing only a limited number of satellites to be visible. (Murphy predicts that the ones that are visible will not be optimal from a GDOP standpoint.)

- During aircraft maneuvering, satellites will come into view momentarily and then drop from view because of antenna masking.

- With the receiver mounted on the wing, manual adjustment will be impossible during flight.

- The GPS antenna, normally on the end of the pod, will not be on the aircraft centerline.

- Since the tracking receiver will also be installed on vehicles other than aircraft, the receiver must be modular so that it may be adapted to targets of various sizes, shapes, and dynamics.

These unique installation requirements of a GPS receiver utilized for range tracking applications will force severe design constraints on the GPS receiver.

It should be apparent that a GPS receiver designed specifically for navigation applications may not be satisfactory for range tracking. To expand on this point, consider how the preceding operational constraints drive the GPS range receiver´s design:

- The instrumentation receiver must be capable of being mounted within a five-inch-diameter pod (e.g., an AIM-9 pod) and requires minimum volume.

- Because the pod containing the test receiver may be mounted on a weapon pylon, it will have a limited choice of power availability. Typically available power is 28 volts DC ±10% and 115 volts AC 400 Hz ±10%. This is at best a very crude power source.

- As the receiver may be pod mounted and installed on a wing tip, the G forces that it will experience are much more severe than those that would be experienced if the receiver were mounted near the aircraft centerline. For example, typical operating characteristics are vibration of 2g 5 to 2000 Hz and shocks up to 20g for 11 milliseconds. In addition, the temperatures to be experienced range from -54°C to +95°C. These temperature extremes would not be experienced by a navigation receiver mounted within the test vehicle.

- As the instrumentation receiver will not be capable of adjustment during flight, any adjustments required must be accomplished via a datalink.

- Because of the severe antenna masking that will be experienced, few satellites will be visible at any one time. All satellites required for optimum GDOP at any location and time will not be visible. Therefore, the receiver must know what satellites will be in view with existing aircraft attitude at the existing location. Furthermore, of those satellites in view, it must select those satellites that provide the best obtainable GDOP.

- As the satellites will come in and out of antenna view rather frequently, the instrumentation GPS receiver must be capable of rapid satellite acquisition and reacquisition.

- The instrumentation receiver will often not be mounted on the test vehicle centerline. In fact, a single test receiver may be moved from vehicle to vehicle with a different mounting configuration on each vehicle. With the antenna position being moved with each installation, the lever arm corrections input to the navigation Kalman filter will have to be modified for each installation. With a permanently installed receiver, these corrections would be fixed at installation.

Therefore, it is apparent that the design parameters for a GPS receiver to be used for range tracking applications are much more severe than those for a navigation receiver. A modern GPS range tracking receiver will have the following characteristics:

- It will be an all-digital, modular GPS receiver using CMOS VLSI to realize a small, lightweight, highly reliable unit. The modularity will allow easy configuration for various types of test platforms with varying dynamics requirements.

- It will have a versatile power supply providing precision operating voltages from highly unstable power sources.

- It will be laid out on printed-circuit boards with short beam lengths to help reduce amplification of shock and vibration loads. In addition, copper clad boards will be mounted in assemblies that will provide conduction cooling.

- It will contain a modular interface to adapt to a datalink that will be capable of adjusting the receiver parameters during a test operation.

- The receiver´s processor must possess adaptive masking capabilities that will keep track of the antenna masking angles for each test vehicle on which the receiver is installed. The receiver will then keep track of the test vehicle attitude and determine which satellites are in view. The receiver then determines which of the satellites in view provide the optimum GDOP. This will allow the receiver to attempt to lock onto the "best" satellite in view.

- The instrumentation receiver will also utilize unique signal acquisition and tracking correlation techniques such as an eight-point correlator to acquire and reacquire satellites rapidly.

- The instrumentation receiver will also contain a programmable navigation filter to enable it to be optimized for each test installation and each test situation. This will permit modification and optimization of the navigation solution for various antenna locations and target dynamics.

- The receiver/processor unit needs to have the ability to collect and store "extra" data (e.g., differential corrections, local weather data, environmental data, etc.) for non-real-time postmission analysis.

- The software for the instrumentation receiver needs to be flexible enough to be readily modified to accommodate new hardware or special test requirements. In this regard it should be understandable and supportable by range personnel.

The preceding arguments have been presented to focus attention on those requirements that are unique to the instrumentation environment as contrasted to the more conventionally considered design drivers for a permanently installed navigation set. The U.S. Air Force Space Division has contracted for the development of GPS user equipment to be installed on a variety of platforms. These GPS receivers have been specifically designed as navigation devices. They have not been optimized for the peculiar requirements of range tracking. Therefore, if GPS receivers are to be used effectively for range tracking, they must be designed by taking into consideration the unique problems addressed here.

KINEMATIC POSITIONING WITH AN INTEGRATED INS-DIFFERENTIAL GPS

J.M. Goldfarb and K.P. Schwarz
Division of Surveying Engineering
The University of Calgary
Calgary, Alberta T2N 1N4
Canada

ABSTRACT. New approaches to precise aircraft positioning with applications in aerotriangulation, airborne gravimetry, and airborne laser profiling, have become feasible through the use of GPS; two strategies are compared in this paper. In the first, differential GPS P-code measurements are combined with the output of a stable-platform inertial navigation system (INS). In the second, GPS carrier phase single differences are used with a strapdown INS to bridge gaps caused by cycle slips. Error models for GPS and INS are given. A simulation program has been written to test the feasibility of using the proposed methods to position the aerial exposure stations for medium-scale photomapping, thus eliminating the need for the usual ground control. Simulations have been performed for a variety of error scenarios. The results indicate that positional accuracies of one-half metre or better can be obtained with either of the proposed methods. Validation tests with real data are planned later this year.

INTRODUCTION

With the development of the NAVSTAR Global Positioning System, precise positioning is feasible where before it was impractical or impossible. One such situation is that of positioning an aircraft in flight.

The ability to position an aircraft with accuracy at the metre or sub-metre level will facilitate several emerging survey applications, and will have a significant impact on other, more traditional applications. Examples of the former are airborne gravimetry and airborne laser profiling; an example of the latter is the use of airborne control for medium-scale photomapping. Typical accuracy requirements are: 1 m in height for gravimetry, a few decimetres in height and about half a metre in horizontal coordinates for laser profiling, and 1 to 2 m in all coordinates for medium-scale photomapping.

The accuracies cited above cannot be obtained using GPS alone. For single-receiver P-code measurements, resulting positional accuracies will be on the order of 15 to 20 m or worse. This accuracy can be improved using differential pseudoranges, but uncertainties in position will still be in the 5 to 10 m range. The use of phase measurements could reduce uncertainties to the sub-metre level, but the presence of cycle slips creates difficulties in kinematic positioning. The required accuracies can be obtained, however, if an auxiliary system is used in conjunction with GPS. An inertial navigation system (INS) is well suited for this purpose as its performance characteristics are complimentary to those of GPS.

Two different strategies for the combination of GPS and INS data will be examined. In the first approach, a stable-platform INS is used along with differential pseudorange (P-code) measurements. In the second approach, an inexpensive strapdown INS augments GPS carrier phase difference measurements.

Figure 1 illustrates the concept behind the first strategy. Typical error behavior for an INS and for GPS is shown. It is seen that while the INS exhibits a very smooth error curve, its (unaided) errors grow very large with time. On the other hand, although the GPS-derived positions are much noisier, their expected values (means) are close to the true trajectory. These properties suggest that the INS can be exploited for its interpolative abilities, while the GPS can be used to assure that the derived trajectory does not stray far from the true trajectory.

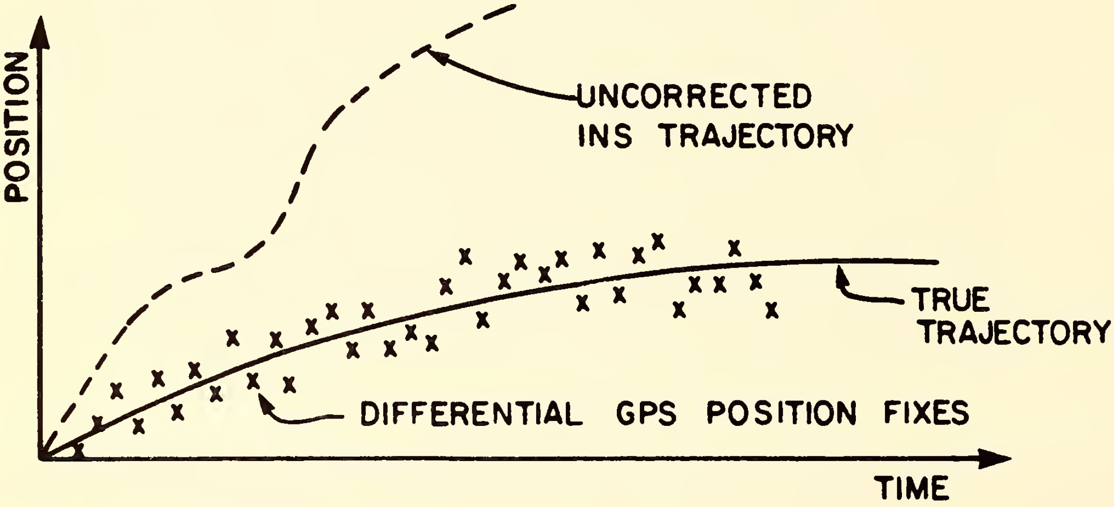

Figure 1: INS-Differential GPS Concept

The above procedure is not without difficulties. In order for the GPS positions to be of sufficient accuracy, the P-code would have to be used; this may be impossible under the DOD's policy of selective availability. Furthermore, stable-platform INS's are very expensive, and the available hardware is often unreliable. The second strategy would alleviate these difficulties. The use of GPS carrier phase measurements alone may result in accuracies sufficient for the planned applications if the effects of cycle slips can be eliminated. Once again, the interpolative ability of the INS can be used to advantage. Because loss of lock will usually occur over very short time intervals, an inexpensive strapdown inertial system can be used to bridge the gaps which result. In order to apply this procedure, however, a technique must be developed to resolve integer phase ambiguities for a moving vehicle. In addition, synchronization of receiver clocks is more difficult.

ERROR MODEL FOR AN INERTIAL NAVIGATION SYSTEM (INS)

The error behaviour of a dynamic system is usually modelled by a linear system of first-order differential equations. This so-called state space model is of the general form

$$\dot{\underline{x}} = \underline{F}\,\underline{x} + \underline{w}$$
$$\underline{x}(t_o) = \underline{x}_o \qquad (2.1)$$

where $\underline{x}$ ... is the state vector
$\underline{F}$ ... is the dynamics matrix
$\underline{w}$ ... is a set of forcing functions
$\underline{x}_o$ ... is the vector of initial values.

The solution of this system of equations

$$\underline{x}(t) = \underline{\Phi}(t,t_o)\,\underline{x}_o + \int_{t_o}^{t} \underline{\Phi}(\tau,t_o)\,\underline{w}(\tau)\,d\tau \qquad (2.2)$$

describes the system errors as functions of time. They are characterized by the transition matrix $\underline{\Phi}(t,t_o)$ and the vector of initial values $\underline{x}(t_o)$. The second term on the right-hand side of equation (2.2) expresses the uncertainty in the determination of $\underline{x}(t)$. For a well-modelled system, this term can usually be described statistically, as having a zero mean over a certain time period and a time-dependent covariance function. Conditions under which a solution to the system (2.1) exists are given in textbooks, e.g. Hochstadt (1975) or Arnold (1978).

Equation (2.2) is thus the error model for a dynamic system. The behaviour of individual errors in time is described by the transition matrix $\underline{\Phi}$ while their amplitude is determined by the initial values $\underline{x}_o$. Every dynamic system has specific error characteristics. If $\underline{\Phi}$ is known, the dominant frequencies governing individual errors can be obtained.

The state space model for inertial navigation systems (INS) is well-known. It is most simply described by a state vector of the form

$$\underline{x} = \{\underline{\delta r},\ \underline{\delta \dot{r}},\ \underline{\delta \varepsilon},\ \underline{\delta \dot{\varepsilon}}\}^T \qquad (2.3)$$

where $\underline{\delta r}$ ... describes three position errors
$\underline{\delta \dot{r}}$ ... describes three velocity errors
$\underline{\delta \varepsilon}$ ... describes three platform alignment errors
$\underline{\delta \dot{\varepsilon}}$ ... describes three linear platform drift rates.

A more detailed discussion of these errors and their relation to the actual sensor errors can be found in Britting (1971) or Schwarz (1985). The latter also discusses an extension of this basic state vector. Since the twelve states given in equation (2.3) usually are responsible for more than 95% of the position errors, special attention will be given to them.

To obtain the position errors as functions of time, the transition matrix of the system (2.1) with state vector (2.3) must be determined. Its form depends on the specific mechanization of the inertial navigation system. We will in the following assume a stable platform system of local-level type. In this case, an analytical form of $\underline{\Phi}$ can be found and the discussion of the dominant frequencies is thus considerably simplified. The derivation of an analytical expression for $\underline{\Phi}$ is a rather cumbersome task. Methods are discussed in Wong and Schwarz (1979) where the basic equations for the case at hand are given. Further details are contained in Wong (1982). If the initial states were known, the error behavior of the inertial system could be predicted from these formulas within the uncertainty given by the system noise. Since the vector $\underline{x}_o$ is unknown, a different route must be taken.

The principle applied in the following was proposed in Schwarz (1983) and further developed in Vassiliou (1984). It consists in reordering the error equations in terms of base functions in the dominant frequencies and to replace the unknown $\underline{x}_o$ by a set of parameters $\underline{y}$ which can be determined by external measurement. The three equations then take the form

$$\begin{aligned}\delta\lambda(t_i) = a_o + a_1 t_i + a_2 \sin\omega_E t_i + a_3 \cos\omega_E t_i + a_4 \sin\omega_s t_i \\ + a_5 \cos\omega_s t_i + a_6 t_i \sin\omega_s t_i + a_7 t_i \cos\omega_s t_i + \varepsilon_\lambda\end{aligned} \tag{2.4a}$$

$$\begin{aligned}\delta\phi(t_i) = b_o + b_1 t_i + b_2 \sin\omega_E t_i + b_3 \cos\omega_E t_i + b_4 \mathrm{sub}\omega_s t_i \\ + b_5 \cos\omega_s t_i + b_6 t_i \sin\omega_s t_i + b_7 t_i \cos\omega_x t_i + \varepsilon_\phi\end{aligned} \tag{2.4b}$$

$$\begin{aligned}\delta h(t_i) = c_o + c_2 \sinh\kappa t_i + c_2 \cosh\kappa t_i + c_3 \sin\omega_E t_i \\ + c_4 \sin\omega_s t_i + c_5 \cos\omega_s t_i + c_6 t_i \cos\omega_s t_i + \varepsilon_h\end{aligned} \tag{2.4c}$$

or

$$\underline{\delta r}_i = \underline{A}_i \, \underline{y} \tag{2.5}$$

where

$$\underline{\delta r}_i = \begin{pmatrix} \delta\lambda(t_i) \\ \delta\phi(t_i) \\ \delta h(t_i) \end{pmatrix} \qquad \underline{y} = \begin{pmatrix} \underline{a} \\ \underline{b} \\ \underline{c} \end{pmatrix}$$

$$\underline{A}_i = \begin{pmatrix} \underline{B}_1 & \underline{0} & \underline{0} \\ \underline{0} & \underline{B}_1 & \underline{0} \\ \underline{0} & \underline{0} & \underline{B}_2 \end{pmatrix}$$

with

$$\underline{a} = (a_0, a_1, a_2, a_3, a_4, a_5, a_6, a_7)^T$$

$$\underline{B}_1 = (1, t_i, \sin\omega_E t_i, \cos\omega_E t_i, \sin\omega_s t_i, \cos\omega_s t_i, t_i \sin\omega_s t_i, t_i \cos\omega_s t_i)$$

and the corresponding expressions for $\underline{b}$, $\underline{c}$, and $\underline{B}_2$. The terms ω_E and ω_s denote the earth rate and the Schuler rate, respectively. The term κ is a damping factor and ε_λ, ε_ϕ, ε_h are stochastic variables with zero mean and known autocorrelation. It should be noted that this formulation neglects the correlation between the three equations, assumes no major acceleration changes occur, and, as an approximation, treats trigonometric functions of latitude as constants.

Equations (2.4) and (2.5) express the time dependent behaviour of the position errors in an inertial navigation system. These errors are dependent on the Schuler rate, having a period of about 84 minutes, and the earth's rotation rate. Errors in all three channels can grow unbounded with time, although error growth in the height channel is usually more rapid.

Besides the time dependent errors, there are a number of errors which in first approximation depend on the coordinate differences from the initial point. The most important of these are accelerometer scale factor errors and nonorthogonalities of the accelerometer frame. They can be added to equation (2.5) by writing

$$\underline{\delta r}_i = \underline{G}_i \underline{z} \qquad (2.6)$$

where

$$\underline{z} = \begin{bmatrix} \underline{y} \\ \underline{d} \end{bmatrix} \qquad \underline{G}_i = \begin{bmatrix} \underline{A}_i & 0 \\ 0 & \underline{D}_i \end{bmatrix}$$

$$\underline{d} = [s_\lambda, s_\phi, s_h, \alpha_1, \alpha_2, \alpha_3, \alpha_4, \alpha_5, \alpha_6]^T$$

$$D_i = \begin{bmatrix} \Delta\lambda_i & 0 & 0 & -\Delta\phi_i & \Delta h_i & 0 & 0 & 0 & 0 \\ 0 & \Delta\phi_i & 0 & 0 & 0 & \Delta\lambda_i & -\Delta h_i & 0 & 0 \\ 0 & 0 & \Delta h_i & 0 & 0 & 0 & 0 & -\Delta\lambda_i & \Delta\phi_i \end{bmatrix}$$

$1 + s_\lambda$, $1 + s_\phi$, $1 + s_h$ ... are three accelerometer scale factors

α_1 to α_6 ... are the six non-orthogonalities of the accelerometer axes

$\Delta\lambda_i$, $\Delta\phi_i$, Δh_i ... are coordinate differences from the initial point at which the INS was aligned.

and $\underline{y}$ and $\underline{A}_i$ are the vector and matrix from equation (2.5). For details see Schwarz (1983).

Equation (2.6) is the final error model of the inertial system. In general, the coefficients $\underline{z}$ are unknown. If position measurements from an external source are available, they can be determined. Thus, each known position gives three observation equations for the determination of the unknown parameters. In our application, position measurements from GPS are available at rather short time intervals, typically every 3 to 4 seconds. Thus, the 30 unknown parameters can be determined by a least-squares adjustment from a large number of redundant observations.

Once the parameters in equation (2.6) have been estimated, precise positions can be obtained for any epoch for which uncorrected INS positions are available. In practice, this can be as often as every 50 milliseconds. These precise positions are obtained for an epoch t_i by using equations (2.6) to calculate $\underline{\delta r}$ and subtracting these computed quantities from the raw INS output. These positions will be accurate if the GPS-derived positions are not biased, i.e., if the mean of their errors equals zero.

THE ERROR MODEL FOR GPS PSEUDORANGES, DIFFERENTIAL PSEUDORANGES AND PHASE MEASUREMENTS

Error sources for GPS positioning may be subdivided into three categories: errors associated with the satellite, errors arising during signal propagation, and errors associated with the GPS receiver. Position uncertainties resulting from the first, and to a lesser extent, from the second category of errors can be largely eliminated if range differences are used. Errors of the third group are minimized if code measurements are replaced by carrier phase measurements.

The error equation for a pseudorange ρ measured from receiver 1 to satellite S can be written

$$\rho_1 - \varepsilon_1 = \sqrt{(x_s-x_1)^2 + (y_s-y_1)^2 + (z_s-z_1)^2} + c'\delta t_s - c'\delta t_1 - \delta_{ion_1} - \delta_{trop_1} \tag{2.7}$$

where

ρ_1 ... is the measured pseudorange

ε_1 ... is the sum of all unmodelled measurement errors

x_s, y_s, z_s ... are Cartesian coordinates of satellite S - as determined from an ephemeris

x_1, y_1, z_1 ... are Cartesian coordinates of receiver 1

c' ... is the average signal propagation speed

δt_s ... is the part of the satellite clock error that can be computed from parameters included in the navigation message.

δt_1 ... is an instantaneous receiver clock bias, usually included as a parameter to be determined

δ_{ion_1} ... is the computed ionospheric delay

δ_{trop_1} ... is the computed tropospheric delay

The model for a differential pseudorange, with reference to Figure 2 is

$$\Delta\rho_{12} - \Delta\varepsilon_{12} = (\rho_1 - \varepsilon_1) - (\rho_2 - \varepsilon_2)$$

$$= \frac{\vec{e}_1 + \vec{e}_2}{1 + \vec{e}_1 \cdot \vec{e}_2} \Delta\vec{r}_{12} - c'\Delta\delta t_{12} - \Delta\delta_{ion_{12}} - \Delta\delta_{trop_{12}} \tag{2.8}$$

where

$\vec{e}_1$ and $\vec{e}_2$ ... are unit vectors pointing from receiver 1 and 2 toward satellite S

$\Delta\vec{r}_{12}$ ... is the baseline vector from receiver 1 to receiver 2

$\Delta\delta_{ion_{12}} = \delta_{ion_2} - \delta_{ion_1}$

$\Delta\delta_{trop_{12}} = \delta_{trop_2} - \delta_{trop_1}$

and all other terms have the same meaning as before. Note that this equation is linear in the baseline components, and its solution can be obtained by the method of successive substitutions.

A single-difference phase measurement may be expressed as

$$\Delta\phi_{12} - \Delta\varepsilon_{\phi_{12}} = \frac{f}{c}\left[\frac{\vec{e}_1 + \vec{e}_2}{1 + \vec{e}_1 \cdot \vec{e}_2} \Delta\vec{r}_{12} - c'\Delta\delta t_{12} - \Delta\delta_{ion_{12}} - \Delta\delta_{trop_{12}}\right] - N_{12} \tag{2.9}$$

$\Delta\phi_{12}$ ... is the fractional portion of the difference between the instantaneous phase measurements at receivers 1 and 2

f ... is the carrier frequency

c ... is the speed of light in vacuum

N_{12} ... is the difference in the integer number of wavelengths in the rays from receivers 1 and 2 to the satellite [plus an arbitrary bias]

$\Delta\varepsilon_{\phi_{12}}$ ... is the sum of all unmodelled errors.

If the integer, or 2π, ambiguity N_{12} is known, equation (2.9) can be transformed into equation (2.8) simply by multiplying both sides by c/f.

The error terms ε, $\Delta\varepsilon$, and $\Delta\varepsilon_\phi$ contain components resulting from a variety of sources. The major ones are:

a. Satellite
   - orbit prediction errors
   - satellite clock errors

b. Propagation
  - ionospheric group delay uncertainties
  - unmodelled tropospheric delay

c. Receiver
  - multipath effects
  - receiver noise and resolution

Each of these residual error sources will be discussed in turn.

Orbit prediction errors arise for several reasons. Firstly, satellite perturbations are not completely predictable. Uncertainties are due to incomplete knowledge of the perturbing forces, especially solar radiation pressure. Secondly, for expediency, a simplified ephemeris representation is broadcast. Finally, the relative positions of stations in the tracking network are not known exactly, and errors in the tracking station measurements propagate into the orbit.

GPS was designed for single receiver operation, and, therefore, the allowable spatial distribution of orbit prediction errors in the broadcast ephemeris is dictated by the contribution of these errors to the "user range error" (URE). Since range measurements are less affected by tangential and cross-track errors than they are by radial errors, the allowable magnitude of the first two components can be rather high. Since residual satellite clock errors contribute directly to the URE, an effort has been made in the system design to keep these errors small.

The effects of orbit prediction and satellite clock errors are virtually eliminated when the differential technique is applied over a short baseline (Beser and Parkinson, 1984).

For single-receiver pseudoranges, ionospheric delay uncertainties can arise from, among other things; (a) the use of only a single frequency for measurements, or (b) the truncation of the series representing group delay as a function of frequency if a dual frequency receiver is used. If single-frequency differential measurements are employed, as was the case in this study, uncertainties in the difference in ionospheric delays, $\Delta\delta_{ion}$, are due to the fact that the received signals traverse paths of different lengths through the ionosphere. In addition, uncorrelated random scintillations may occur along independent paths (Denaro, 1984).

Tropospheric delay uncertainties primarily result from the inadequacy of surface measurements of humidity for the prediction of the wet delay component (Remondi, 1984). The troposphere above 12 km contributes virtually nothing to the wet component. Therefore, because this study concerns an aircraft flying at a moderately high altitude (7.6 km), little benefit can be derived from the differential technique with respect to these uncertainties. This, however, would be different for low flying aircraft (< 1 km) as used e.g. in airborne gravimetry and airborne laser profiling.

Multipath errors arise when a portion of the received signal is reflected off nearby objects; therefore their effect on the measured range is a function of the receiving antenna's directionality and surroundings. Because the receivers in this study are so far apart, the multipath errors at each of the receivers will be independent. These errors will affect both ranges and range differences.

Receiver noise is a function of the receiver's design and operating environment. Receiver resolution is also a function of the receiver design,

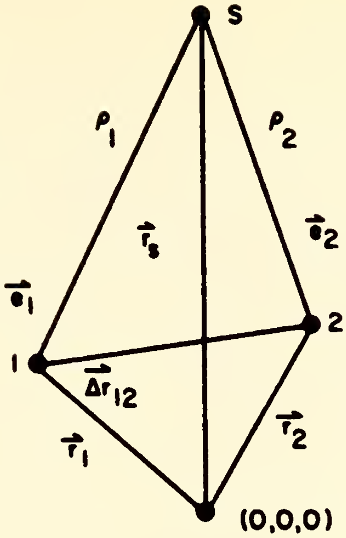

Figure 2: Range Difference Geometry

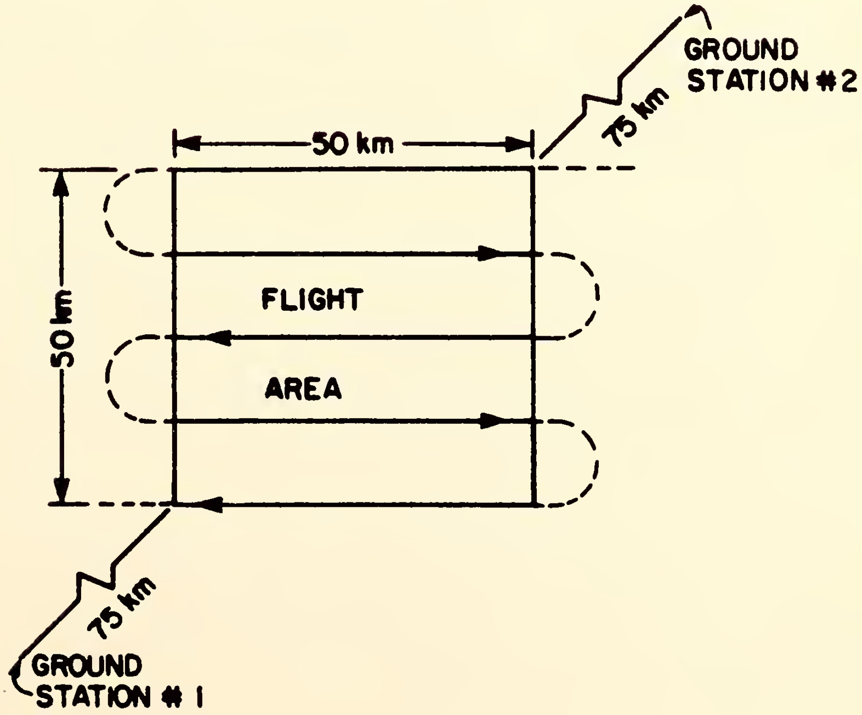

Figure 3: Simulated Flight Pattern

but it depends as well on the type of measurement used. In terms of resolution, phase measurements are far superior to code measurements.

SIMULATION STRATEGY

A computer program has been developed to simulate INS and GPS data for an aircraft in flight and GPS data for any number of ground receivers. An effort has been made to keep the program as flexible as possible so that a variety of possible error combinations can be investigated. The numerical results presented in the next section were obtained when studying the feasibility of replacing ground control for aerotriangulation by exposure station control. A detailed discussion of this application is given in Schwarz et al (1984) where it has been shown that, for an image scale of 1:50 000, standard errors of about 1 m can be obtained for the ground coordinates if the aircraft can be positioned with a standard error of 1-2 m. It was therefore the objective of this study to show that this positioning accuracy is possible. A diagram of the simulation area and the flight plan is shown in Figure 3.

The INS errors are generated using equations (2.4) which account for more than 95% of the total INS error. The refinement given by equation (2.6) has not been implemented. It will, however, not change any of the conclusions significantly. The coefficients a_i, b_i, and c_i are generated as normal deviates with given standard deviations. The terms ε_λ, ε_ϕ, and ε_h can be generated as either white noise or correlated noise (Markov process), or they can be accumulated as random walk processes.

For the GPS data, the 18 satellite constellation given, for example, in Fullenwider and Jorgensen (1984) is used. It is assumed that the receivers can use only four satellites at a time. They are selected using the minimum GDOP at the average ground receiver location as the selection criterion. Errors in the mean anomaly, orbital inclination, and orbital semi-major axis are generated randomly for each satellite, but are applied as biases for each pass. This is realistic, as actual broadcast ephemeris data exhibits a high degree of internal consistency as a consequence of the curve-fitting procedure used by the control segment.

The single-frequency ionospheric delay model given in Martin (1980) is used, as an option, to apply the group delay to the simulated ranges. An uncertainty in the knowledge of the partial water vapor pressure at the ground receiver locations can also be simulated. Receiver clock flicker is added to the measured ranges as correlated or uncorrelated noise; these instantaneous biases are solved for explicitly during processing. Finally, correlated or uncorrelated noise is added to the ranges themselves.

A summary of the particular simulation scenarios used in this report is given in Table 1. Of particular note is the high uncertainty applied to the satellite mean anomaly for the standard orbit. Such a high value would be acceptable under the current specifications because the single receiver navigation solution is least sensitive to tangential and cross-track orbit errors; see Divine and Francisco (1984).

The nature of the local-level INS mechanization requires some form of real-time error control. Usually, external measurements are incorporated by means of Kalman filtering. A simple filter using P-code pseudoranges as update

Flight

location - $\phi = 50°$, $\lambda = -100°$
altitude - 7 620 m
speed - 76.2 m/s
duration - 5 040 s (84 min)

GPS Utilization

satellite constellation - 18 satellites in 6 orbital planes, 40° phasing orbital inclination = 55°
satellite selection - 4 satellites/epoch; minimum GDOP criterion 10° elevation angle cutoff
average GDOP - 4.3
update rate - every 3 seconds
number of updates - 1 680

Errors Simulated

A. Applied in all cases
- 1. code measurement noise - 2.0 m, 1σ, uncorrelated
  phase measurement noise - 0.05 m, 1σ, uncorrelated
- 2. receiver clock flicker - 100 m range-equivalent, 1σ 1st order Markov process, 3 s correlation time
- 3. INS
  - a. systematic - errors grow to ~5-6 km for all three channels
  - b. random - 0.01 m/s, 1σ, accumulated as random walk for position errors.

B. Applied in specific cases
- 1. orbit prediction errors*
  - a. standard - 3m, 1σ, in semi-major axis, 1.13×10^{-7} radians (3m), 1σ, in inclination, 1.38×10^{-6} radians (36.6m), 1σ, in mean anomaly
  - b. improved - 2 m, 1σ, in semi-major axis, 7.53×10^{-8} radians (2m), 1σ, in orbital inclination and mean anomaly
- 2. ionosphere** - single frequency model vertical electron content = 2×10^{17} electrons/m^2
- 3. wet troposphere* - 10 mb, 1σ, uncertainty introduced in the partial water vapor pressure for the ground receiver(s)

* introduced as randomly generated biases

** note that no ionospheric corrections were applied during processing

Table 1: Simulation Summary

measurements is in this case sufficient to assure the linearity of the error equations. For details, see Wong and Schwarz (1983) and Schwarz et al (1984).

The use of carrier phase measurements requires the resolution of the integer ambiguities. This can be achieved before the start of the mission, either by setting up the receivers on very short baselines of known lengths or by obtaining a baseline solution . This will resolve the ambiguities for the initial set of satellites. If the observed satellites change during the mission, the problem becomes more complicated. In this case additional ground stations may help. For our simulations, this problem has been disregarded, i.e. it has been assumed that the ambiguities have been resolved.

RESULTS

In light of the error models developed earlier, post-mission processing is a simple procedure. It requires uncorrected positional data from the INS and positional information from the GPS. The processing may then be summarized as a three-step procedure:

(a) Compute differential GPS positions for each update epoch.

(b) Estimate the parameters of equation (2.6) as

$$\hat{\underline{z}} = (\underline{G}^T \underline{G})^{-1} \underline{G}^T \underline{\delta r}_i \qquad (4.1)$$

where the observed values $\underline{\delta r}_i$ are calculated by subtracting the GPS-derived positions from the uncorrected INS positions. (Note that the simpler equation (2.4) has been used in this case.)

(c) Use the estimated parameters $\hat{\underline{z}}$ in equation (2.6) to obtain $\underline{\delta \hat{r}}_i$ for each epoch of interest, and subtract these values from the uncorrected INS position for the best estimate of the true position.

Simulations have been performed to test both of the proposed strategies. Tables 2 and 3 summarize the results for a number of different observation and error scenarios. The figures given are average rms values from five simulation runs. Table 2 gives the accuracy obtained using GPS code measurements alone. The results of combining GPS and INS data are shown in Table 3 along with the results of using GPS phase single differences. The first three numbers given in each table location are rms errors in x, y, and z in the Average Terrestrial (AT) system, also known as the Conventional Terrestrial (CT) system (Vanicek and Krakiwsky, 1982). The last number, in parentheses, gives the standard deviation of the vector magnitudes of these errors over the five simulation runs, and is thus a measure of the variability of the results from run to run.

The most significant result in Table 2 is the improvement which is obtained when the differential technique is used. The rms error in each coordinate is 8 to 21 m for single-receiver pseudoranges, but drops to 3 to 8 m when one ground receiver is used in conjunction with the aircraft receiver. These error estimates agree with actual results given in Lachapelle et al (1984) where standard errors of 10 to 25 m were obtained for single receiver positioning and 5 to 10 m for differential P-code positioning. An examination of the single-receiver results reveals that orbit prediction errors are a major cause of uncertainty. Ionospheric effects are also significant for single receiver operation but these errors could be greatly reduced it the dual-frequency correction is applied. The large standard error of the single-receiver errors, indicated by the bracketed numbers, is an indication that large biases are present in the individual runs. The homogeneity of the errors for differential positioning indicates that this technique effectively eliminates the influence of orbital errors and ionospheric effects and thus the biasedness of the individual runs.

Errors / Configuration	standard orbit errors only	ionospheric effects only	standard orbit + ionosphere	standard orbit + ionosphere + wet troposphere	improved orbit + all errors
Single Receiver Code	8.85 12.17 18.83 (12.05)	3.00 11.42 14.38 (0.10)	8.45 14.53 20.91 (12.31)	(no ground receiver)	3.94 11.55 17.16 (5.23)
Differential Code 1 Ground Receiver	3.23 5.55 8.46 (0.26)	3.23 5.55 8.45 (0.25)	3.23 5.55 8.46 (0.25)	3.23 5.56 8.46 (0.25)	3.23 5.55 8.46 (0.25)
Differential Code 2 Ground Receivers	2.81 4.69 7.27 (0.08)	2.81 4.69 7.28 (0.08)	2.81 4.69 7.27 (0.08)	2.81 4.69 7.27 (0.08)	2.81 4.69 7.47 (0.08)

Table 2: GPS rms Position Errors (m)
(AT Cartesian)

A common characteristic of all these results is the spatial distribution of the errors, with the largest errors being in the z-coordinates and the smallest occuring in the x-coordinates. This can be explained as follows. Because all the satellites used are above the horizon, the determination of height is somewhat weaker than that of the other coordinates. For the location used in these simulations ($\phi = 50°$, $\lambda = -100°$), the vertical axis, and hence the height uncertainty, has its largest projection on the AT z-axis, and its smallest projection on the x-axis.

A comparison of Tables 2 and 3 reveals the effect of adding the INS. The accuracy of the differential GPS positions increases by an order of magnitude while the single-receiver results show no improvement. Once again, this is an indication of the biasedness of the single-receiver positions. In terms of accuracy, the differential phase measurements are better than the differential code measurements. Considering that this approach has imposed less stringent requirements on the accuracy of the inertial system, it offers a promising avenue to precise aircraft positioning. It should be kept in mind, however, that these results assume a satisfactory solution of the ambiguity problem. By comparison, the use of differential code measurements is without this problem and the resulting accuracy is sufficient for most applications mentioned in the introduction.

Errors Configuration	standard orbit errors only	ionospheric effects only	standard orbit + ionosphere	standard orbit + ionosphere + wet troposphere	improved orbits + all errors
Single Receiver Code	8.09 10.89 16.87 (12.67)	1.79 10.58 12.96 (0.08)	7.68 13.50 19.09 (12.71)	(no ground receiver)	2.76 10.56 15.77 (5.44)
Differential Code 1 Ground Receiver	0.27 0.36 0.60 (0.13)	0.26 0.29 0.52 (0.09)	0.28 0.36 0.59 (0.12)	0.29 0.35 0.58 (0.11)	0.27 0.31 0.54 (0.06)
Differential Code 2 Ground Receivers	0.23 0.35 0.58 (0.12)	0.23 0.36 0.59 (0.11)	0.23 0.35 0.58 (0.11)	0.23 0.37 0.58 (0.15)	0.23 0.38 0.59 (0.14)
Phase Single Differences 1 Ground Receiver	0.13 0.22 0.36 (0.11)	0.12 0.15 0.22 (<0.01)	0.16 0.24 0.36 (0.09)	0.16 0.26 0.33 (0.18)	0.13 0.22 0.29 (0.08)
Phase Single Differences 2 Ground Receivers	0.07 0.12 0.20 (<0.01)	0.07 0.12 0.18 (<0.01)	0.08 0.12 0.20 (<0.01)	0.08 0.21 0.29 (0.09)	0.08 0.21 0.27 (0.09)

Table 3: GPS-INS rms Position Errors (m)
(AT Cartesian)

For our purposes, the effect of the improved orbit is negligible. With phase measurements of higher precision than those simulated (i.e. $\sigma < 0.05$m), the effect may be more significant. Adding a second ground receiver resulted in only a small reduction of errors; a second receiver may be desirable, however, to aid in phase ambiguity resolution and to increase the system reliability.

In conclusion, both methods studied are capable of achieving sub-metre accuracy and should therefore be tested using actual data. Validation tests using a land vehicle on a calibration line are planned later this year and a full-scale airborne test could take place as early as spring 1986.

CONCLUSIONS

Simulation studies presented in this paper show that aircraft positioning at the sub-metre level is possible by combining differential GPS with an inertial navigation system, but not by GPS alone. Typical rms coordinate errors are 12 m for GPS single point positioning, 5 m for GPS differential positioning, and 0.5 for a combined differential GPS/INS.

Two combination methods have been studied. The first integrates differential GPS P-code measurements with the output of a high-quality local-level INS. The second depends on GPS carrier phase differences for accuracy and bridges cycle slips with a medium quality strapdown INS. Both methods achieve coordinate accuracies at the half metre level. Results are in general better for the second method. However, the problem of ambiguity resolution for a changing satellite configuration needs further consideration.

Application of these results to aerotriangulation is straightforward. By positioning all exposure stations with the above accuracy, ground control is not needed. A previous study has shown that the accuracy of the derived terrestrial positions is as good or better than the accuracy achieved at flight level. Validation tests for this application are planned in the near future.

ACKNOWLEDGEMENTS

Support for this research was made available by an EMR Research Agreement, monitored by the Topographic Engineering Section, Surveys and Mapping Branch. Discussions with C.C. Goad during his visit to The University of Calgary are gratefully acknowledged.

REFERENCES

Arnold, V.I., 1978, Ordinary Differential Equations. The M.I.T. Press, Cambridge, Mass.

Beser, J. and B.W. Parkinson, 1984, The application of NAVSTAR differential GPS in the civilian community. In Global Positioning System, 2, 167-196, The Institute of Navigation, Washington.

Britting, K.R., 1971. Inertial Navigation Systems Analysis. Wiley Interscience, New York.

Denaro, R.P., 1984, Simulation and analysis of differential GPS. In Proceedings of the National Technical Meeting of the Institute of Navigation, San Diego, 225-239.

Divine, D. and S.G. Francisco, 1984, Synchromesh, a practical enhancement to GPS service. In IEEE Position Location and Navigation Symposium Record, San Diego, 169-174.

Fullenwider, E.D. and P.S. Jorgensen, 1984, The updated NAVSTAR/GPS test and operational constellations. In IEEE Position Location and Navigation Symposium Record, San Diego, 315-320.

Hochstadt, H. 1975, Differential Equations. Dover, New York.

Lachapelle, G., J. Lethaby and M. Casey, 1984, Airborne single point and differential GPS navigation for hydrographic bathymetry. The Hydrographic Journal, 34, October 1984.

Martin, E.H., 1980, GPS user equipment error models. In Global Positioning System, 109-118, The Institute of Navigation, Washington.

Remondi, W.R., 1984, Using the Global Positioning System phase observable for relative geodesy: modeling, processing, and results. Doctoral Dissertation, Center for Space Research, University of Texas at Austin.

Schwarz, K.P., 1983, Inertial surveying and geodesy. Reviews of Geophysics and Space Physics, 21(4), 878-890.

Schwarz, K.P., C.S. Fraser and P.C. Gustafson, (1984), Aerotriangulation without ground control. International Archives of Photogrammetry and Remote Sensing, 25, Part A1, Rio de Janeiro, June 16-29, 1984.

Schwarz, K.P., R.V.C. Wong, J. Hagglund and G. Lachapelle, 1984, Marine positioning with a GPS-aided inertial navigation system. In Proceedings of the National Technical Meeting of the Institute of Navigation, San Diego.

Schwarz, K.P., 1985, A unified approach to post mission processing of inertial data. Bulletin Géodésique, 59(1).

Vanicek, P. and E.J. Krakiwsky, 1982, Geodesy: The Concepts. North-Holland, Amsterdam.

Vassiliou, A., 1984, Processing of unfiltered inertial data. Division of Surveying Engineering Publication 20006, The University of Calgary.

Wong, R.V.C., 1982, A Kalman filter-smoother for an inertial survey system of the local level type. Division of Surveying Engineering Publication 20001, The University of Calgary.

Wong, R.V.C. and K.P. Schwarz, 1983, Dynamic positioning with an integrated GPS-INS formulae and baseline tests. Division of Surveying Engineering Publication 30003, The University of Calgary.

Wong, V.C. and K.P. Schwarz, 1979, Investigations on the analytical form of the transition matrix in inertial geodesy. Technical Report 58, Department of Surveying Engineering, The University of New Brunswick, Fredericton.

GPS/IMU NAVIGATION
IN A HIGH DYNAMICS ENVIRONMENT

Dr. Donald Eller
Computing Applications Software Technology (CAST), Inc.
5450 Katella Avenue
Los Alamitos, CA 90720

ABSTRACT. An overview of a GPS/IMU integrated navigation system design for high dynamics applications is presented. Simulation results compare three Kalman filter configurations, and the advantages of each are described for various applications. A design for the Kalman filter process noise is developed, and the practical considerations of model selection and filter "tuning" are discussed.

INTRODUCTION

A GPS receiver integrated with a low cost, strapdown Inertial Measurement Unit (IMU) provides a high quality navigation system for a variety of applications. The capabilities of these diverse sensors can be combined in a synergistic fashion which uses the short term accuracy and rapid response of the IMU to aid the navigation solution in between GPS updates, and the high accuracy GPS range and range rate data to calibrate the IMU error parameters. The resulting navigation system overcomes many of the weaknesses of a stand alone GPS set by providing:

a) high rate/accuracy position and velocity estimates (suitable for weapon delivery) during high dynamics

b) reduced position/velocity error growth during GPS signal outage

c) improved jamming resistance through code loop aiding

d) availability of vehicle attitude

This makes GPS suitable for a much wider range of applications than would otherwise be available.

The following sections present an overview of a GPS/IMU integrated navigation system design. A detailed evaluation of the navigation performance as a function of Kalman filter state configuration is presented in conjunction with a new approach for the design and tuning of the process noise model.

SYSTEM OVERVIEW

A functional representation of the system under consideration is shown in Figure 1, with the navigation and Kalman filter processing expanded in Figure 2. The GPS receiver is a multi-channel continuous tracking set which provides simultaneous measurements to four satellites; however, the ideas presented apply equally well to slow sequencing and fast multiplexing designs. The GPS receiver performs

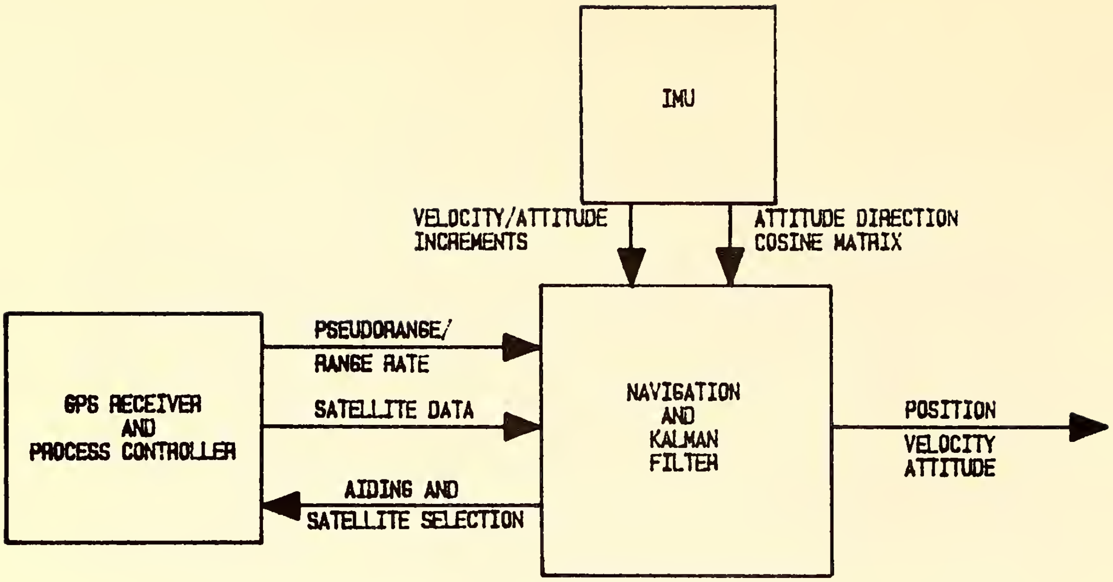
IMU
VELOCITY/ATTITUDE INCREMENTS
ATTITUDE DIRECTION COSINE MATRIX
GPS RECEIVER AND PROCESS CONTROLLER
PSEUDORANGE/ RANGE RATE
SATELLITE DATA
AIDING AND SATELLITE SELECTION
NAVIGATION AND KALMAN FILTER
POSITION
VELOCITY
ATTITUDE

FIGURE 1. GPS/IMU INTEGRATED SYSTEM

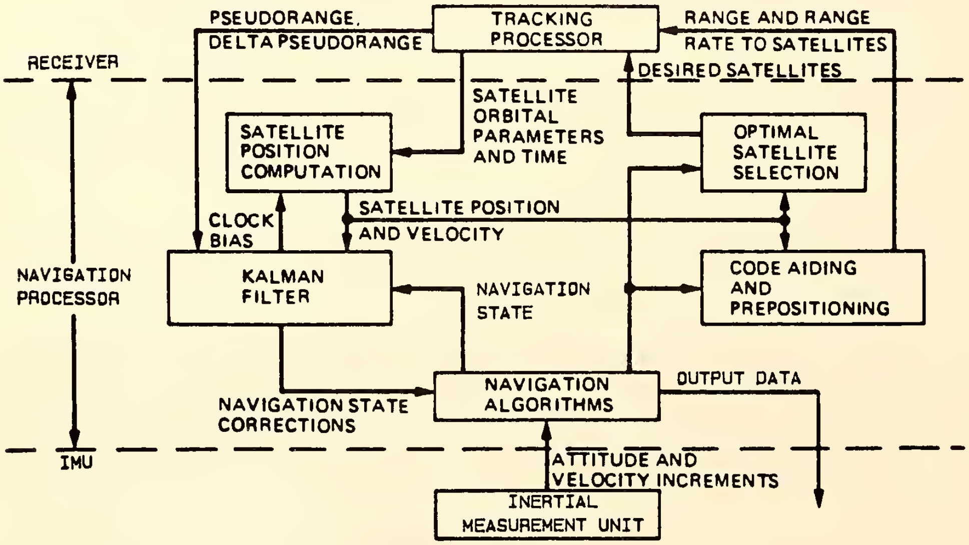
PSEUDORANGE, DELTA PSEUDORANGE
TRACKING PROCESSOR
RANGE AND RANGE RATE TO SATELLITES
RECEIVER
DESIRED SATELLITES
SATELLITE ORBITAL PARAMETERS AND TIME
SATELLITE POSITION COMPUTATION
OPTIMAL SATELLITE SELECTION
SATELLITE POSITION AND VELOCITY
CLOCK BIAS
NAVIGATION PROCESSOR
KALMAN FILTER
NAVIGATION STATE
CODE AIDING AND PREPOSITIONING
OUTPUT DATA
NAVIGATION STATE CORRECTIONS
NAVIGATION ALGORITHMS
IMU
ATTITUDE AND VELOCITY INCREMENTS
INERTIAL MEASUREMENT UNIT

FIGURE 2. NAVIGATION AND KALMAN FILTER PROCESSING

both code (or envelope) tracking and carrier tracking on the received satellite signals. The carrier tracking loop (3rd order), with a bandwidth in excess of 15 Hz, is designed to maintain lock during high vehicle dynamics, and provides aiding to the lower order (first or second), narrower bandwidth (.01 Hz to 1 Hz) code loop. If the signal to noise (SNR) ratio drops below a minimum level, the carrier loop can no longer maintain lock, and the code loop must, due to its narrow bandwidth, receive aiding from another source. The IMU provides this support and extends the GPS operational capability in low SNR by 15 dB.

The IMU is a strapdown unit which provides outputs of integrated specific force and angular rate (ΔV and $\Delta\theta$) represented in the vehicle body frame. The velocity data (ΔV) is transformed at a high rate (100 Hz) into an inertially stabilized reference frame, where it is accumulated for use at the slower data rate (20 Hz) of the inertial navigation processing algorithms. This involves the use of two coordinate transformations, one (C_B^I) from the vehicle body frame to the inertially stabilized reference frame, and the second (C_I^N) from the inertially stabilized reference frame to the navigation frame. C_B^I is generated from the $\Delta\theta$ s in a special purpose processor associated with the IMU, and C is established and maintained within the navigation and Kalman filter processing. The combination of these two transformations is used to express the measured vehicle velocity increments in the navigation frame. An error results in this operation when the I in C_B^I and the I in C_I^N are not identical. This is equivalent to platform tilt errors in a gimballed mechanization, and the error angles between the two frames represent three of the Kalman filter states which must be included in an integrated design.

KALMAN FILTER PROCESS NOISE DESIGN

The primary purpose of the process noise matrix in the Kalman filter is to account for non-linear effects and error parameters not modeled as states. This represents the single most important aspect of the Kalman filter design and development process. The Kalman filter must be capable of establishing a cause and effect relationship between the measurements provided by the sensors (effect) and the states it is trying to estimate (cause). Modeling approximations tend to interfere with this process and can result in the filter making improper error allocations. One purpose of the process noise matrix is to prevent this from occurring. It is better that the filter is unable to establish the cause of a given effect rather than make an incorrect association.

The process noise model for the GPS/IMU integrated design is partitioned into three components as shown in Figure 3. Q_0 represents the dynamics-independent IMU and clock errors (e.g., bias, correlated and white accelerometer and gyro errors, and correlated and white clock noise). Q_1 represents an apriori model for the dynamics dependent IMU and clock errors assuming a steady state low level of vehicle maneuvering. Q_2 is the aposteriori model for dynamics dependent IMU and clock errors (e.g., scale factors, misalignments, g sensitivity). The elements of Q_2 are a function of the actual dynamic outputs of the IMU in conjunction with the statistical representation of the IMU error parameters. Q_1 is unaffected by the actual vehicle motion but retains the basic structure of Q with a nominal assumed level of dynamics. This accounts for any mismodeling effects which are unaccounted for, and uses the results of the chi-squared measurement residual testing to scale the level of application.

The effects modeled by the process noise are in theory supposed to be random, with short time constants relative to the filter time update interval. This assumption is violated in all designs involving inertial systems, since most of the error sources are bias like. In order to mitigate the effects of this assumption, the manufacturer's values for the IMU error sources are not used directly in the process noise design, only the basic model structure is maintained. The error coefficients, used to represent the IMU, are adjusted via simulation to provide optimal performance. This results in error parameter values, within the process noise model, which are much larger than the actual value of the IMU error sources.

The overall design objective is to provide just enough flexibility in the parameter adjustment process to satisfy the design goals without increasing the complexity to the extent that the final tuning process becomes unmanageable. Most of the parameter adjustment is accomplished using detailed computer simulations and laboratory testing; leaving only a few scaling and threshold values for the final tuning operation which is performed during field tests.

KALMAN FILTER STATE SELECTION

One of the major Kalman filter design decisions is the selection of the error states. Most systems contain such a large quantity of error parameters that it would be prohibitive, in terms of computational requirements, to model them all as states. This is especially true for inertial units, and a trade-off study between system performance and computational capability is required. The final decision results in a system which satisfies the performance requirements in the most economical fashion possible. This requires the designer to develop a design for each of the proposed configurations and to individually optimize the estimation procedure to extract the best possible performance from each.

In order to accomplish this process at CAST, a detailed computer simulation (GINS) was developed (Figure 4) to study the performance of the various designs being considered. The simulator includes a variety of aided and unaided Kalman filter configurations which can be selected by input along with the associated tuning parameters.

The GPS measurement model includes all of the standard error sources associated with the space, control, and user segments; however, for the purpose of our study only the following effects are included:

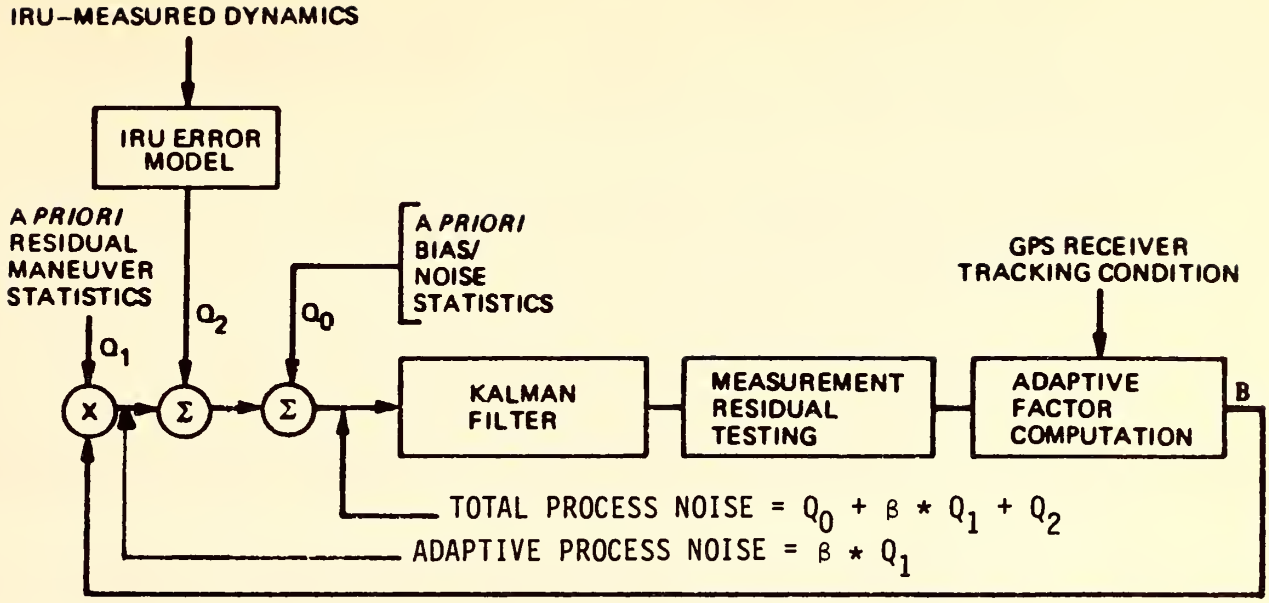
IRU–MEASURED DYNAMICS
IRU ERROR MODEL
A PRIORI RESIDUAL MANEUVER STATISTICS
Q_1
Q_2
Q_0
A PRIORI BIAS/ NOISE STATISTICS
GPS RECEIVER TRACKING CONDITION
X
Σ
Σ
KALMAN FILTER
MEASUREMENT RESIDUAL TESTING
ADAPTIVE FACTOR COMPUTATION
B
TOTAL PROCESS NOISE = $Q_0 + \beta * Q_1 + Q_2$
ADAPTIVE PROCESS NOISE = $\beta * Q_1$

FIGURE 3. PROCESS NOISE MODEL FOR AIDED HDIS

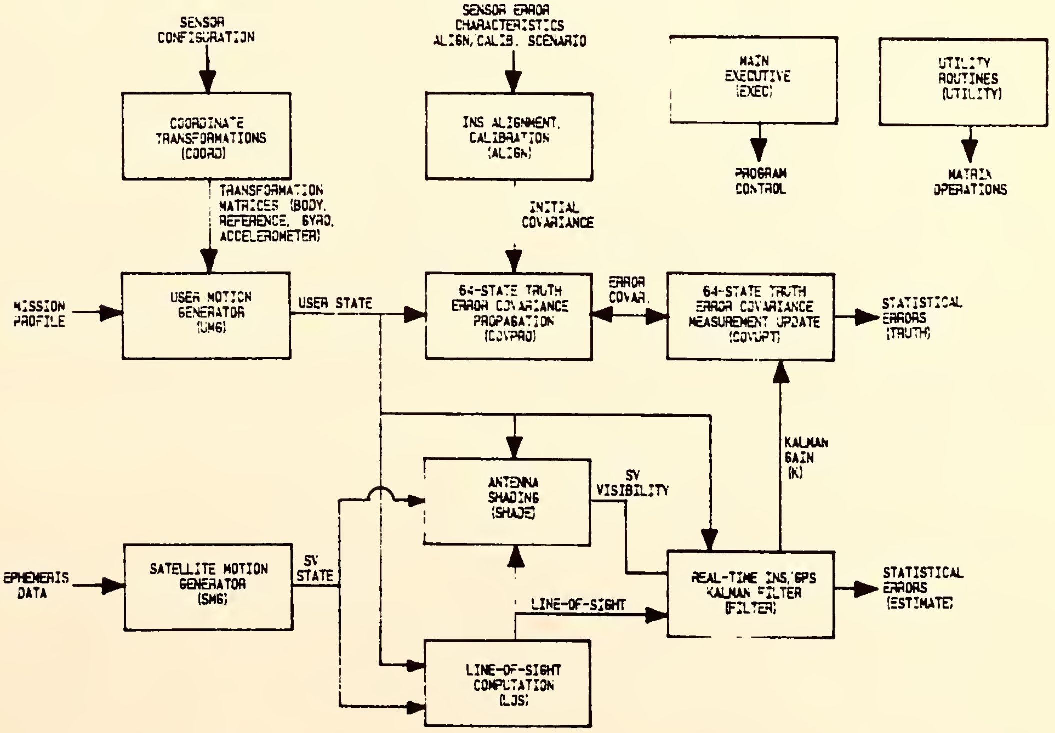
SENSOR CONFIGURATION
COORDINATE TRANSFORMATIONS (COORD)
TRANSFORMATION MATRICES (BODY, REFERENCE, GYRO, ACCELEROMETER)
SENSOR ERROR CHARACTERISTICS ALIGN, CALIB. SCENARIO
INS ALIGNMENT, CALIBRATION (ALIGN)
INITIAL COVARIANCE
MAIN EXECUTIVE (EXEC)
PROGRAM CONTROL
UTILITY ROUTINES (UTILITY)
MATRIX OPERATIONS
MISSION PROFILE
USER MOTION GENERATOR (UMG)
USER STATE
64-STATE TRUTH ERROR COVARIANCE PROPAGATION (COVPRO)
ERROR COVAR.
64-STATE TRUTH ERROR COVARIANCE MEASUREMENT UPDATE (COVUPT)
STATISTICAL ERRORS (TRUTH)
KALMAN GAIN (K)
ANTENNA SHADING (SHADE)
SV VISIBILITY
EPHEMERIS DATA
SATELLITE MOTION GENERATOR (SMG)
SV STATE
LINE-OF-SIGHT
REAL-TIME INS/GPS KALMAN FILTER (FILTER)
STATISTICAL ERRORS (ESTIMATE)
LINE-OF-SIGHT COMPUTATION (LOS)

FIGURE 4. GPS/INS INTEGRATED SYSTEM SIMULATOR (GINS)

Receiver Clock
Allan Variance Model
white noise 2.0x10-21 } Power Spectral
flicker noise 7.2x10-21 | Density Coefficients
random walk 1.5x10-25 }
G-sensitivity 1x10-9 per G

Receiver Measurement Noise
(Including multipath & lever arm effects)
Pseudorange 1.5 m
Delta-pseudorange 10 cm

Atmospheric Effects
Residual Tropospheric Error 0.1 m (at zenith)

The remaining bias-like errors have been omitted, since they affect all configurations identically and can be removed through differential operation.

The IMU model includes the error parameters shown in Table 1, and represents all of the conventional error sources provided by inertial manufacturers to specify their instruments.

The GPS/IMU integrated design requires, as a minimum, eleven Kalman filter states including; position (3), velocity (3), clock (2), and error angles (3). This represents a baseline and any alternate selection will be an augmentation to this basic configuration. Based upon the IMU error parameters shown in Table 1, and a sensitivity analysis conducted using GINS, the navigation performance improvement as a function of state augmentation was studied for a variety of scenarios. The greatest performance payoff was achieved through the inclusion of three gyro bias states (14 states), followed by a 17 state design including the addition of three accelerometer biases.

If the IMU were gimballed, accelerometer bias states would not be considered since their effect is cancelled by platform tilt. This would also be true for a strapdown system, if the vehicle maintained a fixed orientation (as the platform does for a gimballed system), however, a 180 degree turn results in an error effect as if the accelerometer bias had undergone a step change of twice its value. For our system (1 mg accelerometer bias) this would appear as a 2 milliradian change in the platform tilt each time the vehicle makes a 180 degree turn.

Each of the three Kalman filter designs was "tuned" to provide optimal performance; and the resulting position and velocity errors are shown in Figure 5. The flight profile is shown in Figure 6, where only one satellite was available during the turns. The performance improvement available through state augmentation is quite dramatic under these circumstances, primarily due to the loss of GPS updates during the turns. If no GPS signal loss is assumed, the results are much more comparable among the three designs. The flight profile shown in Figure 7 was exercised assuming four satellites were tracked continuously and the RMS error over the flight, for the three configurations, is shown in Table 2. Peak position/velocity errors are reduced by approximately 10% for each addition of three states.

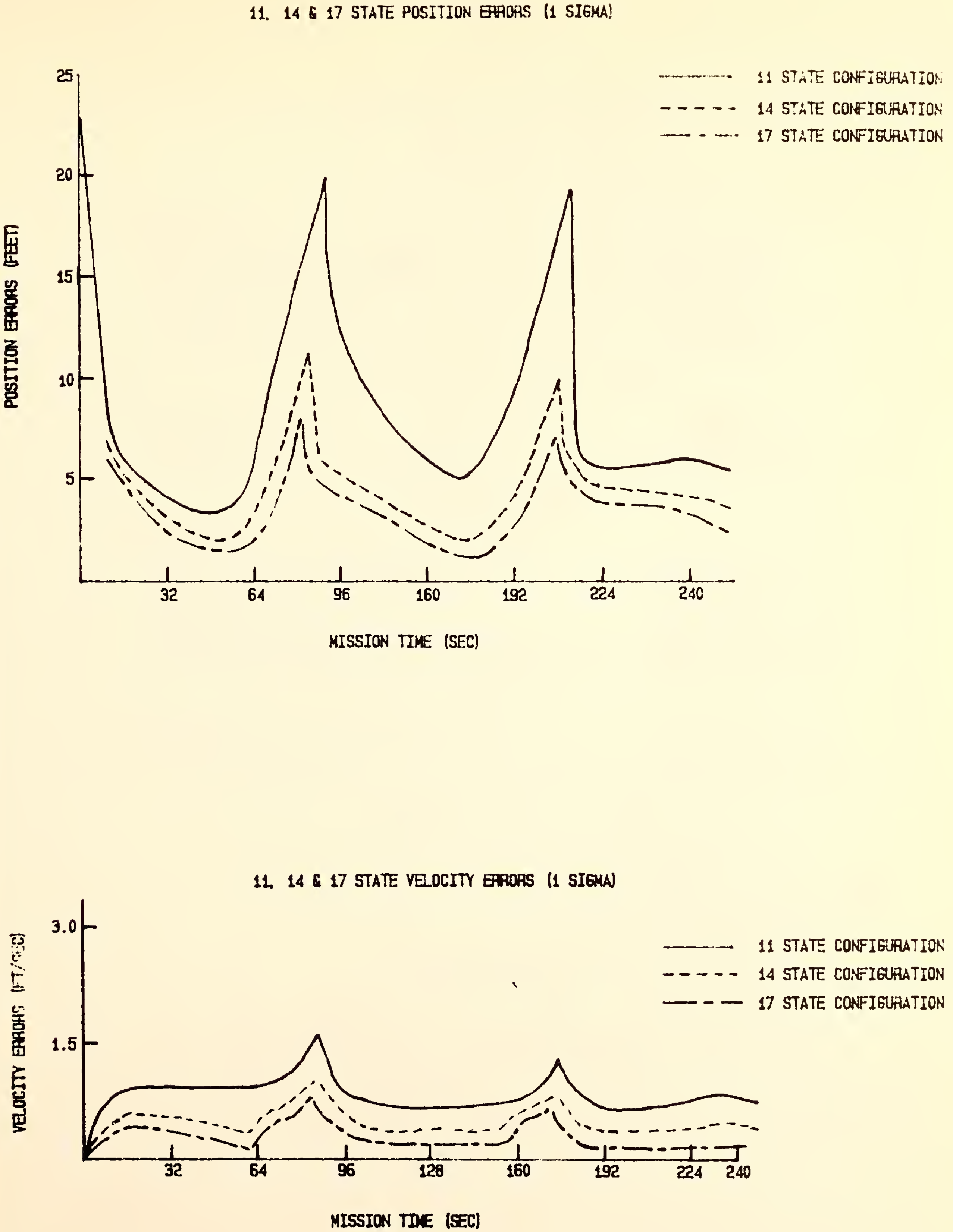

FIGURE 5. STATE ERROR TRADE-OFF

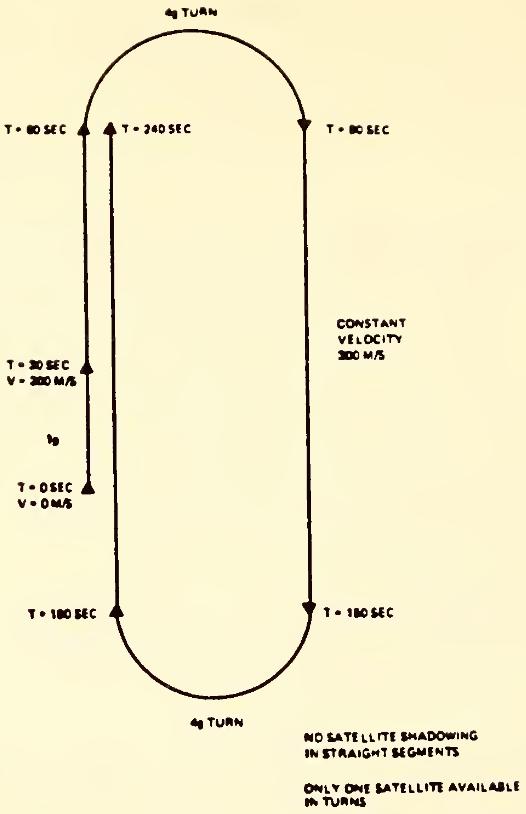

FIGURE 6. FLIGHT PROFILE WITH ANTENNA SHADOWING

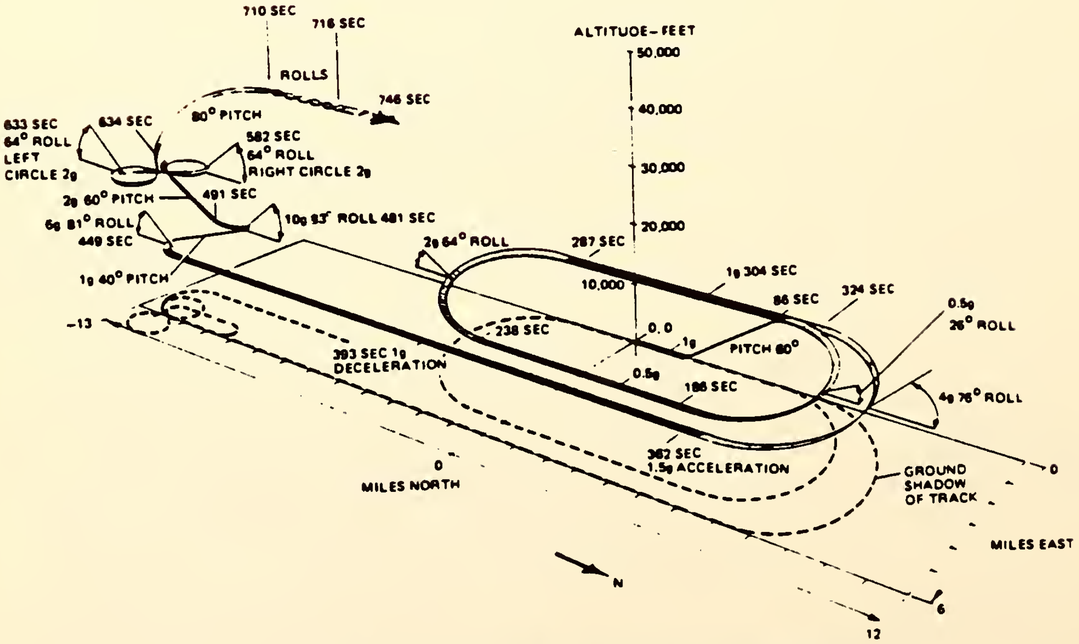

FIGURE 7. HIGH DYNAMICS FLIGHT PROFILE WITHOUT ANTENNA SHADOWING

TABLE 1

IMU ERROR SOURCES

SYSTEM LEVEL SENSOR ERRORS (ONE SIGMA)	
GYRO	
G-INSENSITIVE	
BIAS STABILITY	24.000 deg/hr
SCALE FACTOR STABILITY	1000.000 ppm
SCALE FACTOR ASYMMETRY	200.000 ppm
NON-ORTHOGONALITY	60.000 arc sec
WHITE NOISE	0.250 deg/hr/sqr (hz)
CORRELATED NOISE	0.050 deg/hr
(correlation time)	2.000 min
G-SENSITIVE	
MASS UNBALANCE	3.000 deg/hr/g
QUADRATURE	3.000 deg/hr/g
ANISOELASTIC	1.000 deg/hr/g••2
ACCELEROMETER	
G-INSENSITIVE	
BIAS STABILITY	1000.000 micro g
SCALE FACTOR STABILITY	500.000 ppm
SCALE FACTOR ASYMMETRY	300.000 ppm
NON-ORTHOGONALITY	60.000 arc sec
WHITE NOISE	20.000 micro g/sqr (hz)
CORRELATED NOISE	10.000 micro g
(correlated time)	5.000 min
G-SENSITIVE	
DIRECT-AXIS NON-LINEARITY	50.000 micro g/g••2
CROSS-AXIS COUPLING	50.000 micro g/g••2

TABLE 2

FILTER STATE PERFORMANCE TRADE-OFF

ERROR (1σ) / # OF STATES	POSITION (FT)			VELOCITY (F/S)		
	NORTH	EAST	VERTICAL	NORTH	EAST	VERTICAL
ELEVEN	0.86	1.61	4.03	0.24	0.38	0.75
FOURTEEN	0.82	1.51	3.90	0.21	0.33	0.72
SEVENTEEN	0.74	1.29	2.44	0.17	0.26	0.39

There is an increase of 50% to 75% in the computational requirements for each three-state expansion; and typically the Kalman filter represents 30% to 50% of the total throughput required in an integrated GPS/IMU system. This additional complexity must be traded off against performance for the application being considered.

If GPS outages and antenna shadowing are unlikely to occur, the eleven state design is probably the preferred choice. For applications where navigation performance is critical during periods of antenna shadowing or jamming, then the fourteen or seventeen state will be more appropriate. If additional performance improvements are necessary, scale factors and instrument axis alignment states are the next in order of importance. This will be the subject of future studies; however, the computational requirements rapidly become prohibitive.

CONCLUSIONS

The fundamental design of an integrated GPS/IMU navigation system has been discussed. The Kalman filter state selection is seen to be closely related to the need for periods of automonous inertial operation. For applications where GPS is always available, an eleven state filter is usually adequate.

The basic philosophy for Kalman filter process noise design is one of reduced complexity and parameter adjustment via simulation. The number of tuning parameters to be adjusted during flight tests is kept to a minimum. The process noise matrix is divided into three components, one of which is adjusted real time using IMU measurements and error models to represent the effects of vehicle dynamics. The remaining two components are constants representing nominal levels of vehicle dynamics and maneuver independent error sources. This design provides a basic structure which takes advantage of detailed IMU error modeling and chi-squared measurement residual testing, and can be successfully applied to any GPS/IMU integrated navigation system.

RADIO INTERFEROMETRY IN A MOVING-BASE APPLICATION

R.C. Merenyi, S.J. Brzezowski and W.G. Heller
The Analytic Sciences Corporation
One Jacob Way
Reading, MA 01867

ABSTRACT. An examination of radio interferometric error sources associated with a moving-receiver scenario has been undertaken. Independent research, coupled with published data, established rms values for receiver noise, clock jitter, timing drift, multi-path errors, and ionospheric and tropospheric refractivity effects. Statistical error models for the significant effects are being included in a simulation of a moving-base radio interferometer system to assess the measurement accuracy of receiver kinematics. This system is assumed to consist of two dual-frequency receivers which are equipped with atomic clocks. Doppler shift detection techniques and a cross-correlation algorithm can be applied in a post-mission reduction of recorded GPS signal phase to determine baseline distance and vehicle kinematics. Preliminary analysis results indicate that moving-base radio interferometry will provide navigation accuracies on par with or even better than can be obtained with current inertial navigation technology.

BACKGROUND

Radio interferometric techniques have been successfully applied to measure baseline distances between stationary receivers. Recent experiments have demonstrated that centimeter-level rms accuracies can be attained (Bock, et al. 1984; Goad, et al. 1984; Greenspan, et al. 1984). A moving-base application of radio interferometry is presently being studied. This application consists of one receiver located at a fixed ground site and a second receiver aboard an aircraft (see Fig. 1). The receivers are equipped with atomic clocks which are periodically synchronized to each other. In addition, both receivers operate in a passive mode; i.e., there is no decoding of the coarse acquisition (C/A) GPS signal. Analyses suggest that post-mission processing of the recorded phase data be performed using Doppler shift detection and cross-correlation techniques. The objectives of this paper are to 1) identify the error sources unique to moving-base radio interferometry applications, 2) present statistical models appropriate for these error sources and 3) provide preliminary estimates of rms errors associated with measuring position and velocity quantities with this system.

It is envisioned that radio interferometric measuring systems can be used in survey applications to determine separations between a base station and host aircraft. The key advantage of this application is that it would enable the gathering of exceedingly well-positioned geophysical data over wide areas in a timely, efficient manner. In addition, this system can serve to supplement post-

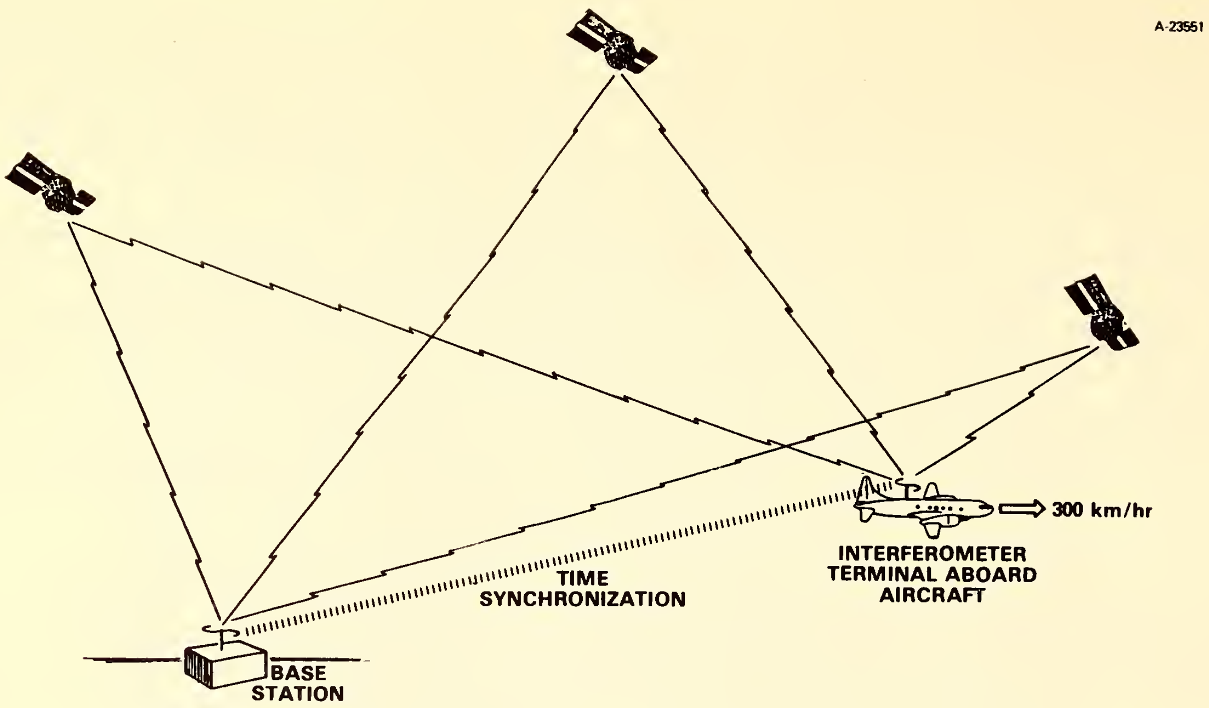

Figure 1 Moving-Receiver Radio Interferometry Scenario

mission reduction of host aircraft inertial navigation system (INS) data by providing a new external velocity reference. Furthermore, by subtracting host vehicle INS and radio interferometric-derived accelerations, one can obtain a new kind of measurement of gravity. This is theoretically appealing since the accelerometers in the INS actually measure only the difference between vehicle and gravitational accelerations, whereas using radio interferometry, vehicle acceleration can be measured directly.

MEASUREMENT TECHNIQUE

The method of Doppler shift detection can be employed in conjunction with the statistical modeling of the cross-correlated phase shift results (the C4 method described in Greenspan, et al. 1984) to process the time-tagged recorded signal. This technique has proven to be an effective means of measuring fixed-baseline distances (Bock, et al. 1984; Greenspan, et al. 1984) and has the advantage of eliminating common-mode atmospheric errors. Furthermore, for receivers equipped with atomic clocks, analysis results indicate that a three-satellite configuration is sufficient for reconstructing aircraft kinematics.

However, the above data reduction approach has theoretical limitations. The post-mission processing is computer-intensive. Published results (Greenspan, et al. 1984) indicate that an hour of CPU time was required on a mini-computer to process 30 minutes of collected data. Accurate statistical modeling of atmospheric properties is also required when measuring baseline distances greater than a kilometer. In addition, the aircraft-to-satellite pointing angle must be greater than 10 degrees to eliminate significant ground/multi-path effects and some refractivity-induced error. This implies that the satellite mask angle must also be greater than 10 degrees which results in an average geometrical dilution of precision (GDOP) of about 7.5 for the planned 18-satellite constellation. However, a GDOP of about 4.5 is possible if a user can selectively choose to operate the system only during predicted times of "good geometry."

The strategy presented here for measuring baseline distances was described in Greenspan, et al. 1984 and applied in this study to evaluate the accuracy potential for measurement of host aircraft kinematics. This strategy consists of converting the 1.5 GHz frequency C/A code to a zero to two megahertz "video" frequency signal. This signal is sampled once every 250 nanoseconds and clipped to preserve only the signal sign. The single bit of time-tagged data is stored on magnetic tape. The statistical modeling of the cross-correlated data is described in Greenspan, et al. 1984 and will serve to yield baseline distance measurements. Similarly, measurement of aircraft kinematics can be obtained using Doppler shift analysis and statistically modeling the timing and atmospheric errors.

DESCRIPTION OF ERROR SOURCES

All of the error sources inherent to fixed-site applications are also present in moving-base radio interferometry operations. These include receiver noise and clock jitter which have been analyzed previously (Bock, et al. 1984; Goad, et al. 1984). In addition, there are mechanical and environmental error sources which are unique to the moving-receiver application. Timing drift, or loss of synchronization between clocks, can be appropriately modeled using a random ramp structure. The refractive properties of the troposphere (which are functions of humidity, air pressure and temperature throughout the lower 40 kilometers of the atmosphere) can vary significantly over distances a kilometer apart. Presently, a Markov process is being used to model tropospheric refraction; however, this does not account for possible pressure gradients in the local region, which is the subject of a current analysis effort. Ionospheric signal path differences, expected to be a significant error source only for situations involving very long baseline measurements (greater than 1000 km), can be computed using dual-frequency receivers. For these long baseline distances, satellite ephemeris error will need to be accounted for. Finally, multi-path propagation effects produced by the aircraft dynamics as the signals are temporaily reflected from the aircraft wing or fuselage can be treated as a random process and can be adequately modeled as white noise.

RESULTS

The models described above are being used to support covariance analysis of moving-base radio interferometry. In this analysis, a coplanar base station, host aircraft trajectory and satellite flight path are simulated. Baseline distances on the order of one kilometer and static atmospheric conditions are considered. Furthermore, the aircraft moves in a straight line at a constant velocity of 300 km/hr in the satellite along-track direction. Optimal Kalman smoothing (Gelb, 1974) is used in the covariance analysis to estimate the uncertainties associated with position, velocity and acceleration errors.

Preliminary root-sum-square (rss) analysis results based on Doppler shift and cross-correlation techniques are encouraging. Over a usable range of aircraft-to-satellite pointing angles for a single-satellite scenario, the rms baseline distance measurement accuracy varies between 20 and 60 cm. As illustrated in Fig. 2, the accuracy potential degrades quite rapidly for pointing angles greater than about 50 degrees since the aircraft trajectory becomes more parallel to the GPS signal wavefront. Since velocity measurement rms accuracies are determined in the same manner, a similar result is evident. As an example, a 20 degree pointing angle yields an rms velocity measurement accuracy of 40 cm/sec, which is approximately 0.5 percent of the aircraft velocity. These preliminary results indicate

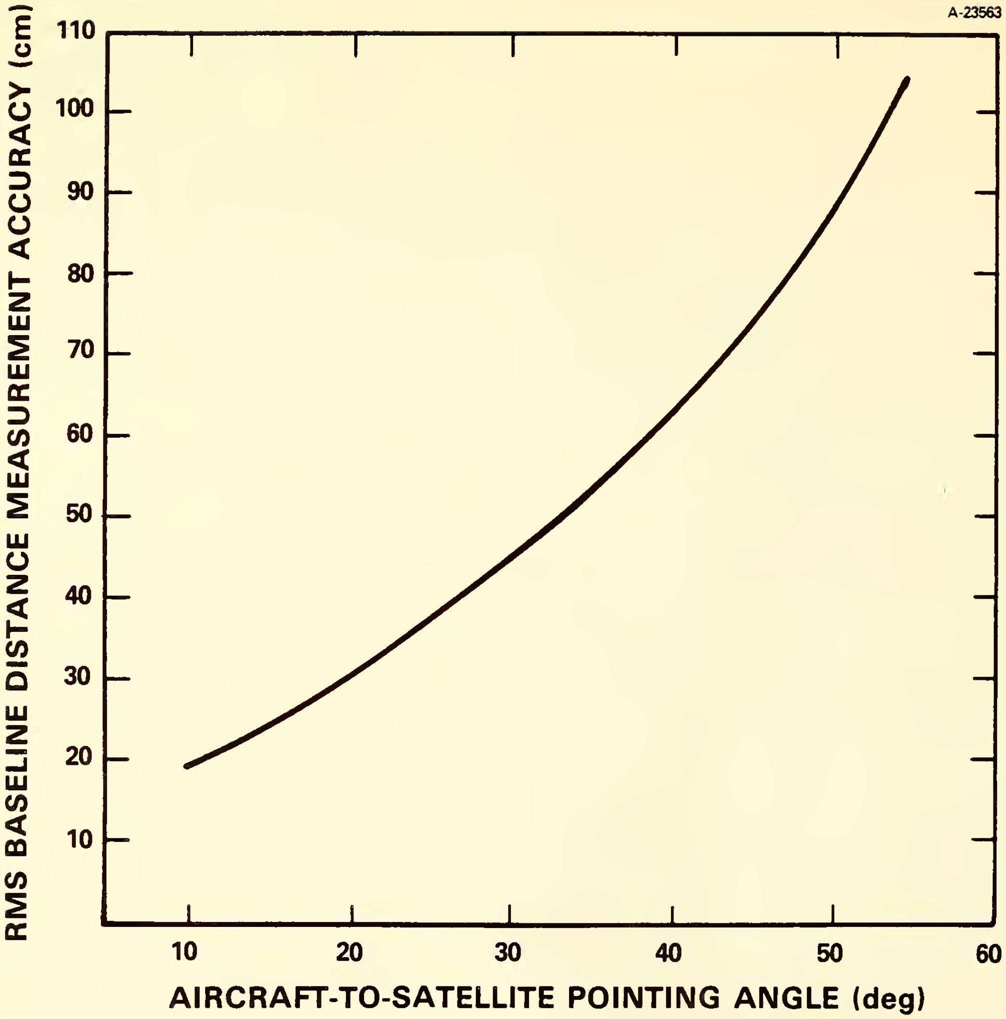

Figure 2 Sensitivity of Distance Measurement Accuracy to Aircraft-to-Satellite Pointing Angle

that moving-base radio interferometry will provide navigation accuracies as good as or even better than current inertial navigation technology can yield and thus, its benefits to navigation and survey will be significant.

SUMMARY

In summary, an examination of error sources associated with moving-base radio interferometry has been conducted and appropriate statistical models have been formulated. It has been determined that a three-satellite configuration is adequate to provide reconstruction of aircraft velocity, provided that the receivers are equipped with atomic clocks. In order to minimize ground/multi-path effects and some refractivity-induced errors, a mask angle of at least 10 degrees is appropriate for the planned 18-satellite constellation. This corresponds to a GDOP of about 7.5.

As reported in Bock, et al. 1984, fixed-base phase data averaged over several days and analyzed using the cross-correlation technique have demonstrated about a 2 ppm position measurement accuracy for very long baseline distances (i.e., thousands of kilometers). Preliminary results from a first-look moving-base scenario indicate distance measurement rms accuracies on the order of tens of centimeters and velocity measurement rms accuracies on the order of tens of centimeters/second or better are possible over baseline distances less than 10 km. Furthermore, for the single-satellite scenario, the analysis indicates moderate sensitivity of the baseline distance and velocity measurement accuracies to the aircraft-to-satellite pointing angle. Analyses involving multiple-satellite configurations are expected to reduce this sensitivity.

Ongoing work in this area involves determining the acceleration measurement accuracy potential and then estimating the error associated with measuring gravity based on a comparison of INS and radio interferometry outputs. In addition, the errors associated with non-uniform tropospheric signal paths and satellite positional uncertainties are being incorporated into the analysis.

REFERENCES

1. Bock, Y., Abbot, R.I., Counselman, C.C., Gourevitch, S.A., King, R.W., and Paradis, A.R., 1984: "Geodetic Accuracy of the Macrometer Model V-1000, Bulletin Geodesique, Vol. 58, pp. 211-221.

2. Gelb, A., Ed., 1974: Applied Optimal Estimation, MIT Press.

3. Goad, C. and Remondi, B.W., 1984: Initial Relative Positioning Results Using the Global Positioning System, Bulletin Geodeseque, Vol. 58, pp. 193-210.

4. Greenspan, R.L., Ng, A., Przyjemski, J., Veale, J., Counselman, C.C., and Gourevitch, S.A., 1984: "Accurate Baseline Determination By Radio Interferometry on NAVSTAR GPS Satellite Transmissions," Report No. AFGL-TR-84-0156.

ACKNOWLEDGMENT

The work reported in this paper was performed under the sponsorship of the U.S. Air Force Geophysics Laboratory and Defense Mapping Agency under Contract No. F19628-83-C-0146.

PERFORMING CENTIMETER ACCURACY RELATIVE SURVEYS IN SECONDS USING GPS CARRIER PHASE

Benjamin W. Remondi
National Geodetic Survey
Charting and Geodetic Services
National Ocean Service, NOAA
Rockville, Maryland 20852

ABSTRACT. Since 1980 the geodetic community has witnessed the development of GPS receiver systems which measure the phase of the L-band carriers at the 1 mm level of accuracy. Typically, receivers are placed at each end of a geodetic base line for 1 to 4 hours for the simultaneous measurement of carrier phase from many GPS satellites. These base lines vary in length from a few meters to tens or even hundreds of kilometers. Although centimeter-level relative geodesy (using GPS) has been proven, and is now routine, one cannot easily justify spending 1 hour, or more, measuring a short base line (e.g., 50 m). This paper describes an approach which permits subcentimeter-accuracy surveys to be performed in seconds. More precisely, local surveys can be performed in the time it takes to physically move the receiver from point to point provided carrier phase tracking is maintained during the transition.

INTRODUCTION

At this point in the development of GPS technology, geodetic relative positioning is being performed routinely at the 1 part per million (ppm) level of accuracy. There is considerable confidence that 0.1 ppm will soon be achieved. In fact, there is widespread belief that 0.01 ppm will ultimately be achieved using GPS in static relative positioning mode.

Although the capability of measuring a 100-km base line in 2 to 5 hours, to the subdecimeter level, using portable equipment, is a remarkable technological achievement, there are certain applications where this static relative positioning technology is not economical. Spending 2 to 5 hours measuring a 200-km base line, or even a 20-km base line, is sensible and economical; spending hours measuring a 20-m or 300-m base line using GPS in static relative mode is not necessarily the logical approach. If only a few short base lines are required this might be acceptable. On the other hand, if one needs to survey hundreds or thousands of points, in a local area of a few kilometers-squared, at the subcentimeter level of accuracy, it would be prohibitive to spend hours measuring each base line. It might be more realistic to employ advanced terrestrial systems. An economical method for performing hundreds of subcentimeter-accuracy local surveys, one which uses GPS receivers, is the subject of this paper.

Two antennas would, initially, be situated at the ends of a known base line. (In fact, for certain applications, this starting vector might be portable.) Once carrier phase tracking begins, one of the two antennas is moved to each of the marks to be surveyed. Carrier phase tracking must be maintained during the transitions. When a survey mark is reached, and after the antenna is plumbed over the mark, GPS phase measurements are recorded. The total occupation time might vary from seconds to minutes depending on the sophistication of the transport vehicle and the accuracy desired. For a well rigged survey vehicle, this process could be completed in seconds. Real-time applications would be straightforward since the required data transfer rate would often be low (e.g., 300 baud). In fact one could "navigate" to an unlimited number of preassigned points (to the subcentimeter level) using the technique described herein.

MODELING THE OBSERVATIONS

In this section the basic modeling equations which describe the raw phase measurements will be briefly developed. In the next section the resulting equations will be adapted to the applications which form the subject of this paper. These equations have been more fully explained in another paper of these proceedings by the same author (Remondi 1985).

Suppose a GPS receiver is scheduled to make phase measurements of GPS satellites at time t_i. Let us assume that the phases of all GPS satellites are measured simultaneously. Because receiver oscillators are imperfect, the true measurement time will be $t_i+\delta t_i$. The carrier phase measurement for the j-th GPS satellite can be described as:

$$m^j(i) = \phi_s^j(t_T^j(i)) - \phi_R(t_i+\delta t_i) + N^j(t_1) + \varepsilon^j(i) \qquad (1)$$

where $m^j(i)$ is the [relative] carrier phase measurement whose time tag is the scheduled time, t_i; $\phi_s^j(t)$ is the instantaneous phase of the carrier signal transmitted by satellite j. $t_T^j(i)$ is the true transmission time of the satellite j phase [event] which was later received at the true receipt time $t_i+\delta t_i$; δt_i is the difference between receiver time and true time at receiver time t_i;

$\phi_R(t)$ is the instantaneous phase of the carrier signal generated by the receiver oscillator; $N^j(t_1)$, hereafter N^j, is an integer ambiguity; $\varepsilon^j(i)$ represents measurement noise.

This carrier phase model appears a bit more complex when many receivers are involved. For the M-th receiver and satellite j the i-th phase measurement can be described as:

$$m_M^j(i) = \phi_s^j(t_{T_M}^j(i)) - \phi_R^M(t_i+\delta_M t_i) + N_M^j + \varepsilon_M^j(i) \tag{2}$$

Notice that since $t_i+\delta_M t_i$ is assumed identical for all j, measured by receiver M, the true transmission time

$$t_{T_M}^j(i) = t_i + \delta_M t_i - \tau_M^j(t_i+\delta_M t_i) \tag{3}$$

is satellite dependent. $\tau_M^j(t_R)$ is the transit time (in a vacuum) of the satellite j carrier phase event received at $t_R = t_i+\delta_M t_i$ (true time). If the geometric instantaneous slant range is given by $\rho(t)$ where

$$\rho^2(t) = (x_R-x_s(t))^2 + (y_R-y_s(t))^2 + (z_R-z_s(t))^2 \tag{4}$$

then

$$\tau(t_R) = \frac{1}{c}\rho[t_R - \frac{1}{c}\rho(t_R - \frac{1}{c}\rho(\cdots))] \tag{5}$$

where ρ, here, is a function of all that follows it. Substituting eq. 3 into eq. 2 and expanding about $t=t_i$ yields:

$$m_M^j(i) = \phi_s^j(t_i) + \dot{\phi}_s^j(t_i)\cdot(\delta_M t_i-\tau_M^j(i)) - \phi_R^M(t_i+\delta_M t_i) + N_M^j + \varepsilon_M^j(i) \tag{6}$$

where $\dot{\phi}_s^j \equiv f_s^j$, the carrier frequency, and $\tau_M^j(i)$ symbolizes $\tau_M^j(t_i+\delta_M t_i)$. When two such phase measurements, taken [nearly] simultaneously by two receivers, are differenced, the resulting observable is a "single difference" phase observation of satellite j defined by $S(j,i) \equiv m_2^j(i)-m_1^j(i)$. A "delta single difference" observation of satellite j is defined as $DS(j,i) \equiv S(j,i+1)-S(j,i)$. A "double difference" observation, based on satellites j and k, is defined as $DD(j,k,i) \equiv S(k,i)-S(j,i)$. Finally, a "triple difference" observation can be defined either by $T(j,k,i) \equiv DS(k,i)-DS(j,i)$ or by $T(j,k,i) \equiv DD(j,k,i+1)-DD(j,k,i)$. In either case

$$T(j,k,i) = S(k,i+1) - S(k,i) - S(j,i+1) + S(j,i). \tag{7}$$

If one substitutes the observation model for the single difference components of this equation and neglects the terms $(f_s^k-f_s^j)\cdot(\delta_2 t-\delta_1 t)$, one arrives at the basic triple difference model of interest:

$$\begin{aligned} T(j,k,i) = {} & f_s^k(i+1)\cdot[\tau_1^k(i+1)-\tau_2^k(i+1)] - f_s^k(i)\cdot[\tau_1^k(i)-\tau_2^k(i)] \\ & -f_s^j(i+1)\cdot[\tau_1^j(i+1)-\tau_2^j(i+1)] + f_s^j(i)\cdot[\tau_1^j(i)-\tau_2^j(i)] + \varepsilon_T(j,k,i) \end{aligned} \tag{8}$$

where

$$\varepsilon_T(j,k,i) \equiv [\varepsilon_2^k(i+1)-\varepsilon_1^k(i+1)]-[\varepsilon_2^k(i)-\varepsilon_1^k(i)]-[\varepsilon_2^j(i+1)-\varepsilon_1^j(i+1)]+[\varepsilon_2^j(i)-\varepsilon_1^j(i)] .$$

The $(f_s^k-f_s^j)\cdot(\delta_2 t-\delta_1 t)$ terms are negligible since $\delta_2 t-\delta_1 t$ is, typically, a few microseconds and $f_s^k-f_s^j$ is, typically, a few Hertz. Neglecting these two products results, therefore, in an error far smaller than the measurement error. The remaining modeling terms comprise a frequency multiplied by a difference of transit times. For the applications under consideration, here (local surveys within, say, 20 km), these transit time differences are less than 100 μs. The frequencies of the GPS satellite oscillators are maintained to within a few Hertz of the nominal values. Thus, for most applications, use of the nominal frequency values will result in a negligible error contribution. Precise values of these frequencies can be obtained or determined, however, if they are required. On the assumption that the transmitted frequency of a given GPS satellite carrier is constant over the survey period, and neglecting measurement noise, triple difference observations can be accurately modeled as:

$$\begin{aligned} T(j,k,i) = {} & f_s^k\cdot[\tau_1^k(i+1)-\tau_2^k(i+1)-\tau_1^k(i)+\tau_2^k(i)] \\ & -f_s^j\cdot[\tau_1^j(i+1)-\tau_2^j(i+1)-\tau_1^j(i)+\tau_2^j(i)] \end{aligned} \tag{9}$$

USING TRIPLE DIFFERENCES FOR SUBCENTIMETER-LEVEL TRAJECTORY DETERMINATION AND PERFORMING SUBCENTIMETER-LEVEL RELATIVE POSITIONING IN SECONDS

Consider the case where receiver 2 is moving. Suppose that receiver 1 is fixed at a known point and that the receiver 2 location is known at t_i. The objective, here, is to determine the receiver 2 location at t_{i+1} regardless of the path taken by receiver 2 during the interval from t_i to t_{i+1}. First of all, a triple difference observation over the interval t_i to t_{i+1}, for satellites j and k, is equivalent to the satellite k delta single difference minus the satellite j delta single difference over the same interval. This is pointed out because a delta single difference is equivalent to a change in range. For one station (Remondi 1984: 31) the continuous Doppler count can be integrated as follows:

$$\int_{t_i}^{t_{i+1}} f_d^j dt \doteq \frac{1}{c} f_s^j \cdot \left(\rho^j(t_{i+1}) - \rho^j(t_i) \right) + \text{relativistic effects} . \qquad (10)$$

For two nearby stations the relativity term is negligible and

$$\int_{t_i}^{t_{i+1}} (f_{d_2}^j - f_{d_1}^j) dt = \frac{1}{c} f_s^j \cdot \left(\rho_2^j(t_{i+1}) - \rho_2^j(t_i) - \rho_1^j(t_{i+1}) + \rho_1^j(t_i) \right) \qquad (11)$$

The corresponding delta single difference observables have a large clock drift component, however. The triple difference observable, on the other hand, has only a small clock drift component which can (adequately) be modeled linearly. Notice that delta single differences (from t_i to t_{i+1}) are path independent and, consequently, so is the triple difference formed by their difference. We shall assume, herein, that the clock drift between the two receivers is accurately measured so that its estimation is not required. Only $\tau_2^j(i+1)$ and $\tau_2^k(i+1)$ of eq. 9 are unknown since they depend on the location of receiver 2 at t_{i+1}. Moving the known terms to the left hand side (LHS) results in:

$$LHS(j,k) \equiv T(j,k,i) - f_s^k \cdot \left(\tau_1^k(i+1) - \tau_1^k(i) + \tau_2^k(i)\right)$$

$$+ f_s^j \cdot \left(\tau_1^j(i+1) - \tau_1^j(i) + \tau_2^j(i)\right) . \qquad (12)$$

Ignoring measurement noise, the nonlinear model would be:

$$LHS(j,k) = f_s^j \tau_2^j(i+1) - f_s^k \tau_2^k(i+1) . \qquad (13)$$

The corresponding linearization would be:

$$LHS(j,k) \doteq \frac{1}{c} f_s^j \cdot \left[\rho_2^j(t_{i+1}+\delta t_{i+1}) + \dot{\rho}_2^j(t_{i+1}+\delta t_{i+1}) \left(- \frac{1}{c} \rho_2^j(t_{i+1}+\delta t_{i+1}) \right) \right]$$

$$- \frac{1}{c} f_s^k \cdot \left[\rho_2^k(t_{i+1}+\delta t_{i+1}) + \dot{\rho}_2^k(t_{i+1}+\delta t_{i+1}) \left(- \frac{1}{c} \rho_2^k(t_{i+1}+\delta t_{i+1}) \right) \right]$$

where $j=1$ and $k=2,3,4,\cdots$. (14)

At least three triple differences are required to determine all three station 2 coordinates at t_{i+1}. If RHS symbolizes the right hand side of eq. 13, then

$$LHS(j,k) = RHS(j,k,\vec{x}_2(i+1)) \qquad (15)$$

$$LHS(j,k) \doteq RHS(j,k,\tilde{\vec{x}}_2(i+1)) + \frac{\partial RHS(j,k,\tilde{\vec{x}}_2(i+1))}{\partial \vec{x}_2} \Delta\vec{x}_2 \qquad (16)$$

where $\Delta\vec{x}_2 = \vec{x}_2(i+1) - \tilde{\vec{x}}_2(i+1)$, and $\tilde{\vec{x}}_2(i+1)$ is the a priori value of $\vec{x}_2(i+1)$. In the first iteration, one could initialize $\tilde{\vec{x}}_2(i+1)$ to $\vec{x}_2(i)$. Let

$y_k = LHS(j,k) - RHS(j,k,\tilde{\vec{x}}_2(i+1))$, where $j=1$ and $k=2,3,4,\cdots$.

Then,

$$\Delta\vec{x}_2 = \left(A^T R^{-1} A\right)^{-1} A^T R^{-1} \vec{y} \qquad (17)$$

where

$$A = (A_k) = \left[\frac{\partial RHS(k)}{\partial \vec{x}_2} \right], \ \vec{y} = (y_k) \qquad (18)$$

and R^{-1} is the correlated weight matrix between triple differences. The partial derivative computations given by

$$\frac{\partial RHS}{\partial \vec{x}_2} \doteq -\frac{1}{c} f_s^j \cdot \frac{\vec{\rho}_2^{\,j}}{\rho_2^j} + \frac{1}{c} f_s^k \cdot \frac{\vec{\rho}_2^{\,k}}{\rho_2^k} \qquad (19)$$

should suffice. Thus it should be straightforward to determine the new position of receiver 2 (to subcentimeter accuracy) at t_{i+1} provided: (1) lock is maintained on four or more satellites; (2) the geodetic position of station 1 is fixed and known; (3) the position of station 2 at t_i is known relative to station 1; (4) the linear clock drift between receiver 1 and receiver 2 is known to approximately 1 μs/hr; and (5) the satellite positions are approximately known.

It should be pointed out that although this formulation was based on triple differences, it could have been based on double differences, delta single differences, etc. In double difference mode the "integer" biases would be determined based on measurements taken before receiver 2 departed; these biases would be applied at the subsequent positions of receiver 2. In triple difference mode these biases need not be determined and receiver 2 can depart as soon as tracking is established and carrier phases, at one instant, are recorded.

RESULTS - SIMULATED AND REAL

A computer program was written to simulate phase data for a moving antenna. Antenna 1 was situated permanently at mark A. Antenna 2 was initially situated at mark B. The coordinates of mark A and mark B were precisely known. After phase tracking had begun at both receivers, antenna 2 departed from mark B at time t_1 and arrived at mark C at time t_2. Regardless of the travel path used, the resulting simulated phase measurements were the same. These data were used to create five triple difference observations T(j,k,i), j=1, k=2,3,4,5. These triple difference observations were then input to the least-squares program described in the previous section. The result was an exact recovery of mark C.

Satisfied that the least-squares program was functioning correctly, real triple difference data were taken from static relative positioning surveys (over base lines 100 m to 25 km long) and processed. The program was aware that mark A and mark B were fixed on a rotating Earth but did not know what motion antenna 2 underwent from time t_1 (mark B) to time t_2 (mark C). The least-squares program determined that mark C was within 2 to 3 mm of mark B, as expected.

In both the simulated and real data situations described above, a considerable error in the geodetic coordinates of the reference station can be tolerated--naturally this depends on the distance between marks B and C. Also, a small error in the starting vector, from mark A to mark B, can be tolerated depending, again, on the distance between marks B and C. Finally, a rather large receiver clock drift can be ignored. (As noted, a linear clock drift model, based on pre- and post receiver clock comparisons, would satisfy most applications.) It should be clear, however, that one could determine the relative clock drift parameters $\delta_2 t_i - \delta_1 t_i$ precisely, if desired, from four or more delta single differences.

IMPLEMENTATION

Practically speaking, two receivers are required (the second one, however, might be owned, maintained, and continuously operated by a local government.) Approximate geodetic coordinates (e.g., ±10 m) are required for the fixed station (mark A). A [starting] reference base line vector between the fixed station (mark A) and the initialization station (mark B) of the roving antenna is required. The mark A to mark B starting vector need not be as accurately known as the desired survey results from mark B to the unknown survey marks. For optimum results, receiver 2 should return, periodically, to mark B for re-initialization.

Although optional, the receiver 1 oscillator and the receiver 2 oscillator should be synchronized and tuned. If it is inconvenient to physically bring these units together, synchronization and tuning could be accomplished remotely. One could exploit the known starting base line vector for subnanosecond time interval transfer. The roving receiver could either remain at the initialization mark long enough for synchronization and tuning or one could proceed with the survey and return to the initialization mark for another time transfer. In this latter case one would have the required data for a linear model. If code receivers are used, then GPS time to better than 1 μs is available at all times. This would further simplify the timing.

This technique requires continuous carrier phase tracking of four or more GPS satellites during the transition from known survey marks to unknown marks. Although such surveys could theoretically be performed with one receiver and three GPS satellites, that is not the point of this paper. More realistically, four are mandatory and five (or more) are desirable. If only four satellites are tracked there is no redundancy, so that measurements would have to be repeated and/or closure carefully monitored.

Although the technology described herein would be economical if implemented in postprocessing mode, its greatest value will be for real-time applications. Thus, to fully exploit this technique, a low data rate (real-time) telecommunications link will be required.

A final requirement is with regard to logistics or rigging. Briefly, whether the roving unit is a manual apparatus or a well-rigged vehicle, the antenna will need to be mounted so that the antenna phase center can be situated vertically over the survey mark quickly and accurately. The antenna will have to be mounted high (2-3 m) to avoid signal blockage during operations and on a table which can be easily leveled.

REFERENCES

Remondi B. W., (Center for Space Research, The University of Texas at Austin, Austin, Texas), 1984: Using the Global Positioning System (GPS) phase observable for relative geodesy: modeling, processing, and results. Ph.D. Dissertation. 360 pp.

Remondi B. W., 1985: Modeling the GPS carrier phase for geodetic applications. Proceedings of the First International Symposium on Precise Positioning with the Global Positioning System, (NOAA), Rockville, Maryland, April 15-19, 1985.

PRECISE SHIP'S VELOCITY FROM GPS: SOME TEST RESULTS

David E. Wells
Alfred Kleusberg
See Hean Quek
Department of Surveying Engineering
University of New Brunswick
Fredericton, New Brunswick
Canada E3B 5A3

James McCullough
United States Geological Survey
Woods Hole Oceanographic Institution
Woods Hole, MA 02543

John Hagglund
Nortech Surveys (Canada) Inc.
309 2nd Avenue SW
Calgary, Alberta
Canada T2P 0C5

ABSTRACT. GPS data from Texas Instruments Model 4100 receivers were used to test the determination of ship's velocities from single-receiver carrier phase measurements. Two data sets were used: data from a stationary receiver, and data from a receiver on a moving ship (using Syledis as the reference positioning system). The static test results indicate that (a) single frequency phase differences provide the best range rate measurements, and (b) instantaneous solutions for two components of horizontal receiver velocity, and for relative clock frequency offset recover the known zero velocity to within a few cm/sec. The ship test results indicate that GPS ship velocity equals Syledisvelocity to an accuracy of about 10 cm/sec, while the ship changed speed by 150 cm/sec (3 knots), and executed a 180 degree turn at 400 cm/sec (8 knots). Planned extensions to these tests are described.

INTRODUCTION

Precise ship's velocity from GPS will be useful for gravity, ocean flowmeter studies, and positioning. Marine gravimetry technology has progressed to the stage where the limiting accuracy in shipboard gravity measurements is due to imprecise velocities used to compute the Eotvos correction. Physical oceanographers using advanced acoustic systems to track ocean currents from on board ship are limited in their observation of these currents by their inability to determine the ship's velocity over the ground as accurately as they can determine the current relative to the ship. Marine positioning systems (including GPS) would benefit, in terms of filtering procedures for example, from a direct measurement of velocity. The purpose of the tests reported here was to ascertain to what extent, and by what methods, GPS velocities can meet these needs.

Two test data sets were selected, one using a fixed receiver, the other on board ship. Both sets were obtained using Texas Instruments 4100 GPS receivers owned by Nortech Surveys. The static test data is from station 6A of the Canadian National Geodetic Baseline in Ottawa, and was acquired on day 140 (May 19) 1984, as part of a campaign sponsored by the Geodetic Survey of Canada. Other results from this campaign are reported in Kleusberg at al (1985). The ship test data was acquired on board Canadian Survey Ship MAXWELL in Mahone Bay Nova Scotia on day 318 (November 14) 1983, as part of a campaign sponsored by the Canadian Hydrographic Service. Other results from this campaign are reported in Goldfarb and Schwarz (1985). Polar plots of the GPS satellite constellations during these two tests are shown in Figure 1.

STATIC TEST RESULTS

The purpose of the static test data was to determine what observations and what solution technique to use in obtaining horizontal velocities from GPS.

Several varieties of the GPS observations available from the TI 4100 were studied. Some of the results are illustrated in Figure 2, which shows the range rate misclosure time series (observed range rate minus range rate computed using the broadcast ephemeris and the receiver's known coordinates) to a single satellite over the same 15 minute period, but using different data. The carrier frequency observable had misclosures as great as 20 cm/sec, and was not considered further. Range rates obtained from paired carrier phase measurements 0.16 seconds apart provided better results. For this test, one 0.16-second phase measurement pair was sampled every three seconds. Misclosures using the L1 carrier only were smaller than those using the L1/L2 combination to correct L1 for ionospheric refraction. (This was expected since applying covariance propagation to the dual frequency correction equation suggests a magnification of the single frequency noise). Taking the L1 and L2 observations, uncorrected for ionospheric refraction, as independent observations and averaging them did not result in misclosures significantly different from those using L1 alone. Finally, results obtained by applying and by neglecting tropospheric refraction corrections did not differ significantly. For the remainder of our tests we used only L1 range rates, uncorrected for either ionospheric and tropospheric refraction, determined from the 0.16 second carrier phase pair measurements.

In selecting a model for the velocity solution, the main problem is how to handle clock frequency biases and drifts. For both test data sets, the TI 4100 receivers were controlled by cesium frequency standards. However some problems were

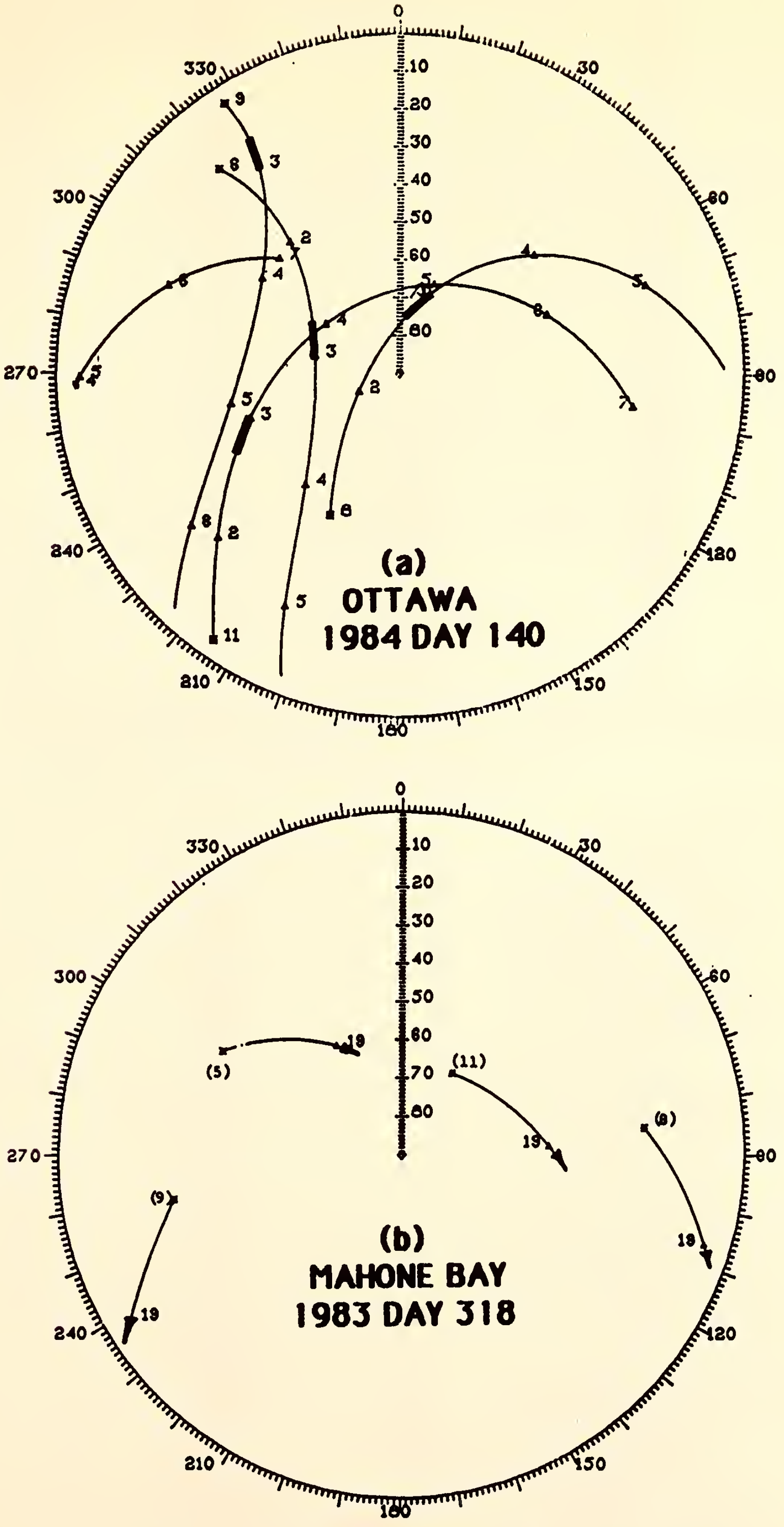

FIGURE 1. GPS SATELLITE POLAR PLOTS

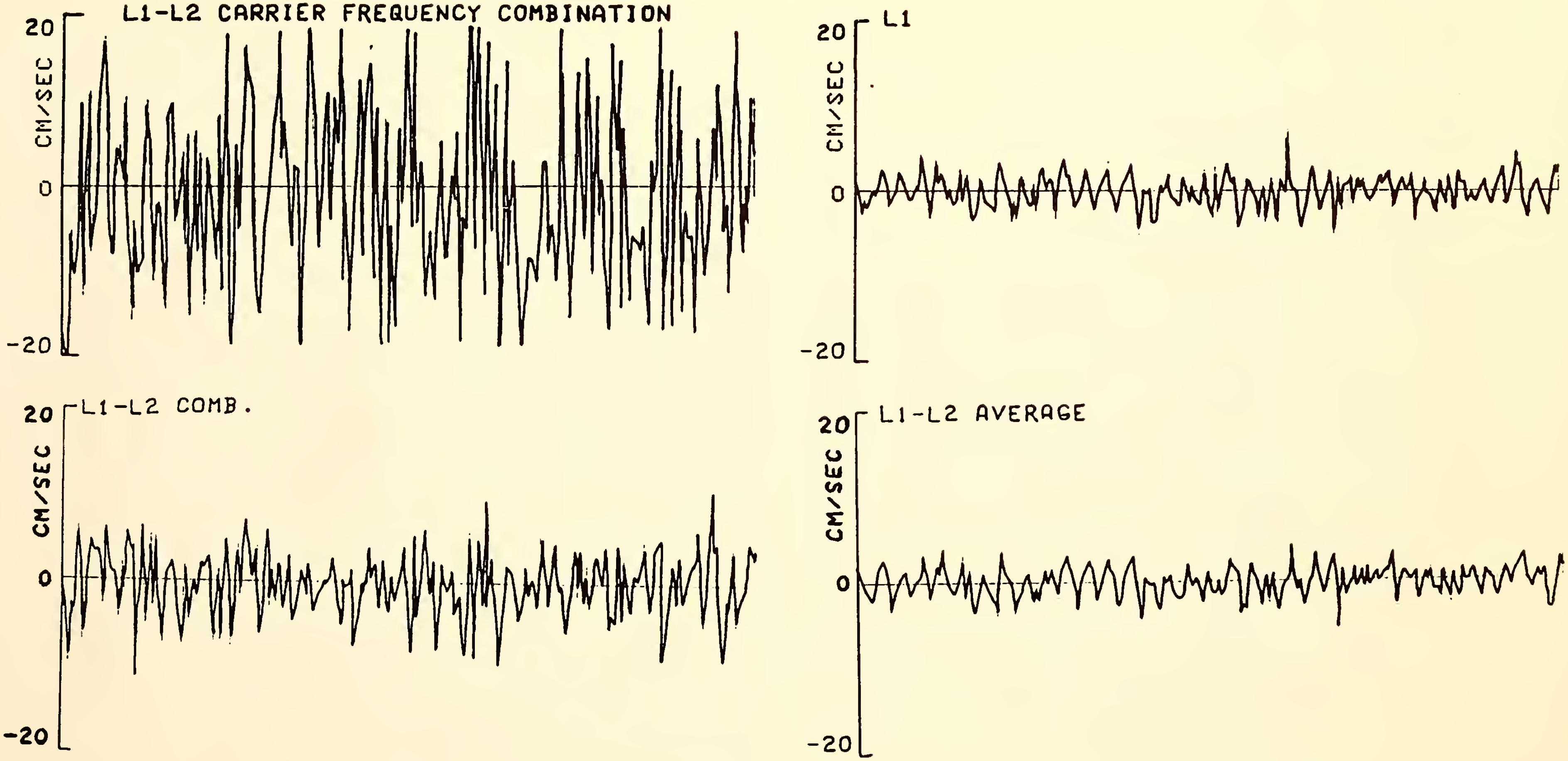

STATION 6A DAY 140 0140-0155

FIGURE 2. VELOCITY MISCLOSURE SATELLITE 8

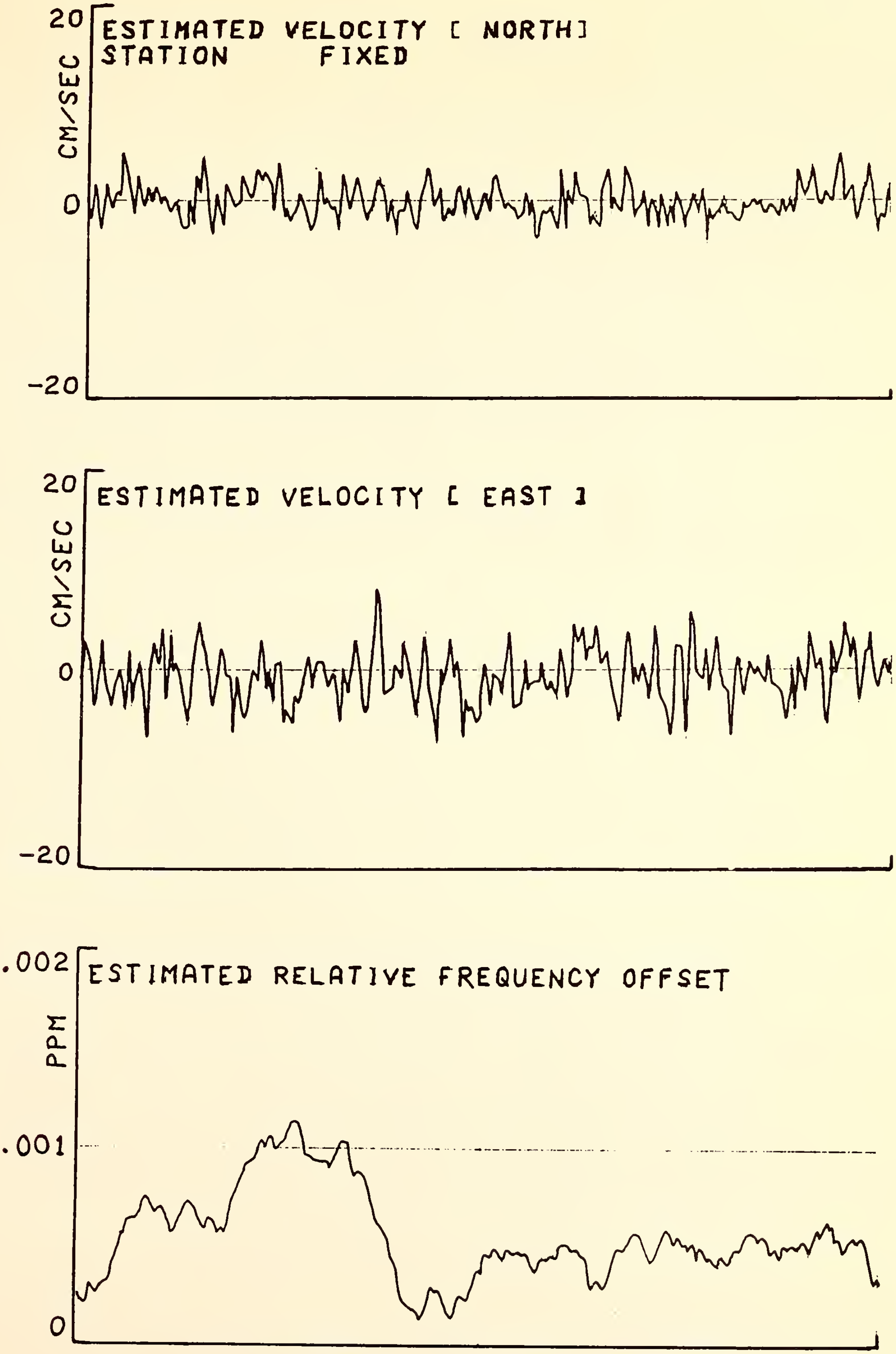

STATION 6A DAY 140 0245-0300

FIGURE 3. FIXED STATION VELOCITY SOLUTION

experienced during both campaigns such that performance typical of cesium standards could not necessarily be assumed. In our solution algorithm, we assume that differences between GPS satellite clock frequencies are adequately modelled by the clock parameter terms in the broadcast ephemeris. Receiver clock (and any possible "common mode" satellite clock) frequency behavior is modelled by including the receiver frequency offset as a "nuisance parameter" in the velocity solution. The results presented here treat each observation epoch independently to provide "instantaneous" estimates of receiver horizontal velocity and frequency offset (no filtering or smoothing has been applied). The vertical receiver velocity was weight-constrained to zero, with a standard deviation of one mm/sec. Figure 3 shows some typical results for the static data set, based on observations of the four GPS satellites shown in Figure 1a. Most encouraging was the fact that the velocity solution shows no biases about the (known) zero velocity. The rms errors in this case are 3 cm/sec in north velocity, and 5 cm/sec in east velocity. The clock frequency variation shown, of one part in ten to the ninth, is more typical of quartz oscillators than cesium standards. This may be due in part to the frequency standard problems referred to, and in part to the absorption of other effects into this nuisance parameter.

SHIP TEST RESULTS

The purpose of the ship test was to determine how well GPS velocities agree with actual ship's velocities. As often the case with GPS, it is difficult to find a system or technique which is sufficiently accurate to be used as reference. For our test, we selected data from a campaign on which GPS, Syledis, Miniranger III, and Ferranti Inertial Navigation System data were all collected simultaneously. In this paper, we report only on the comparison between GPS and Syledis-derived velocities.

The test data selected is a one hour hairpin-shaped track (18:00 to 19:00 UT on day 318) which includes a 1.5 m/sec speed change at 18:28, and a 180 degree course change at 18:38. Syledis ranges were recorded only at 30 second intervals during this period. Syledis velocities were derived by simple differencing between positions. Other tests indicate they are probably accurate at the 10 cm/sec level. GPS velocities were obtained as described above, sampled every three seconds. Figure 4 shows the results of the GPS and Syledis velocity solutions for the one-hour period. Figure 5 shows a subset at larger scale. The two velocities agree in general within 10 cm/sec, however the recovery from the 180 degree course change is markedly different.

CONCLUSIONS AND FUTURE PLANS

Our tests so far indicate that:

- Differencing the 0.16-second phase measurement pairs provides the best range rate observations obtainable from the TI 4100 GPS receiver.

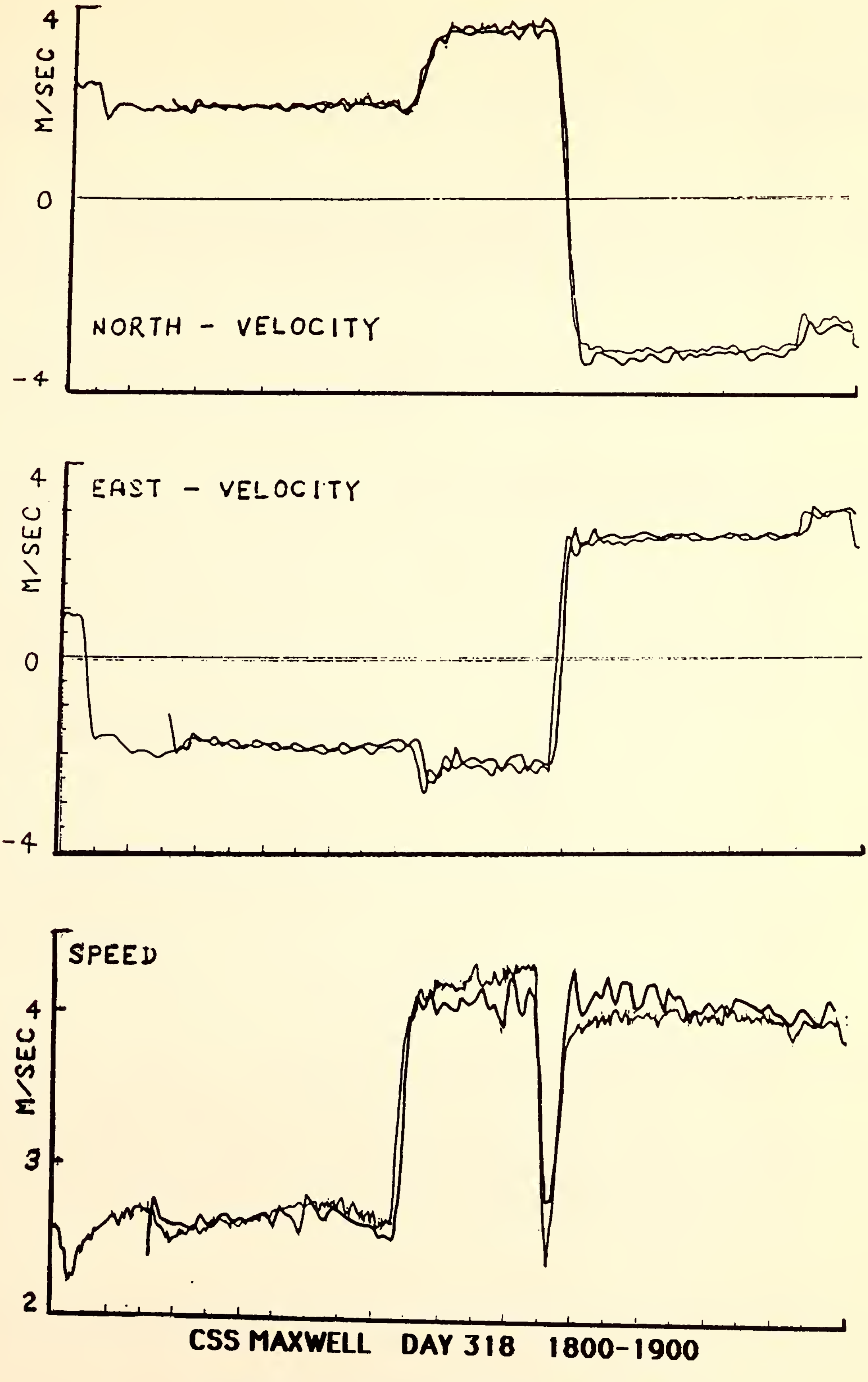

FIGURE 4. SHIP VELOCITY SOLUTION

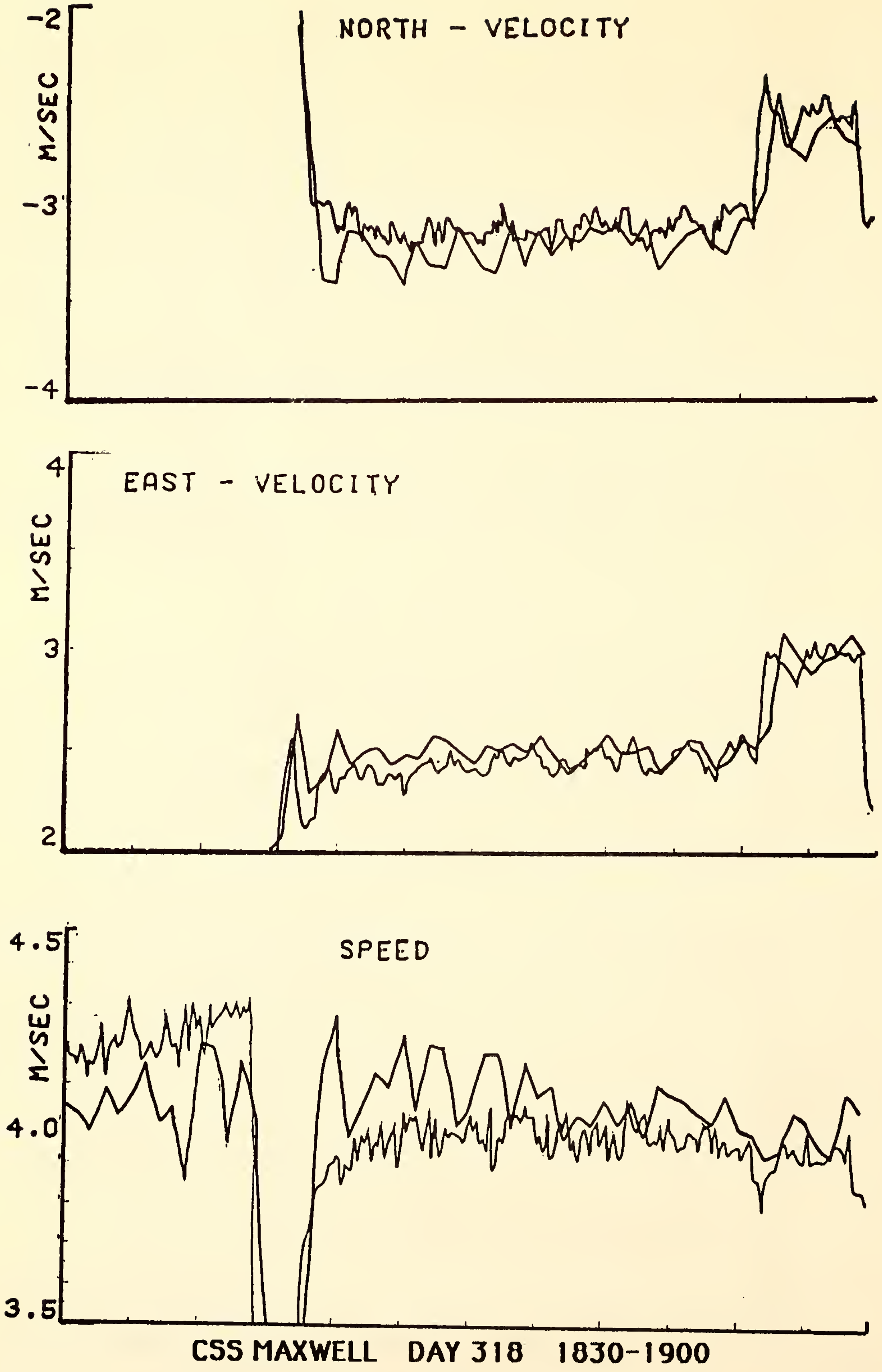

FIGURE 5. SHIP VELOCITY SOLUTION

- L1 single frequency range rates, uncorrected for either ionospheric or tropospheric refraction cannot be significantly improved by refraction corrections, or by averaging with L2 observations.

- Solutions for instantaneous horizontal receiver velocities, based on such L1 range rate observations, for which the vertical velocity is weight constrained to zero, and the receiver clock frequency offset is estimated, recover the known zero horizontal velocity to within five cm/sec.

- GPS-derived ship velocities agree with Syledis-derived velocities to within the expected Syledis accuracy of about 10 cm/sec.

We plan to compare GPS velocities with INS velocities obtained during the campaign described in this paper. The source of the anomalous clock frequency behavior will be investigated in two ways: by constraining the frequency (to behavior consistent with cesium clocks), and observing the influence on the horizontal velocity solution, and by comparing the behavior at pairs of simultaneously observing stations (to identify common ephemeris or refraction effects). The sensitivity of the velocity solution to ship position errors, ephemeris errors, and orbit constellation geometry will be studied both by perturbing our data, and through simulations. Considerations of roll, pitch, yaw and heave sensors, and of filtering techniques, are necessary to exploit the full capable of precise GPS ship's velocities.

ACKNOWLEDGEMENTS

We are indebted to Mike Eaton of the Bedford Institute of Oceanography, and to Demitris Delikaraoglou of the Geodetic Survey of Canada for providing the data upon which this paper is based.

REFERENCES

Goldfarb, J.M., and K.P. Schwarz, 1985: Kinematic positioning using an integrated GPS-INS, these proceedings.

Kleusberg, A., R.B. Langley, R. Santerre, P. Vanicek, and D.E. Wells, 1985: Comparison of survey results from different GPS receiver types, these proceedings.

ORBIT DETERMINATION OF HIGH-ALTITUDE EARTH SATELLITES: DIFFERENTIAL GPS APPROACHES

Sien-Chong Wu
Jet Propulsion Laboratoty
California Institute of Technology
4800 Oak Grove Drive
Pasadena, CA 91109

ABSTRACT. This paper investigates the capabilities of three different types of differential GPS measurements for precise orbit determination of high-altitude earth satellites. A covariance analysis is performed to assess the orbit determination accuracy of these measurement types at various satellite altitudes. The results of this analysis identify the best measurement types for satellites within different ranges of altitudes. Error sources and other factors affecting the orbit determination accuracy are examined and the relative merits of these measurement types are compared.

I. INTRODUCTION

The NAVSTAR Global Positioning System (GPS), which will be in full operation by 1989, was developed for precise positioning of ground sites and of moving vehicles near the earth surface (Milliken and Zoller 1978). Application to the navigation of earth-orbiting satellites has also been investigated (Van Leeuwen, *et al.* 1979, Farr 1979). Two of the major error sources limiting the accuracy of positioning using GPS are the imperfect time and frequency standards on board the GPS satellites and the GPS ephemerides. The former can be removed and the latter reduced by using differential measurements relative to known sites on the earth surface. Such differential GPS measurements yield high-precision relative positioning (MacDoran, *et al.* 1982, Counselman and Steinbrecher 1982, Ondrasik and Wu 1982, Yunck and Wu 1983). Due to the finite altitude and antenna beamwidth of GPS satellites, investigations on the applications to user satellites have been concentrated at lower altitudes. When the altitude of a user satellite is greater than 3,500 km, it will be outside of the antenna mainbeam illumination of a given GPS satellite for a fraction of the time. Eventually when the altitude of a user satellite is greater than that of GPS satellites (~20,000 km) there will be no GPS illumination from above. For such higher user satellites, orbit determination using conventional ("*up-looking*") differential GPS is not suitable; two alternative approaches can be adopted.

The first alternative approach is called "*down-looking*" differential GPS. It makes use of the "spilled" GPS illumination from below when the user satellite and a GPS satellite are on the opposite sides of the earth. The second alternative approach requires the user satellite to transmit a suitably tailored signal which can be observed by the same ground receivers observing GPS satellites; differential measurements at a ground station can then be made between the user satellite and the GPS satellites in common view. This approach is called "*inverted*" differential GPS. It was first suggested and briefly studied in (Yunck and Wu 1983).

This paper presents the results of a covariance analysis comparing the capabilities of the three (including the conventional) differential GPS approaches for the orbit determination of high earth satellites. It is shown that each approach is best suited for user satellites of altitudes in a specific range. When proper approaches are used, orbit determination to sub-meter accuracy can be achieved for user satellites lower than ~7,000 km in altitude. The accuracy degrades to a few meters for higher satellites up to the geosynchronous distance. Error sources and other factors affecting the orbit determination accuracy are examined. The relative merits of the three approaches are compared.

II. DIFFERENTIAL GPS MEASUREMENTS

Fig. 1 provides a brief description of the three types of differential GPS range measurements for the orbit determination of user satellites. Here, only one GPS satellite, denoted GPS1, is shown which is visible from the single ground station ST1. The four user satellites, EO1, EO2, EO3 and EO4, are at different altitudes and separated from GPS1 by different angles.

EO1 is at a lower altitude; it observes GPS1 in a conventional (up-looking) way and forms conventional differential GPS measurements when differenced with the ground observations. EO2 is at a higher altitude and farther separated from GPS1; it is outside of the GPS1 antenna mainbeam illumination and, hence, no GPS measurements can be made. EO3 is also at a higher altitude but is on the opposite side of the earth from GPS1 and is illuminated from below by the "spilled" signal of GPS1; it observes GPS1 in a down-looking way and, when differenced with the ground observations, forms down-looking differential GPS measurements. EO4 is at an altitude above the GPS constellation but is angularly close to GPS1 so that no observations can be made between EO4 and GPS1; however, differential measurements can still be formed using an alternative observing scheme as shown in Fig. 1. EO4 is to be equipped with a transmitter (in place of a GPS receiver) sending a suitably tailored signal which can be observed by the same receiver at the ground station ST1. When such ground observations of the user satellite are differenced with observations of GPS satellites from the same ground station, inverted differential GPS measurements are formed. These measurements are called "inverted" because the positioning of the user satellite is now relative to the GPS satellite, instead of the ground station as in the previous two types of differential GPS measurements.

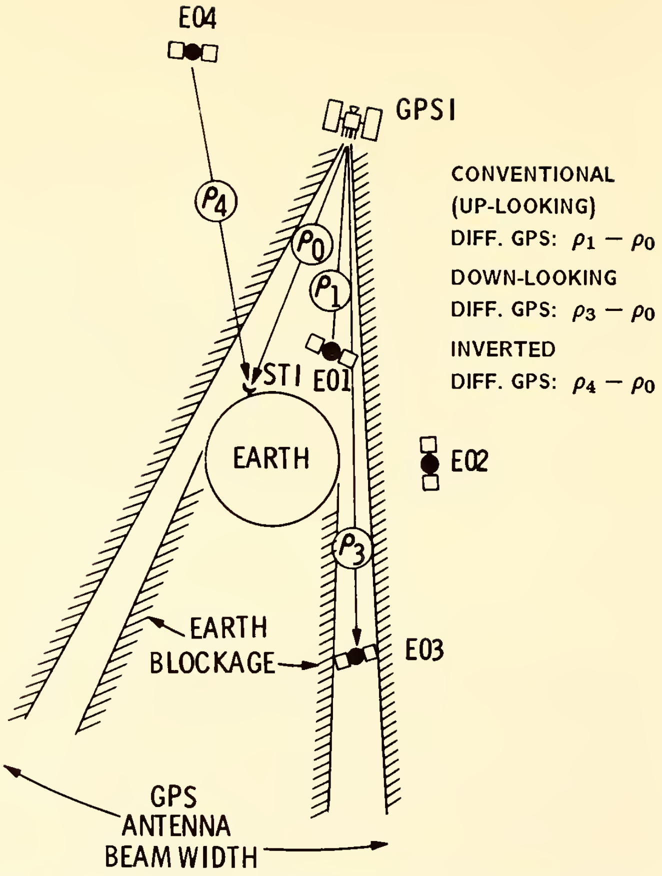
E04
GPS1
CONVENTIONAL (UP-LOOKING) DIFF. GPS: $\rho_1 - \rho_0$
DOWN-LOOKING DIFF. GPS: $\rho_3 - \rho_0$
INVERTED DIFF. GPS: $\rho_4 - \rho_0$
ρ_4
ρ_0
ρ_1
ST1
E01
EARTH
E02
ρ_3
EARTH BLOCKAGE
E03
GPS ANTENNA BEAM WIDTH

Fig. 1. Three types of differential GPS measurements

Differential GPS measurements eliminate any clock errors on GPS satellites (clock errors on ground stations for inverted differential GPS). However, such differential GPS measurements will be subject to clock descrepancies between the user satellite and the ground stations (between the user satellite and GPS satellites for inverted differential GPS). One way to eliminate these clock descrepancies is to form a second difference of these measurements: For up-looking and down-looking differential GPS, the second difference is formed between differential measurements taken from the user satellite and the same ground station but observing different GPS satellites. For inverted differential GPS, the second difference is formed between differential measurements taken at different ground stations observing the user satellite and the same GPS satellite. Such double differential GPS measurements are completely insensitive to any clock discrepancies between the user satellite, the ground stations and the GPS satellites. In the following analysis double differential GPS measurements will be assumed.

III. FACTORS AFFECTING ORBIT DETERMINATION ACCURACY

For fixed values of measurement noise and uncertainties of other model parameters, the accuracy of geometrical point positioning using instantaneous measurements depends heavily on the geometrical aspects of the user satellite and the GPS constellation, i.e., the Position Dilution Of Precision (PDOP) (Milliken and Zoller 1978). In practice, orbit determination requires measurements over a longer period of time. For such dynamical orbit determination, a low PDOP is not critical. Rather, the major factors affecting the accuracy include the number of GPS satellites (or ground stations in the case of inverted differential GPS) in common view of the user satellite, the data gap within the observation period and the sensitivities to GPS ephemeris error and ground station location error. We shall examine the magnitudes of these factors, for the three types of differential GPS measurements, as a function of user satellite altitude before going into detailed covariance analysis.

A. Number of Common-View GPS Satellites or Ground Stations

The antenna beamwidths of GPS satellites are designed to illuminate near earth sites. The half-width of the beams are ~22° and ~27° at L_1 and L_2 frequencies, respectively (Masson, *et al.* 1982). For the purpose of this study, the narrower half-width of 22° is assumed. For simplicity, we also assume a constellation of 18 GPS satellites, uniformly distributed over a spherical shell of radius 26,560 km.

For an up-looking user satellite of altitude h, GPS satellites in common view are confined within a cone defined by a maximum zenith angle of the user satellite. This maximum zenith angle is specified by the GPS antenna beamwidth and is given by

$$\zeta_{\max} = \sin^{-1}\left[(R_{GPS}/R_{\text{user}})\sin 22^\circ\right] \tag{1}$$

where $R_{\text{user}} = h + 6{,}378$ km is the geocentric distance of the user satellite and $R_{GPS} = 26{,}560$ km that of GPS satellites. The average number of GPS satellites in common view of such an up-looking user satellite is

$$\#GPS = 9\left[1 - \cos(\zeta_{\max} - 22^\circ)\right] \qquad \text{(up-looking diff. GPS)} \tag{2}$$

For a down-looking user satellite, GPS satellites in common view are confined within a conical shell defined by a maximum and a minimum nadir angle. The maximum nadir angle is, again, specified by the GPS antenna beamwidth and is given by

$$\nu_{\max} = \sin^{-1}\left[(R_{GPS}/R_{\text{user}})\sin 22^\circ\right] \tag{3}$$

The minimum nadir angle is specified by the earth blockage and is given by

$$\nu_{\min} = \sin^{-1}(R_E/R_{\text{user}}) \tag{4}$$

where $R_E = 6{,}378$ km is the earth's radius. The average number of GPS satellites in common view of such a down-looking user satellite is

$$\#GPS = 9\left\{\cos\left[\nu_{\min} + \sin^{-1}(R_E/R_{GPS})\right] - \cos(\nu_{\max} + 22^\circ)\right\} \qquad \text{(down-looking diff. GPS)} \tag{5}$$

For inverted differential GPS measurements, the user satellite is observed by ground stations. Hence the corresponding factor affecting the orbit determination is the average number of ground stations from which the user satellite is visible. For a net of ten ground stations uniformly distributed over the surface of the earth with a viewing cone of 2 × 80° (a cutoff elevation angle of 10°), the average number of stations in common view of the user satellite is given by

$$\#STN = 5\left\{1 - \cos\left[80^\circ - \sin^{-1}(R_E \sin 80^\circ/R_{\text{user}})\right]\right\} \qquad \text{(inverted diff. GPS)} \tag{6}$$

The average numbers of GPS satellites in common view of an up-looking and a down-looking user satellite, and the average number of ground stations in common view of a transmitting user satellite are shown in Fig. 2 as a function of user satellite altitude. It is surprising that more GPS satellites are visible from a down-looking user satellite than from an up-looking one at the same altitude.† The average number of GPS satellites in common view of an up-looking user satellite drops to less than two at ~5,000 km while there are more than two GPS satellites in common view of a down-looking user satellite at all altitudes up to ~15,000 km. For inverted differential GPS, two or more ground stations, on the average, are in common view of a user satellite higher than ~7,000 km, and this number increases with the user satellite altitude. Note that a simultaneous common view of two GPS satellites (or ground stations in the case of inverted differential GPS) from the user satellite is essential to form a double differential GPS measurement. Therefore, up-looking differential GPS is not suitable for orbit determination of user satellites well beyond 5,000 km in altitude while inverted differential GPS is not suitable for user satellites well below 7,000 km, unless a tracking net consisting of more ground stations is used.

B. Data Gap Within Observation Period

Precise dynamical orbit determination requires measurements distributed over the entire observation period. When there are long data gaps within the observation period, the orbit will have to be mapped over these gaps and large systematic errors will occur. Hence, a good measurement scheme should avoid long data gaps. One

---

† Below $h = 3{,}500$ km, both $\cos(\zeta_{\max} - 22^\circ)$ and $-\cos(\nu_{\max} + 22^\circ)$ are to be replaced by R_{user}/R_{GPS}. More GPS satellites will be visible from an up-looking user satellite than from a down-looking one for $h < 1{,}635$ km.

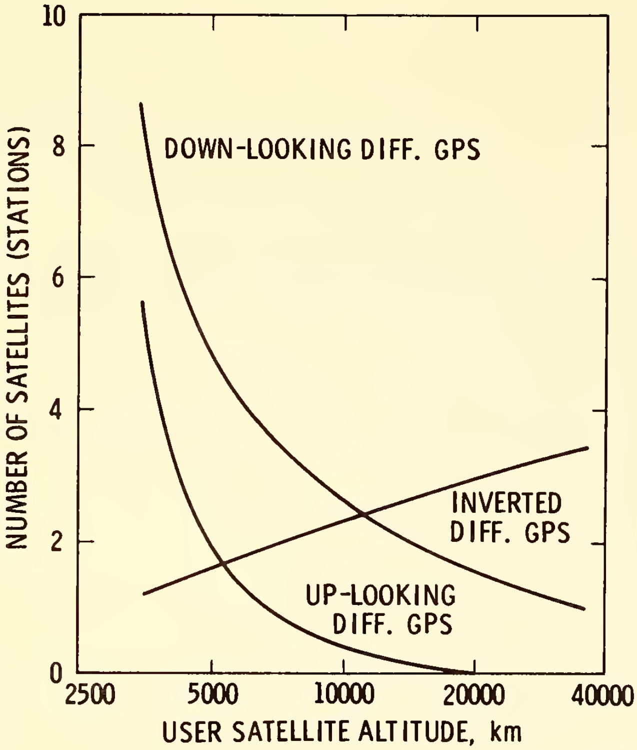

Fig. 2. Average number of GPS satellites and ground stations in common view of a user satellite

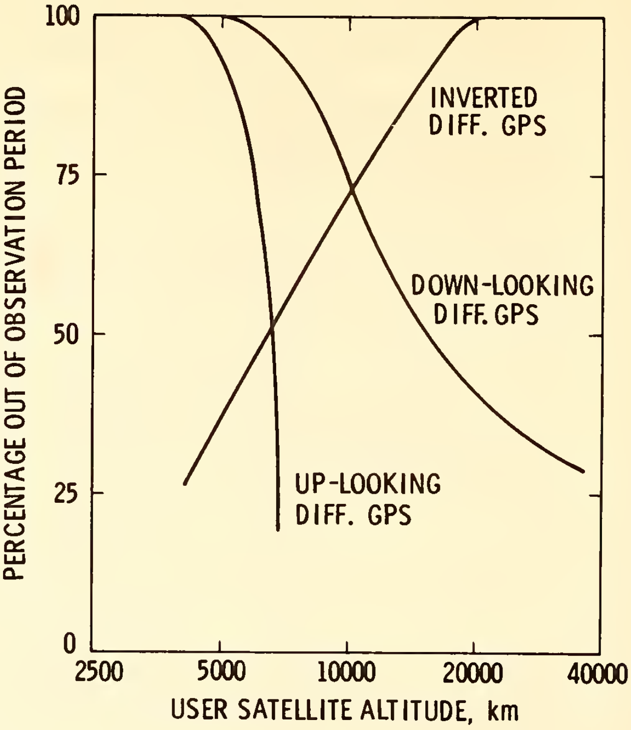

Fig. 3. Percentage of time when there are double differential GPS measurements

way to assess this factor is to examine the view periods for all three types of differential GPS measurements out of a given net of ground stations and the actual constellation of GPS satellites.

Fig. 3 presents the percentage of time, out of the entire observation period, when there are double differential GPS measurements, as a function of user satellite altitude. A net of ten ground stations, as shown in Fig. 4 is assumed. Also assumed is an observation period covering a full orbit of the user satellite. Fig. 3 suggests up-looking and down-looking differential GPS for lower user satellites and inverted differential GPS for higher ones. In this respect, it accords with the factor given in Subsection A above.

C. Sensitivity to GPS Ephemeris Error

Even though GPS ephemerides are to be independently determined on a regular basis, an error of a few meters is not unrealistic. For positioning using non-differential GPS, this error will translate one-for-one into positioning error. Differential GPS reduces or increases this error by a factor roughly equal to the ratio of effective baseline length to GPS altitude. For up-looking differential GPS, the effective baseline length is roughly twice the user satellite altitude; hence the sensitivity to GPS ephemeris error is, roughly,

$$\beta = 2h/H_{GPS} \qquad \text{(up-looking diff. GPS)} \qquad (7)$$

where H_{GPS} = 20,182 km is the altitude of GPS satellites. For down-looking differential GPS, the effective baseline length is roughly the sum of earth's diameter and the user satellite altitude; hence,

$$\beta = (2R_E + h)/H_{GPS} \qquad \text{(down-looking diff. GPS)} \qquad (8)$$

For inverted differential GPS, the GPS satellites serve as the reference points relative to which the user satellite is positioned. Hence GPS ephemeris error will translate one-for-one into user satellite positioning error:

$$\beta = 1 \qquad \text{(inverted diff. GPS)} \qquad (9)$$

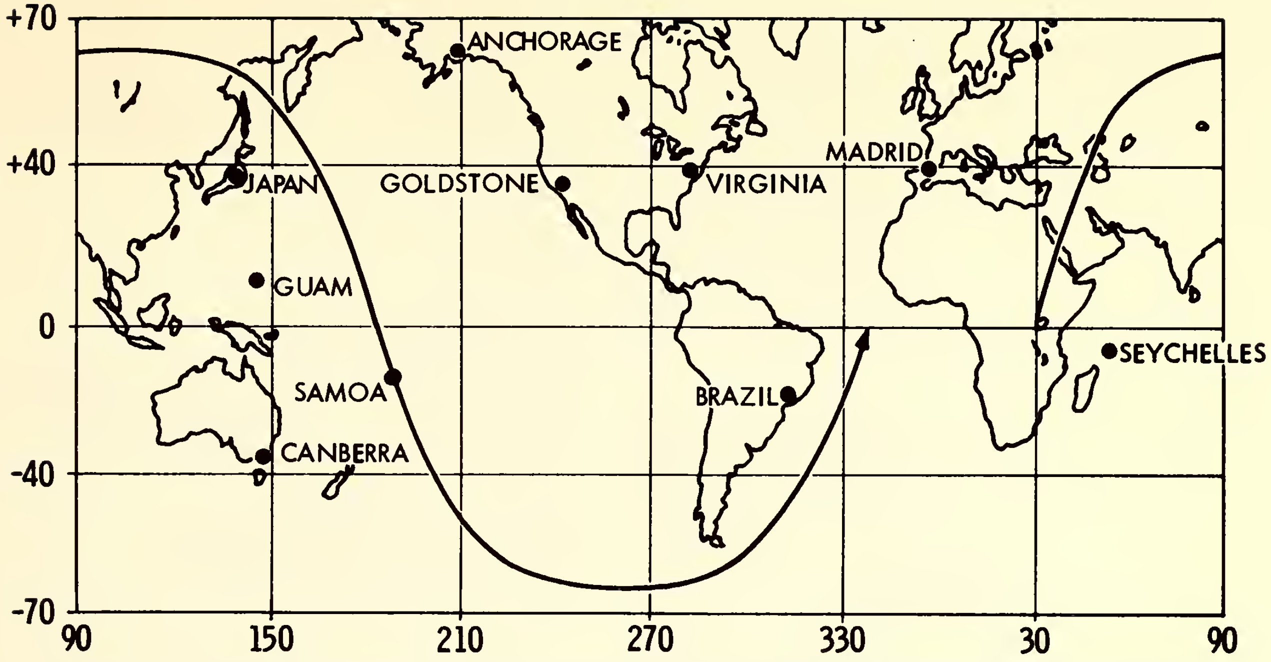

Fig. 4. Network of ground stations and ground track of a user satellite at 5000-km altitude

The sensitivities to GPS ephemeris error for the three differential GPS measurements are shown in Fig. 5 as a function of user satellite altitude. This figure, once again, indicates that up-looking differential GPS is best suited for lower user satellites and inverted differential GPS for higher ones.

D. Sensitivity to Ground Station Location Error

Ground station location error translates one-for-one into user orbit determination error when up-looking or down-looking differential GPS is used. When inverted differential GPS is used, the sensitivity is to be scaled by a factor

$$\frac{\text{user satellite to GPS satellite distance}}{\text{user satellite altitude}} \tag{10}$$

Since station location can be pre-determined to an accuracy an order of magnitude better than GPS ephemerides, the effects of its error is significant only when determining orbits of lower user satellites using inverted differential GPS.

IV. COVARIANCE ANALYSIS

In the previous section, factors affecting the accuracy of orbit determination for earth satellites using the three different types of differential GPS were qualitatively investigated. To predict the overall orbit determination accuracy, a covariance analysis is performed in this section. In this analysis, the actual constellation of 18 GPS satellites, arrayed in 6 orbit planes (Parkinson and Gilbert 1983), is used. The tracking network consists of 10 ground stations, as shown in Fig. 4. User satellites are placed in circular orbits, 65° inclined to the equator, and at altitudes between 4,000 km and 20,000 km. The key parameters of GPS and user satellites are summarized in Table 1. A geostationary satellite, TDRS-East (altitude $h = 35{,}783$ km, inclination $I = 0°$, longitude $\lambda = 41°$ West), is also studied. The ground track of a 5,000-km user satellite for a complete orbit cycle is shown in Fig. 4.

All three types of differential GPS range measurements are made, whenever possible, over a complete cycle of each orbit (half the orbit for the geostationary TDRS-East). The data rate ranges from one every 10 minutes for lower satellites to one every 30 minutes for higher ones. Second differences are made of these measurements to form double differential GPS range measurements, as outlined in the last paragraph of Section II above. A cutoff elevation angle of 10° is assumed at the ground stations. The solution strategy and the error models used in the analysis are summarized in Table 2. Dual-frequency (L_1 and L_2) measurements are assumed so that ionospheric delay errors are removed and not included in Table 2.

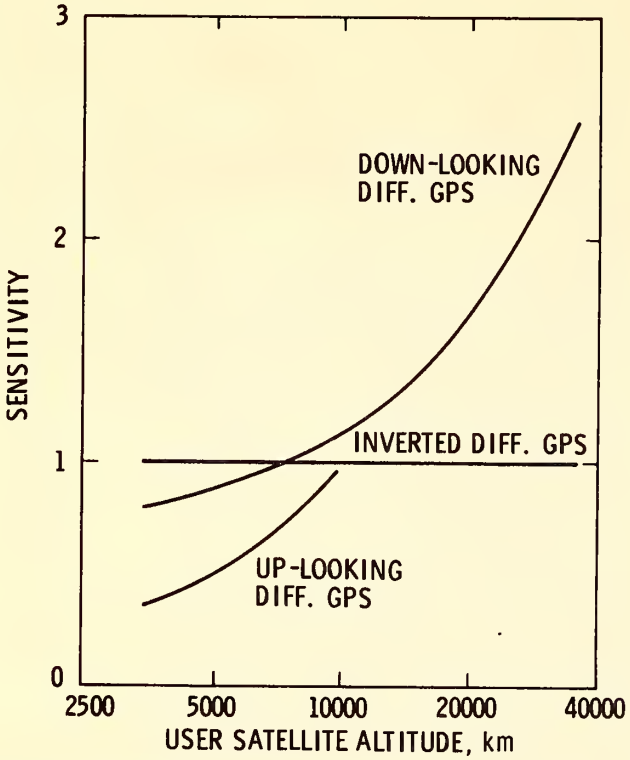

Fig. 5. Sensitivity of user satellite orbit determination to GPS ephemeris error

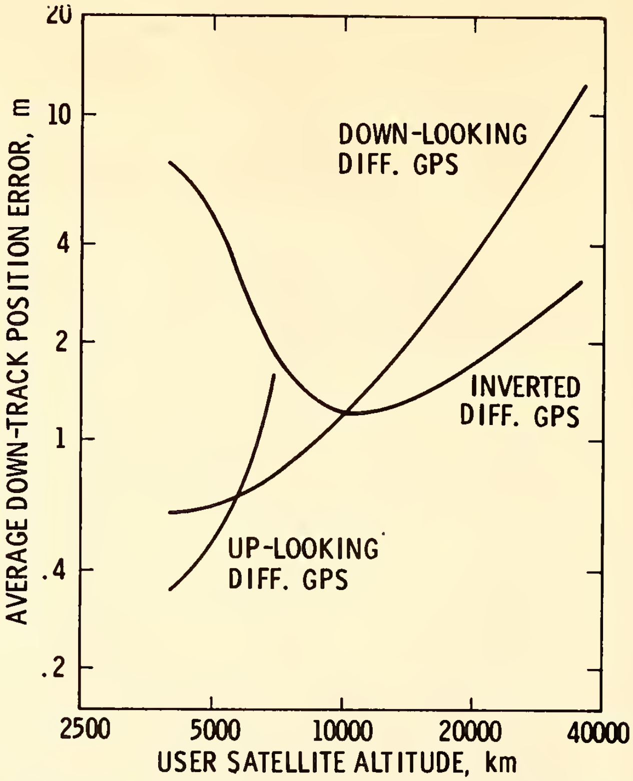

Fig. 6. Down-track position determination errors of a user satellite

Table 1. GPS and User Satellite Parameters

GPS Satellites:	Constellation	Walker 18/6/2 (Walker 1977)
	Semi-major axis, a	26,560 km
	Eccentricity, e	0
	Inclination, I	55°
User Satellite:	Altitude, h	4,000 km 5,000 km 7,000 km 10,000 km 20,000 km 35,783 km (TDRS-East)
	Eccentricity, e	0
	Inclination, I	65° 0° (TDRS-East)
	Longitude of ascending node, Ω	30° East 41° West (TDRS-East)
	Mean anomaly, m	0°
	Argument of peregee, ω	0°
	Area to mass ratio, A/M	0.042 m^2/kg

Table 2. Solution Strategy and Error Models

Solution Strategy:	Data type	Double differential GPS range
	Data span	1 orbit cycle of user satellite (0.5 cycle for TDRS-East)
	Data interval	10 min. for $h \leq 5,000$ km 13 min. for $h = 7,000$ km 14 min. for $h = 10,000$ km 30 min. for $h \geq 20,000$ km
	Estimated parameters	6 components of user satellite state at epoch
Error Sources:	Data noise	20 cm
	Station location	20 cm each component
	Tropospheric delay	5 cm @ zenith
	GPS ephemeris	1.5 m radial 1.5 m cross-track 3.0 m down-track
	Solar radiation pressure	5% @ 1.5 solar reflectivity coefficient
	Earth's gravitation, GM	1 part in 10^8

The epoch-state error covariances of each user satellite are mapped over the entire observation period. The three components (altitude, cross-track, and down-track) of the satellite position error are then averaged over that period. Comparisons are then made between solutions using different types of differential GPS range measurements. Fig. 6 summarizes such a comparison for the down-track component of user satellite position determination errors, as a function of user satellite altitude. In general, down-track error is larger than the other two components. Hence, Fig. 6 can be considered as a comparison of the orbit determination capabilities of the three types of differential GPS measurements. We observe, from Fig. 6, that conventional (up-looking) differential GPS performs better at lower altitudes up to ~6,000 km, and then degrades very rapidly beyond that altitude. Inverted differential GPS is best suited for higher satellites above ~10,000 km. Down-looking differential GPS bridges the gap between ~6,000 km and ~10,000 km.

To investigate the effects of data gaps, two extreme cases are examined. When measurements are plenty over the entire observation period, the orbit determination errors remain low over that period, as shown in Figs. 7 and 8 for a lower and a higher satellite, respectively. On the other hand, when there are large data gaps within the observation period, the error may grow wildly due to mapped systematic errors as shown in Figs. 9 and 10, again for a lower and a higher satellite, respectively. In Figs. 7 to 10, each component of the user satellite position error is plotted with a different symbol and connected by a solid line when data are available; dotted lines are shown for the mapped solutions over data gaps. The severe degradation of orbit determination accuracy over data gaps is observed. Station location error and tropospheric delay error are the major mapped systematic errors for the 4,000-km satellite using inverted differential GPS (Fig. 9); for the TDRS-East using down-looking differential GPS (Fig. 10), it is the GPS ephemeris error.

Fig. 6 indicates that when the proper differential GPS measurement type is used, sub-meter accuracy can be achieved for satellites lower than ~7,000 km in altitude. The accuracy degrades monotonically to a few meters up to the geosynchronous distance. To provide a better perspective, the down-track position errors at epoch are broken down into their contributing components as shown in Fig. 11 for three different altitudes using the best measurement types. GPS ephemeris error contributes almost the entire error for the two lower satellites and also is the major error source for TDRS-East at the geosynchronous distance.

The high sensitivity to GPS ephemeris error suggests that, when measurements are plenty, GPS orbits could be simultaneously estimated together with that of the user satellite. Under such circumstances, precision orbit

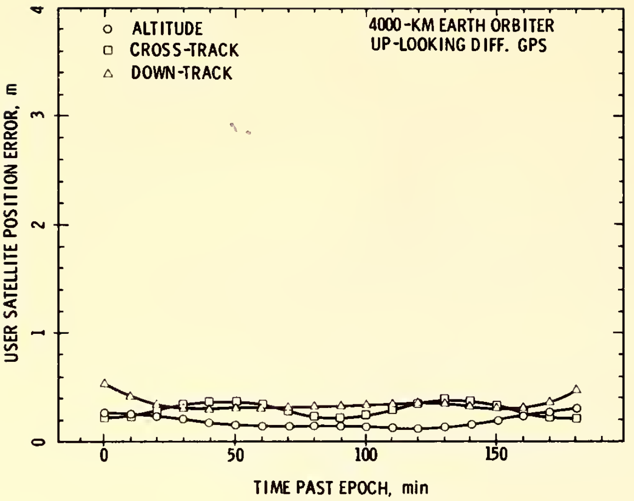

Fig. 7. Orbit determination error of a 4,000-km user satellite using up-looking differential GPS range measurements

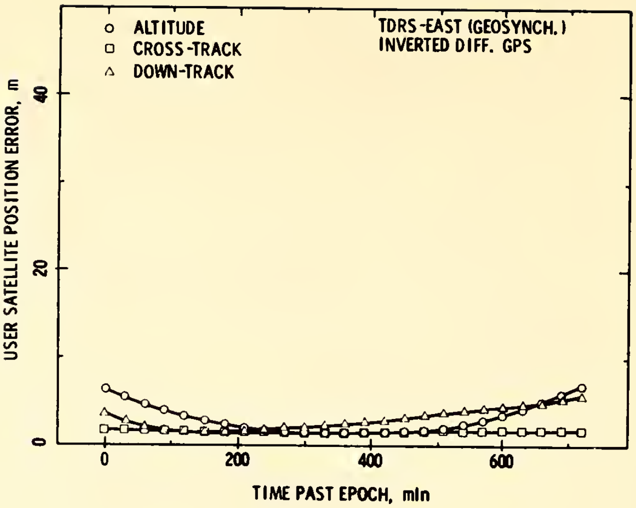

Fig. 8. Orbit determination error of a geosynchronous satellite (TDRS-East) using inverted differential GPS range measurements

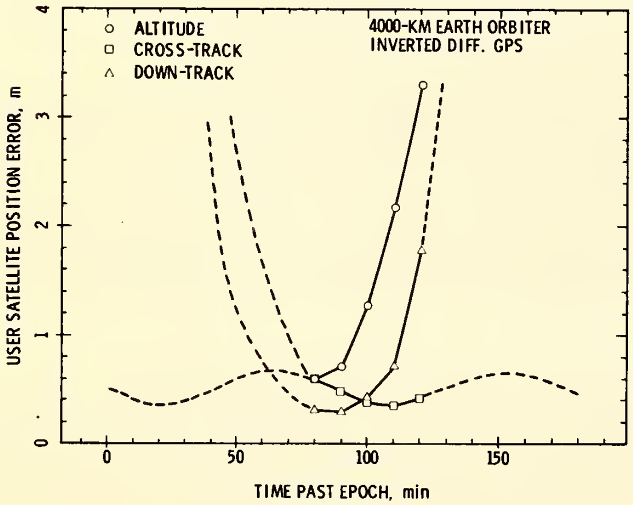

Fig. 9. Orbit determination error of a 4,000-km user satellite using inverted differential GPS range measurements

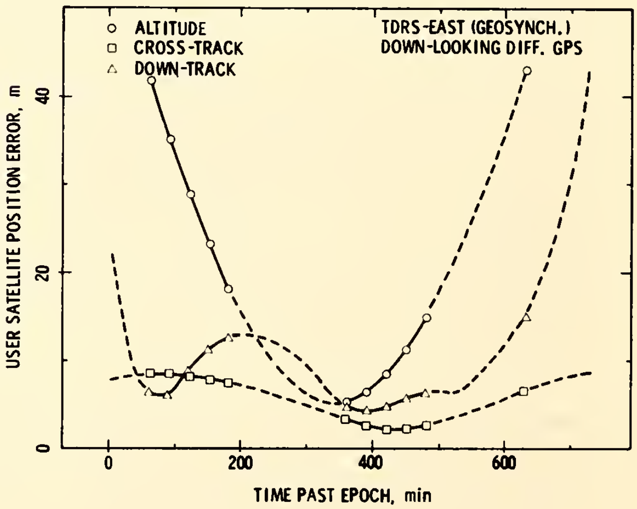

Fig. 10. Orbit determination error of a geosynchronous satellite (TDRS-East) using down-looking differential GPS range measurements

determination of user satellites can still be achieved even with poor *a priori* knowledge of GPS ephemerides. To illustrate this, the covariance analysis is repeated with GPS satellite orbits being simultaneously estimated, for three different cases when measurements are plenty. The *a priori* knowledge of GPS ephemerides is now degraded by a factor of three (5 m radial and cross-track, and 10 m down-track). The mapped orbit determination accuracies for the user satellites are examined and compared. The solutions for a 4,000-km user satellite using up-looking differential GPS and for the TDRS-East using inverted differential GPS degrade only very sightly. The solutions for a 4,000-km user satellite using down-looking differential GPS actually improve and are now better than those using up-looking differential GPS. This is mainly due to the stronger sensitivity to GPS ephemerides and the more measurements available when down-looking differential GPS is used. It should be pointed out that, in the

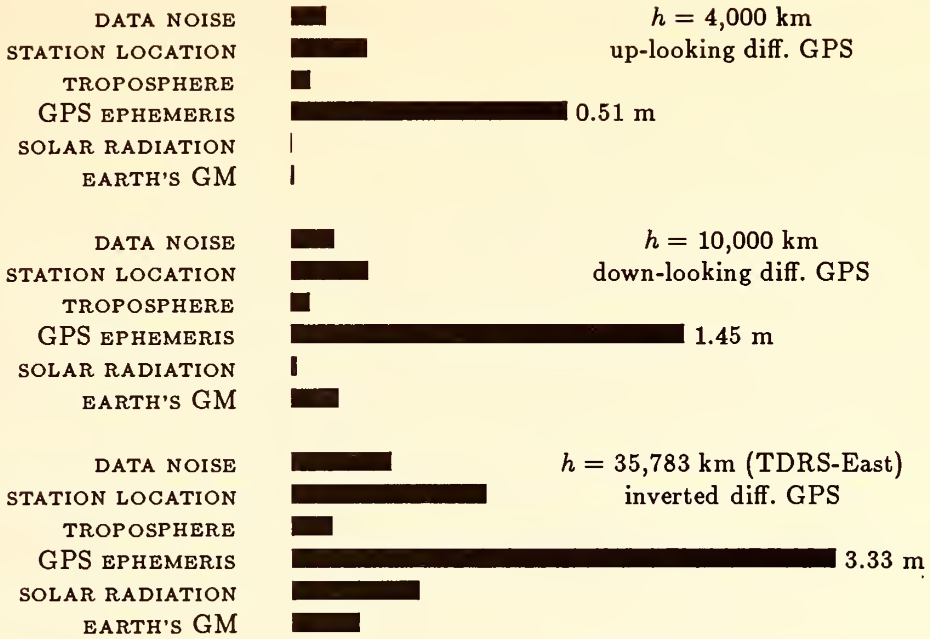

Fig. 11. Breakdown of user satellite down-track epoch position errors at three different altitudes using the best types of differential GPS range measurements

above analysis, only measurements involving the user satellite are included. In practice, when GPS orbits are to be estimated, measurements not involving the user satellite will also be included. Such measurements are the double differential ranges between ground stations observing GPS satellites in common view.

Differential GPS *delta-range* (integrated doppler) measurements derived from GPS carrier phase are inherently much more accurate than differential range measurements derived from GPS *P*-code pseudo-range. They are much less vulnerable to multipath and, also, their acquisition is simpler. Hence, their utility in precise satellite orbit determination should not be ignored. Although earlier studies (Wu and Ondrasik 1982) have indicated a promising potential of differential delta-range for orbit determination of low-altitude earth satellites, its extension to high-altitude satellites is not straightforward. The information of delta-range type measurements is embedded in the "history" of the relative motion between the user satellite and its tracking sites (GPS satellites or ground stations). Low-inclination satellites at or near geosynchronous distance have little motion relative to ground stations; hence inverted differential GPS delta-range (for which ground stations are the tracking sites) is almost useless. In the case of down-looking differential GPS, the visible GPS satellites from a user satellite are confined within a conical shell. This shell becomes thiner when the user satellite is higher; hence only short, broken arcs of delta-range measurements can be made and the "history" information of the user satellite motion is poor. For these reasons, differential GPS delta-ranges are impractical for higher user satellites. A covariance analysis for a user satellite at 4,000-km altitude indicates a 60% degradation in accuracy when 2-cm double differential down-looking GPS delta-range is used in place of its range counterpart (at 20 cm); up-looking differential GPS delta-range shows an accuracy degradation by nearly a factor of 4.

V. CONCLUSION

Three different types of differential GPS measurements for precision orbit determination of high earth satellites have been investigated. The results of a covariance analysis based on realistic error models agree with qualitatively predicted performances of the three measurement types. With a net of ten ground stations, conventional (up-looking) differential GPS range is found best suited for orbit determination of earth satellites up to an altitude of ~6,000 km. Down-looking differential GPS range performs better for satellites of altitudes between ~6,000 and ~10,000 km. Inverted differential GPS range takes over as the logical approach to precision orbit determination of higher earth satellites beyond ~10,000 km. When proper approaches are used, orbit determination to sub-meter accuracy can be achieved for satellites lower than ~7,000 km in altitude. The accuracy degrades to a few meters for higher satellites up to the geosynchronous distance. Differential GPS delta-ranges are inferior to their range counterparts by a factor of 1.5 to 4 at lower altitudes and are practically useless at higher altitudes due to lack of "history" information of the user satellite motion relative to its tracking sites.

Up-looking and down-looking differential GPS are both receive-only systems. User satellites and ground stations are to be equipped with GPS receivers and to observe only GPS satellites; they will not observe each other. The number of ground stations and their data load are independent of the number of user satellites to be tracked; hence, as many user satellites as desired can be tracked with the same systems without increasing the station work load. However, data received at user satellites need to be relayed back to ground for processing (forming double differential GPS data and performing orbit determination). User satellites using inverted differential GPS are to transmit properly tailored signals so that ground stations equipped with GPS receivers can also receive their signals. Station work load will increase with the number of user satellites to be tracked; and the number of such user satellites to be tracked by a given net of ground stations will be limited. However, all tracking data are received at ground stations; no data relaying links more than ground telephone lines are needed.

ACKNOWLEDGEMENT

The author would like to express his thanks to T. P. Yunck for his encouragement and constructive suggestions. The research described in this paper was carried out by the Jet Propulsion Laboratory, California Institute of Technology, under contract with the National Aeronautics and Space Administration.

REFERENCES

Counselman, C. C. and D. H. Steinbrecher, 1982: "The Macrometer: A Compact Radio Interferometry Terminal for Geodesy with GPS," 3rd Int. Geod. Symp. on Satellite Doppler Positioning, Las Cruces, NM.

Farr, J. E., 1979: "Space Navigation Using the Navstar Global Positioning System (GPS)," *Control and Guidance*, Vol. 39, pp. 3–28, published by American Astronautical Society.

MacDoran, P. F., D. J. Spitzmesser and L. A. Buennagel, 1982: "SERIES: Satellite Emission Range Inferred Earth Surveying," 3rd Int. Geod. Symp. on Satellite Doppler Positioning, Las Cruces, NM.

Masson, B. L., M. P. V. Ananda and J. Young, 1982: "Functional Requirements of Next Generation Spaceborne Global Positioning System (GPS) Receivers," IEEE National Telesystems Conference, Galveston, TX.

Milliken, R. J. and C. J. Zoller, 1978: "Principle of Operation of NAVSTAR and System Characteristics," *J. Inst. Navigation*, Vol. 25, No. 2, pp. 95–106.

Ondrasik, V. J. and S. C. Wu, 1982: "A Simple and Economical Tracking System with Subdecimeter Earth Satellite and Ground Receiver Position Determination Capabilities," 3rd Int. Symp. on the Use of Artificial Satellites for Geodesy and Geodynamics, Ermioni, Greece.

Parkinson, P. W. and S. W. Gilbert, 1983: "NAVSTAR: Global Positioning System—Ten Years Later," *Proc. IEEE*, Vol. 71, No. 10, pp. 1177–1186.

Van Leeuwen, A., E. Rosen and L. Carrier, 1979: "The Global Positioning System and Its Applications in Spacecraft Navigation," *J. Inst. Navigation*, Vol. 26, No. 2, pp. 118–135.

Walker, J. G., 1977: "Continuous Whole-Earth Covrage by Circular-Orbit Satellite Patterns," Royal Aircraft Establishment (Farnborough), Technical Report 77044.

Wu, S. C. and V. J. Ondrasik, 1982: "Orbit Determination of Low-Altitude Earth Satellites Using GPS RF Doppler," *IEEE Position Location and Nav. Symp. Record*, Atlantic City, NJ, pp. 85–91.

Yunck, T. P. and S. C. Wu, 1983: "Ultra-Precise Orbit Determination by GPS," AAS/AIAA Astrodynamics Specialists Conference, Lake Placid, NY.

The Use of GPS for Determining the Position of Small Buoys

by

Edwin E. Westerfield

The Johns Hopkins University
Applied Physics Laboratory
Laurel, MD 20707

ABSTRACT. Several DoD programs make use of small expendable buoys as part of instrumentation test systems. An important use of these buoys is determining the at-sea impact points of reentry bodies released by ballistic missiles. It is essential that the buoy positions be accurately known with respect to time. The Global Positioning System (GPS) provides an ideal means for obtaining these position data.

A method will be described that provides accurate buoy position using an instrumented, expendable buoy. The buoy is equipped with a device, known as a transdigitizer, that amplifies and filters the received GPS signals and down converts them to baseband where they are hard limited and sampled at a 2 MHz rate. The digital data stream is then transmitted to an overhead aircraft.

The aircraft is equipped with a receiver/decoder to receive the buoy transmissions, and a multiple channel tracker to track the transmissions from each GPS satellite (whose signals are received by the buoy). The trackers generate precise pseudorange and pseudorange rate measurements from the received signals. Onboard computers are used to calculate the position of each buoy in real time. Both the processed data and the raw digital data are recorded onboard the aircraft. These data can then be processed in a post flight processing facility to provide additional information and further precision of position.

The system, known as the GPS/SMILS (Global Positioning System/-Sonobuoy Missile Impact Location System), is described in this paper. In addition, some results obtained from at-sea tests of the system are provided.

BACKGROUND

The Sonobuoy Missile Impact Location System has been used for a number of years to determine where reentry bodies, released by ballistic missiles, impact in ocean target areas. An Air Force program was initiated over two years ago to develop an improved system to provide the required information at lower cost. The second phase of the three-phase development program is nearing completion.

Figure 1 is an overview of the original Deep Ocean Transponder/Sonobuoy Missile Impact Location System (DOT/SMILS), which makes use of several types of sonobuoys that are dropped by mission support aircraft. A typical sonobuoy is 4.5 inches in diameter and less than 36 inches long. As the buoy falls free from the aircraft, a small drag parachute deploys and stabilizes the descent

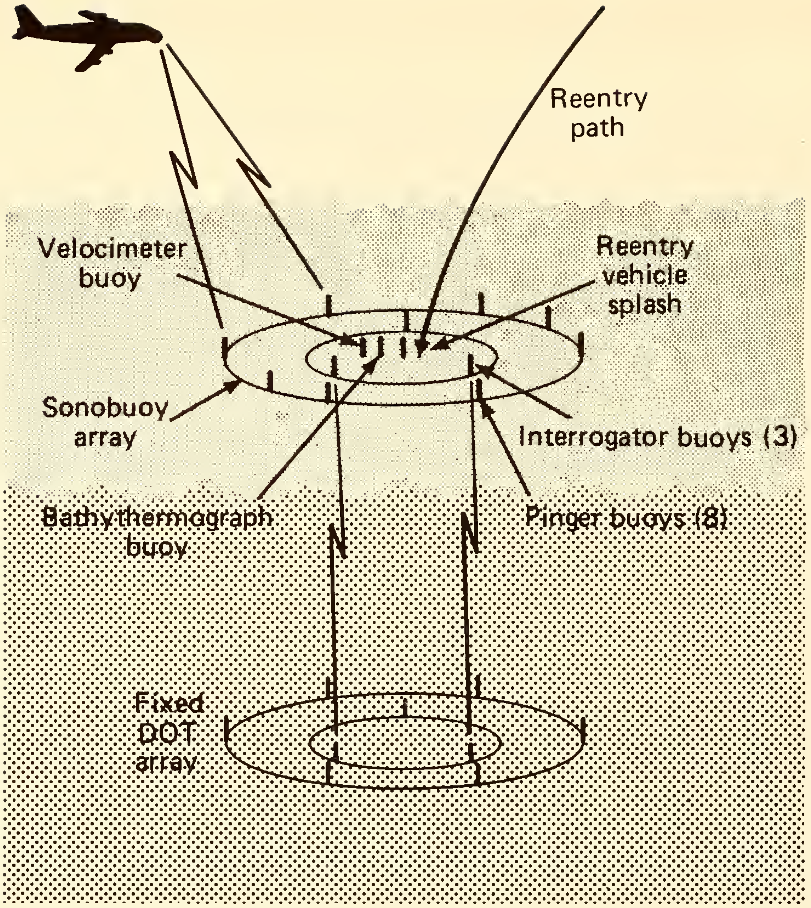

Fig. 1 Overview of the DOT/SMILS system.

of the buoy into the water. At the time of impact, the parachute is released and an antenna is erected. In some buoys, the antenna is located in a small balloon (float) assembly that is inflated by gas from a pressure bottle in the sonobuoy. The balloon provides extra flotation for the buoy and protects the antenna from salt spray.

Concurrent with balloon inflation, the buoy releases a hydrophone assembly that descends to a depth of about 30 feet. The hydrophone picks up acoustic signals generated by other buoys and the sound of each reentry vehicle impact and transmits that information by means of a VHF radio link to the mission support aircraft circling overhead. Some buoys within the array deploy a second hydrophone that injects an acoustic transponder command signal into the water.

Various types of buoys are used in the missile impact location system shown in Figure 1. The velocimeter buoy measures the velocity of sound in water, while the bathythermograph buoy measures the temperature of the water as a function of depth. The interrogator buoys are equipped with sonic transmitters that transmit acoustic command signals to DOTs located at known positions on the ocean floor. Ten transponders typically are used in a target area to provide the necessary coverage. The DOTs respond to interrogations by generating an acoustic signal, each DOT responding on a different acoustic frequency. The pinger buoys on the surface are key system components, both receiving and generating acoustic signals. They receive acoustic transmissions from all buoys equipped with acoustic transmitters and also detect the loud acoustic signals generated by the reentry bodies as they strike the water.

Electronic equipment aboard the aircraft is used to monitor the RF signals transmitted by all of the buoys in the water. After being processed, these transmissions allow us to determine the time of arrival of each acoustic signal received by each buoy, as well as the time of acoustic pulse transmission by each buoy. This information can be processed mathematically to yield the position of each buoy relative to the others. In addition, whenever an interrogator buoy generates a command transmission, all transponders within range respond with a high-frequency reply. The responses as received at the interrogator buoy enable an accurate estimation to be made of the slant range from the buoy to each DOT. When the transponders were originally implanted on the ocean floor, their geodetic positions were determined accurately, typically by means of the Navy Navigation Satellite System. By combining that position information with the slant range measurements, the geodetic position of each interrogator buoy can be determined accurately. When the positions of two or more interrogator buoys have been derived, the geodetic positions of all the buoys in the system can be determined because their relative positions are already known.

When a reentry body impact occurs, the resulting acoustic signal is picked up by all buoys. If the relative times of arrival of the signals at the buoys are compared, the impact position can be determined to a high degree of precision.

The DOT/SMILS system described above requires that relatively large ships be used to plant the DOTs, survey their positions, and perform essential maintenance in the target areas far from land. Currently, the transponder position survey requires nearly a week, principally because the Navy Navigation Satellite System is used as the primary position source. To obtain the required accuracy, data from a minimum of 20 satellite passes should be taken and averaged; this requires a number of days because of the system's orbital configuration. In the future, by using the Global Positioning System (GPS) to perform the survey function, the on-station time should be reduced significantly. Relatively large ships will continue to be required for survey and implant, however, because of the remote locations. It is possible to replace inactive DOTs in the array by means of aircraft. Such a system is the Air Launch Deep Ocean Transponder system under development for the Navy. It will reduce maintenance costs for the DOT/SMILS array.

DEVELOPMENT OF THE GPS/SMILS SYSTEM

Several years ago, the Air Force Western Space and Missile Center at Vandenberg AFB investigated alternative approaches to the current system with the aim of reducing or eliminating the cost of implanting the DOTs. A concept called the Global Positioning System/Sonobuoy Missile Impact Location System (GPS/SMILS) (Figure 2) was found to be very promising, and the Air Force selected APL to develop it.

In that system, the interrogator buoys and the DOTs are replaced by buoys known as GPS transdigitizer buoys (Figure 3). The buoys not only perform the functions of the pinger buoys, but also receive signals from the GPS satellites and amplify, filter, and down-convert the signals to a low frequency of 20 kilohertz. The signals are then fed via a voltage comparator into a

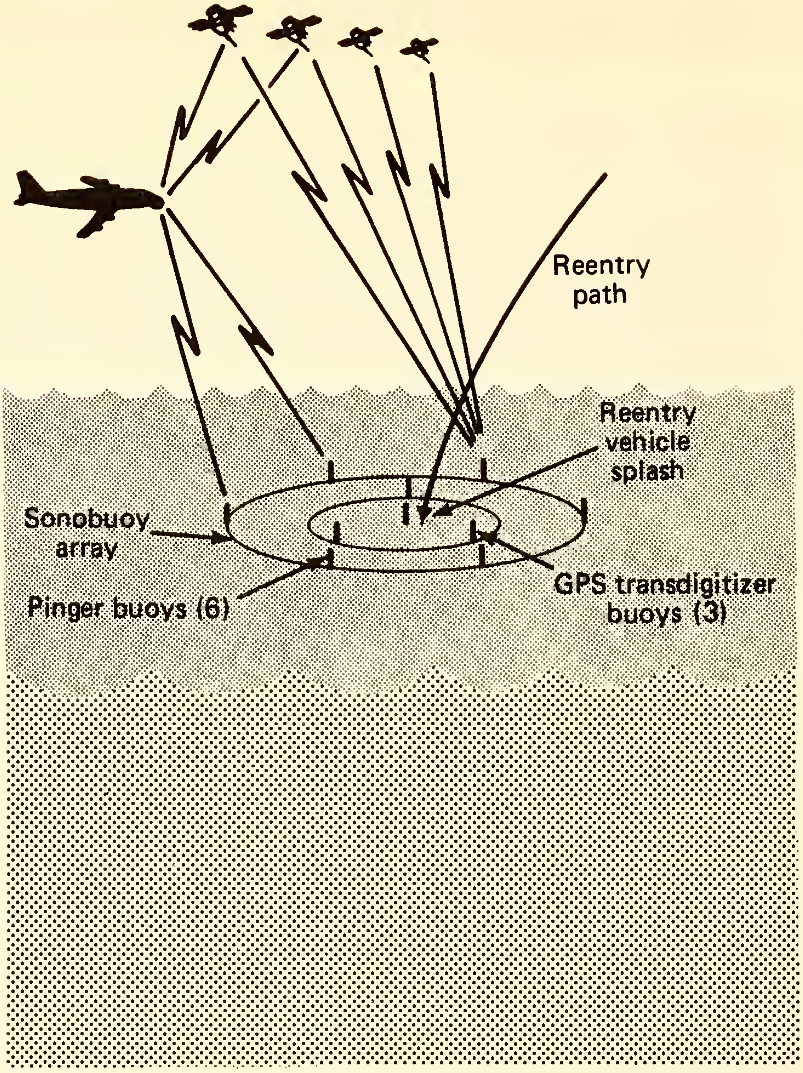

Fig. 2 Overview of the GPS/SMILS system.

1-bit latch circuit to generate a digital data stream. These data, along with digitized acoustic data, are used to modulate a carrier for transmission of the signals to the system aircraft over a VHF link.

Equipment in the aircraft receives the signals from the transdigitizer buoys, separates out the acoustic data from the GPS data, and processes all the data. The GPS data are fed into a number of tracking channels, each of which tracks the signal from one satellite. The output of the channels is pseudorange and pseudorange-rate for the satellite-buoy-aircraft path and GPS message data that describe the satellite orbits. The data can be processed mathematically to provide accurate position data for the transdigitizer buoys. The positions of the pinger buoys in relation to the transdigitizer buoys are then obtained using acoustics, in a fashion similar to that used for the original system. The GPS/SMILS system will function more automatically than the earlier system. The advantages are that no ship is required and there is target flexibility, thereby reducing costs.

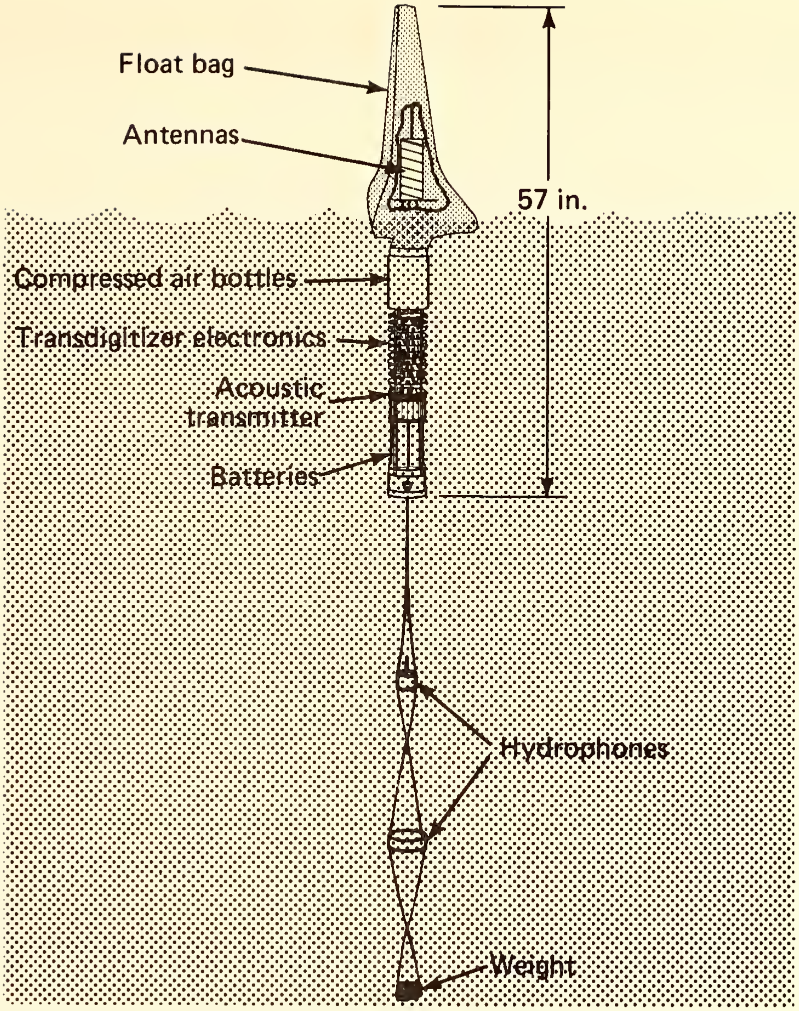

Fig. 3 The GPS/SMILS transdigitizer buoy.

DESCRIPTION OF THE TRANSDIGITIZER BUOY

Figure 3 is an exploded view of the transdigitizer buoy following inflation of the float bag and release of the hydrophones (acoustic transducers). The antenna system, located in the float bag, must provide for receipt of signals from the GPS satellites, receipt of VHF command signals from the aircraft, and transmission of the data back to the aircraft at VHF. The antenna system consists of a backfire helix antenna for reception of the 1575.42 megahertz (MHz) transmission from the satellites. A monopole antenna located at the center of the helix is used both for reception of VHF command signals and transmission of data to the aircraft. The tops of both the helix and the monopole antennas are tied to the top of the float assembly. At the time the buoy is dropped from the aircraft, the float bag and antenna are folded into a compartment at the top of the buoy. When the buoy strikes water, the float is inflated by the release of air from bottles of compressed air located underneath the float storage area, and the antennas are erected automatically.

Underneath the float storage area is a group of boards containing the electronics for the transdigitizer, including the transmitter and the command receiver. There is also a board containing circuitry for processing the acoustic data received from the hydrophone. The board at the bottom of the stack houses the acoustic transmitter. Below the electronics is a compartment housing the batteries.

At the bottom of the buoy is a chamber that houses the acoustic transducer, a damper, and the cable prior to deployment. One transducer serves as a damper. Part of the cable connecting the buoy to the damper is elastic and can readily be stretched. The function of the damper and the cable is to keep the hydrophones stationary while the buoy rides up and down on the ocean swells, in order to reduce the water noise that would occur if the hydrophones were riding up and down in the water following the vertical motion of the buoy.

Figure 4 is a block diagram of the electronics within the transdigitizer. The 1575.42 MHz signals received by the antenna are filtered, amplified, and heterodyned to a first IF frequency of 75.42 MHz. This signal is further amplified and heterodyned down to a frequency of 20 kilohertz. It is then passed through a 1 MHz low-pass filter/amplifier and thence to a zero crossing detector that provides a digital output. This signal is sampled by means of a flip-flop that is clocked by a 2 MHz signal. The digital signal is then fed into one input of a quadraphase modulator where it modulates one phase of the uplink carrier.

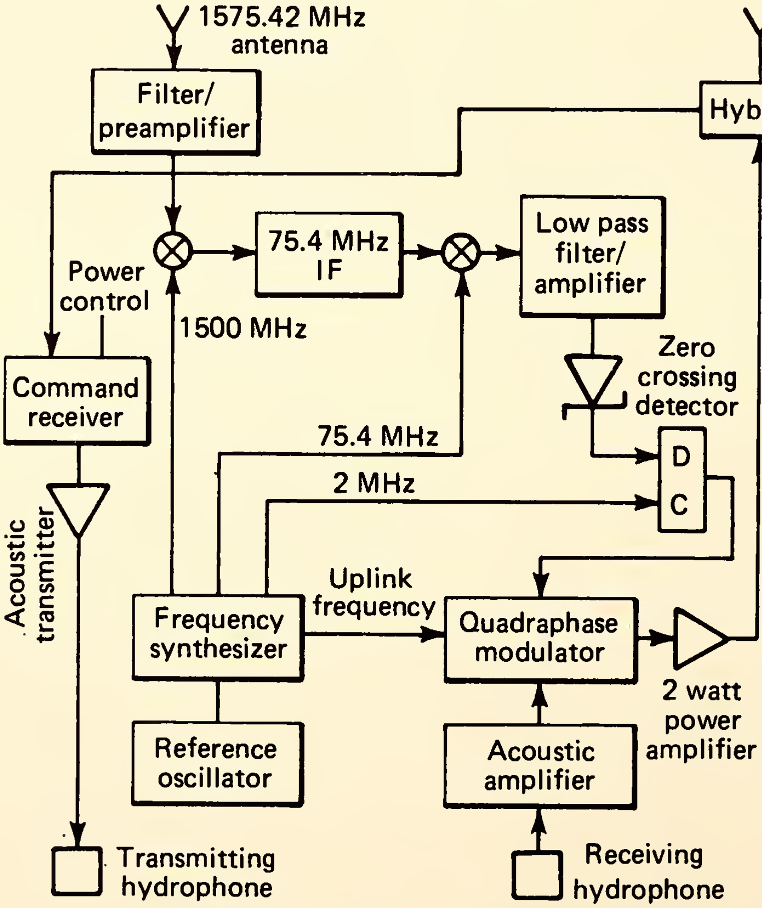

Fig. 4 Block diagram of the buoy electronics.

The second input to the quadraphase modulator is an asynchronous digital data stream generated by processing the acoustic data received by the hydrophone. The signal from the modulator is amplified to provide an RF output power of 2 watts to the antenna.

AIRCRAFT EQUIPMENT

Figure 5 is a block diagram of the equipment required in the aircraft to support the operation of the system. The equipment will be housed in a modified Boeing 707 aircraft along with other range equipment. The aircraft will be equipped with the electronics shown in the diagram and also with the facilities to carry and launch sonobuoys. It will also have special antennas to receive the signals from the buoys and an antenna to receive signals directly from the GPS satellites. The former antennas will be mounted under the fuselage, while the latter will be top mounted.

The signals received from the buoys are fed to two receiver groups. The first is a standard antisubmarine warfare receiver used for receiving the signals from all buoys except the transdigitizers. The transmissions from the transdigitizer buoys are processed by a specially designed 6-channel uplink receiver that filters and amplifies the signals and separates the acoustic data from the GPS data. The GPS and acoustic data are recorded by a standard 14-track analog recorder.

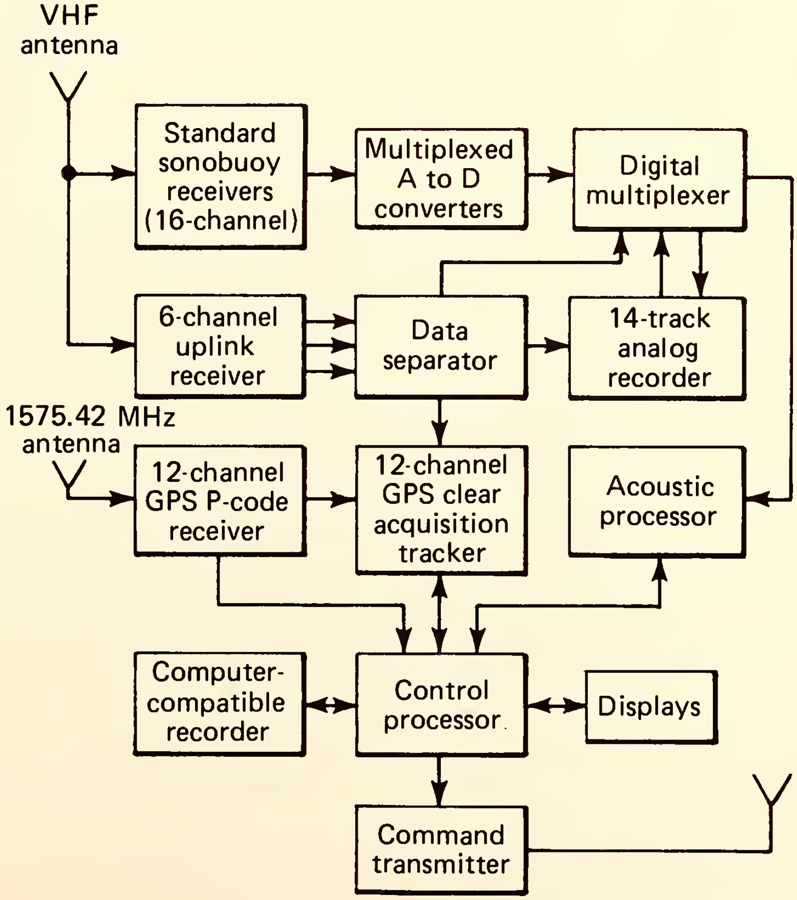
VHF antenna
Standard sonobuoy receivers (16-channel)
Multiplexed A to D converters
Digital multiplexer
6-channel uplink receiver
Data separator
14-track analog recorder
1575.42 MHz antenna
12-channel GPS P-code receiver
12-channel GPS clear acquisition tracker
Acoustic processor
Computer-compatible recorder
Control processor
Displays
Command transmitter

Fig. 5 Block diagram of the aircraft SMILS system.

The GPS data are also fed to a 12-channel digital tracking system. Twelve channels are required in order to allow the simultaneous processing of four satellite signals received from three transdigitizer buoys. The system also computes the position of each transdigitizer buoy.

A second bank of digital trackers is used to process the signals received directly from the satellites. The principal function of this subsystem is to determine the effect that ionospheric refraction has on the 1575.42 MHz transmission from each satellite. This is accomplished by processing the 1575.42 and 1227.6 MHz pseudorange and range-rate signals from each spacecraft to estimate the refraction effect. The refraction data are used to correct the 1575.42 MHz signals received at the transdigitizer buoys. Studies have indicated that at the maximum range of the aircraft from the buoy, the refraction effects at the aircraft and at the buoy will be essentially identical, allowing the technique to be used. In addition to providing the refraction data, the receiver will also provide the aircraft's position; these data will be used to ensure accurate dropping of the sonobuoys in the intended reentry area.

The acoustic processer determines the acoustic transmission time between the various buoys in the array. The information is used to compute the relative position of the buoys. The position data and the transdigitizer position data are fed to the control processor, which combines the information to provide the geodetic position of the buoy. The acoustic processor also processes the splash data from the reentry bodies and computes the geodetic coordinates of the reentry body splash points. The computed results are recorded on a computer-compatible magnetic tape recorder. Displays of buoy status are provided for the operator. There is also a command transmitter that is used to control the transdigitizer buoys.

POSTMISSION PROCESSOR

A postmission processing system will also be developed. The processing facility will use many of the same hardware and software modules as the aircraft systems and will be equipped with a large minicomputer for performing the various acoustic and position computations. A larger computer will allow more sophisticated software to be used in the calculations, resulting in improved accuracy.

STATUS OF THE PROGRAM

The program has been under way for over two years and is in phase two of a three-phase development program. During phase one, two sonobuoys were designed and fabricated, along with a rudimentary version of the aircraft equipment. For the phase one test, only GPS-related equipment was provided. During that phase, it was felt that there was no need to test the acoustic portion of the system because similar techniques have been used in the past.

Testing of the phase one system was performed at the St. Croix, V.I., test range in February 1983. Although two buoys were available, only one was deployed in the ocean at a time. However, a second transdigitizer was operated at the land-based collection site to provide reference data. The recording subsystem was capable of recording signals simultaneously from both transdigitizers. Only a single-channel tracker was available at the field site; it provided for system checkout, but detailed processing had to be performed after the test.

The results of the phase one test were very satisfactory. Figure 6 is a bullseye pattern showing a number of typical fixes. The difference between the position determined by GPS and a survey is shown. The slight bias in the data can readily be seen; the source of the bias has yet to be determined. Figure 7 is a bullseye plot showing the error in the translocated buoy positions. To generate the plot, the positions of the reference transdigitizer and the buoy were first determined by tracking the recorded signals from three or more GPS satellites as received by each transdigitizer. The data were processed, and the error in the computed position of the land-based antenna was subtracted from the computed position of the floating transdigitizer buoy. These positions were compared with the acoustic position data provided by the St. Croix range through the use of pinger buoys attached to the transdigitizer buoys via a 10 foot tether. The resulting differences are plotted in Figure 7. A significant part of the error shown is due to the fact that the range buoy could be as much as 10 feet from the transdigitizer buoy. Note, however, that there is essentially no bias in these data.

The second phase of the program consists of developing an improved buoy that has full capability (including the reception and generation of acoustic signals) and prototype aircraft equipment. Testing of the complete system, including developmental buoys and aircraft equipment, was carried out at St. Croix in October of 1984. Operation of the full system concept was proven in this test series.

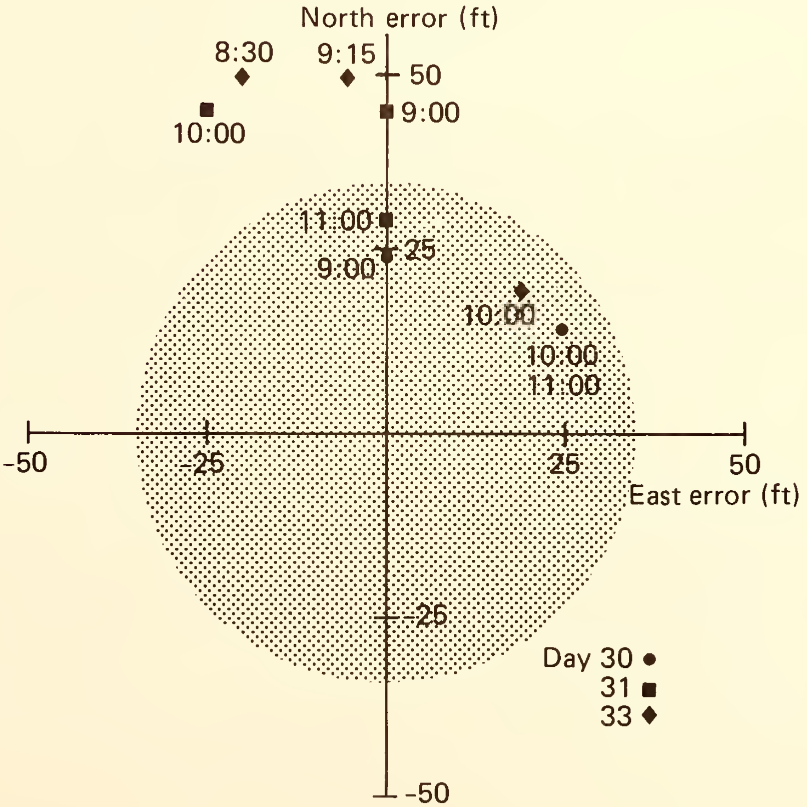

Fig. 6 Typical results from fixed site.

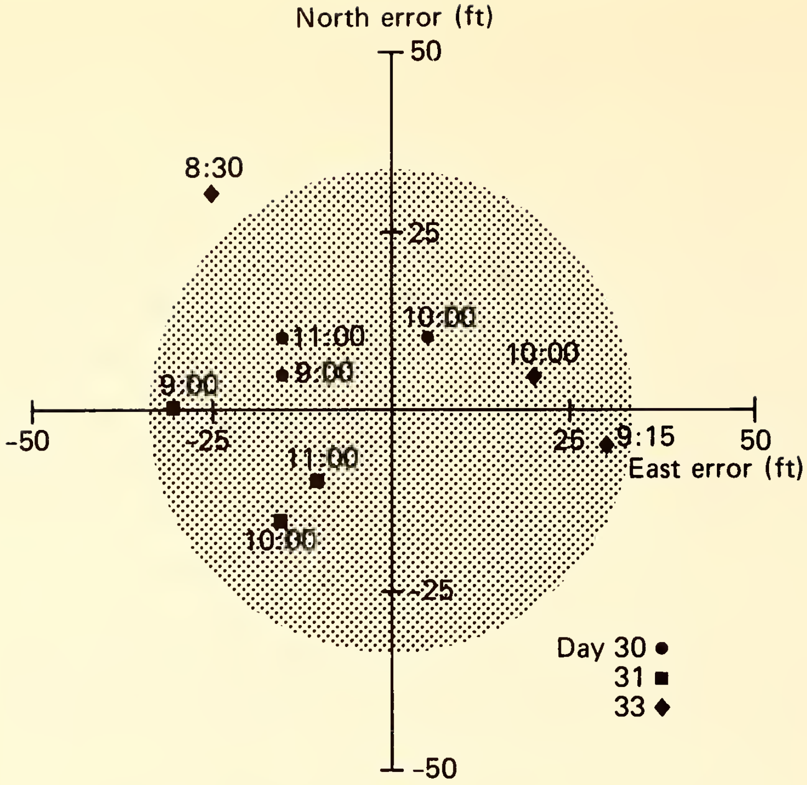

Fig. 7 Typical relative position results.

During the third phase of the program, operational hardware will be fabricated. APL will generate a full set of specifications that the Air Force will use to procure commercial production quantities of transdigitizer and pinger buoys. APL personnel will serve as technical advisors to the Air Force for that procurement. APL personnel will also oversee the fabrication of six sets of aircraft equipment and will generate the operational software.

An Application Study for Using Differential GPS In Airborne Gravity Surveying

William R. Gumert
Gregg F. Wertz
Robert M. Iverson
Carson Geoscience Company
32-H Blooming Glen Road
Perkasie, Pennsylvania 18944

ABSTRACT. Carson Geoscience operates an airborne gravity surveying system in the international arena. One of the major difficulties with this system is obtaining X, Y, and Z position data. Presently much time and expense are expended to provide survey control and to install and operate a groundbased line-of-sight ranging system. As the GPS satellites become more available, it will become necessary to consider their use.

Carson has selected a four-channel Trimble Model 4000A GPS receiver to collect the necessary data for this unique application. Two options of the system are being developed. Initially, Carson will deploy one remote unit to collect data that will be processed differentially with a ground based unit. This option will replace transit satellite positioning that is currently used. Survey time will greatly decrease.

The second option will be to completely replace the present ranging navigation system and to use differential GPS in the dynamic mode. A receiver system has been designed, softfware has been developed, and tests are currently underway.

One of the primary requirements for airborne gravity surveying is the Eotvos correction. This well known correction is a function of the earth's latitude, true ground speed and heading. Tests were conducted by Carson in July 1984 using three Texas Instruments Model 4100 receivers to determine if this correction could be measured. An area over water was selected where the four-satellite GPS positions were compared to data from a Motorola Falcon 484 navigation system. Vertical position of the helicopter was measured by a laser calibrated radar. Adequate Eotvos corrections were obtained from the GPS data during portions of the test.

Carson Geoscience Company operates an airborne gravity surveying system for geophysical exploration and geodetic surveying. This system is used throughout the world. Very precise positioning information is required in latitude (or Y), longitude (or X) and elevation (or Z) because of the nature of gravity measurement. Presently a ground-based ranging system is used to provide the X and Y part of this requirement, and a combination of radar, laser, and precise pressure measurements are used for the Z. Much effort is required to install and position the ground system for navigation control. An auxiliary helicopter must travel to remote locations several times to install towers and other equipment, and to support the Transit satellite equipment used to position this reference station.

One of the primary corrections for airborne gravity surveying is made necessary by the Eotvos effect. This well known correction is a function of the earth's latitude and the aircraft's true ground speed and heading. In order to provide the necessary accuracy for airborne gravity surveying, the heading must be known to better than .05 degree, and the speed to better than .05 knot.

Carson Geoscience decided in early 1984 to investigate the use of the GPS satellites currently deployed and available receivers for measuring the data to compute this Eotvos correction. A test was set up in conjunction with Texas Instruments (T.I.) and the National Geodetic Survey to install a T. I. 4100 receiver on one of Carson's helicopter systems operating in the vicinity of Georgetown, Bahamas.

One unit was placed in the navigation instrument rack of the S-61 survey helicopter. The antenna was located above the rotor blades to avoid any problems with interference of the satellite signals. An area over water was selected where the GPS four-satellite constellation would be available during one of Carson's survey time periods. The regular Carson ground-based navigation system was already deployed in the survey area with good Transit-positioned reference points.

Four ranges from this Motorola Falconer 484 system were received each second during the test flights. Vertical control was established by use of a vertical laser profiler reflecting from the sea surface.

A second T.I. 4100 was located at the airport in Georgetown. Several flights were made. Data from the user solution is all that is available at this time.

This shows the data from the ground station at Georgetown on Julian Day 199. The variation of the position is 25 meters in the north/south direction and 10 meters in the east/west direction. That is a 2 sigma number. There are some larger variations which are due to the loss of lock. Another data day (J.D. 200) at Georgetown shows the same basic distribution of positions, and the 2 sigma values are 25 meters north/south and 10 meters east/west. Each of these data sets represents a time period of about 3 hours when the four-satellite constellation was optimum for the area. A position has been plotted every 5 seconds from the basic user solution information.

One segment of a survey track line is shown here as a plot of the Eotvos correction used for the gravity measurement. The vertical scale is in increments of 10 milligals, a milligal being an acceleration of .001 centimeter per second squared. The black line is the Eotvos correction computed from the Motorola Falconer system which is known to have an accuracy of .02 milligal. The Eotvos correction from the GPS data with the same filter applied corresponds well with the truth data. The maximum departure is 5 milligals with an RMS value of 1.1 milligal.

In this plot of the Eotvos corrections, the general trends are the same but the GPS data displayed a large deviation from the Motorola-derived data in one particular area.

In general the agreement between northings and eastings from both systems is within the 10 to 25 meters that we have seen from the ground station. In one area the GPS position shows a variation over a 10- to 12-minute time period of up to 250 meters. This created an Eotvos correction "bump". It is believed that this variation was created by the poor GDOP of the satellite constellation. In general, it can be concluded that the GPS system, even with current limitations, will give good Eotvos corrections for the airborne gravity system around the 7-milligal range when good satellite geometry exists.

On 3 days of data collected with the user solution at the ground station in Georgetown there was a significant shift in the data. This variation was -50 meters in Z, +60 meters in Y, and -20 meters in X. This change occurred at the midpoint in time of viewing for the four-satellite constellation, and may represent unfavorable geometry when the satellites were at the apex of their orbits with respect to the horizons.

Here is a graphical representation of this change. As can be seen before and after the slope, the X, Y, and Z are relatively constant. In the helicopter at the same time there is a similar variation, but the magnitude is greater, in the order of 3 to 4 times greater. This is what created the Eotvos "bump" shown previously.

These are simply interesting data of a navigation system in its development for a user such as Carson Geoscience. Again, the system will very likely give us excellent Eotvos correction information when GPS is fully deployed.

Carson is developing a system for its airborne geophysical program that starts with a Trimble Model 4000A, C/A code, four-channel receiver. This uinit will form the basis for a ground system that will perform the functions currently carried out by Carson's conventional Transit receivers, and will thus support our Motorola ground-based transponder system. This GPS differential ground system will allow the operator to compute submeter X, Y, and Z position in a short period of time.

This system will be deployed in a small helicopter that will land at a chosen site, and will be left unattended for the time required to determine the position with satisfactory accuracy. Data will be recorded, and when it is returned to the base camp where the second master unit is recording, this information will be processed on site. This equipment will reduce the field time for establishing geodetic control from 5 days to 1 day per site.

Furthermore, Carson is developing a dynamic GPS system to be used as primary navigation when the entire GPS satellite constellation is available. This system, being jointly developed with Theory and Applications Unlimited Corp., will provide real-time navigation to a degree of accuracy sufficient to fly stringent survey grid lines at a selected ground speed. Post-processing, using differential techniqaues, will enhance the data and extract the best accuracy in order to compute position, Eotvos correction, and vertical acceleration.

PERFORMANCE EXPERIENCE OF AND DESIGN GOALS FOR THE SATRACK I & II MISSILE TRACKING SYSTEMS

D. J. Duven, C. W. Meyrick, J. R. Vetter, & M. M. Feen
Johns Hopkins University
Applied Physics Laboratory
Laurel, Maryland 20707

ABSTRACT. SATRACK I was developed for the Strategic Systems Program Office of the U. S. Navy for tracking the Trident I missile test flights. The system uses the GPS L1 signals, a missile-born frequency translator, ground-based receiver/recording stations, and a specialized post-mission processing facility at The Johns Hopkins University Applied Physics Laboratory (JHU/APL) to produce optimal estimates of the missile initial conditions, trajectory, and guidance system errors. The system has been in operation since 1978, and has produced missile performance estimates for over 50 test flights.

The performance characteristics of the SATRACK I system relative to its design accuracy goals of 40 ft and .05 fps (1σ per axis) are reviewed. Since the SATRACK I satellite/missile links are single frequency, a mathematical electron density model must be used to correct for ionospheric range and Doppler errors. The nature and performance characteristics of the model that have been employed are described.

The SATRACK II system is currently being designed for tracking and evaluation of the Trident II missile test flights. The system accuracy goals are 20 ft and .01 fps (1σ per axis). To achieve these goals, it will be necessary to use dual frequency satellite/missile links and other system improvements. The GPS L3 signal has been chosen for this second frequency. The reasons for this choice plus a description of the other system improvements are also reviewed.

The U. S. Navy has been using the GPS satellites to conduct performance evaluations of the Trident I Submarine-Launched Ballistic Missile (SLBM) system since 1978. The system for performing these evaluations is known as SATRACK I. The concept of using a satellite navigation system to perform missile tracking and evaluation was proposed to the Navy by the JHU/APL in 1973 (Thompson 1980). Approval to begin development of the system was granted in 1974, and the system became operational in 1978 during the latter part of the Trident I developmental flight test program. The Navy is now preparing to upgrade the system so that it will be capable of providing similar tracking and evaluation of the Trident II SLBMs. This system will be known as SATRACK II. The goals, structure, performance, and analysis results for both of these systems are described in the remainder of this paper.

SATRACK I

The background behind the development of the SATRACK I system, a description of the system that was implemented, a discussion of the ionospheric and tropospheric compensation techniques that were employed, and a summary of the performance results that have been obtained are described in the following subsections.

System Description

In 1973, the U. S. Navy initiated an "Improved Accuracy Program" to gather detailed information on the accuracy performance of the Trident I SLBM system. The objective of this program was to obtain sufficient information on the missile design factors which affect accuracy such that future designs could achieve improved accuracy. One of the many difficulties in doing this was the requirement to gather accurate information on the in-flight performance of the missile's guidance system during realistic test flights. The Applied Physics Laboratory proposed that this information could best to obtained via a satellite-based navigation system which would provide ranging information of sufficient accuracy to determine the error characteristics of the missile's guidance system. It was initially proposed that a constellation of modified Transit-type satellites be used for this purpose, but the program was subsequently directed to employ the GPS satellites that were being developed at that time.

The basic concept behind the operation of the system is shown in Figure 1. The satellites radiate phase modulated signals at the GPS L1 frequency (1575.42 MHz). These signals are received by the missile, translated up in frequency to S-band, and re-radiated to a pair of support stations in the missile test area. The support stations receive the translated signals, heterodyne them down to base-band, and record the signals on high-rate tape recorders. The recorded signals are then tracked via a multi-channel Post-Flight Receiver (PFR) which contains digital phase-locked loops (PLLs) and delay-locked loops (DLLs) for extracting the Doppler and range information from the signals.

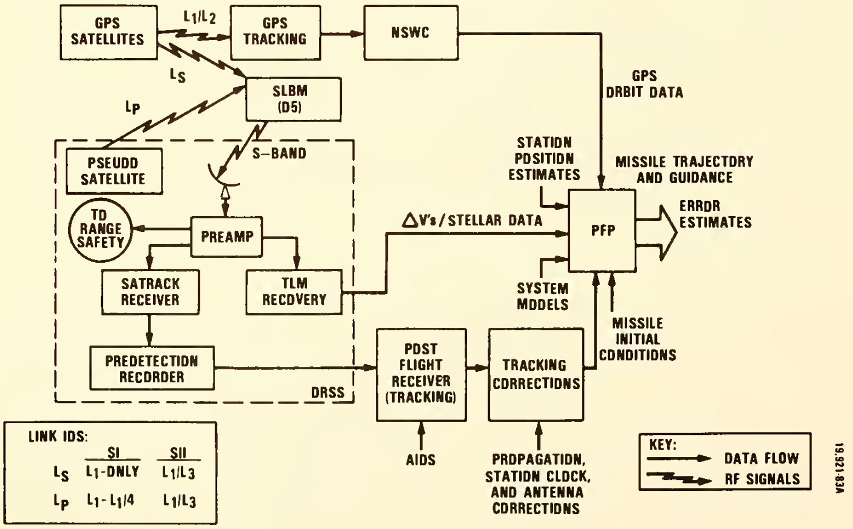

Fig. 1 SATRACK I(SI) and SATRACK II(SII) system configurations.

The missile-borne equipment was chosen to be a simple frequency translator, rather than a full receiver, for several reasons. First, the cost of a translator is considerably less than the cost of a full receiver, which is important because the equipment cannot be recovered and reused. Secondly, the translator is capable of translating and relaying to the support stations all the signals that are incident on the missile; in other words, the number of signals that can be used is not dependent on the number of channels that are implemeneted as would be the case if a full receiver were used. Thirdly, the system is not dependent on the ability of the missile hardware to quickly acquire and track the signals. The tracking can be done post-flight, and can be retracked many times, if necessary, to gather the maximum amount of available data.

The translator responds to the GPS L1 frequency (±1 MHz). This bandwidth is sufficient to pass the C/A portion of the L1 signal, but not the P-code modulation. This restriction was necessary because the downlink bandwidth allocation for the missile was not wide enough to permit translation of the full 20 MHz wide P-code. In addition, the RF output power that would have been required to transmit the wider P-code bandwith would not have been feasible. The translator was also designed to respond to a second frequency at 393.855 MHz (1/4 th the GPS L1 frequency) with a bandwidth of ±100 kHz. This signal, plus a companion signal at the L1 frequency (with a C/A code which is different from satellite C/A codes), is transmitted from one or more ground-based pseudosatellites (PSs) for the purpose of obtaining electron content data for the ionosphere. The GPS L2 signal (@1227.6 MHz) was not chosen for this purpose because the satellites ordinarily use only the P-code modulation for this signal, and therefore would require too much downlink bandwidth. There are provisions to switch the L2 signal from P-code only to C/A-code only, but this option was considered to be too disruptive to other users of the GPS system to be viable for the baseline SATRACK system. The RF links from the satellites are therefore single frequency L1, whereas the links from the ground-based PSs are dual frequency L1-L1/4. The pseudosatellites had the added benefit of providing additional RF links to the missile which tended to improve the GDOP and supplement the GPS constellation when it was in the early phases of build-up.

The antenna system on the missile consists of four discrete slot antennas for the L1 signals, two slots for the L1/4 signals, and four slots for the S-band transmitting antennas. The antennas are mounted under the nose cone in the Equipment Section of the missile. The L1 and S-band antennas are uniformly spaced at 90° increments around the roll-axis of the missile, and the L1/4 antennas have 180° spacing. The signals from opposite pairs of L1 antennas are electrically summed, thus forming a pair of L1 signals that are then multiplexed (@ 434 Hz) into a single signal for the L1 channel of the translator. The L1/4 signals are likewise summed and applied to the L1/4 channel of the translator. The summing process results in interference phenomena for both input signals. However, the partial shielding provided by the body of the missile to the antennas that are oriented away from the incident signal reduces this effect somewhat, and results-in reasonably interference-free reception for one L1 pair or the other over a substantial portion of the test flight. The S-band output from the translator is equally divided and applied to each of the four transmitting antennas. This, of course, also results in interference of the received downlink signal at the surface station receivers, and tends to be somewhat more severe because at least two S-band transmitting antennas are generally visible to each receiver at all times. These interference effects were identified as program risks at the time of the SATRACK I system design, but were considered necessary because of the need for minimal impact on the missile design which was nearing completion at the time that the SATRACK program began.

The post-flight processing system at APL consists of the post-flight digital receiver (PFR), software for correcting and editing the tracked data produced by the PFR, and a large extended Kalman filter/smoother (the Post-Flight Processor, or PFP) which compares the range and Doppler data produced by the SATRACK system with what would have been expected based on the guidance system telemetry information, and allocates those differences to approximately 50 different error states (see Figure 2). The result is both an optimal estimate of the actual trajectory flown by the missile, and estimates of the guidance system and initial condition errors. The guidance system errors include such items as accelerometer biases and scale factor

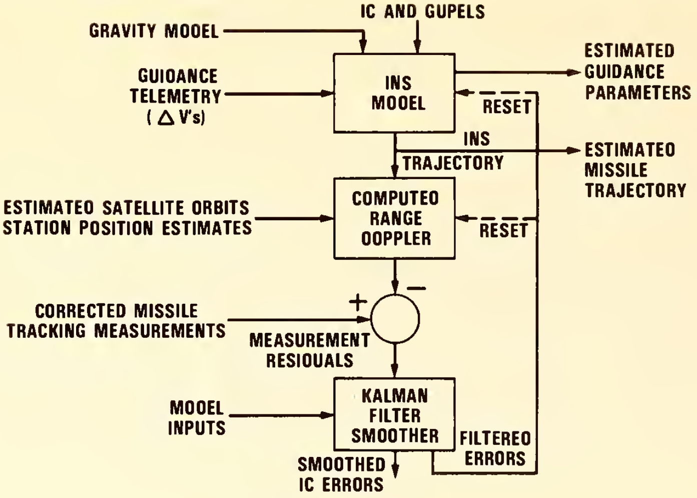
IC AND GUPELS
GRAVITY MODEL
GUIDANCE TELEMETRY (ΔV's)
INS MODEL
RESET
ESTIMATED GUIDANCE PARAMETERS
INS TRAJECTORY
ESTIMATED MISSILE TRAJECTORY
ESTIMATED SATELLITE ORBITS
STATION POSITION ESTIMATES
COMPUTED RANGE DOPPLER
RESET
+
−
CORRECTED MISSILE TRACKING MEASUREMENTS
MEASUREMENT RESIDUALS
MODEL INPUTS
KALMAN FILTER SMOOTHER
FILTERED ERRORS
SMOOTHED IC ERRORS

Fig. 2 Post flight processor block diagram.

errors, gyro drifts, non-orthogonalities, etc; whereas the initial condition errors include the errors in initial position, velocity, and orientation. This information is examined on each flight, and over an ensamble of flights, to arrive at the accuracy assessment for the Trident I system.

Iono/Tropo Compensation

Both the ionospheric and tropohsheric portions of the Earth's atmosphere cause variations in the velocity of propagation of the SATRACK RF signals. As a result, the range and Doppler measurements obtained from the system are perturbed from the values that would have been obtained in a pure vacuum, and require compensation.

The ionospheric effect results from the free electrons which occupy the upper atmosphere. The first-order group and phase path-length effects have opposite sign, and the effects are inversly proportional to the square of the carrier frequency. As a result, it is possible to either measure or perfectly compensate for the first-order ionospheric effect on an RF link if two carrier frequencies are used. This fact is often exploited in radio-navigation systems, but for the reasons listed in the previous section, this was not possible for the SATRACK I system on the satellite/missile links. It was therefore necessary to calculate the ionospheric compensations for these links from a mathematical model of the electron density of the ionosphere. The model used is a complex function of latitude, longitude, altitude, time, season, and solar activity, and is described in detail in the references (Pisacane and Feen 1972 and 1974).

The model is adjusted to match the characteristics of the ionosphere in the area and time of the missile test by adjusting the solar activity parameter to obtain a best fit to the dual frequency PS-to-missile range and Doppler measurements. The corrections that are obtained on the single frequency satellite-missile links are very sensitive to the vertical structure of the ionosphere. For example, two Chapman profiles which differ by only 1.7% or 5 km in the height at which maximum density occurs (which would ordinarily be considered good) can result in rate errors of as much as 0.14 fps for links with low elevation angles. These types of errors are inconsistent with the 0.05 fps accuracy goal for missile velocity determination. As a result, it has been necessary to establish a 15° cutoff in elevation angle for the satellites, and to edit-out substantial portions of the collected data so that it does not corrupt the PFP estimates. The only way to assure that the ionospheric corrections have the required accuracy is to have dual frequency data on all links, which is what is being implemented for the SATRACK II system.

The tropospheric effect, since it is not dispersive, must be compensated via a mathematical model. The model that is used in SATRACK I is the Hopfield two-quartic model (Hopfield 1969, 1971 and 1976), which gives the refractivity of the troposphere as function of height with surface temperature, pressure, and relative humidity as parameters. The range corrections are based on straight line integration of this profile between the two end-points of a link, and special curvature and profile error corrections are applied when the elevation angle is less than 15° (which is allowed on the dual frequency PS-missile links). Experience, to date, with this model has been satisfactory and is expected to continue to be so even with the tighter accuracy requirements of the SATRACK II system.

Performance Results

An assessment of more than fifty flight test results from the PFP has allowed a precise evaluation of the trajectory errors observed during the powered flight phase. These evaluations, conducted on a per-flight basis, have shown remarkable consistency in providing RSS position and velocity accuracies of better than 35 ft and 0.09 fps, respectively, over the ensemble of flights since the inception of the program. These meet the original (1σ) accuracy goals for trajectory estimation of 40 ft and 0.05 fps (per axis), and reflect the present state of understanding of the SATRACK system as represented by its mathematical model in the PFP.

The most significant source of error during the boost phase of flight is the single frequency ionospheric residuals on the satellite links. This is particularly true during the period of flight between 150 - 300 seconds for satellite links with low elevation angles. The range-rate residuals are particulary critical since the range-rate measurements are the predominant data type for recovery of estimated guidance parameters during the high dynamic portion of flight. Because of only partial success in compensating for these single frequency ionospheric effects, the data is judiciously discarded whenever the PFP residuals are too large. Typically, residuals greater than 0.05 - 0.10 fps are not tolerated, and are weighted out of the solution. With the present GPS Block I constellation, at least one satellite is generally at a sufficiently low elevation angle to result in data that is unusable for approximately half of the test-flight period.

Independent assessment of performance is obtained from a wide range of consistency tests performed on various sub-categories in the test program. These include consistency of the PFP estimates with other independent measurement systems, observability and separability of fundamental guidance error sources, and statistical tests conducted on the tracking residuals. The results of the consistency analysis performed in the launch regions in widely different operating areas in the Atlantic and Pacific oceans have shown accuracies to the level of 50 ft. Comparisons of the estimated predeployment state vectors (projected to impact) with transponders in the impact areas have shown consistencies to better than 500 feet. Bayesian estimation recovery ratios of better than 0.50 have been determined across the board for all grouped error categories with best observability experineced in the position, gyro, total guidance, and total initial condition categories. The impact residuals show a relatively small bias (that is not statistically significant for the current sample population size) and a standard deviation that appears to be completely consistent with the PFP covariance results. It therefore appears that the SATRACK I system has achieved its initial 1σ accuracy goals of 40 ft and 0.05 fps (per axis).

SATRACK II

The SATRACK I system is currently being upgraded to the SATRACK II system for support of the accuracy assessment of the Trident II missiles. The accuracy requirements have been substantially tightened [20 ft(1σ) in position and .01 fps(1σ) in velocity, per axis], and the processing turn around times have also been reduced. The following sections describe the system that is being implemented and provide some simulation-analysis results that have been obtained for the system.

System Description

The basic configuration of the SATRACK II system is identical to SATRACK I: satellite and pseudosatellite radiators, missile-born translators, high-rate recording of the data at the surface stations, and post-flight processing at APL. The system will be modified to reduce or eliminate the two principal error contributors in SATRACK I: ionospheric residuals on the satellite-missile links and missile antenna residuals.

The ionospheric errors on the satellite-missile links will be eliminated by the addition of a second frequency, the GPS L3 signal at 1381.05 MHz. This signal can be commanded into the C/A-only mode for several hours per day without substantial impact on other users of the system. Therefore, the second channel of the SATRACK II translator will be designed to pass the GPS L3 frequency (±1 MHz) rather than L1/4. Unfortunately, the frequency separation between L1 and L3 is rather small. As a result, the thermal jitter noise and antenna phase residuals are magnified considerably when the dual frequency correction is made. However, it has been found that the elimination of the systematic ionospheric residuals at the price of increased noise is an advantageous tradeoff, particularly for the portion of the trajectory when the missile is passing through the peak electron density portion of the ionosphere.

The missile antenna system is also being revised. The slot-type antennas will be replaced by ring antennas. The receiving antenna will be a dual freuqency L1/L3 microstrip antenna, and the S-band transmitting antenna will be a slotted waveguide. It is anticipated that this change will greatly reduce the interference effects that were observed in the SATRACK I system. The PFR trackers should therefore be able to maintain lock for longer spans of time, and the residuals that remain after compensation for antenna phase effects should be smaller.

The larger number of satellites that will be available from the GPS Block II constellation will also be of benefit. When the constellation is fully established, the 1-2 hr windows that are now characteristic of the SATRACK I system will be lengthened to nearly 24 hrs. Also, the average PDOP will be reduced by a factor of 1.5 - 2.0 on the surface, and even more at higher altitudes when more satellites are visible to the missile. Some of these satellites will, of course, be at very low elevation angles. The ionospheric effect on these links will consequently be very large, and could not be adequately compensated without the use of dual frequency measurements.

The SATRACK processing facility at APL is also being revised to enhance the accuracy and turn around capabilities of the system. The Post Flight Receiver will be upgraded so that up to 12 dual frequency links can be tracked simultaneously. Also, for increased accuracy, the basic design of the loops will be modified to be nearly identical to the system that has been implemented for the GPS/SMILS system (see the companion paper by Westerfield in this conference). The processing software will be modified to use the dual frequency link measurements to full advantage and to enhance the system turn around time. This will principally be accomplished through the use of automatic editing and interactive user interfaces.

The ionospheric compensation procedure will be a three step process. The first step will be the extraction of the ionospheric range and delta-range refraction effects at L1 from the dual frequency measurements:

$$\rho_I^* = (\rho_2^* - \rho_1^*)/(\gamma^2 - 1) \tag{1}$$

$$\Delta\rho_I^* = (\Delta\rho_2^* - \Delta\rho_1^*)/(\gamma^2 - 1), \tag{2}$$

where ρ_1^*, ρ_2^*, $\Delta\rho_1^*$, and $\Delta\rho_2^*$ are the measured L1 and L3 range and delta-range values, ρ_I^* and $\Delta\rho_I^*$ are the calculated ionospheric range and delta-range refraction effects, and γ is the L1/L3 frequency ratio with a numeric value of 1.14074. Since this value is so close to 1, the $(\gamma^2 - 1)$ factor in the denominator of these equations is very small and causes the noise components in the range and delta-range measurements to be magnified. The second step will be to smooth the resulting ionospheric range and delta-range values. The ionospheric ranges will be smoothed via a process called "Doppler smoothing of range" which is described by the following two equations:

$$\hat{\rho}_I(t_o) = (N + 1)^{-1} \sum_{i=o}^{N} \left[\rho_I^*(t_i) - \sum_{k=1}^{i} \Delta\rho_I^*(t_k)\right] \tag{3}$$

$$\hat{\rho}_I(t_i) = \hat{\rho}_I(t_o) + \sum_{k=1}^{i} \Delta\rho_I^*(t_k) . \tag{4}$$

This process uses the ionospheric delta-range values to define the shape of the ionospheric range compensation curve, and the measured ionospheric ranges are only used to define the initial starting value. The procedure to be used in smoothing the ionospheric delta-ranges has not yet been selected. The third step in the compensation process will be to subtract the smoothed ionospheric range and delta-range values obtained in step two from the L1 range and delta-range measurements, respectively. Small higher-order terms in the ionospheric refraction model will also be calculated and passed on to the PFP Kalman filter for ionospheric residuals modelling.

The system will also be required to compensate the ionospheric effect on the single frequency Block I satellites. This will be done via the mathematical model that was used for SATRACK I, and will be subject to the same difficulties that were experienced in that system. However, the results are expected to be somewhat better since the dual frequency Block II satellites, as well as the ground-based pseudo-satellites, are used to estimate the solar index parameters.

Performance Analysis

Much of the system design activity, to date, has been concerned with the specification of subsystem performance requirements and processing software requirements to enable the SATRACK II system to meet its basic accuracy and turn around requirements. The results of some of the analyses that have been conducted in support of this activity are summarized in this section.

One of the areas of concern has been the trackability of the translated signals. The GPS signals, particularly the L3 signal, are rather weak and require the use of narrow bandwidth tracking loops. In SATRACK I, 10 Hz second-order PLLs were used to track the GPS L1 signals. For SATRACK II, analysis of the link noise characteristics indicates that PLL bandwidths of 3 - 6 Hz will be required to track the L3 signals with high reliability. In both systems, aiding information derived from the telemetered guidance data are required to help the loops follow the high translational dynamics of the missile's motion. In SATRACK II, the loops will probably be increased to third-order to ease the aiding requirements somewhat. However, the unpredictability of the antenna phase effects places a lower limit on the PLL bandwidths which is not much less than the 3 Hz lower limit for achieving satisfactory noise performance.

The gain and phase characteristics of an engineering mockup of the ring antenna have been analyzed for their impact on SATRACK II performance. The gain is variable and has a range of approximately -3 to -15 dBic. The gain is reasonably constant in the equatorial portion of the missile's radiation sphere, but significant variations do occur in the nose and tail regions. This is probably due to interference effects between the front and back sides of the ring. Also, because of other mechanical constraints within the equipment section, an 8-inch section of the ring has had to be deleted, and this causes some variation of gain with respect to the roll angle in all portions of the radiation sphere. The net effect is a 90% coverage gain of -12 dBic for the L1 and L3 frequencies, and -11.5 dBic for the S-band antenna. The antenna phase characteristics, at all three frequencies, are dominated by a sinusoidal variation with respect to the angle from the nose of the missile to the line-of-sight (LOS) vector for the signal, which indicates that the effective phase center of the antenna is near the edge of the ring. The processing software will compensate for this when the Doppler measurements are processed. The phase residual that remains has an RMS uncertainty of approximately 14° for L1-only processing and 52° for dual frequency combined processing. Other phase compensation models will be investigated in the future to attempt to reduce these residuals somewhat.

A detailed simulation of the operation of the PFR in response to the SATRACK II signals has recently been completed. The simulation includes the effects of missile translation, antenna phase and gain variation, ionospheric and tropospheric errors, and thermal noise. The purpose of the simulation was to verify that the signals are trackable and to investigate the performance of the proposed ionospheric processing algorithm. Other questions such as the advisability of cross-aiding the L3 loops from the L1 loops are also being investigated. It has been found that the signals are generally trackable, although some difficulty may be expected when the LOS vectors pass through the region of the 8-inch missing section of the ring antenna. The "Doppler smoothing of range" algorithm has been found to work well as long as the Doppler measurements are continuous. An algorithm to "fill in the gaps" is currently being developed to handle the dropouts. This algorithm will probably also be used to perform data smoothing on the ionospheric delta-range measurements. The dominant error source in this case appears to be the antenna phase residuals rather than thermal noise.

Covariance analyses have also been conducted with a preliminary version of the SATRACK II PFP. The results indicate that the system will meet its accuracy goal of 20 ft and .01 fps (1σ, per axis) when the GPS constellation is fully established. However, in the early phase of testing the constellation will be only partially established, and the position and velocity uncertainties will be several times greater than the desired accuracy goal values. The coverage and accuracy performance is also strongly influenced by the sequence in which the 18 slots of the constellation are filled. This is primarily because of time-of-day constraints imposed by other testing considerations in the Trident II test program. The build-up scenario is part of the Navy/Air Force coordination activity.

CONCLUSIONS

The SATRACK I program has been successful in providing accuracy assessments of the Trident I SLBM system. The SATRACK II program is currently being designed to provide similar accuracy assessments of the Trident II test missiles. Preliminary analyses indicate that the accuracy goals that have been established for this system will be met.

REFERENCES

Hopfield, H. S., 1969: Two-Quartic Troposheric Refractivity Profile for Correcting Satellite Data, J. Geophys. Res., 74(18), 4487-4499.

Hopfield, H. S., 1971: Troposphric Effect on Electromagnetically Measured Range: Prediction from Surface Weather Data, Radio Science, vol. 6, 357-367.

Hopfield, H. S., 1976: Tropospheric Effects on Signals at Very Low Elevation Angles, Rep. TG-1291, Appl. Phys. Lab. Johns Hopkins Univ., Laurel, Md.

Pisacane, V. L. and Feen, M. M., 1972: Prediction Techniques for the Effect of the Ionosphere on Pseudoranging from Synchronous Altitude Satellites, Rep. TG-1197, Appl. Phys. Lab. Johns Hopkins Univ., Laurel, Md.

Pisacane, V. L. and Feen, M. M., 1974: Propagation Effects at Radio Frequency on Satellite Navigation Systems, Proc. AIAA 5th Communications Satellite Systems Conference, 22-24 April 1974, Los Angeles, Cal.

Thompson, T., 1980: Performance of the SATRACK/Global Positioning System Trident I Missile Tracking System, Position Location and Navigation Symposium, December 1980, pp. 445-449.

REAL-TIME GPS TRACKING FOR PEACEKEEPER TEST FLIGHTS

Edward P. Oppenheimer,
Dennis J. Duven and
Edwin E. Westerfield
Johns Hopkins University,
Applied Physics Laboratory,
Laurel, MD 20707

John B. McConnell
U.S. Air Force, Headquarters
Western Space and Missile Center,
Vandenberg AFB, CA 93437

ABSTRACT. Recently JHU/APL completed a study investigating real-time GPS tracking of Peacekeeper (MX) missile test flights. Since strict accuracy requirements were dictated by range-safety constraints for flights into the Kwajalein Lagoon, various tracking configurations were analyzed. Following a brief description of missile tracking experience, system configurations are described. Remote site processing concepts are discussed and attention is directed to ionospheric error correcting methods and receiver phase lock loop thermal noise. Finally, temporal covariance simulation results for the instantaneous impact point (IIP) are presented.

INTRODUCTION

In December of 1981 the Western Space and Missile Center (WSMC), Vandenberg AFB, CA, requested that the Johns Hopkins University/Applied Physics Laboratory (JHU/APL) investigate the feasiblity of real-time tracking of the Peacekeeper missile test flights with the GPS. The purpose of the tracking system would be to provide data for the range-safety missile flight control function, and possibly for post-flight weapon system error analysis. The missile-borne GPS Translator concept was considered, in view of the APL experience with SATRACK (SAtellite missile TRACKing system) which supports the U.S. Navy Trident accuracy evaluations. Any design concept was to be universal and adaptable to other ballistic missile programs. Stringent tracking accuracies, solution rates and timing requirements consistent with test flights into the Kwajalein Lagoon were suggested and other support system parameters were furnished for the study.

EXPERIENCE

SATRACK is a unique system developed for the Strategic Systems Program Office of the U.S. Navy, providing range metric tracking instrumentation for the Trident Improved Accuracy Program. It has been configured to provide precision post-flight trajectory reconstruction of Trident I missile test flights. Signals from the GPS (L1 C/A) are received by the in-flight missile, amplified, two MHz band-limited, hard-limited, frequency translated to the downlink telemetry frequency, and wideband recorded at remote data collection sites for post-flight playback and processing.

System testing began in mid-1978 with Trident I development missiles launched from Cape Canaveral. Submarine launched test flights began in early 1979 and continue to the present date. As depicted in Figure 1, the LASS and DRSS (Launch Area and Down Range Support "Ships") serve as data collection sites for the translated GPS signals. The DRSS also functions as a "pseudosatellite", transmitting GPS-like L1 and L1/4 C/A signals for the additional purpose of post-flight ionospheric sounding and refraction modeling. Missile tracking is accomplished by measurements relative to the GPS, including both code tracking (range) and despread carrier tracking (delta-range or integrated Doppler phase). The measurements are employed in a large scale Kalman filter for post-flight weapon system error analysis. An improved SATRACK II system is currently under development at APL for the Trident II Program (reported in these proceedings).

In contrast to the SATRACK Translator implementation, a new concept employing a "Transdigitizer" is under development at APL for the U.S. Air Force GPS/SMILS Project (reported in these proceedings), where the received GPS signals are amplified, band-limited, hard-limited, and digitized at a two MHz rate. The digital data stream is then similarly transmitted on a downlink frequency.

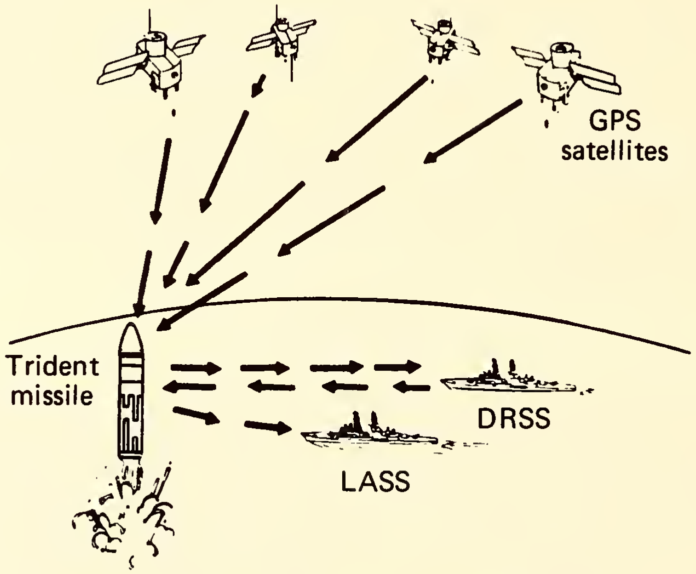

Fig. 1 SATRACK measurement concept.

SYSTEM CONFIGURATIONS

Various system configurations were considered in the MX real-time tracking feasibility study. To a large extent, the study thrust was driven by the system requirements:

Missile rms point estimate accuracies
position - 100 ft.
velocity - 0.1 fps
Estimation rate - 20 sps
Estimation delay - 100 ms or less
Estimate time tags - 100 microsec. of range (abs.)
Preferred tracking - independent of MX IG data
Solution duration - 500 sec. after launch

As a result of APL experience in post-flight GPS tracking of Trident test flights, the large dynamic ionospheric refraction effects on range and delta-range measurements for a ballistic missile traveling through the ionosphere became an immediate concern. Dual-frequency systems were therefore included for first-order correction of ionospheric refraction. On the other hand, because combining dual-frequency code and carrier measurements to remove ionospheric effects results in a magnification of thermal noise (tracking jitter), single-frequency systems employing ionospheric model corrections were necessarily included.

System Hardware

Hardware for the various system configurations may be subdivided into missile-borne, remote receiving site, and central processing facility categories. These are discussed briefly in the following subsections.

a. Missile-Borne

All system configurations assume that the MX IFSS (in-flight safety subsystem) Triband ring antenna will be available. Three distinct electronic mechanizations were included:

1) The analog SATRACK type Translator, which functions to receive L-band C/A GPS transmissions, amplify, two MHz band-limit, hard-limit, heterodyne to S-band, and then amplify for downlink transmission to the remote receiving sites. The L1 and L3 dual-frequency implementation can be configured for overlay, where the second input frequency is initially heterodyned to a frequency near L1 and then summed with L1 for the usual Translator function. Or, separate L1 and L3 or L1/4 Translators may be flown where each has its own center-frequency on the S-band downlink. In all cases, the missile oscillator pilot carrier is also placed on the downlink.

2) The Transdigitizer, which receives the L-band C/A GPS signals, amplifies, down converts to baseband and band-limits, and then separates to I and Q (in-phase and quadrature) components which are each zero-crossing detected at a two MHz rate and placed on the downlink as a digital data stream by 80 degree phase modulation, preserving a small carrier residual. In this sense, the in-flight Transdigitizer performs part of a remote receiving site function. Dual-frequency operation could employ overlay or separate channel techniques with the attendant eight MHz downlink bandwidth (double the digital and quadruple the analog, single-frequency operations).

3) The Transmodulator, where the L1 C/A GPS signals are down-converted to baseband and directly phase modulate the downlink S-band carrier. Information bandwidths (BWs) are the same as the Transdigitizer cases.

In contrasting the three forms, the field proven Translator requires high DC powered Class A output stages while the other techniques can employ efficient Class C operation. (Recent testing has demonstrated that under special circumstances, the Translator can also be operated Class C. See reference SDO-7377.) The Translator requires half the transmission BWs while the Transmodulator complexity is minimal. The Transdigitizer, presently undergoing field testing, lends itself to encryption if required.

b. Remote Receiving Sites

The proposed systems assume that the remote telemetry receiving sites are also available for real-time tracking purposes. These are located at Pillar Point (near San Francisco), Point Mugu, and Oak Mountain (near Vandenberg). The hardware at these sites will uniquely depend on the missile-borne mechanization. In each case a diplexor will be necessary to separate the missile telemetry stream from the translated, transdigitized, or transmodulated tracking signals in the S-band downlink. (Details of the Translator and Transmodulator remote site front-end receiving operations are contained in reference SDO-6990.)

Once the "Pilot Carrier" and I and Q signals are separated and formed, they are fed to a formatter/8-phase modulator which drives a two MHz BW microwave link. ("Pilot Carrier" here implies that a synch word is included with the original pilot carrier. The synch word is used at the microwave link terminus to identify and separate the I and Q data.) Dual microwave links will be necessary for transmission of both RHCP and LHCP single-frequency operation data and quad microwave links will be required if dual-frequency operation is also implemented. The latter would be the case where high accuracy post-flight metric tracking is to be accomplished.

c. Central Processing Facility

Data from each remote site microwave link is received at the central facility where it is fed to an 8-phase demodulator. The demodulator output is fed into digital receiver groups (6-satellite capability) where the signals from each satellite are tracked, providing pseudo range and delta-range measurements. Incorporated within each receiver group is a fast-acquisition channel which is multiplexed among the six satellite receivers to provide very fast (less than one second) acquisition or re-acquisition for the individual receivers.

A central facility microprocessor and data multiplexer will provide automatic decisions, controlling which remote receiving site tracking data is desired and transmitting this data to the real-time navigation computer. As an additional function to insure that the system is highly reliable, a premission readiness mode will be incorporated which includes self-tests of each major equipment within the operating system. The premission tests will also include tracking of simulated signals which are generated by a satellite signal simulator.

System Analyses/Tests

Various analyses, simulations and tests were conducted in support of this study. Since APL has a complete Trident I test flight data base, certain tests could be conducted with actual recorded GPS/ballistic missile data. Similarly, simulation could be conducted employing real geometries. The results of some of these analyses are discussed in the following paragraphs.

a. Tests

Two tests were conducted with the existing SATRACK I digital post-flight receivers (PFRs). Since it was preferred that the real-time system be independent of IG data, the first test was conducted to explore performance of the PFR when the phase lock loops (PLLs) were configured 3rd-order (a software option). The results demonstrated successful tracking without link path-length aiding. (Occasional dropouts were caused by discrete Trident I non-ring antenna interferrometer effects.) The dynamic link tested was for NS-5 (NavStar 5) recorded at Grand Bahamma Island (GBI) for the 1980 DASO-5 (Demonstration And Shakedown Operation 5) test.

A test depicting delayed aiding was conducted with the PFR configured for 2nd-order PLL operation. (Aiding MX IG data would be delayed at least 50 ms due to the telemetry system operation.) OT-2W (Operational Test 2, missile "W") data from the 1980 flight were used and aiding delays of 0, 50, 100 and 150 ms were tested. Results demonstrated unacceptable real-time tracking performance with aiding delays of 100 ms or more.

b. Simulation

Concern for the performance of a tracking system which functions without MX IG data, especially during dynamic missile staging events, prompted a simulation study of 2nd and 3rd-order PLL performances. Analog PLLs were formulated in linearized discrete state-variable form where the input signal is total satellite/pseudosatellite to missile path length phase. The linearized PLLs are depicted in the frequency domain by the block diagram of Figure 2, where $F(s)=(1+a/s)^p$, and p=1 or 2 for 2nd or 3rd-order.

The input data was obtained from the 1980 DASO-6 flight. The PLLs were designed for 0.707 damping ratios, which constrains the amplifier gain (a) and the VCO gain (K). If these are selected to limit the transient and steady-state PLL error responses to a maximum of 30 degrees (based on typical missile dynamics), the loop equivalent BWs are so large that thermal jitter will be a problem. Therefore, reasonable 2nd and 3rd-order BWs were selected as 20 and 15 MHz, which defines the gain values.

Figure 3 provides the noise-free simulation PLL error responses for a dynamic link (GBI to missile) time interval which includes the 3rd staging event. It is apparent that without aiding the 2nd-order PLL fails severely, while 3rd-order is satisfactory.

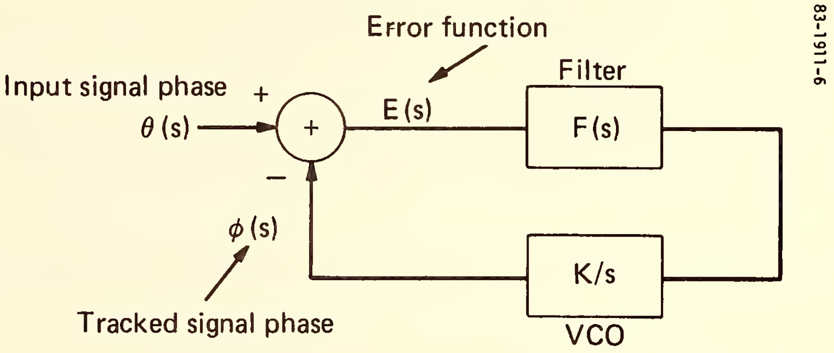

Fig. 2 Linearized PLL block diagram.

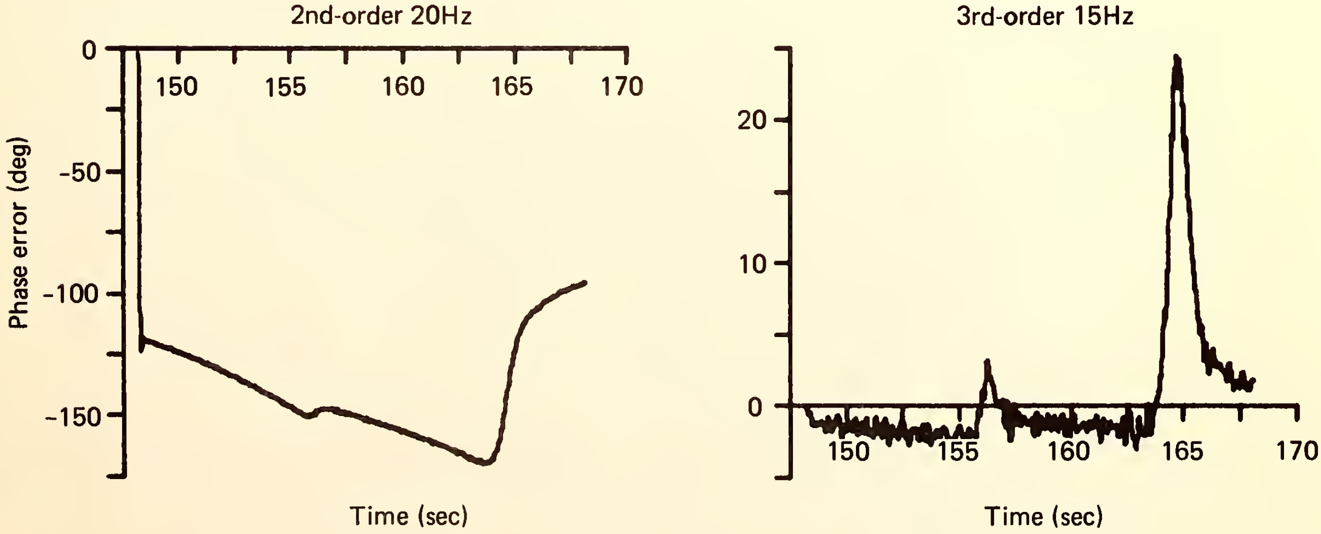

Fig. 3 Simulated unaided 2nd and 3rd-order PLL errors.

c. Analyses

The various analyses conducted to support this study are discussed briefly in the following paragraphs. It was necessary to complete certain ancillary tasks in support of the IIP covariance simulations and these are also included in the discussion.

Because the full GPS constellation would not be initially available for MX tracking, a Positional Dilution of Precision (PDOP) study was conducted to determine the pseudosatellite enhancement to the current satellite performance levels. The constellation of five GPS satellites available on the day of the 1982 DASO-14 test was "rotated" for support of the WSMC furnished MX KMRN-6 (Kwajalein Missile Range North) simulated flight. Augmenting pseudosatellites were assumed at Point Mugu, Pillar Point and Makaha Ridge, Kauai, Hawaii. The missile exceeded four degrees elevation angle for these sites and entered the PDOP solution at 45, 70, and 390 seconds into the flight, respectively. Figure 4 demonstrates the substantial improvement in tracking PDOP when the three pseudosatellites (PSATS) are added to the given five satellite GPS (SATS) coverage.

In order to conduct the weighted least squares point estimation covariance analyses, it is necessary to determine the statistical range and delta-range measurement one-sigma noise levels. These are the composite effect of the missile-borne electronics front-end thermal noise, the low GPS effective incident power at the missile, L-band antenna loss, downlink loss, receiver DLL (delay lock loop) and PLL equivalent BWs, and sampling loss. (Development of topics mentioned in this section would be too extensive to be included here. They are fully described in reference SDO-6990.)

The raw one Hz DLL single (1f) and dual (2f) frequency range noises are given in the following table:

1f	Range(ft.)	2f	Range(ft.)
GPS(L1)	30.1	GPS(L1-L3)	226
GPS(L3)	55.4	PSAT(L1-L1/4)	6
PSAT(L1,L3,L1/4)	5.4	PSAT(L1-L3)	29

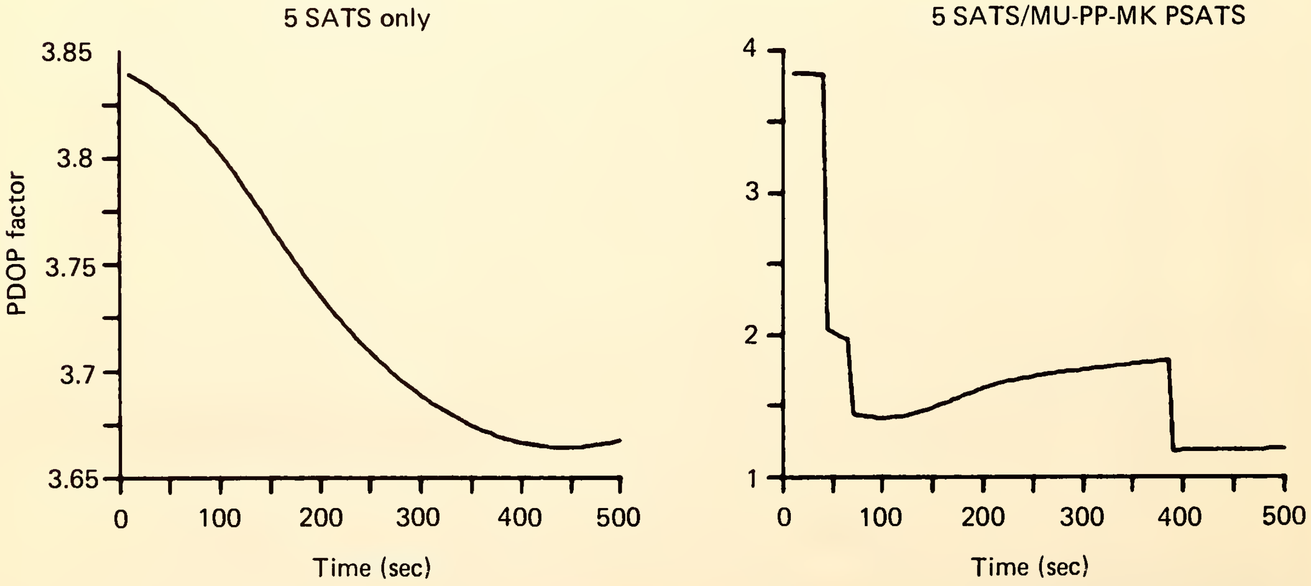

Fig. 4 PDOPs for MX KMRN-6 simulated flight.

The closeness of the GPS frequencies causes large dual-frequency combined noises, while the greater pseudosatellite signal strength results in values lower than GPS. Since the estimation rates are greater than one sps, the one Hz DLL BW correlation prevents smoothing of either single or dual-frequency thermal noise levels.

Compared to range, the delta-range noises are very small. For a GPS(L1) link the 20 Hz PLL value is 0.014 ft. Dual-frequency combining to correct 1st-order refraction magnifies the noise levels. Then, combining the dual-frequency combined PLL errors at each end of the Doppler count interval results in total delta-range GPS(L1-L3) noise of 0.162 ft. When expressed as a velocity for a 20 sps (50 ms) solution rate, this is seen to be an excessive 3.24 fps, relative to the required system accuracy. However, the higher PLL BWs (shorter decorrelation times) and the system 100 ms estimation delay limit permits some simplified smoothing of the phase errors. Expressed as range-rates, the 100 and 200 ms smoothed noises for the GPS(L1-L3) case would be 1.62 and 0.73 fps respectively, with corresponding solution delays of 50 and 100 ms. (The smoothing technique also takes advantage of the anticorrelation of common phase errors in adjacent cycle count intervals.) The four GPS/PSAT single and dual-frequency configurations studied are enumerated as L1/L1, L1/L1-L1/4, L1-L3/L1-L1/4 and L1-L3/L1-L3, where, e.g., L1/L1-L1/4 denotes the single-frequency L1 GPS and dual-frequency L1-L1/4 PSAT case.

The single-frequency ionospheric refraction effects on the satellite to missile links, expressed in range (IONO) and range-rate (IONO-DOT) domains, are shown in Figure 5 (DASO-5 datum). Covariance analyses demonstrated that these errors could not be ignored and still meet the system requirements. Thus ionospheric effects must be modeled for single-frequency links. The pseudosatellite links exhibit an effect (not shown) which is opposite the GPS links, since the refraction effect increases with lengthening ionospheric path exposure as the missile rises. For the single-frequency cases, the FW (fit World) ionosphere was modeled with a spherically symmetric Chapman model using the predicted solar flux value for the day and the RW (real World) model was produced by the large scale SATRACK software. Differences (model errors) are aliased in the estimation.

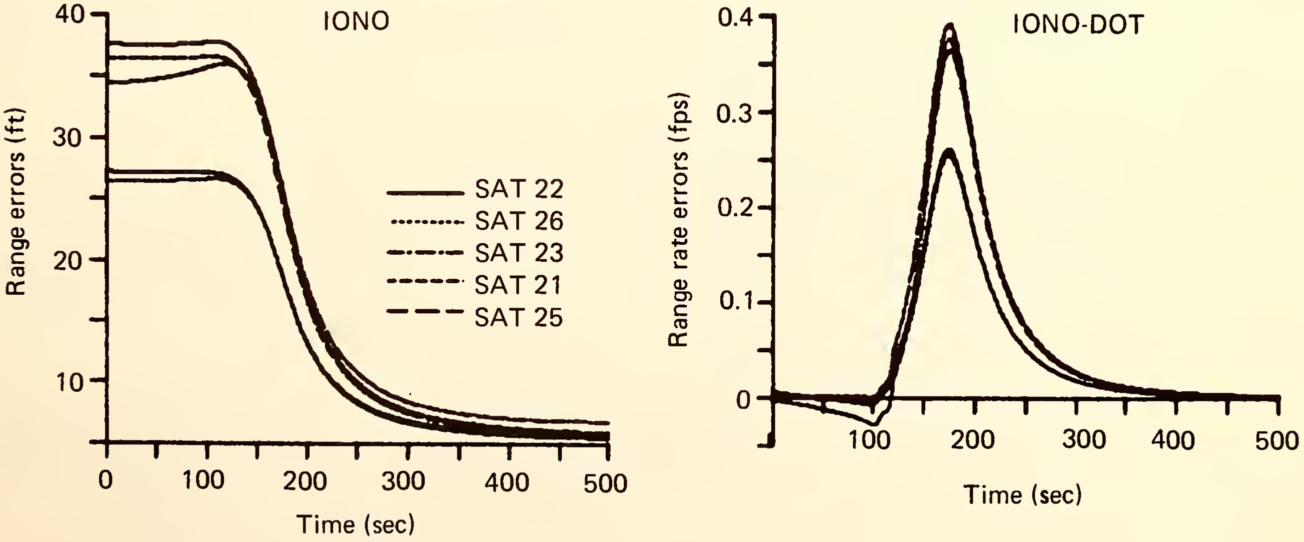

Fig. 5 GPS-to-missile ionospheric refraction effects.

Initial simulation results demonstrated that, early in the flight, point estimate error covariances or ionospheric model error aliasings frequently exceeded state vector accuracy requirements. In view of these results, the accuracy requirements were reexamined and shifted to the thrust-terminated IIP domain - a superior performance criteria. To implement this new performance measure, capabilities to generate IIP partials and propagate covariances and aliased errors were incorporated in the simulation.

Satellite ephemerides were transformed to the HLC (Height, aLong-track, Cross-track) coordinate system from TOD (True Of Date) coordinates. The covariance simulation error budgets for HLC satellite position/velocity errors (inferred from SATRACK experience) were 10,25,25 feet and .001,.001,.003 fps. The pseudosatellite error budgets were expressed in NED (North, East, Down) coordinates and these values were 10,10,10 feet and 0,0,0 fps.

IIP RESULTS

Various tracking system weighted least squares point covariance/estimation simulations were conducted in support of the real-time study. The four configurations enumerated in the previous section became the primary candidates for a base-line system selection. Each configuration was simulated for 50, 100, and 200 ms interval smoothing of the integrated Doppler (delta-range) measurement noises, with corresponding solution delays of 0, 50, and 100 ms. In the single-frequency cases, ionospheric refraction model errors aliased into the estimation error. In the dual-frequency cases, while the ionospheric refraction error was negligible, the higher PLL measurement noises resulted in increased estimation error covariances (uncertainties).

The Kwajalein Lagoon range-safety IIP accuracy requirement is most severe in the cross-track direction, since the reentry bodies must remain well clear of radar stations to the left and right of the nominal trajectory. Figure 6 shows CR (cross-range) estimation "corridors" for the KMRN-6 trajectory, for 100 and 200 ms delta-range noise smoothing of the four candidate systems. (CR "corridor" means half the width of the rectangle which bounds the one-sigma impact covariance ellipse.)

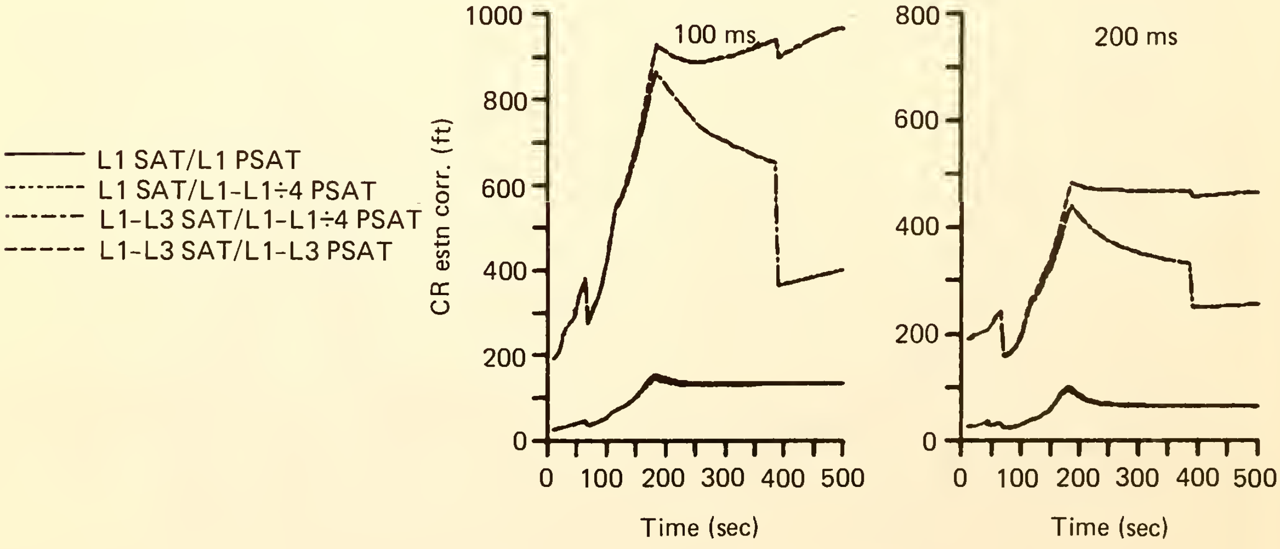

Fig. 6 Cross-range estimation corridors.

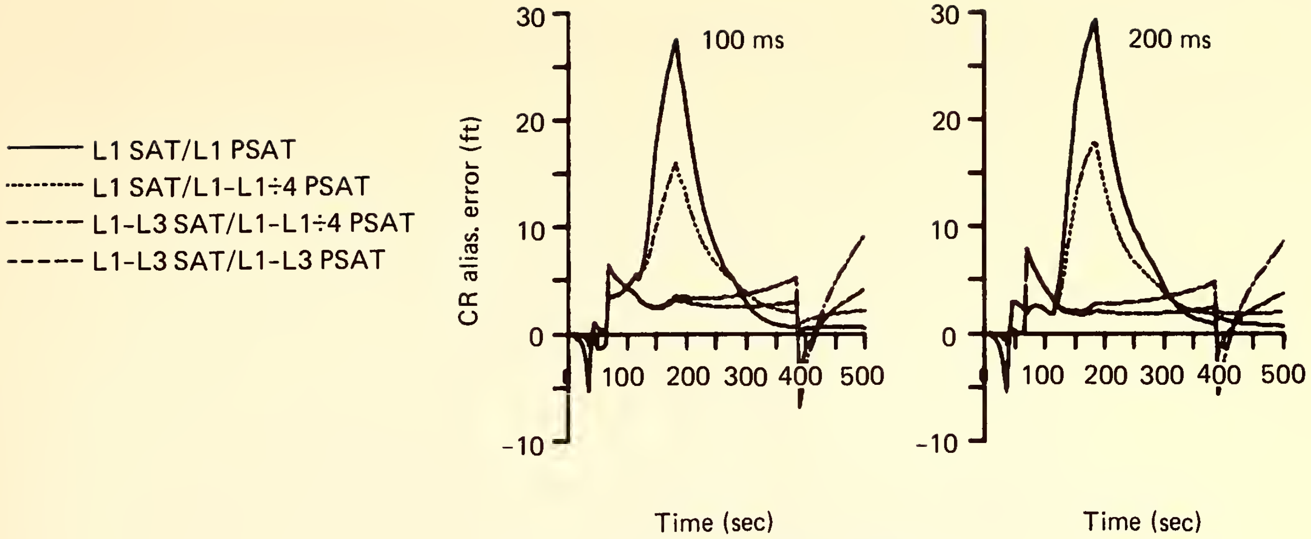

Fig. 7 Cross-range estimation aliasing.

Curves for the two systems using single-frequency GPS are at the bottom of each plot, while the dual-frequency GPS systems are at the top because of their large combined thermal noises. Entry of Makaha Ridge at 390 seconds is noticeable (but not as dramatic as the down-range case). Figure 7 shows the corresponding estimation aliasing, with the larger single-frequency ionospheric modeling error effects.

SUMMARY

The study has concluded that real-time single-frequency GPS tracking of MX test flights targeted to the Kwajalein Lagoon is feasibile for support of the range-safety function. A missile-borne transdigitizer would be preferable, and three remote receiving sites would be linked to a central processing facility. Real-time signal tracking would require a multiplexed fast acquisition channel, as well as 3rd-order PLLs. If post-flight metric data is required, a dual-frequency tracking system must be implemented. Also, until the full GPS constellation is available, pseudosatellites would be needed to "fill the gaps" in the existing satellite coverage.

REFERENCES

Space Department, JHU/APL, March 1984, Real Time Tracking Study, SDO-6990

Space Department, JHU/APL, September 1984, Class C Ampifier Study for Missile Instrumentation, SDO-7377

PREDICTED TOPEX POSITIONING ACCURACY WITH DIFFERENTIAL GPS TECHNIQUES

Stephen M. Lichten
Sien-Chong Wu
Jiun-tsong Wu
Thomas P. Yunck

Jet Propulsion Laboratory
California Institute of Technology
4800 Oak Grove Drive
Pasadena, CA 91109

ABSTRACT. The satellites of the U.S. Defense Department's Global Positioning System (GPS) will provide a basis for demonstrating highly precise tracking of NASA's Ocean Topographic Experiment (TOPEX) proposed for launch in 1990. The goal is to determine TOPEX altitude continuously to better than 10 cm. This paper reports on analysis underway at the Jet Propulsion Laboratory to predict tracking performance for TOPEX using differential GPS measurement techniques. The analysis looks at configurations of three to ten ground receivers expected to be used in a worldwide tracking network, and takes careful account of the expected limitations of the GPS receiver to fly on TOPEX. Station–GPS and TOPEX–GPS measurements are differentially combined to eliminate station and satellite clock errors; the orbits of TOPEX and of all 18 GPS satellites are then simultaneously estimated. Tracking performance is significantly affected by the ground station configuration, by the number of GPS signals which the flight receiver can process simultaneously, by the field of view provided by the GPS antenna on TOPEX, by the receiver noise figure, and by the method chosen for differentially combining GPS measurements. Strategies are discussed which are effective in reducing or eliminating major error sources for two data types: integrated doppler from GPS carrier phase, and pseudo-range from the GPS P-codes. The covariance analysis shows that when realistic observing limitations are taken into account, average TOPEX altitude accuracies of 5–10 cm can be expected over data arcs of slightly less than two hours.

INTRODUCTION

The mission of NASA's Ocean Topographic Experiment (TOPEX), proposed for launch in late 1990, is measurement and study of worldwide ocean topography. To map the topography, TOPEX will carry a radar altimeter precise to approximately 2.5 cm. From the topographic data, investigators will be able to extract mean global circulation and long wavelength variability of the oceans, with implications for weather prediction, world food supplies, and ocean navigation. To achieve this, knowledge of mean ocean height, when averaged over many days, is desired with an accuracy of approximately 5 cm. This in turn requires highly accurate determination of the TOPEX orbit.

The baseline tracking system for TOPEX will be an upgraded TRANET ground based doppler system consisting of approximately 40 stations operated by the Defense Mapping Agency (DMA). TRANET tracking data is expected to yield TOPEX altitude with an accuracy of about 13 cm. However, as a demonstration, the spacecraft will also carry a GPS receiver which, in conjunction with a relatively small set of ground receivers, could improve this accuracy substantially. GPS-based tracking will have experimental status on TOPEX as this will be the first demonstration of decimeter-level tracking by a GPS technique. If the demonstration is successful, GPS-derived orbits may well become the orbits of choice for TOPEX scientists, and the GPS-based tracking system will likely be used on future earth observation missions with very accurate positioning requirements.

The major error sources for TOPEX tracking using differential GPS range and integrated doppler data types have been identified through covariance analyses. In this paper, those errors are described, and various strategies designed to minimize the final TOPEX altitude error through efficient data collection and data processing are discussed.

DATA TYPES

Ground based conventional tracking systems are limited by the short view periods of low Earth orbiters. Typically, many ground terminals are required for good coverage. Even with the favorable combination of a relatively high TOPEX altitude of 1334 km and 40 ground receivers, TRANET tracking of TOPEX will suffer significant coverage gaps. The much higher GPS satellites at slightly more than 20000 km altitude are visible for relatively long periods both from the ground and from low Earth orbiters. The distribution of 18 satellites in the GPS constellation ensures continuous coverage of any low earth orbiter. The GPS satellites emit signals at two L-band frequencies, 1575.42 MHz (L1) and 1227.60 MHz (L2). The two carriers are phase-modulated at a rate of 10.23 MHz with a pseudo-random bit sequence known as the precise or P-code. The P-code transmitted by each satellite is orthogonal to those of all the others so that each satellite's signals are distinguishable. The L1 carrier is also phase-modulated in quadrature at a rate of 1.023 MHz by a pseudo-random square wave code known as the clear acquisition (C/A) code.

When GPS signals are received by a user, they are correlated with a code model which is generated by the GPS receiver. By aligning the code model with the received code, the time delay between transmission and reception is determined. This time delay is a measure of the range between GPS satellite and receiver. However the user clock and GPS clock will in general have a time offset, so the range derived in this way is called a pseudo-range since it is in error by the amount of this offset. Fig. 1 shows how four pseudo-range measurements can yield the three components of user position and the user clock offset from GPS time. (All GPS satellites are said to be synchronized to within several nanoseconds and thus are effectively all on GPS time.)

Using the C/A code, about 100 m position accuracy is possible; using the P-code on both L-band frequencies, an instantaneous position accuracy of about 15 m can be achieved. With a set of measurements made over several hours and with sufficiently accurate dynamical models, an orbiting user could expect position accuracies from direct GPS tracking (Fig. 1) comparable to the GPS ephemeris accuracy. Although GPS ephemeris errors are approximately 10–20 m at this time, by 1990 they are expected to be 1–2 m.

In anticipation of future missions such as TOPEX in which sub-meter accuracies will be required, several methods of further reducing the user position error have been investigated at the Jet Propulsion Laboratory (JPL). One of these, the differential GPS measurement, is shown in Fig. 2. GPS instrumental errors, including the clock error common to both pseudo-ranges, are cancelled. Compared to the distance to the GPS, the distance between the two receivers is small if both are on or near the surface of the earth. Because of this, the effect of GPS ephemeris error is substantially reduced, typically by a factor of ten for TOPEX geometries, and the instantaneous position accuracy using differenced pseudo-range is improved to about 1 m. With differenced GPS measurements, the remaining clock offset between the user satellite and the ground station, and the remaining GPS ephemeris error, limit the positioning accuracy. Note that if a second differential measurement with a second GPS satellite can be made simultaneously, using the same two receivers, the clock offset between receivers can be cancelled

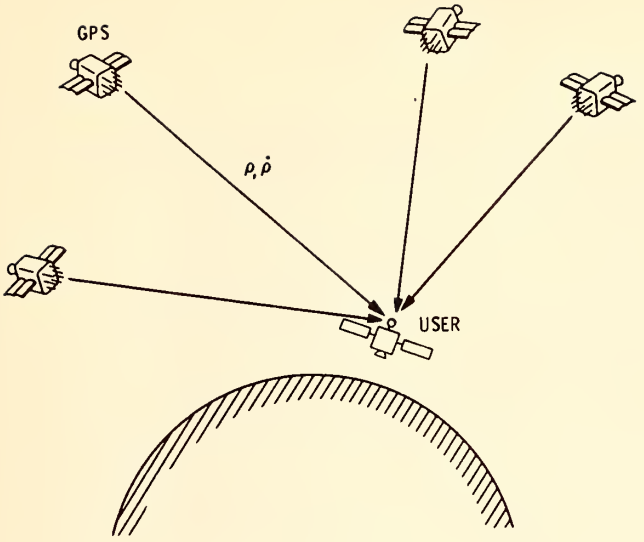

Fig. 1. Direct satellite tracking by GPS

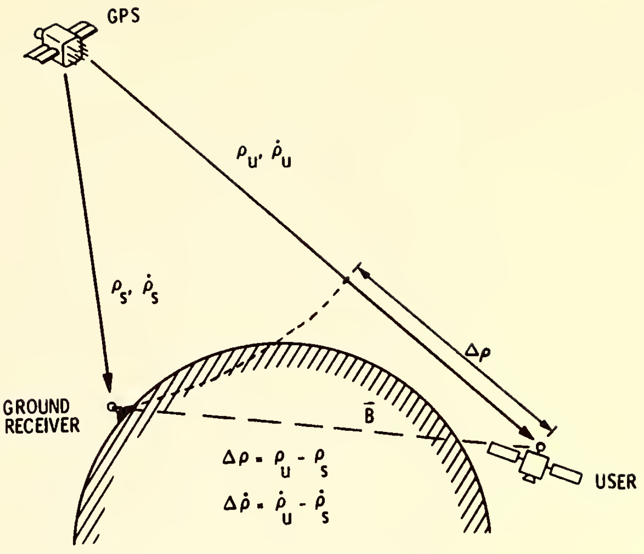

Fig. 2. Satellite tracking by differential GPS observation

by subtracting the second differential measurement from the first. Thus the clock offsets between the GPS transmitters and receivers can be completely eliminated with appropriate combinations of GPS observations. The method used in this study was that of Wu (1984), a generalized linear combination method using the Householder transformation. As with the non-differential tracking method, the orbit error can be further reduced by taking long arcs — several hours — of differential data and performing dynamical orbit solutions. This is the strategy to be employed for TOPEX.

For the analysis in this paper, two data types were studied: pseudo-range, and integrated doppler from GPS carrier phase. The analysis assumes for each data type that the measurement rate is once per 300 seconds. P-code pseudo-range data noise was nominally taken to be 10 cm. This is equivalent to approximately 75 cm receiver noise at L2 in 1 second, increased by a factor of 2.3 by dual frequency ionospheric calibration (based on continuous L1/L2 tracking and L2 3dB weaker than L1) and averaged over the 300 second measurement interval. Measurement of carrier phase has the potential to provide range measurement precision of better than 1 cm for a 1 second observation. However, due to the difficulty in resolving integer cycle ambiguities in carrier phase, precise range changes are recorded instead. The resultant integrated doppler data type is comparable to a very accurate range measurement with additional range biases to solve for. The range biases are analagous to integration constants left over from integrating delta range to compute range. Although there are these extra parameters to solve for, integrated doppler provides an opportunity to exploit the inherently higher precision of carrier phase. Because the carrier is at a higher frequency with a much narrower bandwidth than the codes, it is relatively insensitive to multipath effects which can degrade GPS pseudo-range measurements. For integrated doppler, the data noise assumed in this analysis was 0.4 cm per 300 second count interval. If we assume 7° of phase noise over 4 seconds (rather conservative for a modern GPS receiver), and include a factor of 2.3 for dual frequency ionospheric calibration, thermal receiver data noise over a 300 second count interval is very low, about 0.15 cm. The value of 0.4 cm was chosen in order to partially compensate for random tropospheric variations

TABLE 1. TOPEX ANALYSIS ASSUMPTIONS

ONE TWO-HOUR TOPEX ORBIT, ALTITUDE = 1334 KM
18 GPS SATELLITES IN 6 ORBIT PLANES

A PRIORI UNCERTAINTIES:

2E+06 M (RSS)	TOPEX POSITION	ADJUSTED
2 M/S (RSS)	TOPEX VELOCITY	ADJUSTED
4 M (RSS)	GPS POSITIONS	ADJUSTED
0.5 MM/S (RSS)	GPS VELOCITIES	ADJUSTED
(20,20,20) CM	NON-DSN STATIONS	ADJUSTED
(5, 5, 5) CM	DSN STATIONS	CONSIDERED
5 CM	TROP AT ZENITH (NO WVR)	CONSIDERED
1 CM	TROP AT ZENITH (WVR)	CONSIDERED
50% GEM10-GEM10B	GEOPOTENTIAL	CONSIDERED
1.0E-08	GM	CONSIDERED
10%	ALBEDO	CONSIDERED
10% ($C_D = 2.00$)	DRAG	CONSIDERED
5% ($C_R = 1.77$)	SOLAR RAD PRESSURE	CONSIDERED

DATA NOISE (300 SEC COUNT TIME): 10 CM P-CODE PSEUDO-RANGE
0.4 CM INTEGRATED DOPPLER FROM CARRIER PHASE

NOMINAL GROUND TERMINALS:

1. GOLDSTONE (DSN)
2. MADRID (DSN)
3. CANBERRA (DSN)
4. BRAZIL
5. SEYCHELLES
6. JAPAN
7. ANCHORAGE
8. SAMOA
9. NRAO VIRGINIA
10. GUAM

ALTERNATE POLARIS U.S. SITES FOR STATIONS 7, 8, 9:

7. RICHMOND, FLA
8. WESTFORD, MA
9. FORT DAVIS, TX

which could increase the effective data noise during the scan. If water vapor radiometers (WVRs) are used to calibrate the potentially large systematic troposphere errors, the data noise would still be limited by noise from the calibration technique, also about 0.4 cm.

RESULTS

A covariance analysis was carried out to predict TOPEX positioning accuracy with differential GPS pseudo-range and integrated doppler under a variety of conditions which might be expected during the TOPEX mission. Table 1 shows the assumptions and input *a priori* values for a square root information filter which was used for the analysis. The number of ground terminals in the analysis ranged from a minimum of three NASA Deep Space Network (DSN) stations to a maximum of ten stations, which included the three DSN sites and seven additional TRANET stations. The ground stations are listed in Table 1 and plotted in Fig. 3. In all cases, the states of TOPEX and the 18 GPS satellites were

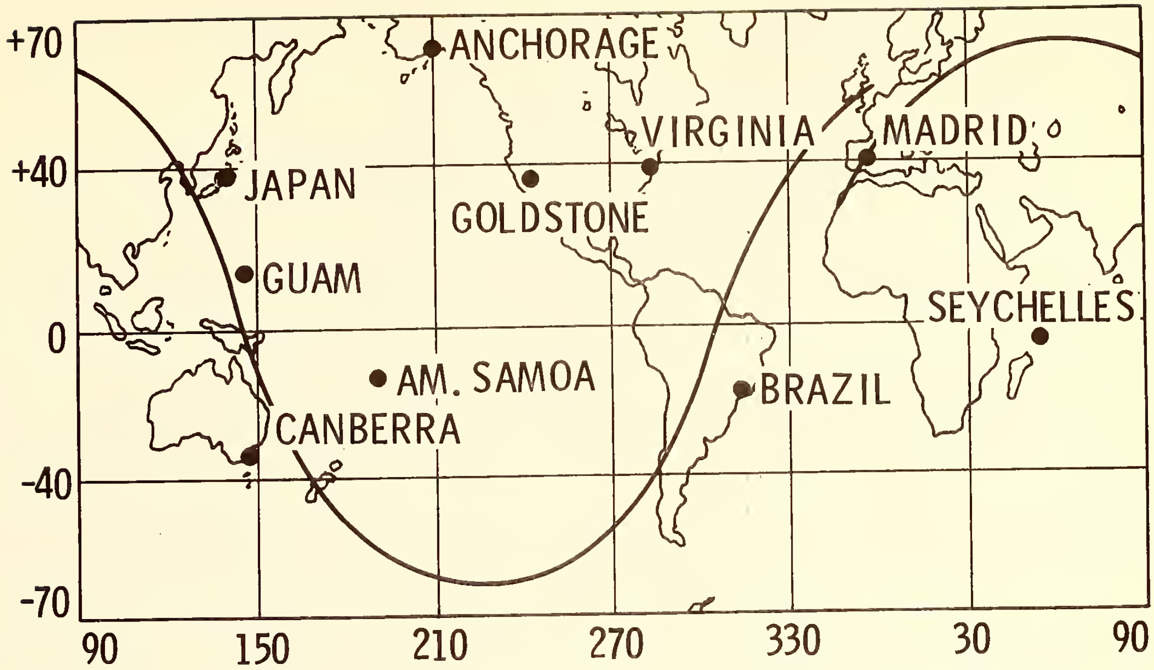

Fig. 3. Ground track of TOPEX over two hours superimposed over locations of ten ground stations used in TOPEX covariance analysis

estimated simultaneously along with the non-DSN station locations. The three DSN locations were considered (not estimated) as they are expected to be very well determined (within 5 cm) from years of VLBI observation of extragalactic sources. Other parameters which might be difficult to model accurately were also considered, as indicated in Table 1.

Several factors can restrict the amount of data available for differential GPS-based orbit determination of TOPEX. The first is the number of ground receivers. During actual operation, between six and ten ground receivers are expected to be in use. A second factor is the capacity of the flight receiver for simultaneous processing of GPS data. A number of receiver designs are under consideration to fly on TOPEX. Some of these receivers can process four GPS signals simultaneously, while others can process as many as eight. A third limitation is the field of view of the GPS antenna on TOPEX; it is expected that the antenna will have a hemispheric (180°) field of view. Variations on these factors can drastically affect the amount of data available. For example, with 13 ground stations and no restrictions on TOPEX-GPS visibility, after Householder differencing there are approximately 1200 measurements available during a two hour arc; however, with only six ground stations, hemispheric antenna field of view, and a four GPS flight receiver processing capability, the number of measurements is reduced to 270.

Previously reported results of similar analyses at JPL have predicted TOPEX altitude errors of about 9 cm (Yunck 1984; Yunck, Melbourne, and Thornton 1985). The results reported here show substantially lower tracking errors. Part of the improvement is due to the use of a full covariance matrix to specify the GPS *a priori* uncertainties. The inclusion of off-diagonal terms which have information about correlations between GPS satellite states strengthens the solution. There is some additional

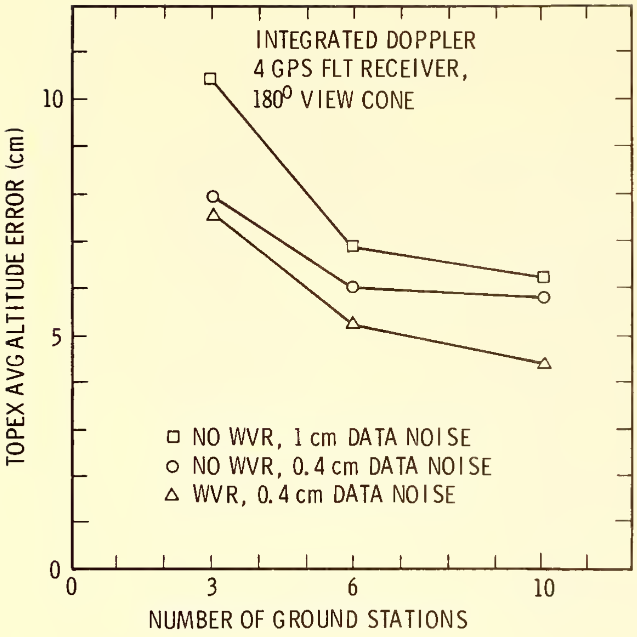

Fig. 4a. TOPEX altitude error analysis for integrated doppler from GPS carrier phase

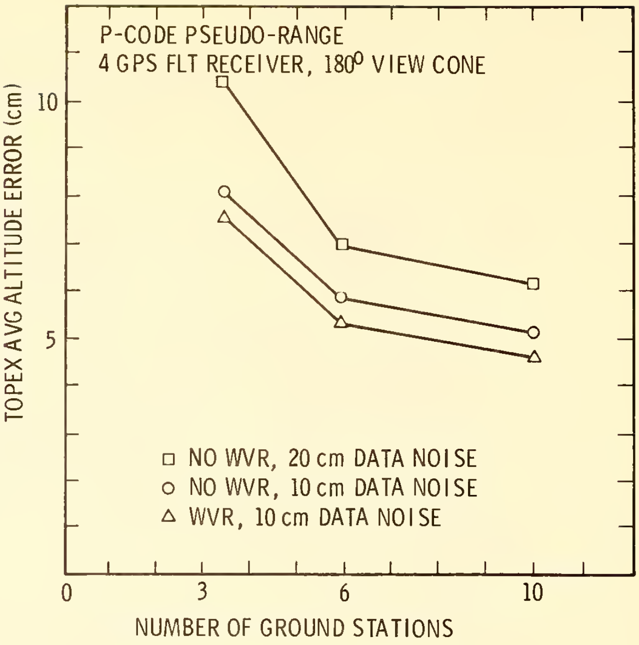

Fig. 4b. TOPEX altitude error analysis for pseudo-range from GPS P-codes

improvement due to slightly lower GPS *a priori* assumed in this study — 4 m instead of the previous 7 m. Most of the improvement, however, is due to use of a generalized linear combination technique (Wu 1984) which more efficiently eliminates clock errors when compared to the simpler differencing scheme employed in the earlier analyses.

Fig. 4a shows how tracking performance with integrated doppler depends on the number of ground stations, the flight receiver capability, and troposphere calibration with WVRs. With six ground terminals, a four GPS flight receiver capability, and a 180° TOPEX antenna viewing cone, the average TOPEX altitude error is about 5 cm over the central 80 minutes of a two hour data arc (slightly more than one revolution). Three cases were analyzed with integrated doppler: 1) WVR case — 1 cm troposphere error at zenith, 0.4 cm data noise; 2) no WVRs case — 5 cm troposphere error at zenith, 0.4 cm data noise; 3) no WVRs, pessimistic case — 5 cm troposphere error at zenith, 1 cm data noise. For pseudo-range, the cases with 1 cm and 5 cm troposphere errors at zenith are compared in Fig. 4b along with several values for the data noise. Also shown in Fig. 5 are error decompositions showing the major contributions to the overall integrated doppler and pseudo-range errors with the six ground station tracking network. Comparison of the curves in Fig. 4a shows that with only three tracking stations, integrated doppler is very sensitive to data noise and relatively insensitive to troposphere errors; however with ten stations, there are so many measurements that data noise is no longer a major factor and the results become sensitive to the troposphere. Pseudo-range is moderately affected by the troposphere (Fig. 4b), but is sensitive to data noise for any number of ground stations. Gravity is a major error source for both data types.

Figs. 6a and 6b compare tracking performance using six ground terminals with performance from a network of the original six stations supplemented by three POLARIS ground stations in the continental United States (the three alternate stations in Table 1). POLARIS stations are presently operated by the National Geodetic Survey for VLBI studies relating to Universal Time (UT), polar motion, and

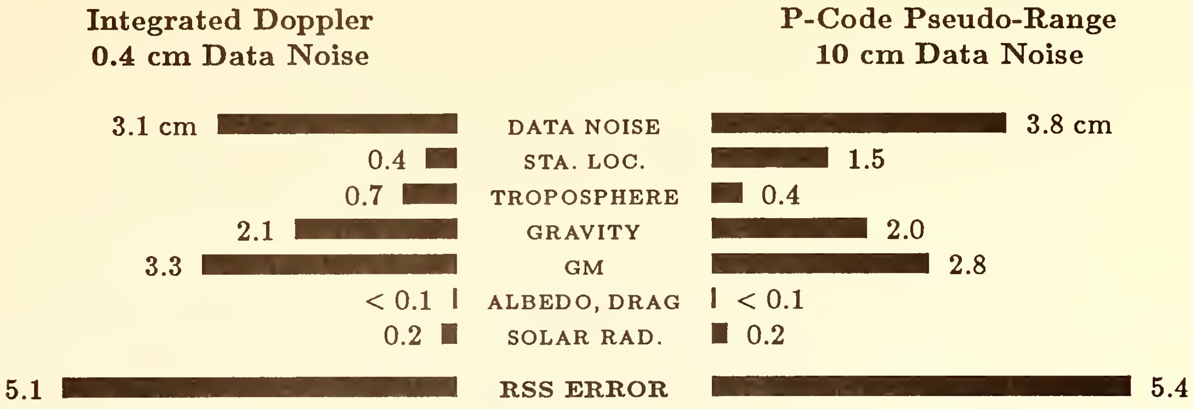

Fig. 5. Breakdown of predicted TOPEX altitude error (cm) for nominal configuration of six ground receivers with WVRs, 4 GPS capacity flight receiver, and 180° flight antenna view cone.

other geodetic parameters. Also shown in Fig. 6 is the increase in TOPEX altitude errors when the TOPEX flight antenna viewing cone is reduced from from 180° to 160°, the reduction of errors possible with a flight receiver which can process up to eight GPS signals simultaneously instead of only four, and the increase in errors when no WVRs are available and the data noise is higher.

EFFECT OF GPS EPHEMERIS ERRORS

The TOPEX solution depends to some degree on the *a priori* knowledge of the GPS satellite positions. The sensitivity to GPS *a priori* uncertainties is noticable in a single two hour arc because the geometrical information may not be sufficient to estimate all the GPS equally well.

The errors for TOPEX quoted above were based on full matrix *a priori* uncertainties (Table 1), 4 m RSS for each GPS satellite. By 1990, GPS orbits accurate to 1.5–3 m may be routinely available with the Block III GPS (Milliken and Zoller 1978; Martin 1978). However, even if such information is not available, TOPEX–GPS data can estimate GPS orbits to very high accuracy. A covariance analysis shows that with initial GPS orbit uncertainties greater than 100 m, after three or four TOPEX orbits (less than 12 hours), the GPS solutions on average are better than 1 m in each positional component. Therefore the assumed 4 m RSS GPS *a priori* uncertainties can be considered reasonable.

LIMITATIONS OF THIS STUDY

The tracking network planned for TOPEX will include at least six ground terminals, a flight receiver with a hemispheric viewing cone and capability for processing four or more GPS signals. It is also likely that WVRs will be installed at most if not all the tracking stations. With reasonable assumptions about data noise for pseudo-range and integrated doppler, the covariance analysis predicts altitude positioning errors for TOPEX comfortably below 10 cm.

There are several factors omitted from this analysis which could cause these error estimates to increase. First, satellite attitude uncertainties, expected to produce about a 1 cm error in knowledge of satellite centers of gravity with respect to the GPS antennas, have not been modeled or included in the filter because these effects are not well understood at this time. Second, effects of uncalibrated antenna phase center variations (multipath) also have not been included because quantitative evaluation of these effects is currently unavailable both for the GPS satellite transmitters as well as for the TOPEX flight and ground receivers. The P-code pseudo-range derived data type is much more sensitive to

(a) Integrated Doppler from GPS Carrier Phase

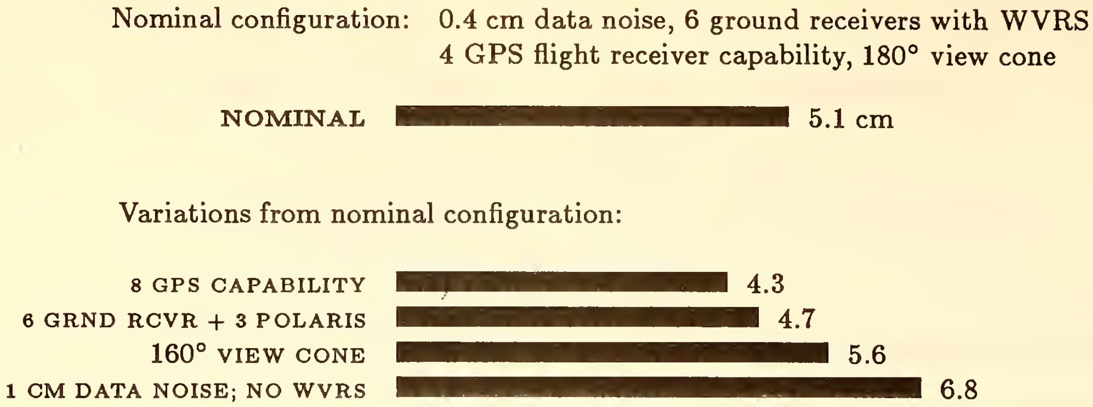

(b) Pseudo-Range from GPS P-Codes

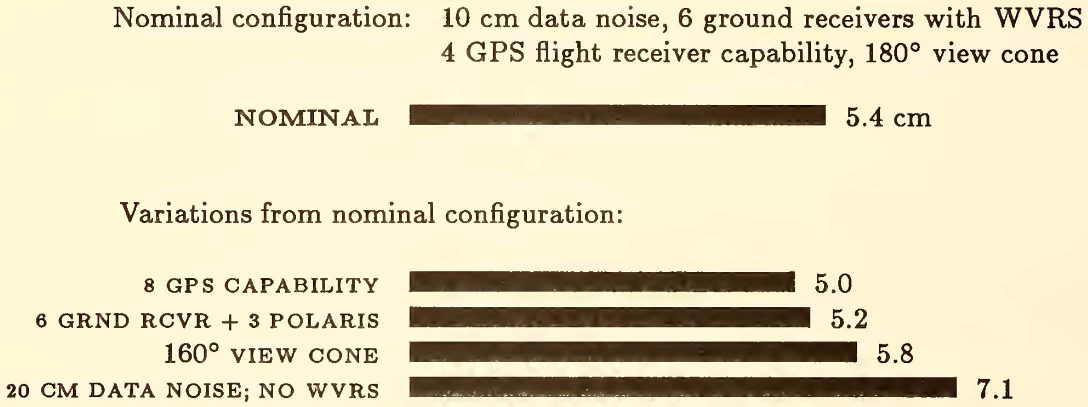

Fig. 6. Comparison of TOPEX altitude tracking performance

multipath than is carrier phase data; if the antenna phase center variations with P-code cannot be calibrated as well as with carrier phase, P-code pseudo-range may give significantly higher positioning errors. Calibrations for carrier phase should be accurate to the order of 1 cm. Multipath errors for GPS satellite transmitters and receivers are currently being studied at JPL (Young, Neilan, and Bletzacker 1985).

A third area of some uncertainty is the effect of the geopotential in the covariance analysis. The assumed *a priori* uncertainties were based on one half the difference between the GEM10 and GEM10B gravity models for 21 selected gravity terms. This approach was chosen to represent the expected improvement in gravity modeling by 1990. It is, of course, difficult to predict how well determined the Earth's geopotential will be in 1990. On the other hand, the TOPEX mission will provide a large amount of data which might be used to improve knowledge of the geopotential to the level assumed here if indeed that level has not been reached at the time of TOPEX launch. Several different strategies could be tried, including tuning of selected gravity terms. Fig. 5 shows that TOPEX positioning errors could potentially be limited by the effects of gravity mismodeling.

There are also reference frame related topics which have not been addressed by the covariance studies. The TOPEX errors discussed above are meaningful only in the context of a self-consistent reference frame. In practice, however, it will be necessary to reconcile the reference frame defined from VLBI radioastronomy observations, the World Geodetic Survey (WGS) reference frame (relevant to GPS positions), and the reference frame defined by the geocenter. It is possible that some of the parameters pertinent to the reference frame ties, such as UT and polar motion constants and the geocenter, could be determined from TOPEX data. Others could be determined from data taken at ground stations used both for VLBI and GPS observations. These topics are being studied at JPL, but they were not included in the TOPEX covariance analyses.

A new JPL software package for precise error analysis, OASIS (Orbiter Analysis and SImulation Software), described more completely by Wu and Thornton (1985), is now nearing completion. It features centimeter level accuracy in the covariance analysis and improved modeling capability, and is specifically designed for GPS-related problems. TOPEX analysis will continue at JPL with the new OASIS software and a number of topics will be examined in the near future which could not be properly treated with the older software. The improvements include: general process noise capability, especially incorporation of process noise for troposphere and clock errors; improved representation of troposphere, solar radiation pressure, and atmospheric drag effects; more extensive representation of the Earth's gravity field; ability to assign different data noises for different satellites and receivers; capability for cases with different data types from different receivers. It is hoped that at least some of the limitations of the present analysis discussed above will be remedied with the new OASIS software.

SUMMARY

Covariance analysis of positioning errors for the TOPEX satellite predicts typical altitude errors of 5–10 cm with linear combinations of GPS pseudo-range or integrated doppler data. These results hold for a tracking network of only six ground stations; care has been taken to incorporate realistic data noise values and flight antenna/receiver restrictions. The predicted TOPEX altitude errors are similar for the two data types, although pseudo-range is somewhat more sensitive to station location errors and data noise, and integrated doppler is more sensitive to troposphere errors. With either data type, gravity mismodeling is expected to be a major factor. Tracking errors for both data types are also slightly worse if WVR troposphere calibrations are not available at the ground stations.

Actual TOPEX tracking errors may be somewhat higher than predicted by the covariance analysis because of several unmodeled effects, including satellite attitude and center of gravity uncertainties, antenna phase center variations on GPS transmitters and GPS receivers, and complications arising from different reference frames. Phase center variations are likely to be substantially worse for pseudo-range data than for carrier phase data, which may give carrier phase an overall edge in tracking performance. In addition, gravity could become a more significant error source if assumed improvements in the gravity model are not achieved by TOPEX launch, although it is likely that GPS data from TOPEX could remedy this. Future work will focus on improving the error models used in the covariance analysis and devising strategies to compensate for these additional errors. If TOPEX tracking accuracy is limited by gravity errors, the two data types will be nearly equally effective in determining TOPEX altitude; however if antenna phase center variations and multipath are the major error sources for differential GPS tracking of TOPEX, integrated GPS doppler derived from carrier phase will have the advantage.

ACKNOWLEDGMENTS

The authors wish to thank Dr. Gerald Bierman for his helpful suggestions relating to the covariance analysis. The research described in this paper was carried out by the Jet Propulsion Laboratory, California Institute of Technology, under contract with the National Aeronautics and Space Administration.

REFERENCES

Martin, E. H., 1977: "GPS User Equipment Error Models," *Navigation*, Vol. 25, pp. 201–210.

Milliken, R. J., and Zoller, C. J., 1978: "Principle of Operation of NAVSTAR and System Characteristics," *Navigation*, Vol. 25, pp. 95–106.

Wu, J. T., 1984: "Elimination of Clock Errors in a GPS Based Tracking System," AIAA/AAS Astrodynamics Conference, Seattle, Washington.

Wu, S. C., and Thornton, C. L., 1985: "OASIS — A New GPS Covariance and Simulation Analysis Software System," First International Symposium on Precise Positioning With GPS, Rockville, Maryland (this conference).

Young, L., Neilan, R., and Bletzacker, F., 1985: "GPS Satellite Multipath: An Experimental Investigation," First International Symposium on Precise Positioning With GPS, Rockville, Maryland (this conference).

Yunck, T. P., 1984: "A GPS Measurement System for Precise Satellite Tracking and Geodesy," Conference on Precision Electromagnetic Measurements, Delft, The Netherlands.

Yunck, T. P., Melbourne, W. G., Thornton, C. L., 1985: "GPS-Based Satellite Tracking System for Precise Positioning," to appear in *IEEE Transactions on Geoscience and Remote Sensing*.

THE PRESENT STATUS AND THE PLAN OF GEODETIC APPLICATIONS OF SPACE TECHNOLOGY INCLUDING THE GLOBAL POSITIONING SYSTEM IN JAPAN

Yoshio Baba
Geographical Survey Institute
Ministry of Construction
Kitazato-1, Yatabe-Machi, Tsukuba-Gun, Ibaraki-Ken, 305 Japan

ABSTRACT. Aiming at higher accuracy and efficiency of the geodetic survey in Japan, Geographical Survey Institute (GSI) has been introducing space technology in addition to the improvement of the conventional surveying methods. As a part of researches and development of geodetic applications of space technology, GSI has been carrying out geodetic positioning with NNSS and has completed a transportable VLBI system, the antenna of which is 5 meters in diameter.

GSI is also much interested in the Global Positioning System (GPS) considering the expected usefulness of its applications to geodetic survey in Japan, where the more accurate and more efficient detection of the crustal movement in and arround the country is essentially important from the viewpoint of earthquake prediction.

In this paper, present status and the plan of geodetic applications of GPS as well as other techniques in Japan is briefly reported.

INTRODUCTION

In Japan, GSI (Geographical Survey Institute), Ministry of Construction, is in charge of planning and carrying out the fundamental surveying and mapping all over the country except ocean area where HD (Hydrographic Department) of Maritime Safety Agency, Ministry of Transportation has responsibility for.

The fundamental geodetic survey by GSI consists of maintenance and revision of existing geodetic control points as well as the establishment of new minor control points. These points are served as references for mapping and any other public surveys. Besides the repetition of the fundamental surveying provides important basic information on the crustal movement essentially related to the earthquake prediction.

Though the land of Japan is small, topographical complexty and other circumstances make it difficult to survey efficiently and precisely with conventional methods of surveying, especialy for the coverage of wide area including the geodetic connection of isolated islands. GSI takes therefore it important to apply space technology, i.e. satellite geodesy and VLBI, to geodetic survey, and has been promoting researches and development on these new techniques for the sake of progress of fundamental control points survey in the country.

Presently GSI has developed a transportable VLBI system in addition to positioning with NNSS. Experimental satellite observation by optical methods is also planned.

Considering the situation of the scheduled development of GPS in U.S. and its prospects for the possibility of the application to geodetic survey, GSI is also planning to apply GPS to the fundamental survey in Japan combining it with VLBI and with the conventional methods. Principal GPS navigation method is also considered to be used to the navigation for aero-photographic survey and aerogeomagnetic survey performed by GSI.

PRESICE GEODETIC SURVEY AND NETWORK IN JAPAN

Since 1973 the fundamental survey called " The precise geodetic network survey" has been carried out with a trilateral method using high precision electro-optical distance measuring instruments in place of the old triangulation method and the old network was rearranged into a new one, the precise geodetic network of Japan islands.

The new network is consisted of primary control points network and the secondary control points network. The former includes old first and second order triangulation points and the latter old third order points. Figure 1(a) shows the old first order triangulation network and Figure 1(b) a part of the new primary control points network.

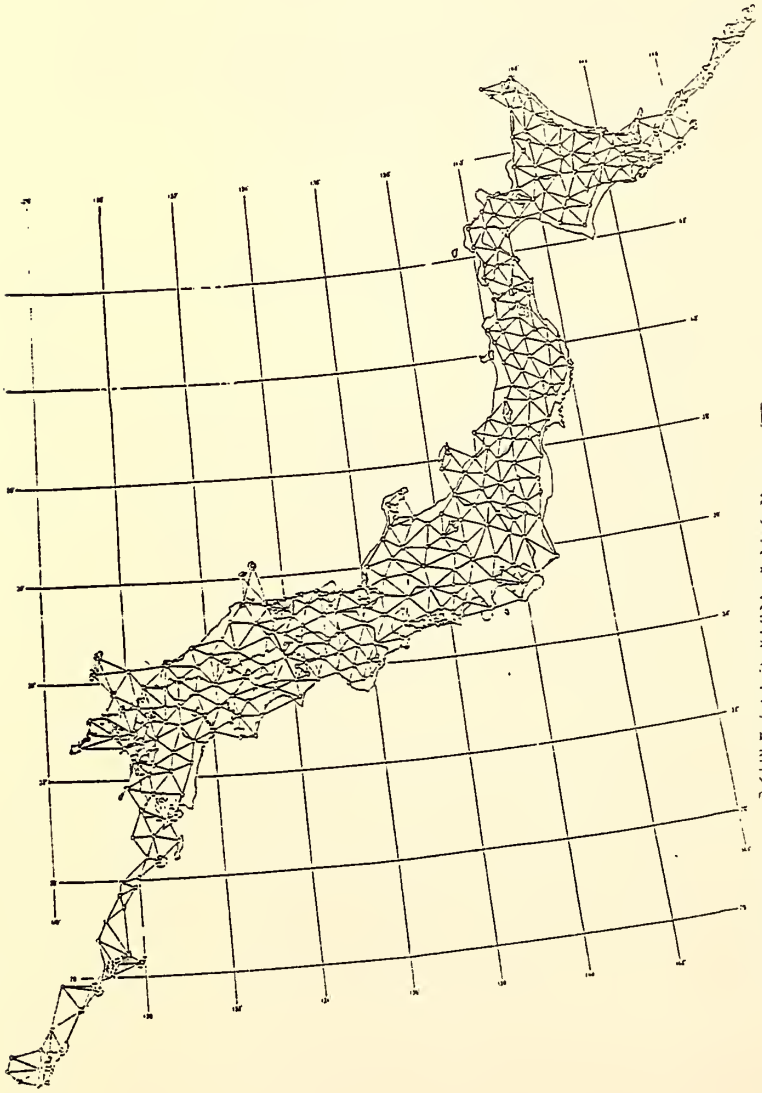

Figure 1(a). First order triangulation network.

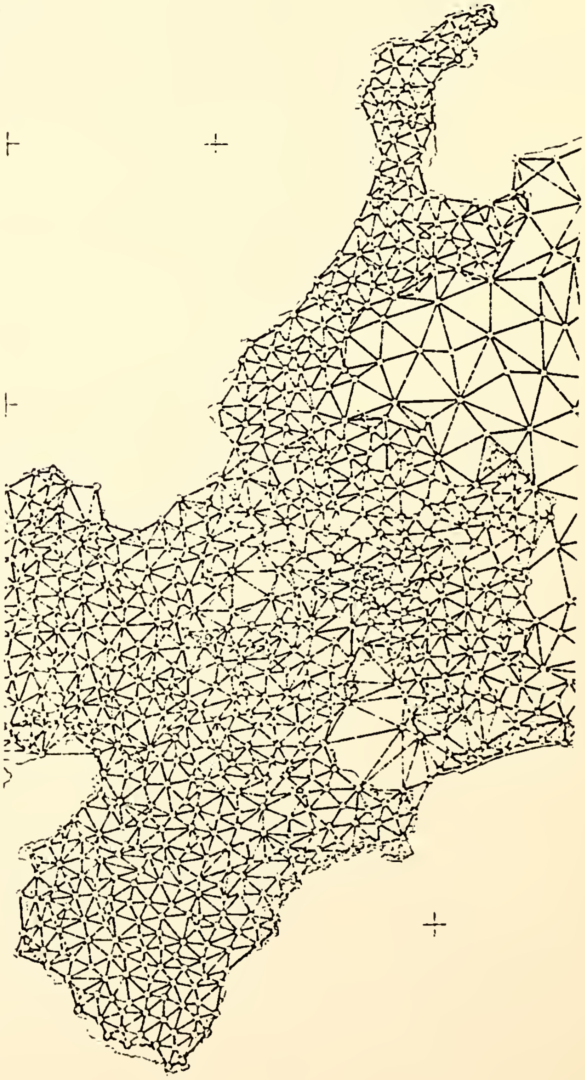

Figure 1(b). A part of the primary control points network.

The primary control points network consists of about 6,000 points and most of side lengths in the network are about 10 kilometers on the average and the rest is partly as long as a few tens of kilometers. All the surveys over the network are considered to have the relative precision of about 10^{-6}. The first whole survey by the new method of trilateration with electro-optical distance measuring instruments was completed in 1984 and the second repetition term survey has been started in 1985. Together with these horizontal control points survey, precise leveling has been performed along the highways about 20,000 kilometers long in total as shown in Figure 2 in about 5 years period except a part of Hokkaido district.

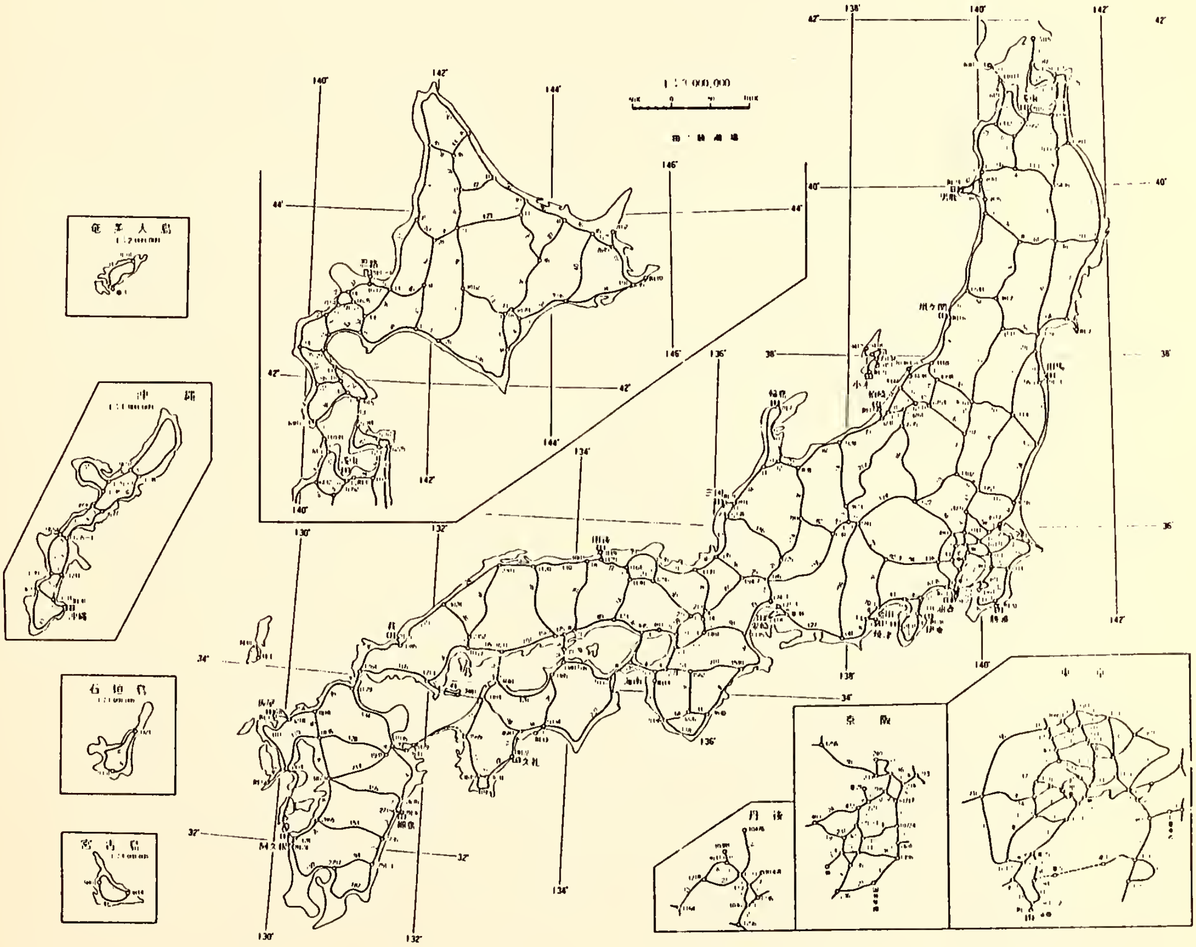

Figure 2. First order leveling network.

From the viewpoint of earthquake prediction, it is desirable to repeat the whole survey more effectively without losing precision or even with higher precision. In the specific areas with possibility of great earthquakes denoted in Figure 3, geodetic survey is performed more often or densely. Among them Tokai and South Kanto areas are the most important ones specified as the intensified observation areas. Especially, Tokai area is considered to be in danger of the occurrence of M8 class earthquake. For further study and higher certainty of earthquake prediction, it is desired to monitor the large scale crustal movement sorrounding Japan islands relating to local crustal movement.

Therefore, the network is required to be correctly adjusted by some other independent methods of survey which can determine long baselines directly with high accuracy as VLBI or satellite geodesy. Long baselines observations are also very useful for the precise determination of positions of many isolated islands which are not geodetically connected to the main lands. Repetition of these long baselines observations will as a result contribute to detect the crustal movement including plate motions strongly related to earthquakes arround Japan islands.

All the surveys in Japan are referred to the Tokyo Datum which is not necessarily precisely related to international geodetic systems, which is another subject to be solved.

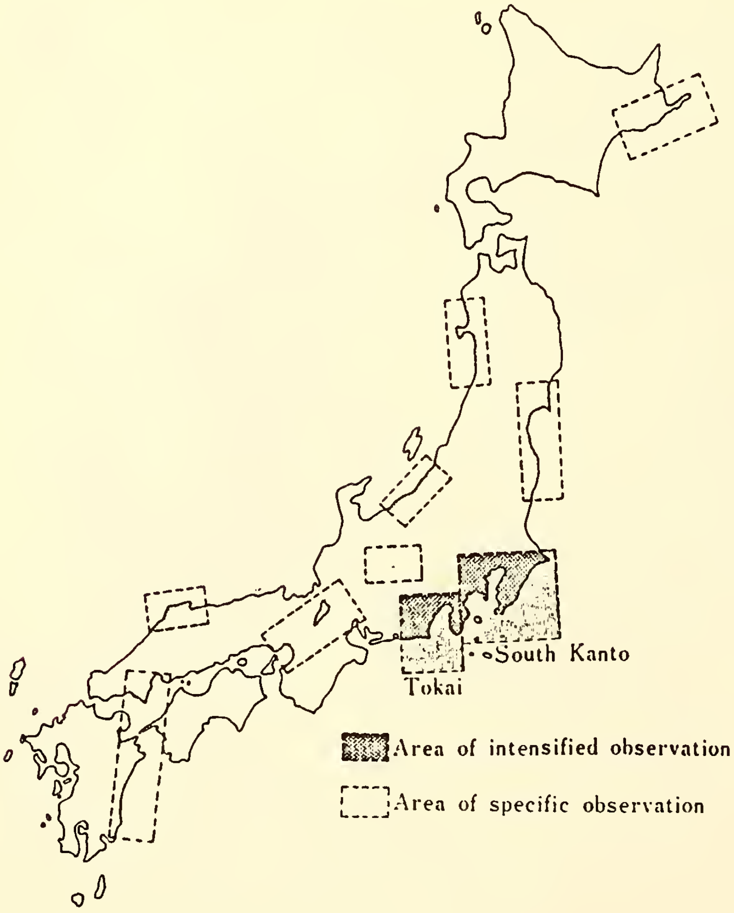
South Kanto
Tokai
▨ Area of intensified observation
☐ Area of specific observation

Figure 3. Areas of specified observation after Coordinating Committee for Earthquake Prediction of Japan.

In order to establish techniques for the precise positioning and direct measurment of long baselines relating to solve the problems as mentioned above, following practical researches and development of geodetic applications of space technology are under promotion in Japan.

Positioning with NNSS

GSI carries out positioning with NNSS (Navy Navigation Satellite System) in determination of some of isolated islands to make or revise basic maps of these islands. HD also uses NNSS in its oceanographical survey. In addition GSI uses NNSS for researches of the geoid near Japan islands and the control of the network. Figure 4 shows observed points with NNSS by GSI.

Estimated parameters of translation of the NSWC-9Z2 geodetic system relative to the Tokyo Datum based on the data hitherto obtained by GSI are $\Delta X=-148.33$m, $\Delta Y=+507.74$m, $\Delta Z=+676.59$m, where scale and rotation of the NSWC-9Z2 system are corrected after C.F.Leroy and L.D.Hothem (Komaki and Kaidzu 1983).

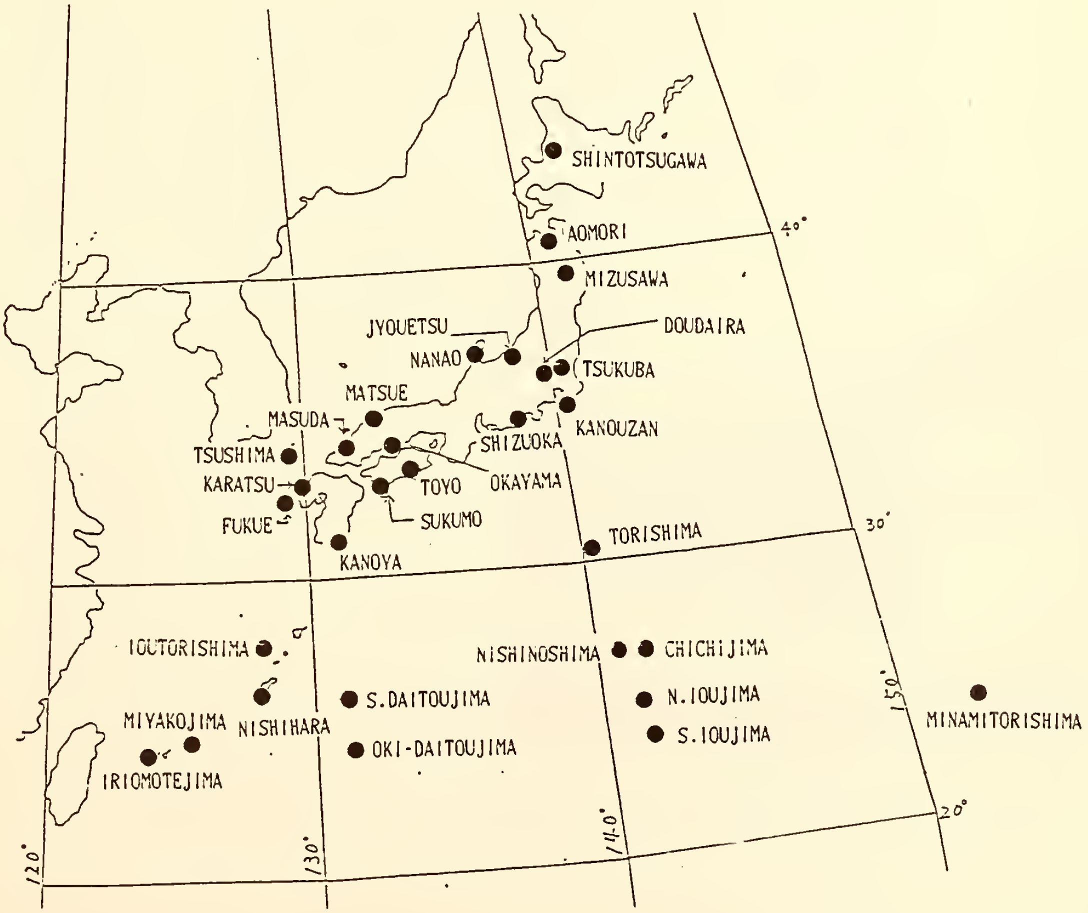

Figure 4. Observed points using NNSS by GSI

Development of a transportable VLBI

GSI has developed a transportable VLBI system under the 4-year program started in 1981. The system having an antenna of 5 meters in diameter was completed March of this year. Figure 5 shows the antenna installed in the grounds of GSI at Tsukuba. The antenna is designed to be disassembled as depicted in Figure 6 for transportation.

After the experimental observations and confirmation of its function at Tsukuba the system is scheduled to be transported to some points including isolated islands to determine long baselines of near 1,000 kilometers in length cooperating with RRL (Radio Research Laboratory), Ministry of Post and Telecommunication. RRL has a VLBI station with an antenna of 26 meters in diameter which is located in Kashima branch of RRL at Kashima and has succeeded in joint experiments with stations in the U.S.A.

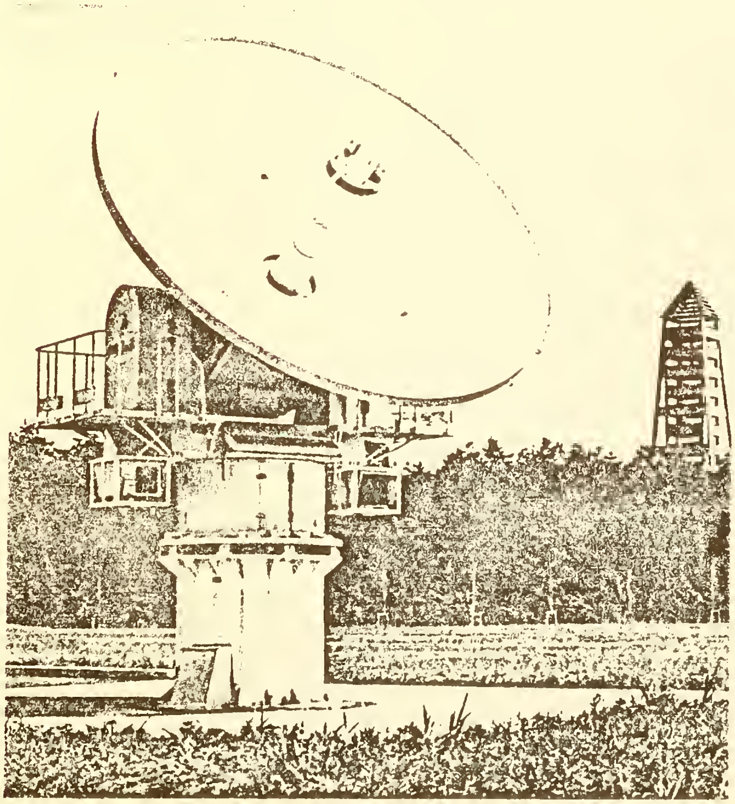

Figure 5. Transportable VLBI system installed in the grounds of GSI at Tsukuba.

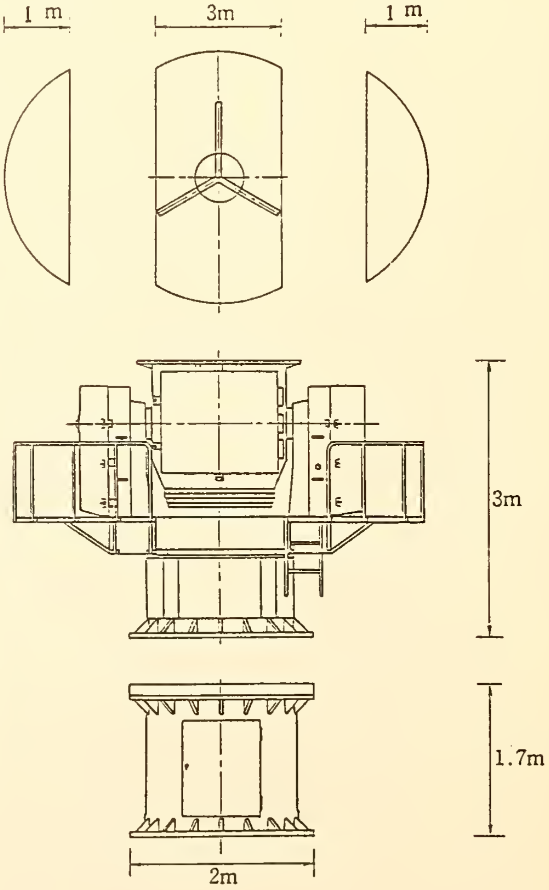

Figure 6. Disassemblement of the antenna.

Preparation of experimental observation of the EGP (Experimental Geodetic Payload)

As an experiment of optical observation of a satellite with both laser ranging and photographic direction measurement at the same time, EGP (Experimental Geodetic Payload) will be launched on a test vehicle of the H-1 rockets by NASDA (National Space Development Agency of Japan) in February, 1986. The EGP which is under development by NASDA is a spherical passive type equipped with corner cube reflectors and mirrors on its surface to be observed with a laser ranging instrument and a satellite camera at the same time (Figure 7). Table 1 gives major specification of the payload.

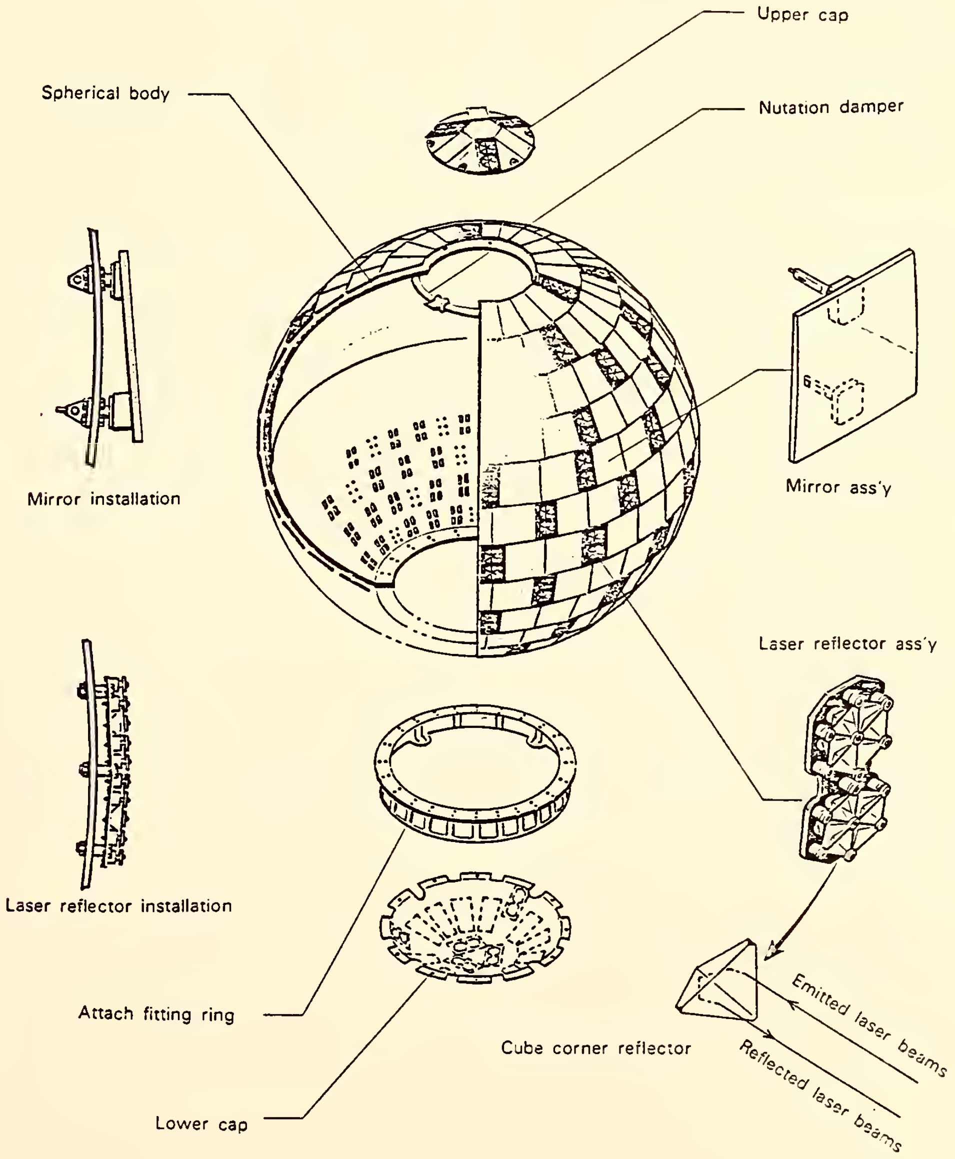

Figure 7. System Construction of the EGP
(By courtesy of NASDA)

Table 1. Major Specification of the EGP

Orbit	Altitude approx. 1500km Inclination approx. 50deg.
Weight	Approx. 700kg
Configuration	Polyhedron inscribed in a sphere with the diameter of 2.15 meters
Mirrors	318 pieces
Laser reflectors	120 sets (1436 cube corner reflectors)
Attitude control	Spin stabilization

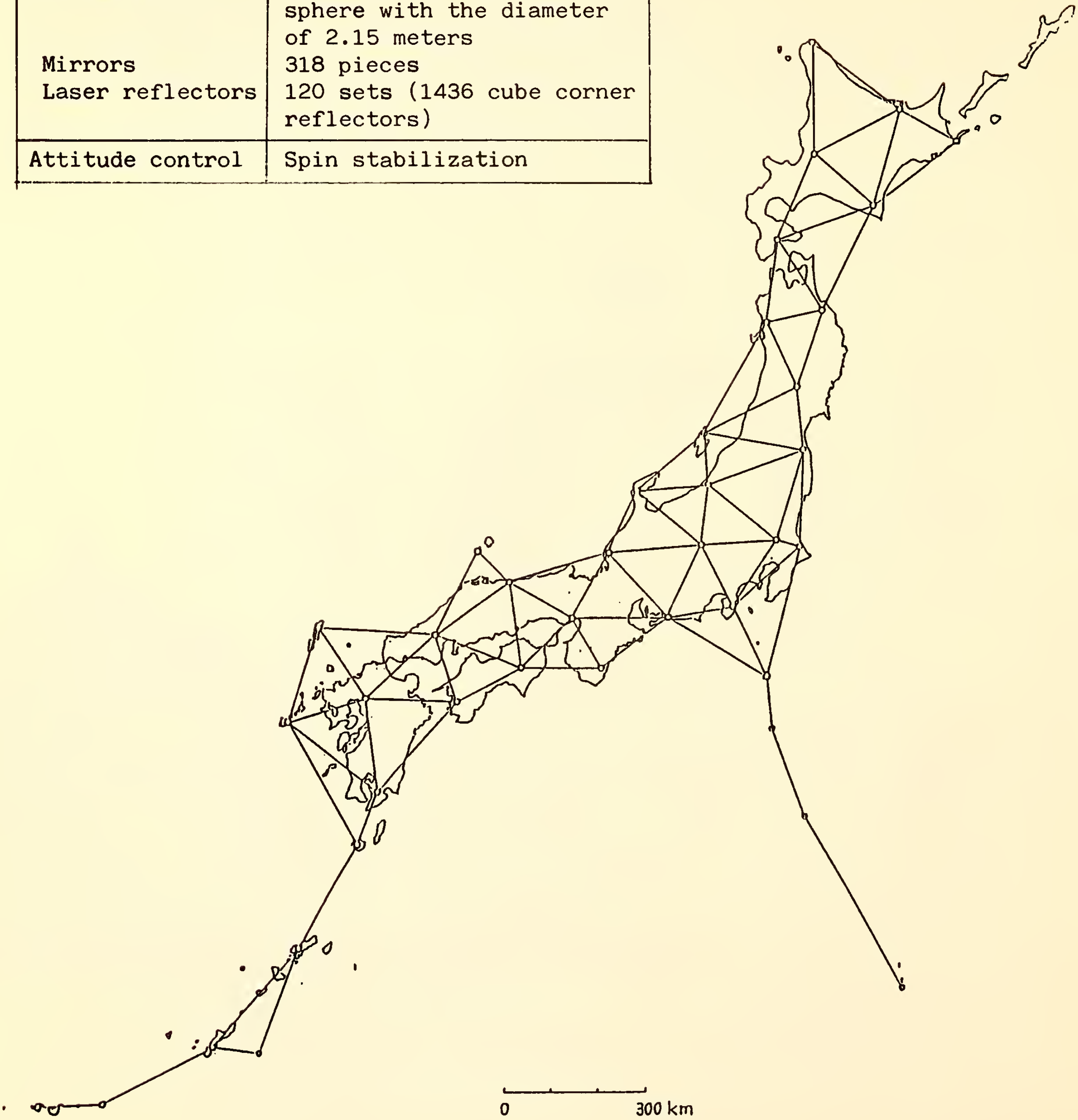

Figure 8. A probable example of a large scale network using precise positioning with GPS in Japan

PROBABLE GEODETIC USE OF GPS IN JAPAN

Though the above mentioned researches and development has been being promoted, NNSS is not sufficient in accuracy for our high precision geodetic control points survey as well as detection of crustal movement, and VLBI system or optical observation instruments of satellites are not suited for frequent movement to many points in Japan. Therefore, it is required to incorporate another new technique which can survey from relatively short distances less than several tens of kilometers to a few hundreds of kilometers with effectiveness and accuracy into the surveying system in the future.

According to the hitherto reported results of theoretical and experimental researches, GPS is expected to be very prospective for our objects. Relative accuracy better than 10^{-6}, which is comparative to the present trilateral methods by electro-optical distance measuring instruments, is very usefull for the nationwide control points surveying. GPS will also effectively contribute to the monitoring crustal movements in local specified areas as shown in Figure 3. Tokai area, for example, where about 1 meter shrinkage in about 90 years between Omaezaki and Izu peninsula separated about 55 kilometers has been observed by conventional methods, will be a test field for an application of the detection of crustal movement with GPS.

A probable example of a large scale network using precise positioning with GPS is shown in Figure 8. Vertical movements of the grounds will be also expected to be more convenientry monitored with a high precision surveying method with GPS.

All the stations of the VLBI observations as well as optical observation stations of the satellites will be colocated with GPS observation points. After experiments on lines of within 10 kilometers, colocated observation experiments will be carried out with VLBI on a baseline between Tsukuba and Kashima.

The surveys in the antarctic region by GSI using NNSS will also be replaced by GPS in the future.

SUMMARY

Considering the expected possibility of geodetic use of GPS, GSI is promoting and planning the combined effective use of space technology including GPS as a whole with colocation of GPS observation stations and others.

Though any demonstrations of experiments of geodetic application have not yet been taken place in Japan, GSI will start these experiments in the near future and detailed planning of effective use of GPS for local and nationwide surveys.

REFERENCE

Komaki, K. and Kaidzu, M.,1983 : Results of positioning with NNSS (2), Kokudochiriin Jihou (GSI chronicle), 57, 12-19 (in Japanese)

RESULTS FROM GPS - RESEARCH PROJECTS IN NORWAY

Jan Chr. Blankenburgh, Statoil/NTH, PB 300, 4000 Stavanger
Roger Ekseth, Norwegian Hydrographic Service
Torbjørn Hals, Continental Shelf Institute
Stian Holte, Kongsberg Våpenfabrikk

ABSTRACT. There is a tremendous interest in Norway for application of GPS for precise positioning. Several industries and institutes have undertaken research projects to clarify limiting factors and to investigate to which extent GPS can be applied to solve existing positioning problems in connection with the exploration and exploitation of the Norwegian continental shelf.

This paper deals with results of investigations and future activities.

INTRODUCTION

The exploration and exploitation of the Norwegian continental shelf has caused an acute need for more advanced positioning technology. High precision positioning is needed for, for example: three-dimensional seismic surveying, positioning of rigs and boreholes, delimitation of boundaries, mapping of the seabottom, hydrographic surveying, laying of pipelines, etc.

Main limitations of existing operational systems are: coverage, continuity, atmospheric effects, geometry, cost effectivity, etc. Improvement of these systems is still possible, however, very expensive. The present state of positioning technology is therefore regarded as to be a limiting factor for more effective offshore exploration and development.

It is generally expected that GPS will solve nearly all surface positioning problems. There is consequently a tremendous interest in Norway for application of the system. Supported by oil-companies operating offshore and by the Norwegian Government, main activities have been undertaken (or are initiated) by Kongsberg Våpenfabrikk (Kongsberg), the Continental Shelf Institute (IKU) and the Norwegian Hydrographic Service.

THE KONGSBERG OPERATIONAL SYSTEM

Kongsbergs activities concerning civil applications of GPS include two main projects: NAVREC and DIFFSTAR.

The NAVREC project is a cooperation with the german firm Prakla-Seismos GmbH in the development of a GPS-navigation receiver. So far two first-generation lab models have been built and tested with good results. A second generation receiver adequate for differential GPS will be presented later this year.

The DIFFSTAR project aims at the development of an operational system for offshore positioning and precise navigation, based on the differential application of the Global Positioning System. It includes the following activities:

- the development of adequate receivers
- the development of differential GPS software
- the testing and evaluation of differential GPS-methods
- the establishing of a permanent system of reference stations for coverage of the North Sea and the Norwegian Sea
- the development of a (long wave) broadcasting system for the transmission of differential corrections to an unlimited number of GPS-users.

SECOND-GENERATION KONGSBERG RECEIVER

A second-generation receiver is now under construction. A complete prototype will be tested already this summer.

The Kongsberg GPS-receiver has the following specifications:

- adequate for offshore differential positioning (accepts differential corrections)
- five channels, fast multiplexing, one frequency
- displays latitude, longitude, GDOP, satellitenumber, date, time, speed, heading, off track, course, distance, time to go
- service-routines for range, bearing, geodetic datumshift, choice of computed, automatic or manual speed and heading
- automatic or manual input of differential correctiondata
- option for raw data output (for post processing)
- self-test
- remote display output

THE DIFFSTAR - FIELD TEST PROJECT

The aim of this project was to investigate fundamental relations for the use of differential GPS based on the analysis of measured data. The task was to carry out a field campaign to collect measurements from two simultaneously operating receivers, to perform a statistical analysis of these data and to evaluate different methods for the differential correction of positioning results. The Continental Shelf Institute (IKU) was subcontractor for this project.

The campaign was organised as a short baseline test (2-3 days of observation) and a long baseline test (10 days of observation). The short baseline test included:

- the calibration of two receivers and antenna (1-10 m baseline)
- a study of receiver-dependent errors
- the collection of data for high precision result application
- the collection of data for tropospheric correction studies
- test measurements on a moving station.

The long baseline test (figure) included:

- the collection of data for the study of differential correction as a function of distance between stations
- at least one day with observations at each station
- observation under variable meteorological (tropospheric) conditions at the stations

The fieldtest was carried out in April 1984 with two TI-4100 receivers owned and operated by Nortech Surveys.

DIFFSTAR - RESULTS

On basis of pseudo-range measurements to four satellites, at two stations simultaneously, the following results were attained from the computations and analyses (among others):

- deviations from reference position were of the same size at both stations
- the biases at both stations varied in a similar way
- the random errors were different at both stations and dependent on local antenna conditions
- the differential errors did not vary noticeably with distance (0-570 km)
- the results were similar for the dynamic and the stationary test
- the 3-dimensional positioning results were to a high degree dependent on good observer-satellite geometry
- the 2-dimensional positioning results were less dependent on geometry and the gaussian noise was reduced significantly
- the use of two frequencies (L1 and L2) did not result in noticeably better differential positionaccuracy compared with the use of L1 only
- typical accuracies were in the order of 1 meter with a few minutes of averaging

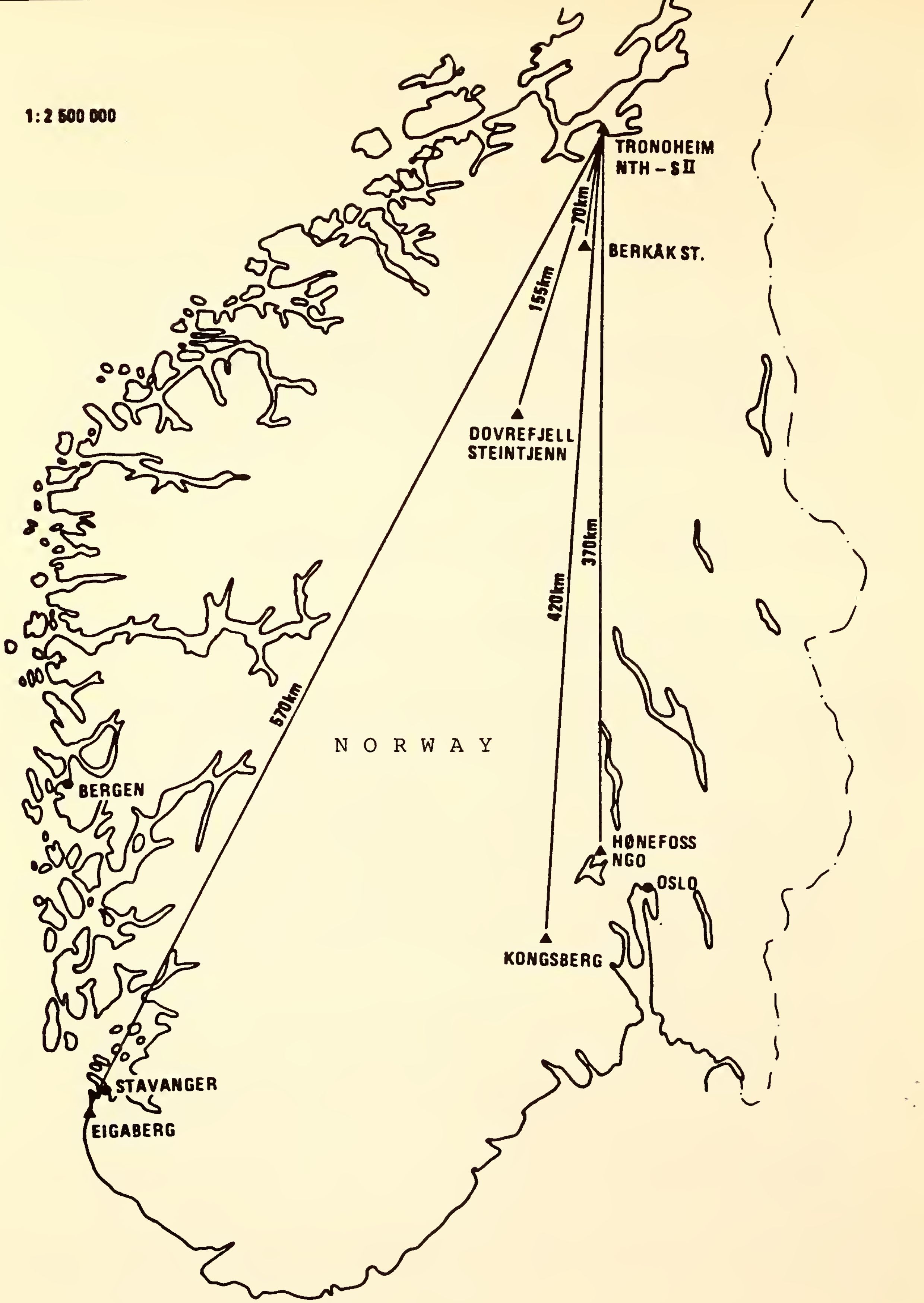

Differential G P S - test stations

DIFFSTAR - CONCLUSIONS

Based on the above mentioned results the following conclusions were drawn (or confirmed):

- the differential GPS-method works satisfactory for both dynamic and stationary positioning, systematic errors in single position results are nearly neutralized
- the size of the residual differential errors is practically independent of the distance between stations (0-570 km)
- the location of the antenna is decisive for the position accuracy, probably due to multipath errors
- direct correction of positions gives the same level of accuracy as correction of pseudo-ranges
- a suitable interval for correction update presently seems to be less than one minute
- for offshore applications it seems sufficient to use the L1-signal only
- the 2-dimensional differential positioning method may be preferred at sea provided the geodetic height is known a-priori.

NAVIGATION LABORATORY

The Norwegian Hydrographic Service has initiated the establishing of a navigation laboratory on board of its survey vessel M/S "LANCE".
The aims are, among others:

- to build up a national center for professional competence in the field of positioning and navigation
- to control geographically conditioned systematic errors of classical navigation and positioning systems
- to calibrate radiopositioning systems
- to use the GPS-system as an overall reference
- to stimulate education and research.

So far classical instrumentation for positioning and navigation is available and a NAVSTAR GPS TI 4100 receiver, a VAX 750 in-house computer and computersoftware have been purchased. In 1985 another TI 4100 will become available in addition to an on-board computer and additional software. It is planned to purchase an inertial system in 1987.

The navigation laboratory will make possible an improved application of existing classical systems, an active participation in national and international research projects and it may contribute to better conditions for academic education in positioning and navigation in Norway.

REFERENCES

Blankenburgh, J.C., 1983	High-Precision Marine Positioning - Requirements, Limitations and Possible Problem Solutions. Marine Geodesy Vol. 7, Nr. 1-4
Davidsen, R., 1985	NAVSTAR/Norsk navigasjonslaboratorium. Nautisk Forum, Oslo
Fossum, B.A., Hals, T., 1984	Resultater for differensiell GPS fra Diffstar feltmålingene. Servicereport IKU nr. 01.6371.00/02/84
Holte, S., 1985	A/S Kongsberg Våpenfabrikks NAVSTAR - engasjement. Nautisk Forum, Oslo

TIME FROM GPS

William J. Klepczynski and Kerry A. Kingham
U. S. Naval Observatory
Washington, D. C.

Michito Imae and Makoto Urazuko
Radio Research Laboratories
Tokyo, Japan

INTRODUCTION

Because precision clocks are the heart of its navigational capabilities, GPS is an important contributor to the precise time and time interval (PTTI) community. It serves them in two ways: first, as a worldwide time dissemination system, and secondly, as a time transfer system which allows the precise synchronization of widely separated clocks. These features are not unique to GPS. However, among operational systems which can also be used for time transfer, it provides these capabilities with the greatest precision and accuracy. Of the many factors contributing to this the most important is the use of cesium beam and rubidium vapor cell frequency standards in the spacecraft to control the navigation signals. Also important is the choice of transmission frequencies which while not removing all atmospheric effects on the transmitted signals, overcome some of the deficiencies of other systems used by the PTTI community, i. e., the seasonal variations in the propagation path delay of the LF navigation system, Loran-C.

GPS timing receivers which recover the time disseminated by the navigation system are now commercially available. In their simplest form, the timing receivers generate an output pulse (IPPS) which is synchronized to the time reference of the GPS system. These receivers also have the capability to compare a local clock to the GPS reference time. When two of these receivers are used simultaneously at widely separated sites, the clocks at these sites can be intercompared.

This paper will discuss the time reference for the GPS system and how it is reconstructed from the navigation message. It will also discuss common-view GPS time transfers and present data which show the capabilities of the system.

REFERENCE TIME FOR GPS

From January, 1983, the time reference for the GPS system is UTC(USNO). UTC(USNO) is a time scale determined at the U. S. Naval Observatory. It is based on the performance of about 25 selected, commercially manufactured cesium beam frequency standards. It is one of the most stable time scales in the world. It receives about 25% of the weight in the formation of International Atomic Time (TAI) by the Bureau International de l'Heure in Paris, France. The Master Clock (MC) of the U. S. Naval Observatory is the real-time, physical realization of UTC(USNO). Presently, the two Master Clocks of the USNO, designated MC1 and MC2, respectively, are driven by two different kinds of frequency standards. MC1 is driven by a cesium beam frequency standard, while MC2 is driven by an hydrogen maser (Klepczynski et al, 1984). Figures 1 and 2 are presented to show the relative performance of the present two Master Clocks. Figure 1 shows the differences between MC1 (cesium based) and UTC(USNO) after removal of a bias. The root mean square (R.M.S.) differences are 4.3 ns. Figure 2 shows the differences between MC2 (hydrogen maser based) and UTC(USNO) after removal of a bias. The RMS differences are 1.2 ns.

The time transmitted by GPS is known as GPS System Time. It is physically maintained to within 1 microsecond of UTC(USNO). Corrections, in the form of coefficients of a polynomial, are transmitted in the navigation message to allow the user to determine UTC(USNO) to within 100 nanoseconds. GPS System Time now differs from UTC(USNO) by 3 seconds because GPS System Time is not affected by leap seconds. Thus, when it is stated that GPS time is within 1 microsecond of UTC(USNO), it means "after the proper number of seconds (2 + number of leap seconds since 1983) have been taken into account".

As with the USNO Master Clock, there is a physical clock which keeps GPS System Time. However, because GPS is a navigation system which must have a high degree of reliability, the system has been designed to allow for the switching of a clock which has been designated as the reference clock with a backup clock. Thus, in the event of a clock failure, another can be designated the reference clock without upsetting the system. This means that clocks from which the reference clock can be chosen must be continually monitored. A unique feature of the system is that these clocks are located at widely separated locations, the GPS Monitor Stations or the GPS Master Control Station.

GPS AS A TIME DISSEMINATION SYSTEM

As mentioned earlier, GPS timing receivers, in their simplest form, are designed to give the user a signal which is synchronized to the GPS time reference. The process starts by deriving the time difference between an internal receiver clock and the space vehicle clock which is being tracked. By noting the range to the satellite, the internal receiver clock can be offset to agree with the SV clock, t_{sv}. GPS System Time, t, is then obtained from the following expression:

$$t = t_{sv} - a_o - a_1(t-t_{oc}) - a_2(t-t_{oc})^2 + t_r + \text{other corrections}$$

where a_o, a_1, a_2 are contained in the navigation message and represent the coefficients of a polynomial that gives the difference between the SV clock and GPS System Time; t_{oc} represents the reference time for the clock coeficients; t_r is a relativistic term which the user must calculate from other information in the navigation message; and the other corrections are for the tropospheric and ionospheric delays and any other systematic affects which can be modelled by the user.

The user then gets UTC(USNO) from GPS System Time by evaluating the expression:

$$\text{UTC(USNO)} = t - t_{LS} - A_o - A_1(t-t_{ot})$$

where t_{LS} is the Leap Second correction; A_o and A_1 are the coefficients for the polynomial that represents the difference between UTC(USNO) and GPS System Time; and t_{ot} is the reference time for coefficients A_o and A_1. It should be noted that the coefficients A_o and A_1 are computed at the U. S. Naval Observatory from data obtained by its monitoring receivers. These coefficients are then transferred, electronically, to the Master Control Station which is now located at Vandenberg AFB. They are then incorporated into the navigation message which is uploaded into the different spacecraft.

In this fashion, then, the GPS timing units generate a signal which is synchronized to the GPS time reference. As a check on the integrity of the system, the USNO derives an estimate for UTC(USNO) from GPS system time with its GPS Time Transfer Units and compares it with UTC(USNO, MC). The differences are available on the USNO Automated Data Service (Miranian, 1983) in a file which has been designated @GPSB6. Table

I is a sample of this file. Barring any sudden frequency changes in the reference clock for GPS System Time, the differences usually run less than 40 nanoseconds. Thus, the user can recover time to well within the specified 100 nanoseconds and anywhere in the world. Figure 3 shows the residuals, after a quadratic fit, to the differences between MC2 and the clock of Space Vehicle (SV) 13 over a 24-day period, starting at MJD = 46096, 31 Jan 85. The RMS of the residuals is 11 ns. The clock on SV 13 is a Cesium Beam Frequency Standard.

GPS COMMON-VIEW TIME TRANSFER

The GPS Time Transfer Units currently available have some special options. For instance, the difference between an external clock and the reconstructed GPS reference time can be evaluated by an internal time interval counter in the TTU and the results displayed as "Local Clock - GPS". This is a very important capability for some applications. Allan and Weiss (1980) pointed out the advantages of using simultaneous observations of the same GPS spacecraft to attain a very high precision time transfer. The technique is usually referred to as common-view time transfer.

Two users, A and B, with GPS Time Transfer Receivers, each observe the same space vehicle at the same time. Each determines the difference between his local clock and that of the spacecraft clock, i. e., A-SV and B-SV. Each user must share his information with the other. Upon subtracting the two sets of numbers, one gets A-B, the difference between the two clocks. What makes this method very accurate is the fact that many of the errors common to the spacecraft clock are eliminated in forming the difference. Ephemeris errors are not eliminated by this technique. However, their effect on the time transfer results are greatly reduced and are a function of the geometry between the two stations. Errors in the ephemeris of a satellite of about 15 meters could have a 5 nanosecond or less effect on the time transfer results (Allan and Weiss, 1980). Unmodelled ionospheric and tropospheric effects are greatly reduced. It is only the unmodelled differential delay between the two sites which affects the results. By carefully selecting the time of day when the observations are made, further reduction in the differential error can be made.

RRL-USNO TIME TRANSFER EXPERIMENT

In December of 1984, Radio Research Laboratories (RRL) and the U. S. Naval Observatory began a program of evaluating some high-precision intercontinental time transfer techniques. One part of the program was to calibrate and verify a time transfer made by Very Long Baseline Interferometry (VLBI). Part of the calibration and verification was done with a Portable Clock (PC) which was transported between Washington and Tokyo. GPS common view was used to monitor and check the performance of the PC while it was in Tokyo. When the PC was not at the VLBI site partaking in the VLBI experiment, it was used to provide an input signal to a GPS Time Transfer Unit which was built by RRL (Imae and Urazuku, 1984). The data obtained consisted of values of PC - SV. Simultaneously, values of USNO MC - SV were obtained in Washington using a STI 502 Time Transfer Unit. The two sets of values were differenced and a constant bias to account for the systematic differences between the two receivers and other unmodelled systematic effects was applied to the results. This then gave estimates for the difference between the PC and USNO MC. Figure 4 shows values for MC-PC obtained by the USNO Data Acquisition System before and after the trip. A noticeable change in frequency of the portable clock took place upon the return of the PC to Washington. Figure 5 shows the values for MC-PC obtained from the GPS common-view measurements superimposed on Figure 4. It appears that the PC behaved well during the trip.

The VLBI results (still to be reduced) will provide further information about the PC behavior. It is important to note that some of the GPS time transfer data obtained using SV6 had to be discarded. The scatter in the data was greater than any that had been seen before using this technique. It was assumed that the excessive scatter was caused by the ionosphere. At the time of the experiment, SV6 was being observed in the early evening in Tokyo and in the morning at Washington, a time when the total electronic content (TEC) of the atmosphere was undergoing its most rapid change.

DISCUSSION

In regard to Figure 3, it should be pointed out that the comparison of SV13 Clock is made against MC2 (H-maser). Therefore, one should not see the quasi-periodic two day terms of 10 ns amplitude that is perceived in Figure 1. The source of the somewhat periodic noise exhibited in Figure 3 is still subject to question. Klepczynski (1983) has conjectured that it is due to minor deficiencies in the transmitted ephemeris. The apparent two-day quasi-periodic term exhibited in Figure 1 can be traced to the daily procedures used in steering MC1(Cs) to follow UTC(USNO). It should be pointed out that the clock of SV13 is a cesium beam frequency standard and it exhibits good performance characteristics.

Figure 4 shows the performance of a cesium beam frequency standard which has been used as a Portable Clock. The performance of a PC is sometimes marred by sudden frequency changes. The downward drift of the values of MC1-PC1 observed before the clock left Washington seems to be confirmed by the GPS Common-View monitoring of the PC. However, as mentioned earlier, only the VLBI Time Transfer measurements will confirm this. There is a noticeable change in frequency which occurred after the clock returned to Washington. No definitive cause can be given for this behavior. But, it should be mentioned that this particular PC has frequently exhibited this kind of behavior.

The values for MC1-PC derived from GPS common-view measurements were based on observations of SV9 and SV13. There is only limited common-view time between Washington and Tokyo. This explains the somewhat apparent paucity of points. During the time the PC could be connected to the RRL GPS Time Transfer Unit, SV6, SV9 and SV13 were tracked continuously. The points shown in Figure 5 are 13 minute averages during the time of common-view. The data for SV9 and SV13 exhibited rather uniform dispersion and it is the data shown in Figure 5. However, the data for SV6 was extremely noisy and could not be used in the analysis. As mentioned earlier, it is conjectured that ionospheric noise was the principle dispersing agent. At the time of the observations for SV6, evening had just started at one of the sites and morning had started at the other site. Thus, it is extremely important to carefully select the time at which common-view GPS measurements are made for time transfers, keeping in mind the relative separation and location of the participating stations.

CONCLUSIONS

GPS is an effective tool for the PTTI community. It is useful for the worldwide dissemination of time at the sub-microsecond level. It is also an high-precision method for the precise synchronization of widely separated clocks using the common-view technique. It is also a cost-effective method. In the few short years that the system has been operational for time transfer, the commercial time transfer units have dropped in price from $52,000 to about $25,000. It is expected that in the coming years we should see this trend continue.

REFERENCES

Allan, D. W. and Weiss, M. A., May, 1985, "Accurate Time and Frequency Transfer During Common-View of a GPS Satellite", Proceedings of the 34th Annual Frequency Control Symposium.

Miranian, M., September, 1982, "The U. S. Naval Observatory Automated Data Service", presented at HP1000 User's Group Meeting.

Imae, M. and Urazuku, M., May, 1985, "Development of a GPS Time Transfer Receiver and Time Comparison Results", to be presented at the 39th Annual Frequency Control Symposium.

Klepczynski, W. J., October, 1985, "Modern Navigation Systems and Their Relation to Timekeeping", Proceedings of the IEEE, Vol. 71, No. 10, 1193-1195.

Klepczynski, W. J., Wheeler, P. J., Kubik, A. J. and Clarke, R. T., 1984, "An Improved U. S. Naval Observatory Master Clock", paper presented at CPEM 84 Conference, Delft, Holland.

Table 1 - Listing of file @GPSB6. This file contains in the last column, the difference between UTC(USNO) and the estimate for UTC(USNO) obtained from GPS System Time using the coefficients, A0 and A1, which are transmitted in the navigation message. In the absence of any sudden frequency changes to GPS System Time, these differences usually run less than 40 ns.

```
--------------------------------------------------------------------------------

USNO GPS TRACKING-
DATA REDUCTION TO UTC(USNO):
SV CL MJD' HH MM SS TRCK AG EL AZM ION   GPS-MC     SLOPE  RESIDUALS  GPS-UTC
                                        MEASURED               RMS     ERROR
                    SEC  HR DG DEG  NS     NS        PS/S       NS       NS

 8 99 6136  3 56  0  780 21 20 193  24    -213        10        18       19
 8 99 6136  4  9  0  780 22 27 195  20    -210         0        17       16
 8 99 6136  4 22  0  780 22 33 197  18    -214         0        13       20
 8 99 6136  4 35  0  780 22 40 199  15    -214         9        15       20
 8 99 6136  4 48  0  780 22 46 202  13    -208        -9        14       14
 8 99 6136  5  1  0  186 23 53 207  12    -208       -29        15       14
 8 99 6136  5  8  0  780 23 57 209  11    -213        -1        12       19
 8 99 6136  5 21  0  780 23 63 216  10    -221        16        14       27
 8 99 6136  5 34  0  132 23 69 225   9    -210       -13         9       16
 6 99 6136  5 48  0  378 23 28 325  16    -203        37        15        9
 8 99 6136  6  4  0  780  0 80 280   9    -211        -4        12       17
 8 99 6136  6 17  0  780  0 79 319   9    -210         0        14       16
 8 99 6136  6 30  0  780  0 75 344   9    -210       -12        15       16
11 99 6136  6 54  0  780  0 46 252  13    -225         0        13       31
11 99 6136  7  7  0  780  0 50 261  12    -227         9        12       32
 9 99 6136  7 26  0  780  0 25 327  17    -215         0        15       20
 8 99 6136  7 42  0  780  1 46  32  12    -228        23        23       33
 6 99 6136  7 58  0  780  1 63 239  10    -219         6        14       24
11 99 6136  8 18  0  780  1 62 324  10    -225         0        13       30
11 99 6136  8 31  0  780  1 61 338  10    -235        18        12       40
 9 99 6136  8 50  0  780  2 48 285  12    -216         1        12       21
 9 99 6136  9  3  0  780  2 47 274  12    -217         0        11       22
11 99 6136  9 30  0  780  3 54  31  11    -229         9        19       34
11 99 6136  9 43  0  780  3 51  40  12    -227         8        15       32
11 99 6136  9 56  0  780  3 49  49  12    -225         0        16       30
13 99 6136 10 12  0  780  2 47 319  12    -229        -4        13       34
12 99 6136 21 40  0  372 12 11  38  23    -247       106        22       51

DATA FROM USNO GPS STI 502 RECEIVER (USNO STANDARD RECEIVER)
```

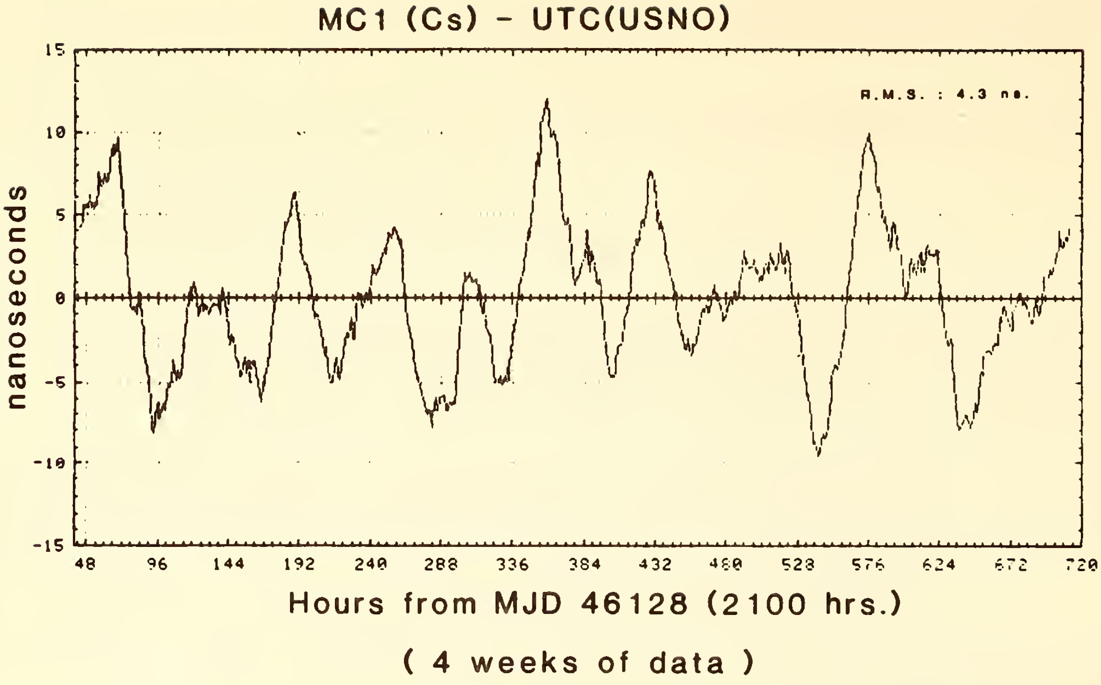

MC1 (Cs) - UTC(USNO)

Figure 1 - Differences between cesium based MC1 and UTC(USNO) after removal of a bias term. R.M.S. of differences is 4.3 ns.

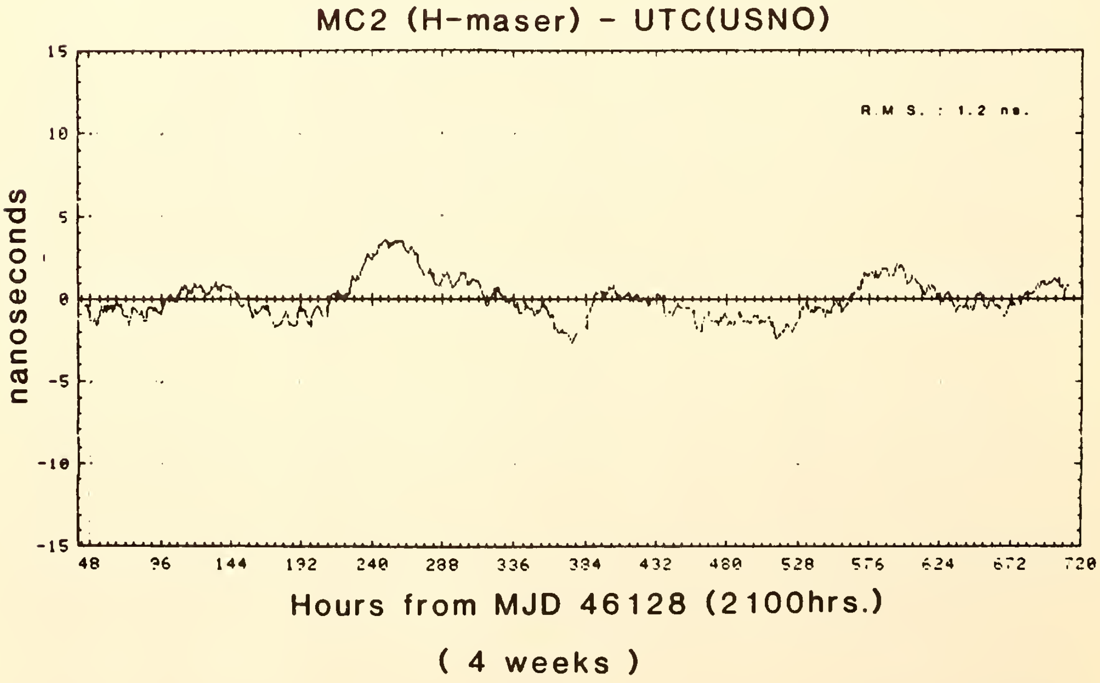

MC2 (H-maser) - UTC(USNO)

Figure 2 - Differences between hydrogen maser based MC2 and UTC(USNO after removal of a bias term. R.M.S. of differences is 1.2 ns.

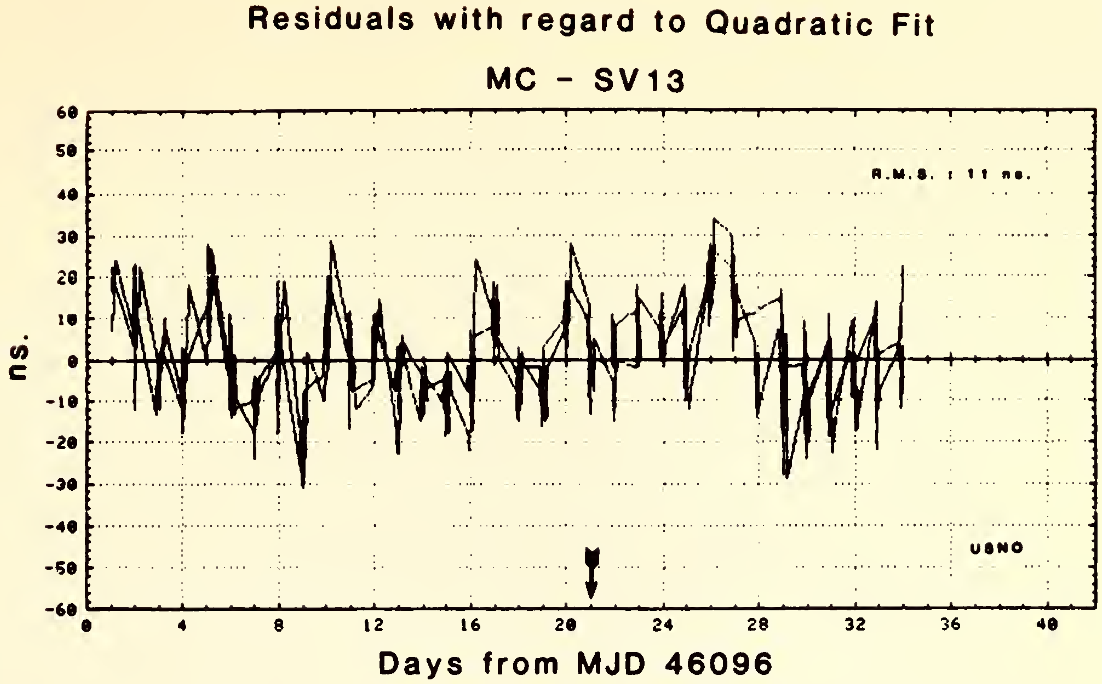

Figure 3 - Residuals with respect to a quadratic fit to MC2 - SV13 clock. R.M.S. of differences is 11 ns.

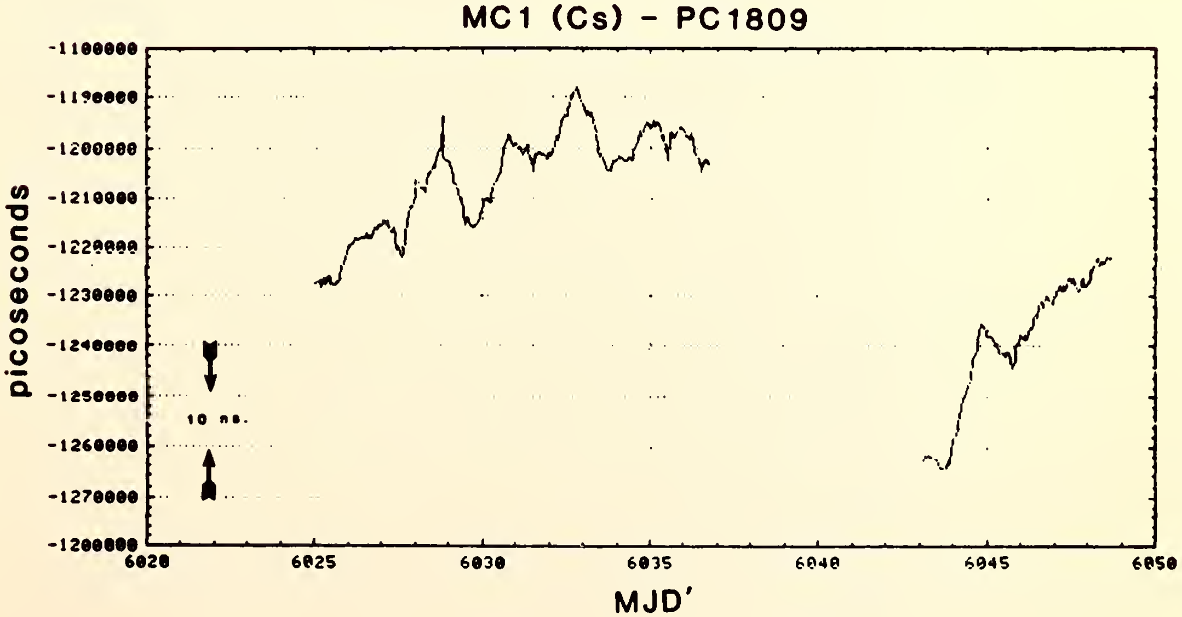

Figure 4 - Differences between MC1 and PC1809 before and after Washington-Tokyo-Washington trip, as monitored at USNO

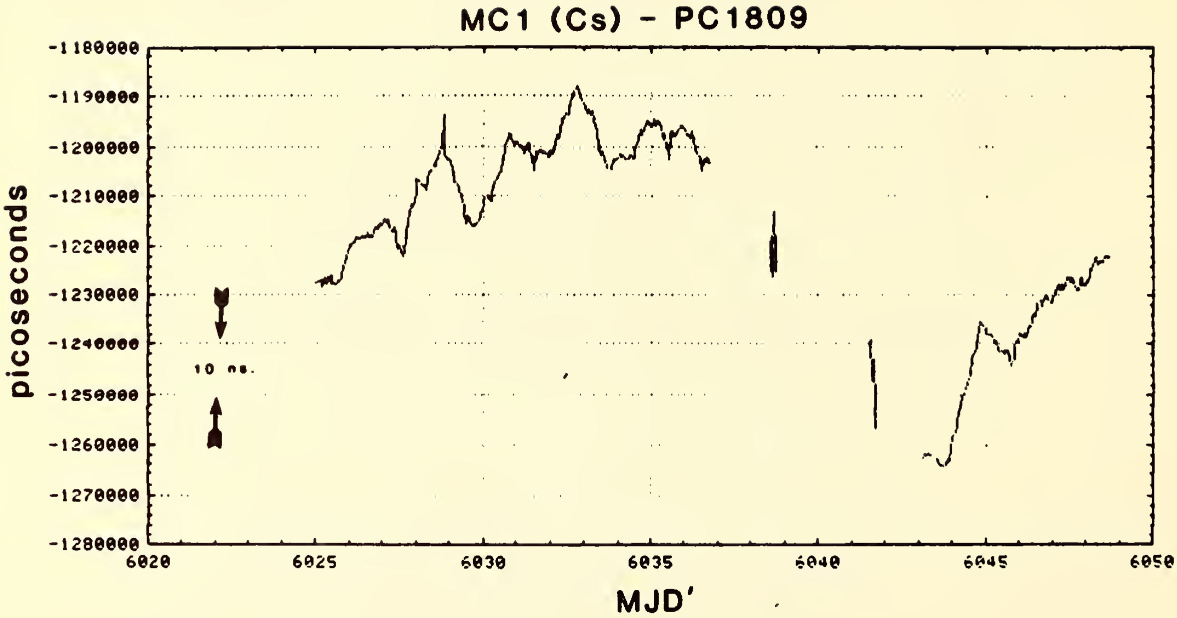

Figure 5 - Differences between MC1 and PC1809 as derived from GPS Common-View measurements superimposed on Figure 4.

GEODETIC CONSTRAINTS ON STRAIN RATES IN THE VICINITY OF THE 1886 CHARLESTON, SOUTH CAROLINA, EARTHQUAKE

William H. Prescott
U. S. Geological Survey
345 Middlefield Road, MS/977
Menlo Park, CA 94025

Scot W. Krueger
University of California, Berkeley
Berkeley, CA 94720

Mark D. Zoback
Stanford University
Stanford, CA 94305

ABSTRACT. An analysis of triangulation data in the vicinity of the 1886 Charleston, South Carolina earthquake reveals no evidence of detectable shear strain accumulation. The resolution of the data set is such that shear strain rates as low as 0.1 μrad/yr average would have been detectable. Most of the angles were first observed in the 1930's and then reobserved between 1950 and 1970. One angle was observed prior to the 1886 earthquake. No significant change was observed in this angle. In order to improve the resolution in the data set the U.S. Geological Survey and the South Carolina Geodetic Survey have reobserved a portion of the triangulation with Global Positioning System receivers. Results of this resurvey are not available yet but the improved precision and spatial coverage should allow reduction of the shear strain rate uncertainty to about 0.04 μrad/yr at the 95% confidence level.

INTRODUCTION

Earthquake hazard is generally associated with the western United States rather than the eastern part of the country. Although earthquakes in the eastern 2/3 of the nation tend to be much less frequent, there have been some major events even during the short period for which records are available. Some of the more notable historical events are listed in Table 1.

Table 1

Large historic earthquakes in eastern North America

Location	Date	Intensity
St. Lawrence River	1663	X
Cape Ann, Mass.	1755	VIII
New Madrid, Mo.	1811-12	XII
Charleston, S.C.	1886	IX-X
St. Lawrence River	1925	VIII

Data from Coffman and van Hake (1982).

In 1886 a large and damaging shock occurred near Charleston, South Carolina. Microseismicity which persists to this day has not been clearly associated with any known structure despite considerable study (Gohn et al., 1983).

The question of the probability of a repeat of the 1886 earthquake is relevant to a seismic hazards assessment of the area. In fact, a significant question in the eastern United States is whether earthquakes like the 1886 Charleston earthquake are only likely in places where they are known to have occurred in the past, or whether similar events can occur anywhere. The process of storing strain energy is very directly related to the earthquake generation process. It has long been assumed that strain rates are low in intraplate regions, but few attempts have been made to measure them. In a companion study to this one Zoback et al. (1985) obtained surprisingly high estimates of the average shear strain rate in southern New York state. In this paper we have analyzed historic triangulation data in the vicinity of the Charleston seismic area in an attempt to put constraints on the rates of crustal strain in this intraplate seismic region. The precision and coverage of the available triangulation data were far from optimal. In cooperation with the South Carolina Geodetic Survey, we have also reoccupied a subset of the triangulation stations in the area. Global Positioning System (GPS) receivers were used for this resurvey. These data were not available in time for the preparation of this report. Consequently, the results obtained thus far are derived exclusively from triangulation surveys.

DATA AND ANALYSIS

Since survey stations are located on the surface of the earth, their position, and consequently the angles formed by them, will change when the crust of the earth is distorted. Frank (1966) suggested a technique for using survey measurements to infer this strain. Prescott (1976) extended Frank's method to allow the use of heterogenous data and to allow the inclusion of the covariance of the observations. This paper utilizes triangulation observations of the National Geodetic Survey (NGS). The area of study and the observed angles are located on the map in Figure 1. Computer listings of observed directions for the area were obtained from the NGS. Although one angle had an observation as early as 1853 (prior to the 1886 earthquake) most of the angles were first observed between 1930 and 1935. The second observation of most angles was made between 1955 and 1970. Shear strain rates were calculated from a least squares inversion of the observed angle changes (Prescott, 1976). The shear strain rate obtained in this way is an average rate over the time and space spanned by the observations. Because the scale of the triangulation surveys is much less accurately determined than are the angles, we did not attempt to estimate changes in dilatation or areal change. Rather we only estimated the deviatoric components of the strain tensor.

In this paper all strain rates refer to engineering (as opposed to tensor) shear and will be given in units of µrad/year. When error bars are given they indicate the one standard deviation uncertainty level. All of the angles used in this study are from triangulation surveys carried out between 1853 and 1981 by the U.S. Coast and Geodetic Survey (now called NGS). A total of 49 angles had more than one observation and thus were potentially of value for the detection of crustal motion. Only one of the angles was first observed before the 1886 earthquake.

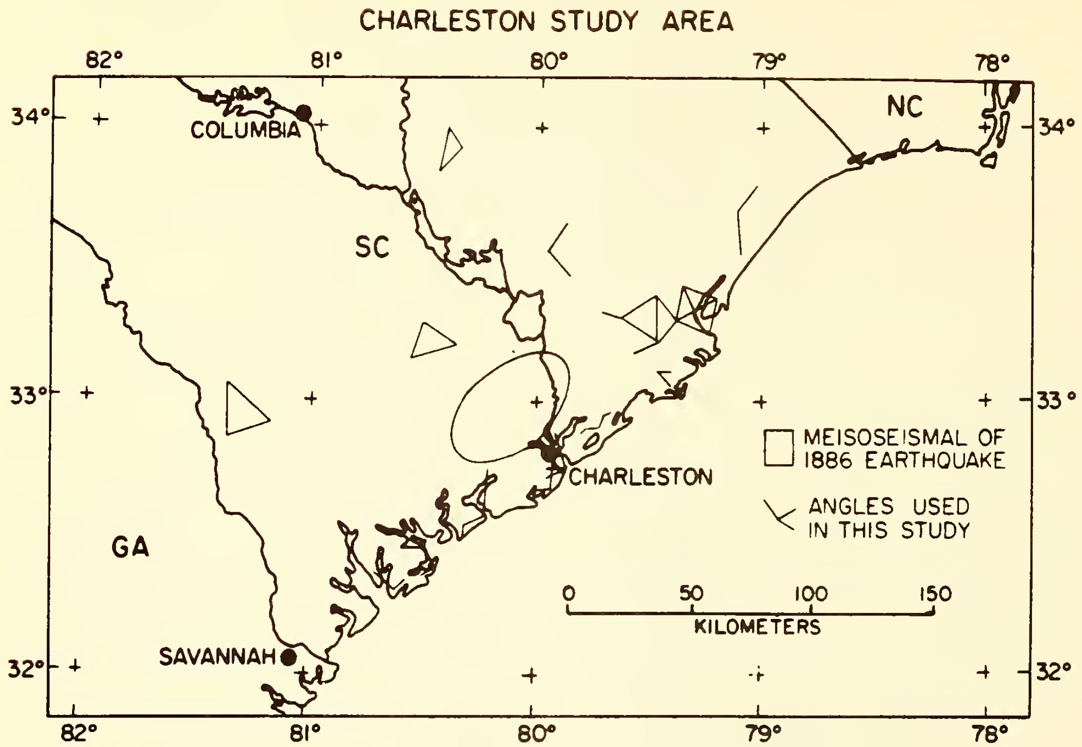

Figure 1. Map of coastal South Carolina. The oval is the meizoseismal area of the 1886 Charleston, South Carolina, earthquake (Dutton, 1889). Lines and triangles indicate the location of the triangulation data that was analyzised.

RESULTS

The first line of Table 2 gives the results of an inversion of the entire set of 50 angle differences. The resulting best fit shear strain rate is 0.061±0.045 µrad/yr corresponding to a N66°W compression direction. The value for the magnitude of the strain rate does not differ significantly from zero at even a one standard deviation level. The data set contained a number of third order observations. The second line of Table 2 contains strain rates calculated using only those angles for which all observations were first order. There is almost no difference in the results, and the results do not indicate any evidence of strain accumulation.

Table 2

Data Set	No.	γ_1	γ_2	γ	ψ
All data	50	-0.041	0.045	0.061	23.6
(Sigma)		0.040	0.046	0.045	19.6
Better data	27	-0.038	0.047	0.061	25.4
(Sigma)		0.042	0.051	0.051	20.2
Near data	22	-0.017	0.053	0.055	36.3
(Sigma)		0.126	0.097	0.091	67.7
Far data	26	-0.041	0.054	0.067	26.5
(Sigma)		0.043	0.053	0.053	18.7

Notes:

γ_1	Shear strain rate on NW-SE or NE-SW planes (µrad/yr).
γ_2	Shear strain rate on E-W or N-S planes (µrad/yr).
γ	Total shear strain rate (µrad/yr).
ψ	Azimuth of maximum extension (clockwise from N).

There were no repeated angles in the vicinity of the 1886 earthquake. If the data are split into two groups, those near the seismic zone and those distant from the seismic zone, the near group gives a value of 0.055±0.091 µrad/yr corresponding to N54°W, and the distant group gives a value of 0.067±0.053 corresponding to N55°W. Neither value differs significantly from zero at even the one standard deviation level, but their orientations agree quite well. It is somewhat surprising that all of the azimuths of maximum extension agree so well, given that none of the strain rates are significant.

In addition to the post-earthquake data analyzed above, one angle was observed prior to the 1886 earthquake. Figure 1 contains a plot of the data for this angle. This angle was far removed from the epicenter of the 1886 earthquake and does not show any obvious effects from it. The observations neither require nor preclude the possibility of a strain step during the interval containing 1886. The simplest explanation for the linearity of the three points is a constant change in angle with time as a result of a constant strain rate acting over the entire time period. However, they can be fit by a horizontal line (no change of angle) within the uncertainty of the observations.

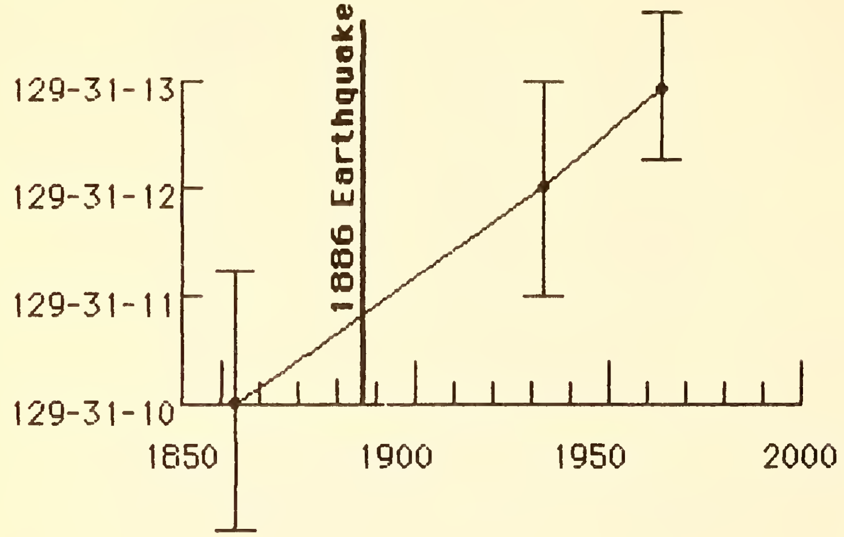

Figure 2. Observations at Edisto Island East Base of the angle (degrees-minutes-seconds) between Edisto Island West Base and New Cut. The error bars are ± one standard deviation.

DISCUSSION

All of the calculated strain rates (Table 2) are within their uncertainty, an uncertainty derived from the precision of the observations. Consequently there is no evidence from this study to suggest that deformation is occurring in the study area. Of course, there is also no way to exclude the possibility of strain accumulation at some lower, undetectable, rate. Note that although the data have a precision of $1{:}10^5$, the strain is determined to within $5{:}10^8$, an improvement in resolution by a factor of 200. This improvement in resolution is a consequence of the fact that we are averaging 50 angles (a factor of about 7) and the fact that the data span a time period of about 35 years. Typical strain rates in the more tectonically active parts of the world are of the order of $3{:}10^7$. If deformation were occurring at these rates in the region covered by the angles in Figure 1, it would be clearly detectable.

One of the troubling features of the data set is the persistence of the results in light of the low signal-to-noise ratio. Given that none of the strain rates is significant at even the one sigma level, we would expect to see more scatter in the results from different subsets than is evident from Table 2. There are really only two independent data sets in Table 2, those labeled "near data" and "far data". The first and second lines of Table 2 are derived from these two. It is a little surprising how well these two agree given the size of the error estimates. A bootstrap technique of estimating the standard deviations (Diaconis and Efron, 1983) would produce a much smaller estimate than the those given in Table 2. Consequently it is worth expanding on how the error estimates of Table 2 were obtained, and considering whether these standard deviations could be seriously overestimated. The standard deviations given in Table 2 were obtained from estimates of the uncertainty in the observed directions provided by the NGS. These direction uncertainties were then propagated through the inversion (a linear process) to obtain corresponding estimates in the strain rate uncertainties. About half of the angles were first or second order with standard deviations of 0.6" or 0.7". The remainder generally had standard deviations of 1.2" to 1.7", although in one case the standard deviation was 3.0". These estimates are based on a very broad base of experience (by NGS) and it is unlikely that the angles are significantly more accurate than the quoted uncertainties. Additional evidence confirming that the standard deviations are correctly estimated comes from the residuals in the strain rate inversion.

The quantity

$$\sigma_0 = \left[\frac{\sum (o_i - c_i)^2 \sigma_i^{-2}}{\sum \sigma_i^{-2}} \right]^{1/2} \qquad (1)$$

has an expected value of 1 if the σ's are reasonable estimates of the uncertainty in the observations ("o" in the above expression). For the "far" data $\sigma_0 = 0.7$ and for the "near" data $\sigma_0 = 0.9$. This implies that a slight reduction in the size of the error estimates might be in order, but the effect is not nearly large enough to account for the good agreement between the "near" and "far" data. (Note: The above expression is actually only correct for the case of uncorrelated observations. The correct expression is slightly more involved in the present case since the angles are not independent.)

One problem with the data set is that it does not contain any angles in the most interesting area, that is, near the inferred epicenter of the 1886 earthquake. In order to obtain a data set with better coverage of the meizoseismal area, the U.S. Geological Survey and the South Carolina Geodetic Survey have undertaken a resurvey of the 1935 first order triangulation arc shown in Figure 3. Global Positioning System receivers were used for determining the 1985 position of the stations. The GPS field work was completed in January 1985. An adjustment of the GPS survey closed within $1:10^6$ (Steve Bell, Geo-Hydro, pers. comm. 1985). However many of the stations occupied by the GPS receivers were eccentric to the original triangulation stations. Ties to the original stations have been carried out (by the South Carolina Geodetic Survey) but this information was not available in time to include the results in this report. Addition of the new data should have two consequences: It will provide better coverage of the area of interest; and it will produce a reduction in the uncertainty of the determination of strain rate. The GPS data is more precise than the triangulation data ($1:10^6$ instead of $1:10^5$). A back of the envelope calculation indicates that the strain rate uncertainty for the comparison of the 1935 triangulation to the 1985 GPS survey should be about $2:10^8$ or 0.02 µrad/yr.

The 1886 earthquake occurred along the Atlantic margin, an area with relatively flat lying sediments covering a preCambrian basement. Extensive work has been undertaken to study the crustal structure (Gohn 1983), but there is still no clear understanding of the structures responsible for the seismicity of the region. Much of the discussion of the tectonics of the area has focused on the direction of maximum of compression since this is a feature that can be estimated in a number of ways. Zoback et al. (1978) found an in situ stress orientation with N25°W compression near Charleston from hydro-fracture measurements in the Clubhouse Crossroads well. Wentworth and Mergner-Keefer (1983) infer that the predominant mode of deformation has been NW-SE compression throughout all of the Cenezoic up to including the 1886 earthquake. From focal mechanisms of modern earthquakes Talwani (1982) concluded that, although the mechanism and locations fell into two distinct groups, both groups were characterized by an maximum compressive direction of N60°E. Subject to the (large) uncertainty noted above, the geodetic observations seem consistent with Zoback et al.'s and Wentworth and Mergner-Keefer's results and they appear inconsistent with the focal mechanisms of Talwani.

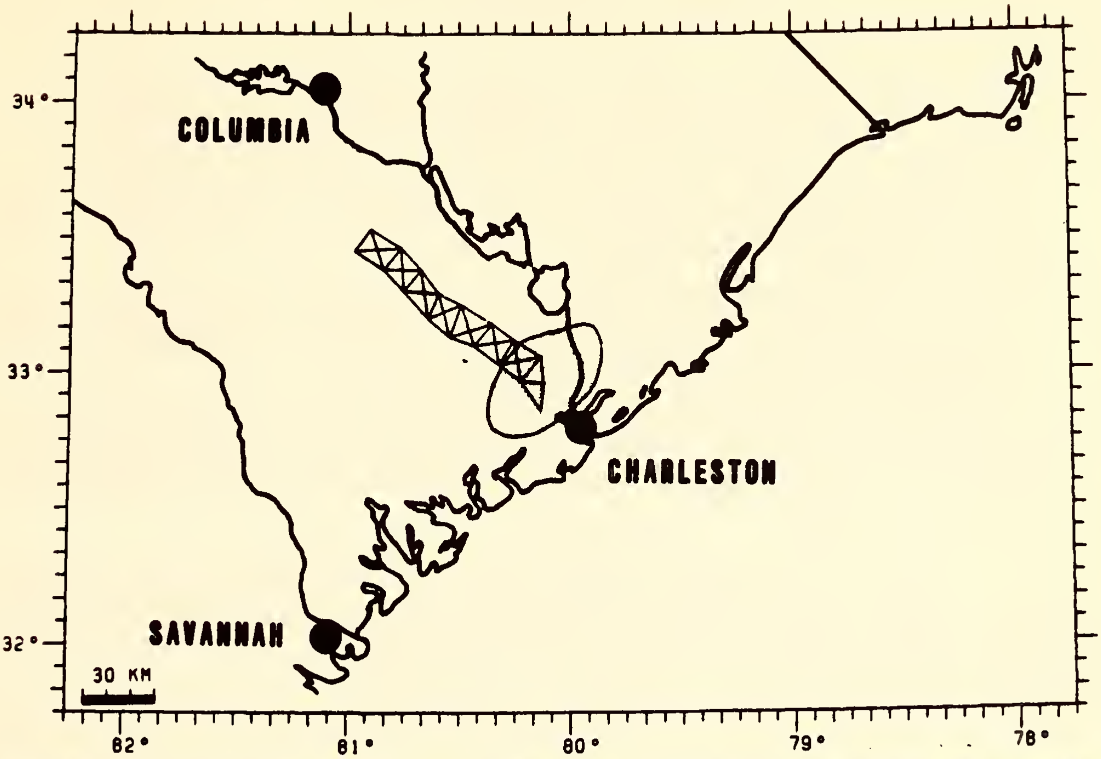

Figure 3. Map of coastal South Carolina. The angles shown were observed by conventional triangulation techniques in 1935, and the station positions were redetermined by GPS in January 1985.

ACKNOWLEDGEMENTS

This study would not have been possible without the generous help of Michael Cline and Richard Snay of the National Geodetic Survey who supplied the direction lists.

REFERENCES

Coffman, Jerry L. and Carl A. von Hake, 1982: Earthquake history of the United States, NOAA, Publ. No. 41-1.

Dutton, C.E., 1889: The Charleston earthquake of August 31, 1886, U.S. Geol. Surv. Ann. Rep., 1887-1888, 203-528.

Diaconis, P. and B. Efron, 1983: Computer-intensive methods in statistics, Sci. Am., 248(5), 116-130.

Frank, F.C., Deduction of earth strains from survey data, 1966: Bull. Seis. Soc. Amer., 56(1), 35-42.

Gohn, Gregory S., Editor's Preface, 1983: U.S. Geol. Surv. Prof. Pap. 1313, vii.

Prescott, W.H., An extension of Frank's method for obtaining crustal shear strains from survey data, 1976: Bull. Seis. Soc. Amer., 66(6), 1847-1853.

Talwani, P., Internally consistent pattern of seismicity near Charleston, South Carolina, 1982: Geology, 10, 654-658.

Wentworth, Carl and Marcia Mergner-Keefer, 1983: Regenerate faults of small Cenozoic offset—Probable earthquake sources in the Southeastern United States, 1983: U.S. Geol. Surv. Prof. Pap. 1313, S1-S20.

Zoback, M.D., J.H. Healy, J.C. Roller, G.S. Gohn, and B.B. Wiggins, Normal faulting and in situ stress in the South Carolina coastal plain near Charleston, Geology, 1978: 6, 147-152.

Zoback, M.D., W.H. Prescott, and S.W. Krueger, Crustal deformation and intraplate seismicity in southern New York: Evidence for lower crustal ductile strain localization?, 1985: submitted to Nature, 12 ms pages.

A 406 MHZ GPS/EMERGENCY LOCATION TRANSMITTER (ELT) FOR SARSAT OPERATIONS

Kristine P. Maine
Navigation Satellite Systems Directorate, Programs Group
The Aerospace Corporation
El Segundo, CA 90245

ABSTRACT. The SARSAT (Search and Rescue Satellite) has demonstrated the use of 121.5/243.0 MHz beacons to locate victims of aircraft and marine accidents. An experimental 406 MHz Emergency Location Transmitter (ELT) has been developed by NASA allowing a digital message containing identification and timing information as an alternative to the tone modulation signal provided on the 121.5/243.0 MHz ELT. Utilization of Global Positioning System (GPS) information with the 406 MHz ELT could greatly enhance the accuracy of the SARSAT system by including GPS position coordinates within the digital message. Location accuracies of less than 100 meters could be provided worldwide, which is ten times better than that available with the experimental 406 MHz ELT.

INTRODUCTION

Rapid detection of an aircraft crash or a marine distress is the most important feature to the survival of the victim. Studies have shown that those who have survived the initial crash have less than a 10 percent chance of survival if rescue is delayed beyond 2 days. If the rescue is accomplished within 8 hours, survival rate increases to 50 percent (Ref. 1). The SARSAT system contains 121.5/243.0 MHz and 406 MHz transponders on a low earth-orbiting spacecraft which can detect emergency signals from aviation or maritime vessels on a worldwide basis (including the polar regions). At this time of writing, two proposed SARSATs (from the United States) and three COSPAS satellites (from the Soviet Union) will carry these transponders. A joint agreement between Canada, France, the Soviet Union, and the United States has been established to provide emergency signal detection from 1985 to the end of the next decade.

Current technology of ELTs or Emergency Position Indicating Radio Beacons (EPIRB) used by civilian and military vehicles emits a tone modulated beacon on 121.5 MHz and 243.0 MHz frequencies. These signals are detected by receivers on low-orbiting SARSAT/COSPAS satellites yielding a position accuracy of 10 to 20 km (rms). An experimental 406 MHz ELT is being tested by the SARSAT/COSPAS project (Ref. 2) where the signal contains a digital message format indicating identification and elasped time information. SARSAT position accuracy is estimated to be between 2 to 5 kilometers for 406 MHz without any position reporting information within the digital message. Positioning is determined by utilizing the beacon identification from each transmission burst of the ELT. The frequency is measured and time tagged in the spacecraft processor. These parameters provide time and frequency values as input to a weighted least-mean-squares (WLS) position determination algorithm, yielding an accuracy of 2 to 5 km (rms). Hardware tests conducted by the Soviet Union yielded a position accuracy of 3 km (rms) (see Ref. 3).

USE OF GPS DATA

GPS receivers are expected to be used widely in the military aviation, civilian aviation, and maritime communities because of their accurate position locating capability. A GPS receiver contacts all GPS satellites within view in order to determine time and position information. The receiver software controls the activities of the receiver, maintains a navigation data base, estimates location, and monitors system performance. Time, latitude, and longitude come from the receiver software.

NAVSTAR satellites (GPS satellites) will be launched beginning in 1986 with a full operational system by 1988. Approximately 10,000 military user receivers are expected to be deployed over the same period. The majority of military GPS users will be aircraft, ships, ground vehicles, and ground troops. At this time, the number of civilian users has not been defined; however, civil aviation (commercial and private), maritime vessels (commercial and private), and ground vehicles are expected to use GPS navigation. The Federal Aviation Administration has committed to use GPS navigation as a secondary system for enroute navigation, with ongoing studies toward incorporating GPS for primary navigation. Several shipping industries and automobile companies have expressed interest in using GPS navigation capabilities. Positioning with a GPS receiver is expected to be within 100 meters (2) for civilian applications and 30 meters (2) for military applications.

SYSTEM DESIGN

Combining the accuracy of GPS receivers and the rapid detection capability provided by the SARSAT will reduce time locating victims from hours to within a few minutes and the area of search from 2 to 5 kilometers to 30 to 100 meters. Figure 1 illustrates the concept of using the 406 MHz ELT with an onboard GPS receiver. When a ship or an aircraft is in distress, an activation device initiates the ELT. Assuming the GPS receiver is working at the moment of impact, the position (latitude and longitude) and universal time (UTC) coordinates are incorporated within the digital message. The ELT will transmit the digital message containing identification of the aircraft (or ship), position, and time from an omni antenna to SARSAT. The SARSAT package receives and relays the digital messages to the Local User Terminal (LUT). No satellite processing for positioning will be necessary because the LUT will receive the exact loaction of the ELT. Digital messages can be stored within the satellite if a LUT is not within receiving range. Precise positioning is most beneficial to distressed aircraft or ships in remote regions where even the 3 km (rms) area provided by SARSAT would be too large to ensure prompt rescue (see Fig. 2). The GPS/ELT values are based upon the assumption that the GPS receiver is operating at the moment of impact. Small discrepancies may exist if the GPS deactivates less than 10 minutes before impact. If the GPS receiver is not operating under 10 minutes before an emergency occurs, nominal SARSAT processing will be needed for position determination.

The block diagram of the GPS/ELT, shown in Figure 3, consists of using a typical GPS receiver (see Ref. 4) and a modified 406 MHz ELT. The current time and position data generated by the GPS receiver enters a modified 406 MHz ELT through a RS232 or similar data bus, and is generated as part of the digital message. Aircraft (or ship) identification, country, and position coordinates are formulated and transmitted from a 406 MHz omni-directional antenna to SARSAT. The 406 MHz ELT also consists of a remote monitor and controller for testing and manual control of the unit. The activation sensor acts as a switch for automatic startup of the ELT during impact. Both the remote monitor and activation sensor interact with the power control, supplying the battery power to the 406 MHz electronics. The ELT memory is an active unit for storing the most recent GPS position information. An internal clock inside the ELT compares time with the GPS receiver time. If the time differential is greater than 10 minutes, no position information from the GPS receiver is used within the digital message. Therefore, normal SARSAT position processing will be necessary in determining the location of the ELT. The digital message is modulated over the 5k Hz bandwidth with a central frequency of 406.025 MHz. The signal is phase-modulated with bi-phased "L" (Manchester) data encoding with a specified data rate of 400 bps. Modifications in the digital message format extend transmission time to 605 msec.

The message generated by the ELT follows a format set up by the participating nation in the SARSAT/COSPAS program and is illustrated by Figure 4 (Ref. 5). However, it has been modified to adopt to GPS positioning accuracy by increasing the number of bits in the latitude and longitude slots. A bit synchronization pattern consisting of "1's" occupies the first 15 bits position, followed by a frame synchronization pattern occupying the 9 bits position. The format flag following the frame synchronization is a flag bit used to indicate the short or long message format. The long message format is designed to transmit 56 bits for latitude, 64 bits for longitude. and 4 bits for time (UTC). The short message format is the same as the long message format except it does not include the last 132 bits. This format would be used if the time differential were greater than 10 minutes. Type of vehicle and country are indicated within the message with an individual identification code unique for each user. Error correction coding is based upon the Bose-Chaudhuri parity code. Following code correction, the nature of emergency or elapsed time since activation is coded within the digital message. A special code may also be provided by indicating testing of the ELT, thereby reducing the large amount of false alarms plaguing ELT detection today. Latitude, longitude, and time [Universal Coordinated Time (UTC)] coordinates are received directly from the GPS receiver and coded into the message format. However, the choice of geodetic datum has not been determined at this time.

CONCLUSION

The SARSAT/COPSPAS project has already demonstrated its usefulness by detecting 121.5/243.0 MHz ELT signals leading to rescue of crash victims. Nevertheless, SARSAT operations can be improved by using GPS accuracy, provided by GPS receivers, within the digital message detected by SARSAT. Thus, SARSAT acts as a relay by sending the message to the Local User Terminals within the Search and Rescue operation centers. Using the GPS concept requires no modification to the GPS set and small modifications in the 406 MHz ELT in the form of a data bus hookup, active memory, internal clock. No modification is necessary to the SARSAT/COSPAS transponders or processing system. The digital message format has been established to incorporate future position and time information where the position slots have been extended to accommodate GPS accuracy. The combination GPS/ELT offers prompt rescue from a marriage of two space system--NAVSTAR and SARSAT/COSPAS.

References

1. COSPAS-SARSAT System Summary, December, 1981. National Aeronautics and Space Administration.

2. Douglas R. Kahle "Development of Satellite Location System for Aircraft and Boat Distress Beacon" (IEEE Aerospace and Electronic Systems, New York, NY, 1982) p 1-4.

3. Y. Zurabov, V. Bogdanov, Y. Makarov, and V. Rogalskiy, "The First Results of the COPSPAS-SARSAT System Flight Test" (IEEE, Aerospace Electronic System, New York, NY, 1982) p. 310-313.

4. Anthony Buige, Raymond R. LaFrey, and Steve D. Campbell, "The Design and Measured Performance of an Experimental GPS Navigation Receiver for General Aviation." (IEEE, Aerospace and Electronic Systems, New York, NY, 1982), p 5-12

5. Specification for the SARSAT Experimental 406-MHz ELT and EPIRB Electronics; National Aeronautics and Space Administration, October, 1981.

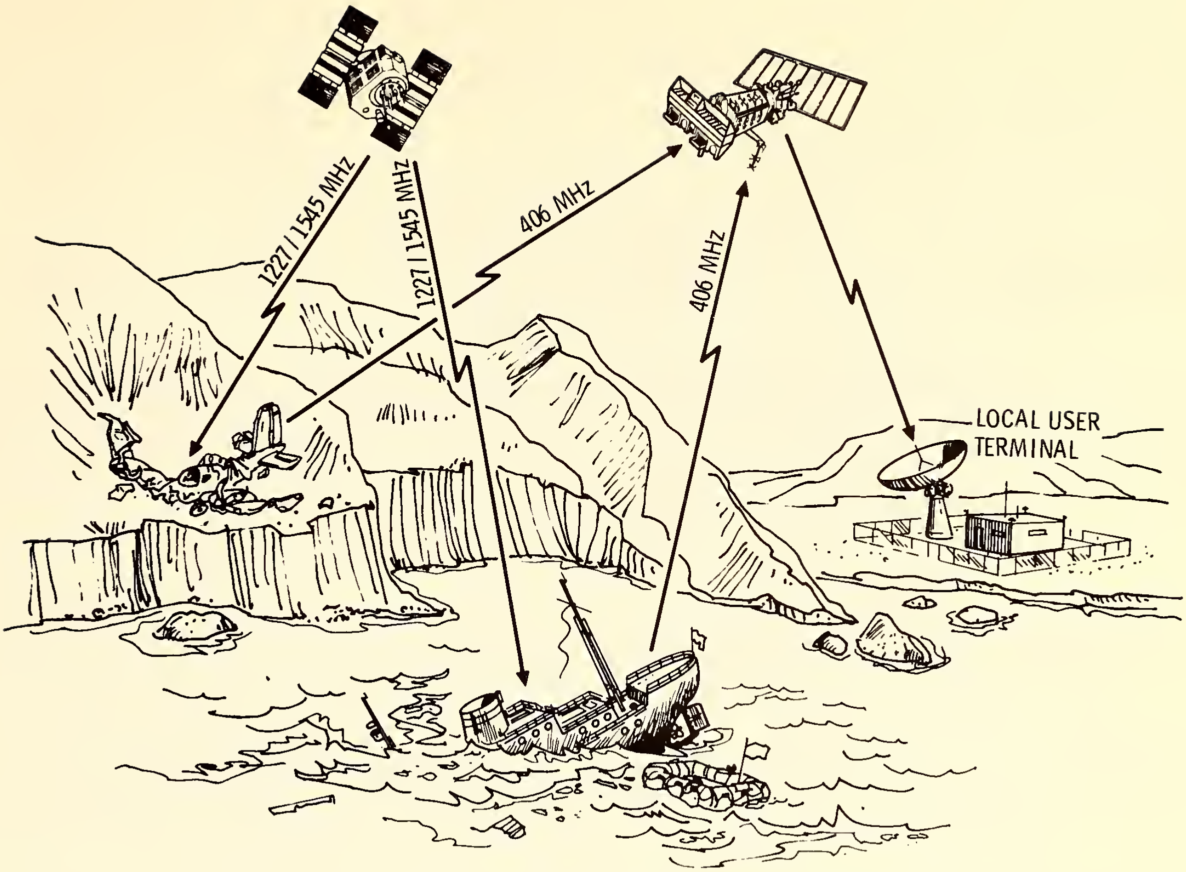

Figure 1. GPS/ELT System Overview

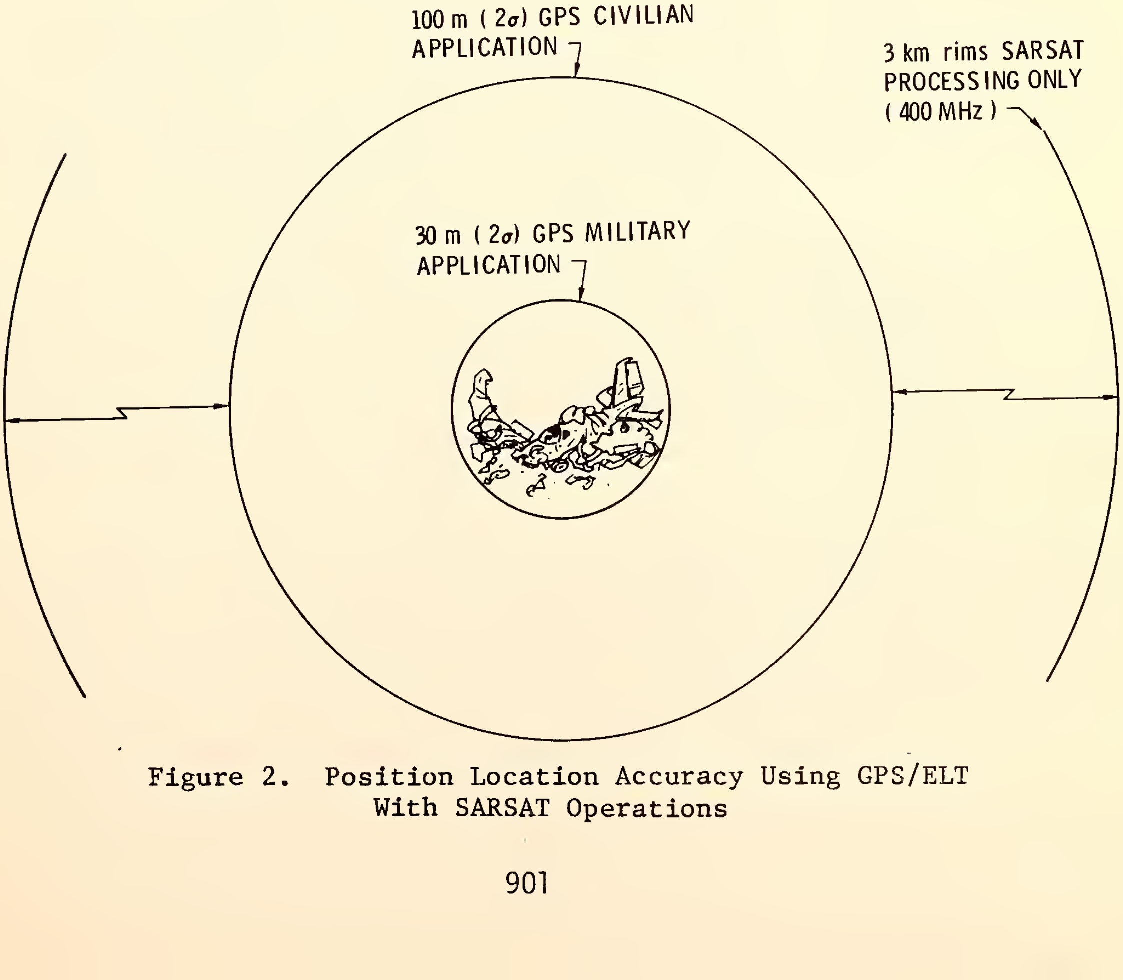
100 m (2σ) GPS CIVILIAN APPLICATION
3 km rims SARSAT PROCESSING ONLY (400 MHz)
30 m (2σ) GPS MILITARY APPLICATION

Figure 2. Position Location Accuracy Using GPS/ELT With SARSAT Operations

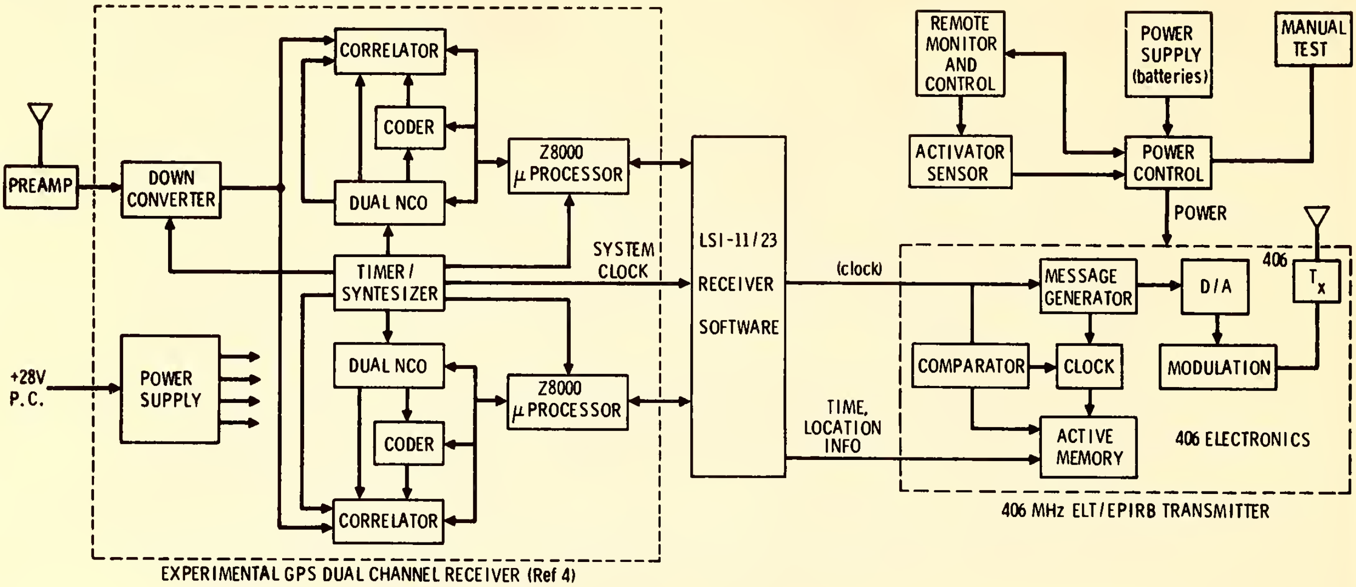

Figure 3. Block Diagram of GPS/ELT System

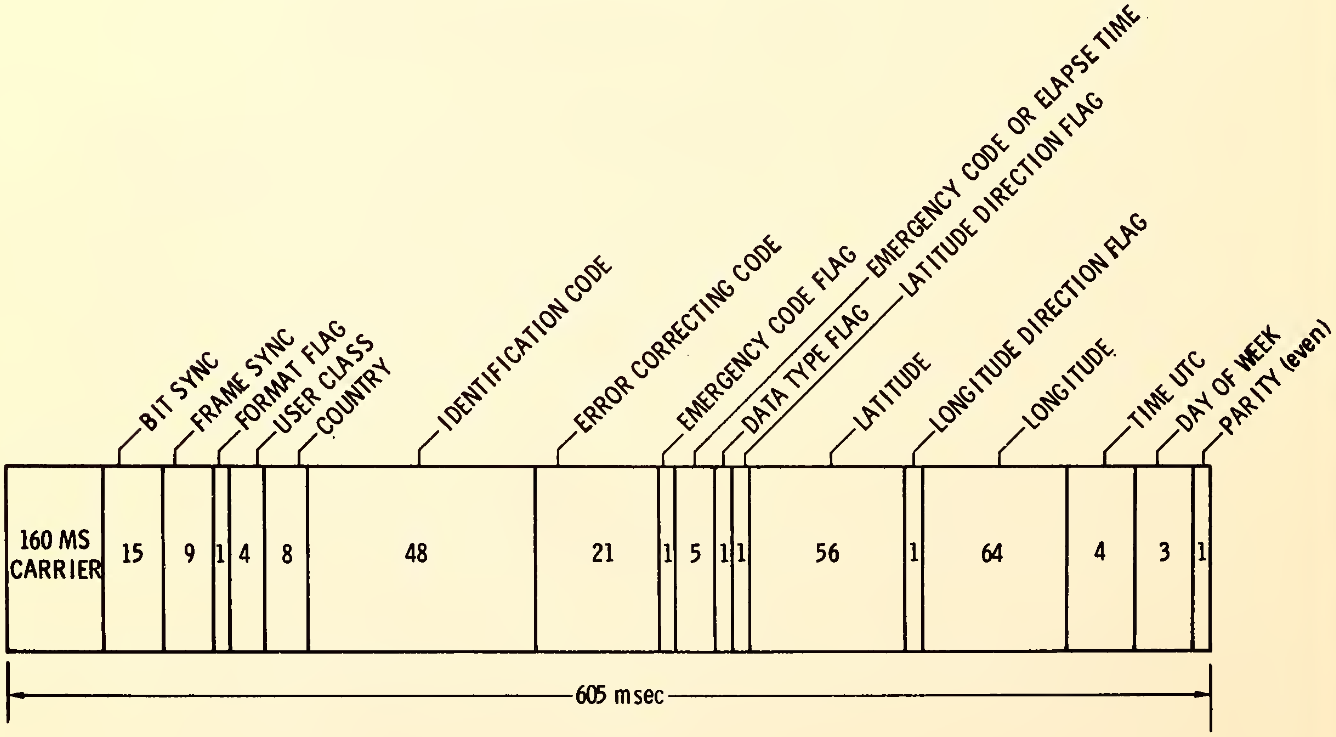

Figure 4. 406 MHz Digital Message Format

RECOMMENDED GPS TERMINOLOGY

David E. Wells
Department of Surveying Engineering
University of New Brunswick
Fredericton, New Brunswick
Canada E3B 5A3

ABSTRACT. A proposal for standardized GPS terminology is presented. The concepts behind the terms are defined, and the reasons for selecting particular terms are given. A Glossary of terms is appended.

INTRODUCTION

It is probable that the Global Positioning System (GPS), and perhaps other similar systems such as GLONASS, GEOSTAR and NAVSAT (McDonald and Greenspan, 1985), will find wide applications in surveying and geodesy over the next several years. The community of users and variety of equipment are both likely to be very heterogeneous. The establishment of standards is necessary to permit communication and cooperation among these users, who may employ various kinds of equipment and software.

Such communication and cooperation (and hence such standards) should exist on at least three levels. A common understanding of the concepts involved in GPS positioning requires standard terminology. The possibility for exchange of observed data requires standard data structures. The combination of results from various GPS campaigns requires consistency among these results, which would ideally be achieved by use of standard processing algorithms. In this paper an attempt is made to deal with only the first of these, a standard terminology.

Many new concepts and terms have begun to appear in the surveying literature as a result of the complexity and flexibility of GPS. This paper recommends a standard terminology for GPS which is specific enough to describe the complexities, but general enough to accomodate the flexibility of GPS and the possible use of other similar systems. A Glossary of terms, both recommended and otherwise, drawn from the recent GPS literature, appears as an Appendix.

A standard terminology is no more than a set of conventions, assigning specific meanings to a set of terms. We have tried to keep these terms as few and as simple as possible, and have included enough discussion to place them in context, and to give reasons why they are preferred over alternatives. The proposed terms are presented under eight headings: applications, satellites, signal, measurements, receivers, differencing, network solutions, and uncertainties.

As GPS continues to evolve, so will the most appropriate terminology used to describe it. This proposal should be considered as only one step in this evolutionary process. Comments and suggestions for future versions are welcome, and should be sent to the author.

A word of acknowledgement. The original version of this paper was prepared by the author and Demitris Paradissis, and presented by the latter at a meeting in Sopron Hungary in July 1984 of the Subcommission on Standards of the Committee on Space Techniques for Geodynamics. Subsequent comments and corrections were provided by Gerhard Beutler, Nick Christou, Charles Counselman, Mike Eaton, Ron Hatch, Larry Hothem, Patrick Hui, Hal Janes, Alfred Kleusberg, Richard Langley, Richard Moreau, Ben Remondi, Fred Spiess, Rock Santerre, Tom Stansell, Petr Vanicek, Richard Wong, and Larry Young. The present version was compiled from their comments, and further revised with the help of Yehuda Bock, Claude Boucher, Ron Hatch, Hal Janes, Alfred Kleusberg, and Ben Remondi. Without this extensive help, this proposal would not exist. However, errors and misconceptions which remain are the sole responsibility of the author.

APPLICATIONS

KINEMATIC (or DYNAMIC) POSITIONING refers to applications in which a trajectory (of a ship, ice field, tectonic plate, etc.) is determined.

STATIC POSITIONING refers to applications in which the positions of points are determined, without regard for any trajectory they may or may not have.

Consideration was given to basing these definitions on whether there was significant receiver motion or not, or in terms of the required accuracies. However, in the first case, the existance of receiver motion, *per se,* did not seem to introduce a fundamental difference from static applications, so long as the accuracy obtainable for instantaneous positioning is adequate. In the second case, there are examples of kinematic applications (e.g. marine 3D seismic) which may have higher accuracy requirements than some static applications (e.g. small scale mapping control).

Formally, kinematics is that branch of mechanics which treats motion without regard to its cause, which is the case here. Dynamics relates the motion to its cause. However, the term dynamic positioning has become so firmly rooted in common (mis)usage, that it may be unrealistic to expect a switch to the term kinematic positioning.

RELATIVE POSITIONING refers to the determination of relative positions between two or more receivers which are simultaneously tracking the same radiopositioning signals (e.g from GPS).

Alternatives to the term "relative" which were considered were "differential" and "interferometric". While both are valid, "differential" may be misconstrued to imply some infinitesimal process, and "interferometric" has specific, as well as general, connotations (see the discussion on this point in the Receivers section below). As well, "interferometric" emphasizes the measurement technique rather than the relative positioning application.

Real time relative positioning implies that signals (containing sufficient information for relative positioning) from all receivers are somehow broadcast in real time for processing at a central site (which may be at one of the receivers).

Because many GPS errors (clock errors, ephemeris errors, propagation errors) are correlated between observations obtained simultaneously at different sites, the relative positions between these sites can be determined to a higher accuracy than the absolute positions of the sites. In its simplest form, relative positioning involves a pair of receivers. For **kinematic relative positioning**, where the trajectory is of interest, one of these will be a monitor receiver at a known stationary location, and the other will be a mobile receiver tracing out the trajectory of interest. **Static relative positioning** involves determination of the difference in coordinates between pairs of points of a network. In this case, there is no restriction that one receiver remain at the same control point throughout the network survey (although that may be one feasible strategy). Usually at present independent baseline vectors between pairs of these points are computed as an intermediate step. When only two receivers are used for relative positioning (one baseline at a time), baselines can be considered independent. In general, using **n** receivers, the number of combinations of receiver pairs (baselines) is **n (n-1) / 2**. However, only **(n-1)** of these are rigorously independent (see the Network Solutions section below for more on relative static positioning).

SATELLITES

One confusing issue concerning GPS terminology is the numbering or identification of the GPS satellites. Several systems are used: the launch sequence number, an orbit position number, a number identifying which week of the 37-week long P-code has been assigned to the satellite (the PRN number), as well as more conventional NASA and International satellite identification numbers. Table 1 lists all these numbers for the eleven GPS Block I (prototype) satellites. Since the satellite ephemeris message uses the PRN number to identify satellites, that is the one which has gained widest use.

TABLE 1. GPS SATELLITE IDENTIFICATION

LAUNCH SEQUENCE NUMBER	ORBITAL POSITION NUMBER	ASSIGNED VEHICLE PRN CODE	NASA CATALOGUE NUMBER	INTERNATIONAL DESIGNATION	LAUNCH DATE (YY-MM-DD)	STATUS
1	0	4	10684	1978-020A	78-02-22	crystal clock
2	4	7	10893	1978-047A	78-05-13	not operating
3	6	6	11054	1978-093A	78-10-07	operating
4	3	8	11141	1978-112A	78-12-11	operating
5	1	5	11690	1980-011A	80-02-09	not operating
6	5	9	11783	1980-032A	80-04-26	operating
7					81-12-18	launch failed
8	2	11	14189	1983-072A	83-07-14	operating
9	1	13	15039	1984-059A	84-06-13	operating
10	4	12	15271	1984-097A	84-09-08	operating
11					85-08-??	launch plan

SIGNAL

The GPS signal has a number of components, all based on the fundamental frequency F = 10.23 MHz (see Figure 1). Two carriers are generated at 154 F (called L1), and 120 F (called L2). Pseudorandom noise codes are added to the carriers as binary biphase modulations at F (P-code) and F/10 (S-code, previously called C/A-code). A 1500-bit-long binary message is added to the carriers as binary biphase modulations at 50 bits per second.

> **PSEUDORANDOM NOISE CODE** (PRN code) is any of a group of binary sequences that exhibit noise-like properties, the most important of which is that the sequence has a maximum autocorrelation at zero lag.
>
> **BINARY BIPHASE MODULATIONS** on a constant frequency carrier are phase changes of either 0° (to represent a binary 0) or 180° (to represent a binary 1). These can be modelled by

$$y = A(t) \cos (\omega t - \phi) \tag{1}$$

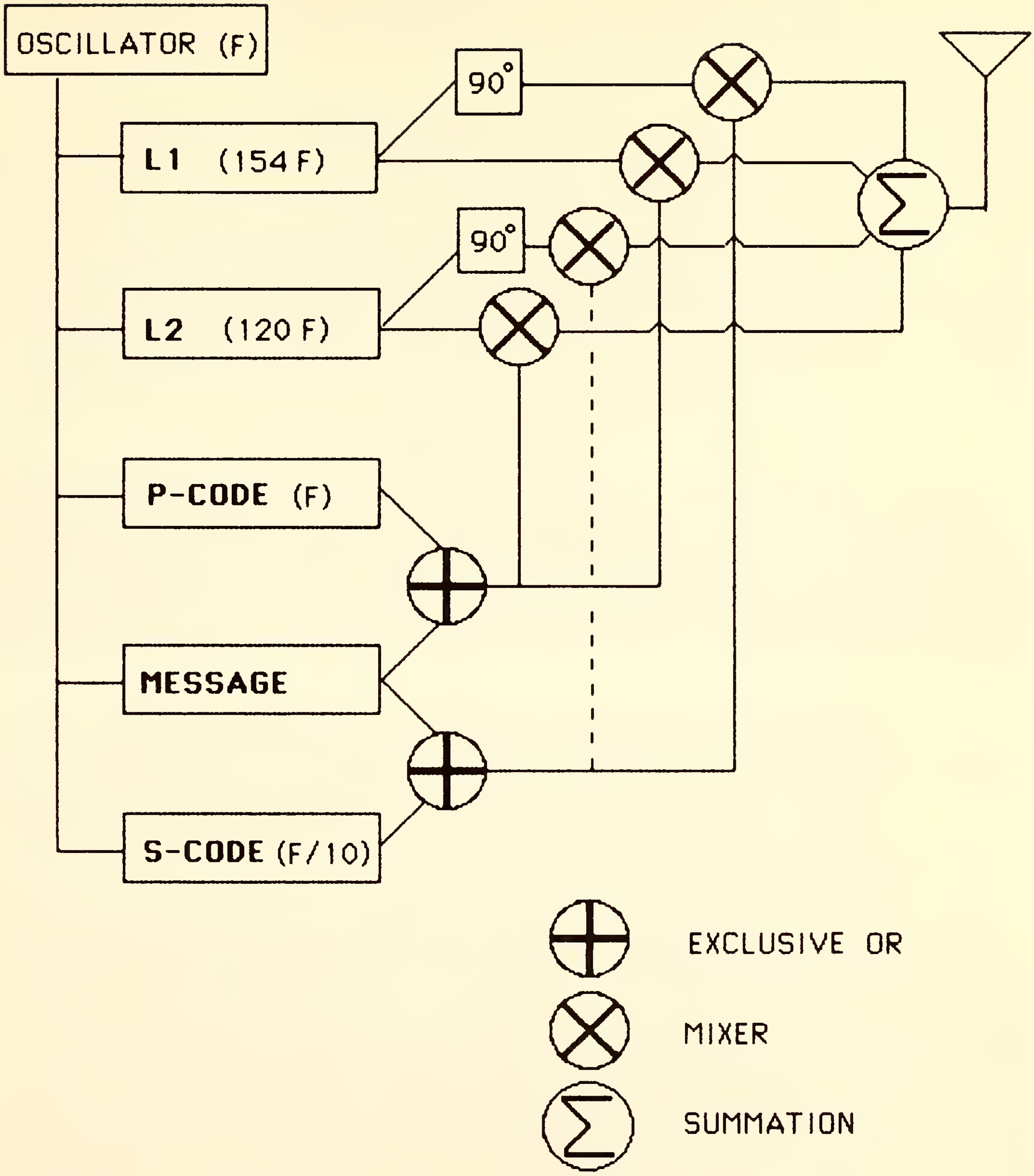

GPS SATELLITE SIGNALS

FIGURE 1

where the amplitude function **A(t)** is a sequence of +1 and -1 values (to represent 0° and 180° phase changes, respectively).

The P-code is a long (about 10^{14} bits) sequence, and the S-code is a short (1023 bit) sequence. The two codes are impressed on separate carriers that are in quadrature (the carriers are 90° apart in phase). For the present prototype (Block I) GPS satellites, and those to be used for the next decade (Block II), the S-code is normally available only on the L1 frequency. It is likely that access of civilian users to the P-code will be restricted, once the present prototype GPS satellites are replaced by production versions. Other similar systems (e.g. GLONASS) will undoubtedly have signal structures different to GPS.

MEASUREMENTS

Either the carrier or the code can be used to obtain GPS observations. In the case of carrier observations, phase is measured. In the case of code observations, usually pseudoranges are measured, but phase of the code can also be measured. Carrier measurements are subject to ionospheric phase advance, and code measurements to ionospheric group delay.

> **CARRIER BEAT PHASE** is the phase of the signal which remains when the incoming Doppler-shifted satellite carrier signal is beat (the difference frequency signal is generated) with the nominally-constant reference frequency generated in the receiver.

This term is preferable to the four alternatives "phase", "carrier phase", "reconstructed carrier phase" and "Doppler phase" for the following reasons. "Phase" does not distinguish between carrier and code measurements, for each of which phase measurements can be made (by very different techniques). "Carrier phase" implies that the phase of the GPS signal carrier itself is observed, which is not the case. "Reconstructed carrier phase" emphasizes the technique by which the signal to be observed is obtained, rather than emphasizing the signal itself. "Doppler phase" implies that the signal to be observed is due solely to the Doppler shift of the satellite carrier signal, which may not be the case (if, for example, the receiver reference frequency is intentionally offset significantly from the unshifted satellite carrier frequency).

Measurements of the carrier beat phase can be either **complete instantaneous phase measurements**, or **fractional instantaneous phase measurements**. The distinction between the two is that the former includes the integer number of cycles of the carrier beat phase since the initial phase measurement, and the latter is a number between zero and one cycles.

CARRIER BEAT PHASE AMBIGUITY is the uncertainty in the initial measurement, which biases all measurements in an unbroken sequence. The ambiguity consists of three components

$$\alpha_i + \beta^j + N_i^j \tag{2}$$

where

α_i is the fractional initial phase in the receiver,

β^j is the fractional initial phase in the satellite, (both due to various contributions to phase bias, such as unknown clock phase, circuit delays, etc.), and

N_i^j is an integer cycle bias in the initial measurement.

The carrier beat phase can be related to the satellite-to-receiver range, once the phase ambiguity has been determined. A change in the satellite-to-receiver range of one wavelength of the GPS carrier (19 cm for L1) will result in one cycle change in the phase of the carrier. Carrier beat phase measurement resolutions of a few degrees of phase are possible. Hence the measurements are sensitive to sub-centimetre range changes.

The complete instantaneous phase measurement differs from the more familiar continuously integrated Doppler measurement only because the latter does not include this ambiguity (assumes it to be zero).

Depending on receiver design, the phase samples are made at either epochs of the receiver clock, or at epochs of the satellite clock (as transferred through the modulations imbedded in the received satellite signal). I am not aware of a receiver which uses satellite timing, however.

Delta Pseudorange is a commonly used term which incorrectly implies it is somehow associated with code measurements. In fact Delta Pseudorange is the difference between two carrier beat phase measurements, made coincidently with (code) pseudorange epochs.

PSEUDORANGE is the time shift required to align (correlate) a replica of the GPS code generated in the receiver with the incoming GPS code, scaled into distance by the speed of light. This time shift is the difference between the time of signal reception (measured in the receiver time frame) and the time of emission (measured in the satellite time frame).

Pseudoranges change due to variations in the satellite-to-receiver propagation delay, and are biased by the time offset between satellite and receiver clocks. The resolution of pseudorange measurements depends on the accuracy with which the incoming and replicated codes can be aligned. An alignment accuracy of a few nanoseconds is equivalent to metre-level range resolution.

RECEIVERS

GPS receivers have one or more channels. Two kinds of channels are useful for static positioning using carrier phase measurements: squaring type channels, and correlation type channels.

> A **CHANNEL** of a GPS receiver consists of the radiofrequency and digital hardware, and the software, required to track the signal from one GPS satellite at one of the two GPS carrier frequencies.
>
> A **SQUARING-TYPE CHANNEL** multiplies the received signal by itself to obtain a second harmonic of the carrier, which does not contain the code modulation.

The squaring concept is simply shown by squaring equation (1) to obtain

$$y^2 = A^2 \cos^2(\omega t + \phi) = A^2 \; [1 + \cos(2\omega t + 2\phi)] \,/\, 2 \qquad (3)$$

Since $A(t)$ is the sequence of +1 and −1 values representing the code, $A(t)^2 = A^2$ is always equal to +1 and may be dropped from equation (3). The resulting signal y^2 is then pure carrier, but at twice the original frequency. Note that for a simple squaring loop, any noise on the signal is also squared. In practice as shown in Figure 2, the incoming signal is first differenced with a local reference frequency to obtain the carrier beat phase signal, at an intermediate frequency much lower than the original carrier frequency.

This is a simple conceptual description of the squaring process which, in practice, is implemented by one of several proprietary techniques which have been developed. These proprietary techniques often involve some method of narrowing the GPS signal bandwidth from 20 MHz (due to the P-code "spreading"), to a bandwidth the order of several Hertz. Only the carrier is obtained from a squaring-type channel. Pseudoranges and the message cannot be obtained. An example of such a receiver is the Macrometer™ V-1000, a six channel receiver which does not require any knowledge of the code, capable of continuously tracking the L1 carrier beat phase second harmonic, from six satellites.

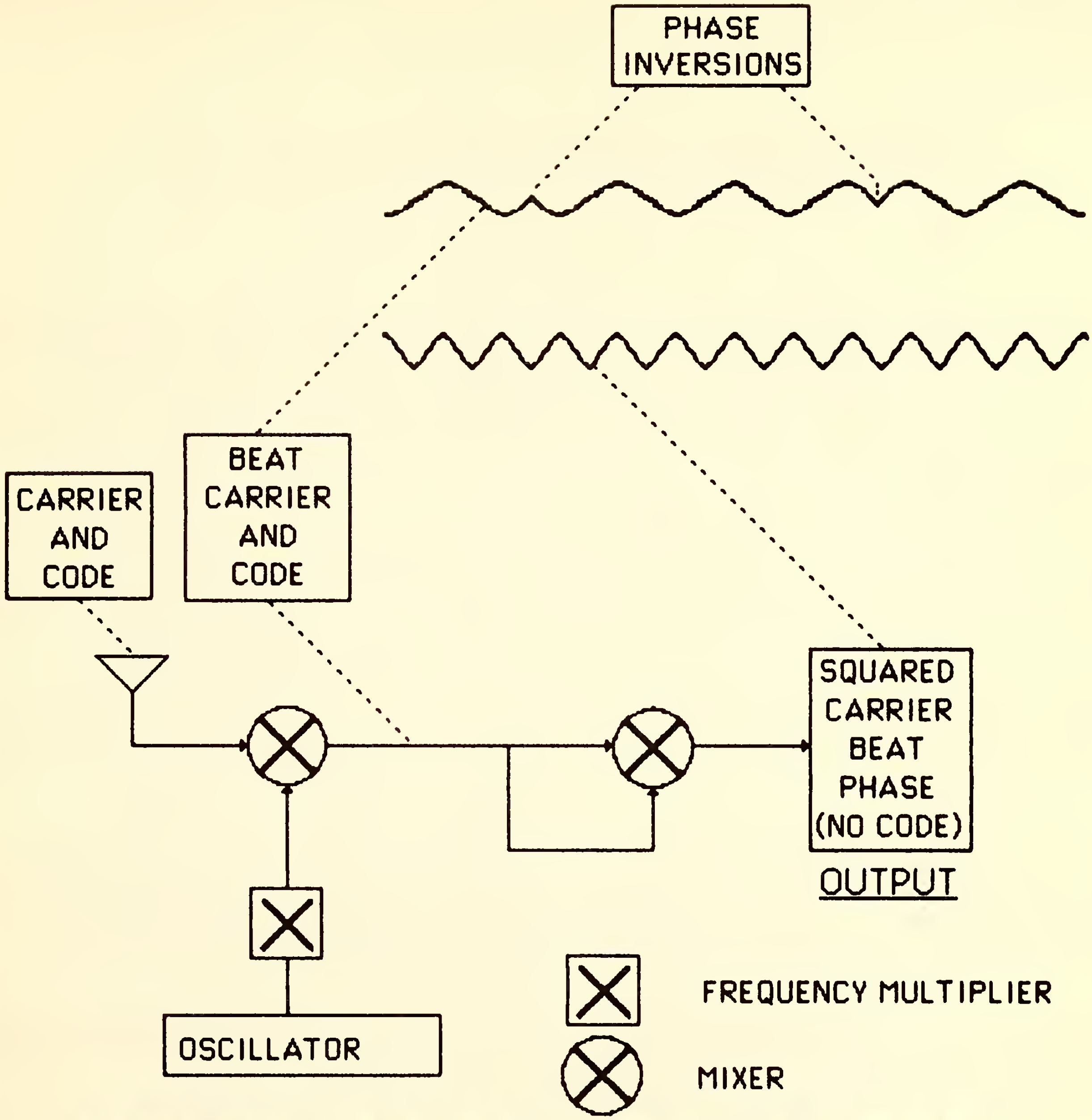

GPS SQUARING-TYPE CHANNEL

FIGURE 2

An alternative to the squaring process, which also does not require detailed knowledge of the code, is the SERIES technique [Buennagel et al., 1984] in which the GPS signal is despread by tracking the Doppler shift of the code modulation transitions, without detailed knowledge or recovery of the actual code sequences or use of the carrier.

> A **CORRELATION-TYPE CHANNEL** uses a delay lock loop to maintain an alignment (correlation peak) between the replica of the GPS code generated in the receiver, and the incoming code.

In simple terms, the code correlation concept involves generating a replica of the code sequence [the sequence of +1 and -1 values represented by **A(t)** in equation (1)] within the receiver, and to align this replica in time (correlate) with the incoming signal. Once aligned, multiplying the two codes together results in only +1 values for the resulting amplitude function. In Figure 3, the incoming signal is first reduced in frequency by differencing with a local carrier (point A). The signal resulting from multiplying this incoming signal by the local code replica (point B) will have the code removed, but only if the two codes are aligned. The correlation peak detector tests for the presence of the code, and corrects the delay (point C) of the locally generated code replica to maintain alignment, completing the delay lock loop. This time delay is the pseudorange measurement (see above). Also, once the receiver code generator is aligned to the incoming code, its output is a reading of the satellite clock at the time of signal transmission. The fourth and final kind of information obtained from a code correlation channel is the 50 bit per second message containing the ephemeris.

This is a simple conceptual description of a correlation-type channel. In practice, details of the correlation process may involve any of a number of advanced techniques (e.g. tau dither, early minus late gating), and may be implemented predominantly in hardware, or predominantly in software, depending on receiver design.

Code correlation channels may be either multiplexing or switching, depending on how the satellite message bits are accumulated.

> A **MULTIPLEXING CHANNEL** is sequenced through a number of satellite signals (each from a specific satellite and at a specific frequency) at a rate which is synchronous with the satellite message bit-rate (50 bits per second, or 20 milliseconds per bit). Thus one complete sequence is completed in a multiple of 20 milliseconds.

> A **SWITCHING CHANNEL** is sequenced through a number of satellite signals (each from a specific satellite and at a

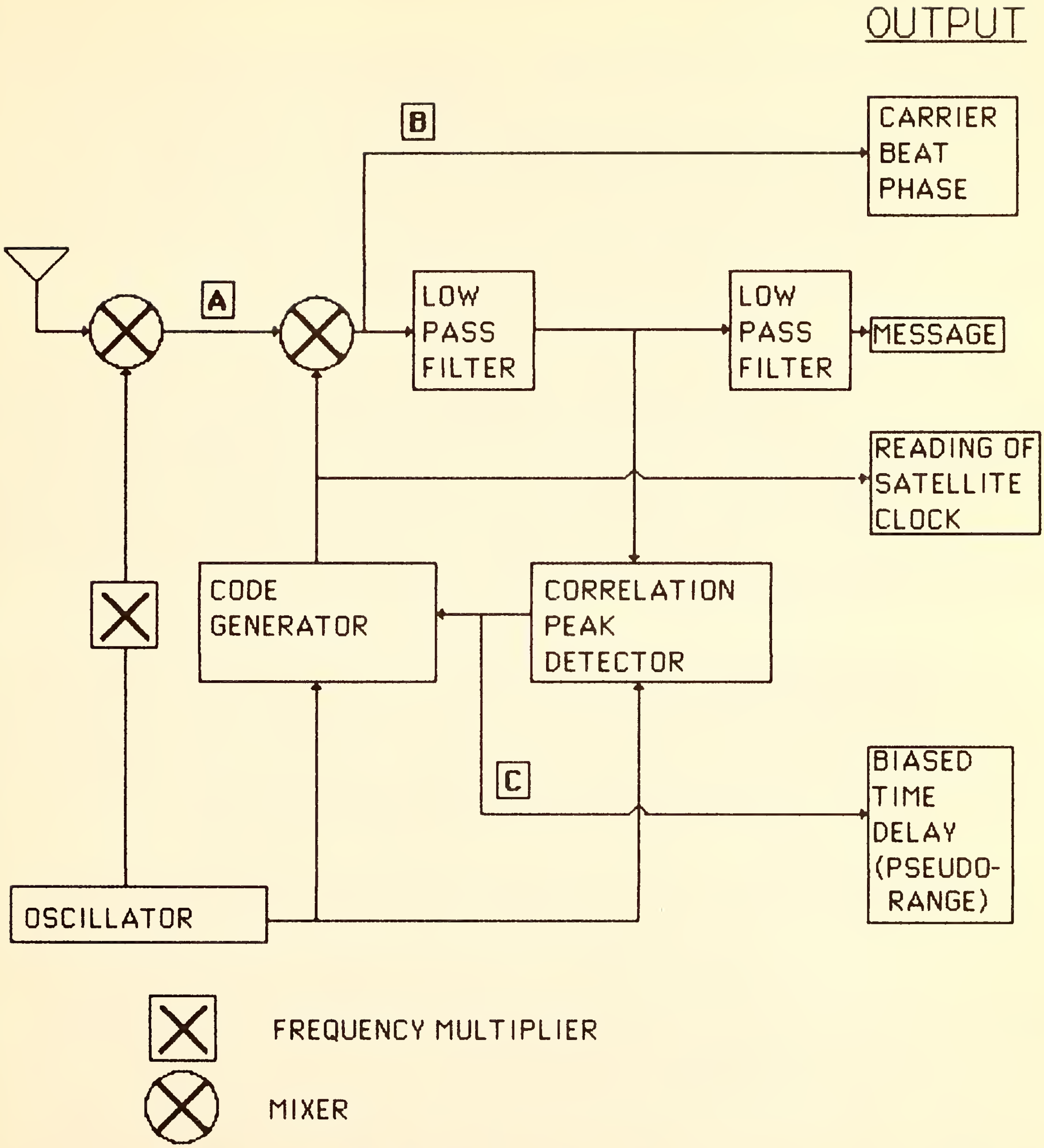

GPS CORRELATION CHANNEL

FIGURE 3

specific frequency) at a rate which is slower than, and asynchronous with, the message data rate.

A multiplexing channel builds up a map of the message from each satellite one bit (for each satellite) per sequence cycle. An example of a multiplexing receiver is the Texas Instruments 4100, which has one multiplexing channel which tracks both L1 and L2 signals from up to four satellites (a total of eight signals), dwelling on each for five milliseconds, hence taking two bit-periods (40 milliseconds) to complete one sequence. Each satellite is visited once per bit period (on alternating frequencies), in order not to lose any message bits. Software in the receiver tracks all signals in such a way that values for all signals, referred to the same epoch, can be obtained.

Switching channels may dwell on each signal for relatively short (less than a second) or relatively long (tens of seconds to hours) periods. If the sequence time is short enough for the channel to recover (through software prediction) the integer part of the carrier beat phase (in practice no more than several seconds), then the channel is a **fast-switching channel**. A switching channel builds up a map of the message from each satellite many bits per signal dwell time. In order that all parts of each satellite message are sampled, the dwell times must progress through the message (that is the sequencing must be asynchronous with the message data rate).

A receiver with many channels is a multichannel receiever. It may be that these channels are of the same type (all code correlation, or all squaring), or of different types. For example, since civil access to the P-code is expected to be restricted in the future, and the S-code is not expected to be available on the L2 carrier, a civilian dual frequency receiver must either have squaring channels for both L1 and L2, or code correlation channels for L1 and squaring channels for L2.

A multichannel switching receiver may have more or less flexibility in how the channels are used. For example, three possible scenarios are

- All channels track the same signal continuously (while the satellite is visible). For highly kinematic applications, where the receiver motion over even a fast-switching sequence period is significant, this may be the only feasible strategy.
- All channels fast-sequence through a subset of the signals to be tracked. This reduces the number of channels required (perhaps to one).
- Some channels track one signal continuously, with other channels switching through the signals (perhaps to collect ephemeris data from all visible satellites).

A very different alternative is to simply record the total GPS received signal as a "noise" signal (although it consists of carriers and codes from all visible satellites) at each station in a network, and then to extract between-receiver differences (see below) by correlating the recorded data station-pair by station-pair, and satellite by satellite. This is the interferometric approach. The receiver in this case would be very simple and inexpensive. The lack of real time quality control, however, makes this an

MULTIPLEXING CHANNEL

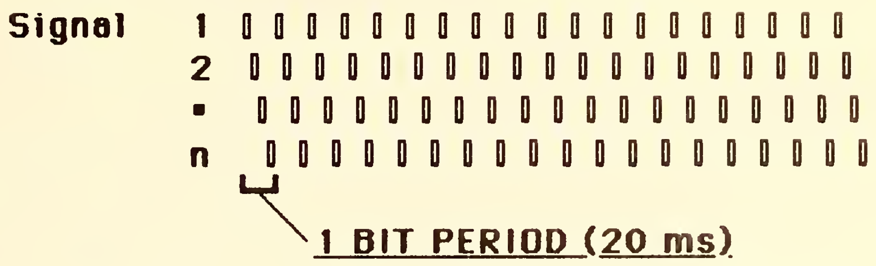

FAST SWITCHING CHANNEL

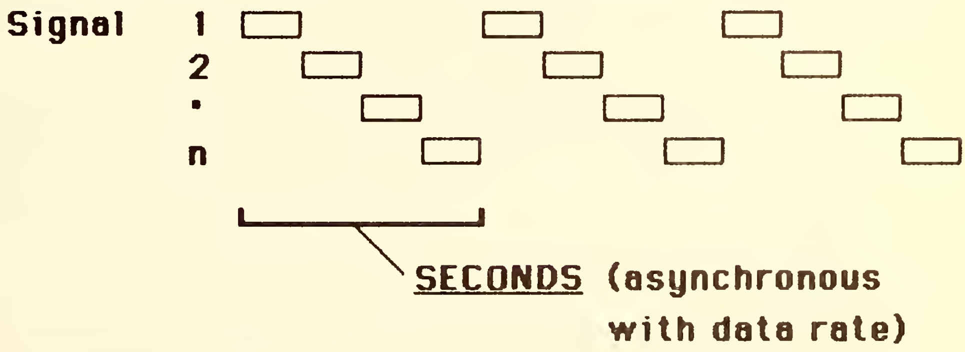

SLOW SWITCHING CHANNEL

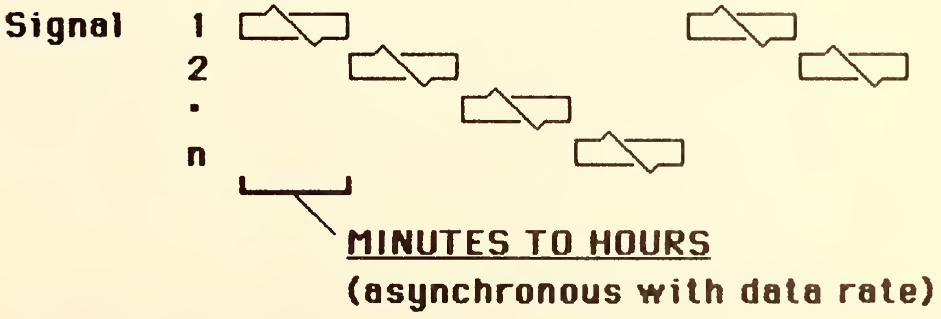

MULTIPLEXING AND SWITCHING CHANNELS

FIGURE 4

impractical option. Note that, in principle, any technique involving comparison of measurements made by two receivers could be called an interferometric technique. We have noted above the preference for using "relative positioning" in place of this more general meaning for interferometry.

DIFFERENCING

For relative static positioning, many of the errors are correlated among the various measurements which are made. One approach is to attempt to model this correlation through bias parameter estimation and correlated weighting of the observations. Another commonly used approach for processing carrier measurements involves taking differences between measurements, since this removes or reduces the effect of errors which are common to the measurements being differenced. GPS measurements can be differenced in several ways: between receivers, between satellites, between time epochs, and between L1 and L2 frequencies. Figure 5 illustrates the first three of these. All but between-epoch differences involve the concept of simultaneity.

> **SIMULTANEOUS MEASUREMENTS** are measurements referred to time frame epochs which are either exactly equal, or else so closely spaced in time that the time misalignment can be accomodated by correction terms in the observation equation, rather than by parameter estimation.
>
> A **BETWEEN-RECEIVER** carrier beat phase difference is the instantaneous difference in the complete carrier beat phase measurement made at two receivers simultaneously observing the same received signal (same satellite, same frequency).
>
> A **BETWEEN-SATELLITE** carrier beat phase difference is the instantaneous difference in the complete carrier beat phase measurement made by the same receiver observing two satellite signals simultaneously (same frequency).
>
> A **BETWEEN-EPOCH** carrier beat phase difference is the difference between two complete carrier beat phase measurements made by the same receiver on the same signal (same satellite, same frequency).
>
> A **BETWEEN-FREQUENCY** carrier beat phase difference is the instantaneous difference between (or, more generally, any other linear combination involving) the complete carrier beat phase measurements made by the same receiver observing signals from the same satellite at two (or more) different frequencies.

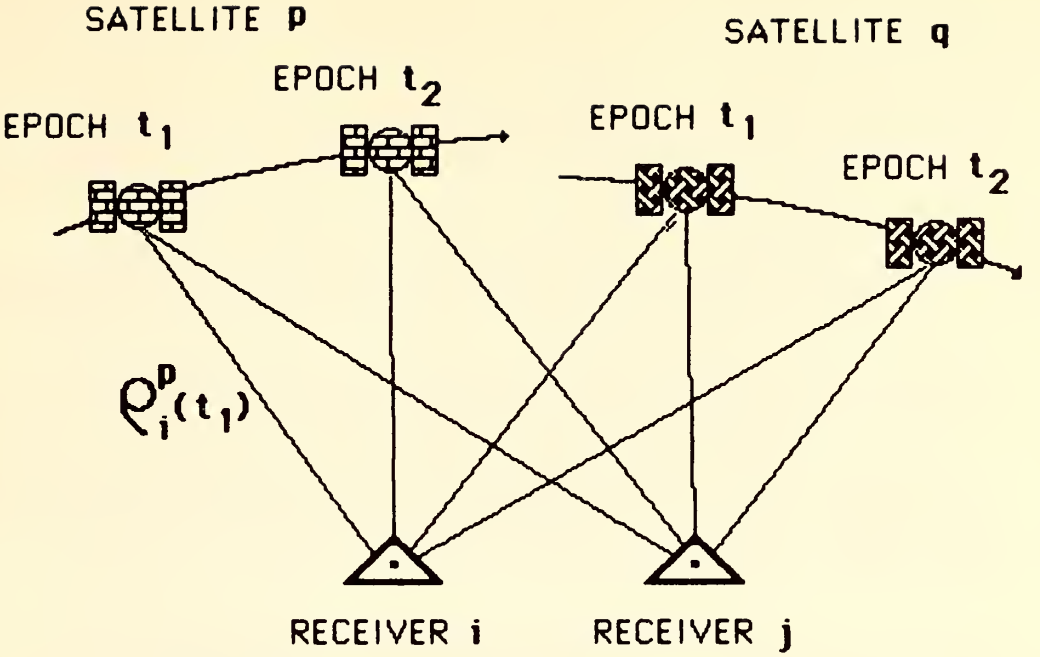

BETWEEN-RECEIVER	BETWEEN-SATELLITE	BETWEEN-EPOCH
$[\rho_i^p(t_1) - \rho_j^p(t_1)]$	$[\rho_i^p(t_1) - \rho_i^q(t_1)]$	$[\rho_i^p(t_2) - \rho_i^p(t_1)]$
$[\rho_i^q(t_1) - \rho_j^q(t_1)]$	$[\rho_i^p(t_1) - \rho_i^q(t_1)]$	$[\rho_j^p(t_2) - \rho_j^p(t_1)]$
$[\rho_i^p(t_2) - \rho_j^p(t_2)]$	$[\rho_i^p(t_2) - \rho_i^q(t_2)]$	$[\rho_i^q(t_2) - \rho_i^q(t_1)]$
$[\rho_i^q(t_2) - \rho_j^q(t_2)]$	$[\rho_j^p(t_2) - \rho_j^p(t_2)]$	$[\rho_j^q(t_2) - \rho_j^q(t_1)]$

GPS PHASE MEASUREMENT DIFFERENCING

FIGURE 5

Between-receiver differences remove or reduce the effect of satellite clock errors (and cancel the β^j term in the ambiguity expression of equation 2, which is common to both measurements). For baselines which are short compared to the 20,000 km GPS satellite height, between-receiver differences also significantly reduce the effect of satellite ephemeris and atmospheric refraction errors. **Between-satellite** differences remove or reduce the effects of receiver clock errors (and cancel the α_i term in the ambiguity expression of equation 2, which is common to both measurements). **Between-epoch** differences are the same as integrated Doppler measurements (and cancel all three terms $\alpha_i + \beta^j + N_i^j$ in the ambiguity expression of equation 2, all of which are common to both measurements). However, clock errors remain in this case. **Between-frequency** differences are not made for the purpose of ionospheric refraction correction, but rather to generate a signal which is a linear combination of L1 and L2, and hence has a coarser (or finer) wavelength (Hatch and Larson, 1985).

Many combinations of these differences are possible. It is important that which differences, and their order, be specified in describing a processing method. For example, **Receiver-Satellite Double Differences** refers to differencing between receivers first and between satellites second; **Receiver-Time Double Differences** refers to differencing between receivers first, then between time epochs; **Receiver-Satellite-Time Triple Differences** refers to differencing between receivers, then satellites, and finally time.

Figure 5 illustrates differences between receivers, satellites and epochs for the simplest possible case (two receivers, two satellites, two epochs, and one frequency). A total of eight carrier beat phase measurements are made. Each of the three possible single differences reduces this to four. Double differencing further reduces this to two measurements. These measurements correspond to only one triple difference measurement. In practice, many more receivers, satellites and epochs are involved. In this case, there are, for example, many ways in which Receiver-Satellite Double Differences can be formed.

NETWORK SOLUTIONS

GPS network processing techniques are still in their infancy, and it is probably too early to fully define the terminology required to describe and distinguish between them. However some of the simple concepts can be stated.

The simplest static relative positioning observation strategy, to survey a network of points, is to use one pair of receivers which occupy, in some sequence, all the baselines desired to determine the network. Most of the work done to date has used this method. In this case, two concepts are well defined:

A **BASELINE** consists of a pair of stations for which simultaneous GPS data has been collected.

A two-receiver **OBSERVING SESSION** is the period of time over which GPS data is collected simultaneously at both ends of one baseline.

When more than two receivers are used simultaneously, the baseline and session concepts must be extended:

A **n**-receiver **OBSERVING SESSION** is the period of time over which GPS data is collected simultaneously at **n** stations.

Two **SESSIONS** are **INDEPENDENT** to the extent that we can ignore any common biases affecting the observations in both cases.

Two **BASELINES** are **INDEPENDENT** if they have been determined from independent sessions.

Once enough GPS satellites are in orbit to provide continuous coverage, the definition of a multi-receiver observing session will become more blurred, since the definite break between sessions now provided by the limited periods of satellite availability will no longer exist.

To obtain a network solution, either the GPS observations can be taken directly into a network adjustment program, or else the baseline solutions can be obtained individually first, and taken as vector pseudo-observations into a simpler three dimensional network adjustment. The advantage of the former approach is that biases and correlations affecting the data can more easily be taken into account. In each case, the network adjustment may use either a batch algorithm (processing the entire set of observations in one run), or a sequential algorithm (in which the data can be processed and results obtained on a session by session, or even observation by observation, basis). The most important practical property of a sequential alogorithm is that the data can be processed in a sequence of computer runs, rather than in one large run. Programs having this property are said to have a "restart" capability.

UNCERTAINTIES

Uncertainties in surveying are conventionally expressed in terms of covariance matrices. The uncertainty in a set observations $\boldsymbol{\ell}$ is contained in the covariance matrix $\mathbf{C}_{\boldsymbol{\ell}}$ for those observations. In general this quantity will be the sum of the contributions from many error sources. Each error source will have its own properties, such as dependence on geometry, correlations in various ways between observations, etc. Accounting for these properties is not a simple task, and to date has not been fully addressed for GPS.

The uncertainty in a solution **X** is contained in the solution covariance matrix $\mathbf{C_x} = (\mathbf{P_x} + \mathbf{A}^T \mathbf{P_\ell} \mathbf{A})^{-1}$ where $\mathbf{P_x}$ = the *apriori* solution weight matrix, **A** = the design matrix, and $\mathbf{P_\ell} = \mathbf{C_\ell}^{-1}$.

For planning and preanalysis, it is often convenient to separate the geometric factors affecting the solution (contained in **A**) from the measurement uncertainties (contained in $\mathbf{P_\ell}$). One scalar measure of these geometrical factors is the dilution of precision

The **DILUTION OF PRECISION (DOP)** is given by

$$\mathbf{DOP} = \sqrt{\mathrm{Trace}(\mathbf{A}^T\mathbf{A})^{-1}} \ .$$

The smaller the DOP, the stronger the geometry.

In the case of kinematic point positioning, several kinds of DOP exist, depending on the parameters of the solution:
- **GDOP** = geometrical DOP (three position coordinates plus clock offset)
- **PDOP** = position DOP (three coordinates)
- **HDOP** = horizontal DOP (two horizontal coordinates)
- **VDOP** = vertical DOP (height only)
- **TDOP** = time DOP (clock offset only)
- **HTDOP** = horizontal-time DOP (two horizontal coordinates and clock offset).

When the DOP factor exceeds a specified maximum value at some location for some period of time, it indicates that the normal equation matrices in those circumstances have become ill-conditioned to some extent. This is sometimes referred to as an "outage" of the GPS system.

For static positioning applications, what is important are the variations in the geometry of the satellite configuration over the entire time span of the data, and over the network of receivers simultaneously tracking the signals. This may not be adequately represented by the geometrical configuration at one instant at a single location. However, it may be impractical to attempt to evaluate a more rigorous DOP.

Standard methods of expressing kinematic application accuracies recently adopted by NATO [1983] are presented here without recommendation, for comment:
- For one dimensional error, the interval in metres containing 95% of the observations.

- For two or three dimensional radial error, the number which represents the radial distance in metres centred on the mean position of a large number of trials of the actual or desired system, which includes 95% of the observations.
- To express performance independant of geometrical factors, a 95% measure in terms of portions of a cycle or of a second.
- Speed accuracy as a dimensioned number (e.g. cm/sec) including 95% of observations from a large number of trials.

REFERENCES

Bauersima, I. (1983). "NAVSTAR/Global Positioning System (GPS) III: Erdvermessung durch radiointerferometriche satellitenbeobachtungen." Miteilungen der satelliten-beobachtungstation Zimmerwald Nr. 12, Drucherei der Universitat Bern.

Bossler, J.D., C.C. Goad and P.L. Bender (1980). "Using the Global Positioning System (GPS) for geodetic positioning." Bulletin Geodesique, 54, pp. 553-563.

Bowditch, N. (1981). "Useful tables, calculations, glossary of marine navigation." Vol. II of The American Practical Navigator, Publication No. 9, DMAHTC, Washington, D.C.

Buennagal, L.A., P.F. MacDoran, R.E. Neilan, D.J. Spitzmesser and L.E. Young (1984). "Satellite emission range inferred earth survey (SERIES) project: Final report on research and development phase, 1979 to 1983." JPL publication 84-16, March.

Counselman, C. and S. Gourevitch (1981). "Miniature interferometer terminals for earth surveying: Ambiguity and multipath with Global Positioning System." IEEE Transactions on Geoscience and Remote Sensing, Vol. GE-19, No. 4, pp. 244-252.

Davidson, D., D. Delikaraoglou, R. Langley, B. Nickerson, P. Vanicek and D. Wells (1983). "Global Positioning System differential positioning simulations." Department of Surveying Engineering Technical Report 90, University of New Brusnwick, Fredericton.

Dixon, R.C. (1975). Spread Spectrum Systems. John Wiley.

Goad, C.C. and B.W. Remondi (1983). "Initial relative positioning results using the Global Positioning System." Paper presented at the XVIII General Assembly of the IUGG, IAG Symposium D, Hamburg, F.R.G., August.

Hatch, R. and K. Larson (1985). "MAGNET-4100 GPS survey program test results." These proceedings.

Johnson, C.R., P.W. Ward, M.D. Turner and S.D. Roemerman (1981). "Applications of a multiplexed GPS user set." In: Global Positioning System. Papers published in Navigation, reprinted by The (U.S.) Institute of Navigation, Vol. II, pp. 61-77.

Jorgensen, P.S. (1980). "NAVSTAR/Global Positioning System 18-satellite constellations." In: Global Positioning System. Papers published in Navigation, reprinted by The (U.S.) Institute of Navigation, Vol. II, pp. 1-12.

Kalafus, R.M. (1984). "RTCM SC-104 progress on differential GPS standards." Presented at the Annual Meeting of the U.S. Institute of Navigation, Cambridge, MA, June.

Martin, E.H. (1980). "GPS user equipment error models." In: Global Positioning System. Papers published in Navigation, reprinted by The (U.S.) Institute of Navigation, pp. 109-118.

McDonald, K.D. and R. L. Greenspan (1985). "A survey of GPS satellite system alternatives and their potential for precise positioning" These proceedings.

Mertikas, S. (1983). "Differential Global Positioning System navigation: A geometrical analysis." M.Sc. thesis, Department of Surveying Engineering, University of New Brunswick, Fredericton, May.

Milliken, R.J. and C.J. Zoller (1980). "Principle of operation of NAVSTAR and system characteristics." In: Global Positioning System. Papers published in Navigation, reprinted by The (U.S.) Institute of Navigation, pp. 3-14.

NATO (1983). "Method of expressing navigation accuracies." North Atlantic Treaty Organization Standardization Agreement 4278.

Remondi, B.W. (1984). "Using the Global Positioning System (GPS) phase observable for relative geodesy: Modelling, processing, and results." Ph.D. dissertation, The University of Texas at Austin, May.

Scott, V.D. and J.G. Peters (1983). "A standardized exchange format for NAVSTAR GPS geodetic data." Applied Research Laboratories, The University of Texas at Austin, March.

Spilker, J.J. (1980). "GPS signal structure and performance characteristics." In: Global Positioning System. Papers published in Navigation, reprinted by The (U.S.) Institute of Navigation, pp. 29-54.

Stiffler, J.J. (1966). "Telecommunications." Vol. V of Space Technology, NASA.

United States Department of Defense/Department of Transportation (1982). Federal Radionavigation Plan. Vols. I-IV, March.

van Dierendock, A.J., S.S. Russell, E.R. Kopitzke and M. Birnbaum (1980). "The GPS navigation message." In: Global Positioning System. Papers published in Navigation, reprinted by The (U.S.) Institute of Navigation, pp. 55-73.

Ward, P. (1981). "An inside view of pseudorange and delta pseudorange measurements in a digital NAVSTAR GPS receiver." Presented at the ITC/USA/'81 International Telemetering Conference, San Diego, October.

Wells, D. (1974). "Doppler satellite control." Department of Surveying Engineering Technical Report 29, University of New Brunswick, Fredericton, N.B.

Wells, D., P. Vanicek and D. Delikaraoglou (1981). "Application of NAVSTAR/GPS to geodesy in Canada: Pilot study." Department of Surveying Engineering Technical Report 76, University of New Brunswick, Fredericton, N.B.

APPENDIX 1
GLOSSARY OF GPS TERMINOLOGY

Ambiguity

see Carrier Beat Phase Ambiguity

Bandwidth

A measure of the width of the spectrum of a signal (frequency domain representation of a signal) expressed in Hertz (Stiffler, 1966).

Baseline

A baseline consists of a pair of stations for which simultaneous GPS data has been collected.

Beat frequency

Either of the two additional frequencies obtained when signals of two frequencies are mixed, equal to the sum or difference of the original frequencies, respectively. For example, in the identity,

$$\cos A \cos B = (\cos(A+B) + \cos(A-B))/2,$$

the original signals are **A** and **B** and the beat signals are **A+B** and **A-B**. The term Carrier Beat Phase refers only to the difference **A-B**, where **A** is the incoming Doppler-shifted satellite carrier signal, and **B** is the nominally-constant reference frequency generated in the receiver.

Between-epoch difference

The difference between two complete carrier beat phase measurements made by the same receiver on the same signal (same satellite, same frequency), but at different time epochs.

Between-frequency difference

The instantaneous difference between (or, more generally, any other linear combination involving) the complete carrier beat phase measurements made by the same receiver observing signals from the same satellite at two (or more) different frequencies.

Between-receiver difference

The instantaneous difference in the complete carrier beat phase measurement made at two receivers simultaneously observing the same received signal (same satellite, same frequency).

Between satellite difference

The instantaneous difference in the complete carrier beat phase measurement made by the same receiver observing two satellite signals simultaneously (same frequency).

Binary pulse code modulation

Pulse modulation using a string (code) of binary numbers. This coding is usually represented by ones and zeros with definite meanings assigned to them, such as changes in phase or direction of a wave (Dixon, 1975).

Binary biphase modulation

Phase changes on a constant frequency carrier of either 0° or 180° (to represent binary 0 or 1 respectively). These can be modelled by $\mathbf{y = A(t) \cos (\omega t + \phi)}$, where the amplitude function $\mathbf{A(t)}$ is a sequence of +1 and −1 values (to represent 0° and 180°phase changes respectively) (Dixon, 1975).

Carrier

A radio wave having at least one characteristic (e.g., frequency, amplitude, phase) which may be varied from a known reference value by modulation (Bowditch, 1981, Vol. II).

Carrier frequency

The frequency of the unmodulated fundamental output of a radio transmitter (Bowditch, 1981, Vol. II).

Carrier beat phase

The phase of the signal which remains when the incoming Doppler-shifted satellite carrier signal is beat (the difference frequency signal is generated) with the nominally-constant reference frequency generated in the receiver.

Carrier beat phase ambiguity

The uncertainty in the initial measurement, which biases all measurements in an unbroken sequence. The ambiguity consists of three components

$$\alpha_i + \beta^j + N_i^j$$

where

α_i is the fractional initial phase in the receiver

β^j is the fractional initial phase in the satellite (both due to various contributions to phase bias, such as unknown clock phase, circuit delays, etc.), and

N_i^j is an integer cycle bias in the initial measurement.

Channel

A channel of a GPS receiver consists of the radiofrequency and digital hardware, and the software, required to track the signal from one GPS satellite at one of the two GPS carrier frequencies.

Chip

The minimum time interval of either a zero or a one in a binary pulse code.

C/A-code

see S-code.

Complete instantaneous phase measurement

A measurement of carrier beat phase which includes the integer number of cycles of carrier beat phase since the initial phase measurement. See fractional instantaneous phase measurement.

Correlation-type channel

A GPS receiver channel which uses a delay lock loop to maintain an alignment (correlation peak) between the replica of the GPS code generated in the receiver and the incoming code.

Delay lock

The technique whereby the received code (generated by the satellite clock) is compared with the internal code (generated by the receiver clock) and the latter shifted in time until the two codes match. Delay lock loops can be implemented in several ways, for example, tau dither and early-minus-late gating (Spilker, 1980).

Delta pseudorange

The difference between two carrier beat phase measurements, made coincidentally with (code) pseudorange epochs.

Differenced measurements

see Between-epoch difference; Between-frequency difference; Between-receievr difference; Between-satellite difference.

Many combinations of differences are possible. Which differences, and their order, should be specified in describing a processing method (for example Receiver-Satellite Double Differences).

Differential positioning

see Relative Positioning

Dilution of precision (DOP)

A description of the purely geometrical contribution to the uncertainty in a dynamic position fix, given by the expression

$$\mathrm{DOP} = \sqrt{\mathrm{TRACE}(A^{T}A)^{-1}},$$

where **A** is the design matrix for the solution (dependent on satellite/receiver geometry). The DOP factor depends on the parameters of the position fix solution. Standard terms in the case of kinematic GPS are:

GDOP (three position coordinates plus clock offset in the solution)
PDOP (three coordinates)
HDOP (two horizontal coordinates)
VDOP (height only)
TDOP (clock offset only), and
HTDOP (horizontal position and time).

Doppler shift

The apparent change in frequency of a received signal due to the rate of change of the range between the transmitter and receiver. See carrier beat phase.

Dynamic positioning

see Kinematic positioning

Fast switching channel

A switching channel with a sequence time short enough to recover (through software prediction) the integer part of the carrier beat phase.

Fractional instantaneous phase measurement

A measurement of the carrier beat phase which does not include any integer cycle count. It is a value between zero and one cycle. See complete instantaneous phase measurement.

Frequency band

A range of frequencies in a particular region of the electromagnetic spectrum (Wells, 1974).

Frequency spectrum

The distribution of amplitudes as a function of frequency of the constituent waves in a signal (Wells, 1974).

Handover word

The word in the GPS message that contains time synchronization information for the transfer from the S-code to the P-code (Milliken and Zoller, 1980).

Independent baselines

Baselines determined from independent observing sessions.

Independent observing sessions

Sessions for which any common biases affecting the observations can be ignored.

Ionospheric refraction

A signal travelling through the ionosphere (which is a nonhomogeneous and dispersive medium) experiences a propagation time different from that which would occur in a vacuum. Phase advance depends on electron content and affects carrier signals. Group delay depends on dispersion in the ionosphere as well, and affects signal modulation (codes). The phase and group advance are of the same magnitude but opposite sign (Davidson et al., 1983).

Interferometry

see Relative positioning

Kinematic positioning

Kinematic positioning refers to applications in which a trajectory (of a ship, ice field, tectonic plate, etc.) is determined.

Lane

The area (or volume) enclosed by adjacent lines (or surfaces) of zero phase of either the carrier beat phase signal, or of the difference between two carrier beat phase signals. On the earth's surface a line of zero phase is the locus of all points for which the observed value would have a exact integer value for the complete instantaneous phase measurement. In three dimensions, this locus becomes a surface.

L-band

The radio frequency band extending from 390 MHz to (nominally) 1550 MHz (Bowditch 1981, Vol. II).

Multipath error

An error resulting from interference between radiowaves which have travelled between the transmitter and the receiver by two paths of different electrical lengths (Bowditch, 1981, Vol. II).

Multichannel receiver

A receiver containing many channels.

Multiplexing channel

A receiver channel which is sequenced through a number of satellite signals (each from a specific satellite and at a specific frequency) at a rate which is synchronous with the satellite message bit-rate (50 bits per second, or 20 milliseconds per bit). Thus one complete sequence is completed in a multiple of 20 milliseconds.

Observing session

The period of time over which GPS data is collected simultaneously by two or more receivers.

Outage

The occurrence in time and space of a GPS Dilution of Precision value exceeding a specified maximum.

Phase lock

The technique whereby the phase of an oscillator signal is made to become a smoothed replica of the phase of a reference signal by first comparing the phases of the two signals and then using the resulting phase difference signal to adjust the reference oscillator frequency to eliminate phase difference when the two signals are next compared (Bowditch, 1981, Vol. II). The smoothing time span occurs over approximately the inverse of the bandwidth. Thus a 40 hertz loop bandwidth implies an approximately 25 millisecond smoothing time constant.

Phase observable

See carrier beat phase.

P-code

The Precise (or Protected) GPS code--a very long (about 1014 bit) sequence of pseudorandom binary biphase modulations on the GPS carrier at a chip rate of 10.23 MHz which does not repeat itself for about 267 days. Each one-week segment of the P-code is unique to one GPS satellite, and is reset each week.

Precise positioning service (PPS)

The highest level of dynamic positioning accuracy that will be provided by GPS, based on the dual frequency P-code (U.S. DoD/DOT, 1982).

Pseudolite

The ground-based differential GPS station which transmits a signal with a structure similar to that of an actual GPS satellite (Kalafus, 1984).

Pseudorandom noise (PRN) code

Any of a group of binary sequences that exhibit noise-like properties, the most important of which is that the sequence has a maximum autocorrelation, at zero lag (Dixon, 1975).

Pseudorange

The time shift required to align (correlate) a replica of the GPS code generated in the receiver with the received GPS code, scaled into distance by the speed of light. This time shift is the difference between the time of signal reception (measured in the receiver time frame) and the time of emission (measured in the satellite time frame).

Pseudorange difference
See carrier beat phase.

Receiver channel
See channel

Reconstructed carrier phase
see Carrier Beat Phase

Relative positioning
The determination of relative positions between two or more receivers which are simultaneously tracking the same radiopositioning signals (e.g. from GPS).

Restart capability
The proprerty of a sequential processing computer program, that data can be processed rigorously in a sequence of computer runs, rather than only in one long run.

S-code
The Standard GPS code (formerly the C/A, Coarse/Acquisition, or Clear/Access code) -- a sequence of 1023 pseudorandom binary biphase modulations on the GPS carrier at a chip rate of 1.023 MHz, thus having a code repetition period of one millisecond.

Satellite constellation
The arrangement in space of the complete set of satellites of a system like GPS.

Satellite configuration
The state of the satellite constellation at a specific time, relative to a specific user or set of users.

Simultaneous measurements
Measurements referred to time frame epochs which are either exactly equal, or else so closely spaced in time that the time misalignment can be accomodated by correction terms in the observation equation, rather than by parameter estimation.

Slow switching channel
A switching channel with a sequencing period which is too long to allow recovery of the integer part of the carrier beat phase.

Spread spectrum systems

A system in which the transmitted signal is spread over a frequency band much wider than the minimum bandwidth needed to transmit the information being sent (Dixon, 1975).

Squaring-type channel

A GPS receiver channel which multiplies the received signal by itself to obtain a second harmonic of the carrier, which does not contain the code modulation.

Standard positioning service (SPS)

The level of kinematic positioning accuracy that will be provided by GPS based on the single frequency S-code (U.S. DoD/DOT, 1982).

Static positioning

Positioning applications in which the positions of points are determined, without regard for any trajectory they may or may not have.

Switching channel

A receiver channel which is sequenced through a number of satellite signals (each from a specific satellite and at a specific frequency) at a rate which is slower than, and asynchronous with, the message data rate.

Translocation

See relative positioning.

User equivalent range error (UERE)

The contribution to the range measurement error from an individual error source, converted into range units, assuming that error source is uncorrelated with all other error sources (Martin, 1980).

Z-count word

The GPS satellite clock time at the leading edge of the next data subframe of the transmitted GPS message (usually expressed as an integer number of 1.5 second periods) (van Dierendock et al., 1980).

LIST OF REGISTERED PARTICIPANTS

LEENDERT AARDOOM
GEODESY
DELFT UNIV. TECHNOLOGY
P.O. BOX 581
7300 AN APELDOORN
NETHERLANDS

RICHARD I. ABBOT
EARTH, ATMOSPHERIC AND
PLANETARY SCIENCES
MIT 54-627
MASSACHUSETTS INSTITUTE OF
TECHNOLOGY
CAMBRIDGE, MASSACHUSETTS 02139

JAMES R. ACKERET
DMAHTC
SATELLITE TRACKING BRANCH
5516 SWIFT CURRENT CT.
BURKE, VA 22015

TONY W. ADAMS
ARCO EXPLORATION
GEOPHYSICAL DATA ACQ.-LAND
P.O. BOX 2819
DALLAS, TX 75221

M. T. ALLISON
LEEDS UNIVERSITY U.K.
DEPT. ELECTRICAL ENGINEERING
LEEDS LS2 9JT
U.K.

RAY ALLISON
USDA FOREST SERVICE
ENG., 1101 RP-E
P.O. BOX 2417
WASHINGTON, D.C. 20013

HAMED SALEH AL-MERRI
ARAMCO
BOX 0302
UDHAIYLIYH
SAUDI ARABIA

ABDULLAH ALSHAMMARI
OSU
5225 HOLLISTER ROAD
COLUMBUS, OHIO 43220

RICHARD J. ANDERLE
GENERAL ELECTRIC
SPACE SYSTEMS DIVISION
BOX 469
SOUTHEASTERN, PA 19399

JOHN M. ANDERSON
MD STATE HIGHWAY
707 N. CALVERT ST.
BALTIMORE, MD 21202

LARRY A. ANDERSON
PACIFIC MISSILE TEST CENTER
CODE 3452
POINT MUGU, CA 93042

WILLIAM K. ANDERSON
W. D. USHER & ASSOCIATES
101 10335 172ND STREET
EDMONTON, ALBERTA
CANADA T5S 1K9

M. JAEGLE ANDRE
I.G.N.
2, AVENUE PASTEUR
94160 SAINT-MANDE, FRANCE

PETER ANGUS-LEPPAN
DEPARTMENT OF LANDS - THAILAND
PHRA PHIPHIT ROAD
BANGKOK 10200, THAILAND

JOHN APPLEGATE
TEXAS INSTRUMENTS
1500 BAFFIN BAY
PLANO, TX 75075

JAVAD MA. ASHJAEE
TRIMBLE NAVIGATION
1077 INDEPENDENCE
MOUNTAIN VIEW, CA 94043

VIDAL ASHKENAZI
UNIVERSITY OF NOTTINGHAM
DEPT. OF CIVIL ENGINEERING
UNIVERSITY PARK
NOTTINGHAM NG72RD
UNITED KINGDOM

ANTHONY P. ATKINSON
ORDNANCE SURVEY
ROMSEY ROAD
SOUTHAMPTON, 5094DH
UNITED KINGDOM

PAUL AUDET
PHOTOSUR I LAVALIN
1130
MONTREAL, QUEBEC
CANADA H3A 2R5

YOSHIO BABA
GEOGRAPHICAL SURVEY INSTITUTE
KITASATO-1, YATABLE-MACHI,
TSUKUBA-GUM, IBARAKI-KEN
JAPAN 305

ALICE BABCOCK
U.S. NAVAL OBSERVATORY
TIME SERVICE DEPARTMENT
34TH AND MASSACHUSETTS AVE., N.W.
WASHINGTON, DC 20390

RICK BADEWITZ
CUBIC CORPORATION
9333 BALBOA AVENUE
SAN DIEGO, CA

LEONARD S. BAKER
JANET BAKER
SAM BAKER CONSULTING
8612 FOX RUN
POTIMAC, MD 20854

PHILLIP J. BAKER
OSD/C3I
PENTAGON - ROOM 30174
WASHINGTON, DC

ANGEL A. BALDINI
USA-ETL RESEARCH INSTITUTE
ETL RI
VIRGINIA

VAIOS BALIS
NATIONAL TECHNICAL UNIVERSITY
9 HEROON POLYTECHNIOU
ZOGRAPHOS, GREECE GR 15773

WILLIAM E. BALL, JR.
USDI BUREAU OF LAND MANAGEMENT
BLDG 50 DENVER FEDERAL CENTER
DENVER, CO 80225

HERB BANSBACH
LITTON AERO PRODUCTS
6101 CONDOR DRIVE
MOORPARK, CA 93021

MOUSTAFA A. BARAKA
GEODETIC SCIENCE AND SURVEYING
THE OHIO STATE UNIVERSITY
1958 NEIL AVENUE
404 COCKINS HALL
COLUMBUS, OH 43210

NEVEN EL-SWEFY BARAKA
GEODETIC SCIENCE AND SURVEYING
THE OHIO STATE UNIVERSITY
1958 NEIL AVENUE
COLUMBUS, OH 43210

MARK J. BARDAKJIASN
ARAMCO
BOX 5347
DHAHRAN 31311, SAUDI ARABIA

RICHARD A. BARKER
JOHN E. CHANCE AND ASSOC.
P.O. BOX 52029
LAFAYETTE, LA 70505

CRAIG D. BARNES, P. ENG.
GEODETIC COMPUTATION
4949-94B AVE.
EDMONTON, ALBERTA T6B 2T5
CANADA

IVO BAUERSIMA
UNIVERSITY OF BERNE
ASTRONOMICAL INSTITUTE
SIDLERSTRASSE 5
3006 BERN, SWITZERLAND

COLIN M.D. BEATTY
MAGNAVOX INT. OPS, LTD.
470 LONDON ROAD
SLOUGH, BERKSHIRE, SL38QY
UNITED KINGDOM

NORMAN BECK
GEODETIC SURVEY OF CANADA
615 BOOTH ST.
OTTAWA, ONTARIO
CANADA K1A 0E9

JEAN-MARIE BECKER
NATIONAL LAND SURVEY OF SWEDEN
LANTMATERIGATAN 2
GAVLE, SWEDEN

JOHN F. BEEKMAN
GEODETIC INTERNATIONAL, INC.
5635 NORTHWEST CENTRAL DRIVE -101
HOUSTON, TX 77092

MOHAMED AIT BELAID
SC. GEODESIQUES ET TELED.
UNIVERSITE LAVAL
PAVILLON CASAULT
STE FOY, QUEBEC G1K 7P4
CANADA

STEVE BELL
GEO/HYDRO
2115 E. JEFFERSON
ROCKVILLE, MD 20852

PETER L. BENDER
NATIONAL BUREAU OF STANDARDS
DIV 525
325 BROADWAY
BOULDER, CO 80303

DAVID W. BENNETT
USGA
1400 INDEPENDENCE RD
ROLLA, MO 65559

GLENN BERGEY
USDA FOREST SERVICE
1621 N. KENT STREET
ARLINGTON, VA

KNUTE A. BERSTIS
N/CG16
NOAA/NATIONAL GEODETIC SURVEY
6001 EXECUTIVE BLVD.
ROCKVILLE, MD 20852

GILLES M. BESSERO
SERVICE HYDRO-ET OCEANO-DE LA
MARINE (SHOM)
BREST, FINISTERE
FRANCE 2g275 BP 426

GERHARD BEUTLER
UNIV. OF BERN - ASTRO. INST.
SIDLERSTRASSE 5BERNE CH-3012
SWITZERLAND

ROGER BILHAM
JILA - UNIVERSITY OF COLORADO
BOULDER, CO 80309

NGUYEN KIM BINH
UNIVERSITY LAVAL
1056 DUCHESNEAU
STE-FOY
QUEBEC, CANADA G1W 4H9

JOHN B. BISHOP
NAVAL INTELLIGENCE SUPPORT LTR
4301 SUITLAND ROAD
WASHINGTON, DC

HAROLD D. BLACK
JHU APL
SPACE ANALYSIS & COMPUTATIONS
JOHNS HOPKINS ROAD
LAUREL, MARYLAND 20707

ZEB BLACKMAN
SIDNEY B. BOWNE & SON
235 E. JERICHO TPKE
MINEOLA, NY 11501

WALTER F. BLANCHARD
RACAL POSITIONING SYSTEMS
KINGSTON ROAD
LEATHERHEAD, SURREY
UNITED KINGDOM

J. BLANCHETTE
BENDIX FIELD ENGINEERING
CORPORATION
ONE BENDIX ROAD
COLUMBIA, MARYLAND 21045-1897

JAN C. BLANKENBURGH
STATOIL/NTH
RESEARCH & DEVELOPMENT
P.O. BOX 300 - 4000 STAVANGER
NORWAY

FRANK BLETZACKER
CAST
5450 KATELLA AVE., STE. 102
LOS ALAMITOS, CA 90720

ZHIPENG
WUHAN TECHNICAL UNIVERSITY OF
SURVEYING AND MAPPING
23 LOYU ROAD
WUHAN, CHINA

YEHUDA BOCK
EARTH, ATMOS. & PLANETARY SCI.
MIT 54-627
MASS. INST. OF TECHNOLOGY
CAMBRIDGE, MASSACHUSETTS 02139

H.L. BONNET
USCG - RADIONAVIGATION DIV.
2100 SECOND STREET, S.W.
WASHINGTON, D.C. 20593

GEORGE H. BORN
UNIVERSITY OF TEXAS AS AUSTIN
CENTER FOR SPACE RESEARCH WRW414
AUSTIN, TX

JOHN D. BOSSLER
NOAA/NOS
6001 EXECUTIVE BLVD.
ROCKVILLE, MD

JOHN M. BOSWORTH
NASA GODDARD SPACE FLT CENTER
GREENBELT, MD 20771

CLAUDE BOUCHER
INSTITUT GEOGRAPHIQUE NATIONAL
SGNM/DTIG
2 AVENUE PASTEUR
SAINT-MANDE 94160, FRANCE

WADE BRADFORD
TEXAS INSTRUMENTS
P.O. BOX 405 MS 3418
LEWISVILLE, TX 75067

PATRICK T. BRASSARD
BYTOWN MARINE LTD.
P.O. BOX 11397 STN.H
OTTAWA, ONTARIO
CANADA K2H 7V1

THOMAS K. BRAY
U.S. GEOLOGICAL SURVEY
2845 PARFET DRIVE
LAKEWOOD, CO

LAWRENCE C. BRADLEY
GEOSPACE SYSTEM CORP.
WELLESLEY OFFICE PARK
40 WILLIAM ST. - SUITE 95
WELLESLEY, MA 02181

MAJOR MARK C. BREACH
DEF. MAP. AGENCY - HYDRO TOPO
UK 512
6500 BROOKES LANE
WASHINGTON, D.C. 20315

MIKE BRESLIN
N.S.W.C., DAHLGREN
DAHLGREN, VA 22448

ROBERT BROCK
SUNY-ESF
312 BRAY HALL
SYRACUSE, NY

STEVEN M. BRIGGS
FLORIDA LEVEL AND TRANSIT CO.
809 PROGRESSO DRIVE
FORT LAUDERDALE, FL

ALISON KAY BROWN
LITTON AERO PRODUCTS
6101 CONDOR DRIVE
MOORPARK, CA 93021-2699

DUANE C. BROWN
GEODETIC SERVICES, INC.
1511 RIVERVIEW DRIVE
MELBOURNE, FL 32901

PHILIP BROXHAM
WILD HEERBRUGG (UK) LTD.
REVENGE RD. LORDSWOOD
CHATHAM, KENT ME7 8TE
UNITED KINGDOM

JOHN BROZENA
NAVAL RESEARCH LABORATORY
WASHINGTON, DC 20375

NORMAN E. BRUNELL
AERO SERVICE
4249 SAN RAFAEL
LOS ANGELES, CA 90042

RONALD D. BRUNELL
INTERSTATE ELECTRONICS CORP.
D 4460
1001 E. BALL RD.
ANAHEIM, CALIFORNIA 92803

FRITZ K. BRUNNER
WILD HEERBRUGG LTD.
CH-9435 HEERBRUGG
SWITZERLAND

STEVEN J. BRZEZOWSKI
TASC - SYS. DEVELOPMENT
DIV./GEOSCIENCES DEPT.
1 JACOB WAY
READING, MA 01876

ROBERT C. BURTCH
SURVEYING AND MAPPING BRANCH
FERRIS STATE COLLEGE
SWAN 106
BIG RAPIDS, MI 49307

QINGJUN BU
XIAN RESEARCH INSTITUTE OF
SURVEYING AND MAPPIING
17 YAN TA ROAD
XIAN, CHINA

AL BUENNAGEL
ISTAC
444 W. ALTADENA DR.
PASADENA, CA

JAMES BUISSON
NAVAL RESEARCH LAB. - CODE 7773
WASHINGTON, DC

PAUL JOSEPH CABION
COUNCEL FOR SCI. IND. RESEARCH
18A GILLSTR OBSERVATORY
JOHANNESBURG, TRANSVAAL
SOUTH AFRICA

JIMMY D. CAIN
AERO SERVICE DIV. - LITTON
8100 WEST PARK DR.
HOUSTON, TX 77063

ALESSANDRO CAPORALI
DEPT. OF PHYSICS
UNIVERSITY OF PADOVA
VIA MARZOLA 8
PADOVA 35131, ITALY

RICHARD W. CARROLL
ROCKWELL/COLLINS
400 C AVENUE, NE
CEDAR RAPIDS, IA

RON A. CARROUTH
CARROUTH & ASSOC. INC. - SUR.
9100 JEFFERSON DAVIS HIGHWAY
RICHMOND, VA 23234

NANCY CARROUTH
CARROUTH & ASSOC. INC.
SURVEYING
P.O. BOX 34366
RICHMOND, VA 23234

WILLIAM E. CARTER
NES
ROCKVILLE, MD

MRS. MARILYN CARTER
NGS
ROCKVILLE, MD

LAVERN R. CELESTINO
LARSEN ENGINEERS
136 AMSDEN DRIVE
ROCHESTER, NY

CHARLES CHALLSTROM
NOAA
6001 EXECUTIVE BLVD.
ROCKVILLE, MD

MICHAEL E. CHAMBERLIN
ARCO EXPLORATION
BOX 2819 PRC 1159
DALLAS, TX 75042

THOMAS S. CHANCE
NAVIGATION ELECTRONICS, INC.
BOX 52047
LAFAYETTE, LA

BEN F. CHAO
NASA/GODDARD SPACE FLIGHT CENTER
GEODYNAMICS BRANCH
CODE 621, GSFC
GREENBELT, MD 21046

WILLIAM M. CHAPMAN
NATIONAL MAPPING DIVISION
U.S. GEOLOGICAL SURVEY
3802 HOWARD ST.
ANNANDALE, VA 22003

FRANK J. CHARLES
MAGNAVOX
SURVEY SYSTEMS - MARINE DIV.
2829 MARICOPA ST.
TORRANCE, CALIFORNIA 90503

LAURA G. CHARRON
U.S. NAVAL OBSERVATORY
34TH AND MASSACHUSETTS AVE., N.W.
TIME SERVICE DEPARTMENT
WASHINGTON, DC 20390

MIRANDA M. CHIN
NATIONAL GEODETIC SURVEY
DEPT. OF COMMERCE
6808 TAMMY COURT
BETHESDA, MD 20817

JACQUELINE CHOVITZ
U.S. DEPARTMENT OF COMMERCE/NOAA
NATIONAL GEODETIC SURVEY, N/CGx2
6001 EXECUTIVE BLVD.
ROCKVILLE, MD 20852

BERNARD H. CHOVITZ
U.S. DEPARTMENT OF COMMERCE, NOAA
NATIONAL GEODETIC SURVEY, N/CGx2
6001 EXECUTIVE BLVD.
ROCKVILLE, MD 20852

JOHAN HENRIK CHRISTIANSEN
A/S WORSKE SHELL E&P
BOX 10, 4033 FORUS
STAVANGER, NORWAY

LUIGI CIRAOLO
IROE - CNR
V. PANCIATICHI 75
FLORENCE, ITALY,

JOHN F. CLARK
CAST
5450 KATELLA AVE., STE. 102
LOS ALAMITOS, CA 90720

RANDOLPH CLARKE
U.S. NAVAL OBSERVATORY
TIME SERVICE DEPARTMENT
34TH AND MASSACHUSETTS AVE., N.W.
WASHINGTON, DC 20390

JAMES R. CLYNCH
APPLIED RESEARCH LABORATORY
P.O. BOX 8029
AUSTIN, TX

ROBERT J. COATES
CRUSTAL DYNAMICS PROJ./CODE 601
GODDARD SPACE FLIGHT CENTER
CODE 601
GREENBELT, MD 20771

DAVID COCO
UNIVERSITY OF TEXAS
10000 BURNET
AUSTIN, TX

RONALD COLER
BOSTON SURVEY CONSULTANTS
647 SUMMER STREET
BOSTON, MA 02210

ANN COLLIER
TEXAS INSTRUMENTS
P.O. BOX 405 M/S 3418
LEWISVILLE, TX 75067

JAMES COLLINS
GEO/HYDRO
2115 E. JEFFERSON ST.
ROCKVILLE, MD

O.W. CONWAY
ARCO EXPLORATION
GEOPHYSICAL DATA ACQ.-LAND
2300 WEST PLANO PARKWAY
PLANO, TX

STAN COPELAND
SEA SYSTEMS CORPORATION
230 S. POWERLINE ST.
DEERFIELD BEACH, FL 33441

ROBERT C. COTTINGHAM
NAVAL WEAPONS CENTER
PRODUCT ASSURANCE DIV.
(CODE 3683)
CHINA LAKE, CA 93555

CHARLES C. COUNSELMAN, III
EARTH, ATMOSPHERIC AND PLANETARY
SCIENCES
MIT 54-620
MASSACHUSETTS INSTITUTE OF
TECHNOLOGY
CAMBRIDGE, MASSACHUSETTS 02139

CAROLINE COVER
1435 PRINCE OF WALES DRIVE
APT #1616
OTTAWA, ONTARIO
CANADA K2C IN5

ARTHUR COX
PACIFIC MISSILE TEST CENTER
POINT MUGU, CA 93042

DUNCAN B. COX, JR
CS DRAPER LABORATORY
RADIO COMMUNICATIONS AND
NAVIGATIONS DIV.
555 TECH SQ.
CAMBRIDGE, MA 02139

MARVIN D. CRABTREE
INTERNATIONAL BOUNDARY COMM.
425 I STREET, NW., ROOM 150
WASHINGTON, DC 20001

JOHN CRITCHLEY
GEODESY DIVISION
MCE RE
ELMWOOD AVENUE
FELTHAM, MIDDLESEX
UNITED KINGDOM, TW137AF

JAMES K. CROSSFIELD
CALIF. STATE UNIVERSITY
FRESNO
DEPT. OF CIVIL AND SURV. ENGR.
FRESNO, CA 93740-0094

ALEJANDRO CUARTIN
ESTUDIOS DE FOTOGRAMETRIA C.A.
GEODETIC DEPARTMENT
AV. LA HAYA QTA. MERCEDES ELENA
CARACAS, D.F. 1070
VENEZUELA

GARY T. CUPPELS
GILBERT/COMMONWEALTH INC.
P.O. BOX 1498
READING, PA 19606

ROBERT ANTHONY CURLEY
GEOPHYSICAL SERVICES, INC.
MANTON LANE
BEDFORD, ENGLAND
MK41 7PA

EDWARD J. CYRAN
U.S. GEOLOGICAL SURVEY
NATIONAL MAPPING DIVISION
MS-526
12201 SUNRISE VALLEY DR.
RESTON, VA 22092

MRS. C.J. DALY
KINGSTON ROA, LEATHERHEAD
SURREY, KT227ND
UNITED KINGDOM

PETER J. DALY
RACAL SURVEY LIMITED
KINGSTON ROAD, LEATHERHEAD
SURREY, KT227ND
UNITED KINGDOM

DR. P. DALY
UNIVERSITY OF LEEDS
DEPT. OF ELECTRICAL ENGINEERING
LEEDS, UNITED KINGDON, L52 9J7

SANDRAL DANIELL
DMAAC/STS
3200 SOUTH 2ND STREET
ST. LOUIS, MO 63118

JOHN M. DAVIDSON
JET PROPULSION LABORATORY
4800 OAK GROVE DR.
PASADENA, CA

E.S. DAVIS
JET PROPULSION LAB
TELECOMMUNICATIONS SCI. & ENGRG.
4800 OAK GROVE DR. 233-540
PASADENA, CA 91109

JOSE BITTENCOURT DE ANDRANDE
PARANA FEDERAL UNIVERSITY (BR)
RUA JOAO PAROLIN, 645
CURITIBA, PARANA
BRAZIL 80000

MELVIN DE GREE
USGS
NAT. CENTER MS 526
RESTON, VA

BARBARA J. DE NOYER
DMAHTC
6400 BROOKES LANE
WASHINGTON, DC 20315

ETTORE DELMONTE
OF. TEC. DEL MONTE AND ASSOC.
P.O. BOX 330
PUERTO ORDAZ, BOLIVAR
VENEZUELA

STEPHEN R. DELOACH
U.S. ARMY ENGINEER TOPO. LABS
ETL-TD-EA
FORT BELVOIR, VA 22060-5546

DELIKARAOGLOU DEMITRIS
GEODETIC SURVEY OF CANADA
615 BOOTH STREET
OTTAWA, ONTARIO
CANADA K1AOE9

PARADISSIS DEMITRIS
DIREL - ING.
DIONYSOS SATELLITE TRACKING CTR.
9, HEROON POLYTECHNIOU STR
ZOGRAPHOS, GREECE GR-15773

LUC DEMONIE
NATIONAL GEOGRAPHICAL INSTITUTE
DEPARTMENT OF GEODESIC
ABDIJ TER KAMEREN 13
1050 BRUSSELS, BELGIUM

ROBERT P. DENARO
TAU CORPORATION
10 JACKSON STREET
SUITE 101
LOS GATOS, CA 95030

CHRIS DISE
U.S. NAVAL OBSERVATORY
TIME SERVICE DEPARTMENT
34TH AND MASSACHUSETTS AVE., N.W.
WASHINGTON, DC 20390

JAMES G. DONAHUE
ESPEY HUSTON & ASSOC., INC.
P.O. BOX 519
AUSTIN, TX

DON DONOFRIO
NATIONAL GEODETIC SURVEY
3601 C ST. SUITE 980
ANCHORAGE, AL 99503

MARK D. DOSS
TRANSCONTINENTAL GAS PIPE LINE
ENGINEERING CONSTRUCTION/SURVEY
2800 POST OAK BOULEVARD
HOUSTON, TEXAS 77056

BRUCE C. DOUGLAS
NOAA/NOS
ROCKVILLE, MD 20852

T.P. DRAKE
BRITISH PETROLEUM CO. LTD.
MOOR LANE - BRITANNIC HOUSE
LONDON ECS
UNITED KINGDON ECSY 9BU

EDWARD J. DRELICH
VEP ASSOCIATES, INC.
1140 BLOOMFIELD AVENUE
W. CALDWELL, NJ 07006

STEPHEN DUNCOMBE
HARVEY LYNCH INC.
10777 WEST HEIMER S-965
HOUSTON, TX 77429

MICHAEL LEONARD DURANT
WIMPOL, LTD.
HARGREAVES ROAD
GROUNDWELL IND. ESTATE
SWINDON, WILTSHIRE
UNITED KINGDOM

I. NEWTON DURBORAN, III
MOTOROLA
2100 E. ELLIOT RD.
TEMPE, AZ

DENNIS J. DUVEN
APPLIED PHYSICS LABORATORY/JHU
JOHNS HOPKINS ROAD
LAUREL, MD 20707

DELF EGGE
ASSISTANT PROFESSOR
CIVIL ENGINEERING, FX-10
UNIVERSITY OF WASHINGTON
SEATTLE, WA 98195

DR. KLAUS EICHHOLZ
WESTFAELISCHE BERGGEWERUSUASSE
HERNER STR 45
D-4630 BOCHUM
GERMANY

ROGER EKSETH
NORWEGION HYDROGRAPHIC SERVICES
POSTBOKS 60
4000 STAVANGER
NORWAY

LEIF ELIASSON
NATIONAL LAND SURVEY OF SWEDEN
S-801 12 GAVLE
GAVLE,
SWEDEN

DON ELLER
CAST
5450 KATELLA AVE., STE. 102
LOS ALAMITOS, CA 90720

BARRY ELSON
U.S. NAVAL OBSERVATORY
TIME SERVICE DEPT.
WASHINGTON, DC 20390

EMMANUEL EMENIKE
UNIVERSITY OF NIGERIA NSUKKA
ENUGU CAMPUS ENUGU NIGERIA
ENUGU, ANAMBRA
NIGERIA

RALPH ESCHENBACH
TRIMBLE NAV
1077 INDEPENDENCE
MOUNTAIN VIEW, CA

MAX M. ETHRIDGE
DEFENSE MAPPING AGENCY
US NAVAL OBSERVATORY ATTN: PPS
WASHINGTON, DC

ALAN G. EVANS
NAVAL SURFACE WEAPONS CENTER
DAHLGREN, VA 20646

MRS. ALAN G. EVANS
SPACE FLIGHT SCIENCE
DAHLGREN LAB (K13)
DAHLGREN, VA 22448

JON FALKENBERG
NAVIGATION
GEOPHYSICAL CO OF NORWAY
VERITASVEIEN 1
1322 HOVIK
NORWAY

JAMES I. FELIX
U.S. BUREAU OF RECLAMATION
DENVER FEDERAL CENTER
P.O. BOX 25007
DENVER, CO 80225

JAMES T. FELKERSON
U.S. GEOLOGICAL SURVEY
1400 INDEPENDENCE ROAD
ROLLA, MO

PATRICK FELL
DMAHTC
4612 JACKSON ROAD
FREDERICKSBURG, VA 22401

REMI FERLAND
THE MCELHANNEY GROUP, LTD.
MARINE SURVEYS DIVISION
#450, 999 - 8TH STRET S.W.
CALGARY, ALTA.
CANADA T2R1J5

CHARLES J. FINLEY
NASA HQ
OSSA/RRG
WASHINGTON, DC 20546

THOMAS L. FISCHETTI
NASA - GEODYNAMICS BRANCH
600 INDEPENDENCE AVE., S.W.
WASHINGTON, D.C. 20546

HENRY S. FLEMING
US NAVAL RESEARCH LAB
WASHINGTON, DC 20375

BRUCE L. FLETCHER
ENERGY & NATURAL RESOURCES
4949-49 B AVE.
EDMONTON, ALBERTA
CANADA T6A1T5

HENRY F. FLIEGEL
AERO SPACE
EL SEGUNDO BLVD.
EL SEGUNDO, CA

ANGEL FONSECA
ESTUDIOS DE FOTOGRAMETRIA C.A.
GEODETIC DEPARTMENT
AV. LA HAYA QTA. MERCEDES ELENA
CARACAS, D.F. 1070, VENEZUELA

GEORGE MICAHEL FRANK
NATIONAL GEODETIC SURVEY
11400 ROCKVILLE PIKE
ROCKVILLE, MD

J. ED FRENCH
RCA
MTP/TECHNICAL ANALYSIS
BLDG. 989, Mu 645
PATRICK AFB, FLA 32925

PETER FRICKER
WILD HEERBRUGG LTD.
CH-9435 HEERBRUGG
SWITZERLAND

CHARLES J. FRONCZEK, JR.
NATIONAL BUREAU OF STANDARDS
GAITHERSBURG, MD

ADESTE E. FUENTES
U.S. COAST GUARD HQ
RADIONAVIGATION DIVISION
2100 SECOND ST., S.W.
WASHINGTON, D.C. 20593

RUDOLF J. FURY
NOAA, NOS, C&GS
NATIONAL GEODETIC SURVEY
6001 EXECUTIVE BLVD.
ROCKVILLE, MD 20852

JOHN T. FURZE
CS DRAPER LABORATORY
RADIO COMMUNICATION & NAVIGATION
555 TECHNOLOGY SQUARE
CAMBRIDGE, MA 02717

PIERRE GAGNON
SC. GEODESIQUES ET TELED.
UNIVERSITE LAVAL
PAVILLON CASSAULT
STE FOY, QUEBEC G1K 7P4
CANADA

BEVERLY GAIL
U.S. GOVERNMENT
APT. 707 - 1435 4TH ST. SW
WASHINGTON, DC 20024

CDR. ROLAND GARCIA
NAVAL OCEANOGRAPHY COMMAND
NSTL STATION, ME 39579

ALAN R. GARDNER
WILD HEERBRUGG (UK) LTD.
REVENGE ROAD, LORSWOOD
CHATHAM, KENT ME5 8TE
UNITED KINGDOM

DAVID GARIEPY
BROWN & ROOT INTERNATIONAL
HYDROGRAPHIC SURVEY DIV.
4130 DIRECTORS ROW
HOUSTON, TX 77092

DAVID S. GASVODA
USDA-FOREST SERVICE MEDC
FORT MISSOULA - BLVD. 1
MISSOULA, MT 59801

JOHN P. GAY
MOBIL OIL
P.O. BOX 456540
DALLAS, TX 75245

LEE GAZLAY
U.S. COAST GUARD
RADIONAVIGATION INFORMATION
2100 SECOND STREET, S.W.
WASHINGTON, D.C. 20593

ALAIN GEIGER
ETH-HONGGERBERG
INSTITUTE OF GEODESY AND
PHOTOGRAMMETRY
8093 ZURICH
SWITZERLAND

JEAN GERVAISE
CERN
CHIEF APPLIED GEODESY GROUP
SITE DE PREVESSIN
F-01631 CERN CEDEX
FRANCE

LTC. JOHN I. GERZEL
DMA HTD
WASHINGTON, DC 20315

RICHARD T. GIBSON
CAST
5450 KATELLA AVE., STE. 102
LOS ALAMITOS, CA 90720

DR. CLYDE C. GOAD
N/CG14
NATIONAL GEODETIC SURVEY
6001 EXECUTIVE BLVD.
ROCKVILLE, MD 20852

JAY GOLDFARB
UNIVERSITY OF CALGARY
2500 UNIVERSITY DR.
CALGARY, ALBERTA
CANADA T2N 1NA

MICHEL GONTHIER
EDO CANADA
8-6320 11TH STREET S.E.
CALGARY, ALTA. T2H 2L7
CANADA

RENE GONZALEZ
INSTITUTO GEOGRAFICO MILITAR
AV LAS AMERICAS 5-76 Z-13
GUATEMALA, GUATEMALA

ARTIE GOODWIN
TEXAS INSTRUMENTS
P.O. BOX 405 MS 3418
LEWISVILLE, TX 75067

DHANVANT H. GORADIA
SPERRY CORP.
ROUTE 29N
CHARLOTTESVILLE, VA 22906

DAVID M. GORG
STATE OF MINN DEPT. OF TRANS.
4819 CENTRAL AVE.
WHITE BEAR LAKE, MN

M. WENDEL GOULDMAN
NAVAL SURFACE WEAPONS CENTER
CODE K12
DAHLGREN, VA 22448

SERGEI A. GOUREVITCH
STEINBRECHER CORP.
185 NEW BOSTON ST.
WOBURN, MA

R. GOVIND
DIVISION OF NATIONAL MAPPING
CJAMD:ER STREET
CANBERRA
A.C.T.
AUSTRALIA 2616

RICHARD O. GREENMAN
ENG. CONSTRUCTION - SURVEY
TRANSCONTINENTAL GAS PIPE LINE
P.O. BOX 1396
HOUSTON, TX 77251

RICHARD GREENSPAN
CS DRAPER LABORATORY
RADIO COMMUNICATION & NAVIGATION
555 TECH SQ.
CAMBRIDGE, MASSACHUSSETTS 02139

TIMOTHY GRIFFIN
WIMPOL, INC.
8850 JAMEEL RD. #100
HOUSTON, TX 77040

XINGJUN GUAN
XIAN RESEARCH INSTITUTE OF
SURVEYING & MAPPING
17 YANTA ROAD XIAN
XIAN
CHINA

ERICH GUBLER
FED OFF OF TOPOGRAPHY - GEOD
SEFTIGEN STRASSE 264
CH-3084 WABERN
SWITZERLAND

TONG KIAT GUOY
HYDROGRAPHIC DEPT. (RMN)
MINISTRY OF DEFENCE
JLN PADANG TEMBAK
KUALA LUMPUR 15-03
MALAYSIA

WERNER GURTNER
UNIV OF BERNE - ASTRO INST.
SIDLERSTRASSE 5
CH-3012 BERNE
SWITZERLAND

CARL J. GUSTAFSON
INTERNATIONAL BOUNDARY COMMISSION
CANADIAN SECTION
615 BOOTH STREET #134
OTTAWA, ONT. K1A 0E9
CANADA

IUAR HAARSTAD
IKU
P.O. BOX 1883 JAARESLETTA
7001 TRONDHEIM
NORWAY

DR. D. P. HAJELA
OSU
DEPT. GEODETIC SCIENCE
1958 NEIL AVENUE, #404
COLUMBUS, OHIO 43210-1247

ROBERT N. HALLENBECK
OFFSHORE NAVIGATION INC.
5728 JEFFERSON HIGHWAY
HARAHAN, LA 70123

CHARLES A. HAMILTON
DMAAC
SYSTEMS AND TECHNOLOGY
3200 SOUTH 2ND
ST. LOUIS, MO 63118

JOHN HANNAH
DEPT. OF LANDS & SURVEY
PRIVATE BAG
WELLINGTON,
NEW ZEALAND

JANIS HARBUS
TEXAS INSTRUMENTS
P.O. BOX 405 M/S 3418
LEWISVILLE, TX 75067

NICK W. HARRISON
PROFESSIONAL SURVEYOR MAGAZINE
918 F STREET NW, SUITE 410
WASHINGTON, D.C.

RONALD G. HARTSOCK
NATIONAL BUREAU OF STANDARDS
GAITHERSBURG, MD 20988

SAYED HASHIMI
CONSTRUCTION DEPT./SURVEY
FERRIS STATE COLLEGE
SWAN 202 A
BIG RAPIDS, MI 49307

LOWELL HEATON
BUREAU OF RECLAMATION
941 E. MILLITTE AVE.
MESA, AZ

BRUCE E. HEDQUIST
GEODETIC SURVEYS CO, INC.
2100 W. LOOP SOUTH #1550
HOUSTON, TX

VICTOR H. HEDMAN
U.S. FOREST SERVICE
310 W. WISCONSIN AVE.
MILWAUKEE, WI

MADELEINE C. HEIDKAMP
JHO/APPLIED PHYSICS LABORATORY
JOHN HOPKINS ROAD
LAUREL, MD 20707

GUNTER W. HEIN
UNIVERSITY FAF MUNICH
WERNER-HEISENBERG-WEG 39
D-8014 NEUBIBERG
FEDERAL REPUBLIC OF GERMANY

DENNIS HENSON
TEXAS INSTRUMENTS
P.O. BOX 405 m/s 3418
LEWISVILLE, TX 75067

EDWARD H. HERBRECHTSMEIER
NATIONAL GEODETIC SURVEY, N/CG15
ROCKVILLE, MD 20852

BRUCE R. HERMANN
K-13
NAVAL SURFACE WEAPONS CENTER
DAHLGREN, VA 22448

PEIRRE HEROUX
GEODETIC SURVEY OF CANADA
142-E VALLEY STREAM DR.
NEDEAN, ONTARIO
CANADA K2H GC6

RAFAEL HERRERO
INSTITUTO GEOGRAFICO NACIONAL
C/GENERAL IBANEZ DE IBERO, 3
MADRID, SPAIN

EVAN F. HERRIN
SHELL OFFSHORE INC.
ONE SHELL SQUARE
NEW ORLEANS, LA 70160

KJELL HERVIG
NAVIGATION SYSTEM DEPARTMENT
KONGSBERG VAAPENFABRIKK
P.O. BOX 25
KONGSBERG N3601
NORWAY

HOWARD HEUBERGER
NASA/GODDARD SPACE CENTER
CODE 552
GREENBELT, MD 20771

LANNY HEYMANN
SPACE BUSINESS NEWS
1401 WILSON BLVD.
SUITE 910
ARLINGTON, VA 22209

ALEX HITTEL
NORTECH SURVEYS
309 2ND AVE. SW
CALGARY, ALBERTA
CANADA T2P 0C5

YIN-HSIN HO
MCDONNELL DOUGLAS CO.
P.O. BOX 516
ST. LOUIS, MO 63166

DENNIS HOAR
OPERATIONS BRANCH
NATIONAL GEODETIC SURVEY
11400 ROCKVILLE PIKE
ROCKVILLE, MD 20852

CARL E. HOEFENER
INTERSTATE ELECTRONICS
1001 BALL ROAD
ANAHEIM, CA 92803

DAG HOGVARD
A/S GEOTEAM
GML. DRAMMENSV. 48
N1320 STABEKK
NORWAY

JOHN E. HOHOL
BERNSTEN, INC.
P.O. BOX 8666
MADISON, WI 53708

MARK HOLDRIDGE
FORD AEROSPACE
4920 NIAGRA RD.
COLLEGE PARK, MD

NORMAN C. HOLMES
EUROPEAN SPACE AGENCY
KEPLERLAAN
NOORDWIJK
NETHERLANDS

H. D. HOLSCHER
C/O C. HIDE COUNCELLOR (SCIENCE)
SOUTH AFRICAN EMBASSY
SUITE 350
4801 MASSACHUSETTS AVENUE, N.W.
WASHINGTON, D.C.

ARTHUR W. HOLT, JR.
NAVAL RESEARCH LABORATORY
4555 OVERLOOK AVE., SW
WASHINGTON, DC 20375

LARRY D. HOTHEM
ASTRONOMY AND SPACE GEODESY
BRANCH
NATIONAL GEODETIC SURVEY, N/CG142
6001 EXECUTIVE BLVD.
ROCKVILLE, MD 20852

CHERYL A. HOWARTH
MARKETING
GEOSTAR CORPORATION
101 CARNEGIE CENTER, SUITE 302
PRINCETON, NJ 08536

DR. GUYEN DAN HUA
STANFORD TELECOMMUNICATIONS, INC.
GPS - NAVIGATION & TRACKING
2421 MISSION COLLEGE BLVD.
SANTA CLARA, CA 95050

ART HUMBLE
MAGNAVOX
2829 MARICOPA STREET
TORRANCE, CA 90503

KEN HURST
LDGO-SEISMOLOGY
PALISADES, NY 10964

RON C. HYATT
TRIMBLE NAVIGATION
GPS INSTRUMENTATION
1944 ALFORD
LOS ALTOS, CA

R. M. IVERSON
CARSON GEOSCIENCE
32H BLOOMING GLEN ROAD
PERKASIE, PA 18944

LEONARD J. JACOBSON
INTERSTATE ELECT. CORP.
MARKETING
1001 E. BALL RD.
ANAHEIM, CA 92803

JAEGLE
INSTITUT GEOGRAPHIQUE NATIONAL
2 AV PASTEUR
SAINT MANDE
FRANCE G4160

OTOOLE JAMES
NS WC
DAHLGREN, VA

ASHJAEE JAVAD
TRIMBLE NAVIGATION
1077 INDEPENDENCE AVE
MOUNTAIN VIEW, CA 94043

CHRISTOPHER JEKELI
AIR FORCE GEOPHYSICS LAB
HANSCOM AFB
BEDFORD, MA

JAMES JESPERSEN
NATIONAL BUREAU OF STANDARDS
325 BROADWAY
BOULDER, COLORADO 80303

WILLIAM MALCOLM JOHNSON
JATCO/ARAMCO
P.O. BOX 2713
DAMMAM, SAUDI ARABIA

KEN J. JOHNSTON
NRL CODE 4130
WASHINGTON, D.C. 20375

ANDREW C. JONES
SURVEY DIVISION
SOUTH AUSTRALIAN DEPT. OF LANDS
P.O. BOX 1047 G.P.O
ADELAIDE, SOUTH AUSTRALIA 5001
AUSTRALIA

BO JONSSON
NATIONAL LAND SURVEY OF SWEDEN
801 12
GAVLE, SWEDEN

RUDY JUNKE
GEOMAR ENG. INC.
181 VINEYARD ROAD
HUNTINGTON, NY 11743

MRS. RUDY JUNKE
GEOMAR ENG. INC.
181 VINEYARD ROAD
HUNTINGTON, NY 11743

HERIBERT P. KAHMEN
GEODETIC INSTITUTE
UNIVERSITY OF HANNOVER
NIENBURGER STR. 1
D3000 HANNOVER
FEDERAL REPUBLIC OF GERMANY

RUDOLPH M. KALAFUS
U.S. DEPT. OF TRANSPORTATION/TSC
KENDALL SQUARE
CAMBRIDGE, MA 02142

ALEX KALISH
GEODETIC INTERNATIONAL, INC.
16138 NEW FIELD DR.
HOUSTON, TX 77082

KLAUS KANIUTH
DEUTSCHES GEODATISCHES
FORSCHUNGSINSTITUT
MARSTALLPLATZ 8
MUNCHEN 22
D-8000 MUENCHEN 22
FEDERAL REPUBLIC OF GERMANY

FRED KARKALIK
SYSTEMS CONTROL TECHNOLOGY, INC.
1801 PAGE MILL ROAD
PALO ALTO, CA 94304

BILL KASS
NOAA/NOS/NGS
9001 GREEN RUN WAY
GAITHERSBURG, MD 20879

WILLIAM M. KAULA
CHIEF, NATIONAL GEODETIC SURVEY.
DIV.
N/CG1
NOS/NOAA
6001 EXECUTIVE BLVD.
ROCKVILLE, MD 20852

JOHN A. KELMELIS
U.S. GEOLOGICAL SURVEY
12201 SUNRISE VALLEY DRIVE 515
RESTON, VA

ROBERT V. KEMPEL
TRANSCONTINENTAL GAS PIPE LINE
ENGINEERING/SURVEY
P.O. BOX 1396
HOUSTON, TEXAS 77251

KERRY W. KEMPER
PENTAX CORPORATION
SURVEY DIVISION
35 INVERNESS DR. EAST
ENGLEWOOD, CO 80112

STANLEY E. KING
INTERNATIONAL TECHNOLOGY
3127 COMMERCIAL DRIVE
ANCHORAGE, AK 99501

KERRY KINGHAM
U.S. NAVAL OBSERVATORY
TIME SERVICE DEPARTMENT
34TH AND MASSACHUSETTS AVE., N.W.
WASHINGTON, DC 20390

JOHN G. KIRK
GEODYNAMICS CORP.
5290 OVERPASS RD., BLDG. D
SANTA BARBARA, CA 93111

WILLIAM J. KLEPCZYNSKI
U.S. NAVAL OBSERVATORY
TIME SERVICE DEPARTMENT
34TH AND MASSACHUSETTS AVE., N.W.
WASHINGTON, DC 20390

ALFRED KLEUSBERG
UNIVERSITY OF NEW BRUNSWICK
P.O. BOX 4400
FREDERICTON
NEW BRUNSWICK, CANADA E3B 5A3

JOHN A. KLOBUCHAR
A.F. GEOPHYSICS LAB
HANSCOM AFB, MA

DR. CURTIS A. KNIGHT
INTERFEROMETRICS INC.
8150 LEESBURG PIKE
VIENNA, VA 22180

RONALD KOLENKIEWICZ
NASA GODDARD SPACE FLIGHT CENTER
CODE 621
GREENBELT, MD 20221

FRED KORKALIK
SYSTEMS CONTROL TECHNOLOGY
1801 PAGE MILL RD.
PALO ALTO, CA 94303

JAN KOUBA
EMR CANADA, EARTH PHYSICS BR.
1 OBSERVATORY CRESCENT
OTTAWA K2H-5T8
CANADA KIA 0Y3

CAPT. KARL L. KOVACH
GPS MASTER CONTROL STATION
SD/OL-AQ (GPS)
VANDENBERG AFB, CA 93437

JOHN H. KRAEMER
U.S. DEPARTMENT OF TRANSPORTATION
55 BROADWAY
CAMBRIDGE, MA 02192

CHARLES KRINSKY
NAVAL SURFACE WEAPONS CENTER
DAHLGREN, VA

PETER M. KROGER
JET PROPULSION LAB
4800 OAK GROVE DR.
PASADENA, CA

ZDZISLAW J. KRYSINSKI
SPACE RESEARCH CENTER
POLISH ACADEMY OF SCIENCE
UL. ORDONA 21
01-237
WARSAW, POLAND

WOLF KUEBLER
ITTRJ
THOMAS POINT 3740
ANNAPOLIS, MD

JOHN KUKOWSKI
ARABIAN AMERICAN OIL COMPANY
DHAHRAN
SAUDI ARABIA

RALPH L. KULP
NSWC
DAHLGREN, VA 22448

DR. M. KUMAR
DEFENSE MAPPING AGENCY
6500 BROOKES LANE
WASHINGTON, DC 20315

GERALD LACHAPELLE
NORTECH SURVEYS
309 2ND AVE., NW
CALGARY, ALTA
CANADA T2P 0C5

JONATHAN W. LADD
AERO SERVICE
8100 WESTPARK DR.
HOUSTON, TX

LEWIS A. LAPINE
NOAA NATIONAL OCEAN SERVICE
HERBERT C. HOOVER BLDG., RM 4018
WASHINGTON, DC

MARIE LARGAY
NAVAL RESEARCH LABORATORY
4555 OVERLOOK AVE
WASHINGTON, DC

DR. HANS-JVERGEN LARISCH
GEOSAT
LOEHBERG 78
D 4330 MUELHEIM/RUHR
GERMANY

JEAN-GUY LECLERC
UNIVERSITY LAVAL
DEPT. SCI. GEODESIQUES
PAVILLON CASAULT
STE FOY, QUEBEC
CANADA G0A1 1N0

ROGER W. LEEMAN
W.D. USHER & ASSOC. LTD
#101, 10335 - 172 STREET
EDMONTON, ALBERTA
CANADA T5S 1K9

CHAD LEFFERSON
COCHRANE SUBSEA ACOUSTICS
OPERATIONS
108 RIDONA STREET
LAFAYETTE, LA 70508

DAVID J. LEHMAN
INTERAMERICAN GEODETIC SURVEY
DRAWER K
APO MIAMI, FL 34004

PROF. ALFRED M. LEICK
AFGL/LWG
HANSCOM AFB, MA 01731

WAYNE R. LEONARD
RAMSEY COUNTY
PUBLIC WORKS DEPARTMENT
3377 N. RICE ST.
ST. PAUL, MN 55112

NORMAN A. LEPPARD
DIRECTORATE OF MILITARY SURVEY
ELMWOOD AVENUE
FELTHAM, MIDDLESEX TW13 7AE
UNITED KINGDOM

YULIN LI
RESEARCH INSTITUE OF SURVEYING
AND MAPPING
7 YONGDING ROAD
BEIJING, CHINA

ZHENGHANG LI
WUHAN TECHNICAL UNIVERSITY OF
SURVEYING AND MAPPING
23 LOYU ROAD
WUHAN, CHINA

STEPHEN M. LICHTEN
JET PROPULSION LABORATORY
NAVIGATION & EARTH ORBITER
SYSTEMS
JPL 264-737
4800 OAK GROVE DRIVE
PASADENA, CALIFORNIA 91109

STEVEN H. LIEBER
HARVEY LYNCH INC.
10777 WEST HEIMER
HOUSTON, TX 77042

DONALD L. LIGHT
U.S. GEOLOGICAL SURVEY
NATIONAL MAPPING DIV.
13105 MEMORY LANE
FAIRFAX, VA 22033

DIPL.-ING. W. LINDLOHR
DEPARTMENT OF GEODETIC SCIENCE
STUTTGART UNIVERSITY
KEPLERSTR 11
D-7000 STUTTGART 1
FEDERAL REPUBLIC OF GERMANY

JACK E. LINDSEY
TENNESSEE DEPT. OF TRANSPORTATION
P.O. BOX 58
KNOXVILLE, TN

MR. DONALD W. LITTLE
VA. DEPT. HYWS. & TRANSP.
LOCATION & DESIGN DIV.
1401 E. BROAD STREET
RICHMOND, VA 23219

ZHEN-TING LIU
INSTITUTE OF SPACE PHYSICS
P.O. BOX 2701
BEIJING, CHINA

SANDRA LIVGARD
SAINT LOUIS COUNTY SURVEYOR
SURVEYOR'S OFFICE
COURTHOUSE
DULUTH, MN 55718

NORMAN B. LIVGARD
SAINT LOUIS COUNTY SURVEYOR
SURVEYOR'S OFFICE
COURTHOUSE
DULUTH, MN 55718

D.G. LIVINGSTONE
BRITISH PETROLEUM CO. LTD.
EXPLORATION
BRITANNIC HOUSE, MOOR LANE
LODON EC249BU
UNITED KINGDOM

KEVIN P. LOGAN
COMMANDER AND DIRECTOR
US ARMY ENGINEER TOPOGRAPHIC
LABORATORIES
ATTN: ETL-TD-EA
FORT BELVOIR, VA 22060-5546

BRUCE M. LOHREY
TIME SERVICE DIVISION
USNO
34TH AND MASSACHUSSETTS AVE. NW.
WASHINGTON, D.C. 20390

JEFF LONELL
BOSTON SURVEY CONSULTANTS
467 SUMMER STREET
BOSTON, MA 02210

W. J. LOUNSBERY
NOS/OMA
6001 EXECUTIVE BLVD.
ROCKVILLE, MD

CARL LUKAC
U.S. NAVAL OBSERVATORY
TIME SERVICE DEPARTMENT
34TH AND MASSACHUSETTS AVE., N.W.
WASHINGTON, DC 20390

THORD LUNDGREN
SCAIS AB
GAMLATORG 5
27500 SJOBO
SWEDEN

CHOPO MA
NASA/GODDARD
GEODYNAMICS BRANCH, CODE 621.9
GREENBELT, MD 20771

JUDY MACDORAN
ISTAC, INC.
SUITE 101
444 N. ALTADENA DR.
PASADENA, CA 91107

PETER F. MACDORAN
ISTAC, INC.
SUITE 101
444 N. ALTADENA DR.
PASADENA, CA 91107

DR. MARK M. MACOMBER
HQ DEFENSE MAPPING AGENCY
DEPUTY DIRECTOR FOR SYSTEMS AND
TECHNIQUES
BLDG. 56, U.S. NAVAL OBSERVATORY
WASHINGTON, D.C. 20305

GERALD L. MADER
N/CG114
NATIONAL GEODETIC SURVEY
11400 ROCKVILLE PIKE
ROCKVILLE, MD' 20852

FREDE MADSEN
DANISH GEODETIC INSTITUTE
GAMLEHAVE ALLE 22
CHARLOTTENLUND,
DENMARK
DK 2920

BRUCE MAGNELL
EG & G OCEANOGRAPHIC SERVICES
77 RUMFORD AVENUE
WALTHAM, MA

KRISTINE P. MAINE
THE AEROSPACE CORPORATION
P.O. BOX 92957
LOS ANGELES, CA 90009

ANDRE MAINVILLE
GEODETIC SURVEY OF CANADA
615 BOOTH STREET
OTTAWA, ONTARIO
CANADA K1A 0E9

RAJENDRA P. MALLA
INTERSTATE ELCTRONICS CO.
ENGINEERING
707 E. VERMONT AVE.
ANAHEIM, CALIFORNIA 92803

CAROL W. MALYEVAC
NAVAL SURFACE WEAPONS CENTER
CODE K12
DAHLGREN, VA 22448

ANGELA MARCHIONDA
GEOMAR ENG. INC.
181 VINEYARD ROAD
HUNTINGTON, NY 11743

CHARLES F. MARTIN
DEFENSE MAPPING AGENCY
USN OBS GROUNDS-BLDG. 36
WASHINGTON, D.C. 20305

CHRESTON F. MARTIN
EG&G WASHINGTON ANALYTICAL SFR
5000 PHILADELPHIA WAY
LANHAM, MD 20706

RUSSELL E. MARTIN
PACIFIC MISSLE TEST CENTER
CODE 3442
POINT MUGU, CA 93010

ROBERT H. MARTIN
THE LIETZ CO.
VICE PRESIDENT - PRODUCTS
9111 BARTON BOX 2934
OVERLAND PARK, KANSAS 66213

EMIL J. MATEKER, JR.
AERO SERVICE
8100 WESTPARK DR.
HOUSTON, TX 77079

MIKE MATHWIG
OPERATIONS BRANCH
NATIONAL GEODETIC SURVEY N/CG 161
ROOM 26, ROCKWALL BLDG.
ROCKVILLE, MD 20852

PAMPALONI MAURIZIO
ISTITUTO GEOGRAFICO MILITARE
VIA CESARE BATTISTI 10
FIRENZE, ITALY

KURTIS L. MAYNARD
JOHN E. CHANCE & ASSOC., INC.
200 DULLES BLVD.
LAFAYETTE, LA 70505

MICHEL MAYOUD
CERN-
1211-GENEVA-23
SWITZERLAND

DAVID J. MCARTHUR
CANADIAN GEODETIC SURVEY
615 BOOTH ST.
OTTAWA, ONTARIO, CANADA K2B 5A8

DENNIS D. MCCARTHY
U.S. NAVAL OBSERVATORY
TIME SERVICE DEPARTMENT
34TH AND MASSACHUSETTS AVE., N.W.
WASHINGTON, DC 22180

THOMAS B. MCCASKILL
NAVAL RESEARCH LAB
4555 OVERLOOK AVE., S.W.
WASHINGTON, D.C. 20375

RAULLO J. MCCONAHY
JOHNS HOPKINS/APP. PHYSICS LAB
JOHNS HOPKINS ROAD
LAUREL, MD 20707

JAMES MCCULLOUGH
WOODS HOLE OCEANO
37 SACONESSET ROAD
FALMOUTH, MA 02540

KEITH D. MCDONALD
FEDERAL AVIATION ADMIN.
800 INDEPENDENCE AVENUE
WASHINGTON, DC

MICHAEL L. MCGINLEY
NOAA/NOS
PHOTOGRAMMETRY
6001 EXECUTIVE BLVD.
ROCKVILLE, MD 20851

JAMES D. MCNAMARA
NOAA, NOS. PHOTO BRANCH
6001 EXECUTIVE BLVD.
ROCKVILLE, MD 20852

GILBERT P. MEAD
NASA/GSFC
CODE 601
GREENBELT, MD 20771

B.K. MEADE
JOHN E. CHANCE & ASSOC., INC.
5903 MT. EAGLE DRIVE #404
ALEXANDRIA, VIRGINIA 22303

NYLE V. MEADE
VA. DEPT. HWYS. & TRANSP.
1401 E. BROAD STREET
RICHMOND, VA 23219

WILLIAM G. MELBOURNE
TELECOMMUNICATIONS SCIENCE AND
ENGINEERING
JPL
4800 OAK GROVE DR.
PASADENA, CA 91109

JERRY MERCURE
BDM MANAGEMENT SERVICES CO.
8200 MOPAC SUITE 300
AUSTIN, TX

ROBERT C. MERENYI
NDE
TASC
1 JACOB WAY
READING, MA 01867

ROGER L. MERRELL
TEXAS DEPT. OF HIGHWATS AND
PUBLIC TRANSP.
AUTOMATION DIVISION
11TH AND BRAZO'S STREETS
AUSTIN, TX 78701

ROBERT W. MERRIAM
PRESIDENT
MERRIAM INSTRUMENTS, INC.
627 TILLINGHAST ROAD
EAST GREENWICH, RI 02818

BRETT D. MERRITT/CODE GSGT
DEFENSE MAPPING AGENCY/HTC
6500 BROOKS LANE
WASHINGTON, D.C. 20315

TED E. MEYER
DEFENSE MAPPING AGENCY/HTC
6500 BROOKS LANE
WASHINGTON, D.C.

DAVID F. MEZERA
UNIV. OF WISCONSIN
1214 ENGR. BLDG.
1415 JOHNSON DR.
MADISON, WISCONSIN 53706

SZABOLCS MIHALY
FOLDMERESI INTEZET
SATELLITE GEODETIC OBSERVATORY
H-1051, GUSLEV U. 19.
BUDAPEST, HUNGARY

DENNIS MILBERT
NATIONAL GEODETIC SURVEY
N/CG112, NOAA
ROCKVILLE, MD 20852

MOODY K. MILES
US ARMY CORPS OF ENGINEERS
20 MASSACHUSETTS AVE.
WASHINGTON, D.C.

LEON M. MILLER
GREIMER ENGINEERING
ONE VILLAGE SQUARE
BALTIMORE, MD

ROBERT B. MILLER
ISTAC
444 N. ALTADENA DR. #101
PASADENA, CA

MIHRAN MIRANIAN
U.S. NAVAL OBSERVATORY
TIME SERVICE DEPARTMENT
34TH AND MASSACHUSETTS AVE., N.W.
WASHINGTON, DC 20390

AIT BELAID MOHNED
UNIVERSITY LAVAL
886 AVE NYRAND
QUEBEC, CANADA G1V2V9

MICHAEL MONET
CERN
GEODESY GROUP
SITE DE PREVESSIN
F-01631 CERN CEDEX
FRANCE

BRAD MONTGOMERY
TEXAS INSTRUMENTS
P.O. BOX 405 M/S 3418
LEWISVILLE, TX 75262

CLYDE R. MOORE
INTERNATIONAL BOUNDARY COMMISSION
US-CANADA
425 I STREET, N.W. ROOM 150
WASHINGTON, D.C. 20001-2599

GARRETT R. MOORE
DEFENSE MAPPING SCHOOL
SURVEY DEPT.
FT. BELVOIR, VA 22060-5828

RICHARD MOREAU
QUEBEC GOV.
1995 BD CHAREST O.
SAINTE FOY
QUEBEC, CANADA GIN4H9

CHARLES P. MORGAN
ROCKWILL INTERNATIONAL
400 C AVENUE, N.E.
CEDAR RAPIDS, IOWA

STEVE MOSELEY
TEXAS INSTRUMENTS
P.O. BOX 405 MS 3418
LEWISVILLE, TX 75023

CAPT. RAY MOSES
NOAA/OAR
6010 EXECUTIVE BLVD.
ROCKVILLE, MD 20852

ACHIM MUELLER
UNIVERSITY BONN
NUSSALLEE 17
53 BONN, W. GERMANY

IVAN I. MUELLER
OHIO STATE UNIVERSITY
GEODETIC SCIENCE AND SURVEYING
1958 NEIL AVENUE
COLUMBUS, OHIO 43210-1247

RICHARD MUNIZ
US ARMY CORPS ENGINEERS
PENTAGON
WASHINGTON, D.C.

ORLAND W. MURRAY
NATIONAL GEODETIC SURVEY
INSTRUMENT AND EQUIPMENT SECTION
P.O. BOX 1
CORBIN, VA 22446

GEORGE NARD
SERCEL
BP 64
NANTES, FRANCE 44471

PAUL E. NEEDHAM
NAT'L. MAPPING, U.S.G.S.
525 NATIONAL CENTER
RESTON, VA 22092

RUTH E. NEILAN
JPL MS138-208
4800 OAK GROVE AVENUE
PASADENA, CA 91042

MADHU NERLIKER
TEXAS INSTRUMENTS
P.O. BOX 405 M/S 3418
LEWISVILLE, TX 75023

SCOTT WILLIAM NESBITT
COMAP GEOSURVEYS
11391 MEADONGLEN LANE
HOUSTON, TX 77082

K. BINH NGUYEN
SC. GEODESIQUES ET TELED.
UNIVERSITE LAVAL
PAVILLON CASSAULT
STE FOY, QUEBEC G1K 7P4
CANADA

WOLFGANG NIEMEIER
GEODETIC INSTITUT
UNIVERSITY OF HANNOVER
NIENBURGER STRASSE 1
HANNOVER 3000
FEDERAL REPUBLIC OF GERMANY

JEFFREY NOBLET
U.S. COAST GUARD
RADIONAVIGATION DIVISION
2100 SECOND STREET S.W.
WASHINGTON, D.C. 20593

PHILIP S. NOE
TEXAS A&M UNIV.
ELECTRICAL ENGR. DEPT.
COLLEGE STATION
TEXAS

DON O. NORMAN
NOS
11801 ROCKVILLE PIKE
ROCKVILLE, MD 20852

TIMOTHY G. NORTON
DIVISION OF SURVEY & MAPPING
2 TREASURY PLACE
MELBOURNE
VICTORIA, AUSTRALIA 3002

ROBERT W. NOVACK
NAVAL RESEARCH LAB.
4555 OVERLOOK AVE.
WASHINGTON, D.C. 20375

ARNE EDMUND OFSTAD
HYDROGRAPHIC SERVICES
OF NORWAY
KLUBBGATA 1
4000 STAVANGER
NORWAY

JOE OLLIVER
OXFORD UNIVERSITY
EARTH SCIENCES
62 BANBURY ROAD
OXFORD OX2 6PN
ENGLAND

RANDLE W. OLSEN
U.S. GEOLOGICAL SURVEY
NAT'L MAPPING DIVISION
510 NATIONAL CENTER
RESTON, VA 22092

EDWARD P. OPPENHEIMER
JOHNS HOPKINS APPLIED PHYSICS
LABORATORY
JOHNS HOPKINS ROAD
LAUREL, MD 20707

JOSE J.S.P. OSORIO
INST. INV. CIENTIFICA TROPICAL
OBSERVATORIO ASTRONOMICO
UNIVERSIDADE DO PORTO
MONTE DA VIRGEM
4400 VILA NOVA DE GAIA
PORTUGAL

TERRY N. OSTERDOCK
STANFORD TELECOMMUNICATIONS, INC.
2421 MISSION COLLEGE BLVD.
SANTA CLARA, CA 95054

JOHN H. OSTRANDER
BETA HI INC
4104 OFFUT DRIVE
SUITLAND, MD 20746

JOHN H. PAINTER
TEXAS A & M UNIVERSITY
DEPT. OF ELECTRICAL ENG.
COLLEGE STATION, TX 77843

JOSEPH V.R. PAIVA
UNIVERSITY OF MO/CIVIL
ENGINEERING
1038 ENGINEERING BLDG
COLUMBIA, MD 65211

RICHARD M. PAUL
VITRO CORPORATION
14000 GEORGIA AVENUE
SILVER SPRING, MD 20910

JOSEPH A. PAVELKA
ESSO ESPL INC.
3616 RICHMOND
HOUSTON, TX 77046

RICHARD PEARSALL
USGS
NATIONAL CENTER
RESTON, VA

PETER PESEC
INST. FOR SPACE RESEARCH
SATELLITE GEODESY
LUSTBUEHELSTRASSE 46
GRA7, AUSTRIA 8042

LEROY M. PETERSON
SUBMARINE TECHNOLOGY PROGRAM
APPLIED PHYSICS LAB./JOHN HOPKINS
JOHNS HOPKINS ROAD
LAUREL, MD 20707

FRED W. PHILLIPS
SPERRY MARINE
RT 29 NORTH
CHARLOTTESVILLE, VA 222906

KIRVAN H. PIERSON
VITRO CORPORATION
14000 GEORGIA AVENUE
SILVER SPRING, MD 20910

PENELOPE S. PIETRAS
MAGNAVOX
MARINE SYSTEMS DIVISION
2829 MARICOPA
TORRANCE, CA 90503

DAVID J. PIETRASZEWSKI
USCG R & D CENTER
AVERY POINT
GROTON, CT 06340

COLIN R. PIKE
POSITIONING RESOURCES LTD
54 COMMERCE STREET
ABERDEEN, SCOTLAND AB1 2BP

JERRY L. PINKERTON
U.S. BUREAU OF LAND MNGT.
CADASTRAL SURVEY
701 C ST.
BOX 13
ANCHORAGE, AK 99513

ROBERT E. PODLESNY
NAVAL COASTAL SYSTEMS CENTER
COMBAT SYSTEMS DIVISION
SYSTEMS DEPT.
HWY 98
PANAMA CITY, FL 32407-5000

WILLIAM H. PRESCOTT
U.S. GEOLOGICAL SURVEY
345 MIDDLEFIELD ROAD, MS/977
SAN FRANCISCO, CA 94025

GERALD PREZALAR
VITRO CORPORATION
14000 GEORGIA AVENUE
SILVER SPRING, MD 20910

MIKHAIL T. PRILEPIN
SOVIET GEOPHYSICAL COMMITTEE
MORODEZHNAJE
MOSCOW, USSR

DR. SERGIO PUGNAGHI
GEOPHYSICAL OBSERVATORY MODENA
G. CAMPI
MODENA, ITALY I41100

BARNEY PUTZIGER
NATIONAL GEODETIC SURVEY
65 AVIATION CIRCLE
ATLANTA, GA 30336

SEE HEAN QUEK
UNIVERSITY OF NEW BRUMSWICK
BOX 4400
FREDERICTION
NEW BRUNSWICK, CANADA E3B 5A3

JOHN QUILL
US COAST GUARD
G-DST-2154
WASHINGTON, D.C. 22152

KNUT REED
A/S GEOTEAM
GAMLE DRAMMENSVEI 48
1321 STABEKK
NORWAY

CHRISTIAN REGNIER
ATELIERS DE CONSTRUCTIONS DU
CENTRE
RUE DU PRE LA REINE
CLERMONT FERRAND
FRANCE 6300

HEINRICH W. REHMERT
PRAKLA-SEI SMOS GMBH
BUCHHOLZERSTR 100
3000 HANNOVER 51
W. GERMANY

SVEIN REKKEDAL
GEODETIC DEPT.
GEOGRAPHICAL SURVEY OF NORWAY
3500 HONEFOSS
NORWAY

FERLAND REMI
THE MCELHANNEY GROUP LTD
450-999 8TH STREET, S.W.
CALGARY, ALBERTA, CANADA T2R 1J5

DR. BENJAMIN W. REMONDI
NOAA-NGS
6001 EXECUTIVE BLVD.
ROCKVILLE, MD 20852

JEAN G. RIEMERSMA
TOPOGRAPHICAL
SHELL INTERNATIONAL
OOSTDUINLAAN 75
THE HAGUE
NETHERLANDS

JOHN G. RISCH
TEXAS INSTRUMENTS
S HWY 121
LEWISVILLE, TX 75067

GEORGE F. RITCHIE
POSITIONING RESOURCES LTD
54 COMMERCE STREET
ABERDEEN, SCOTLAND
UK AB2 1BP

J.F. ROEBER
SPERRY
CHARLOTTESVILLE, VA 22906

JOHN W. ROTH
SHELL OFFSHORE INC.
ONE SHELL SQUARE
NEW ORLEANS
LOUISIANA 70160

PAUL F. ROWANE
5799-62 RAYBURN AVENUE
ALEXANDRIA, VA

CARYL L. ROWLAND
APL/JHU
JOHNS HOPKINS ROAD
LAUREL, MD 20708

ROBERT RULAND
STANFORD UNIVERSITY
P.O. BOX 4349
STANFORD, CA 94402

TIMOTHY A. RULON
NATIONAL OCEAN SERVICE
6001 EXECUTIVE BLVD.
ROCKVILLE, MD 20852

GRAEME JAMES RUSH
DEPT. MAPPING & SURVEYING QLD
P.O. BOX 234 NORTH QUAY
BRISBAHE
QUEENSLAND, AUSTRALIA

STELLA RUSH
ITECH
3127 COMMERCIAL DRIVE
ANCHORAGE, AK 99501

GERALD F. SAGE
NAVIGATION TECH INC.
2327 DOUBLE O MINE TRAIL
COOL, CA 95614

SANDEE SAGE
NAVIGATION TECH INC.
2327 DOUBLE O MINE TRAIL
COOL, CA 95614

GERALD C. SALADIN
NATIONAL GEODETIC SURVEY
OPERATIONS BRANCH
11400 ROCKVILLE PIKE
ROOM 26, ROCKWALL BLDG.
ROCKVILLE, MD 20852

PAUL H. SALAMONOWICZ
NATIONAL MAPPING DIVISION
U.S. GEOLOGICAL SURVEY
RESTON, VA 22092

ROCK SANTERRE
UNIVERSITY OF NEW-BRUNSWICK
SURV. ENGG. DEPT. P.O. BOX 4400
FREDERICTON, N.B. CANADA E3B 5A3

NARENDRA K. SAXENA
DEPT. OF OCEANOGRAPHY
NAVAL POSTGRADUATE SCOOL
CODE 68ZX
MONTEREY, CA 93943

DON SCHEIBE
DMAAC
3200 S. SECOND ST.
ST. LOUIS, MO

DR. HANS WERNER SCHENKE
ALFRED-WEGENER-INSTITUTE
COLUMBUS CENTER
D-2850 BREMERHAVEN
WEST-GERMANY

RENE SCHERRER
WILD HEERBRUGG LTD.
SWITZERLAND

JOHN B. SCHLEEPE
THE MCELHANNEY GROUP LTD.
MARINE SURVEYS DIVISION
450-999 - 8TH STREET S.W.
CALGARY, ALBERTA
CANADA T2R1J5

KEVIN SCHNEIDER
TEXAS INSTRUMENTS
P.O. BOX 405 M/S 3418
LEWISVILLE, TX 75067

PROF. ALBERT SCHOEDLBAUER
UNIVERSITAT DER BUNDESWEHR
WERNER-HEISENBERG-WEG 39
MUENCHEN, GERMANY

JAMES W. SCHOONMAKER, JR.
U.S. GEOLOGICAL SURVEY
NATIONAL MAPPING DIVISION
MS 521 NATIONAL CENTER
RESTON, VA 22092

THOMAS F. SCHREIER
EXXIN PRODUCTION RES CO.
P.O. BOX 2189
HOUSTON, TX 77001

BOB E. SCHUTZ
CENTER FOR SPACE RESEARCH
UNIVERSITY OF TEXAS
AUSTIN, TX 78712

SCHWENDENER
WILD HEERBRUGG
HEERBRUGG, SWITZERLAND

DR. OTMAR SCHUSTER
GEOSTAT GMEA
LOEHBERG 78
4330 MUELHEI M.A.D.R.
FED. REP. OF GERMANY

KLAUS-PETER SCHWARZ
UNIVERSITY OF CALGARY
2500 UNIVERSITY DR.
CALGARY, ALBERTA, CANADA T2N-1N4

GREG SCHLUGE
SPERRY MARINE SYSTEMS
RT 29 N
CHARLOTTESVILLE
VA 22906

JANUSZ SCIEGIENNY
M I T LINCOLN LAB
LEXINGTON, MA

DAVID C. SCULL
DEPT. OF TRANSPORTATION
2112 WITTINGTON BLVD
ALEXANDRIA, VA

ANDREW J. SEDLOCK
U.S. COAST GUARD
RADIONAVIGATION DIVISION
10652 PORTER LANE
JUNEAU, AK 99801

GUENTER G. SEEBER
UNIVERSITY HANNOVER
NIENBURGER STR. 6
FEDERAL REPUBLIC OF GERMANY

HERMANN SEEGER
UNIVERSITY OF BONN
NUSSALLEE 17
BONN, FED. REP. GERMANY

STEVE SHEARD
MOTOROLA
2100 E. ELLIOT RD.
TEMPE, AZ 85282

ROBERT P. SHORT
DEFENSE MAPPING AGENCY
6500 BROKES LANE
WASHINGTON, D.C.

MICHAEL L. SIMS
U.S. NAVAL SURFACE WEAPONS CENTER
K13
DAHLGREN, VA 22448

EARL SINES
LOCUS, INC.
2560 HUNNINGTON AVE.
ALEXANDRIA, VA 22303

JOSEPH W. SIRY
NASA GODDARD SPACE FLIGHT CENTER
GREENBELT, MD 20771

LARS E. SJOEBERG
THE ROYAL INSTITUTE OF TECHNOLOGY
STOCKHOLM
SWEDEN 100 44

JAMES A. SLATER
DEFENSE MAPPING AGENCY HTC
6500 BROOKES LANE
WASHINGTON, D.C. 20315

PIET G. SLUITER
GEODETIC
WILLEM PIJPEKLAAN 16
LEIDSCHENDAM
NETHERLANDS 2264 VM

MRS. PEIT G. SLUITER
16 WILLEM PYPERLAAN
LEIDSCHENDAM 2264VM
NETHERLANDS

CHESTER M. SMITH
METRO ENGINEERS
186 LUCKIE ST
ATLANTA, GA

RANDALL W. SMITH
HQ DEFENSE MAPPING AGENCY
CHIEF, GEOPHYSICAL DEVELOPMENT
DIV.
BLDG. 56, US NAVAL OBSERVATORY
WASHINGTON, D.C. 20305

J. KEITH SMITH
STEWART, WEIR & CO
11405 163 STREET
EDMONTON, ALBERTA, CANADA T5R5X6

RONALD H. SMITH
PACIFIC MISSILE TEST CENTER
PT MUGU, CA 93042

DAVID T. SMITHSON
U.S. ARMY ENGINEER SCHOOL
ATZA-TD-I-T
FORT BELVOIR, VA 22060

TOMAS SOLER
NOAA/NOS/NGS
ROCKVILLE, MARYLAND 20852

MS. GRACE SOLLERS
NOAA
NATIONAL GEODETIC INFORMATION
CENTER
NATIONAL GEODETIC SURVEY
6001 EXECUTIVE BLVD.
ROCKVILLE, MD 20852

GERHARD SOLTAU
GEODETIC BRANCH
INSTITUT FUER ANGEW
GEODAESIE
RICHARD STRAUSS ALLEE
FRANKFURT
WEST GERMANY

MICHAEL L. SORRENTINO
DECISIONS AND DESIGNS
8400 WESTPARK DRIVE
MCLEAN, VA 22101

DONALD F. SPENCER
DECISIONS AND DESIGNS INC.
1800 WEST PARK DRIVE SUITE 600
MCLEAN, VA 22101

JOHN H. SPENCER
NRL CODE 4134
WASHINGTON, D.C. 20375

LARRY SPICE
NATIONAL SECURITY AGENCY
SAVAGE ROAD
FORT G. G. MEADE
MARYLAND 20755

T. STALDER
ALLIED/BENDIX
5707 THUNDERHILL RD.
COLUMBIA, MD 21045

LOWELL E. STARR
45 GEOLOGICAL SURVEY
NATIONAL CENTER 519
RESTON, VA 22092

SARAH B. STEBBINS
NAVAL RESEARCH LAB
4555 OVERLOOK AVE
WASHINGTON, D.C.
CODE 7773

BARRY A. STEIN
MITRE CORP.
NAVY SYSTEMS ENGINEERING
1820 DOLLEY MADISON BLVD.
MCLEAN, VA 22102

WILLIAM STEIN
NAVAL SURFACE WEAPONS CENTER
CODE K13
DAHLGREN, VA 22448

C. ERIK O. STENBORG
SWEDISH HYDROGRAPHIC DEPT.
S-601 78 NORRKOEPING
SWEDEN

SCOTT A. STEPHENS
JPL
4800 OAK GROVE DRIVE
PASADENA, CA 91109

MRS. EMILIA R. STENTZ
DEFENSE MAPPING AGENCY AC
3200 S. SECOND STREET
ST. LOUIS, MO 63118

GEORGE T. STENTZ
DEFENSE MAPPING AGENCY AC
3200 S. SECOND STREET
ST. LOUIS, MO 63118

WOLFGANG STOESSEL
BAYER LANDESVERMESSUNGSAMT
ALEXANDRIA STREET 4
MUNICH, BAVARIA, GERMANY
D-8000

ART STOLZ
DEPT. OF SURVEYING
UNIVERSITY OF NEW SOUTH WALES
KENSINGTON, NSW, AUSTRALIA 2033

JAMES L. STOWELL
GEOPHYSICAL SERVICES INC. GSI
P.O. BOX 225621 MS 3988
DALLAS, TX

WILLIAM E. STRANGE
NGS/NOAA
6001 EXECUTIVE BLVD
ROCKVILLE, MD 20852

BRYANT STURGESS
STATE LANDS COMMISSION
1807 13TH STREET
SACRAMENTO, CA 95814

MARK STURZA
LITTON AERO PRODUCTS
6101 CONDOR DRIVE
MOORPARK, CA

DENISE E. STUTZMAN
DMAHTC
ATTN: GST
WASHINGTON, D.C.

FRED W. STYER
COCHRANE SUBSEA ACOUSTICS
OPERATIONS DEPT.
108 RIDONA STREET
LAFAYETTE, LA 70508

JOHN SUMNER
GEOSCIENCES
UNIV. OF ARIZONA
TUCSON, AZ 85721

JOHN SUNDSBY
NORGES GEOGRAFISKE OPPMALING
3500 HONEFOSS
NORWAY

S. LEIF SVENSSON
GEODATISCHES INST.
UNI. STUTTGART
KEPLERSTRASSE 11
STUTTGART
FEDERAL REPUBLIC OF GERMANY

COURTNEY H. SWANSON
U.S. GEOLOGICAL SURVEY
NATIONAL MAPPING DIV.
BOX 25046 MJ 509 D.F.C.
DENVER, CO 80225

R.B. SWART
U.S. COAST GUARD
RADIONAVIGATION DIVISION
2100 SECOND STREET, S.W.
WASHINGTON, D.C. 20593

RICHARD W. SWARTS
SUMMIT COUNTY ENGINEER
538 E. SOUTH STREET
AKRON, OHIO 44311

EVERETT R. SWIFT
NAVAL SURFACE WEAPONS CENTER
SPACE SYSTEMS DIVISION
K12
DAHLGREN, VIRGINIA 22448

JOHN H. TAMURA
GUIDANCE AND CONTROL SYSTEMS
LITTON SYSTEMS
5500 CANOGA AVE.
WOODLAND HILLS, CA 91367

EUGENE A. TAYLOR
VIRGINIA TECH.
103 PEARMAN RD.
BLACKSBURG, VA 24060

PAUL H. TAYLOR
U.S. NAVAL OCEANOGRAPHIC OFFICE
601
100 RABBIT HILL LANE
CARRIERE, MS 39426

GEORGE T. TENNIS
GSG/GSGT
DMAHTC
WASHINGTON, D.C. 20315

PIERRE TESSIER
QUEBEC GOVERNMENT
1995 QUEST BOUL CHAREST
STE-FOY
QUEBEC GIN-4H9

STEVEN THEBO
TEXAS INSTRUMENTS
P.O. BOX 45 MS 3418
LEWISVILLE, TX

KARL-HEINZ THIEL
INSTITUT FUR NAVIGATION
KEPLERSTRASSE 11
7000 STUTTGART 1
GERMANY

ROBERT H. THOMAS
THOMAS LAND SURVEYING
135 N. HIGH ST. P.O. BOX 930
MILLVILLE, NJ 08332

DAVID K. THOMMEN
LITTON GCSD
5500 CANOGA AVE.
WOODLAND HILLS, CALIFORNIA 91365

JUNE M. THORMODSGARD
U.S. GEOLOGICAL SURVEY
EROS DATA CENTER
TECHNIQUE DEVELOPMENT & APPL. B.
SIOUX FALLS, S.D. 57198

CATHY THORNTON
JPL
4800 OAK GROVE DR.
PASADENA, CA 91103

LOUIS G. THORSEN
DMA IAGS
BLDG. 144
FT. SAM HOUSTON, TX 78234

HANS THURNHEER
SONNENSTR 5
9434 AU
SWITZERLAND

ULRIKE H. TILK
GEODETIC INSTITUTE
UNIVERSITY OF HANNOVER
NIENBURGER STRASSE 1
HANNOVER 3000
LOWER SAXONY
FEDERAL REPUBLIC OF GERMANY

MARTI TIURI
HELSINKI UNIV OF TECHNOLOGY
OTANIEMI
ESPOO
FINLAND 02130

MARK H. TORRENCE
EG & G WASC INC.
5000 PHILADELPHIA WAY, SUTTE J
LANHAM, MD

REYNALDO M. TREVINO
PACIFIC MISSLE TEST CENTER
RANGE DEVELOPMENT DEPARTMENT
(3141)
POINT MUGU, CA 93042

CHARLES TRIMBLE
TRIMBLE NAVIGATION
1077 INDEPENDENCE AVE.
MT. VIEW, CA 94043

ARNOLD J. TUCKER
APPLIED RESEARCH LABORATORY
10000 BURNET RD.
AUSTIN, TX 78759

GREGORY M. TUTTLE
BUREAU OF RECLAMATION
505 S. 43RD AVENUE
PHOENIX, AZ 85068

PROF. MARCO UNGUENDOLI
INSTITO DI. TOPOGRAFIA, GEODESIA
E GEOFISICA MINERARIA
FACOLTA DI INGEGNERIA
UNIVERSITA DEGLI STUDI
VIALE RISCORGIMENTO, 2
40136 BOLOGNA ITALY

HANS VAN DER WAL
RYKSWATERSTAAT
KANAALWEG 3B
DELFT, NETHERLANDS

PETR VANICEK
UNB
FREDERICTON, N.B.
CANADA E3B 5A3

JEROME R. VETTER
APPLIED PHYSICS LABORATORY
JOHN HOPKINS ROAD
LAUREL, MD

MARK A. VINCENT
JILA
UNIVERSITY OF COLORADO
BOULDER, CO 80309

JACK WAANANEN
U.S. GEOLOGICAL SURVEY
MAIL STOP 510
RESTON, VA 22092

GREGORY K. WAGSTAFF
METRO ENGINEERING
186 LUCKIE ST.
ATLANTA, GA

BRENT ALAN WANLESS
UNIVERSITY OF CALGARY
4836 NORTH HAVEN DR.
CALGARY, ALBERTA, CANADA T2K-2J7

RANIN B. WARD
NOAA/NGS
1532 TANYARD HILL ROAD
GAITHERSBURG, MD

RANDOLPH WARE
UNIVERSITY NAVSTAR CONSORTIUM
UNIVERSITY OF COLORADO
BOULDER, CO 80309

HUGH WARREN
BENDIX/NRL
4555 OVERLOOK AVE.
WASHINGTON, D.C. 20375

ATTALLAH M. WASSEF
UNIVERSITY OF TORONTO
ERINDALE CAMPUS
TORONTO, ONTARIO M6P2T4
CANADA

DR. KERMIT R. WAY
BENDIX FIELD ENGINEERING CORP.
1 BENDIX ROAD
COLUMBIA, MD 21045

N. RHODUS WAYNE
AEROSPACE CORP
4350 E. EL SEGUNDO BLVD
EL SEGUNDO
CA 90001

DENNIS A. WEGENAST
NATIONAL GEODETIC SURVEY
80 21 52ND AVE. WEST
MUKILTEO, WASHINGTON

WILLIAM L. WEHLING
WEHLING ENGINEERS
221 SOUTH SUMNER STREET
BEATRICE, NEBRASKA 68310

ZIQING WEI
OHIO STATE UNIVERSITY
GEODETIC SCIENCE AND SURVEYING
1958 NEIL AVENUE
COLUMBUS, OHIO 43210

JACK A. WEIGHTMAN
BRITOIL
150 SAINT VINCENT STREET
GLASGOW, SCOTLAND G25LJ

MARC A. WEISS
NATIONAL BUREAU OF STANDARDS
325 BROADWAY
BOULDER, CO 80303

DAVE WELLS
UNIVERSITY OF NEW BRUNSWICK
538 SQUIRES ST.
FREDERICTON
N.B., CANADA E3B 3V4

DR. WALTER M. WELSCH
UNIVERSITAET DER BUNDESWEHR
WERNER-HEISENBERG-WEG 39
8014 NEUBIBERG
FEDERAL REPUBLIC OF GERMANY

ROBERT G. WELSHE
AERO SERVICE
8100 WESTPARK
HOUSTON, TX 77024

DANNY A. WEST
U.S. BUREAU OF LAND MNGT.
541 LEDORA CIRCLE
ANCHORAGE, ALASKA

EDWIN E. WESTERFIELD
APPLIED PHYSICS LABORATORY/JHU
JOHNS HOPKINS ROAD
LAUREL,MD 20707

JAMES H. WHITCOMB
ISTAC, INC.
SUITE 101
444 N. ALTADENA DRIVE
PASADENA, CA 91107

HASCHAL L. WHITE
DMA AEROSPACE CENTER
GDT
3200 SOUTH SECOND STREET
ST. LOUIS, MISSOURI 63118

LARRY WHITING
INTERNATIONAL TECHNOLOGY LTD.
3127 COMMERCIAL DRIVE
ANCHORAGE, ALASKA 99501

CHARLES A. WHITTEN
NOAA (RET.)
9606 SUTHERLAND RD.
SILVER SPRING, MD 20901

LAWRENCE F. WIEDERHOLT
INTERMETRICS, INC.
733 CONCORD AVE.
CAMBRIDGE, MA

BRUCE I. WILLIAMS
NGS/NOAA
1633 BRADLEY AVE.
HUMMELSTOWN, PA 17036

GEORGE E. WILLIAMS
NOAA, NOS, NGS
11440 EXECUTIVE BLVD.
ROCKVILLE, MD 20852

RICHARD WILLIAMS
WIMPOL INC.
8850 JAMEEL #100
HOUSTON, TX 77040

PASCAL R. WILLIS
INSTITUT GEOGRAPHIQUE NATIONAL
5 ALLEE DES BRUNETTES
POITIERS 86000
FRANCE

HERBERT WILMES
ABT. 1, THEOR. GEODASIE
DEUTSCHES GEODAT.
FORSCHUNGSINSTITUT
MARSTALLPLATZ 8
8000 MUNCHEN 22
FEDERAL REPUBLIC OF GERMANY

RACHEL WILMES
ABT. 1, THEOR. GEODASIE
DEUTSCHES GEODT.
FORSCHUNGSINSTITUT
MARSTALLPLATZ 8
8000 MUNCHEN 22
FEDERAL REPUBLIC OF GERMANY

ERNEST L. WILSON
FORD AEROSPACE
4920 NIAGARA RD.
COLLEGE PARK, MD

CHARLES T. WHALEN
NATIONAL GEODETIC SURVEY
NOAA/NOS N/CG1
ROCKVILLE, MD 20852

GERNOT M.R. WINKLER
U.S. NAVAL OBSERVATORY
DIRECTOR, TIME SERVICE DEPARTMENT
34TH AND MASSACHUSETTS AVE., N.W.
WASHINGTON, DC 20390

DONALD D. WINTER
NOAA-OCEAN ASSESSMENTS DIV.
11400 ROCKVILLE PIKE, RM652
ROCKVILLE, MD 20852

J. WINTERMYRE
NGS
1801 FAIRVIEW AVE. E.
SEATTLE, WA 98177

JOHN J. WISE
BONNEVILLE POWER ADMIN.-ETRS
P.O. BOX 3621
PORTLAND, OR 97208

HELMNT WIST
BWB KOBLENZ
KONRAD ADENAUER UFER
5400 KOBLENZ
FEDERAL REPUBLIC OF GERMANY

FRANCES NEVILLE WITHINGTON
U.S. NAVAL OBSERVATORY
TIME SERVICE DEPARTMENT
34TH AND MASSACHUSETTS AVE., N.W.
WASHINGTON, DC 20390

WILLIAM H. WOODEN
DEFENSE MAPPING AGENCY
P.O. BOX 92960, WPC
LOS ANGELES, CA 90009-2960

PETER B. WORSNOP
SOHIO PETROLEUM
5400 LBJ FUY #1200
DALLAS, TX 75240

ALAN F. WRIGHT
GLOBAL SURVEYS LIMITED
2, RIDGACRE LANE
QUINTON, BIRMINGHAM B321ES
UNITED KINGDOM

SIEN-CHONG WU
JET PROPULSION LAB.
TRACKING SYSTEMS & APPLICATION
4800 OAK GROVE DR.
PASADENA, CALIFORNIA 91109

GERHARD WUEBBENA
UNIVERSITY HANNOVER
INSTITUT FUR ERDMESSUNG
NIENBURGER STR. 6
D3000 HANNOVER 1
FEDERAL REPUBLIC OF GERMANY

DAVID WYMAN
BUOY TECHNOLOGY
134 HALL STREET
P.O. BOX 922
CONCORD, NH 03301

QIFENG XU
ZHENGZHOU INSTITUTE OF SURVEYING
AND MAPPING
59 WEST LONGHAI ROAD
ZHENGZHOU, CHINA

MIKE YAKOS
ROCKWELL COLLINS
400 COLLINS RD., NE
CEDAR RAPIDS
IOWA 52406

RICHARD YORCZYK
NATIONAL GEODETIC SURVEY
11400 ROCKVILLE PIKE
ROCKVILLE, MD

GARY YOUNG
VERTICAL NETWORK BRANCH
N/CG13, ROOM 313 A, ROCKWALL
BLDG.
NATIONAL GEODETIC SURVEY
ROCKVILLE, MD 20852

LAWRENCE E. YOUNG
CALTECH/JET PROPALSLON LAB
4800 OAK GROVE AVE.
PASADENA, CA 91101

FRED ZEDECK
OSD C3I
PENTAGON
WASHINGTON, D.C. 20301

JAMES H. ZEIGLER
TENN. TRANSPORTATION DEPT.
1100 JAMES K POLK BLDG.
NASHVILLE, TN

NIKITA ZELENSKY
EG&G/WASC
5000 PHILADELPHIA WAY
LANHAM, MD

CHENGZE ZHANG
INSTITUTE OF GEODY & GEOPHYSICS
XIAO HONG SHAN
WUCHUANG, HUBEI, CHINA

JANUSZ B. ZIELINSKI
SPACE RESEARCH CENTRE, P.A.S.
PLANETARY GEODESY
UL. ORDONA 21
01-237
WARSAW, POLAND

GREGORY D. ZIEMER
U.S. COAST GUARD
RADIONAVIGATION DIVISION
2100 SECOND STREET S.W.
WASHINGTON, D.C. 20593

DAVID B. ZILKOSKI
19 NOBLEWOOD CT.
GAITHERSBURG, MD 20878

☆U.S. GOVERNMENT PRINTING OFFICE: 1985 461 135 36604

PENN STATE UNIVERSITY LIBRARIES
A000070941623